Shape optimization for contact and plasticity problems thanks to the level set method

Aymeric Maury

Université Pierre et Marie Curie

Ecole doctorale de sciences mathématiques de Paris centre

Thèse de doctorat

Discipline : Mathématiques

présentée par

Aymeric Maury

Shape optimization for contact and plasticity problems thanks to the level set method

---

dirigée par François Jouve et Grégoire Allaire

Soutenue le 2 décembre 2016 devant le jury composé de :

M. Grégoire Allaire	École Polytechnique	Thesis Advisor
M^{me} Anne-Sophie Bonnet-BenDhia	ENSTA ParisTech	Examiner
M. François Jouve	Université Paris Diderot (Paris 7)	Thesis Advisor
M. Jean-Jacques Marigo	École Polytechnique	Reviewer
M. Édouard Oudet	Université Grenoble Alpes	Examiner
M. Olivier Pironneau	Université Pierre et Marie Curie	Examiner
M. Eduard Rohan	University of West Bohemia	Reviewer

Laboratoire Jacques-Louis Lions, UMR 7598.
Boîte courrier 187
4 place Jussieu
75252 Paris Cedex 05

Université Pierre et Marie Curie.
Ecole doctorale de sciences
mathématiques de Paris centre.
Boîte courrier 290
4 place Jussieu
75252 Paris Cedex 05

Abstract

The main purpose of this thesis is to perform shape optimisation, in the framework of the level set method, for two mechanical behaviours inducing displacement which are not shape differentiable: contact and plasticity. To overcome this obstacle, we use approximate problems found by penalisation and regularisation.

In the first part, we present some classical notions in optimal design (chapter 1). Then we give the mathematical results needed for the analysis of the two mechanical problems in consideration and illustrate these results thanks to some examples.

The second part is meant to introduce the five static contact models (chapter 3) and the static plasticity model (chapter 4) we use throughout the manuscript. For each chapter we provide the basis of the mechanical modeling, a mathematical analysis of the related variational equations and inequations and, finally, explain how we implement the associated solvers.

Eventually the last part, consisting of two chapters is devoted to shape optimisation. In each of them, we state the penalised and regularised versions of the models, prove, for some of them, the convergence to the exact ones, compute shape gradients and perform some numerical experiments in 2D and, for contact, in 3D. Thus, in chapter 5, we focus on contact and consider two types of optimal design problems: one with a fixed contact zone, which can be used or not by the algorithm, and another one with a mobile contact zone. For this last type, we introduce two ways to solve frictionless contact without meshing the contact zone. One of them is new and the other one has never been employed in this framework. In chapter 6, we deal with the Hencky model which we approximate thanks to a Perzyna penalised problem as well as a home-made one.

Keywords: Level set method, shape optimization, contact, friction, plasticity, Hencky model, variational inequations, conical derivative.

Résumé

Le sujet principal de cette thèse est l'optimisation de forme via la méthode des "level sets" pour deux types de comportements mécaniques induisant des déplacements qui ne sont pas différentiables par rapport à la forme: le contact et la plasticité. Afin de surmonter cet obstacle, nous utilisons des problèmes approchés construits à l'aide de méthode de pénalisation et de régularisation.

Dans la première partie, nous présentons quelques notions fondamentales d'optimsation de forme (chapitre 1). Puis nous exposons les résultats qui seront utiles à l'analyse des deux problèmes mécaniques considérés et nous illustrons ces résultats à l'aide de quelques exemples.

La deuxième partie introduit les cinq modèles statique de contact (chapitre 3) et le modèle statique de plasticité (chapitre 4) que nous utilisons tout au long du manuscrit. Pour chaque modèle, nous donnons les bases de la modélisation mécanique, une analyse mathématique des équations et inéquations variationnelles associés et, enfin, nous expliquons quels solveurs nous avons implémentés.

La dernière partie, divisée en deux chapitres, se focalise sur l'optimisation de forme. Dans chacun des chapitres nous donnons les versions pénalisées et régularisées des moddèles, prouvons, pour certains d'entre eux, leur convergence vers les modèles exactes, calculons les gradients de forme respectifs et proposons des exemples numériques 2D et aussi, dans le cas du contact, 3D. Ainsi, dans le chapitre 5, traitons-nous du contact et considèrons deux sortes de problèmes d'optimisation de forme: le premier dans lequel la zone de contact est fixe mais peu ou non être utilisée par l'algorithme, le second dans lequel la zone de contact est optimisable. Pour ce dernier type de problème, nous introduisons deux méthodes différentes pour résoudre du contact sans frottement sans discrétiser la zone de contact. Une de ces méthodes est nouvelles tandis que l'autre n'a jamais été employée dans ce contexte. Dans le chapitre 6, nous abordons le modèle de Hencky que nous approximons grâce à une pénalisation de Perzyna ainsi que grâce à un modèle de notre crue.

Keywords: Méthode de lignes de niveaux, Optimisation de forme, contact, frottement, plasticité, modèle de Hencky, inéquation variationelles, dérivée conique.

Contents

Introduction

This thesis is part of the RODIN (Robust structural Optimization for Design in INdustry) project [1] which gathers 11 industrial and academic partners on the subject of topology optimization. The fundamental working principle of topology optimisation algorithms is to start from an initial domain on which the algorithm can work, adding or removing material, in order to optimise an objective (for instance the mass), while satisfying some performance constraints (such as an upper bound on the compliance). One of the potential advantages of topology optimisation is that it can broaden the range of reachable shapes, formerly restricted by the creative power of the designers.

However, even if commercial softwares exist, their application scope remains limited to not too complex systems. The goal of the RODIN project is to develop a topology optimisation software capable of delivering a manufacturable product. To do so, three major industrial players (Renault, Airbus and Safran) join forces with a software company (ESI-Group), four academic partners (Ecole Polytechnique, Université Pierre et Marie Curie (Paris 6), Université Paris Diderot (Paris 7), INRIA Bordeaux) and three SMEs (Eurodecision, DPS and ALNEOS). The existing commercial softwares are almost all based on the technique of material with variable density or SIMP (Solid Isotropic Material with Penalization) [29], see figures 1 and 2. This method has the drawback to model the object through a density of material between 0 and 1. Whence, it leads to final shapes which contain parts for which the density is neither 0 or 1 but intermediate. These parts are difficult to interpret for the designers. Consequently, there was a room for the development of two shape optimisation algorithms: one using the level set method (which is the framework of this thesis) and another one based on mesh deformations (on this subject see the thesis [84]).

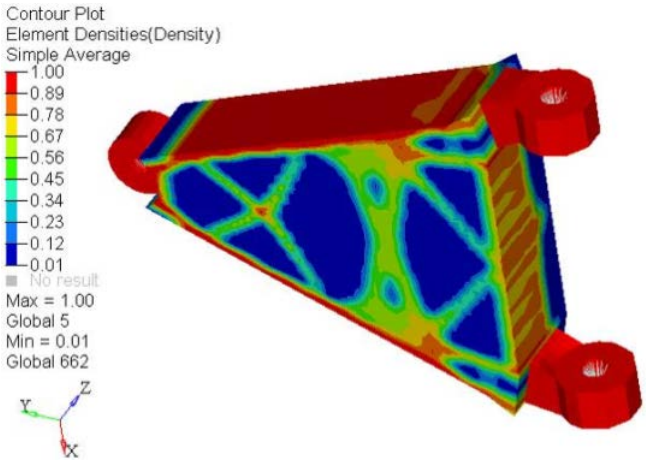

Figure 1: Topology Optimization of an automotive control arm thanks to densities method, obtained with the commercial software Optistruct of Altair Engineering, (extracted from https://www.sharcnet.ca/Software/Hyperworks/help/hwsolvers/hwsolvers.htm?os_2060.htm).

In addition, the project aims to tackle the issues of taking manufacturing constraints into account (see the thesis [202]), using optimisation algorithms of order two (see the thesis [288]) and dealing with complex analyses. This last topic is extremely vast and varied. This thesis endeavours to progress in this way by working on mechanical laws different from the usual linearised elasticity. This mechanical model, which is one of the most used models in topology optimisation, is not able to well describe the great variety of structures. So, if a software strives to be used at an industrial level, it has to be able to work with more complex mechanics. We choose to focus on two non linear problems which enable to extend the applicability of topology optimisation to a large number of structures: contact and plasticity. The difficulty stemming from these two models comes from their inherent nonlinearities which are proved to be complicated to handle.

In the case of contact, these nonlinearities are due to boundary conditions. Typically, if we take an structure in contact with a rigid body, it will not penetrate its support. However, they can separate each other: this leads

(a) Bridge 1 (b) Bridge 2

Figure 2: Results with the SIMP method, for two bridges. The structure is embedded on the left and right bottom side. A force is applied on the upper side, on a the whole side for 2(b) and on just a part 2(a).

to boundary conditions depending on the direction of the displacement, which triggers the nonlinearities. To avoid the ensuing difficulties, in topology optimisation, the contact zones are usually replaced by embedded zones or simply ignored, leading to specious designs. Moreover, taking into consideration friction phenomena adds further complexities. It induces more nonlinearities and the model has to be cautiously chosen:

- It has to correctly model the mechanical phenomena.
- It has to be adapted to topology optimisation.

For example, the well-known Coulomb model is used to model numerous situations. Yet it presents the disadvantage of not having, in general, a unique solution.

In the case of plasticity, the nonlinearities are caused by the law describing the material. The simple linear elasticity is not assumed anymore. Rather, the material will react to mechanical stresses, differently depending on its state. Actually, plasticity covers a vast class of different behaviours which have in common that, for a particular region in terms of mechanical state, the structure will follow laws of linear elasticity. Outside this region it is not the case anymore and a plastic law has to be chosen. At this point, we see that plasticity needs, at least, two steps of modeling:

- the definition of the region where the behaviour is elastic (the elastic zone),
- the behaviour outside this elastic zone, when plasticity occurs.

In this thesis, we focus on a model of static perfect plasticity, also called the Hencky model. As this model is static, it cannot properly illustrate the multiplicity of comportment allowed by perfect plasticity. Indeed, when time is taken into account, plasticity generates hysteresis phenomena: the behaviour of the material is contingent on its history. The fact that plasticity is supposed perfect is also a limitation of our approach: it is a simplified mechanical model which is often replaced by plasticity with hardening for real cases.

However the Hencky model is a first step in the direction of more general plasticity. Thus:

- the quasi-static perfect plasticity, when discretised, can be seen as a sequence of Hencky problems,
- Compared with hardening, the Hencky model presents additional mathematical issues: its solution is not unique and belongs to spaces of less regularity.

The common point of plasticity and contact is that they induce variational inequations. Therefore, mathematical challenges which arise from these models, in the framework of topology optimisation, are, to some extent, comparable. To express them we need to explain a little bit the way the shape optimisation problem is written and how it is solved.

We consider an object whose shape is noted Ω. We want to optimise an objective $J(u(\Omega))$ where $u(\Omega)$ is the displacement of the structure. It characterizes its mechanical deformation and is the solution of a state equation. A consequence is that it depends on Ω. We also ask the object to satisfy some constraints and we note $\mathcal{U}_{ad}$ the set of shapes which fulfill theses constraints. The problem can then be written as:

$$\begin{cases} \min J(u(\Omega)) \\ \Omega \in \mathcal{U}_{ad} \\ u(\Omega) \text{ solution of a state equation.} \end{cases} \tag{1}$$

To solve such an optimisation problem, we want to use a descent gradient type algorithm. The crucial point is that we need to get an information on the sensitivity of the function $J(u(\Omega))$ to small variations of Ω. So, it will be needed to define the variations of Ω and to compute the sensitivities of J (and therefore of u) with respect to the variation of the shape.

However it is utterly possible for u not to be differentiable with respect to Ω and it is, in general, the case when u is solution of a variational inequality (at least when Fréchet or Gateaux differentiability are considered). Thus, plasticity and contact problems lead to solutions which are not shape differentiable. Furthermore, their respective solutions are sometimes not unique. This last point causes supplementary troubles as it urges the computations of derivatives of multi-valued functions.

In this thesis, the guiding philosophy we adopt, is to approximate these variational inequations thanks to regularised and penalised variational equations. This approach is quite common in optimal control theory. It was already used for shape optimisation of contact problems, but not in the framework of the level set method. On the contrary, in shape optimisation of plasticity problems, one rather considers plasticity with hardening as it enables to take advantage of the mathematical properties of the state solution and as it better models the mechanical reality of structures. However, the calculation of the sensitivities is addressed in completely different manners than what we perform in this work. On the Hencky model, very few articles exist and, to our knowledge, no one tries to apply the proposed method to this problem.

The solutions of these regularised and penalised models are, in most of the cases, unique, more regular and enable to compute shape gradients which can then be used inside the optimisation algorithm. In the algorithm, these gradients are coupled with a solver which determines the displacement u of, either the regularised and penalised solutions, or the exact ones.

This thesis contains three parts of two chapters each. The first provides an introduction to shape optimization (chapter 1) and introduces mathematical definitions and results which are used throughtout this thesis (chapter 2). The second part focuses on what we call direct problems. We describe the contact problems which will be used in shape optimisation (chapter 3) and give a brief presentation of plasticity (chapter 4). The third part displays the results we obtained on shape optimisation for contact problems (chapter 5) and for static perfect plasticity (chapter 6).

Part I: Preliminaries

In the first chapter, we give an introduction to shape optimisation, presenting the specific method used all through this work. We also mention other methods to outline the background in this field. The second chapter is a collection of mathematical results on which we rely in the next parts. We also adventure a bit beyond the results useful in this thesis to give a larger overview of the subject.

Chapter 1: Optimal design

The first chapter begins with the principles of shape optimisation and, in particular, its goal. Then, we shortly present the different shape optimisation methods going from parametric optimisation (size of bars, splines, nodes of a boundary) to enhanced methods such as the homogenization [6] and the SIMP method. We define a general optimisation problem and catalogue the classical questions which can be investigated on such problems:

- Existence and uniqueness of optimal solutions.
- Computations of shape gradients.
- Convergence of the discretized shape optimisation to the continuous one.

Then we provide some hints on the existence of optimal solutions. To begin with, we show a counter example of existence. Then we explain how to gain existence properties by adding constraints on the admissible shapes.

In the remainder of the chapter, we focus on the level set method [251] coupled with the Hadamard technique [5] of shape variation to build a shape optimisation algorithm. First we explain how a shape Ω, assumed to be a subset of a fixed domain D, can be implicitly described by the zero level sets of a function ψ. The basic idea is to define the boundary of Ω thanks to the points of D for which ψ has a zero value. The interior of Ω is recovered by finding the points of negative ψ values and the exterior by finding the points of positive ψ values. This can be summed up by the following definition:

$$\begin{cases} \psi(x) = 0 & \text{if } x \in \partial\Omega \cap D \\ \psi(x) < 0 & \text{if } x \in \Omega \\ \psi(x) > 0 & \text{otherwise.} \end{cases} \tag{2}$$

Then we introduce the Hadamard method to compute shape derivatives. The idea is to define the small variations of the shape Ω thanks to a diffeomorphism of the form $Id + \theta$, with θ being small:

$$\Omega_\theta = (Id + \theta)\,\Omega.$$

Thanks to this description of small perturbations, the shape derivative can be defined as the derivative with respect to θ in $\theta = 0$. As our goal is to derive a criterion depending on the solution of a state equation posed in Ω, we explain how the derivative of such a solution can be found. To do that, we define the Lagrangian derivative and display the fundamental difficulty in defining an Eulerian derivative as well as a possible alternate definition. We apply this notion to the exterior unit normal to Ω and give a (formal) theorem on how to compute the shape derivative of criteria of the form used in all this work:

$$J_1(\Omega) = \int_\Omega j(u(\Omega))\,dx,$$

$$J_2(\Omega) = \int_{\partial\Omega} l(u(\Omega))\,ds.$$

Our next step is to detail the method to prove that the solution of a variational equation is differentiable with respect to the shape. We give two methods and, after a very short introduction on elasticity, apply one of them on the linearized elasticity problem.

At this point, the derivation of the criterion $J(u(\Omega))$ includes the shape derivative of u. If we want to evolve the shape during the optimisation process by the means of a descent gradient algorithm, we need to determine a descent direction. This role is played, here, by $Id + \theta$. Thus we need to find a suitable θ. As θ is somehow implicitly present in the gradient through the shape derivative of u, finding a good θ for the optimisation is not convenient. A remedy is the application of the adjoint method which we present, thanks to the example of linearized elasticity. Finally, we introduce the Céa's method of fast differentiation by applying it to the same example.

The last sections explain how to build a shape optimisation algorithm mixing the level set method and the Hadamard method. We interpret the shape gradient as an advection velocity and give its possible expression in the case of a descent algorithm using a Lagrangian formulation with a fixed Lagrange multiplier. Once the gradients and a descent direction θ are computed, it remains to move the shape Ω in this direction. This evolution is done thanks to an Hamilton-Jacobi equation:

$$\frac{\partial \psi}{\partial t}(t,x) + V(t,x(t))\,|\nabla \psi(t,x)| = 0 \text{ in } D,$$

where V is a normal velocity which plays the role of $\theta \cdot n$ with n an extension of the normal to the boundary of Ω.

Eventually, before giving some numerical examples (figure 3 for one of them), we articulate the ersatz material method and the extension and regularisation phase. It enables us to compute the solutions of the mechanical problems with a mesh remaining fixed during the optimisation.

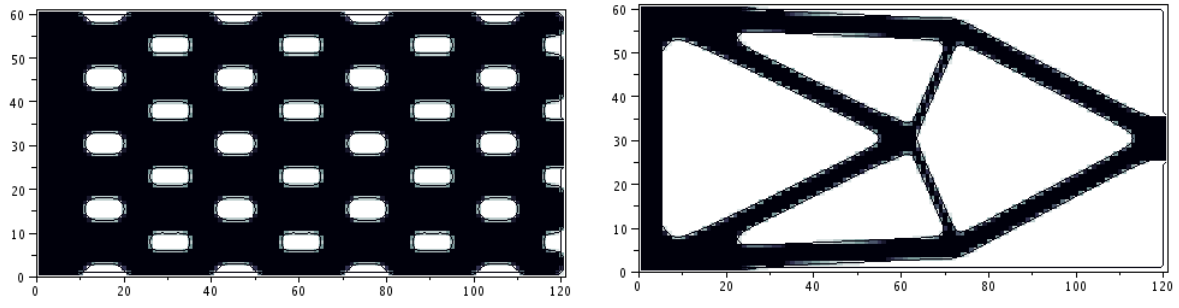

(a) The initialization. (b) The final design.

Figure 3: Results for the cantilever case with the level set method. The structure is embedded on the left side and a force is applied in the middle of the right side.

Chapter 2: Variational inequalities and projection

This chapter is meant to provide some results which will be extensively used in the next parts and references for more details. We can divide these results into two categories. The first ones are destined to be used in the analysis of direct problems. The second ones deal with differentiability.

The first section states some definitions and two important theorems. First we give a theorem [47] which ensures the existence and, sometimes, the uniqueness of a solution to a minimisation problem under convexity, regularity and growth conditions at infinity. This theorem will be used in the contact chapter. Then we define monotone operators [242], some of their possible properties and state an important theorem which will be used in chapter 6, ensuring the surjectivity and, with additional assumptions, the injectivity of such operators. The last part in this section focuses on capacity [137] which is a tool to measure the size of sets and which will intervene when conical derivative will come into question.

The second section focuses on the definition and the properties of the projection operator on a closed convex set K. We prove, [47], that the projection of a point x on K is well-defined and unique. Then we state that the projection is a Lipschitzian funtion which implies some differential regularities. We investigate the C^1 regularity, see [220], of the projection and give theorem 2.3.5 which will be used in the chapter 4 on plasticity. Considering less regular differential properties, we define the conical derivative and state that if K is polyhedric, then the projection is conically differentiable, [205]. This derivative is applied on an example at the end of the chapter. We end the discussion by the particular case of finite dimension, giving two theorems of [260] which we apply on a simple example and by giving some further references.

The last section is a presentation of variational inequalities in the static case. We present three types of variational inequalities and for each one give theorems about existence and uniqueness of their solutions, [264]. We start by variational inequalities of the first kind and variational inequalities of the second kind (used in chapters 3 and 4). It is interesting to note that variational inequalities of the first kind are particular cases of the ones of the second kind. However, we separately prove the existence and uniqueness of a solution to this two types of variational inequalities and underline the fact that the two proofs are quite the same, the first one relying on the projection operator and the second one on the proximal operator. We present an example of variational inequality of the first kind, the well-known obstacle problem for which we give some interesting properties and references. The last type of variational inequalities we introduce is more general: quasi-variational inequalities. Yet, for this type of variational inequalities, contrary to the two first, the existence and uniqueness are not always ensured. For instance, this kind of variational inequalities are, in particular, used to describe some friction models of chapter 3 for which there is no uniqueness result. Still we give two theorems treating of the subject.

The chapter ends with the computation of the conical derivative of the solution to the obstacle problem, with respect to a thickness parameter. We also investigate the literature on the question of sufficient conditions for the conical derivative to be linear.

Part II: Direct problems: Contact and Plasticity

This part is devoted to a concise presentation of the different mechanical models considered in this thesis. Chapter 3 deals with contact mechanics and is mainly based on [298],[98], [100] and [264] whereas chapter 4 treats of plasticity and refers to [199], [283], [277] and [246]. Nevertheless, the penalised and regularised formulations employed to compute the gradients are given in part III.

Chapter 3: Contact mechanics

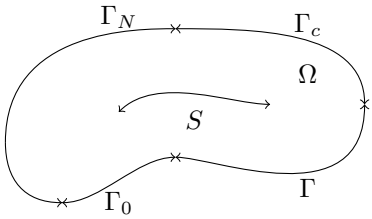

Figure 4: The open set Ω and its boundaries.

The contact problem considered in this thesis can include two different kinds of contact boundary conditions: contact with a rigid body or auto-contact. Thus the shape Ω considered is such that:

$$\partial\Omega = \Gamma_0 \cup \Gamma_N \cup \Gamma_c \cup \Gamma \cup S.$$

where S is a kind of crack in Ω like on figure 4. Its two sides S_+ and S_- can be in contact or separate. Γ_c corresponds to the part in potential contact with the rigid body. Γ_0 is an embedded part, Γ a free part, Γ_N a part where a surface force is applied.

In comparison to the classical linearised elasticity problem, only the type of boundary conditions applied change (on Γ_c and S). We can divide the contact conditions into two parts: the normal part to the boundary and the tangential part. The normal part expresses the non interpenetration condition, for instance on Γ_c:

$$u \cdot n \leq 0,\ Ae(u)n \cdot n \leq 0,\ (u \cdot n)(Ae(u)n \cdot n) = 0$$

where A is the isotropic Hooke tensor, $e(u)$ the symmetric gradient of u and $Ae(u)n \cdot n$ corresponds to the (signed) value of the normal force. The tangential part conveys the information on the friction model chosen. For instance, for the frictionless model the tangential force is taken equal to 0:

$$(Ae(u)n)_t = 0.$$

In the case of the Tresca model, on Γ_c:

$$\begin{array}{ll} \|(Ae(u)n)_t\| \leq s & \text{on } \Gamma_c \\ \|(Ae(u)n)_t\| < s \Rightarrow u_t = 0 & \text{on } \Gamma_c \\ \|(Ae(u)n)_t\| = s \Rightarrow \exists \lambda \geq 0,\ u_t = -\lambda (Ae(u)n)_t & \text{on } \Gamma_c. \end{array}$$

with for a vector v, v_t being its tangential part. The different friction models considered in this thesis are:

1. Tresca
2. Coulomb
3. Norton-Hoff
4. Normal compliance

For each one, we give the associated variational formulation. For the frictionless model and the Tresca model we prove the equivalence with the variational formulation and the existence and uniqueness of a solution to this variational problem. We point out that the frictionless contact problem can be written under the form of a variational inequality of the first kind, the Tresca problem under the form of a variational inequality of the second kind. Thus the proof of existence and uniqueness are quite straightforward with the results of chapter 2. The three other models turn into quasi-variational inequalities and the existence and uniqueness are trickier to get: we refer to some references. In fact, for the Coulomb and Norton-Hoff model the uniqueness is not ensured and the existence is only ensured for small friction coefficients. For the normal compliance model, the existence and the uniqueness are proved as soon as the friction coefficient and the interpenetration coefficient are small enough.

Once the presentation of the contact models made, we concentrate on the way these problems can be numerically solved. This part has not the ambition to draw up a comprehensive list of all the possible solutions, but, rather, to highlight three of them, as they lead to formulations which could give approximate problems of the exact ones, and, so, can potentially be used to compute gradients. The first method introduced is the Lagrangian method. It has no chance to furnish a way to compute shape gradients since the variational inequality has not disappeared: it concerns, now, the Lagrange multiplier. So, this advocates to look for other formulations of the contact problem and to avoid all the formulations derived from the Lagrangian method. The second method consists in a reformulation of the problem called the Nitsche's formulation and results in a non linear equation [69]. We focus more on the third and last one: the penalty and regularisation method. For each problem considered in this chapter, we give the associate penalised and regularised non linear variational equations and give some results of existence and uniqueness of the solutions. We stress that there is still a problem of uniqueness for the Norton-Hoff and the Coulomb models.

To be able to perform some shape optimisation numerical experiments, the first step is to manage to solve the direct problem. The last part of the chapter concentrates on the numerical solvers we implemented for two dimensional cases. We use the finite element method and detail the case of the frictionless contact problem, giving some hints of what was done for the friction cases. As the equations to solve are non linear, we had to develop a non linear solver: we briefly explain which method we choose to implement. The chapter ends with some results of mechanical examples solved with our 6 different solvers. An example is given on figure 5.

Chapter 4: Plasticity

The aim of this chapter is to give the basic foundations of perfect plasticity from a mechanical and a mathematical point of view. We also make short incursions in adjacent topics to situate perfect plasticity inside the more general framework of plasticity. Of course, we focus more on the Hencky model and the different manners to approximate it.

(a) Structure at rest. (b) Deformed structure.

Figure 5: Sliding contact result. The structure is pulled on the right side and embedded on the left side. A contact zone lies in the middle of the structure (in green).

The description of plasticity is based on three ingredients:

- the deformation is separate into two parts: the elastic part e_e and the plastic part e_p. The plastic part appears when the behaviour of the material is not elastic anymore.
- The elastic region K which characterizes the elastic zone and the plastic zone. In this thesis K is taken of the form:
$$K = \left\{\tau \in \mathbb{M}_s^d | \mathcal{F}(\tau) \leq 0\right\}.$$
with $\mathbb{M}_s^d$ the space of symmetric tensors of order two in dimension d and $\mathcal{F}$ the yield function. When the material is such that its mechanical state is on the boundary of K, plasticity can occur.
- An evolution law for the plastic deformation has to be stated: the flow rule.

One important assumption which is made in the laws considered in this work is that the Hill principle is true. This principle, also called the maximum plastic work principle, is a stronger extension of the Drucker-Ilyushin postulate. It implies some important properties on K (convexity) and on the flow rule. Thanks to this principle, the equations of the Hencky model can be written. This mechanical part ends with two classic examples of yield functions and two extensions about non associated plasticity and hardening.

The mathematical analysis of the Hencky model is done, thanks to a duality approach. In fact, e_p and σ, the stress tensor, are, in a certain sense, in duality. This point is proved and used to analyse the Hencky model. We present, first, an approach doomed to fail, which, nevertheless, ensures the existence and uniqueness of σ. The problem comes from the displacement u, which, with this technique, is searched in a too regular space ($H^1(\Omega)$). This prevents the displacement from admitting surface discontinuities and jeopardises the existence of u. With this first method, the analysis of the derived formulation is tantamount to the study of a monotone operator which is not coercive. We give a counter-example of its coercivity.

The issue lies in the possible displacement discontinuities which can appear inside Ω but also at the boundary of Ω. This implies an additional difficulty for the definition of boundary conditions on embedded parts. To address these two problems, we look for u in $BD(\Omega)$ and change the boundary conditions, adding a penalisation term. This leads to a problem which allows the existence of u under a safe-load condition. It basically says that there exists $\overline{\sigma}$, admissible for the loads and lying in the interior of K. Finally we mention another formulation of the Hencky model, tackling the Dirichlet boundary conditions in a different manner. This formulation will be used in chapter 6.

We finish the exploration of plasticity models with regularisations of the Hencky model. We give some results on the convergence of some hardening models and of the Norton-Hoff viscoplasticity model to the Hencky model. We concentrate more on the Perzyna model which will be used in chapter 6. This model can be seen as a regularised or a penalised Hencky model. Its basic formulation is written with respect to σ and u but we manage to find a formulation depending only on the displacement. We give a theorem ensuring the existence and uniqueness of a solution to this model, and, also, its convergence to the solution of static perfect plasticity.

Eventually, we explain how we numerically implement a solver for the Perzyna penalisation model in 2D thanks to finite elements. On an example, we compare the results found for the Perzyna penalisation and for the Hencky model, for different values of the penalisation parameter (figure 6).

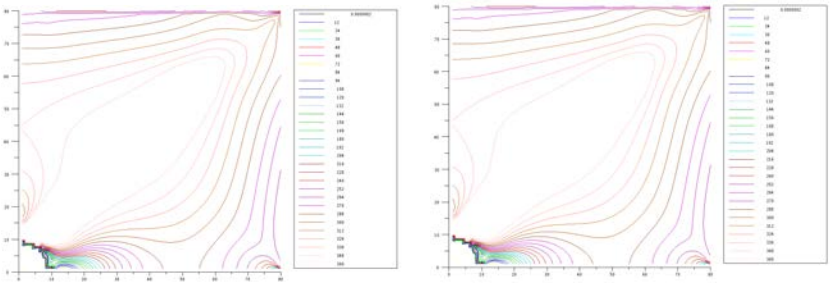

(a) Hencky model. (b) Perzyna model.

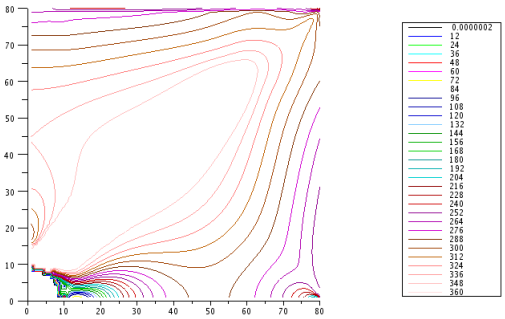

(c) Second regularisation.

Figure 6: Plasticity results for the Hencky model figure 6(a), for the Perzyna penalisation figure 6(b) and for the new regularisation model of chapter 6 figure 6(c). We plot the level set of the Von Mises criterion (the yield criterion). The square is full of material except for a quarter of circle in bottom left corner. The left and bottom side are embedded respectively in the x direction and in the y direction. A surface load is applied on the right side.

Part III: Shape Optimization

In this part we present some original developments in the shape optimisation for contact problems (chapter 5) and for plasticity problems (chapter 6). Compared to the two first parts, it mostly contains novel results. For the contact, we also try to clarify some proofs given in [269] on the conical derivatives of the frictionless contact model and the Tresca model (appendix A).

Chapter 5: Shape optimisation for contact problems

In this chapter, the underlying idea is to use some penalised and regularised versions of the contact problems to perform shape optimisation. We deal with two types of problems. The first one includes contact boundaries and crack which are fixed in the domain D. The algorithm can choose to use them or not. The second one focuses on how an auto-contact zone can be optimised, keeping the mesh fixed.

We begin with the proof of the existence and uniqueness of a conical derivative for the frictionless contact problem. This proof is inspired by [269]. The main idea is to use the results given about the conical derivative of the projection.

After this introductory proof, we give the formulations we want to use to compute shape gradients. These are regularisations of the problems previously given in chapter 3. We prove the existence and uniqueness of a solution in the case of the frictionless and Tresca models. We also prove for these two problems the convergence of the regularised solutions to the exact solutions.

Next we pass to the analysis of the differentiability of the regularised and penalised functions using the theory of superposition operators. This allows us to compute the shape gradient of a general criterion, thanks to the Céa's method.

Then, we introduce the criteria used in numerical examples. Classical ones (compliance, volume) but also criteria depending on the contact pressure. For this last kind of criteria, two types are employed, according to their action on the pressure. The first one aims to make it uniform on the contact zone. The second one endeavours to make the pressure (which is negative) remain under a certain threshold: in other words to ensure a sufficient pressure on the whole contact zone.

All these results are applied on numerous examples in 2D (figure 7 for one case), focusing first on the frictionless model, then on the pressure criteria and finally introducing friction cases. The next series of examples are done in 3D with the industrial software SYSTUS of ESI-Group, see figure 8. For the 3D examples, we implemented in the software the computations of the adjoint methods and use node to node string finite elements to take frictionless and Tresca friction into account. We had also to implement for these elements the penalisation terms corresponding to these two models, ensuring this way that the problems solved by the software correspond to the problems considered in this thesis and are comparable to the 2D results. In this section, the robustness of the mechanical solvers is pointed out if one wants to get successful shape optimisations.

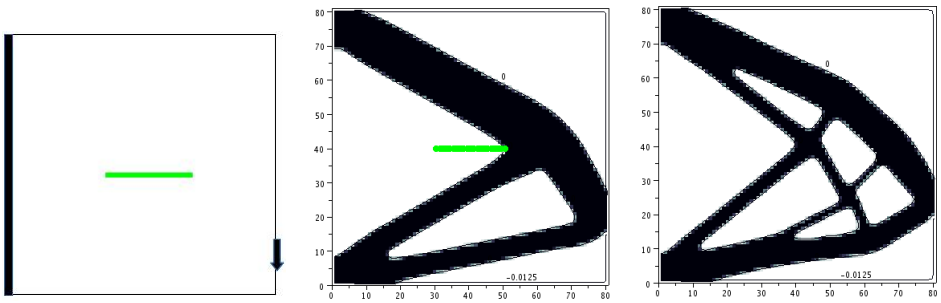

(a) Load case for the cantilever

(b) Final design with contact

(c) Final design without contact

Figure 7: The structure is embedded on the left side, a force is applied in the middle of the right side and the green part is a contact zone. On the right figure, the contact zone has been removed. The volume is optimised under compliance constraint.

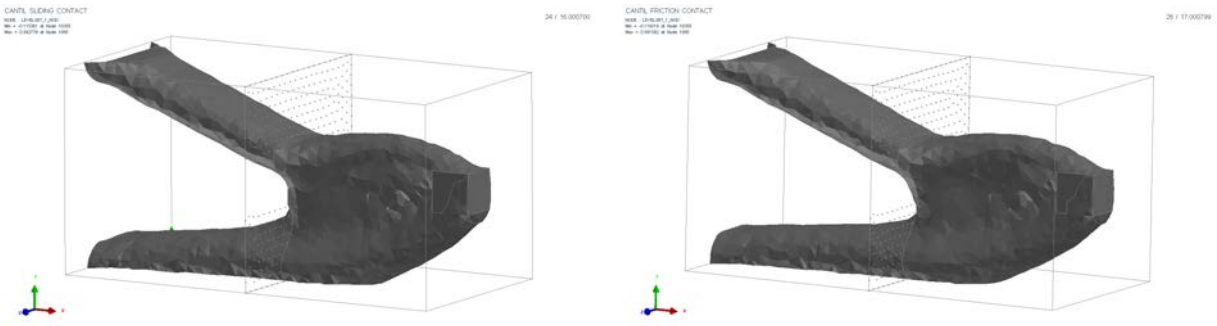

(a) Final design for frictionless contact

(b) Final design for the Tresca model

Figure 8: A 3D case performed with the industrial software SYSTUS of ESI-Group. The case corresponds to a cantilever with two vertical contact zones in the middle of the cube (covered of gray points in the figure).

The next section treats of the contact zone optimising. We limit ourselves to the optimising of a crack with frictionless contact. As we want to work with a fixed mesh, the main question is: how can we solve the contact problem without meshing the contact zone ? We present two new solutions.

- A completely new idea which we call the **enlarging crack method**.
- The application of a technique used in crack evolution theory [16] in the context of shape optimisation: the **phasefield contact method**.

Our first idea is to approximate the crack with an enlarged crack, a hole of small thickness. Using some of the estimations done for the conical differentiability of the frictionless contact model, we prove that the approximate solution converges to the exact one as the thickness of the hole decreases. Following the idea of the previous section, we write the associated penalised and regularised versions of the approximate problem which we use to solve the mechanical problem and to compute shape gradients. After having given some details about the numerical implementation of this 2D solver, we show some simple examples of solutions by the means of this solver, comparing it with the solutions found with the previous solver implemented for frictionless contact. Then we compute the shape gradient of a general criterion (with a mobile Dirichlet zone), thanks to Céa's method, and provide some numerical examples of shape optimisation where the contact zone can be translated in a particular direction.

The analysis is conducted in the same way for the second solution. Here, the idea is to approximate the contact zone with a phasefield [42]. This means that the crack S is replaced by an enlarged open zone ω on which a smooth function α is defined, equal to 1 on the crack and zero outside ω. It can be seen as an evanescent enlarged crack. To account for the contact conditions on S, the usual elasticity energy is changed inside ω. We distinguish between the parts responsible for the shear, the compression and the expansion. The compression part is left unchanged. The two other parts should be deleted on the crack as we authorize the seperation between S_+ and S_- (the expansion) and the sliding (the shear). As we cannot do that exactly, as the contact zone is not discretized, we make this energy depend on α like $(1-\alpha)^2$. If $\alpha = 1$ (the case on the crack) it only remains the compression part in the energy. If $\alpha = 0$ (outside the crack) we recover the classical energy. Then, we write a regularised version of the associated variational (non linear) equation and solve the same problems as for the enlarging crack method to test the algorithm.

To perform shape optimisation on this last model, we need to choose how making α evolve. We could use the phasefield method of shape optimisation but we can also make the most of what was already implemented for the variation of the level set function. Therefore, we decide to define the phasefield through two level set functions which will be taken equal to signed distance functions. The shape optimization will be done with respect to these two level set functions. Consequently, before computing shape gradients with the Céa's method, we make a short investigation of the differentiability property of the signed distance function.

Finally, as the gradients calculated are written in an usual form, we manage to come back to classical formulations, thanks to the coarea formula. This enables us to easily determine shape gradients and to perform shape optimisation on the same examples performed for the enlarging crack case.

Chapter 6: Shape optimisation for static plasticity

In this chapter, in addition to our guideline consisting of utilising regularised versions of the models we want to study, we limit ourselves to problems which can be written exclusively with respect to the displacement: we step the mixed formulations (depending on σ and u) aside for the computation of shape gradients and the numerical solvers. Thus, we propose two approximate versions of the Hencky model for a Von Mises yield function.

The first one is a regularisation of the Perzyna model. We give a result of existence and uniqueness for this model and make the proof of the convergence of its solution to the one of the Hencky model, adapting the proof given for the Perzyna model in [190].

Next, we propose another regularised model. We prove the existence and uniqueness of its solution, thanks to monotone operator theory presented in chapter 2. Then we manage to prove its convergence to the Hencky model by relating it to a kind of regularised Perzyna model and proving that its solution also converges to the one of Hencky model. We illustrate this model by solving the same example as at the end of chapter 4, thanks to our 2D solver.

After a short analysis of the differentiability of the penalisation and regularisation term, we compute the shape gradient thanks to Céa's method. We end the chapter by some numerical examples, comparing the results found in the case of elasticity and the ones found for the two proposed regularisations, see figure 9 for a cantilever.

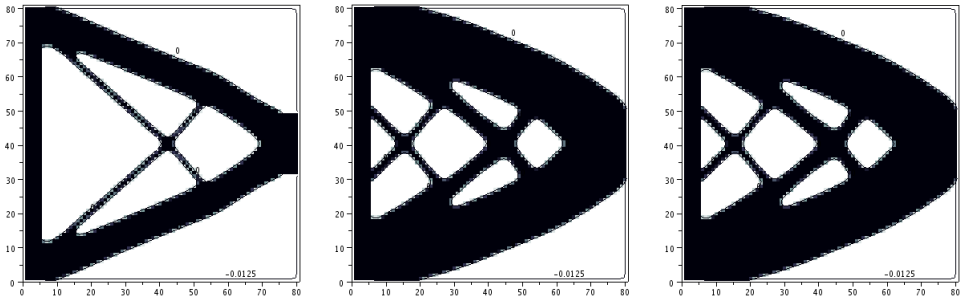

(a) Without plasticity (b) Perzyna penalisation (c) Second regularisation

Figure 9: Cantilever, final designs for elasticity and plasticity

Appendix A: Conical derivative for the Tresca model

In this appendix, we give the proof of the conical derivative of the Tresca model in 2D for particular directions and with regularity assumptions on the solution. We try to clarify the proof done in [269]. We give more details and state clearly the assumptions needed to do the proof. The main idea is to transform the Tresca problem into a saddle-point problem including a problem written in Ω (for the displacement) and one on the contact boundary (for the Lagrange

multiplier). It remains to interpret each problem as projections on closed convex set and apply the same method as for the conical derivative of the frictionless contact problem. The difficult part is the proof of the polyhedricity of the convex associated with the problem solved on the contact boundary.

Based on this work we prepare to submit two preprints:

- G.Allaire, F. Jouve and A. Maury. *Shape optimisation with the level set method for contact problems in linearised elasticity.* (In preparation), 2016,
- G.Allaire, F. Jouve and A. Maury. *Elasto-plastic shape optimisation using the level set method.* (In preparation), 2016.

This work was also the basis of conference presentations:

- Shape optimisation for unilateral contact problem in linear elasticity, SMAI, Les Karellis, France, 2015.
- Shape optimisation for contact problems in linear elasticity, ECCOMAS, Crete, Greece, 2016.
- Shape optimisation in static perfect plasticity, PICOF, Autrans, France, 2016.

Part I

Preliminaries

Chapter 1

Optimal design

Contents

1.1 Introduction

The optimization of the shape was already studied in the Antiquity as Greek people were wondering what was the largest surface which could be drawn for a given perimeter. They had the intuition that a disk was the solution but the mathematical proof has been given much later by Steiner and Carathéodory, proving the isoperimetric inequality [270], [249]. The minimal surface problems, studied first by Euler and Lagrange, are other examples of such types of questions. Euler found that the catenoïde is the minimal surface which lies on two parallel circles and Lagrange investigated the problem of the minimal surface streched across a closed contour which is typically the shape taken by a soap bubble which rests on a closed curve. Since then, the shape optimization has been more and more studied since it can be applied to numerous domains in industry (airplanes, cars, additive manufacturing...). This thesis focuses on structural optimization, which means that we want to design objects which are meant to sustain loads and aim at industrial applications.

In structural optimization, the object is designed in order to optimize some of its mechanical characteristics. It consists in finding the best shape for the object in view of an objective and some constraints. For instance, if we want to design a piece of a car, it could be interesting to build it the lightest as possible with the constraint that it does not break. Finding such a shape is not straightforward as the objective and the constraints are somehow opposite each other. Consequently the use of optimization algorithms is highly relevant in this case and, if adapted to a problem in which the optimization variable is a shape, they can help to improve solutions guessed by the designer.

The structural optimization has been extensively studied in last fifty years and a lot of numerical propositions were made to address the problem of computing "optimal" shapes. One of the key points is which description of the shape is chosen, as it will constraint the admissible shapes and also imply different ways to calculate derivatives with respect to the shape, in case a gradient algorithm is used.

At first, we can think of optimizing the structure by describing the shape with a few parameters. There exists a wide range of examples in which the size of bars in a truss were meant to be optimized [72], [105] and [170], [244], [243] where it is used to study singular topologies or where the boundary of the shapes are parametrized with splines, NURBS... as done in [45], [165] and reviewed in [122]. The boundary of the shape can also be described through its discretization by a mesh in what is called "geometric" optimization. Thus the optimization is made by changing the place of the nodes on the boundary which are the optimization parameters. On this particular technique we mention the monographs of [137], [129], [232] .

(a) The penalty parameter $p = 1$ (b) The penalty parameter $p = 4$

Figure 1.1: Results with the SIMP method, the structure is clamped on the left side and a downward isolated force is applied on the bottom right

To get rid of some of the limitations inherent to these first approaches, the level set or the phase field method can be used. The level set, which will be described in the following, is an implicit description of the boundary, thanks to the zero values of a function. On the other hand, the phase field method [41], [42], [280], [37] uses an explicit smooth function which is a kind of a regularization of the characteristics function of the shape. For both, a way to make the shape evolve is needed when a numerical resolution is performed. For the level set method, an Hamilton-Jacobi equation is employed and a Cahn-Hilliard or an Allen-Cahn for the phase field one.

One of the drawbacks of these two methods is that the changes of topology are difficult to achieve (and for some of them impossible without adpating the method). The notion of topological sensitivity (see [266], [116], [267], [17], [268] or [222]) is one possible answer to this lack. It consists of measuring the sensitivity of the criteria to the creations of small holes inside the shape. This method can be mixed with the level set method and the classic shape derivative (see 1.3.2 for this notion), as for instance in [7]. For phase field method we mention [301] and [304].

Another famous approach the homogenization method introduced in [6], [11], [28]. The idea of the homogenization method is to perform a kind of relaxation of the problem. A "black and white" solution is not searched anymore but a local density is rather defined. In the homogenization method, a domain D is taken where it is allowed to put matter. But instead of just putting matter, we look for solutions under the form of very small microstructures of a given material and void. When the size of microstructures tends to zero, the problem converges to a so-called homogenized problem and the optimization is done with respect to them. This leads to the definition of a density θ and an homogenized tensor A^*. The SIMP method [29] is a simplification which defines a density on each point and instead of taking the elasticity tensor A^*, takes the tensor $\theta^p A$, where p is a penalization parameter used to force the solution to contain as less as possible intermediate densities. It has to be pointed out that this tensor is not necessary the homogenized tensor corresponding to a particular microstructure, A^*, Hooke's law at each point of D .

Finally we want to highlight that all these description choices are most of the time related to optimization algorithms using differentiability properties. However there exist algorithms which does not rely on such objects making part of what we can call stochastic optimization methods. Thus the evolutionary algorithms, presented in chapter 8 of [5], in the monograph [300] or in the review [215], adopt the Darwin principles to apply them to shape optimization. Beginning from a group of solutions, they will evolve, subject to mutations and crossings. We also mention on this subject [117], [158], [189] and [63] (for a stochastic algorithm and the references therein). These methods have the drawbacks that they require a lot of mechanical computations (even if for this point parallel computing can be used [4], [291] or [52]), that the choice of the fitness function being quite heuristic, nothing guarantees that the use of such fitness enables to reach a minimum and, if so, the convergence can be very slow.

To define the optimization problem we need to specify three points:

- The **model** which describes the behaviour of what we want to design. In the cases considered in this thesis, we will design structures analysed through their mechanical characteristics. In linearized elasticity, this will result in a variational equation and for the contact and plastic cases variational inequations.
- The **objective** we want to optimize (for instance the mass or the volume).
- The **set of admissible shapes** which includes the constraints which are inherent to the goal and the mechanical behaviour of the structure and the constraints related to the way the shape is described.

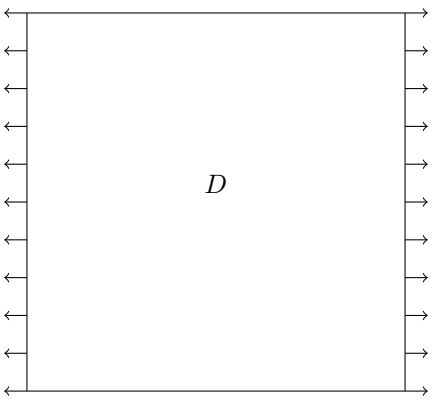

Figure 1.2: Load case of the counter example.

We are then able to state the optimization problem under a general form:

$$\begin{cases} \min J(u(\Omega)) \\ \Omega \in \mathcal{U}_{ad} \\ u(\Omega) \text{ solution of a state equation} \end{cases} \tag{1.1}$$

where Ω is the shape, $u(\Omega)$ is the solution of the equation modeling the behaviour of the structure we optimize, $\mathcal{U}_{ad}$ is the set of admissible shapes and J is the objective function. Like for any optimisation problems, some classical questions can be investigated:

- The existence and uniqueness of optimal solutions and their properties,
- The optimality conditions and the differentiability of the variables with respect to the shape. These conditions are used in numerical algorithms such as descent gradient ones.
- When we numerically want to compute the solutions of an optimization problem, the state equation is solved thanks to a discretization, for instance with a finite element method. So, if there exists a solution to the discretized problem and also to the continuous problem, it raises the question of the convergence of the discretized optimized shape to the continuous optimum.

We will not consider the last one but there exist a lot of articles studying it in the framework of contact and plasticity, see the .

In a first part we curtly discuss about the ill-posedness of shape optimization problems and the different ways to gain some existence properties. Then we present the level set method.

1.2 Existence of optimal shapes

In shape optimization, there is usually no existence of an optimal solution if the admissible shapes are not enough constrained. This raises concern when numerical simulations are performed as it says that the algorithm can only converge to a local minimum. It is the choice of this thesis to only try to improve the initial guess of the shape of an object, without hoping to reach a global minimum, however we briefly present a counter example of existence and give some possible ways to ensure the existence of an optimal shape for some particular cases.

1.2.1 Counter example of existence

This example is taken from [5], 6.2.1 and we only explain the idea on which it is based. We work in dimension 2 and the problem is to chose how to distribute two elastic isotropic materials in a domain $D = (0,1)^2$ modeling a moving membrane. On this domain, forces are put on the left and the right side in the outward normal direction see figure 1.2. We note α and β the elastic coefficients with $0 < \alpha < \beta$. We also note Ω the part of the domain D filled with the material β, χ its characteristic function and:

$$a_\chi = \beta\chi + \alpha(1-\chi). \tag{1.2}$$

We model the displacement u_χ of the membrane by:

$$\begin{cases} -\operatorname{div}(a_\chi \nabla u_\chi) = 0 & \text{in } D \\ a_\chi \nabla u_\chi \cdot n = e_1 \cdot n & \text{on } \partial D \end{cases} \tag{1.3}$$

denoting n the outward normal of D. We stress the fact that this problem is scalar since only the It remains to define the objective and constraints of the optimization problem. For the objective we take the compliance and we constraint Ω to be equal to a certain volume $0 < V_0 < 1$:

$$\begin{cases} \inf J(\chi) = \displaystyle\int_{\partial D} e_1 \cdot n \; u_\chi \, ds \\ \chi \in \mathcal{U}_{ad} \\ u(\chi) \text{ solution of (1.3)} \end{cases} \tag{1.4}$$

and the admissible set is defined by:

$$\mathcal{U}_{ad} = \left\{ \chi \in L^\infty(D; \{0,1\}) \mid \int_D \chi = V_0 \right\} \tag{1.5}$$

Proposition 1.2.1. *There is no optimal solution to* (1.4) *in the space* $\mathcal{U}_{ad}$.

First it is important to remark that the objective corresponds to the work of the forces, therefore to minimize it we would like to put as much as possible of the stronger material β. However the constraint put on the volume of the phase β prevents us from filling D with this material. The problem is then tantamount to find the best way to distribute the weaker material α in D.

The idea of the proof of the proposition is that, since the forces are horizontal and applied on the whole left and right sides, the better way to put the phase α is in horizontal thin lines. This way, the path of the constraints (which are horizontal for the β-full domain) stays quite horizontal and are the least perturbed. Once this saying, we have not yet defined how thin these lines should be and the fact is that we can choose them as thin as we want, as soon as there are enough of them for the shape to fulfill the volume constraint. Making these inclusions of α thinner and thinner produces a minimizing sequence which converges to an homogenized solution which is not in $\mathcal{U}_{ad}$. The minimum is not reached and it can be proved that it cannot be reached.

The idea that smaller and smaller inclusions enable to improve the objective is quite classical and is often the ingredient of counter examples, see [5] chapter 5, [137] chapter 4.2, [51] chapter 4. It also explains the mesh dependency of the numerical solutions which tend, as the mesh is refined, to create more and more small holes and bars.

1.2.2 Gaining existence

Given the counter examples, there are two opposite ways to gain the existence. The first one is to accept the homogenized shapes as admissible shapes, which leads to the homogenization method for shape optimization described earlier. Again this method replaces the characteristic function χ by a density θ which takes its value in the interval $[0,1]$ and the isotropic elasticity tensor A by an homogenized one A^* which has to be compatible with θ in a certain sense. If we note G_θ the set of tensors A^* compatible with θ, the homogenized optimization problem can be written as follows:

$$\inf_{(\theta, A^*) \in \mathcal{U}_{ad}} J(\theta, A^*) \tag{1.6}$$

with

$$\mathcal{U}_{ad} = \left\{ (\theta, A^*) \in L^\infty(\Omega; [0,1] \times \mathbb{R}^{N^2} | A^*(x) \in G_{\theta(x)} \text{ in } \Omega, \int_\Omega \theta \, dx = V_0 \right\} \tag{1.7}$$

It can be proved that in the case of the counter example (and in many other ones), there exists an optimal solution.

The second one is to narrow the set of admissible shapes to forbid the sequences which converge to homogenized solutions and in the meantime gain compactness. There are multiple choices which enable to limit this set and manage to recover existence properties. We give some of them:

- We can add uniform **regularity constraints**. As proved in [67] or in [137] chapter 4.3, the ϵ-cone property or asking the domain to be uniformly Lipschitz (see [217]) ensures the existence of an optimal shape for a wide range of objectives and constraints. See also [5] in the case of the optimal thickness of a membrane.
- **Topological constraints** can also be used to gain the existence of an optimal solution as proved in [278] for the membrane model and [62] in two dimensions elasticity. The basic idea is to compel the number of connected components of the complement of the shape to be bounded.
- A constraint on the perimeter of the shape can also be applied to gain, in particular cases, the existence of a solution to the optimization problem. This idea is developed in [137] or [15].

For more details on this subject we refer to the review done in [137] chapter 4 and book [5] 6.2.

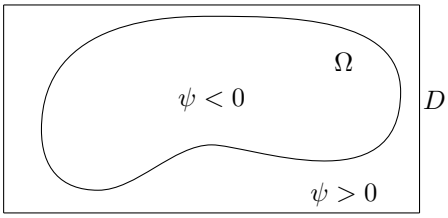

Figure 1.3: Description of a shape by the level set method.

1.3 Level set and shape optimization

The level set method, introduced by Osher and Sethian in [224], [223] and [251], is a powerful tool to describe the shape of an object or interfaces. Its applications cover a wide range of domains going from image analysis ([245], [196] or [106]) to front propagation or the modelization of physical phenomenon like in fluid dynamics [213] or [252]. In the framework of shape optimization, it has been more and more used since the first papers [225], [9], [10], [253] and [293]. The great advantages of this method is that it provides a real black and white description of the shape, contrary to density-based methods, and that it does not necessitate a remeshing of the domain as the shape varies. It is also ideally suited to consider geometric criterion such minimal thickness (see [202]).

First we present how an open set Ω can be described thanks to this method. Then the Hadamard method to calculate sensitivity with respect to the shape is presented and the fast method of computing it, due to Céa [61], is given. Finally we explain how to use the level set method to perform shape optimization coupling the Hadamard derivative with the level set evolution.

1.3.1 Description of a shape by the level set method

The method consists in an implicit definition of shape thanks to a function ψ. Later, when we will consider shape optimization, we will restrain the admissible set to the shapes contained in a working domain D. So we present the level set idea taking this working domain into account. The boundary of the shape Ω corresponds to the points of D where the ψ is equal to zero. The interior of the shape is characterized by $\psi < 0$ and the exterior $\psi > 0$. It follows that:

$$\begin{cases} \psi(x) = 0 & \text{if } x \in \partial\Omega \cap D \\ \psi(x) < 0 & \text{if } x \in \Omega \\ \psi(x) > 0 & \text{otherwise.} \end{cases} \tag{1.8}$$

The normal n to the shape is easily defined and furthermore extended in the whole domain by as soon as ψ is of class C^1 and $\nabla\psi \neq 0$:

$$n = \frac{\nabla\psi}{\|\nabla\psi\|} \tag{1.9}$$

and the mean curvature H, which can be written as the divergence of the normal n, can be computed as soon as ψ is of class C^2:

$$H = \nabla \cdot \frac{\nabla\psi}{\|\nabla\psi\|} \tag{1.10}$$

We conclude this part with an example of function ψ which will be of great importance in the next: the signed distance function. We first note the distance of a point x to the boundary $\partial\Omega$ by $d(x, \partial\Omega)$ and define $d_\Omega(x)$ the signed distance function by:

$$d_\Omega(x) = \begin{cases} 0 & \text{if } x \in \partial\Omega \cap D \\ -d(x, \partial\Omega) & \text{if } x \in \Omega \\ d(x, \partial\Omega) & \text{otherwise.} \end{cases} \tag{1.11}$$

1.3.2 Hadmard method for shape derivative

As we want to perform shape optimization, we will use an optimization algorithm which will make the structure vary iteratively. Our choice is to use a gradient based algorithm, therefore we need to compute a gradient with respect to the shape and to define what we could call "small variations" of the shape. We choose to use the notion introduced by Hadamard and then extensively studied, see for instance [232] or [269], adopting the frameworks of [218], [262] and [5]. Starting from a smooth domain Ω_0, the evolution of the domain takes the form:

$$\Omega_\theta = (Id + \theta)(\Omega_0) \tag{1.12}$$

with $\theta \in W^{1,\infty}(\mathbb{R}^d, \mathbb{R}^d)$ and Id the identity map. When θ is sufficiently small, $Id + \theta$ is a diffeomorphism in $\mathbb{R}^d$, (see [5]). Once the variation of the shape is defined, it is possible to define the notion of Fréchet derivative for a function J depending on the shape:

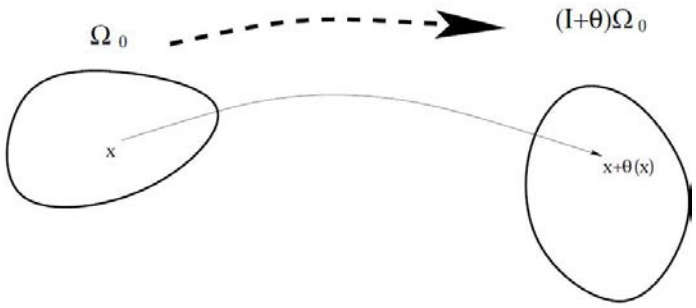

Figure 1.4: Illustration of the diffeomorphism taken from [5].

Definition 1.3.1. *We say that $J(\Omega)$ is shape differentiable at Ω in the direction θ if there exists a continuous linear form $J'(\Omega)$ on $W^{1,\infty}(\mathbb{R}^d,\mathbb{R}^d)$ such that:*

$$J((Id+\theta)(\Omega)) = J(\Omega) + J'(\Omega)(\theta) + o(\theta) \tag{1.13}$$

where $\lim_{\theta\to 0} \dfrac{|o(\theta)|}{\|\theta\|_{W^{1,\infty}}} = 0.$

Remark 1.3.2. *Other notions of differentiability can be defined in the same way such as Gateau differentiability or directional differentiability.*

In the following we recall some classical results about this kind of derivation, see [137]. The first one is an interesting structure theorem which states that the derivative of a functional only depends on the normal part of θ: $\theta \cdot n$. Let first introduce $\mathcal{O}_k$ which will denote the set of open sets of class C^k.

Theorem 1.3.3. *Let $k \geq 1$ be an integer, $J : \mathcal{O}_k \to \mathbb{R}$, $\Omega \in \mathcal{O}_k$ and*

$$\forall \theta \in C^k \cap W^{k,\infty}(\mathbb{R}^d,\mathbb{R}^d),\ \mathcal{J}(\theta) = J((Id+\theta)(\Omega))$$

then, if $\Omega \in \mathcal{O}_{k+1}$ and $\mathcal{J} : C^k \cap W^{k,\infty}(\mathbb{R}^d,\mathbb{R}^d) \to \mathbb{R}$ is differentiable at 0, there exists a linear form l_1 continuous on $C^k(\partial\Omega)$ such that:

$$\forall \xi \in C^k \cap W^{k,\infty}(\mathbb{R}^d,\mathbb{R}^d), \mathcal{J}'(0)(\xi) = l_1(\xi \cdot n)$$

We recall the following classical useful theorem [5]:

Theorem 1.3.4. *Let $\Omega \in \mathcal{U}_{ad}$ be a smooth open domain, ϕ a smooth function defined in $\mathbb{R}^d$,*

$$J_v = \int_\Omega \phi(x)\,dx \quad \text{and } J_s = \int_{\partial\Omega} \phi(x)\,ds.$$

These two functions are shape differentiable at Ω in the direction $\theta \in W^{1,\infty}(\mathbb{R}^d,\mathbb{R}^d)$ and:

$$J_v'(\Omega)(\theta) = \int_{\partial\Omega} (\theta \cdot n)\ \phi\, ds$$

$$J_s'(\Omega)(\theta) = \int_{\partial\Omega} (\theta \cdot n) \left(\frac{\partial\phi}{\partial n} + H\phi\right) ds$$

where H is the mean curvature of $\partial\Omega$.

The idea of the proof of such theorems is to take advantage of the fact that $Id+\theta$ is a diffeomorphism and that we can consequently apply a change of variable.

1.3.3 Compute the derivative of a criterion

In this subsection we show the way to compute the shape derivative of a criterion which depends on a solution of a variational equation. Let Ω be an open bounded subset of $\mathbb{R}^d$ which represents the shape of the structure we want to optimise. Assume the criterion is of the form:

$$J(u) \tag{1.14}$$

with u solution of a variational equation on Ω. This implies that u depends on Ω and that we need to compute its derivative with respect to the shape. To do so, we introduce two notions of derivative: the Lagrangian and the Eulerian ones.

Lagrangian and Eulerian derivatives

We consider a function $u(x,\Omega)$ which depends on Ω with $x \in \Omega$. There are two ways to define a derivative with respect to Ω using the Hadamard framework. First we can follow the point x during the transport by the diffeomorphism $Id+\theta$. That is to say, we want to compare $u(x+\theta(x),(Id+\theta)(\Omega))$ with $u(x,\Omega)$. This is called the Lagrangian derivative refering to the associated approach in mechanics. The Lagrangian derivative of u can then be defined by:

Definition 1.3.5. *Let B be a reflexive Banach set and assume that $u(x,\Omega) \in B$ and $u(x+\theta(x),(Id+\theta)(\Omega)) \in B$. We call $Y(x,\theta)$ the Lagrangian derivative of $u(x,\Omega)$ if it is a linear form in θ from $W^{1,\infty}(\mathbb{R}^d,\mathbb{R}^d)$ to B and it verifies:*

$$u(x+\theta(x),(Id+\theta)(\Omega)) = u(x,\Omega) + Y(x,\theta) + o(\theta) \tag{1.15}$$

where the o is to be understood as $\lim_{\theta\to 0} \frac{\|o(\theta)\|_B}{\|\theta\|_{W^{1,\infty}}} = 0$.

The Eulerian derivative is a bit more natural but it causes some additional difficulties. It is easy to define it for a point x which belongs to both Ω and $(Id+\theta)(\Omega)$. The idea is to compare the value of u at the point x according to whether we consider x in Ω, $u(x,\Omega)$, or in $(Id+\theta)(\Omega)$, $u(x,(Id+\theta)(\Omega))$. Troubles arise for the points which are on the boundary $\partial\Omega$ which are likely not to belong to $(Id+\theta)(\Omega)$ or its boundary. Then we only differentiate the punctual values of $u(x)$, notwithstanding the boundary which prevents from rigorously defining functional spaces for u and its derivative.

Definition 1.3.6. *We call $U(x,\theta)$ the Eulerian derivative of $u(x,\Omega)$ if it is a linear form in θ and it verifies:*

$$u(x,(Id+\theta)(\Omega)) = u(x,\Omega) + U(x,\theta) + o(\theta(x)) \tag{1.16}$$

where the o is to be understood as $\lim_{\theta\to 0} \frac{|o(\theta(x))|}{\|\theta\|_{W^{1,\infty}}} = 0$.

Naturally there is a link between this two notions given by this equality:

$$Y(x,\theta) = U(x,\theta) + (\theta\cdot\nabla)\, u(x,\Omega)(\theta). \tag{1.17}$$

This last equality enables us to define the Eulerian derivative, avoiding the difficulties which arise when we try to define it in the manner of definition 1.3.6.

Remark 1.3.7. *The Lagrangian derivative is also called the material derivative in [269] section* 2.25 *and the that if we define the Eulerian derivative in a weak sense thanks to* (1.17)*, it is called the shape derivative in [269] section* 2.30.

First we give the shape derivative of the normal. We will note for a vector $v \in \mathbb{R}^d$:

$$v_t = v - (v\cdot n)\, n, \tag{1.18}$$

for matrix M we note the transpose matrix ${}^tM$ and for a C^1 function $g : \partial\Omega \to \mathbb{R}$ we define (definition 5.4.5 in [137] its tangential gradient:

$$\nabla_\tau = \nabla\tilde{g} - (\nabla\tilde{g}\cdot n)\, n \tag{1.19}$$

with $\tilde{g} \in C^1(\mathbb{R}^d)$ an extension of g.

Lemma 1.3.8. *If Ω_0 is C^2, its unit normal is differentiable with respect to every direction $\theta \in W^{1,\infty}$ and its Lagrangian derivative in the direction θ is $n_0'(\theta)$ defined by:*

$$n_0'(\theta) = -({}^t\nabla\theta n^0(y))_t = -{}^t\nabla\theta(y)n^0(y) + \left(n^0(y)\cdot\, {}^t\nabla\theta(y)n^0(y)\right) n^0(y). \tag{1.20}$$

If we choose the extension of the normal given by the signed distance function defined on a neighborhood of the $\partial\Omega$, the Eulerian derivative of the normal is (see also [137], proposition 5.4.14, p198-199 and lemma 3.4 *p125 in [269]):*

$$n'(\theta) = -\nabla_\tau(\theta\cdot n) \tag{1.21}$$

Proof. As Ω_0 is C^2 (which means that $\partial\Omega_0$ is a C^2 manifold), we can define the orthogonal vector to the boundary of Ω_0, m^0 (which is not normed) on an open set around $\partial\Omega_0$. See [269] paragraph 2.1. Let O_i^0 an open sets collection of cardinal l covering $\partial\Omega_0$. On each O_i^0 it exists $c_i^0 \in C^2(O_i^0, B)$ where $B \subset \mathbb{R}^d$ is an open ball. If we note $(\xi_1,...,\xi_N)$ the coordinates in B we have: $c_i^0(O_i \cap \Omega_0) = \left\{\xi \in \mathbb{R}^d,\ \xi_d \geq 0\right\}$. It also exists a partition of unity $r_i^0 \in C_0^\infty(O_i^0)$ adapted to the O_i^0. Then we have the expression of the normal:

$$m^0(y) = \sum_{i=1}^{l} r_i^0\, {}^tDc_i^0(y)e_n$$

We transport this construction on Ω thanks to $Id+\theta$. We then have: $c_i(y+\theta(y)) = c_i^0(y)$ and $r_i(y+\theta(y)) = r_i^0(y)$ and the normal:

$$m(x) = \sum_{i=1}^{l} r_i \, {}^t Dc_i(x) e_n$$

We can write:

$$\begin{aligned}
&c_i\left(y+h+\theta\left(y+h\right)\right) = c_i^0\left(y+h\right)\\
&c_i\left(y+h+\theta\left(y\right)+\nabla\theta\left(y\right)h\right) = c_i^0\left(y\right)+Dc_i^0\left(y\right)h+o(h)\\
&c_i\left(y+\theta\left(y\right)\right)+Dc_i\left(y+\theta\left(y\right)\right)\left(I+\nabla\theta\left(y\right)\right)h+o(h) = c_i^0\left(y\right)+Dc_i^0\left(y\right)h+o(h)
\end{aligned}$$

This gives the following equality: $Dc_i(y+\theta(y))(I+\nabla\theta(y)) = Dc_i^0(y)$ and so:

$${}^t Dc_i(y+\theta(y)) =^t (I+\nabla\theta(y))^{-1} \, {}^t Dc_i^0(y) \tag{1.22}$$

By replacing in the normal $m(y+\theta(y))$ we obtain:

$$m(y+\theta(y)) = \sum_{i=1}^{l} r_i(y+\theta(y))^t (I+\nabla\theta(y))^{-1} \, {}^t Dc_i^0(y) e_n$$

and as $r_i(y+\theta(y)) = r_i^0(y)$:

$$m(y+\theta(y)) =^t (I+\nabla\theta(y))^{-1} m^0(y) \tag{1.23}$$

Then we have to analyse the expression of the unit normal and so the norm of $m(y+\theta(y))$:

$$\begin{aligned}
\|m(y+\theta(y))\| &= \left\|^t(I+\nabla\theta(y))^{-1}m^0(y)\right\|\\
&= \left\|(I-^t\nabla\theta)m^0(y)+o(\theta)\right\|\\
&= \left\|m^0(y)-^t\nabla\theta m^0(y)+o(\theta)\right\|\\
&= \left\|m^0(y)\right\| - \frac{\left(m^0(y)\cdot\, {}^t\nabla\theta m^0(y)\right)}{\|m^0(y)\|}+o(\theta)
\end{aligned}$$

which gives:

$$\begin{aligned}
n(y+\theta(y)) &=^t (I+\nabla\theta(y))^{-1} n^0(y)\left(1+\left(n^0(y)\cdot\, {}^t\nabla\theta(y)n^0(y)\right)\right)+o(\theta)\\
&=^t (I+\nabla\theta(y))^{-1} n^0(y) +^t (I+\nabla\theta(y))^{-1} n^0(y)\left(n^0(y)\cdot\, {}^t\nabla\theta(y)n^0(y)\right)+o(\theta)\\
&= \left(I-^t\nabla\theta(y)\right)n^0(y)+\left(I-^t\nabla\theta(y)\right)n^0(y)\left(\left(n^0(y)\cdot\, {}^t\nabla\theta(y)n^0(y)\right)\right)+o(\theta)\\
&= n^0(y)-^t\nabla\theta(y)n^0(y)+\left(n^0(y)\cdot\, {}^t\nabla\theta(y)n^0(y)\right)n^0(y)+o(\theta)
\end{aligned}$$

and the unit normal Lagrangian derivative is:

$$n_0'(\theta) = -({}^t\nabla\theta n^0(y))_t = -^t\nabla\theta(y)n^0(y)+\left(n^0(y)\cdot\, {}^t\nabla\theta(y)n^0(y)\right)n^0(y) \tag{1.24}$$

We have:

$$-({}^t\nabla\theta n^0(y))_t = -\nabla_\tau(\theta\cdot n)+^t\nabla n\theta-\left({}^t\nabla n\theta\cdot n\right)n \tag{1.25}$$

And the Eulerian derivative of the normal is then given by:

$$n'(\theta) = -\nabla_\tau(\theta\cdot n^0)+^t\nabla n^0\theta-\nabla n^0\theta-\left({}^t\nabla n^0\theta\cdot n^0\right)n^0 \tag{1.26}$$

For an extension of the normal defined by the signed distance function, the last term is equal to zero as the norm of n^0 is equal to one in a neighborhood of $\partial\Omega_0$. The term ${}^t\nabla n^0\theta-\nabla n^0\theta$ is also null as ∇n is the Hessian of the signed distance function supposed to be C^2 in the neighborhood of $\partial\Omega_0$. □

We also give the derivative of particular criteria that will be considered in this thesis, the proof can be found in [5] proposition 6.28:

Proposition 1.3.9. *Let Ω be a smooth bounded open set of $\mathbb{R}^d$ and $u(\Omega)$ a function going in $L^1(\Omega)$. We define its transported function from $C^1(\mathbb{R}^d;\mathbb{R}^d)$ to $L^1(\mathbb{R}^d)$:*

$$\bar{u}(\theta) = u((Id+\theta)(\Omega))\circ(Id+\theta) \tag{1.27}$$

assumed to be differentiable at 0. We note Y its derivative corresponding to the Lagrangian derivative of u. We note U the associated Eulerian derivative. Then the functional defined by:

$$J_1 = \int_\Omega j(u(\Omega))\,dx \tag{1.28}$$

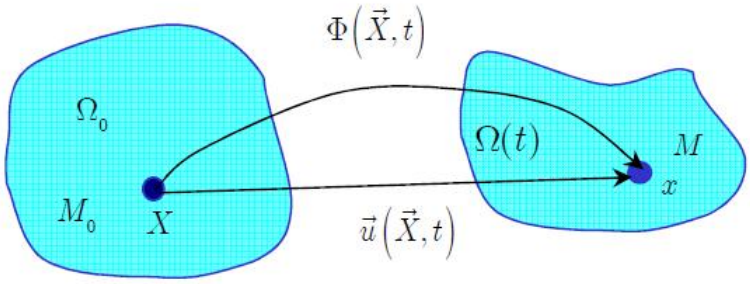

Figure 1.5: The deformation function Φ and the displacement u, (from a course of Frédéric Golay and Stéphane Bonelli).

with j a smooth function, is differentiable at Ω and $\forall\theta \in C^1(\mathbb{R}^d;\mathbb{R}^d)$ we have:

$$J_1'(\Omega)(\theta) = \int_\Omega j(u(\Omega))\mathrm{div}(\theta) + j'(u)Y(\theta)\,dx = \int_\Omega \mathrm{div}(j(u(\Omega))\theta) + j'(u)U(\theta)\,dx \tag{1.29}$$

Moreover if the transported function is derivable at 0 as a function from $C^1(\mathbb{R}^d;\mathbb{R}^d)$ to $L^1(\partial\Omega)$, then the functionnal J_2:

$$J_2 = \int_{\partial\Omega} l(u(\Omega))\,ds \tag{1.30}$$

with l a smooth function, is differentiable at Ω and $\forall\theta \in C^1(\mathbb{R}^d;\mathbb{R}^d)$ we get:

$$J_2'(\Omega)(\theta) = \int_{\partial\Omega} l\left(u\left(\Omega\right)\right)\left(\mathrm{div}\theta - \nabla\theta n\cdot n\right) + l'(u)Y(\theta)\,ds = \int_{\partial\Omega} \theta\cdot n\left(\frac{\partial l(u(\Omega))}{\partial n} + Hl(u(\Omega))\right) + l'(u)U(\theta)\,ds \tag{1.31}$$

The variable $u(\Omega)$ will be in general the solution of a variational equation and, as stated in the proposition, it is needed to prove that u is shape differentiable. The next section gives two ways to do it.

Differentiability of the solution of a PDE

Proving that the solution u of a PDE is differentiable with respect to the shape is not an easy job and it surely exists a large number of possibilities. The two presented here rely on a first common step which is proving the existence of a Lagrangian derivative by writing the equation solved by $\bar{u}(\theta)$:

- First write the PDE for the transported equation on Ω thanks to a change of variable
- Subtract the transported PDE and the PDE solved by $u(x,\Omega)$ to do a Taylor expansion and find the equation solved by the Lagrangian derivative Y and a remainder.
- Prove that the remainder is a $o(\theta)$ and that the solution of Lagrangian equation is unique.

or

- First write the PDE for the transported equation on Ω thanks to a change of variable
- Apply the implicit function theorem to prove that u is differentiable with respect to θ.

Next we apply these schemes to prove that the solution of the linearized elasticity is differentiable with respect to the shape and find the equation solved by the Lagrangian derivative. To do so we first briefly present some basics of the mechanics of deformable solids and linearized elasticity.

Linearized Elasticity

Let Ω_0 be a deformable bounded solid. Due to mechanical stresses, Ω_0 changes shape and we note Ω_t the successive shape taken by Ω_0 during a time interval $[0,T]$. To describe this motion, a deformation function $\Phi : \Omega_0\times\mathbb{R}^+ \to \mathbb{R}^d$ is used. Thus a point $X\in\Omega_0$ is arrived at the time t at the point $\Phi(X,t)$ in Ω_t. From Φ we can define the displacement which is $u(x,t) = \Phi(X,t) - X$ and which also characterizes the motion, see the figure 1.5. For a point $X\in\Omega_0$ we also note $V(X,t)$ its speed at a time t and $\gamma(X,t)$ its acceleration. The next quantity to be defined is the density $\rho(x,t)$ which accounts for how much matter there is at a point x at a time t. The first classic law is the mass conservation which writes:

$$\frac{\partial\rho}{\partial t} + \mathrm{div}(\rho V(X,t)) = 0 \tag{1.32}$$

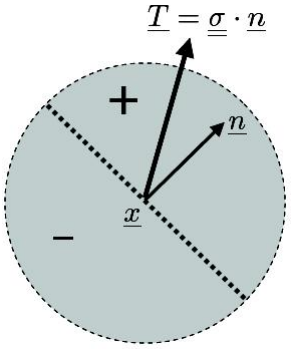

Figure 1.6: The signification of σ, (from [199]).

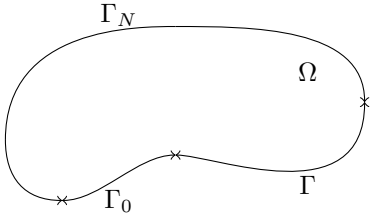

Figure 1.7: The open set Ω.

To model the internal distortion within Ω, the variation of the scalar product is measured thanks to the Cauchy-Green strain tensor $C(\Phi)$ or equivalently the Green-Saint-Venant strain tensor $E(u)$:

$$C(\Phi) = {}^t \nabla\Phi\nabla\Phi, \quad E(u) = \frac{1}{2}\left(C(\Phi) - I\right) = \frac{1}{2}\left(\nabla u + \nabla u + {}^t \nabla u \nabla u\right) \tag{1.33}$$

We make the assumption of small deformations which is tantamount to neglect the quadratic term in $E(u)$:

$$E(u) \simeq e(u) = \frac{1}{2}\left(\nabla u + {}^t \nabla u\right) \tag{1.34}$$

The last quantity to be defined is, contrary to the first cinematic ones, of a dynamic type. It models the internal forces and is called the stress tensor σ. Take a point $x \in \Omega_0$ and a plane surface S such that $x \in S$. We note n the normal to S going from one side noted S_- to the other side noted S_+. Then the force exerted by S_+ on S_- is $T = \sigma n$, see figure 1.6. This tensor is symmetric and of order two. Finally applying the fundamental principle of dynamics it follows that:

$$\begin{cases} \rho\gamma - \operatorname{div}(\sigma) & = f & \text{in } \Omega \\ u & = 0 & \text{on } \Gamma_0 \\ \sigma n & = g & \text{on } \Gamma_N \\ \sigma n & = 0 & \text{on } \Gamma \end{cases} \tag{1.35}$$

where f is a volume force, $\partial\Omega = \Gamma_0 \cup \Gamma_N \cup \Gamma$ is a partition of the boundary and g a surface force. Note that the boundary Γ_0 is a clamped part of the boundary which is assumed to be of positive measure.

In our case the time dependence will be removed: we only consider static cases. That means that Ω_0 instantly deforms into $\Omega_1 = \Omega_T$ as soon as stresses are applied. Furthermore small deformations and small displacements are assumed and the equations (1.32) and (1.35) can be linearized with respect to the displacement u [98] chapter 3 section 2. This leads to the simplified formulation, also called equilibrium equation:

$$\begin{cases} -\operatorname{div}(\sigma) & = f & \text{in } \Omega \\ u & = 0 & \text{on } \Gamma_0 \\ \sigma n & = g & \text{on } \Gamma_N \\ \sigma n & = 0 & \text{on } \Gamma \end{cases} \tag{1.36}$$

assuming a constant ρ.

It remains to make the link between cinematic and dynamics. In elasticity the knowing of $e(u)$ suffices to know σ. In linearized elasticity the link between the strain tensor and the stress tensor is linear:

$$\sigma = Ae(u), \tag{1.37}$$

where A is a fourth order tensor. We will assume isotropic linearized elasticity, so we can in fact write:

$$\sigma = 2\mu e(u) + \lambda tr(e(u)) \tag{1.38}$$

where λ and μ are the Lamé coefficients.

Finally we can state the complete linearized elasticity equations for Ω an open Lipschitz bounded set:

$$\begin{cases} -\operatorname{div}(Ae(u)) &= f \quad \text{in } \Omega \\ u &= 0 \quad \text{on } \Gamma_0 \\ Ae(u)n &= g \quad \text{on } \Gamma_N \\ Ae(u)n &= 0 \quad \text{on } \Gamma \end{cases} \tag{1.39}$$

which is equivalent to the following variational equation: find $u \in H^1_{\Gamma_0}(\Omega)^d$ such that

$$\int_\Omega Ae(u) : e(v)\, dx = \int_\Omega f \cdot v\, dx + \int_{\Gamma_N} g \cdot v\, ds \quad \forall v \in H^1_{\Gamma_0}(\Omega)^d. \tag{1.40}$$

with:

$$H^1_{\Gamma_0}(\Omega)^d = \left\{ v \in (H^1(\Omega))^d,\ v = 0 \text{ on } \Gamma_0 \right\} \tag{1.41}$$

The application of Lax-Milgram theorem, coupled with Korn's inequality gives the existence and uniqueness of u if $f \in L^2(\Omega)^d$ and $g \in L^2(\Gamma_N)^d$. In the following we will suppose $f \in H^1(\mathbb{R}^d)^d$ and $g \in H^2(\mathbb{R}^d)^d$ to compute the Lagrangian and the Eulerian shape derivatives of u. Further regularity results can be proven (see [74]) in the case $\partial\Omega = \Gamma_0$ or $\partial\Omega = \Gamma_N$. For mixed boundary conditions, there can be a lack of regularity in the vicinity of the points near the change of boundary conditions.

Differentiability of the linearized elasticity solution

We start from the variational formulation (1.40) and transpose the formulation which is written on Ω to a formulation written on Ω_0, a reference open set, thanks to the following diffeomorphism: $Id + \theta$ such that $\Omega = (Id + \theta)(\Omega_0)$. Furthermore we also consider that Γ_0 can't change, which means that $\theta = 0$ on Γ_0. We take particular test functions: $v = \phi \circ (Id + \theta)^{-1}$. We will note y the coordinates of points in Ω_0 and x the coordinates of points in Ω. Finally we assume in this section that the solution u and Ω are regular enough.

First we give a relation between the gradient of a function u defined on Ω, taken at the point $(Id + \theta)(y)$, and the gradient of $u \circ (Id + \theta)$ at y.

Lemma 1.3.10.

$$\nabla_y \left[u\left((Id + \theta)(y) \right) \right] = \left[\nabla_x u \right] \circ (Id + \theta)(y)\, (I + \nabla_y \theta) \tag{1.42}$$

Proof. We have:

$$\begin{aligned} u\left((Id + \theta)(y + h) \right) &= u\left((Id + \theta)(y) + h + \nabla_y \theta h + o(h) \right) \\ &= u\left((Id + \theta)(y) \right) + \left[\nabla_x u \right] \circ (Id + \theta)(y)\, (I + \nabla_y \theta)\, h + o(h) \end{aligned}$$

and also

$$u\left((Id + \theta)(y + h) \right) = u\left((Id + \theta)(y) \right) + \nabla_y \left[u\left((Id + \theta)(y) \right) \right] h + o(h)$$

The uniqueness of the derivative gives (1.42) □

Definition 1.3.11. *We note $\overline{u}(\theta)$ the function defined for all $y \in \Omega_0$ by $\overline{u}(\theta)(y) = u\left((Id + \theta)(\Omega_0), y + \theta(y) \right)$*

We perform a change of variable in the integral. By using (1.42) and the symmetry properties of A we have:

$$\int_\Omega Ae(u) : e(v)\, dx = \int_{\Omega_0} A(\nabla \overline{u}(\theta)(I + \nabla\theta)^{-1}) : (\nabla\phi(I + \nabla\theta)^{-1}) |det(I + \nabla\theta)|\, dy \tag{1.43}$$

$$\int_\Omega f \cdot v\, dx = \int_{\Omega_0} f(y + \theta(y)) \cdot \phi |det(I + \nabla\theta)|\, dy \tag{1.44}$$

$$\int_{\Gamma_N} g \cdot v\, ds = \int_{\Gamma_N^0} g(y + \theta(y)) \cdot \phi |det(I + \nabla\theta)| |^t (I + \nabla\theta)^{-1} n|\, ds \tag{1.45}$$

Theorem 1.3.12. *The solution u of the linearized elasticity problem (1.39) admits a Lagrangian derivative $Y(\theta, y)$ with respect to the shape assuming Γ_0 does not vary, $f \in H^1(\mathbb{R}^d)^d$ and $g \in H^2(\mathbb{R}^d)^d$. The existence of an Eulerian derivative follows from (1.17).*

Proof. We want to use the implicit function theorem. Each of (1.43), (1.44) and (1.45) defines an operator from $(\theta,\overline{u}) \in C^1(\mathbb{R}^d,\mathbb{R}^d)\cap W^{1,\infty}(\mathbb{R}^d,\mathbb{R}^d)\times H^1(\Omega)^d$ to $(H^1(\Omega)^d)^*$ respectively noted $A(\theta,\overline{u})$, $F(\theta,\overline{u})$ and $G(\theta,\overline{u})$. With the regularities taken for f and g their differentiability with respect to θ at 0 is proved for $F(\theta,\overline{u})$ and $G(\theta,\overline{u})$ in [137] theorem 5.3.2 and in theorem 5.5.1. For the operator given by $A(\theta,\overline{u})$ the proof can be done exactly as in [137] theorem 5.3.2. Then we apply the implicit function theorem and it exists a C^1 function $\theta\to\overline{u}_\theta$ such that in the neighborhood of 0 $A(\theta,\overline{u}_\theta)+F(\theta,\overline{u}_\theta)+G(\theta,\overline{u}_\theta)=0$. The uniqueness of the solution to the variational equation gives $\overline{u}_\theta=\overline{u}(\theta)$ and the existence of a Lagrangian derivative. For the Eulerian derivative, we need to prove that we can apply (1.17). We note that:

$$u\left(x,\left(Id+\theta\right)\left(\Omega\right)\right)=\overline{u}(\theta)\circ\left(Id+\theta\right)^{-1}. \tag{1.46}$$

and applying lemma 5.3.3 of [137] which remains valid for a function $g\in W^{1,p}(\mathbb{R}^d)^d$, for $p=2$, $g(\theta)=\overline{u}(\theta)$ and $\Psi(\theta)=(I+\theta)^{-1}$, $u\left(x,\left(Id+\theta\right)\right)$ is differentiable in 0 and (1.17) holds. This give

□

Theorem 1.3.13. *The Lagrangian derivative $Y(\theta,y)$ is the solution of the following equation: $\forall\phi\in H^1_{\Gamma_0}(\Omega)^d$*

$$\begin{aligned}
&\int_{\Omega_0} A\nabla Y(\theta,y):\nabla\phi\,dx\\
&=\int_{\Omega_0}\nabla f\cdot\theta(y)\phi+f(y)\cdot\phi\,\mathrm{div}(\theta)\,dx\\
&+\int_{\Gamma_N^0}\nabla g(y)\theta(y)\cdot\phi+g(y)\cdot\phi\,\mathrm{div}(\theta)-\left(g(y)\cdot\phi\right)\left({}^t\nabla\theta n\right)\cdot n\,ds\\
&+\int_{\Omega_0} A\nabla\bar{u}(0):(\nabla\phi\nabla\theta)+A\nabla\bar{u}(0)\nabla\theta:\nabla\phi-Ae(\bar{u}(0)):e(\phi)\mathrm{div}(\theta)\,dx
\end{aligned} \tag{1.47}$$

Proof. We will differentiate each term from (1.43) to (1.45). Let us begin with (1.43).

$$\left[\nabla\bar{u}(\theta)\right]\left(I+\nabla\theta\right)^{-1}=\nabla\bar{u}(0)+\nabla Y(\theta,y)-\nabla\bar{u}(0)\nabla\theta+o(\theta)$$

and

$$\left[\nabla\phi\right]\left(I+\nabla\theta\right)^{-1}=\nabla\phi-\nabla\phi\nabla\theta+o(\theta)$$

which gives:

$$\begin{aligned}
A\left(\nabla\bar{u}(\theta)\left(I+\nabla\theta\right)^{-1}\right):\left(\nabla\phi\left(I+\nabla\theta\right)^{-1}\right)&=A\nabla\bar{u}(0):\nabla\phi-A\nabla\bar{u}(0):(\nabla\phi\nabla\theta)\\
&+A\nabla Y(\theta,y):\nabla\phi-A\left(\nabla\bar{u}(0)\nabla\theta\right):\nabla\phi+o(\theta).
\end{aligned}$$

Moreover we know that

$$det\left(I+\nabla\theta\right)=1+\mathrm{div}(\theta)+o(\theta). \tag{1.48}$$

So the term in the integral which is:

$$A\left(\nabla\bar{u}(\theta)\left(I+\nabla\theta\right)^{-1}\right):\left(\nabla(\phi)\left(I+\nabla\theta\right)^{-1}\right)\left|det\left(I+\nabla\theta\right)\right|$$

has a derivative which is:

$$\begin{aligned}
&A\nabla\bar{u}(0):\nabla\phi+\mathrm{div}(\theta)A\nabla\bar{u}(0):\nabla\phi-A\nabla\bar{u}(0):(\nabla\phi\nabla\theta)\\
&+A\nabla Y(\theta,y):\nabla\phi-A\left(\nabla\bar{u}(0)\nabla\theta\right):\nabla\phi+o(\theta)
\end{aligned} \tag{1.49}$$

Then we have to differentiate the term (1.44) which gives:

$$f\left(y+\theta(y)\right)\left|det\left(I+\nabla\theta\right)\right|=f(y)+\nabla f\theta(y)+f(y)\mathrm{div}(\theta)+o(\theta) \tag{1.50}$$

and the term (1.45):

$$g\left(y+\theta(y)\right)\left|det(I+\nabla\theta)\right|\left|{}^t(I+\nabla\theta)^{-1}n\right|=g(y)+\nabla g(y)\theta(y)+g(y)\mathrm{div}(\theta)-g(y)\left({}^t\nabla\theta n\right)\cdot n+o(\theta) \tag{1.51}$$

using the formula:

$$\left|{}^t(I+\nabla\theta)^{-1}n\right|=1-\left({}^t\nabla\theta n\right)\cdot n+o(\theta). \tag{1.52}$$

By putting the terms (1.49), (1.50) and (1.51) together we find (1.47). □

Theorem 1.3.14. *The Eulerian derivative $U(\theta,y)$ is solution of the following equation: $\forall\phi\in H^1_{\Gamma_0}(\Omega)^d$*

$$\begin{aligned}
&\int_{\Omega_0} A\nabla U(\theta,y):\nabla\phi\,dx+\int_{\Omega_0} A\nabla\left(\nabla\bar{u}(0)\theta\right):\nabla\phi\,dx\\
&=\int_{\Omega_0}\nabla f\cdot\theta(y)\phi+f(y)\cdot\phi\,\mathrm{div}(\theta)\,dx\\
&+\int_{\Gamma_N^0}\nabla g(y)\theta(y)\cdot\phi+g(y)\cdot\phi\,\mathrm{div}(\theta)-\left(g(y)\cdot\phi\right)\left({}^t\nabla\theta n\right)\cdot n\,ds\\
&+\int_{\Omega_0} A\nabla\bar{u}(0):(\nabla\phi\nabla\theta)+A\left(\nabla\bar{u}(0)\nabla\theta\right):\nabla\phi-Ae(\bar{u}(0):e(\phi)\,\mathrm{div}(\theta)\,dx
\end{aligned} \tag{1.53}$$

Proof. It suffices to replace Y by $U + \nabla\bar{u}(0)\theta$. □

This is the first idea to compute the Eulerian derivative of u. But once the existence of a derivative is proved, we can apply a kind of chain rule formula directly on the equation to retrieve another version of the variational equation solved by $U(\theta, x)$. This is done in [5] and in [137] theorem 5 5.2, assuming enough regularity on u in our case.

Theorem 1.3.15. *The Eulerian derivative $U(\theta, y)$ is solution of the following equation with $\Gamma_m = \Gamma_N \cup \Gamma$: $\forall \phi \in H^1_{\Gamma_0}(\Omega)^d$*

$$\int_\Omega A\nabla U(\theta,x) : \nabla\phi \, dx + \int_{\Gamma_m} (\theta\cdot n)\,(Ae(u) : e(\phi))\; ds = \int_{\Gamma_m} (\theta\cdot n)\; f\cdot\phi \, dx + \int_{\Gamma_N} (\theta\cdot n)\left(Hg\phi + \frac{\partial g\phi}{\partial n}\right) ds \quad (1.54)$$

Proof. We differentiate the variational equation (1.40) directly. This can be written as the addition of the partial derivative with respect to Ω with the partial derivative with respect to u taken in the direction of $U(\theta, x)$ ([137] corollary 5.2.5). Using the theorem 1.3.4 we get (1.54). □

Adjoint method to compute the derivative of a criterion I

If we look at the expression of the derivative of a criterion J_1 (or a criterion J_2) as in proposition 1.3.9, the dependency on θ is implicit through the presence of the derivative $U(\theta, x)$. This is not convenient from a numerical point of view since, in a gradient based algorithm, it is θ which needs to be chosen to make the shape Ω vary. To make this dependency explicit and to get rid of the Eulerian derivative, an adjoint method is used. It consists in computing a quantity which will be independent of θ but dependent on the criterion and will contain the information on the variations of the criterion with respect to the shape.

We consider the criterion J_1 for the sake of simplicity and rewrite its derivative:

$$J_1'(\Omega)(\theta) = \int_\Omega j\,(u(\Omega))\,\mathrm{div}(\theta) + j'(u)Y(\theta)\,dx = \int_\Omega \mathrm{div}\,(j\,(u(\Omega))\,\theta) + j'(u)U(\theta)\,dx.$$

The term we want to remove is $\displaystyle\int_\Omega j'(u)U(\theta)\,dx$. Then we will use equation (1.54) to do it. We state the following adjoint problem:

$$\int_\Omega A\nabla\phi : \nabla p = -\int_\Omega j'(u)\cdot\phi\,dx \quad \forall\phi \in H^1_{\Gamma_0}(\Omega)^d \quad (1.55)$$

As for p and $U(\theta, x)$, the test functions are in the same space: we can take $\phi = p$ in (1.54) and $\phi = U(\theta, x)$ in (1.55). Then we get:

$$\int_\Omega j'(u)\cdot U(\theta,x)\,dx = \int_{\Gamma_m} (\theta\cdot n)\,(Ae(u) : e(p))\; ds - \int_{\Gamma_m} (\theta\cdot n)\,(f\cdot p)\; ds - \int_{\Gamma_N} (\theta\cdot n)\left(Hg\cdot p + \frac{\partial g\cdot p}{\partial n}\right) ds \quad (1.56)$$

and the derivative of the criterion is:

$$J_1'(\Omega)(\theta) = \int_{\Gamma_m} j\,(u\,(\Omega))\,(\theta\cdot n)\; ds + \int_{\Gamma_m} \theta\cdot n\,(Ae(u) : e(p))\; ds - \int_{\Gamma_m} (\theta\cdot n)\,(f\cdot p)\; ds - \int_{\Gamma_N} (\theta\cdot n)\left(Hg\cdot p + \frac{\partial g\cdot p}{\partial n}\right) ds$$

So we can state the following theorem:

Theorem 1.3.16. *The derivative of J_1 with respect to the shape is:*

$$J_1'(\Omega)(\theta) = \int_{\Gamma_m} j\,(u\,(\Omega))\,(\theta\cdot n)\; ds + \int_{\Gamma_m} \theta\cdot n\,(Ae(u) : e(p))\; ds - \int_{\Gamma_m} (\theta\cdot n)\,(f\cdot p)\; ds - \int_{\Gamma_N} (\theta\cdot n)\left(Hg\cdot p + \frac{\partial g\cdot p}{\partial n}\right) ds \quad (1.57)$$

with p the solution of the following adjoint problem:

$$\begin{cases} -\,\mathrm{div}(Ae(p)) = -j'(u) & \text{in } \Omega \\ p = 0 & \text{on } \Gamma_0 \\ Ae(p) = 0 & \text{on } \Gamma_m. \end{cases} \quad (1.58)$$

Adjoint method to compute the derivative of a criterion II - Céa method

There exists a method to easily find the derivative and the associated adjoint problem without finding the equation solved by the Eulerian derivative which could be cumbersome. This method is described in [61] or in [5]. The idea is to see the variational equation as a constraint of the optimization problem and so to write a Lagrangian function taking the test function as a Lagrangian multiplier. Still we keep working on shapes for which Γ_0 does not change. If it is not the case we refer to [5] for the method and for the particular case of elasticity to Proposition 1.3.9 [202].

We write the Lagrangian function $L : \mathcal{U}_{ad} \times H^1_{\Gamma_0}(\Omega)^d \times H^1_{\Gamma_0}(\Omega)^d \to \mathbb{R}$:

$$L(\Omega, v, q) = \int_\Omega j(v) + \int_\Omega Ae(v) : e(q)\, dx - \int_\Omega f \cdot q\, dx - \int_{\Gamma_N} g \cdot q\, ds \tag{1.59}$$

where q plays the role of the Lagrangian multiplier. It is important to note that we can express $J_1(\Omega)$ thanks to the Lagrangian:

$$\forall q \in H^1_{\Gamma_0}(\mathbb{R}^d)^d,\ \ J_1(\Omega) = L(\Omega, u, q) \tag{1.60}$$

where u is the solution of the elasticity problem (1.40). We note (u, p) a stationarity point of L. Differentiating the Lagrangian with respect to q yields the equation solved by u which is exactly (1.40).

The equation solved by p can be found by derivating L with respect to v in the direction $\psi \in H^1_{\Gamma_0}(\mathbb{R}^d)^d$:

$$\partial_v L(\Omega, u, q; \psi) = \int_\Omega Ae(q) : e(\psi)\, dx + \int_\Omega j'(u) \cdot \psi\, dx \tag{1.61}$$

and the adjoint problem is:

$$\int_\Omega Ae(p) : e(\psi)\, dx = -\int_\Omega j'(u) \cdot \psi\, dx,\ \ \forall \psi \in H^1_{\Gamma_0}(\mathbb{R}^d). \tag{1.62}$$

Finally we compute the shape derivative of J_1 thanks to (1.60):

$$\begin{aligned} J'(\Omega, \theta) &= L'(\Omega, u_\Omega, q; \theta) \\ &= \partial_\Omega L(\Omega, u_\Omega, q; \theta) + \partial_u L(\Omega, u_\Omega, q; u'(\theta)) \end{aligned} \tag{1.63}$$

for every $q \in H^1_{\Gamma_0}(\mathbb{R}^d)^d$. So taking $q = p$ gives:

$$\begin{aligned} J'(\Omega, \theta) &= \partial_\Omega L(\Omega, u_\Omega, p; \theta) \\ &= \int_{\Gamma_m} j\left(u\left(\Omega\right)\right)\left(\theta \cdot n\right)\, ds + \int_{\Gamma_m} \theta \cdot n\left(Ae(u) : e(p)\right)\, ds - \int_{\Gamma_m} \left(\theta \cdot n\right)\left(f \cdot p\right)\, ds \\ &- \int_{\Gamma_N} \left(\theta \cdot n\right)\left(Hg \cdot p + \frac{\partial g \cdot p}{\partial n}\right)\, ds \end{aligned} \tag{1.64}$$

using theorem 1.3.4.

This method will be used in the following to compute shape gradients due to its great simplicity. However one has to pay attention to the fact that it does not prove itself that there exists a derivative. Applying it to problems which are not differentiable can lead to wrong formulae ([282]).

1.3.4 Optimizing with the level set method

Once the shape gradients of the criteria are computed, one can use them in a descent algorithm. This algorithm produces a sequence of shape $(\Omega^n)_{n\in\mathbb{N}}$ starting from an initial guess denoted Ω^0. Then it follows the steps below:

1. Calculate the solution of (1.39) and the associated adjoint state p if needed on Ω^n.
2. Find a descent direction θ^n.
3. Find a descent step t^n small enough for the objective to be reduced and the constraints to be fulfilled or improved
4. State $\Omega^{n+1} = (Id + t^n\theta^n)(\Omega^n)$.

The scheme presented here is general and highlights the two crucial points to be studied: the choice of a descent direction and the choice of a descent step.

To initiate the discussion we rewrite the formulation into a problem without constraint and give an example. We take Ω an open bounded set, smooth enough, filled with an isotropic elastic material as modeled in 1.3.3. For the optimisation part we note $J(\Omega)$ the objective and $C(\Omega)$ a constraint which can be a volume or a perimeter constraint. Instead of stating a constrained optimization problem, we choose to minimize a weighted sum of J and C:

$$\mathcal{L}(\Omega) = J(\Omega) + \alpha C(\Omega) \tag{1.65}$$

with α a fixed Lagrangian multiplier. This approach is simple but is at the root of more sophisticated algorithm such as the quadratic penalty method or the augmented Lagrangian method...see [219] chapter 17. Moreover it enables to present the difficulties due to the level set method without adding difficulties coming from the optimization algorithm.

As seen in 1.3.3, the shape gradient of $\mathcal{L}$ can be written as:

$$\mathcal{L}'(\Omega) = \int_{\Gamma_m} (\theta \cdot n)\, l(x)\, ds \tag{1.66}$$

with l a function from $\mathbb{R}^d$ to $\mathbb{R}$. Then a simple descent direction defined on $\partial\Omega$ is:

$$\theta(x) = -l(x)n. \tag{1.67}$$

Second order derivatives can also be computed and used in second order algorithms. It is not the goal of this thesis to investigate this subject and we won't use these techniques. We refer the interested reader to [137] and [288].

Extension and Regularization of the descent direction

We note that this defines θ only on the boundary of Ω, whereas θ in the definition of the shape derivative was defined on $\mathbb{R}^d$. So we need to extend θ to stuck to the theory. In fact, for the level set method it will be necessary to have θ extended to be able to change the shape during the optimization process as we will use a front propagation equation. Furthermore this extension leaves place to a regularization of θ which enables to prevent oscillations of the boundary (see 6.5.3 [5]). A way to do this is to identify the direction θ by means of a different scalar product. For instance we can choose a H^1 scalar product:

$$a(\phi, \psi) = \beta^2 \int_\Omega \nabla\phi : \nabla\psi + \int_\Omega \phi \cdot \psi \, dx \tag{1.68}$$

with β a small parameter depending on the mesh size. If we are searching for θ under the form wn we can solve:

$$a(w, q) = \int_{\Gamma_m} l(x)q(x)\, ds \;\; \forall q \in H^1(D) \tag{1.69}$$

and $-w \in H^1(D)$ will be a descent direction which is regularized. Indeed:

$$\int_{\Gamma_m} l(x)w(x) = a(w, w) > 0 \tag{1.70}$$

thanks to the coercivity property of the scalar product a.

It is important to point out that this phase of extension and regularization has to be done such that the new field is still a descent direction. We refer to [5], [86], [53], for further details.

Evolution of the shape

As stated, the shape evolves during the optimization process according to a descent direction. As we have seen before, it is linked to the shape derivative of our criteria and a descent step that has to be adjusted. The question is how we can perform this evolution. The idea is to take a level set function ψ which depends not only on the space but also on the time. So let us introduce $\psi : [0, T] \times D \to \mathbb{R}$ a time dependent level set function with T a fixed parameter.

For $t \in [0, T]$ the boundary of the shape Ω^t is given by the set of points $x(t)$ such that:

$$\psi(x(t), t) = 0 \tag{1.71}$$

We assume that $\psi(t, x)$ and $\theta(t, x)$ are smooth and suppose that the shape evolves according to θ which means that $x'(t) = \theta(t, x(t))$. Then, (as everything is assumed smooth), the equation (1.71) can be differentiated which gives:

$$\frac{\partial\psi}{\partial t}(t, x) + \theta(t, x(t)) \cdot \nabla\psi(t, x) = 0. \tag{1.72}$$

This equation is first stated for $x(t) \in \partial\Omega^t$ but can be extended to the whole domain D as the level set function is supposed to be smooth. If θ is searched under the form $\theta = V(t, x)n(t, x)$, the evolution equation can be rewritten as:

$$\frac{\partial\psi}{\partial t}(t, x) + V(t, x(t))\, |\nabla\psi(t, x)| = 0 \text{ in } D, \tag{1.73}$$

which is an Hamilton-Jacobi equation with V called the velocity field. We will use this equation to make numerically evolve our shape.

Remark 1.3.17. *To get equation* (1.73)*, we made a smoothness assumption which is rarely true. In fact singularities can appear during the evolution, even when it is done with very smooth $\psi(0, \cdot)$ and smooth velocity field. Consequently, if we use this method of evolution, starting from a smooth Ω_0 does not give necessarily at the end a smooth shape. Then the derivation done is not rigorous. The Hamilton-Jacobi equation has to be studied in these cases from a weaker point of view, thanks to the theory of viscosity solutions introduced by M.G. Crandall and P.L. Lions, see [77]. For further details on this subject we refer to [84] and [251].*

From a numerical point of view, it is then straightforward to define the descent step. Starting from Ω^n and a velocity V^n, we solve the Hamilton-Jacobi equation on a time interval $[0, t_f]$ with t_f being the descent step found through a linear search. To solve this equation, we use an explicit second order upwind scheme on a cartesian grid meshing D, with Neumann boundary conditions, [224]. Since the scheme is explicit in time, the time stepping has to satisfy a CFL condition and, in order to regularise the level set which can become too flat or too steep during the successive optimisation iterations, periodical reinitialisations, thanks to an Hamilton-Jacobi equation admitting the signed distance to the shape as stationnary solution, are performed. We refer to [10] and [251] section 5.1 for numerical implementation details. For other possible and more complex ways to solve the Hamilton-Jacobi equation through for instance unstructed meshes fitting the boundary of the shape we refer to [271] or [84].

Finally we point out the fact that the Hadamard method for shape variation prevents the shape from topological changes. Yet this property is not naturally fulfilled when the Hamilton-Jacobi equation is numerically solved. Indeed, it could be enforced in the algorithm by ensuring that the steps chosen are always small enough for the topology not to change. However it is in our interest to get such topological changes and we take advantage of this "default" to be able to reach a larger range of shapes. Still it remains that the shape derivative is not correct when topological changes occur and this can lead to a premature stop in the algorithm. To address this issue, one can use the notion of topological derivative as mentionned in 1.1.

Solving elasticity with the ersatz material

The mesh used to compute the solutions of Hamilton-Jacobi equation is fixed and does not fit the boundary of the shape defined by $\{x \,|\, \psi(x) = 0\}$. In the same way we choose to compute the solution of the mechanical problem on a fixed mesh of the domain D (which can be the same as the grid used for solving (1.73)). To do so, we use the so-called "ersatz-material" approach. It is tantamount to fill $D \setminus \Omega$ with a weak material mimicking void but preventing the stiffness matrix from being singular. This technique is commonly used in topological and in shape optimisation with level sets, [10]. We define a new elasticity tensor $A^* = \rho A$ with ρ:

$$\rho(x) = \begin{cases} 1 \text{ in } \Omega \\ \epsilon \ll 1 \text{ in } D \setminus \Omega \end{cases} \tag{1.74}$$

and solve the equations for u and p with this new tensor A^* on the whole domain D.

1.3.5 Numerical examples

To illustrate this part we give three examples of shape otpimization performed thanks to the procedure described previously. In all examples the goal is to minimize the volume under a compliance constraint for a material which is supposed to solve the linearized elasticity equations (1.40). The volume is defined as:

$$J_{\text{vol}} = \int_\Omega dx \tag{1.75}$$

and the compliance:

$$\int_\Omega f \cdot u \, dx + \int_{\Gamma_N} g \cdot u = \int_\Omega Ae(u) : e(u) \, dx. \tag{1.76}$$

Using 1.3.3, it is straightforward that the adjoint function associated with the compliance is $-u$. The solution u is computed thanks to the finite element method (square Q1 elements) on a regular mesh. As explained during the optimization process, some shapes are accepted and other ones are rejected. That's why for each example both the number of iterations (shapes which were accepted) and the number of evaluations (all the shapes which were evaluated) are given.

Bridge

The mesh is 100 elements long and 50 elements large. We apply a downward force at the middle of the bottom and clamped the structure at the two bottom corners (see figure 1.8 for the load case and for the results figure 1.9 and 1.10). The Lagrangian multiplier is $\lambda = 0.05$. The algorithm converged in 72 iterations making 115 evaluations.

Cantilever

The mesh is 120 elements long and 60 elements large. We apply a downward force at the middle of the right side and clamped the structure on the left side (see figure 1.11 for the load case and for the results figure 1.12 and 1.13). The Lagrangian multiplier is $\lambda = 0.01$. The algorithm converged in 236 iterations and 1379 evaluations.

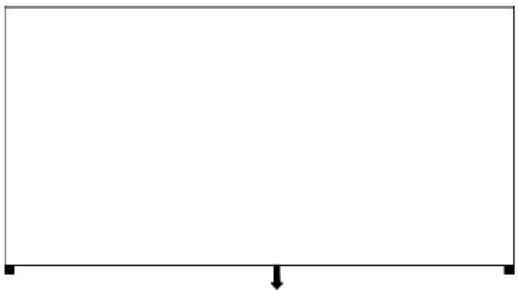

Figure 1.8: Load case for the bridge case.

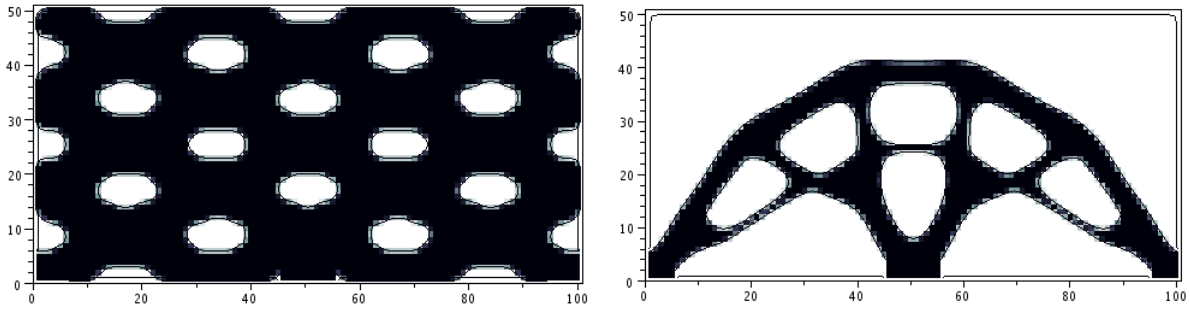

(a) The initialization. (b) The final design.

Figure 1.9: Results for the bridge case.

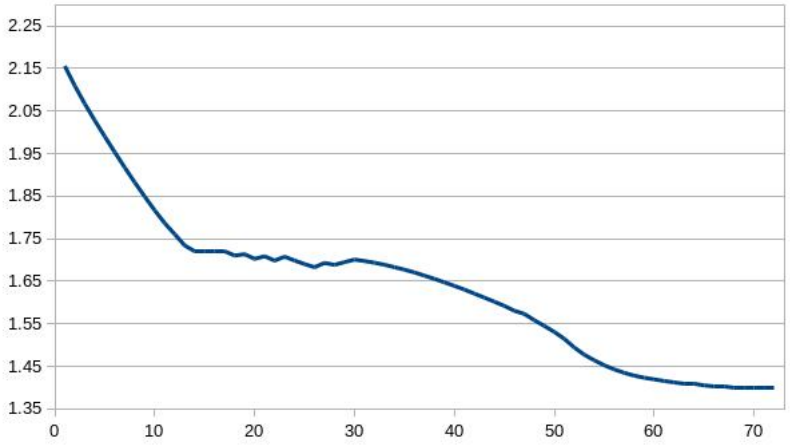

Figure 1.10: The evolution of the Lagrangian function for the bridge case.

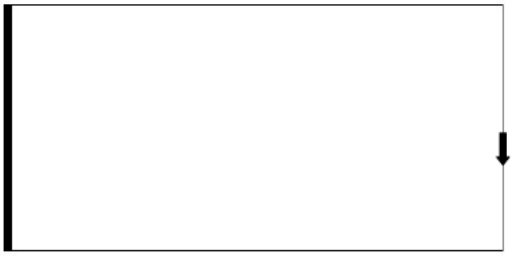

Figure 1.11: Load case for the cantilever case.

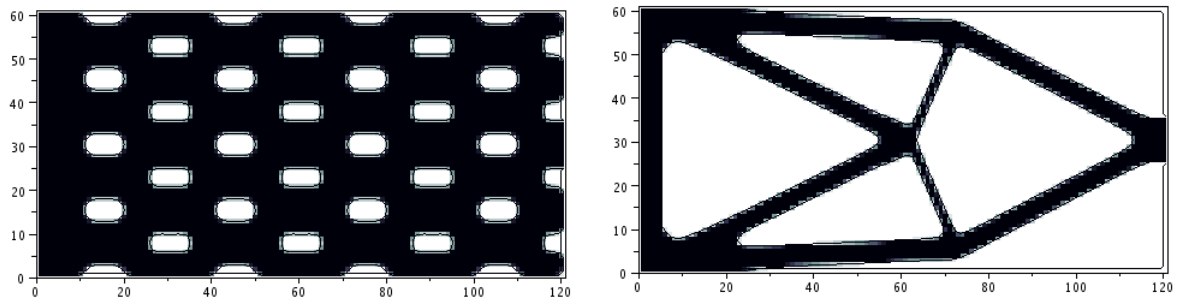

(a) The initialization. (b) The final design.

Figure 1.12: Results for the cantilever case.

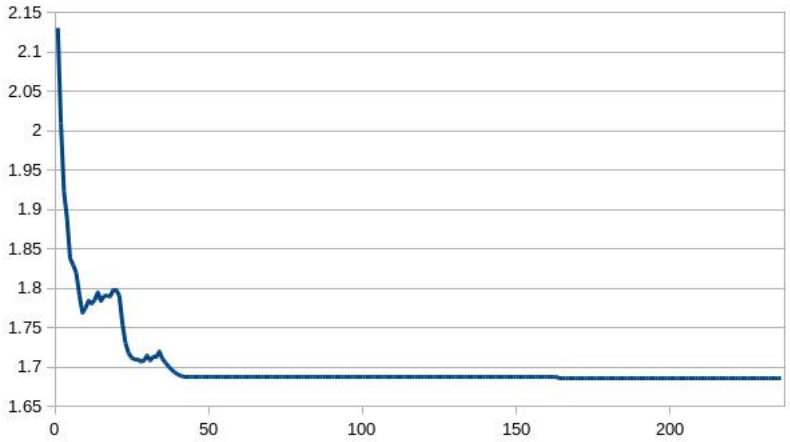

Figure 1.13: The evolution of the Lagrangian function for the cantilever case.

L-shape

The mesh is 100 elements long and 100 elements large. Dirichlet conditions are enforced on the part up to the left part of the L-shape and a downward force is applied on $(2, 1.6)$. (see figure 1.14 for the load case and for the results figure 1.15 and 1.16). The Lagrangian multiplier is $\lambda = 0.01$. The algorithm converged in 131 iterations and 916 evaluations.

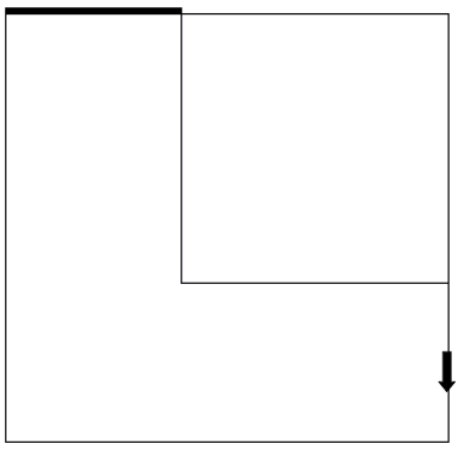

Figure 1.14: Load case for the Lshape case.

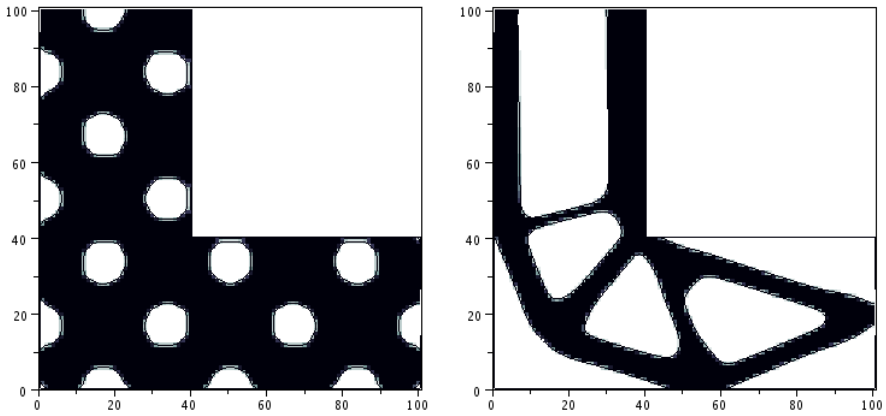

(a) The initialization. (b) The final design.

Figure 1.15: Results for the L-shape case.

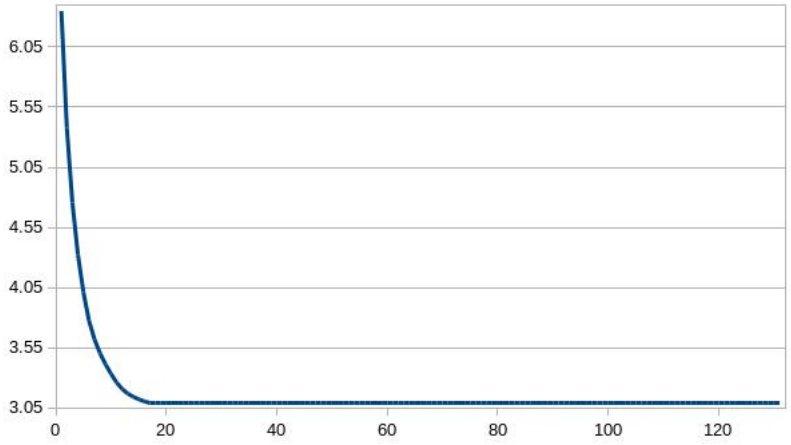

Figure 1.16: The evolution of the Lagrangian function for the L-shape case.

Chapter 2

Variational inequalities and projection

Contents

2.1 Introduction

This chapter is meant to give some results on variational inequalities and the projection operator which will be extensively used in the study of contact mechanics and plasticity. The presentation is very brief and we provide some references in each section if more details or extensions are needed. We start with mathematical preliminaries on minimisation on convex sets, monotone operators and capacity theory. Then we talk about the projection operator and its regularity. Finally we give some results for particular variational inequalities and give a first example of the differentiation of a variational inequality with respect to a parameter (the thickness) accounting for the shape.

2.2 Preliminaries

These preliminaries are divided into three parts. The first part is meant to state theorem 2.2.4 which will be used to prove the existence of a solution to the projection problem 2.3 and the proximal problem (proposition 2.4.6). The second part recall some basic notions on monotone operators which are necessary to understand the part on variational inequalities and some remarks made in the chapter 4 about plasticity. The third part presents some notions on capacity theory which are indispensable to understand the part on conical derivatives and the example of sensitivity analysis given at the end of this chapter.

2.2.1 Minimisation theorem

In all the applications we will place ourselves in Hilbert spaces, but the main theorem of this part is true in reflexive Banach spaces. Consequently we briefly we recall the definition of such spaces:

Definition 2.2.1.
- *X is a Banach space if it is normed and complete. The space of continuous linear form on X is called the dual and is noted X^*. If $f \in X^*$ we note the duality product $\langle \cdot, \cdot \rangle$:*

$$f(x) = \langle f, x \rangle \tag{2.1}$$

- *X is a reflexive Banach space when we can identify the bi-dual X^{**} with X by means of the following injection $J : X \to X^{**}$:*

$$J : x \mapsto [f \mapsto \langle f, x \rangle] \tag{2.2}$$

which is an isomorphism if the identification can be made.

- *Let X be a metric space. X is seperable if there exists a dense countable subset $D \subset X$.*
- *A Hilbert space X is a space with an inner product which is complete for the norm associated with its inner product. A Hilbert space is reflexive and its dual X^* can be identified with X, thanks to the Riesz-Fréchet theorem ([47] 5.2).*

We also need some basic notions of convexity to state the main theorem of this part. The proposition is taken from [264] proposition 1.29. For a complete presentation of the basics of convex analysis we refer to [239].

Definition 2.2.2.
- *A function f from a normed vector space X to $\overline{\mathbb{R}} = \mathbb{R} \cup \{-\infty, +\infty\}$ is said to be positively homogeneous if*
$$\forall x \in X,\ \forall \alpha > 0\ f(\alpha x) = \alpha f(x) \tag{2.3}$$
- *A function f from a normed vector space X to $\overline{\mathbb{R}} = \mathbb{R} \cup \{-\infty, +\infty\}$ is said to be proper if $f(x) < +\infty$ for at least one $x \in X$ and $f(x) > -\infty$ for every $x \in X$.*
- *a function f from X, a Banach space, to $\mathbb{R} \cup \{+\infty\}$ is lower semicontinuous (l.s.c.) if for every sequence $(x_n)_{n\in\mathbb{N}}$ converging to x:*
$$\lim \inf_{n\to\infty} f(x_n) \geq f(x). \tag{2.4}$$
- *a function f from X, a linear space, to $\mathbb{R} \cup \{+\infty\}$ is convex if for every $t \in [0,1]$ and for every $(x,y) \in X^2$:*
$$f(tx + (1-t)y) \leq tf(x) + (1-t)f(y). \tag{2.5}$$
If the inequality is strict (for t not equal to 0 or 1 and $x \neq y$), then f is said strictly convex.

Proposition 2.2.3. *Let X be a normed space, K a non empty closed convex of X and $\phi : K \to \mathbb{R}$ a convex lower semicontinuous function. Then ϕ is bounded from below by an affine function: there exists $l \in X^*$ and $\alpha \in \mathbb{R}$ such that for every $v \in K$ $\phi(v) \geq l(v) + \alpha$.*

We state a minimization theorem, the proof of which can be found in [47] corollary III.20:

Theorem 2.2.4. *Let X be a reflexive Banach space, $K \subset X$ a closed convex set, not empty and $f : K \to \mathbb{R} \cup \{+\infty\}$ a convex, l.s.c. function not identically equal to $+\infty$ such that $\lim_{\substack{x\in K \\ \|x\|\to\infty}} f(x) = +\infty$. Then f reaches its minimum on K, i.e., there exists $x_0 \in K$ such that $f(x_0) = \min_K f$. If f is strictly convex then x_0 is unique.*

For more details on functional analysis we refer to [47]

2.2.2 Monotone operators

For this part we refer to [46], the introduction on non linear analysis chapter 8 in [182], [242] chapter 2 and [103] part III chapter 9. First we give some definitions, then state important theorems. We will denote X a separable reflexive Banach space and X^* its dual. Again the duality product will be written $\langle \cdot, \cdot \rangle$.

Definition 2.2.5. *Let A be a mapping $X \to X^*$.*

- *A is monotone if*
$$\forall (u,v) \in X^2,\ \langle A(u) - A(v), u - v \rangle \geq 0. \tag{2.6}$$
- *A is strictly monotone if for every $(u,v) \in X^2$ such that $u \neq v$, the inequality is strict:*
$$\langle A(u) - A(v), u - v \rangle > 0. \tag{2.7}$$
- *A is strongly monotone if there exists a constant $m > 0$ such that for every $(u,v) \in X^2$:*
$$\langle A(u) - A(v), u - v \rangle \geq m\|u - v\|^2 \tag{2.8}$$
- *A is Lipschitz continuous if there exists $M > 0$ such that for every $(u,v) \in X^2$:*
$$\|A(u) - A(v)\| \leq M \|u - v\| \tag{2.9}$$

Next we define ways to account for the continuity of the operator in weak senses:

Definition 2.2.6. *Let A be a mapping $X \to X^*$.*

- *A is hemicontinuous if for every $(u,v,w) \in X^3$, the function $t \to \langle A(u+tv), w\rangle$ is continuous. It means that A is directionnally weakly continuous.*
- *A is radially continuous if for every $(u,v) \in X^2$ the function $t \to \langle A(u+tv), v\rangle$ is continuous. It is the hemicontinuity with $w = v$.*

It is clear that hemicontinuity implies radial continuity.

Definition 2.2.7. *Let A be a mapping $X \to X^*$. A is coercive if:*

$$\lim_{\|u\|\to+\infty} \frac{\langle A(u), u\rangle}{\|u\|} = +\infty \tag{2.10}$$

Definition 2.2.8. *Let A be a mapping $X \to X^*$. A is bounded if it maps every bounded set in X into a bounded set in X^*.*

We are now able to state theorems which ensure the existence and sometimes uniqueness of solutions to equations including monotone operators.

Theorem 2.2.9. *Let A be a mapping $X \to X^*$. If A is bounded, radially continuous, monotone and coercive then*

- *A is surjective. It means that for every $f \in X^*$, there exists at least one $u \in X$ such that $A(u) = f$. And the set of solutions for this equation is a closed convex set.*
- *If we assume that A is in addition strictly monotone, then for every $f \in X^*$, there exists one and only one $u \in X$ such that $A(u) = f$.*

A more complete version of this theorem can be found in [242], theorem 2.14, chapter 2. In fact we do not need the boundedness property to have the surjectivity, as indicated by the theorem of Browder and Minty in [242] theorem 2.18, chapter 2:

Theorem 2.2.10. *Any monotone, radially continuous and coercive $A : X \to X^*$ is surjective.*

We will not give further details and address the reader to the references given earlier for a deeper insight of non linear analysis thanks to monotone and pseudomonotone operators. We also mention that these references also provide other techniques used for the study of non linear problems (calculus of variations and fixed point theorems in particular).

2.2.3 Capacity

We refer to [19] and [136] chapter 4.4 for results on the capacity or, for another approach, [137] chapter 3.3 which gives a brief of overview of H^1-capacity. First we recall some definitions and facts on bilinear forms:

Definition 2.2.11.

- *The bilinear form a is coercive on X if there exists $m > 0$ such that for every $v \in X$:*

$$a(v,v) \geq m \|v\|^2 \tag{2.11}$$

- *The bilinear form a is continuous if there exists M such that for every $(u,v) \in X^2$:*

$$|a(u,v)| \leq M \|u\| \|v\| \tag{2.12}$$

To every continuous bilinear form a we can associate a linear continuous operator $A : X \to X^*$ such that:

$$a(u,v) = \langle A(u), v\rangle. \tag{2.13}$$

Proposition 2.2.12. *The coercivity of a continuous bilinear form a is equivalent to the coercivity of the operator A in the sense of the definition 2.2.7.*

Proof. It is clear that (2.11) implies the definition 2.2.7. So we prove that the definition 2.2.7 implies (2.11). In fact the definition 2.2.7 implies that $\langle A(u), u\rangle = a(u,u) \to +\infty$ as $|u| \to +\infty$. This means that there exists $R > 0$ such that for every v such that $\|v\| \geq R$, $a(v,v) \geq 1$. Then for every $u \in X$:

$$a\left(\frac{R}{\|u\|}u, \frac{R}{\|u\|}u\right) \geq 1. \tag{2.14}$$

As a is a bilinear form:

$$\frac{R^2}{\|u\|^2} a(u,u) \geq 1.$$

and $a(u,u) \geq \dfrac{\|u\|^2}{R^2}$ which proves the implication. □

We choose to briefly give the definition of the capacity in H^1 with respect to the norm associated with a coercive and continuous bilinear form a, noted $\|\cdot\|_a$, as the capactity will only be used within this framework in the parts dealing with conical derivatives.

Definition 2.2.13.
- *For a compact $K \subset \mathbb{R}^d$ we define:*

$$\mathrm{cap}_a(K) = \inf\left\{\|v\|_a^2 \,|\, v \in C_0^\infty(\mathbb{R}^d),\ v \geq 1 \text{ on } K\right\} \tag{2.15}$$

- *For ω an open subset of $\mathbb{R}^d$ we define:*

$$\mathrm{cap}_a(\omega) = \sup\left\{\mathrm{cap}_a(K) \,|\, K \text{ compact, } K \subset \omega\right\} \tag{2.16}$$

- *For any subset E of $\mathbb{R}^d$ we define:*

$$\mathrm{cap}_a(E) = \inf\left\{\mathrm{cap}_a(\omega) \,|\, \omega \text{ open set, } E \subset \omega\right\} \tag{2.17}$$

Remark 2.2.14. *The 1-capacity corresponds to the bilinear symmetric form $a(u,v) = \displaystyle\int_\Omega \nabla u \cdot \nabla v \, dx$. We note it* cap.

Proposition 2.2.15. *For $E \subset \mathbb{R}^d$, the equality holds:*

$$\mathrm{cap}_a(E) = \inf\left\{\|v\|_a^2 \,|\, v \geq 1 \text{ a.e. on a neighborhood of } E\right\} \tag{2.18}$$

Remark 2.2.16. *A set of null capactity is of Lebesgue measure equal to zero. The inverse is not true and there exist compact sets of null measure but of strictly positive capactiy.*

Following [205], we finally define:

Definition 2.2.17.
- *A function $f : X \to \mathbb{R}$ is said quasi-continuous (respectively lower quasi-semicontinuous (l.q.s.c.)) if there exists a decreasing sequence of open sets ω_n such that $cap_a(\omega_n) \to 0$ and $f_{|X\setminus\omega_n}$ continuous (respectively lower quasi-semicontinuous). We said that f is upper quasi-semicontinuous (u.q.s.c.) if $-f$ is lower quasi-semicontinuous.*

- *A property is true quasi everywhere (noted q.e) if it is true everywhere except in a set of a-capacity equal to zero.*

- *A polar set is a set of null a-capacity.*

Definition 2.2.18. *Let $\phi : X \to [0, +\infty]$ l.q.s.c.. The zero set of ϕ is:*

$$Z(\phi) = \{x, x \in X, \phi(x) = 0\}. \tag{2.19}$$

If ϕ is a class of l.q.s.c. functions and if ϕ_1 and ϕ_2 are two l.q.s.c. elements of this class then $Z(\phi_1)$ and $Z(\phi_2)$ are equal up to a polar set. The class of these sets will be noted $E(\phi)$.

Next we give the theorem 3.3.29 of [137] which is a particular case of the statement which could be found in [205] at the beginning of part 3 valid for any Dirichlet space (V, a) (see [19] or [205] for a definition).

Proposition 2.2.19. *For every $f \in H^1(\mathbb{R}^d)$ there exists f_c in the class of f, quasi-continuous unique for the equivalence relation q.e..*

2.3 The projection operator

In this part we assume that X is a Hilbert seperable space and that K is a non empty closed convex set. The inner product of X is noted $(\cdot,\cdot)_X$ and the associated norm $\|\cdot\|$. First we prove the existence and uniqueness of the projection operator, theorem 2.3.1, and mention its Lipschitzian property. Then we give an overview on the different regularity results which exist on the projection operator. Theorem 2.3.5 is used, in chapter 4, for the Perzyna model 4.4 and theorem 2.3.6 gives the maximal regularity results which can be found about the projection. Passing to lower regularity results we speak about conical differentiability of the projection the main theorem being theorem 2.3.15. Before concluding this part on the projection by a short review of articles speaking about the regularity of the projection, we present a result valid in finite dimensional spaces finding some points on which the projection is differentiable and proving that the remaining points are of null Lebesgue measure.

2.3.1 Definition and characterization

We define the projection thanks to a minimization problem:

Theorem 2.3.1. *For every $f \in X$, there exists a unique $u \in K$ such that:*

$$\|f-u\| = \min_{v\in K} \|f-v\|. \tag{2.20}$$

Moreover u is characterized by the following two properties: $u \in K$ and

$$(f-u, v-u)_X \leq 0 \ \ \forall v \in K. \tag{2.21}$$

In the sequel we note $u = P_K(f)$ the projection of f on K.

Remark 2.3.2. *The given definition of the projection is not independent on the norm and if another inner product of X, making X a Hilbert space, can be found, the projection will be different.*

Proof. The existence is straightforward using theorem 2.2.4 as $v \to \|f-v\|$ is convex continuous and $\lim_{\|v\|\to\infty} \|f-v\| = \infty$. As X is reflexive, the minimum is reached. The uniqueness of this minimum is also ensured as minimizing $v \to \|f-v\|$ is the same as minimising $v \to \|f-v\|^2$ which is in addition strictly convex.
Now we prove the characterization. Let u be the solution of the minimization problem (2.20). For every $v \in K$:

$$\|f-u\| \leq \|f-v\| \tag{2.22}$$

then we pass to the square which implies that:

$$2\,(f, v-u)_X \leq (v,v)_X - (u,u)_X \tag{2.23}$$

Taking $v = (1-t)u + tw \in K$ for any $w \in K$ and $t \in]0,1[$ we get:

$$2t\,(f, w-u)_X \leq t^2\,(w,w)_X + t^2\,(u,u)_X - 2t\,(u,u)_X + 2t\,(u,w)_X - t^2\,(u,w)_X \tag{2.24}$$

Dividing by $2t$ and making t tend to 0 gives (2.21).
Let $u \in K$ be fulfilling the property (2.21). For every $v \in K$

$$\begin{aligned} &(f-u, f-u)_X + (f-u, v-f)_X \leq 0 \\ &\|f-u\|^2 \leq (f-u, f-v)_x \leq \|f-u\|\|f-v\| \\ &\|f-u\| \leq \|f-v\| \end{aligned} \tag{2.25}$$

which means that u is a minimizer of (2.20). □

Remark 2.3.3. *The proof shows that it is not necessary to be in a Hilbert space to define the projection which is not the case of the characterization* (2.21).

For the study of projections in Hilbert spaces we refer to [303] which provides a thorough study on the subject. We mention a last well-known property of projections:

Proposition 2.3.4. *The projection P_K is Lipschitz which means that for every $(f_1, f_2) \in X^2$ we have*

$$\|P_K(f_1) - P_K(f_2)\| \leq \|f_1 - f_2\| \tag{2.26}$$

2.3.2 Differentiability

The question of the regularity of the projection on a closed convex set is the subject of numerous articles. There are two preliminar results which can be proved. The first one says that if X is finite dimensional, then, thanks to the Rademacher theorem [104] section 3.1.2, it is almost everywhere Fréchet differentiable, since the projection is Lipschitz. The second one is a generalization for X of infinite dimension given in [205] theorem 1.2. Every Lipschitzian application from a separable Hilbert space into a Hilbert space is Gateaux differentiable at the point of a dense set. It is the case for the projection P_K.

The basic idea of the study is to relate the regularity of the convex set with the regularity of the projection.

C^1 regularity

We first give high regularity results due to Zarantonello, Holmes, Fitzpatrick and Phelps. The first regularity result is the Fréchet differentiability of the real function:

$$\|x - P_K(x)\|^2 . \tag{2.27}$$

Theorem 2.3.5. *The function* $x \to \frac{1}{2}\|x - P_K(x)\|^2$ *from* X *to* $\mathbb{R}$ *is Fréchet differentiable and its Fréchet derivative is:*

$$x - P_K(x). \tag{2.28}$$

The proof is given in [303] theorem 4.1 and the result is also mentionned in [149]. Then we state a theorem proved in [149] and [109]:

Theorem 2.3.6. *We note* $X[x] = \{y \in X \mid (x - P_K(x), y)_X = 0\}$ *for* $x \in X \setminus K$.

- *If* K *has a* C^k *boundary with* $k \geq 2$ *then* P_K *is* C^{k-1} *in* $X \setminus K$ *and its Fréchet derivative at a point* x *is invertible in X[x] for each* $x \in X \setminus K$.
- *Reciprocally, if* $\mathring{K}$ *is not empty and for* $k \geq 1$, P_k *is* C^k *in* $X \setminus K$ *with its Fréchet derivative at a point* x *invertible in X[x] for every* $x \in X \setminus K$, *then the boundary of* K *is* C^{k+1}

Remark 2.3.7. *On figure 2.1, the vector space* $X[x]$ *is drawn in blue.*

Conical derivative

We discuss now the existence of a directionnal derivative for the projection, assuming less regularity on the closed convex set K. We focus on the work of Zarantonello [303] and Mignot [205] for this part. First we define the conical derivative as in [205]:

Definition 2.3.8. *We say that a continuous function* f *from* V_1 *to* V_2 *(two Banach spaces) admits a conical derivative at* x *if there exists an operator* Q *positively homogeneous such that:*

$$\forall h \in V_1, \forall t > 0,\ f(x + th) = f(x) + tQ(h) + o(t) \tag{2.29}$$

Note that this definition coincides with the definition of weakly directionally differentiable function given in [256]. We define some cones and sets related to the convex set K.

Definition 2.3.9. *If* B *is a convex set and* a *a continuous coercive bilinear form, we define its polar cone (or the normal cone in* 0*) with respect to* a*:*

$$B_a^0 = \{w \in X \mid \forall u \in B,\ a(w, u) \leq 0\} \tag{2.30}$$

Now we define three sets of particular importance adopting the notations of [205]. To have an illustration of what theses sets represent we refer the reader to the figure 2.1 and to remark 2.3.11. We point out the huge difference between the two sets $S_y(K)$ and $S^y(K)$ the last one being included in the first one. Finally we mention that $[\mathbb{R}(v - P_K(v))]_a^0 = X[v]$, keeping then notation $[\cdot]_a^0$ to be able to make the remark 2.3.18.

Definition 2.3.10. *To a closed convex set* K *we associate:*

- *for* $y \in K$,
$$C_y(K) = \{w \in K \mid \exists t > 0,\ y + tw \in K\} \tag{2.31}$$
- *for* $y \in K$, *we define the tangent cone:*
$$S_y(K) = \overline{C_y(K)} = \{w \in H,\ \exists w_n \to w,\ \exists t_n > 0,\ y + t_n w_n \in K\} \tag{2.32}$$
- *for* $y \in K$ *and* $v \in y + [S_y(K)]_a^0$, *implying in particular that* $P_K(v) = y$,
$$S^y(K) = S_y(K) \cap [\mathbb{R}(v - y)]_a^0 \tag{2.33}$$
with the notation $[\cdot]_a^0$ *referring to the definition 2.3.9.*

Remark 2.3.11. *For a particular case, we explain the notations of definition 2.3.10 thanks to figure 2.1. Noting* $y = P_K(v_1)$, *the tangent cone* $S_y(K)$ *is a closed half-space of* X *with the tangent space of* K *at* y *being the boundary of the tangent cone. The space* $[\mathbb{R}(v - y)]_a^0$ *is in fact the set of every* $w \in X$ *such that* $a(w, v - y) = 0$ *which means that such a* w *is in the tangent space of* K *at* y *and that* $S^y(K)$ *reduces to the tangent space of* K *at the point* y.

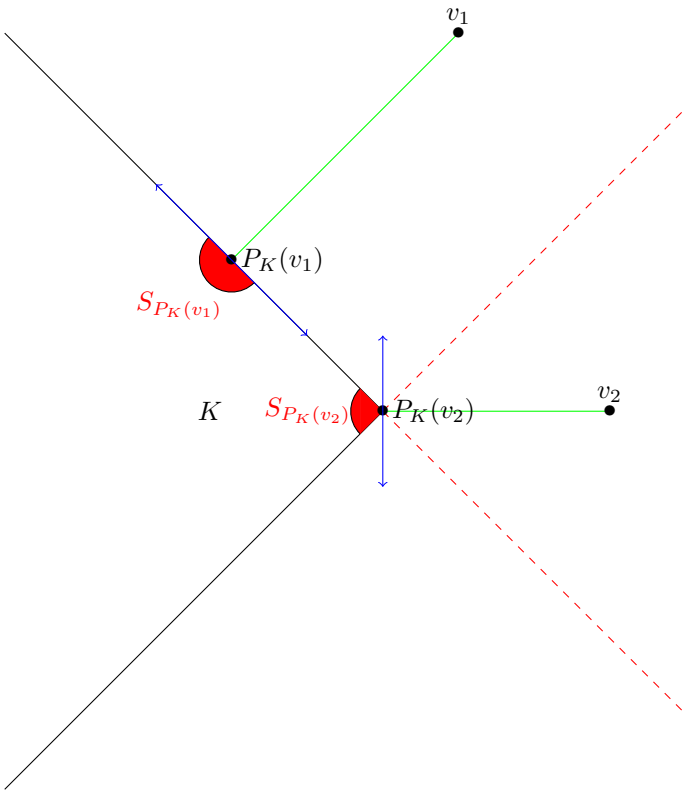

Figure 2.1: Sets involved in the conical derivative definition. In black the boundary of K, the dashed red lines delimit the normal cone at $P_K(v_2)$, the red areas represent the vectors of the cone $S_{P_K(v_i)}(K)$ and in blue the **vector** space $[\mathbb{R}(v_i - P_K(v_i))]_a^0 = X[v_i]$. The set $S^{P_K(v_i)}$ is the intersection between the blue part and the red part. Pay attention to the fact that the red areas represent vector and thus for instance $S^{P_K(v_1)}$ is a whole half-space.

We finish this list of definitions with the one of a polyhedric set

Definition 2.3.12. *A closed convex set K is polyhedric at $v \in X$ if:*

$$S^y(K) = \overline{C_y(K) \cap [\mathbb{R}(v-y)]_a^0} \tag{2.34}$$

where $y = P_K(v)$.

Remark 2.3.13. *The polyhedric sets in finite dimension reduce to the polyhedral ones [195] .*

We are now able to state a theorem of [303] (lemma 4.6) and generalized in [205] for non symmetric bilinear forms:

Theorem 2.3.14. *If $v \in K$, then the projection P_K is conically differentiable in v and its conical derivative is $P_{S^y(K)}$:*

$$\forall w \in X,\ P_K(v+tw) = v + tP_{S^y(K)}(w) + o(t). \tag{2.35}$$

Finally theorem 2.1 in [205] ensures the existence of conical derivative for point where K is polyhedric.

Theorem 2.3.15. *Let $v \in X$ and $y = P_K(v)$. If K is polyhedric at v then the projection is conically differentiable at v and its conical derivative is $P_{S^y(K)}$:*

$$\forall w \in X,\ P_K(v+tw) = v + tP_{S^y(K)}(w) + o(t). \tag{2.36}$$

Remark 2.3.16. *The figure 2.1 also illustrates (in finite dimension) how the conical derivative works. Let's take first the case of the point v_1. The theorem 2.3.15 says that, at first ordrer, if we move v_1 in a direction w, the projection of the point $v_1 + w$ will move on the boundary of K into $P_{S^{P_K(v_1)}(K)}(w)$, with $S^{P_K(v_1)}(K)$ being the intersection between the red half-space and the blue vector space, which is, in this particular case, the blue vector space. For the point v_2, the space $S^{P_K(v_2)}(K) = \{0\}$: moving v_2 a little does not change its projection. Finally on the particular example illustrated by the figure 2.1, the set $S^{P_K(v_3)}(K)$ will not be a vector space if we take a point v_3 on the dashed red line.*

Remark 2.3.17. *Note that the first theorem does not need any regularity assumptions on K. Note also that the second one is a kind of generalization of the first one (for polyhedric sets) which gives a formula valid for every element of X including the ones belonging to K. Indeed, in theorem 2.3.14, the space $S^y(K)$ is in fact equal to $S_y(K)$ when $v = y$.*

Remark 2.3.18. *In all the definitions and the theorems given in this part on conical derivatives of the projection we limited ourselves to the symmetric part. We mention that in [205] the bilinear form can be non symmetric and that the results are unchanged except for the space* $[\mathbb{R}(v-y)]_a^0$ *whic becomes* $[\mathbb{R}(v-y)]_{a^*}^0$ *with* a^* *being the conjugate of* a*:*

$$a^*(u,v) = a(v,u). \tag{2.37}$$

To define the projection the following characterization is used (see the next part on variational inequalities theorem 2.4.1 for existence and uniqueness of u*): for every* $v \in X$*, there exists a unique* $y \in K$ *such that*

$$\forall u \in K \; a(v-y, u-y) \leq 0, \tag{2.38}$$

which is not equivalent to minimizing the functionnal $a(v,v)$ *on* K*.*

A particular case: the finite dimension

As we said, in finite dimension, the Rademacher theorem gives the differentiability almost everywhere. It could be interesting to characterize the points of non differentiability in this case and this is done in [260]. Our goal is to give the two main theorems 2.3.21 and 2.3.21 and apply them to an example. Before giving the results, we need to introduce some notations:

Definition 2.3.19. *For a closed convex set* $K \subset X$ *a Hilbert space of finite dimension* n*, we define*

- *the normal cone to* K *at* y *is:*

$$N_K(y) = \{b \in X \mid (b, z-y)_X \leq 0, \; \forall z \in K\}. \tag{2.39}$$

- *the space* T_r *for* $0 \leq r \leq n$*:*

$$T_r = \{y \in K \mid \dim(N_K(y)) = r\} \tag{2.40}$$

  with $\dim(N_K(y)) = \dim(span(N_K(y)))$*.*

- *The space:*

$$V_r = \cup \{y + N_K(y) \mid y \in T_r\} \tag{2.41}$$

  and $W_r = \mathring{V}_r$*.*

Remark 2.3.20. *The set* T_r *has a geometric representation. Thus* T_0 *is the set of points which are in the interior of* K*,* T_1 *are regular points of the boundary,* T_r *for* $2 \leq r < n$ *are edges and* T_n *are vertices. For the understanding of* W_r *and* V_r *we refer to the example below and the figure 2.2.*

We make two technical assumptions, with ri denoting the relative interior:

Assumption A_r**:** The set T_r is (a possibly empty) $n-r$ dimensional manifold of class C^p with $p \geq 2$.

Assumption B_r**:** If $y \in T_r$ and $z \in \mathrm{ri}(\mathrm{N_K(y)})$, then there exists an $\epsilon > 0$ such that, for all $y' \in T_r$ sufficiently close to y, $\{z' \in N_{T_r}(y) \mid \| z' - z \| < \epsilon\} \subset N_K(y')$.

Now we can state the theorem 2.3.4 of [260]:

Theorem 2.3.21. *Let* r *be an integer such that* $0 \leq r \leq n$ *and assume that* A_r *holds. Then the map* P_K *is* C^{p-1} *on* W_r *and its derivative is invertible.*

The theorem 2.3.4 of [260] gives much more details and especially gives a formula for the derivative. Now we pass to the points where the differentiability is not guaranteed:

Theorem 2.3.22. *Assuming* A_r *and* B_r *for every* $0 \leq r \leq n$ *then* P *is of* C^{p-1} *on the open set* $\cup_{r=0}^n W_r$ *whose complement has null* d *dimensional Lebesgue measure.*

Assuming that A_r and B_r hold for every for every $0 \leq r \leq n$, the first theorem implies that the differentiability is not ensured for the points of $E = X \setminus \cup_{r=0}^n W_r$. The second one says that this set is of null measure, which implies, in particular, that $\cup_{r=0}^n W_r$ is dense.

Example We propose a small application analysing the projection on the convex set of $(\mathbb{R}^+)^n$ in $\mathbb{R}^n$ with respect to the inner product implied by a symmetric positive definite matrix A. The results are illustrated on figure 2.2 for $n = 2$ and $A = I$. As stated in [260], $(\mathbb{R}^+)^n$ fulfills the assumptions A_r and B_r for every $0 \leq r \leq n$. The first remark we made is that T_0 is the set of points in the interior of K, i.e. $(\mathbb{R}^+_*)^n$. Now we determine T_k for every $1 \leq k \leq n$:

Lemma 2.3.23. *Let be $1 \leq k \leq n$, T_k is the set of $y \in K$ such that there exists $(i_j)_{1\leq j\leq k} \in \{1 \dots n\}^k$ with $y_{i_j} = 0$ and its other components strictly positive.*

Proof. Let be $1 \leq k \leq n$. We prove that such a y is in T_k. Let $b \in N_K(y)$ it is equivalent to:

$$(Ab, y - z)_X \geq 0 \ \ \forall z \in K \Leftrightarrow \sum_i (Ab)_i(y_i - z_i) \geq 0 \ \ \forall z \in K$$

If we note e_i the canonical basis of $\mathbb{R}^n$, taking $z = \lambda e_j$ for $\lambda > 0$ and $1 \leq j \leq n$ gives that when $y_j = 0$ then $(Ab)_j \leq 0$ and when $y_j > 0$ then we can find $\lambda > 0$ such that $y_j - z_j$ is either negative either positive therefore $(Ab)_j = 0$. As A is invertible $\dim(N_K(y)) = k$ and the set T'_k, of points $y \in K$ such that there exists $(i_j)_{1\leq j\leq k} \in \{1 \dots n\}^k$ with $y_{i_j} = 0$ and its other components strictly positive, is a subset of T_k.
But the union of all the T_k gives K and it is clear that it is also the case of T'_k so $T_k = T'_k$. □

Then we determine the spaces V_k as the union of subsets which we note V_k^l, with $1 < l \leq \binom{n}{k}$ where we choose to number with the variable l the possible choices for $(i_j)_{1\leq j\leq k} \in \{1 \dots n\}^k$. So, for a fixed $(i_j)_{1\leq j\leq k}$:

$$V_k^l = \left\{ y + b \,|\, y_{i_j} = 0,\ y_{i\neq i_j} > 0,\ (Ab)_{i\neq i_j} = 0,\ (Ab)_{i_j} \leq 0 \right\} \tag{2.42}$$

and V_k is the disjoint union:

$$V_k = \cup_l V_k^l. \tag{2.43}$$

The next step is to find the interior of V_k, W_k. In the same way we define:

$$W_k^l = \left\{ y + b \,|\, y_{i_j} = 0,\ y_{i\neq i_j} > 0,\ (Ab)_{i\neq i_j} = 0,\ (Ab)_{i_j} < 0 \right\} \tag{2.44}$$

which is open and it is clear that:

$$\cup_l W_k^l \subset V_k.$$

So $\cup_l W_k^l \subset W_k$ (for the case $A = I$ the equality holds, see figure 2.2) and the points of non differentiability are in the set $\mathbb{R}^n \setminus \cup_l W_k^l$.

For more details

In [220], the author manages, in particular, to find an equivalence between the conical differentiability (or as it is named in the article, directional Gateaux differentiability) and the Mosco-regularity of the support function of the convex. In [258] the existence and differentiability of metric projections in Hilbert spaces are studied for sets which are not necessarily convex. We also mention the article [195] which studies the particular example of the cones of nonnegative functions in $L^p(0,1)$ and $W^{1,p}(0,1)$ and the article [93] for the differentiability of the projection on moving convex sets at boundary points.

In [177], [257] and [3], counter examples of the directional differentiability of any projection in a finite dimensional Hilbert space is given. In finite dimensional space the differentiability of the projection is often seen as a particular case of the sensitivity analysis of non linear programs:

$$\min_{v\in\Phi(h)} f(v, h), \tag{2.45}$$

where we want to differentiate $u(h)$ the solution of the minimization problem 2.45 with respect to h, Φ describes the admissible set (for the projection it is the set on which the projection is made) and f a cost function (see (2.20) for the projection). So the results given are often more general than the results in infinite dimension as moving sets are generally considered (Φ depends on h). We mention [193], [259], [254], [255], [107], [194] and [154].

2.4 Variational inequalities

The great majority of the mechanical problems studied into this thesis can be written under the form of variational inequalities. We consequently present some results on the subject giving some references if more details are needed. We only treat three particular types of variational inequalities independent of the time and that will be used in the sequel. Variational inequalities of the first kind are used for frictionless contact 3.2 and Hencky plasticity see chapter 4. Variational inequalities of the second kind are used for the Tresca model (3.3.1) and the quasi-variational inequalities for the Norton-Hoff model and the Normal compliance model 3.3.3 and 3.3.4.

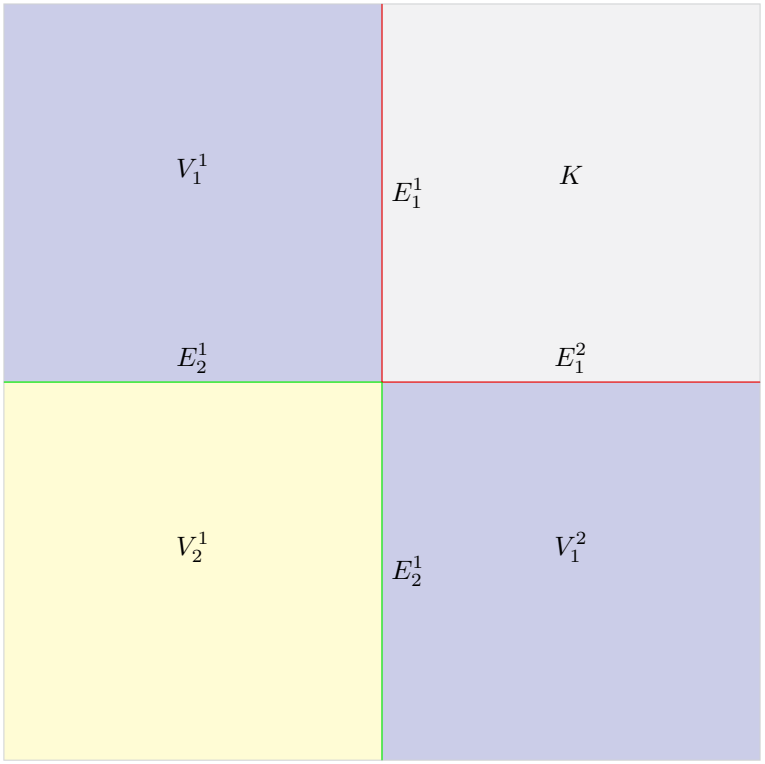

Figure 2.2: Illustration of the theorems 2.3.21 and 2.3.22 in the case of the projection on $(\mathbb{R}^+)^2$ with respect to the canonical inner product. We note $E_k^l = V_k^l \setminus W_k^l$. It is clear that the projection, in this case, is not Fréchet differentiable only on the red and green lines.

2.4.1 Variational inequality of the first kind

Variational inequalities of the first kind are the simplest variational inequalities to be thought of. Yet they enable to model many problems and their mathematical study can be cumbersome. One of the most famous references on the subject is the monograph of Kinderlehrer and Stampacchia [169].

To introduce the form of the variational inequalities we have to take some notations. Let X be a Hilbert space, $a(\cdot,\cdot)$ a bilinear form on X, $f \in X^*$ and K a non empty closed convex set in X. Then the problem is: find $u \in K$ such that

$$\forall v \in K \;\; a(u, v-u) \geq \langle f, v-u \rangle. \tag{2.46}$$

We state an existence and uniqueness theorem due to Kinderlehrer and Stampacchia [169]. The proof presented here can be found in [47] for the existence part:

Theorem 2.4.1. *Let a be a continuous coercive bilinear form. There exists a unique solution u to the problem (2.46). Moreover if a is symmetric, u is also the solution of the minimization problem: $u \in K$ and*

$$u = \underset{v \in K}{\operatorname{argmin}} \left(\frac{1}{2} a(v,v) - \langle f, v \rangle \right) \tag{2.47}$$

Proof. The idea is to use the Banach fixed point theorem and the results proved on the projection operator. First we apply the Riesz-Fréchet theorem to say that there exists $F \in X$ such that: for every $v \in X$,

$$\langle f, v \rangle = (F, v)_X .$$

We also consider the operator A associated with the bilinear for a with respect to the inner product $(\cdot,\cdot)_X$.
Then we can rewrite the inequation (2.46), using the scalar product of X: find $u \in K$ such that

$$\forall v \in K \;\; (A(u), v-u)_X \geq (F, v-u)_X . \tag{2.48}$$

We take $\rho > 0$ and change (2.48) by multiplying it by ρ and adding $u - u$ in the right handside:

$$(\rho F - \rho A(u) + u - u, v - u) \leq 0$$

which exactly means that $u = P_K(\rho F - A(u) + u)$. So we introduce the operator S:

$$S(v) = P_K(\rho F - A(v) + v). \tag{2.49}$$

The next step is to show that there exists a ρ which makes S contracting. Then the Banach fixed point theorem will ensure the existence of a unique u for this specific ρ. As the projection is a Lipschitzian operator (proposition 2.3.4) we have:

$$\|S(v) - S(w)\| \leq \|v - w - \rho\,(A(v) - A(w))\|$$

Computing the square of $\|S(v) - S(w)\|$ it implies:

$$\|S(v) - S(w)\|^2 \leq \|v - w\|^2 - 2\rho\,(A(v) - A(w), v - w)_X + \rho^2\,\|A(v) - A(w)\|^2$$

Then using the coercivity of A for the substracted term and the continuity of A for the last term it implies that:

$$\|S(v) - S(w)\|^2 \leq \|v - w\|^2\left(1 - 2\rho m + \rho^2 M^2\right)$$

Then taking $0 < \rho < \dfrac{2m}{M}$ implies $1 - 2\rho m + \rho^2 M^2 < 1$ and S is contracting. So the existence of u is ensured. The uniqueness is easily proved by taking two solutions u_1 and u_2 corresponding to two f_1 and f_2. Writing the variational inequations with respectively $v = u_2$ and $v = u_1$ produces:

$$a(u_1 - u_2, u_2 - u_1) \geq \langle f_1 - f_2, u_2 - u_1\rangle. \tag{2.50}$$

Then using the continuity of $f_1 - f_2$ and the coercivity of a it follows that:

$$\|u_1 - u_2\| \leq C\|f_1 - f_2\|_{X^*} \tag{2.51}$$

with $C > 0$, which implies the uniqueness.
Now we pass to the case of a being symmetric. Then as a is coercive it defines an inner product on X. Moreover, thanks to the coercivity and the continuity of a, the norm induced by a is equivalent to the one of X. It follows that X is a Hilbert space also for this norm and, thanks to the Riesz-Fréchet theorem, we can find $G \in X$ such that: for every $v \in X$,

$$\langle f, v\rangle = a(G, v). \tag{2.52}$$

and the inequation becomes: find $u \in K$ such that

$$\forall v \in K \;\; a\,(G - u, v - u) \leq 0 \tag{2.53}$$

which is equivalent to find a point $u \in K$ which minimizes:

$$\sqrt{a(G - v, G - v)} \tag{2.54}$$

on K or the square of this quantity:

$$a(v, v) - 2a(G, v) + a(G, G)$$

which is finally equivalent to minimize $\dfrac{1}{2}a(v, v) - \langle f, v\rangle$. □

Remark 2.4.2. *In [205], the author calls the solution of such variational inequalities a-projection even when a is not symmetric. Indeed when a is symmetric it is the projection with respect to another norm and if a is not symmetric the inequation can be written in the same way as the characterization of the projection.*

This result can be generalized to some monotone operators, see [182] theorem 8.1, chapter 5 in [242], chapter 3 of [169], in particular theorem 1.4:

Theorem 2.4.3. *Let $A : K \to X^*$ be a monotone, continuous on finite dimensional subspaces operator. There exists $u \in K$ such that for every $v \in K$,*

$$\langle A(u), v - u\rangle \geq 0. \tag{2.55}$$

If A is strictly monotone then u is unique.

Remark 2.4.4. *A proof similar to the one given for the theorem 2.4.1 can be done if stronger assumptions are made (strongly monotone Lipschitz continuous operator), see [264] theorem* 2.1. *In the same monograph, results on the convergence of a penalized version of the problem is given in* 2.1.2.

An example: the obstacle problem

One of the most famous problems which can be written as a variational inequation of the first kind is the obstacle problem. Let $\Omega \subset \mathbb{R}^d$ be open, smooth, bounded and connected. we consider the bilinear form on $H_0^1(\Omega)$:

$$a(u,v) = \int_\Omega \nabla u : \nabla v \, dx \tag{2.56}$$

and $f \in H^{-1}(\Omega)$. Then let $\psi \in H^1(\Omega)$ be such that $\psi \leq 0$ on $\partial\Omega$ and define the closed convex set:

$$K = \left\{ v \in H_0^1(\Omega) \,|\, v \geq \psi \text{ a.e. } \Omega \right\}. \tag{2.57}$$

The inequation models a membrane in unilateral contact with an obstacle described by ψ. The variable u is the normal displacement of the membrane. The existence of a unique solution comes directly from the theorem 2.4.1. There are numerous questions which can be asked on this problem. For a detailed review we refer to [240], [231] and [234] chapter 2. The first one is the regularity of the solution depending on the regularity of the obstacle and the regularity of Ω. The optimal regularity which can be proved is $C^{1,1}$, theorem 2.3.5 [234] with a counter example of better regularity for smooth Ω and obstacle, theorem 1.1 in [208]. For additional details we refer to [169], [240], [49], [113], [279].

There is a set of particular importance called the coincidence set:

$$E = \Omega \setminus \{ x \in \Omega \,|\, (u-\psi)(x) > 0 \}. \tag{2.58}$$

This set is clearly undetermined a priori and is an unknown of the problem. It is the part of Ω which will be in contact with the obstacle. The part ∂E is called the free boundary part and this problem belongs to the family of free boundary problems. One interesting result is the theorem 6.9 chapter 2 in [169]. Thanks to the Riesz-Schwarz theorem we can define a non negative measure μ such that for every $\xi \in H_0^1(\Omega)$:

$$a(u,\xi) - \langle f, \xi \rangle = \int_\Omega \xi \, d\mu \tag{2.59}$$

and $\text{supp}(\mu) \subset E$. Yet μ is the reaction force on the contact zone and this property only says that the force is possibly not zero only when the obstacle and the membrane are in contact. The theorem 6.11 compares the capacity and the measure:

Theorem 2.4.5. *For $f \in H^{-1}(\Omega)$ and $\psi \in H^1(\Omega)$ such that $\psi \leq 0$ on $\partial\Omega$, there exists $C > 0$ such that: for every compact $B \subset \Omega$,*

$$\mu(B) \leq C\sqrt{\text{cap}_1(B)}. \tag{2.60}$$

This implies amongst others that the coincidence set is defined up to a set of null 1-capacity and that if $\text{cap}_1(E) = 0$, then $-\Delta u = f$ in Ω in the sense of the distributions. We mention section 2.4 in [234] for a review of results on topological properties of E.

Another subject of study on the obstacle problem is the geometry of the free boundary. This last point is the subject of the Schaffer's conjecture [247]:

"We conjecture that generically the weak solution of the (d-dimensional)-obstacle problem that one obtains variationally is a strong solution, by which we mean that the free boundary ∂E is C^∞-smooth $(d-1)$-manifold."

On this problem we mention the work of Caffarelli [55] [56], Caffarelli and Rivière [57] [58], the articles [168] [186] [209] [207] and its generalization in [234] section 2.6, the results in [169] and [240] and the review [208].

2.4.2 Variational inequality of the second kind

We take the same notations and framework as for variational inequality of the first kind and introduce a function $j : K \to \mathbb{R} \cup \{+\infty\}$ convex, non identically equal to $+\infty$ and l.s.c.. The problem we consider in this part is: find $u \in X$ such that for every $v \in X$,

$$a(u, v-u) + j(v) - j(u) \geq \langle f, v-u \rangle. \tag{2.61}$$

We note that for $j = 0$ we find the variational inequality of the first kind.

We will prove that there exists a unique solution to this variational inequality by applying the same method as for the variational inequality of the first kind. The main ingredient was the use of the projection and the Banach fixed point theorem. We replace the use of the projection by the use of the proximal operator (see [264]).

Proposition 2.4.6. *For every $f \in X^*$ there exists a unique element $u \in K$ such that: for every $v \in K$*

$$(u, v-u)_X + j(v) - j(u) \geq \langle f, v-u \rangle \tag{2.62}$$

and we note $u = Prox_j(f)$. The proximal operator is non-expansive.

Proof. We note $F \in X$ the function given by the Riesz-Fréchet theorem such that $(F, v) = \langle f, v \rangle$ for every $v \in X$. We prove that u is the unique solution of the following minimization problem:

$$\min_{v \in K} J(v) = \frac{1}{2}(v, v)_X + j(v) - (F, v)_X. \tag{2.63}$$

We apply the proposition 2.2.3 to j, so there exists $\alpha \in \mathbb{R}$, $l \in X^*$ and consequently $g \in X$ such that:

$$j(v) \geq (g, v)_X + \alpha. \tag{2.64}$$

It is clear that J is strictly convex and l.s.c.. The affine boundedness of j implies that $\lim\limits_{\substack{\|v\| \to \infty \\ v \in K}} J(v) = +\infty$. So we can apply the theorem 2.2.4 and the existence and the uniqueness is proved.

Now it remains to prove that the two problems are equivalent. Suppose that u solves (2.63). For every $t \in]0, 1]$ and for every $v \in K$:

$$J(u + t(v-u)) \geq J(u). \tag{2.65}$$

It follows that:

$$\frac{t^2}{2}(v-u, v-u)_X + t(u, v-u)_X + j(u + t(v-u)) - j(u) \geq t(F, v-u)_X.$$

Using the convexity of j, $j(u + t(v-u)) \leq (1-t)j(u) + tj(v)$:

$$\frac{t^2}{2}(v-u, v-u)_X + t(u, v-u)_X + tj(v) - tj(u) \geq t(F, v-u)_X.$$

Dividing by t and making t go to 0 gives (2.62).
Now taking u as (2.62), we compute for $v \in K$:

$$J(v) - J(u) = \frac{1}{2}(v-u, v-u)_X + (u, v-u)_X + j(v) - j(u) - (F, v-u)_X \geq 0$$

and u is the solution of the problem (2.63).
To prove the non-expansivity of the proximal operator we take $(f_1, f_2) \in X^2$ and their associate function in X, F_1 and F_2. We denote u_1 and u_2 the associated solutions and in their variational inequation respectively take $v = u_2$ and $v = u_1$. Adding the inequations it follows that:

$$(u_1 - u_2, u_2 - u_1)_X \geq (f_1 - f_2, u_2 - u_1)_X$$

and it suffices to apply the Cauchy-Schwarz inequality to get:

$$\|u_2 - u_1\| \leq \|f_2 - f_1\|. \tag{2.66}$$

□

Now we can prove the existence and uniqueness of a solution to (2.61). For more properties on such problem we mention chapter 3.1 in [60].

Theorem 2.4.7. *Let a be a continuous coercive bilinear form. There exists a unique solution u to the problem* (2.61)*. Moreover if a is symmetric, u is also the solution of the minimization problem: $u \in K$ and*

$$u = \underset{v \in K}{\operatorname{argmin}} \left(\frac{1}{2} a(v, v) + j(v) - \langle f, v \rangle \right) \tag{2.67}$$

Proof. We introduce the operator associated with a, A. Then we define for $v \in K$:

$$S(v) = Prox_{\rho j}(\rho f - \rho A(v) + v) \tag{2.68}$$

Note that if u is solution to (2.61) then $S(u) = u$. Indeed as u is the solution of (2.61) then:

$$\rho(A(u), v-u) + \rho j(v) - \rho j(u) \geq \langle \rho f, v-u \rangle. \tag{2.69}$$

Adding $\langle u, v-u\rangle$ on both sides we get:

$$(u, v-u) + \rho j(v) - \rho j(u) \geq \langle \rho f - \rho A(u) + u, v-u\rangle. \tag{2.70}$$

which is the caracterization of the proximal operator found in theorem 2.4.6: $S(u) = u$.
We use the non-expansivity property of the proximal operator:

$$\|S(u) - S(v)\| \leq \|u - v - \rho\left(A(u) - A(v)\right)\|.$$

Then the same calculations as in the proof of theorem 2.4.1 can be done:

$$\|S(v) - S(w)\|^2 \leq \|v-w\|^2 \left(1 - 2\rho m + \rho^2 M^2\right)$$

and we can choose ρ such that S is non-expansive. We apply the Banach fixed point theorem and prove the existence of u. The uniqueness of u is proved in the same way as in theorem 2.4.1. Take two solutions u_1 and u_2 corresponding to f_1 and f_2. Take $v = u_1$ in the variational inequality of u_2 and $v = u_2$ in the other one. Add both and it follows:

$$\|u_1 - u_2\| \leq C\|f_1 - f_2\|_{X^*} \tag{2.71}$$

with $C > 0$, which implies the uniqueness. Finally the equivalence with the minimization problem can be proved exactly as in the proof of the propositon 2.4.6 on the proximal operator. □

Remark 2.4.8. *Again the proof can be done for A being a non linear strongly monotone Lipschitz continuous operator, see [264] theorem* 2.8 *and for more general theorems see chapter* 5.1, 5.2, 5.3 *in [242]. In both monographs results on the convergence of regularized versions of the problem can be found.*

Remark 2.4.9. *Note that the proof is correct when $K = X$, theorem* 3.1 *in [263] is a corollary of theorem 2.4.7.*

2.4.3 Quasi-variational inequality

Quasi-variational inequalities are generalization of variational inequalities of the second kind in which the function j depends on the solution. The new problem is to find $u \in K$ such that for every $v \in K$,

$$a(u, v-u) + j(u, v) - j(u, u) \geq \langle f, v-u\rangle. \tag{2.72}$$

The results of this part are taken from the monographs of Sofonea and Matei [263] and [264]. So we state the problem in a more general manner, as in this book: find $u \in K$ such that for every $v \in K$,

$$\left(A(u), v-u\right)_X + j(u, v) - j(u, u) \geq \langle f, v-u\rangle. \tag{2.73}$$

There are two kinds of results on this problem. Existence and uniqueness results under some assumptions thanks to the Banach fixed point theorem or only existence results thanks to Schauder fixed point theorem [264] or Kakutani fixed point theorem (see [242] chapter 5.4).

Theorem 2.4.10. *Assume that A is a strongly monotone Lipschitz continuous operator, that for every $\eta \in K$, $j(\eta, \cdot) : K \to \mathbb{R}$ is convex and l.s.c., that there exists $\alpha > 0$ such that for every $(\eta_1, \eta_2, v_1, v_2) \in K^4$,*

$$j(\eta_1, v_2) - j(\eta_1, v_1) + j(\eta_2, v_1) - j(\eta_2, v_2) \leq \alpha \left\|\eta_1 - \eta_2\right\| \left\|v_1 - v_2\right\| \tag{2.74}$$

and $\alpha < m$ with m the constant of strong monotonicity of A, then for each $f \in X$ there exists a unique solution to (2.73)

Proof. The proof relies on the Banach fixed point theorem and the results proved for variational inequalities of the second kind. We introduce for a given $\eta \in K$ the following problem: find u_η such that,

$$\left(A\left(u_\eta\right), v - u_\eta\right)_X + j(\eta, v) - j(\eta, u_\eta) \geq \langle f, v - u_\eta\rangle. \tag{2.75}$$

There exists a unique solution to this problem, thanks to the theorem 2.4.7 and the remark 2.4.8. This enables to define an operator:

$$T(\eta) = u_\eta. \tag{2.76}$$

We then prove that under the assumption $\alpha < m$, S is non expansive. We take η_1 and η_2 two elements of K and write the variational inequalities associated with (2.75) taking particular v:

$$\begin{aligned} \left(A\left(u_{\eta_1}\right), u_{\eta_2} - u_{\eta_1}\right)_X + j(\eta_1, u_{\eta_2}) - j(\eta_1, u_{\eta_1}) &\geq \langle f, u_{\eta_2} - u_{\eta_1}\rangle \\ \left(A\left(u_{\eta_2}\right), u_{\eta_1} - u_{\eta_2}\right)_X + j(\eta_2, u_{\eta_1}) - j(\eta_2, u_{\eta_2}) &\geq \langle f, u_{\eta_1} - u_{\eta_2}\rangle \end{aligned} \tag{2.77}$$

Adding the inequalities yields:

$$\left(A\left(u_{\eta_1}\right) - A\left(u_{\eta_2}\right), u_{\eta_2} - u_{\eta_1}\right)_X \geq j(\eta_1, u_{\eta_1}) + j(\eta_2, u_{\eta_2}) - j(\eta_1, u_{\eta_2}) - j(\eta_2, u_{\eta_1}).$$

Using the strong monotonicity of A with the assumption (2.74) it follows:

$$\|u_{\eta_2} - u_{\eta_1}\| \leq \frac{\alpha}{m} \|\eta_1 - \eta_2\| . \tag{2.78}$$

As $\frac{\alpha}{m} < 1$, T is non expansive and we can apply the Banach fixed point theorem. As there is an equivalence between being a fixed point of T and being a solution of the quasi-variational inequality (2.73), the existence and uniqueness of a solution is proved. □

Finally we state the existence theorem 2.22 of [264] without giving its proof which is a bit long.

Theorem 2.4.11. *Assume that A is a strongly monotone Lipschitz continuous operator, $0 \in K$, that for every $\eta \in K$, $j(\eta, \cdot) : K \to \mathbb{R}$ is convex, for every $(v, \eta) \in K^2$, $j(\eta, v) \geq 0$ and $j(\eta, 0) = 0$, that for all sequences $(\eta_n)_{n\in\mathbb{N}}$ and $(u_n)_{n\in\mathbb{N}}$ of elements of K such that they weakly converge in X to η and u and for every $v \in K$ the inequality holds:*

$$\limsup_{n\to\infty} (j(\eta_n, v) - j(\eta_n, u_n)) \leq j(\eta, v) - j(\eta, u), \tag{2.79}$$

then, for every $f \in X$, there exists at least one solution to the quasi-variational inequality (2.73)

For more details and other theorems there exists a huge litterature on quasi-variational inequation. For general references we refer to [24], [156], [212] and [216]. There exist a lot of articles which treat the subject for particular problems, as this type of inequalities arise in many domains such as mechanics [176] and finance [73].

2.4.4 Sensitivity analysis: an example

In this part we analyse the problem (5.1) considered in [5] chapter 5, but with an obstacle $\psi = 0$. The problem corresponds to a membrane on which a force is applied and h models its thickness. We first introduce the problem, prove an existence and uniqueness theorem and then do a sensitivity analysis thanks to the results of [205]. The method is inspired by the one in [269]. For sensitivity analysis and control of variational inequalities we mention [26], [125], [185], [33], [34], [35], [150], [151], [221], [290], [114], [39]...

The Problem

Let $\Omega \subset \mathbb{R}^d$ be bounded and smooth. We introduce the set of admissible thickness:

$$U_{ad} = \{k \in L^\infty,\ \forall x \in \Omega,\ h_{min} \leq k(x) \leq h_{max}\} . \tag{2.80}$$

For every $h \in U_{ad}$, we study the following variational inequation: find $u \in H^+(\Omega) = \left\{v \in H_0^1(\Omega),\ v \geq 0\right\}$:

$$\int_\Omega h\nabla u(h) \cdot \nabla(v - u(h))\, dx \geq \int_\Omega f(v - u(h))\, dx\ \forall v \in H^+(\Omega) \tag{2.81}$$

Theorem 2.4.12. *Problem* (2.81) *is equivalent to the following problem in the sense of distribution:*

$$\begin{cases} -\mathrm{div}(h\nabla u) \geq f & \text{in } \Omega \\ u \geq 0 & \text{in } \Omega \\ (\mathrm{div}(h\nabla u) + f)u = 0 & \text{in } \Omega \\ u = 0 & \text{on } \partial\Omega \end{cases} \tag{2.82}$$

with $f \in L^2(\Omega)$.

Proof. First we prove that (2.82) $\implies$ (2.81). In the sense of distributions $-\mathrm{div}(h\nabla u) \geq f$ in Ω means that:

$$\forall v \in C_c^\infty(\Omega),\ v \geq 0,\ -\int_\Omega \mathrm{div}(h\nabla u)v\, dx \geq \int_\Omega fv\, dx$$

We then use the third line in (2.82) to say that:

$$-\mathrm{div}(h\nabla u)u = -fu$$

and adding the inequality and the equality we get:

$$\forall v \in C_0^\infty(\Omega),\ -\int_\Omega \mathrm{div}(h\nabla u)(v - u)\, dx \geq \int_\Omega f(v - u)\, dx \tag{2.83}$$

By integration by parts we obtain (2.81) with $v \in C_c^\infty(\Omega)$ such that $v \geq 0$. By density of $C_0^\infty(\Omega)$ in $H_0^1(\Omega)$, it implies (2.81) with $v \in H^+(\Omega)$.
Finally we prove that (2.81) $\implies$ (2.82).

Taking $v = u + w$, with $w \in C_c^\infty(\Omega),\ w \geq 0$ in (2.81) gives:

$$\int_\Omega h\nabla u(h) \cdot \nabla w \, dx \geq \int_\Omega f w \, dx$$

which implies in the sense of distributions the first line of (2.82):

$$-\mathrm{div}(h\nabla u) \geq f \text{ in } D'(\Omega) \tag{2.84}$$

Take $v = 0$ in (2.81) to find :

$$\int_\Omega h|\nabla u|^2 \, dx \leq \int_\Omega f u \, dx$$

take $v = 2u$ in (2.81) to obtain the opposite inequality, which implies :

$$\int_\Omega h|\nabla u|^2 \, dx = \int_\Omega f u \, dx$$

An integration by part gives :

$$\int_\Omega (\mathrm{div}(h\nabla u) + f) u \, dx = 0$$

As $u \geq 0$ and $(\mathrm{div}(h\nabla u) + f) \leq 0$ the term under the integral doesn't change its sign and is 0 almost everywhere (third line of (2.82)). □

Theorem 2.4.13. *The problem* (2.81) *admits one and only one solution for $f \in L^2(\Omega)$ (or for $f \in H^{-1}(\Omega)$).*

Proof. We use theorem 2.4.1. First we have $H^+(\Omega) \subset H_0^1(\Omega)$ which is a non empty closed convex cone and $H_0^1(\Omega)$ is an Hilbert space with the norm $\|\nabla u\|_{L^2(\Omega)}$. Let us set :

$$a(u, v) = \int_\Omega h\nabla u \cdot \nabla(v) \, dx \ \forall (u, v) \in (H_0^1(\Omega))^2, \tag{2.85}$$

$$l(v) = \int_\Omega f v \, dx.$$

The bilinear form a is such that :

$$|a(u, u)| \geq h_{min} \|\nabla u\|^2_{L^2(\Omega)} \tag{2.86}$$

which ensures the coercivity, and its continuity is a consequence of the Cauchy-Schwarz inequality. The linear form l is continuous, thanks to the Cauchy-Schwarz inequality and the Poincaré inequality. Using the theorem 2.1 of [169], we get the existence of a unique solution to (2.81). □

Sensitivity with respect to the design variable

We want to differentiate u with respect to the design variable $h \in U_{ad}$, defined in (2.80).

Theorem 2.4.14. *The function u is conically-differentiable at every $h \in U_{ad}$ and its conical derivative at h, $U_h \in S^{u(h)}$, is defined for every $k \in L^\infty(\Omega)$ such that $h + tk \in U_{ad}$ for $t > 0$ small enough, as the solution of the following problem:*

$$\int_\Omega h\nabla U_h(k) \cdot \nabla(v - U_h(k)) \, dx \geq -\int_\Omega k\nabla u(h) \cdot \nabla(v - U_h(k)) \, dx \ \forall v \in S^{u(h)} \tag{2.87}$$

with

$$S^{u(h)} = \left\{ \phi \in H_0^1(\Omega), \phi \geq 0 \ q.e \text{ on } \{u(h) = 0\} \text{ and } \int_\Omega h\nabla u(h) \cdot \nabla\phi \, dx = \int_\Omega f\phi \, dx \right\} \tag{2.88}$$

Remark 2.4.15. *We point out that the condition $\int_\Omega h\nabla u(h) \cdot \nabla\phi \, dx = \int_\Omega f\phi \, dx$ in the set* (2.88) *means that the vector ϕ has to be normal to the vector $w - u(h)$ for the inner product implied by the bilinear form a defined in* (2.85).

Proof. We take $k \in L^\infty(\Omega)$ such that $h + tk \in U_{ad}$ for $t > 0$ small enough. We then have $u(h + tk)$ solution of

$$\int_\Omega (h + tk)\nabla u(h + tk) \cdot \nabla(v - u(h + tk)) \, dx \geq \int_\Omega f(v - u(h + tk)) \, dx \ \forall v \in H^+(\Omega) \tag{2.89}$$

which can be rewritten:

$$\begin{aligned} \int_\Omega h\nabla u(h + tk) \cdot \nabla(v - u(h + tk)) \, dx \quad \geq \quad & \int_\Omega f(v - u(h + tk)) \, dx \\ & - \int_\Omega tk\nabla u(h) \cdot \nabla(v - u(h + tk)) \, dx \\ & - \int_\Omega tk\nabla(u(h + tk) - u(h)) \cdot \nabla(v - u(h + tk)) \, dx \\ & \forall v \in H^+(\Omega) \end{aligned} \tag{2.90}$$

Let $z(k) \in H_0^1(\Omega)$ be the solution of:

$$\int_\Omega h\nabla z(k)\cdot\nabla\phi\,dx = \int_\Omega k\nabla u(h)\cdot\nabla\phi\,dx\ \forall\phi\in H_0^1(\Omega) \tag{2.91}$$

So we can rewrite (2.90):

$$\begin{array}{rcl}\displaystyle\int_\Omega h\nabla u(h+tk)\cdot\nabla(v-u(h+tk))\,dx & \geq & \displaystyle\int_\Omega f(v-u(h+tk))\,dx \\ & & \displaystyle -\int_\Omega th\nabla z(k)\cdot\nabla(v-u(h+tk))\,dx \\ & & \displaystyle -\int_\Omega tk\nabla(u(h+tk)-u(h))\cdot\nabla(v-u(h+tk))\,dx \\ & & \forall v\in H^+(\Omega)\end{array} \tag{2.92}$$

Let us note $P^h_{H^+}$ the projection operator on $H^+(\Omega)$ with respect to the scalar product $a(u,v)=\displaystyle\int_\Omega h\nabla u\cdot\nabla v\,dx$. We also note $w\in H_0^1(\Omega)$ such that

$$\int_\Omega h\nabla w\cdot\nabla\phi\,dx = \int_\Omega f\phi\,dx\ \forall\phi\in H_0^1(\Omega) \tag{2.93}$$

With (2.92) and the lemma 2.4.16, we see that in fact, thanks to theorem 2.3.15:

$$\begin{array}{rcl} u(h+k) & = & P^h_{H^+}(w-tz(k)+o(t)) \\ & = & P^h_{H^+}(w-tz(k))+o(t) \\ & = & P^h_{H^+}(w)+tP^h_{S^{u(h)}}(-z(k))+o(t) \\ & = & u(h)+tP^h_{S^{u(h)}}(-z(k))+o(t)\end{array} \tag{2.94}$$

where we use the conical derivative of $P^h_{H^+}$, $P^h_{S^{u(h)}}$, to pass from the second line to the third line, with $S^{u(h)}$ defined in (2.88) and $P^h_{S^{u(h)}}$ the operator defined as the projection on $S^{u(h)}$ with respect to the bilinear form $a(u,v)=\displaystyle\int_\Omega h\nabla u\cdot\nabla v\,dx$ with $(u,v)\in H_0^1(\Omega)$. In other words, for $f\in L^2(\Omega)$, $P^h_{S^{u(h)}}(f)\in S^{u(h)}$ is the solution of the variational inequation:

$$a(u-f,v-u)\geq 0\ \ \forall v\in S^{u(h)}. \tag{2.95}$$

The form of $S^{u(h)}$ is found, thanks to lemma 3.2 and given in theorem 3.3 in [205]. The fact that the projection is conically differentiable is due to the polyhedric property of $H^+(\Omega)$ proved in theorem 3.2 in [205].
Thanks to (2.94) the existence of a conical shape derivative $U_h(k)$ at h of u is ensured. We have $U_h(k)=P^h_{S^{u(h)}}(-z(k))$ (which ensures the existence and uniqueness of $U_h(k)$ as $S^{u(h)}$ is a non empty closed convex set) and we get the variational inequality (2.87) solved by $U_h(k)$ thanks to the characterization of the projection (2.95). The theorem 2.4.14 is proved. □

Lemma 2.4.16. *The linear form defined on $H_0^1(\Omega)$, by:*

$$\langle L,\phi\rangle = \int_\Omega tk\nabla(u(h+tk)-u(h))\cdot\nabla\phi\,dx \tag{2.96}$$

is a $o(t)$ meaning that $\dfrac{\|L\|_{H^{-1}}}{t}\to 0$.

Proof. We have:

$$\left|\int_\Omega tk\nabla(u(h+tk)-u(h))\cdot\nabla\phi\right| \leq t\,\|k\|_{L^\infty}\,\|u(h+tk)-u(h)\|_{H_0^1}\,\|\phi\|_{H_0^1} \tag{2.97}$$

with (2.97), (2.99) and (2.102):

$$\frac{\left|\int_\Omega k\nabla(u(h+tk)-u(h))\cdot\nabla\phi\right|}{\|\phi\|_{H_0^1}} \leq Ct^2\frac{\|f\|_{L^2}}{h_{min}^2}\,\|k\|_{L^\infty}^2$$

We can then take the sup on ϕ in this inequality and we have:

$$\|L\|_{H^{-1}} \leq Ct^2\frac{\|f\|_{L^2}}{h_{min}^2}\,\|k\|_{L^\infty}^2 \tag{2.98}$$

so we conclude that

$$\frac{\|L\|_{H^{-1}}}{t}\to 0$$

when $t\to 0$, which proves the lemma 2.4.16. □

Lemma 2.4.17. *The following inequality holds for $k \in L^\infty$ such that $h + tk \in U_{ad}$, for $t > 0$ small enough:*

$$\|u(h+tk) - u(h)\|_{H_0^1} \leq t \frac{\|k\|_{L^\infty}}{h_{min}} \|u(h+tk)\|_{H_0^1} \tag{2.99}$$

Proof. We take (2.81) with $v = u(h+tk)$:

$$\int_\Omega h\nabla u(h) \cdot \nabla(u(h+tk) - u(h))\, dx \geq \int_\Omega f(u(h+tk) - u(h))\, dx \tag{2.100}$$

and (2.89) with $v = u(h)$:

$$\int_\Omega (h+tk)\nabla u(h+tk)\nabla(u(h) - u(h+tk))\, dx \geq \int_\Omega f(u(h) - u(h+tk))\, dx \tag{2.101}$$

By adding these two inequalities we get:

$$\int_\Omega h\nabla u(h) \cdot \nabla(u(h+tk) - u(h))\, dx + \int_\Omega (h+tk)\nabla u(h+tk) \cdot \nabla(u(h) - u(h+tk))\, dx \geq 0$$

or

$$\int_\Omega h\nabla(u(h+tk) - u(h)) \cdot \nabla(u(h+tk) - u(h))\, dx \leq \int_\Omega k\nabla u(h+tk) \cdot \nabla(u(h) - u(h+tk))\, dx$$

By using that $h_{min} \leq h \leq h_{max}$:

$$h_{min} \|u(h+k) - u(h)\|_{H_0^1}^2 \leq \int_\Omega k\nabla(u(h+tk) - u(h)) \cdot \nabla(u(h+tk) - u(h))\, dx$$

and also:

$$\int_\Omega k\nabla u(h+tk) \cdot \nabla(u(h) - u(h+tk))\, dx \leq t \|k\|_{L^\infty} \|u(h+tk)\|_{H_0^1} \|u(h+tk) - u(h)\|_{H_0^1}$$

which gives (2.99). □

Lemma 2.4.18. *We have the following inequality for $k \in L^\infty$ such that $h + tk \in U_{ad}$, for $t > 0$ small enough: there exists $C > 0$ such that,*

$$\|u(h+k)\|_{H_0^1} \leq C \frac{\|f\|_{L^2}}{h_{min}} \tag{2.102}$$

Proof. We take (2.89) with $v = 0$ and we obtain:

$$\int_\Omega (h+k)|\nabla u(h+k)|^2\, dx \leq \int_\Omega f u(h+k)\, dx$$

and it follows that:

$$h_{min} \|u(h+k)\|_{H_0^1}^2 \leq C \|f\|_{L^2} \|u(h+k)\|_{H_0^1}$$

and then we get (2.102). □

We keep in mind that we want to perform shape optimization and the fact that the state constraint is a variational inequality prevents us from applying the same methods as the one presented in chapter 1, 1.3.3 to compute the derivative of criterions and find adjoint functions. As a matter of fact, the first method 1.3.3 was relying on the implicit function theorem, which needs an equality of the form $F(h, u) = 0$ with F a sufficiently regular function, and somehow, on the derivation of the variational equality. There is no chance that we manage to complete these two parts since we only work on a variational inequality. The second method was the method of Céa 1.3.3. But the fact that the solution is not Fréchet or Gateaux differentiable forbids its use and a natural question could be: is it easy to characterize the points where the conical derivative of u with respect to the shape is linear? In finite dimension as previously said the theorems 2.3.21 and 2.3.22 of [260] answer the question for a large number of problems (see also [193]). We turn to infinite dimension and make a small survey on the different solutions proposed.

Study of the linearity of the derivative

Definition 2.4.19. *Let us call A the operator defined from $H_0^1(\Omega)$ to $H^{-1}(\Omega)$ by:*

$$\forall (u, v) \in H_0^1(\Omega),\ \langle Au, v\rangle = a(u, v) = \int_\Omega h\nabla u \cdot \nabla v\, dx. \tag{2.103}$$

The problem we want to solve is the same, except for the convex $H^+(\Omega)$ which is now more general:

$$K = \left\{ v \in H_0^1(\Omega),\, v \geq \psi \right\}$$

with ψ a function on which regularity assumptions will be made. We note E_h the coincidence set already defined in (2.58). The results given before were proved for $\psi = 0$. It is easy to adapt the proofs for $\psi \in H^1(\Omega)$ such that $\psi \leq 0$ on $\partial\Omega$ (for the convex to be non empty). Then the conical derivative exists and the space $S^{u(h)}$ rewrites:

$$S^{u(h)} = \left\{ \phi \in H_0^1(\Omega), \phi \geq 0 \text{ q.e on } E_h \text{ and } \int_\Omega h \nabla u(h) \cdot \nabla \phi \, dx = \int_\Omega f \phi \, dx \right\} \tag{2.104}$$

where E_h is now equal to $E_h = \{u(h) = \psi\}$.

Proposition 2.4.20. *If $cap(E_h) = 0$, then U_h is linear with respect to the direction.*

Proof. We take the result of theorem 2.4.14 with the expression (2.104) and note that U_h is the projection on the convex set $S^{u(h)}$ which is now, with the assumptions made, a linear subspace:

$$S^{u(h)} = \left\{ \phi \in H_0^1(\Omega), \int_\Omega h \nabla u(h) \cdot \nabla \phi \, dx = \int_\Omega f \phi \, dx \right\} \tag{2.105}$$

which gives that U_h is now the unique solution of: find $U_h \in S^{u(h)}$ such that,

$$\int_\Omega h \nabla U_h(k) \cdot \nabla v \, dx = -\int_\Omega k \nabla u(h) \cdot \nabla v \, dx \;\forall v \in S^{u(h)} \tag{2.106}$$

and so is linear with respect to k. □

We give a regularity result proved in [48], corollary II.3:

Theorem 2.4.21. *For $p \in]1; +\infty[$, $f \in H^{-1}(\Omega) \cap L^p(\Omega)$ and $\psi \in H^1(\Omega) \cap H^{2,p}(\Omega)$ then $u \in H^{2,p}(\Omega)$. If $p > N$ then $u \in C^{1,\alpha}(\overline{\Omega})$ with $\alpha = 1 - \dfrac{N}{p}$.*

As pointed in [145], the measure μ defined in (2.59) can be represented as $\lambda \in L^p(\Omega)$ such that:

$$\int_\Omega \phi \, d\mu = \int_\Omega \lambda \phi \, dx. \tag{2.107}$$

An important fact is that λ has no better general regularity,whatever the smoothness of f and ψ.

Coming back to our goal, we write the definition of strict complementarity in the sense of [40] and the proposition which follows (Corollary 6.60):

Definition 2.4.22. *$u(h)$ is said to satisfy the strict complementarity condition if;*

$$S^{u(h)} = \left\{ \phi \in H_0^1(\Omega),\, \phi = 0 \text{ q.e. on } E_h \right\}$$

Proposition 2.4.23. *With the assumptions that $f \in L^2(\Omega)$ and $\psi \in H^2(\Omega)$ and strict complementarity, the conical derivative is linear.*

The question could be now to find some sufficient conditions of the strict complementarity property. In finite dimension, the non differentiability comes from the fact that $u = \psi$ at some points with a contact force which is equalled to zero. The contact force is here the function λ in (2.107). We will see that the situation is not as simple in infinite dimension. So first we give some results of [269] chapter 4.3, taking $f \in C^1(\overline{\Omega})$, $\psi \in C^2(\overline{\Omega})$:

Theorem 2.4.24. *If $\Sigma_h = \partial E_h$ is a C^1 manifold, if $f < 0$ in a neighbourhood of Ω, then $u(h)$ is the solution of*

$$\begin{cases} Au(h) = f & \text{in } \Omega \setminus E_h \\ u(h) = 0 & \text{on } \partial\Omega \\ u(h) = \psi & \text{on } \Sigma_h \\ \dfrac{\partial u(h)}{\partial n} = \dfrac{\partial \psi}{\partial n} & \text{on } \Sigma_h \\ u(h) = \psi & \text{on } E_h \end{cases} \tag{2.108}$$

and the set $S^{u(h)}$ is now equal to :

$$S^{u(h)} = \left\{ \phi \in H_0^1(\Omega), \phi \geq 0 \text{ q.e. on } E_h,\, \phi = 0 \text{ a.e. on } E_h \cap \{A\psi - f > 0\} \right\} \tag{2.109}$$

Proof. The first statement in [269] is that E_h is closed (thanks to the regularity of $u(h)$) and $mes(E_h) > 0$ due to the assumptions made. This, with the assumption that Σ_h is a C^1 manifold enables to conclude that $u(h)$ solves (2.108). It remains to compute (2.109). We know that $\lambda \in L^2(\Omega)$ is non negative and its support is in E_h. Furthermore $A\psi = Au_h$ a.e. in E_h as ψ and u_h are at least in $H^2(\Omega)$. But, since $u_h \in H^2(\Omega)$, $Au_h \in L^2(\Omega)$ only.
Let be $\phi \in S^{u(h)}$ then:

$$\langle \lambda, \phi \rangle = \int_\Omega \lambda\phi \, dx = \int_{E_h} \lambda\phi \, dx = \int_{E_h} (Au(h) - f)\phi \, dx = \int_{E_h} (A\psi - f)\phi \, dx = 0 \tag{2.110}$$

and due to the regularity of ψ and f we have $(A\psi - f)$ which is at least continuous. As $\phi \geq 0$ q.e. on E_h and as $A\psi - f \geq 0$ a.e. since λ is non negative (μ was a non negative measure), the last equality in (2.110) gives $\phi = 0$ almost everywhere on $\{A\psi - f > 0\}$ which implies (2.109). □

Remark 2.4.25. *In [269] the space $S^{u(h)}$ found is not the same:*

$$\begin{aligned} S^{u(h)} = \big\{ &\phi \in H_0^1(\Omega), \phi(x) \geq 0 \text{ for } x \text{ such that } u(h)(x) = \psi(x) \text{ and } A\psi(x) - f(x) = 0, \\ &\phi(x) = 0 \text{ for } x \text{ such that } u(h)(x) = \psi(x) \text{ and } A\psi(x) - f(x) > 0 \big\}. \end{aligned} \tag{2.111}$$

In (2.109) *we would obtain* (2.111) *if we managed to get $\phi = 0$ q.e. on $\{A\psi - f > 0\}$, which is not the case as the measure μ is less fine than the capacity.*

The formula (2.111) leads in [269] to the following sufficient condition:

Proposition 2.4.26. *One sufficient condition for U_h to be linear is then $f - A\psi < 0$ a.e. in Ω.*

As $\lambda = -f + A\psi$, the sufficient condition given by Sokolowski could be reduced to $f - A\psi < 0$ in E_h. In our case, starting from (2.109), this condition only gives:

$$S^{u(h)} = \big\{ \phi \in H_0^1(\Omega), \phi \geq 0 \text{ q.e. on } E_h, \, \phi = 0 \text{ a.e. on } E_h \big\} \tag{2.112}$$

which is clearly not sufficient.

The same problem arises in chapter 2.8 of [234]. In 2.8.2 in [234], the author gives the expression of the critical cone (which we have called $S^{u(h)}$):

$$Cr_K(u(h) = \big\{ \phi \in H_0^1(\Omega), \text{ such that } \phi \geq 0 \text{ q.e on } E_h, \, \phi = 0 \text{ q.e on } \mathrm{supp}(\lambda) \big\} \tag{2.113}$$

The expression which can be found in [205] theorem 3.3, in [40] 6.4.4 or in [125] Corollary 7 do not mention the condition:

$$\phi = 0 \text{ q.e on } \mathrm{supp}(\lambda)$$

but the condition $\langle \lambda, \phi \rangle = 0$. Again, to our knowledge, the two conditions are not equivalent since we effectively have that the measure λ of a set E is bounded by $\sqrt{\mathrm{cap}(E)}$ (theorem 2.4.5) but we did not found results on the reverse inequality. In other words, λ a.e. does not seem equivalent to q.e.. This leads to a definition of the strict complementarity in [234] (namely that $\mathrm{supp}(\lambda) = E_h$) which differs from the definition 6.59 in [40]. In [234] it is stated without any proof, that:

Proposition 2.4.27. *Let be $f \in L^2(\Omega)$ and $\psi \in H^2(\Omega)$ then $supp(\lambda) = E_h$ up to a set of null measure is equivalent to the linearity of the conical derivative U_h.*

By the next proof we want to show the difficulties which occur:

Proof. Theorem 2.4.21 implies that $u(h)$ is in $H^2(\Omega)$. As:

$$Au(h) = f + \lambda$$

$\lambda \in L^2(\Omega)$. So for every $\phi \in H_0^1(\Omega)$,

$$\langle \lambda, \phi \rangle = \int_\Omega \lambda\phi \, dx$$

with $\lambda \geq 0$.

We first investigate the implication left to right that $supp(\lambda) = E_h$ up to a set of null measure implies the linearity of the conical derivative U_h. We have:

$$S^{u(h)} = \big\{ \phi \in H_0^1(\Omega), \phi \geq 0 \text{ q.e in } \{u(h) = 0\} \text{ and } \langle \lambda, \phi \rangle = 0 \big\}$$

Let be $\phi \in S^{u(h)}$, then $\displaystyle\int_\Omega \lambda\phi \, dx = 0$. As $\lambda \geq 0$ almost everywhere the set $\{\phi > 0\}$ is such that:

$$\mathrm{meas}(\{\phi > 0\} \cap \mathrm{supp}(\lambda)) = 0$$

But $\text{supp}(\lambda) = E_h = \{u = \psi\}$ up to a set of null measure, so $\phi = 0$ a.e in E_h and $\phi \geq 0$ q.e in E_h. So $\text{cap}(\{\phi > 0\} \cap E_h)$ can be non zero but the set $\{\phi > 0\} \cap E_h$ is of null measure.

$$\phi \in \left\{\phi \in H_0^1(\Omega), \phi = 0 \text{ a.e in } \{u(h) = 0\}\right\}$$

so

$$S^{u(h)} \subset \left\{\phi \in H_0^1(\Omega), \phi = 0 \text{ a.e in } \{u(h) = 0\}\right\}$$

and it remains to be proved the doubtful equality:

$$\left\{\phi \in H_0^1(\Omega), \phi = 0 \text{ a.e in } \{u(h) = 0\}\right\} = \left\{\phi \in H_0^1(\Omega), \phi = 0 \text{ q.e in } \{u(h) = 0\}\right\}.$$

Now we investigate the implication from right to left. Suppose the conical derivative is linear. Then $S^{u(h)}$ should be a linear space ([205]). So:

$$S^{u(h)} = \left\{\phi \in H_0^1(\Omega), \phi = 0 \text{ q.e in } \{u(h) = \psi\}\right\}$$

which means that $\phi \geq 0$ q.e. in E_h and $\langle \lambda, \phi \rangle = 0$ are equivalent to $\phi = 0$ q.e in E_h. Let suppose that there exists an open subset $\mathcal{O}$ of $E_h \setminus \text{supp}(\lambda)$ whose measure is positive, taking a function in $D(\mathcal{O})$ which takes the value one in a ball of $\mathcal{O}$ and is nonnegative contradicts the equivalence. So $E_h \setminus \text{supp}(\lambda)$ is either of null measure either closed without interior. □

Part II

Direct problems: Contact and Plasticity

Chapter 3

Contact Mechanics

Contents

3.1 Introduction

We call contact the touching of two bodies in motion. In mechanics, contact situations occur in almost every mechanical system (just think of someone walking, driving a car or skating on ice) and are responsible for the transmission of loads in the structure. Consequently the study of contact is of great interest for the understanding of the mechanical behavior of such systems, affecting for instance the strain, the repartition of stress or the displacement.

Modelling the contact is not an easy task. The first issue which was investigated by Leonardo Da Vinci, Guillaume Amontons or Charles de Coulomb is the one of the friction. Each of them tried to characterize the friction force applied on an object sliding on an undeformable body, the last two stating eponymous laws. Since then, various friction laws were stated, adapted for different situations: Coulomb law, Stokes law, Norton-Hoff law...

The second difficulty is that, before the loads are applied, the contact surface is not known. In 1933 Signorini wrote the contact problem in linearized elasticity for small strains which he called "a problem with ambiguous boundary conditions". The existence and uniqueness of the solution to this problem was given by one of his students Gaetano Fichera in [108] and is now known as the Signorini problem, which models a sliding contact (without friction). The equations governing the mechanical system take the form of a variational inequation which highlights its non linearity and the resulting computational difficulties. Adding friction to Signorini problem potentially leads to mathematically ill-posed problems.

In the following we give a brief review of the contact problems in the framework of linearized elasticity and small strain. For more details on computational issues, extensions to large deformation, or mathematical analysis we refer to the books [100], [163], [263], [264] and [297]. The starting point of this presentation is the linearized elasticity system given in 1.3.3 and we place ourselves in the following framework: Ω denotes an open bounded smooth subset of $\mathbb{R}^d$ where $d = 2$ or 3 and represents the shape of the structure we want to optimise. Its boundary is divided into five disjoint parts meaning that:

$$\partial\Omega = \Gamma_0 \cup \Gamma_N \cup \Gamma_c \cup \Gamma \cup S. \tag{3.1}$$

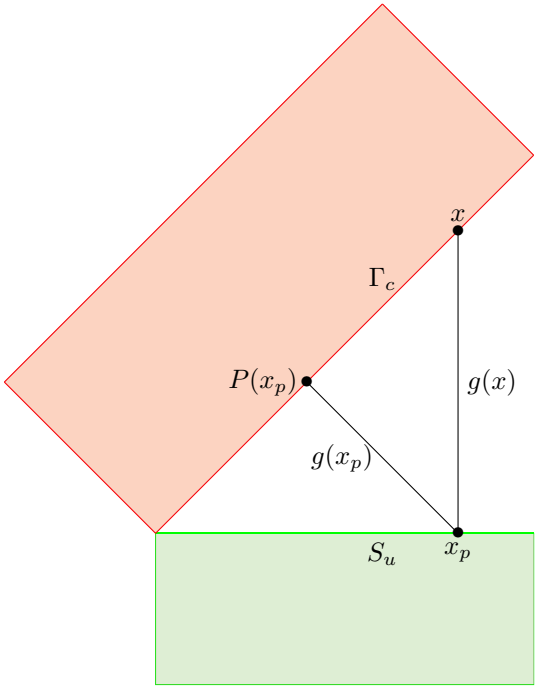

Figure 3.1: The contact zone Γ_c (without assuming small deformation).

The structure Ω is full of a linear isotropic elastic material with a Hooke's law defined by A for any τ symmetric matrix as:

$$A\tau = 2\mu\tau + \lambda Tr(\tau) I_d \tag{3.2}$$

where μ and λ are the Lamé moduli. On Γ_0, the structure is clamped and on Γ_N a force is applied. The free part of the boundary is Γ and the parts where contact conditions are enforced are S and Γ_c. The part Γ_c represents a contact with an undeformable body, whereas S is an auto-contact part (as for instance a crack could be). So S lies in the interior of $\overline{\Omega}$ and we suppose S to be smooth (at least Lipschitz [173]). The displacement field u is then solution of the system of linearized elasticity which we recall:

$$\begin{cases} -\operatorname{div}(Ae(u)) &= f & \text{in } \Omega \\ u &= 0 & \text{on } \Gamma_0 \\ Ae(u)n &= g & \text{on } \Gamma_N \\ Ae(u)n &= 0 & \text{on } \Gamma, \end{cases} \tag{3.3}$$

plus some boundary conditions on Γ_c and S which depend on which type of contact is used. To specify these boundary conditions we introduce first some notations. We note the jump through S of v, noting S_- and S_+ the two sides of S:

$$[v] = v_{|S_-} - v_{|S_+} \tag{3.4}$$

and n_- is the normal to S_- pointing toward S_+.

First we present the sliding contact problem and then the friction formulations which will be used in the thesis. For each of them a mathematical analysis is given. Finally we explain how to compute their solutions with regard to their use in a shape optimization process.

3.2 Sliding contact

3.2.1 Mechanical formulation

Sliding contact assumes there is no friction, which means that $(Ae(u)n)_t = 0$ on Γ_c and $(Ae(u)n)_t = 0$ on S_- and S_+. For the normal conditions we focus on Γ_c, the conditions on S can be derived in the same way. Before the loads are applied, there is an initial gap g between the part Γ_c and the undeformable surface S_u. As we assume small strains and displacements, the gap g has to be small. So if we take a point x on Γ_c and we note x_p its orthogonal projection on S_u, we make the approximation that the projection of x_p, $P(x_p)$ on Γ_c is x again (figure 3.1 displays the general case where the gap is not small so $P(x_p)$ is different from x). Furthermore, if we note n_u the normal to S_u pointing toward Ω, this leads to the fact that $n_u(x_p) = -n(x)$. In the following, the initial gap g is taken equal to 0.

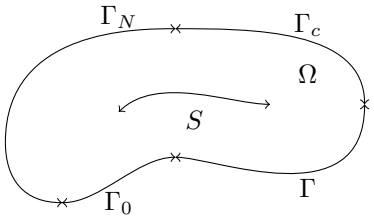

Figure 3.2: The open set Ω.

We would like to say that Γ_c cannot penetrate into S_u. Yet the distance between x and x_p is the smallest distance from x to S_u, what we have called $d(x, S_u)$ in 1.3.1. This means that if we want to prevent interpenetration, we just have to enforce:

$$u \cdot n \leq 0. \tag{3.5}$$

Another important point is that the normal force on the contact surface is always in the sense opposite to the outward normal as it is a reaction force:

$$Ae(u)n \cdot n \leq 0 \tag{3.6}$$

The last normal condition is that, either there is no contact and the force is null, or there is contact and $u \cdot n = 0$. This is summarized by a complementarity condition:

$$(u \cdot n)(Ae(u)n \cdot n) = 0. \tag{3.7}$$

For the normal part on S the conditions are similar adding jumps:

$$\begin{cases} [u] \cdot n_- \leq 0 \\ Ae(u_{|S_-})n_- \cdot n_- = Ae(u_{|S_+})n_- \cdot n_- \leq 0 \\ ([u] \cdot n_-)(Ae(u_{|S_-})n_- \cdot n_-) = 0. \end{cases} \tag{3.8}$$

Coupling these boundary conditions with (3.3), the sliding contact problem can be written as:

$$\begin{cases} -\operatorname{div}(Ae(u)) = f & \text{in } \Omega \\ u = 0 & \text{on } \Gamma_0 \\ Ae(u)n = g & \text{on } \Gamma_N \\ Ae(u)n = 0 & \text{on } \Gamma \\ u \cdot n \leq 0,\ Ae(u)n \cdot n \leq 0,\ (u \cdot n)(Ae(u)n \cdot n) = 0 & \text{on } \Gamma_c \\ [u] \cdot n_- \leq 0,\ Ae(u_{|S_-})n_- \cdot n_- = Ae(u_{|S_+})n_- \cdot n_- \leq 0,\ ([u] \cdot n_-)(Ae(u_{|S_-})n_- \cdot n_-) = 0 & \text{on } S \\ (Ae(u)n)_t = 0 & \text{on } \Gamma_c \cup S \end{cases} \tag{3.9}$$

3.2.2 Variational formulation

Let us set:

$$H^1_{\Gamma_0}(\Omega)^d = \left\{ v \in (H^1(\Omega))^d,\ v = 0 \text{ on } \Gamma_0 \right\} \tag{3.10}$$

$$K(\Omega) = \left\{ v \in H^1_{\Gamma_0}(\Omega)^d,\, v \cdot n \leq 0 \text{ on } \Gamma_c,\, [v] \cdot n_- \leq 0 \text{ on } S \right\} \tag{3.11}$$

Theorem 3.2.1. *Assuming $f \in L^2(\Omega)^d$ and $g \in L^2(\Gamma_N)^d$, the problem* (3.9) *is equivalent to the following variational inequality with $u \in K(\Omega)$:*

$$\int_\Omega Ae(u) : e(v-u)\, dx \geq \int_\Omega f \cdot (v-u)\, dx + \int_{\Gamma_N} g \cdot (v-u)\, ds \ \forall v \in K(\Omega) \tag{3.12}$$

Proof. We make the proof for $S = \varnothing$, for the sake of simplicity. If $S \neq \varnothing$ the same proof can be made, mimicking what was done on Γ_c paying attention to the fact that S is divided into S_+ and S_-. First we prove that : (3.9) $\Longrightarrow$ (3.12).

The first line of (3.9) gives:

$$\forall v \in K(\Omega),\ -\int_\Omega \operatorname{div}(Ae(u)) \cdot (v-u)\, dx = \int_\Omega f \cdot (v-u)\, dx$$

Integration by part implies:

$$\forall v \in K(\Omega),\ \int_\Omega (Ae(u)) : e(v-u)\,dx - \int_{\partial\Omega} (Ae(u))n \cdot (v-u)\,ds = \int_\Omega f \cdot (v-u)\,dx$$

Using the boundary conditions on Γ_0 and Γ_N, it happens that:

$$\forall v \in K(\Omega),\ \int_\Omega (Ae(u)) : e(v-u)\,dx - \int_{\Gamma_c} (Ae(u))n \cdot (v-u)\,ds = \int_\Omega f \cdot (v-u)\,dx + \int_{\Gamma_N} g \cdot (v-u)$$

It suffices now to remark that:

$$Ae(u)n \cdot (v-u) = (Ae(u)n \cdot n)\,(v-u) \cdot n = (Ae(u)n \cdot n)\,v \cdot n \geq 0$$

to find (3.12)

Then we prove(3.12) $\implies$ (3.9).

We take $v = u + w$ with $w \in C_0^\infty(\Omega)$ and we get:

$$\int_\Omega (Ae(u)) : e(w)\,dx \geq \int_\Omega f \cdot w\,dx$$

But w is in a vector space, so the inequality gives an equality. In the sense of distributions we obtain the first line of (3.9):

$$-\mathrm{div}(Ae(u)) = f \tag{3.13}$$

Take $v \in K(\Omega)$ such that $v = 0$ on $\partial\Omega \setminus \Gamma_N$. Using (3.13) and after integrating by part:

$$\int_\Omega (Ae(u)) : e(v)\,dx = \int_\Omega f \cdot v\,dx + \int_{\Gamma_N} Ae(u)n \cdot v\,ds$$

we also notice that (3.12) gives an equality for such a v (v stays in a vector space) and we obtain:

$$\forall v \in K(\Omega),\ v|_{\partial\Omega\setminus\Gamma_N} = 0,\ \int_{\Gamma_N} Ae(u)n \cdot v\,ds = \int_{\Gamma_N} g \cdot v\,ds$$

The densitiy of $C_0^\infty(\Gamma_N)^d$ into $L^2(\Gamma_N)^d$ gives the following equality in $L^2(\Gamma_N)^d$ and then almost everywhere on Γ_N:

$$Ae(u)n = g \text{ on } \Gamma_N. \tag{3.14}$$

The boundary conditions on Γ can be retrieved in the same way.

We now focus on the boundary conditions put on Γ_c. We take $v \in K(\Omega)$ such that $v = 0$ on $\partial\Omega \setminus \Gamma_c$. Using (3.13) and after integrating by part:

$$\int_\Omega (Ae(u)) : e(v)\,dx = \int_\Omega f \cdot v\,dx + \int_{\Gamma_c} Ae(u)n \cdot v\,ds$$

we also notice that (3.12) gives:

$$\forall v \in K(\Omega),\ v|_{\partial\Omega\setminus\Gamma_c} = 0\ \int_\Omega Ae(u) : e(v)\,dx \geq \int_\Omega f \cdot v\,dx$$

and we obtain :

$$\forall v \in K(\Omega),\ v|_{\partial\Omega\setminus\Gamma_c} = 0\ \int_{\Gamma_c} Ae(u)n \cdot v\,ds \geq 0 \tag{3.15}$$

We take $v \in K(\Omega)$ such that $v|_{\partial\Omega\setminus\Gamma_c} = 0$ and such that $v \cdot n = 0$ on Γ_c. Then (3.15) reduces to:

$$\forall v \in K(\Omega),\ v|_{\partial\Omega\setminus\Gamma_c} = 0,\ (v \cdot n)|_{\Gamma_c} = 0,\ \int_{\Gamma_c} (Ae(u)n)_t \cdot v_t\,ds = 0$$

since v belongs to a vector space. So:

$$(Ae(u)n)_t = 0 \text{ on } \Gamma_c \tag{3.16}$$

For the normal condition, take $v \in K(\Omega)$ such that $v|_{\partial\Omega\setminus\Gamma_c} = 0$ and such that $v_t = 0$ on Γ_c. Here v does not belong to a vector space but we still have:

$$\forall v \in K(\Omega),\ v|_{\partial\Omega\setminus\Gamma_c} = 0,\ (v \cdot n)|_{\Gamma_c} = 0,\ \int_{\Gamma_c} (Ae(u)n \cdot n)\,v \cdot n\,ds \geq 0$$

As $v \cdot n \leq 0$ we obtain:

$$(Ae(u)n \cdot n) \leq 0 \tag{3.17}$$

It remains one condition on Γ_c to find. We start from (3.12) with $v = 0$:

$$\int_\Omega Ae(u) : e(u)\,dx \leq \int_\Omega f \cdot u\,dx + \int_{\Gamma_N} g \cdot u\,ds$$

and also take $v = 2u$:

$$\int_\Omega Ae(u) : e(u)\,dx \geq \int_\Omega f \cdot u\,dx + \int_{\Gamma_N} g \cdot u\,ds$$

which implies the equality

$$\int_\Omega Ae(u) : e(u)\,dx = \int_\Omega f \cdot u\,dx + \int_{\Gamma_N} g \cdot u\,ds$$

An integration by part and the use of (3.13) and (3.14) gives :

$$\int_{\Gamma_c} Ae(u)n \cdot u\,ds = 0$$

Using (3.16) it happens that :

$$\int_{\Gamma_c} (Ae(u)n, n)\,u \cdot n\,ds = 0$$

and by the fact that $u \cdot n \leq 0$ and (3.17), we have almost everywhere :

$$(Ae(u)n, n)\,u \cdot n = 0 \tag{3.18}$$

which puts an end to the proof. □

Remark 3.2.2. *The regularity of g can be lowered: g can be taken into one of these two spaces $\left(H^{\frac{1}{2}}(\partial\Omega)^d\right)^*$ or $\left(H^{\frac{1}{2}}_{00}(\Gamma_N)^d\right)^*$. The space $H^{\frac{1}{2}}_{00}(\Gamma_N)^d$ is defined in [188] by:*

$$H^{\frac{1}{2}}_{00}(\Gamma_N) = \left\{ v \in H^{\frac{1}{2}}(\Gamma_N) \,|\, \overline{v} \in H^{\frac{1}{2}}(\partial\Omega) \right\}, \tag{3.19}$$

with $\overline{v}$ which is equal to v on Γ_N and equal to 0 on $\partial\Omega \setminus \Gamma_N$. We point out that the subscript is 00 and not 0 to highlight the fact that $C^\infty_0(\Gamma_N)$ is dense in $H^{\frac{1}{2}}(\Gamma_N)$. So the space (3.19) is not the closure of $C^\infty_0(\Gamma_N)$ and is included into $H^{\frac{1}{2}}(\Gamma_N)$. Finally we mention that the trace operator is surjective from $H^1(\Omega)$ to $H^{\frac{1}{2}}_{00}(\Gamma_N)$.

From (3.12), it follows that (3.9) is the Euler-Lagrange optimality condition of the minimisation problem:

$$u = \underset{v \in K(\Omega)}{\operatorname{argmin}} \frac{1}{2} \int_\Omega Ae(v) : e(v)\,dx - \int_\Omega f \cdot v\,dx - \int_{\Gamma_N} g \cdot v\,ds \tag{3.20}$$

3.2.3 Existence, uniqueness and regularity

The study of the existence and uniqueness of a solution for frictionless contact and its regularity were for instance performed in [98], [38], more recently in [20] and, thanks to the use of pseudo-differential operator, in [248]. For auto-contact problems we refer to [173]. We also mention the work [22] and [23] where lower dimensional obstacle problems are studied, which is a problem not far from the Signorini contact problem. Here we only prove the existence and uniqueness of a solution:

Theorem 3.2.3. *The problem (3.12) admits one and only one solution for $f \in L^2(\Omega)^d$ and $g \in L^2(\Gamma_N)^d$.*

Proof. This is a consequence of theorem 2.4.1. First we have $K(\Omega) \subset H^1_{\Gamma_0}(\Omega)^d$ which is a closed convex cone and $H^1_{\Gamma_0}(\Omega)^d$ is an Hilbert space with the norm $\|\nabla u\|_{L^2(\Omega)^d}$. Let us set :

$$a(u, v) = \int_\Omega Ae(u) : e(v)\,dx \;\forall (u, v) \in (H^1_{\Gamma_0}(\Omega)^d)^2$$

$$l(v) = \int_\Omega f \cdot v\,dx + \int_{\Gamma_N} g \cdot u\,ds \;\forall v \in H^1_{\Gamma_0}(\Omega)^d$$

The coercivity of a is given by the Korn inequality and the continuity is a consequence of the Cauchy-Schwarz inequality.

The linear form l is continuous thanks to the Cauchy Schwarz inequality, the Poincaré inequality and the continuity of the trace operator from $H^1_{\Gamma_0}(\Omega)$ to $L^2(\Gamma_N)$. Using theorem 2.1 of [169], we get the existence of a unique solution to (3.12). □

Remark 3.2.4. *The regularity of f and g can be reduced. We can take $f \in H^{-1}(\Omega)$ and g in one of the follwing spaces: $\left(H^{\frac{1}{2}}(\partial\Omega)^d\right)^*$ or $\left(H^{\frac{1}{2}}_{00}(\Gamma_N)^d\right)^*$).*

3.3 Friction

To add some friction conditions, it is necessary to change the tangential condition $(Ae(u)n)_t = 0$ on Γ_c and S. The most popular friction model is the Coulomb one, but we first state a simpler model derived from it and then present the different models which will be used in the shape optimization part.

3.3.1 Tresca model

The Tresca friction model, also known as the model of given friction, was introduced in [98]. Even if it does not represent a realistic mechanical model, it can be used numerically to obtain the solution of the Coulomb friction model in a fixed point method and is mathematically well-posed. For the normal part (3.8), (3.5), (3.6) and (3.7) are kept and for the tangential part on Γ_c it is stated as:

$$\begin{aligned} &\|(Ae(u)n)_t\| \leq s && \text{on } \Gamma_c \\ &\|(Ae(u)n)_t\| < s \Rightarrow u_t = 0 && \text{on } \Gamma_c \\ &\|(Ae(u)n)_t\| = s \Rightarrow \exists \lambda \geq 0,\ u_t = -\lambda (Ae(u)n)_t && \text{on } \Gamma_c \end{aligned} \tag{3.21}$$

and on S:

$$\begin{aligned} &(Ae(u)n)_t = (Ae(u_{|S_-})n_-)_t = -(Ae(u_{|S_+})n_+)_t && \text{on } S \\ &\|(Ae(u)n)_t\| \leq s && \text{on } S \\ &\|(Ae(u)n)_t\| < s \Rightarrow [u_t] = 0 && \text{on } S \\ &\|(Ae(u)n)_t\| = s \Rightarrow \exists \lambda \geq 0,\ [u_t] = -\lambda (Ae(u_{|S_-})n_-)_t && \text{on } S \end{aligned} \tag{3.22}$$

where $\|\cdot\|$ denotes the classical euclidian norm on $\mathbb{R}^d$, s is a smooth function representing the coefficient of friction. While the tangential force is smaller than the coefficient of friction, there is no sliding. If the tangential force reaches the threshold s, sliding can appear. This model is not well-suited to modelize real phenomena since the tangential force does not take into account the normal force. Yet, like the problem (3.9), (3.21) can be written as a variational inequation and a minimisation problem of respectively the form: find $u \in K(\Omega)$ such that

$$\int_\Omega Ae(u) : e(v-u)\,dx + j_{\text{tr}}(v) - j_{\text{tr}}(u) \geq \int_\Omega f \cdot (v-u)\,dx + \int_{\Gamma_N} g \cdot (v-u)\,ds \quad \forall v \in K(\Omega) \tag{3.23}$$

and:

$$u = \underset{v \in K(\Omega)}{\operatorname{argmin}} \frac{1}{2} \int_\Omega Ae(v) : e(v)\,dx - \int_\Omega f \cdot v\,dx - \int_{\Gamma_N} g \cdot v\,ds + j_{\text{tr}}(v). \tag{3.24}$$

with

$$j_{\text{tr}}(v) = \int_{\Gamma_c} s\,\|v_t\|\,ds + \int_S s\,\|[v]_t\|\,ds \tag{3.25}$$

In the following we prove the equivalence between the variational inequality and the mechanical formulation, assuming $S = \varnothing$ for the sake of simplicity and noting $\sigma_t = (Ae(u)n)_t$:

$$\begin{cases} -\text{div}(Ae(u)) = f & \text{in } \Omega \\ u = 0 & \text{on } \Gamma_0 \\ Ae(u)\cdot n = g & \text{on } \Gamma_N \\ u.n \leq 0 & \text{on } \Gamma_c \\ Ae(u)n \cdot n \leq 0 & \text{on } \Gamma_c \\ (u\cdot n)(Ae(u)n\cdot n) = 0 & \text{on } \Gamma_c \\ \|\sigma_t\| \leq s & \text{on } \Gamma_c \\ \|\sigma_t\| < s \Rightarrow u_t = 0 & \text{on } \Gamma_c \\ \|\sigma_t\| = s \Rightarrow \exists \lambda \geq 0,\ u_t = -\lambda \sigma_t & \text{on } \Gamma_c \end{cases} \tag{3.26}$$

Theorem 3.3.1. *For $f \in L^2(\Omega)^d$ and $g \in L^2(\Gamma_N)^d$, the Tresca model (3.26) is equivalent to the following variational problem: find $u \in K(\Omega)$ such that*

$$\forall v \in K(\Omega),\ a(u, v-u) + j(v) - j(u) \geq \langle F, v-u\rangle \tag{3.27}$$

with

$$K(\Omega) = \left\{ v \in H^1_{\Gamma_0}(\Omega),\ v\cdot n \leq 0 \text{ on } \Gamma_c \right\},$$

$$a(u,v) = \int_\Omega Ae(u) : e(v)\,dx,$$

$$j(v) = \int_{\Gamma_c} s(x)\,\|v_t\|\,ds$$

and

$$\langle F, v\rangle = \int_\Omega f\cdot v\,dx + \int_{\Gamma_N} g\cdot v\,ds.$$

Proof. The proof is a simple rewriting of [98] 5.2.2.
We first prove that (3.27) $\Rightarrow$ (3.26). The proof is exactly the same as the proof of theorem 3.2.1 except for the boundary condition on Γ_c. We take v in $K(\Omega)$ such that its trace is zero on $\partial\Omega \setminus \Gamma_c$ and also the tangent part of its trace on Γ_c. This gives the boundary conditions $Ae(u)n \cdot n \leq 0$ and $(u \cdot n)(Ae(u)n \cdot n) = 0$ on Γ_c (cf the proof of theorem 3.2.1).

Now we take v in $K(\Omega)$ such that its trace is zero on $\partial\Omega \setminus \Gamma_c$ and the normal part of its trace on Γ_c is zero. Then the variational inequality gives, after aplying the Green formula:

$$\int_{\Gamma_c} (Ae(u)n) \cdot (v-u)\, ds + \int_{\Gamma_c} s(\|v_t\| - \|u_t\|)\, ds \geq 0$$

But $(u.n)(Ae(u)n.n) = 0$ on Γ_c so:

$$\int_{\Gamma_c} (Ae(u)n)_t \cdot (v-u)_t\, ds + \int_{\Gamma_c} s(\|v_t\| - \|u_t\|)\, ds \geq 0$$

and rewriting the precedent inequation with σ:

$$\int_{\Gamma_c} \sigma_t \cdot (v-u)_t\, ds + \int_{\Gamma_c} s(\|v_t\| - \|u_t\|)\, ds \geq 0$$

which gives:

$$\int_{\Gamma_c} \sigma_t \cdot u_t + s\,\|u_t\|\, ds \geq 0 \tag{3.28}$$

Taking $v_1 = \lambda\phi$ and $v_2 = -\lambda\phi$ with $\lambda > 0$ and $\phi \in \Psi = \left\{\psi \in H^{\frac{1}{2}}(\Gamma_c)^n, \text{ with support in the interior of } \Gamma_c\right\}$ it happens that:

$$\int_{\Gamma_c} \sigma_t \cdot \phi + s\,\|\phi\|\, ds - \frac{1}{\lambda}\int_{\Gamma_c} \sigma_t \cdot u_t + g\,\|u_t\|\, ds \geq 0$$

since $\|\phi_t\| \leq \|\phi\|$ and

$$\int_{\Gamma_c} -\sigma_t \cdot \phi + s\,\|\phi\|\, ds - \frac{1}{\lambda}\int_{\Gamma_c} \sigma_t \cdot u_t + g\,\|u_t\|\, ds \geq 0$$

then $\lambda \to +\infty$ it follows that :

$$\left|\int_{\Gamma_c} \sigma_t \cdot \phi\, ds\right| \leq \int_{\Gamma_c} s\,\|\phi\|\, ds$$

which means that $\phi \to \displaystyle\int_{\Gamma_c} \sigma_t \cdot \phi\, ds$ is a continuous application from Ψ with the norm $\displaystyle\int_{\Gamma_c} \|\phi\|\, ds$ to $\mathbb{R}$. But Ψ is dense in $(L^1(\Gamma_c))^n$ therefore this application is also continuous from $(L^1(\Gamma_c))^n$ to $\mathbb{R}$. As the dual space of $L^1(\Gamma_c)^n$ is $L^\infty(\Gamma_c)^n$, $\dfrac{1}{g}\sigma_t \in L^\infty(\Gamma_c)^n$ and its norm is smaller than 1: $\|\sigma_t\| \leq g$.

It follows that $\sigma_t \cdot u_t + s\,\|u_t\| \geq 0$ but with (3.28) it happens that:

$$\sigma_t \cdot u_t + s\,\|u_t\| = 0$$

which is equivalent to the tangential boundary conditions on Γ_c.

We now prove that (3.26) $\Rightarrow$ (3.27). We have:

$$\forall v \in K(\Omega),\ \int_\Omega (Ae(u)) : e(v-u)\, dx - \int_{\Gamma_c} (Ae(u)n) \cdot (v-u)\, ds = \int_\Omega f \cdot (v-u)\, dx + \int_{\Gamma_N} g \cdot (v-u)$$

similarly as in the proof of 3.2.1. Then

$$Ae(u)n \cdot (v-u) = (Ae(u)n \cdot n)\,(v-u) \cdot n + (Ae(u)n)_t (v-u)_t$$

and $(Ae(u)n \cdot n)\,(v-u) \cdot n = (Ae(u)n \cdot n)\, v \cdot n \geq 0$. Moreover

$$(Ae(u)n)_t (v-u)_t = \sigma_t v_t - \sigma_t u_t = \sigma_t v_t + s\,\|u_t\|$$

and $\sigma_t \cdot u_t \geq -\,\|\sigma_t\|\,\|u_t\| \geq -s\,\|u_t\|$ therefore

$$\int_{\Gamma_c} (Ae(u)n) \cdot (v-u)\, ds \geq \int_{\Gamma_c} (Ae(u)n)_t \cdot (v-u)_t\, ds \geq \int_{\Gamma_c} s(\|u_t\| - \|v_t\|)\, ds$$

which gives (3.27). □

Remark 3.3.2. *Note that g can also be taken into one of these two spaces $\left(H^{\frac{1}{2}}(\partial\Omega)^d\right)^*$ or $\left(H^{\frac{1}{2}}_{00}(\Gamma_N)^d\right)^*$).*

Theorem 3.3.3. *The Tresca model* (3.23) *has a unique solution $u \in K(\Omega)$ with $K(\Omega)$ defined by* (3.11).

Proof. The proof of the uniqueness and existence of u is a straightforward application of theorem 2.4.7 as j_{tr} is convex and continuous on $H^1_{\Gamma_0}(\Omega)^d$. □

3.3.2 Coulomb friction

The model of Coulomb friction is similar to the Tresca one, changing s into μ, a friction coefficient, times the absolute value of the normal force. For Γ_c:

$$\begin{array}{ll} \|(Ae(u)n)_t\| \leq \mu|(Ae(u)n\cdot n)| & \text{on } \Gamma_c \\ \|(Ae(u)n)_t\| < \mu|(Ae(u)n\cdot n)| \Rightarrow u_t = 0 & \text{on } \Gamma_c \\ \|(Ae(u)n)_t\| = \mu|(Ae(u)n\cdot n)| \Rightarrow \exists\lambda \geq 0,\ u_t = -\lambda(Ae(u)n)_t & \text{on } \Gamma_c \end{array} \tag{3.29}$$

and for S:

$$\begin{array}{ll} (Ae(u)n)_t = (Ae(u_{|S_-})n_-)_t = -(Ae(u_{|S_+})n_+)_t & \text{on } S \\ \|(Ae(u)n)_t\| \leq \mu|(Ae(u)n\cdot n)| & \text{on } S \\ \|(Ae(u)n)_t\| < \mu|(Ae(u)n\cdot n)| \Rightarrow [u_t] = 0 & \text{on } S \\ \|(Ae(u)n)_t\| = \mu|(Ae(u)n\cdot n)| \Rightarrow \exists\lambda \geq 0,\ [u_t] = -\lambda(Ae(u_{|S_-})n_-)_t & \text{on } S \end{array} \tag{3.30}$$

For the normal part there is no change in the boundary conditions: (3.8), (3.5), (3.6) and (3.7). This can be written as the following variational inequation: find $u \in K(\Omega)$ such that

$$\int_\Omega Ae(u) : e(v-u)\,dx + j_{\rm co}(u,v) - j_{\rm co}(u,u) \geq \int_\Omega f\cdot(v-u)\,dx + \int_{\Gamma_N} g\cdot(v-u)\,ds \quad \forall v \in K(\Omega) \tag{3.31}$$

with

$$j_{\rm co}(u,v) = \int_{\Gamma_c} \mu|(Ae(u)n\cdot n)|\,\|v_t\|\,ds + \int_S \mu|(Ae(u)n\cdot n)|\,\|[v]_t\|\,ds. \tag{3.32}$$

which is a function of two variables. The equivalence of the two problems can be proved as in theorem 3.3.1 in a formal sense. We have to pay attention to the fact that $Ae(u)n\cdot n$ belongs to $H^{-\frac{1}{2}}(\Gamma_c)$ which means that its absolute value is not defined. Either we can choose to take a regularisation of the operator giving the normal force as in [76], either we can state that it means that $Ae(u)n\cdot n$ has to be positive in the dual sense of $H^{-\frac{1}{2}}(\Gamma_c)$ as in [100].

The study of this model is done in chapter 1 and 3 of [100]. It is not equivalent to the minimisation of a function. To our knowledge there is no uniqueness results for this problem and the existence is only ensured for small friction coefficient. Yet the uniqueness was proven for the discretized problem in [126]. It is interesting, both for numerical [178] and theoretical [100] reasons, to note that this problem can be seen as the solution of a fixed point problem involving the solution of the Tresca model.

3.3.3 Norton-Hoff model

The Norton-Hoff model ([206]) is a variation of the previous friction model. The boundary condition is now a one to one relation between the tangential force and the tangential jump of the displacement (notwithstanding the normal force). It can be written as:

$$\begin{array}{ll} (Ae(u)n)_t = \mu|(Ae(u)n\cdot n)|\,\|u_t\|^{\rho-1}\,u_t & \text{on } \Gamma_c \\ (Ae(u_{|S_-})n)_t = -(Ae(u_{|S_+})n)_t = -\mu|(Ae(u)n\cdot n)|\,\|[u_t]\|^{\rho-1}\,[u_t] & \text{on } S \end{array} \tag{3.33}$$

where $0<\rho<1$, adding (3.8), (3.5), (3.6) and (3.7). It can be put under the form below: find $u \in K(\Omega)$ such that

$$\int_\Omega Ae(u) : e(v-u)\,dx + j_{\rm nh}(u,v-u) \geq \int_\Omega f\cdot(v-u)\,dx + \int_{\Gamma_N} g\cdot(v-u)\,ds \quad \forall v \in K(\Omega) \tag{3.34}$$

noting

$$j_{\rm nh}(u,v) = \int_{\Gamma_c} \mu|(Ae(u)n\cdot n)|\,\|u_t\|^{\rho-1}\,u_t\cdot v_t\,ds + \int_S \mu|(Ae(u)n\cdot n)|\,\|[u]_t\|^{\rho-1}\,[u]_t\cdot[v]_t\,ds \tag{3.35}$$

which is a function of two variables.

The one to one character of the boundary condition (3.33) makes the model numerically simpler to solve than the Coulomb one. Let us remark that this problem is not equivalent to the minimisation of a function and that the nearer ρ is of 0, the nearer the Norton Hoff-model is of the Coulomb model.

3.3.4 Normal compliance model

The last friction model considered is the normal compliance model presented in [200] and studied in [171]. It is pretty similar to a problem where the normal inequality constraint is penalised with a small penalisation coefficient. On Γ_c it takes the following form:

$$\begin{aligned}
&(Ae(u)n\cdot n)n = -C_N(u\cdot n)_+^{m_N} n && \text{on } \Gamma_c\\
&\|(Ae(u)n)_t\| \le C_T(u\cdot n)_+^{m_T} && \text{on } \Gamma_c\\
&\|(Ae(u)n)_t\| < C_T(u\cdot n)_+^{m_T} \Rightarrow u_t = 0 && \text{on } \Gamma_c\\
&\|(Ae(u)n)_t\| = C_T(u\cdot n)_+^{m_T} \Rightarrow \exists\lambda\ge 0,\ u_t = -\lambda(Ae(u)n)_t && \text{on } \Gamma_c
\end{aligned} \tag{3.36}$$

and on S:

$$\begin{aligned}
&(Ae(u_{|S_-})n\cdot n)n_- = -(Ae(u_{|S_+})n\cdot n)n_- = -C_N([u]\cdot n_-)_+^{m_N} n && \text{on } S\\
&(Ae(u)n)_t = (Ae(u_{|S_-})n_-)_t = -(Ae(u_{|S_+})n_+)_t && \text{on } S\\
&\|(Ae(u)n)_t\| \le C_T([u]\cdot n_-)_+^{m_T} && \text{on } S\\
&\|(Ae(u)n)_t\| < C_T([u]\cdot n_-)_+^{m_T} \Rightarrow [u_t] = 0 && \text{on } S\\
&\|(Ae(u)n)_t\| = C_T([u]\cdot n_-)_+^{m_T} \Rightarrow \exists\lambda\ge 0,\ [u_t] = -\lambda(Ae(u_{|S_-})n_-)_t && \text{on } S
\end{aligned} \tag{3.37}$$

where $(\cdot)_+ = max(0,\cdot)$, C_N and C_T are material coefficients and m_N and m_T are typically equal to 1 or 2 (see [171] for the possible value depending on the dimension d). Contrary to the other friction models the normal part is different from the case of sliding contact. Again it is possible to write a variational inequation equivalent to (3.36): find $u \in H^1_{\Gamma_0}(\Omega)^d$ such that:

$$\int_\Omega Ae(u) : e(v-u)\,dx + j_{N,Nc}(u,v-u) + j_{T,Nc}(u,v) - j_{T,Nc}(u,u) \ge \int_\Omega f\cdot(v-u)\,dx + \int_{\Gamma_N} g\cdot(v-u)\,ds \quad \forall v\in H^1_{\Gamma_0}(\Omega)^d \tag{3.38}$$

where:

$$j_{N,\mathrm{nc}}(u,v) = \int_{\Gamma_c} C_N(u\cdot n)_+^{m_N} v\cdot n\,ds + \int_S C_N([u]\cdot n_-)_+^{m_N}[v]\cdot n\,ds \tag{3.39}$$

$$j_{T,\mathrm{nc}}(u,v) = \int_{\Gamma_c} C_T(u\cdot n)_+^{m_T}\,\|v_t\|\,ds + \int_S C_T([u]\cdot n_-)_+^{m_T}\,\|[v]_t\|\,ds. \tag{3.40}$$

This model allows interpenetration which can represent a material loss at the surface of the material in contact. Existence and uniqueness results are given and discussed in [171] and [143] for smallness conditions on coefficients C_N and C_T but u is still not the solution of a minimisation problem. The proof is also given in [264] chapter 5.3 for the existence and uniqueness using theorem 2.4.10 with still smallness conditions on coefficients C_N and C_T and for the existence without any assumption on C_N and C_T using theorem 2.4.11.

3.4 Solving contact problems

We refer to [297] for a thorough presentation of algorithms solving contact problems. We only briefly present three of them: the Lagrangian method, the Nitsche method and the penalty and regularisation method. As we only use the last one in the thesis, we rapidly pass over the two first and concentrate on the penalty and regularisation method.

3.4.1 Lagrangian method

As this method will not be used in this thesis, we focus on its application to the sliding case, for the friction case we mention the chapter *IV* written by Haslinger in [211]. The idea is to introduce a Lagrange multiplier to account for the constraint that $u \in K$ and search for a saddle point of the Lagrangian function. In the case where $S = \varnothing$, the constraint is that $u\cdot n \le 0$ on Γ_c. The existence and uniqueness of a saddle point is proved in part 3.4 in [163]. So instead of solving (3.20):

$$u = \underset{v\in K(\Omega)}{\operatorname{argmin}} \left(\frac{1}{2}\int_\Omega Ae(v) : e(v)\,dx - \int_\Omega f\cdot v\,dx - \int_{\Gamma_N} g\cdot v\,ds\right),$$

we solve:

$$\sup_{\lambda\ge 0}\inf_{v\in H^1_{\Gamma_0}(\Omega)^d} \left(\int_\Omega Ae(v) : e(v)\,dx - \int_\Omega f\cdot v\,dx - \int_{\Gamma_N} g\cdot v\,ds + \int_{\Gamma_c}\lambda\, v\cdot n\,ds\right). \tag{3.41}$$

This can be done thanks to an Uzawa type algorithm, chapter 4.3 in [118]. We note that we still have a constraint but now on the Lagrangian multiplier. This will prevent us to use this formulation in the optimization process.

3.4.2 Nitsche's method

The Nitsche's method consists in a reformulation of the contact boundary conditions. If we take $\gamma > 0$, the boundary conditions (3.5), (3.6) and (3.7) are equivalent, see [78], to:

$$Ae(u)n = -\frac{1}{\gamma}\max(0, u\cdot n - \gamma Ae(u)n\cdot n)n. \tag{3.42}$$

This results in a variational non linear equation to be solved. The study of this type of method is done for instance in [237], [68], [71] or [69].

3.4.3 Penalty and regularisation method

The idea of penalisation is to change inequations into equation by removing that $u \in K$ and replacing it in the formulation by a term, depending on a small parameter, forcing u not to be too far from respecting the constraint. When the parameter tends to 0, the solution of the penalized problem tends to the solution of the real one.

In the different contact problems presented, there are two kinds of reasons which trigger the appearance of inequations. The first one, concerning the normal part of u on the boundary, is that u belongs to a convex set. This constraint will be penalised. The second one is the singularity in the tangential friction formulation due to the presence of the term $\|\cdot\|$. This term will be regularised thanks to a regularisation of $\|\cdot\|$.

Penalisation for the convex set

In this part we present the penalisation used to get rid of the constraint stating that u needs to be in $K(\Omega)$. This penalisation will be used for every model but the normal compliance one and we explain how to add it to change the inequations into equations, or sometimes into other inequations. As a matter of fact, for the problems comprising friction, to get equations we also need to regularise the friction term (as said before). That is why we only write the penalised equation associated with (3.24) in this part. For the other models, they can be found in the next one.

To add the penalisation, the procedure differs whether the initial problem can be written as a minimisation problem: (3.24) and (3.20) or not: (3.31) and (3.34).

For (3.24) and (3.20), we change the function to minimise and the set to which the solution u belongs. Instead of minimizing on $K(\Omega)$, we minimise on $H^1_{\Gamma_0}(\Omega)^d$. But to force the solution to approximately fullfill the condition $v\cdot n \leq 0$ on Γ_c and $[v]\cdot n_- \leq 0$ on S, we add to the function a term of the form:

$$j_{N,\epsilon}(u) = \frac{1}{\epsilon}\left(\int_{\Gamma_c}\int_0^{u.n}\phi_r(t)\,dt\,ds + \int_S\int_0^{[u].n}\phi_r(t)\,dt\,ds\right) \tag{3.43}$$

where $\phi_r(t) = t \mapsto t\mathcal{H}(t)$ with $\mathcal{H}$ the Heaviside function. We can then deduce a penalised variational formulation associated with (3.20):

$$\int_\Omega Ae(u) : e(v)\,dx + j'_{N,\epsilon}(u,v) = \int_\Omega f\cdot v\,dx + \int_{\Gamma_N} g\cdot v\,ds.\ \ \forall v \in H^1_{\Gamma_0}(\Omega)^d \tag{3.44}$$

and as minimisation problem:

$$u = \underset{v\in H^1_{\Gamma_0}(\Omega)^d}{\operatorname{argmin}}\left(\frac{1}{2}\int_\Omega Ae(v) : e(v)\,dx - \int_\Omega f\cdot v\,dx - \int_{\Gamma_N} g\cdot v\,ds + j_{N,\epsilon}(v)\right), \tag{3.45}$$

noting

$$j'_{N,\epsilon}(u,v) = \frac{1}{\epsilon}\int_{\Gamma_c}\phi_r(u\cdot n)v\cdot n\,ds + \frac{1}{\epsilon}\int_S \phi_r([u]\cdot n_-)[v]\cdot n_-\,ds. \tag{3.46}$$

Its convergence to the exact solution was proved in [97] and [70].

For (3.31) and (3.34), the problems cannot be changed into a minimisation problem, therefore we need to work directly on the variational inequation. The idea is to add a term $j'_{N,\epsilon}(u, v-u)$ on the left hand side and change the spaces of the solutions as done in [100], chapter 3, keeping in mind that to get an equation we still need to regularise the friction term.

Regularisation of the friction term

In (3.23), (3.31), (3.34) and (3.38) to transform the inequation into an equation we also need to regularise $\|\cdot\|$. We note $\mathcal{N}_\eta$ a smooth convex function approximating it (at least twice differentiable), with $\eta > 0$ a small coefficient. For instance [100]:

$$\mathcal{N}_\eta(x) = \begin{cases} \|x\| & \text{for } \|x\| \geq \eta \\ -\dfrac{1}{8\eta^3}\|x\|^4 + \dfrac{3}{4\eta}\|x\|^2 + \dfrac{3}{8}\eta & \text{for } \|x\| \leq \eta \end{cases} \tag{3.47}$$

The new penalised and regularised equations are then given:

- for the Tresca model by

$$\int_\Omega Ae(u) : e(v)\,dx + j'_{\mathrm{tr},\eta}(u,v) + j'_{N,\epsilon}(u,v) = \int_\Omega f\cdot v\,dx + \int_{\Gamma_N} g\cdot v\,ds \quad \forall v \in H^1_{\Gamma_0}(\Omega)^d, \tag{3.48}$$

  where $j'_{\mathrm{tr},\eta}$ denotes the derivative of $j_{\mathrm{tr},\eta}$ with respect to v with:

$$j_{\mathrm{tr},\eta}(v) = \int_{\Gamma_c} s\mathcal{N}_\eta(v_t)\,ds + \int_S s\mathcal{N}_\eta([v]_t)\,ds. \tag{3.49}$$

  We mention that the penalised and regularised Tresca problem can be written as a minimisation problem:

$$u = \underset{v\in H^1\Gamma_0(\Omega)^d}{\operatorname{argmin}} \left(\frac{1}{2}\int_\Omega Ae(v) : e(v)\,dx - \int_\Omega f\cdot v\,dx - \int_{\Gamma_N} g\cdot v\,ds + j_{N,\epsilon}(v) + j_{\mathrm{tr},\eta}(v)\right). \tag{3.50}$$

  It is not the case for the other friction models described in the following.

- for the Coulomb model:

$$\int_\Omega Ae(u) : e(v)\,dx + j'_{\mathrm{co},\epsilon,\eta}(u,v) + j'_{N,\epsilon}(u,v) = \int_\Omega f\cdot u\,dx + \int_{\Gamma_N} g\cdot u\,ds \quad \forall v \in H^1_{\Gamma_0}(\Omega)^d. \tag{3.51}$$

  denoting

$$j'_{\mathrm{co},\epsilon,\eta}(u,v) = \int_{\Gamma_c} \frac{\mu}{\epsilon}\phi_r(u\cdot n)\mathcal{N}'_\eta(u_t)\cdot v_t\,ds + \int_S \frac{\mu}{\epsilon}\phi_r([u]\cdot n_-)\mathcal{N}'_\eta([u]_t)\cdot [v]_t\,ds \tag{3.52}$$

  and $\mathcal{N}'_\eta$ the derivative of $\mathcal{N}_\eta$.

- for the Norton-Hoff model, the regularized variational formulation is:

$$\int_\Omega Ae(u) : e(v)\,dx + j_{\mathrm{nh},\epsilon,\eta}(u,v) + j'_{N,\epsilon}(u,v) = \int_\Omega f\cdot v\,dx + \int_{\Gamma_N} g\cdot v\,ds \quad \forall v \in H^1_{\Gamma_0}(\Omega)^d. \tag{3.53}$$

  noting

$$j_{\mathrm{nh},\epsilon,\eta}(u,v) = \int_{\Gamma_c} \frac{\mu}{\epsilon}\phi_r(u\cdot n)\mathcal{N}_\eta(u_t)^{\rho-1}u_t\cdot v_t\,ds + \int_S \frac{\mu}{\epsilon}\phi_r([u]\cdot n_-)\mathcal{N}_\eta([u]_t)^{\rho-1}[u]_t\cdot [v]_t\,ds \tag{3.54}$$

  Remark 3.4.1. *Note that, for this particular case, the tangential part $j_{\mathrm{nh},\epsilon,\eta}$ is not derived since it was already linear with respect to v.*

- for the normal compliance model, the regularized variational formulation is:

$$\int_\Omega Ae(u) : e(v)\,dx + j_{N,r,Nc}(u,v) + j'_{T,\eta,Nc}(u,v) = \int_\Omega f\cdot v\,dx + \int_{\Gamma_N} g\cdot v\,ds \quad \forall v \in H^1_{\Gamma_0}(\Omega)^d \tag{3.55}$$

  with

$$j_{N,\mathrm{nc,r}}(u,v) = \int_{\Gamma_c} C_N\phi_r(u\cdot n)^{m_N} v\cdot n\,ds + \int_S C_N\phi_r([u]\cdot n_-)^{m_N}[v]\cdot n\,ds$$

$$j'_{T,\mathrm{nc},\eta}(u,v) = \int_{\Gamma_c} C_T\phi_r(u\cdot n)^{m_T}\mathcal{N}'_\eta(u_t)\cdot v_t\,ds + \int_S C_T\phi_r([u]\cdot n_-)^{m_T}\mathcal{N}'_\eta([u]_t)\cdot [v]_t\,ds.$$

  For this model, both the normal and tangential terms were regularised and no penalisation were needed as the initial inequation is already solved into $H^1_{\Gamma_0}(\Omega)^d$.

Existence and uniqueness of the penalised/regularized formulation

For (3.48) and (3.44) the existence and uniqueness results are easily proved by taking advantage of their respective minimisation problem formulation.

Theorem 3.4.2. *The problems* (3.48) *and* (3.44) *admit one and only one solution for* $f \in L^2(\Omega)^d$, $g \in L^2(\Gamma_N)^d$, ϕ_r *positive increasing and* $\mathcal{N}_\eta$ *convex positive.*

Proof. The proof is an application of either theorem 2.4.7 (for (3.48)) or theorem 2.4.1 (for (3.44)) with a strongly monotone Lipschitz continuous operator A defined as:

$$\langle A(u), v\rangle = \int_\Omega Ae(u) : e(u)\, dx + j'_{N,\epsilon}(u, v)$$

and the function $j_{\mathrm{tr},\eta}$ which is convex and continuous. □

For (3.51) the existence is proved in chapter 3 of [100]. A proof similar to the one of (3.51) can be done for (3.53). In the case of the normal compliance model we refer to [123] for a particular case.

Numerical solvers

All penalized and regularised formulations of contact presented here are non linear variational equations which can be discretized thanks to the finite element method, see [297] chapter 8 and [163]. For the sake of simplicity and because we want to perform shape optimization with the level set method on a fixed mesh, we choose to implement a solver using a node-to-node contact algorithm with a square matching grid. This means that the contact surfaces S and Γ_c will be meshed and that on S on one geometrical location two nodes are present to enable the crack to open and the displacement to be discontinuous. The finite elements used are Q_1 elements.

The elasticity equation is discretized as usual. We explain how the normal contact term (3.46) $j'_{N,\epsilon}(u, v)$ is discretized and focus on the boundary part S in 2D. So we want to discretize:

$$B(u, v) = \int_S \phi_r([u]\cdot n_-)[v]\cdot n_-\, ds = \int_S [u]\cdot n_-[v]\cdot n_-\mathcal{H}([u]\cdot n_-)\, ds$$

We call I_S the geometrical location of nodes on S, I_S^- the nodes on S_- and I_S^+ the nodes on S_+. We have $I_S = I_S^+ \cup I_S^-$ and $I_S^+ \cap I_S^-$ are the nodes on the boundary of S. Note that these nodes are not doubled. If we take $i \in S$, the corresponding node on S_+ is noted i^+ and the one on S_-, i^-. We note ϕ_j^x the shape function at the node j for the x component and ϕ_j^y, the same for the component y. As we want to solve the variational equation in the linear span V_h of the shape functions, with h the size of the side of an element, we can write the trace of u on S:

$$u_{|S} = \sum_{i\in I_S} u_{i^+}^x\phi_{i^+}^x + u_{i^-}^x\phi_{i^-}^x + u_{i^+}^y\phi_{i^+}^y + u_{i^-}^y\phi_{i^-}^y. \tag{3.56}$$

So taking $v \in V_h$, we also have:

$$v_{|S} = \sum_{i\in I_S} v_{i^+}^x\phi_{i^+}^x + v_{i^-}^x\phi_{i^-}^x + v_{i^+}^y\phi_{i^+}^y + v_{i^-}^y\phi_{i^-}^y. \tag{3.57}$$

We will not discretize the Heaviside function and focus on the linear part:

$$\begin{aligned} B(u, v) &= \int_S \big(u(x^-) - u(x^+)\big)\cdot n_- \big(v(x^-) - v(x^+)\big)\cdot n_-\mathcal{H}([u]\cdot n_-) \\ &= \sum_{i\in I_S}\sum_{j\in I_S}\int_S \Big(u_{j^-}^x\phi_{j^-}^x + u_{j^-}^y\phi_{j^-}^y - u_{j^+}^x\phi_{j^+}^x - u_{j^+}^y\phi_{j^+}^y\Big)\cdot n_- \\ &\quad \big(v_{i^-}^x\phi_{i^-}^x + v_{i^-}^y\phi_{i^-}^y - v_{i^+}^x\phi_{i^+}^x - v_{i^+}^y\phi_{i^+}^y\big)\cdot n_-\mathcal{H}([u]\cdot n_-)\, ds \end{aligned} \tag{3.58}$$

Then we expand the term inside the integral:

$$\begin{aligned} &u_{j^-}^x v_{i^-}^x\left(\phi_{j^-}^x\phi_{i^-}^x n_x^2 + 2n_xn_y\phi_{j^-}^x\phi_{i^-}^y + \phi_{j^-}^y\phi_{i^-}^y n_y^2\right) \\ &- u_{j^-}^x v_{i^+}^x\left(\phi_{j^-}^x\phi_{i^+}^x n_x^2 + 2n_xn_y\phi_{j^-}^x\phi_{i^+}^y + \phi_{j^-}^y\phi_{i^+}^y n_y^2\right) \\ &- u_{j^+}^x v_{i^-}^x\left(\phi_{j^+}^x\phi_{i^-}^x n_x^2 + 2n_xn_y\phi_{j^+}^x\phi_{i^-}^y + \phi_{j^+}^y\phi_{i^-}^y n_y^2\right) \\ &+ u_{j^+}^x v_{i^+}^x\left(\phi_{j^+}^x\phi_{i^+}^x n_x^2 + 2n_xn_y\phi_{j^+}^x\phi_{i^+}^y + \phi_{j^+}^y\phi_{i^+}^y n_y^2\right) \end{aligned}$$

which enables to easily build the finite element matrix corresponding to B noted $M_N(U)$, highlighting that it depends on U, the vector of the components of u in the shape functions basis. We also remark that these integrals can be exactly computed if an analytical expression of the normal is known.

We choose to sort these components such that, for one node, the different dimensions are one following the other. We also note K the rigidity matrice corresponding to the bilinear form due to the term

$$\int_\Omega Ae(u) : e(v)\, dx.$$

Then, in the case of sliding contact, we have to solve the finite dimensional system:

$$(K + M_N(U))\, U = F \tag{3.59}$$

where F is the discretization of the second member.

For the friction cases, the integral corresponding to the friction is of the form:

$$\int_S k(u)[u_t] \cdot [v_t]\, ds$$

with k a non linear function which depends on the model used. The same calculation can be made to find the associated finite element matrices except for numerical computations. Now, the integrals to calculate cannot be explicitly found as the function k is not as simple as the Heaviside function. We need to numerically approach these integrals, thanks to a quadrature formula like the Simpson rule or Gauss rules, see [85] or [91].

Each of these penalized contact models leads to a non linear equation to solve, which is usually solved by a damped Newton method, see [92] chapter 6 and [219] chapter 11, or a fixed point method. The Newton method has the advantage to be faster but it needs a good choice for the damping and the smoothness of the non linear function to be able to compute their derivatives. On the other hand, the fixed point method despite its relative slowness is easier to implement. We also mention that the robustness of the algorithm which solves the contact equations is crucial in the optimisation process. First because the optimisation can produce structures for which the finite element matrices are nearly singular. Secondly because we are solving problems whose solution is not always unique. Finally, as we will see in the shape optimization part, the use of an adjoint in a non linear problem implies the calculation of the derivatives of the matrices. This advocates in a certain sense for the use of a Newton method. In our algorithms, we make the most of both methods, using a damped Newton method coupled with a fixed point method when the damped Newton method has trouble converging.

Numerical examples

In this last part, we present some computations done with our contact algorithms (for the penalised models). Our goal is to unformally evidence their good behavior and also to qualitatively underline the impact of a change in the parameters of the models. To this end we analyse three different examples. On each example the deformation of the mesh is plotted to show the displacement u, by moving the mesh points with a translation of vector αu with α depending on the examples considered.

First example We consider a square full of elastic material with a crack in the middle going from the upper side to the center of the square. A rightward force is applied in the middle of the right side and the structure is clamped on the left side, see figure 3.3. It is clear that the crack will open and we show that it is the case for every model. An interesting observation is that for the Tresca model the crack opens but the friction prevents the structure from going as down as for the other models. It exemplifies its mechanical non sense: as explained in 3.3.1 even if there is no contact friction can occur. For all the cases the friction coefficient is taken equal to 0.5. For the normal compliance model the other coefficients (C_N, m_N, m_T) are all equal to 1 and in the Norton-Hoff model $\rho = 0.5$.

Second example The case is the same except for the force which is not downward anymore but leftward, see figure 3.5. First we perform some tests on the model without friction for different penalization coefficients to underline that the penalization method allows an interpenetration which decreases with ϵ, see figure 3.6. The interpenetration is of the same magnitude as the penalization ϵ.

In the figure 3.7, some examples are presented for the Norton-Hoff model in which we vary the coefficient ρ. The coefficient of friction is taken equal to 0.5. As ρ goes to 1 the importance of the friction decreases.

In the figure 3.8, some examples are presented for the Normal compliance model in which we vary the coefficient m_N and m_T. The friction coefficient is taken equal to 0.5. We notice that this model allows the interpenetration which is minimal for $m_N = 1$ and that the case in figure 3.8(b) allows more sliding than the other ones.

We also compare the different models, changing the friction coefficient taken 0.04 figure 3.9 and 0.5 figure 3.10. We take $\rho = 0.5$, $C_N = 1$, $m_N = 1$, $m_T = 1$ and $\epsilon = 10^{-7}$. We notice that the sliding is greater with a friction coefficient equal to 0.04.

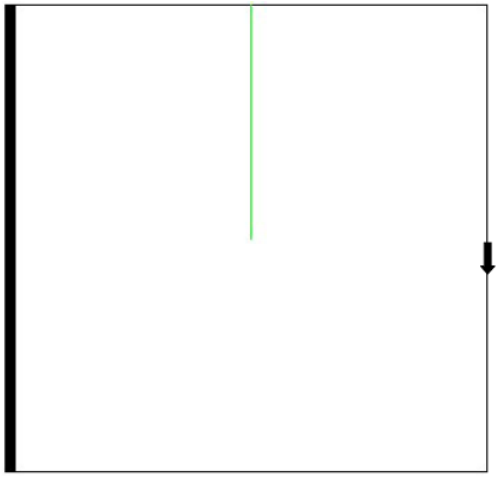

Figure 3.3: Load case for the first contact example.

We also plot the difference between the solutions found with the penalisation for the Coulomb model figure 3.10(e) and the one found with the fixed point method 3.10(f). On figure 3.11(a) the absolute value of the difference between the x-components of the displacement is presented, on figure 3.11(b) the difference between the y-components and respectively on figure 3.11(c) and 3.11(d) the x and y components for the contact nodes (the first value corresponds to the highest node and the last to the lowest one).

Third example On this example we test the contact on the boundary of Ω. The contact zone is in the middle of the bottom side, the structure is clamped on the left side and a force is applied in the middle of the right side, see figure 3.12. We plot the solutions for a friction coefficient equal to 0.5, figure 3.13. We take $\rho = 0.5$, $C_N = 1$, $m_N = 1$, $m_T = 1$ and $\epsilon = 10^{-7}$. The friction produces more bending on the bottom right side (it is particularly obvious on the Tresca case).

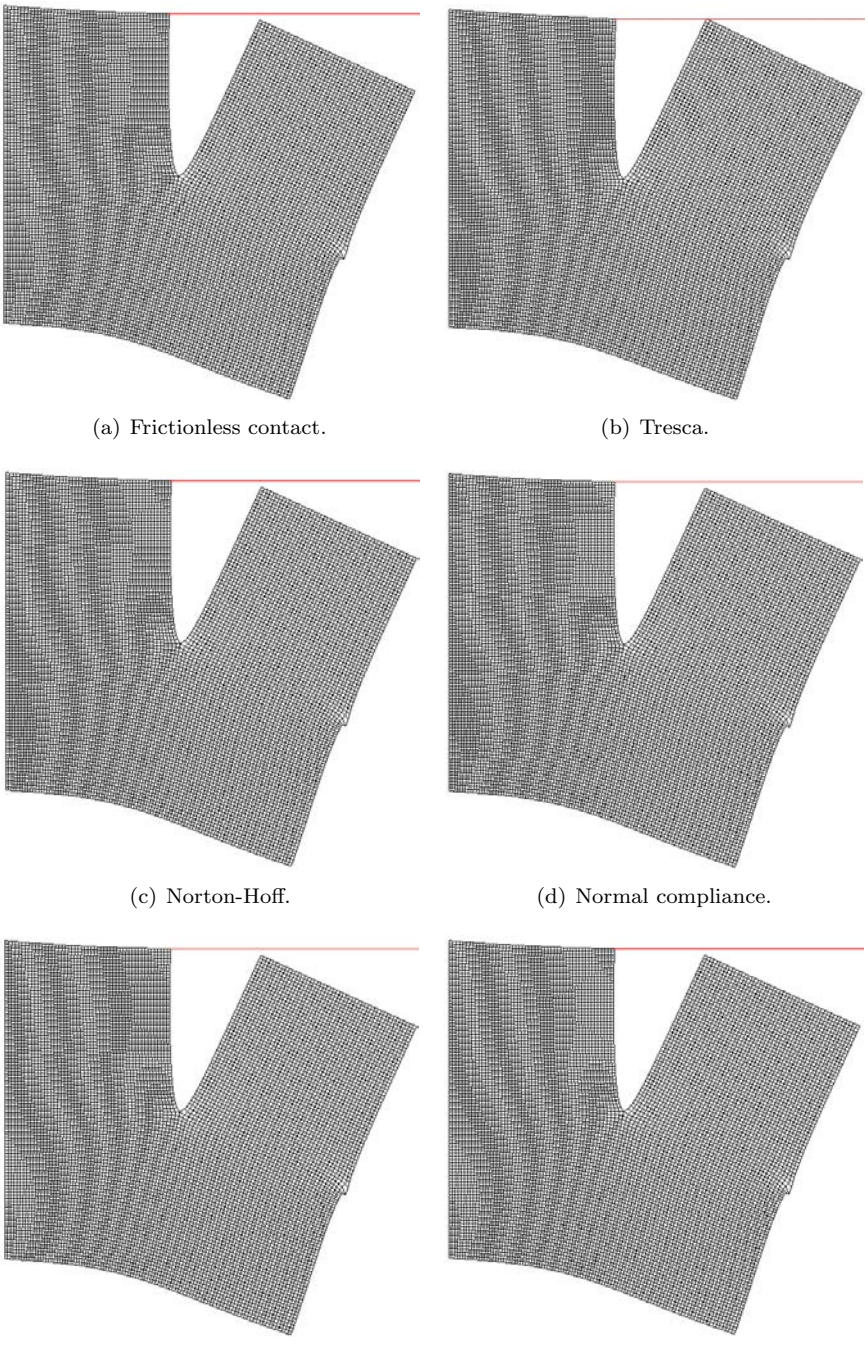

(a) Frictionless contact.

(b) Tresca.

(c) Norton-Hoff.

(d) Normal compliance.

(e) Penalized Coulomb.

(f) Coulomb thanks to the fixed point method.

Figure 3.4: Results for the first contact case.

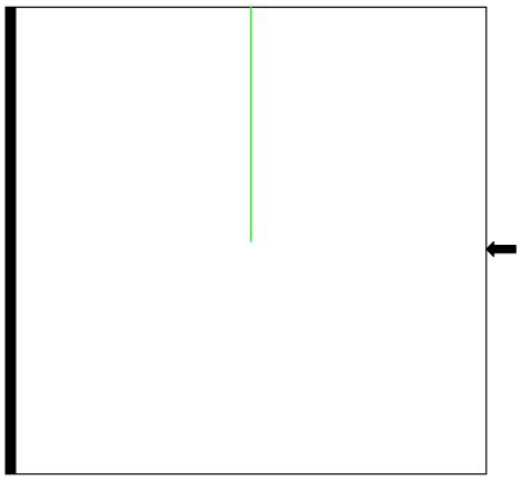

Figure 3.5: Load case for the second contact example.

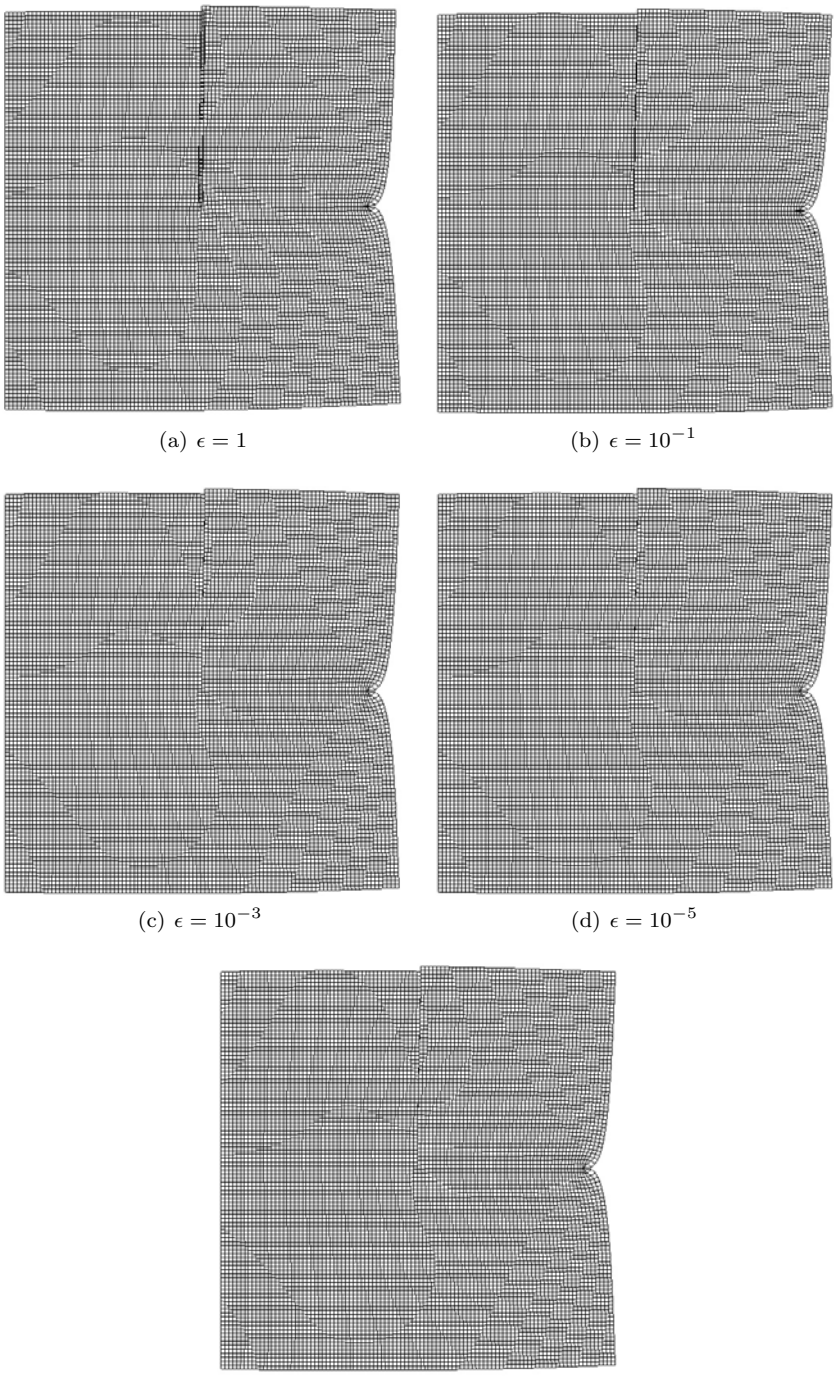

(a) $\epsilon = 1$

(b) $\epsilon = 10^{-1}$

(c) $\epsilon = 10^{-3}$

(d) $\epsilon = 10^{-5}$

(e) $\epsilon = 10^{-7}$

Figure 3.6: Results for the second contact case, varying the penalization coefficients in the frictionless model.

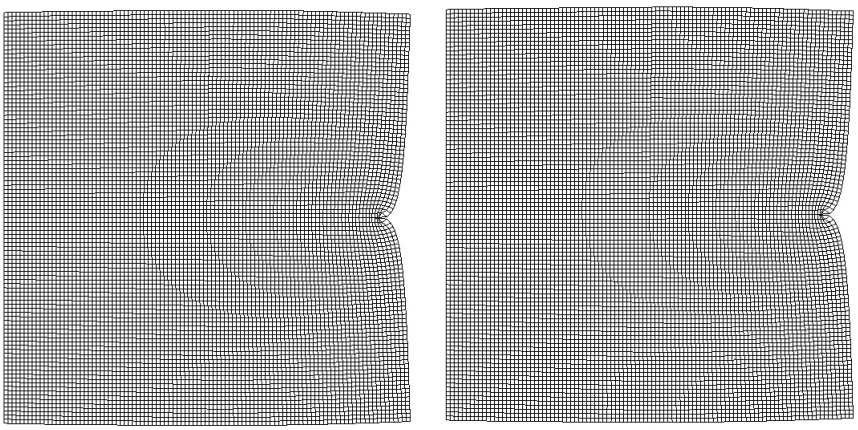

(a) $\rho = 0.4$ (b) $\rho = 0.5$

(c) $\rho = 0.7$ (d) $\rho = 0.9$

Figure 3.7: Results for the second contact case, varying the coefficient ρ in the Norton Hoff model.

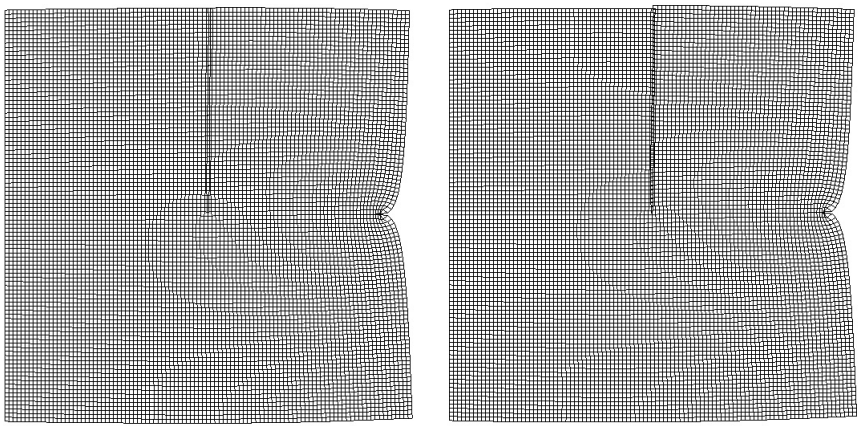

(a) $m_N = 1$ and $m_T = 1$ (b) $m_N = 1$ and $m_T = 2$

(c) $m_N = 2$ and $m_T = 1$ (d) $m_N = 2$ and $m_T = 2$

Figure 3.8: Results for the second contact case, varying the coefficients m_N and m_T in the normal compliance model.

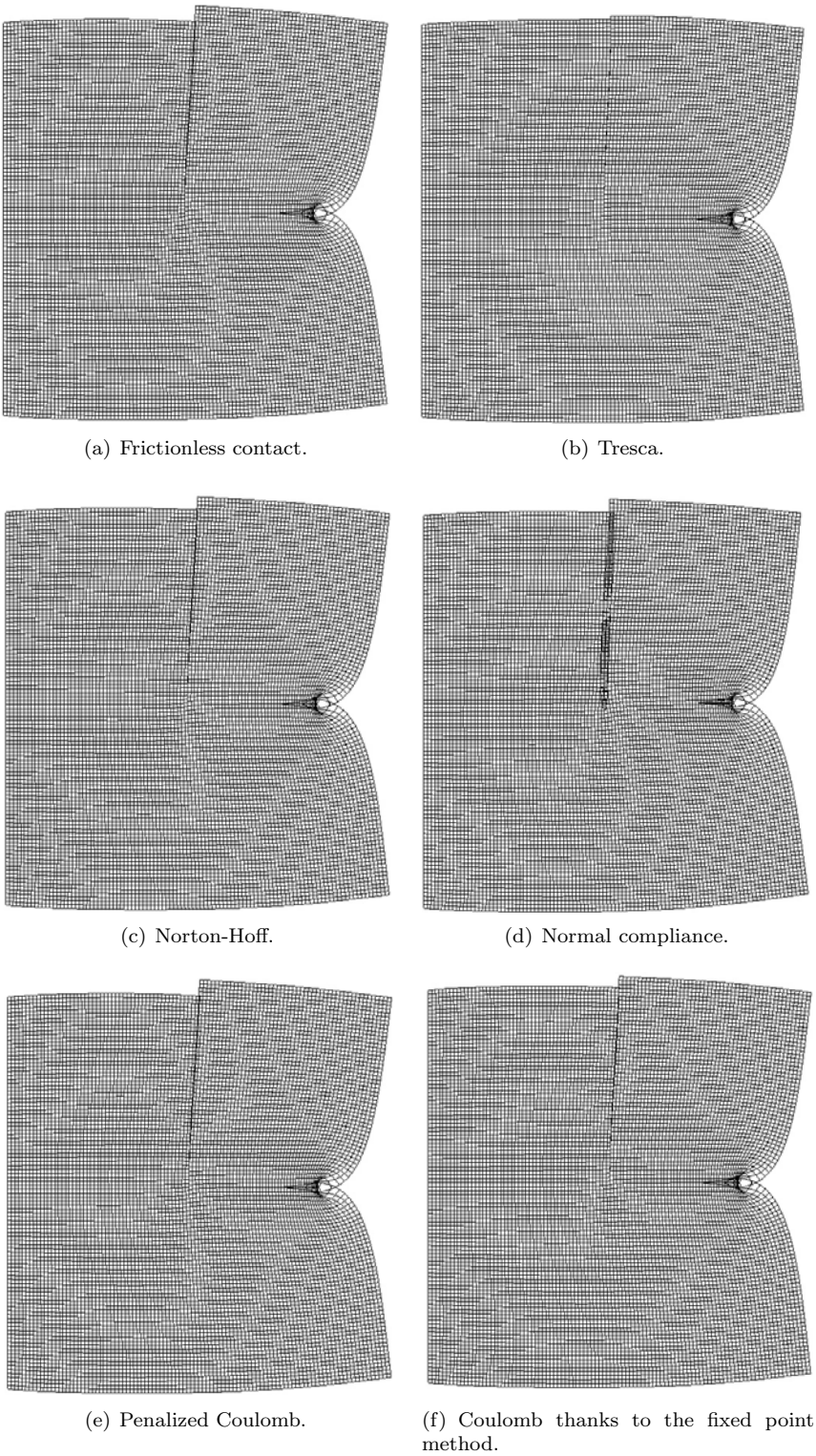

(a) Frictionless contact.

(b) Tresca.

(c) Norton-Hoff.

(d) Normal compliance.

(e) Penalized Coulomb.

(f) Coulomb thanks to the fixed point method.

Figure 3.9: Results for the second contact case with a friction coefficient equal to 0.04

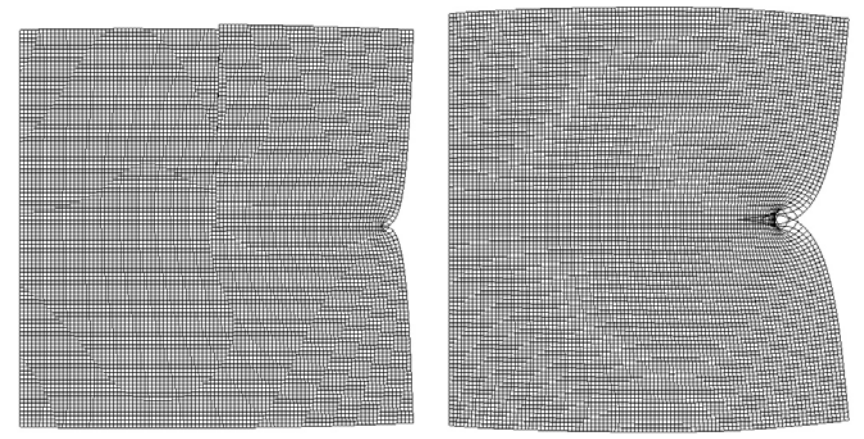

(a) Frictionless contact.

(b) Tresca.

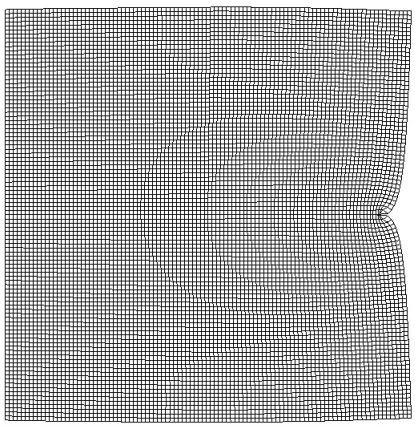

(c) Norton-Hoff.

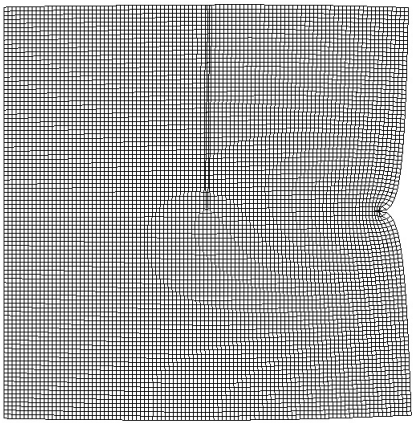

(d) Normal compliance.

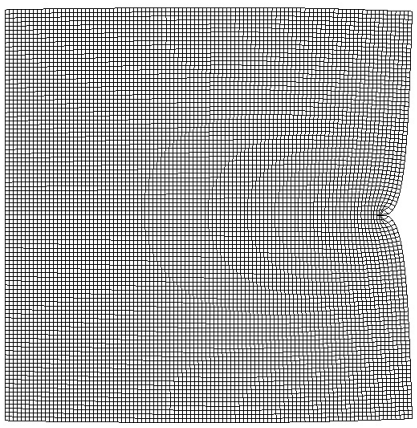

(e) Penalized Coulomb.

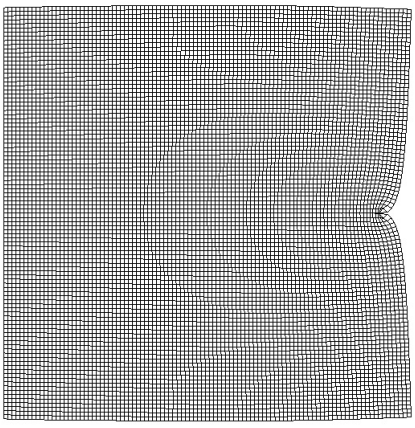

(f) Coulomb thanks to the fixed point method.

Figure 3.10: Results for the second contact case with a friction coefficient equal to 0.5

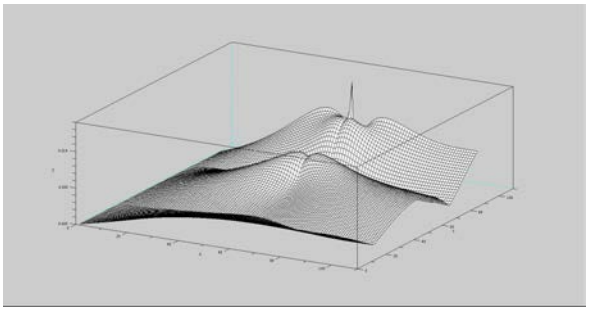

(a) The x-component

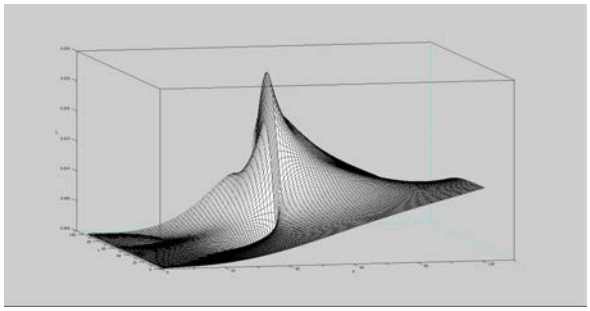

(b) The y-component

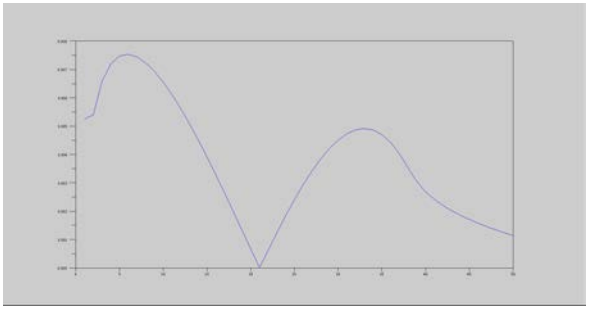

(c) The x-component on the contact zone

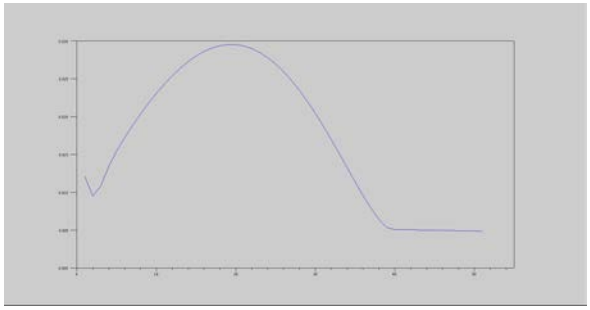

(d) The y-component on the contact zone

Figure 3.11: Comparison between two ways of computing the solution of the Coulomb model for a friction coefficient equal to 0.5

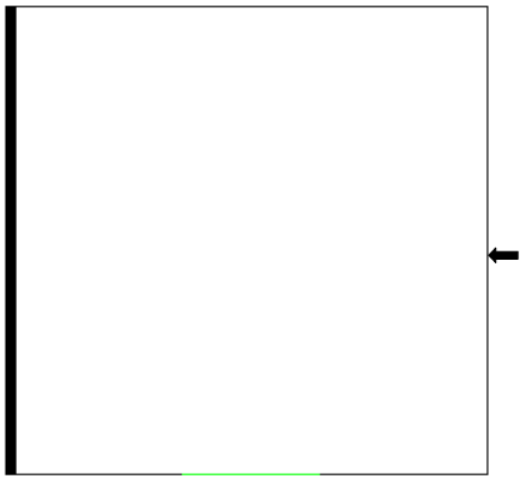

Figure 3.12: Load case for the third contact example.

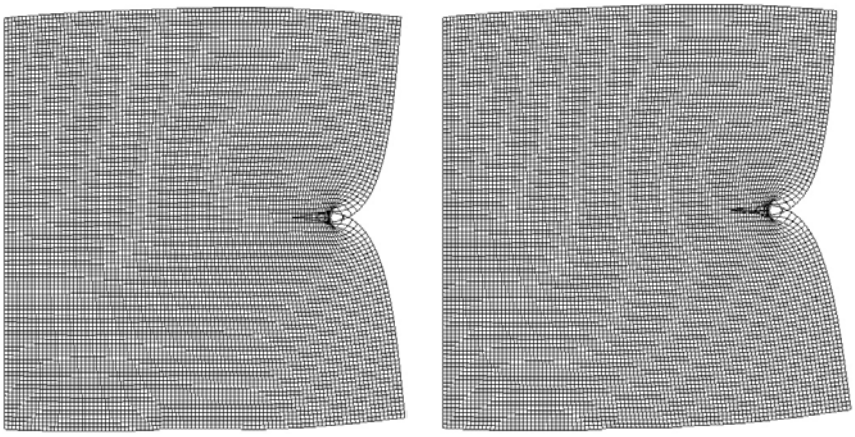

(a) Frictionless contact.

(b) Tresca.

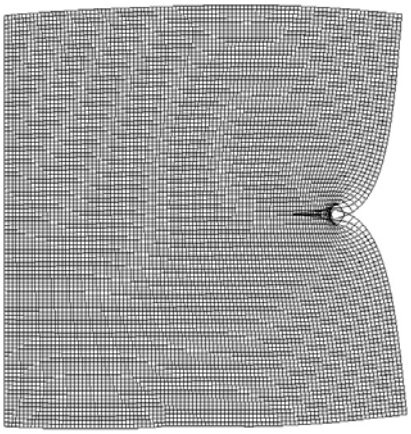

(c) Norton-Hoff.

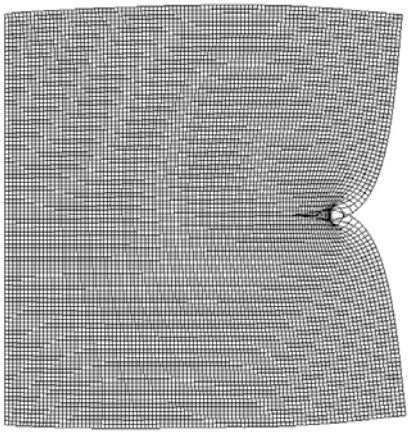

(d) Normal compliance.

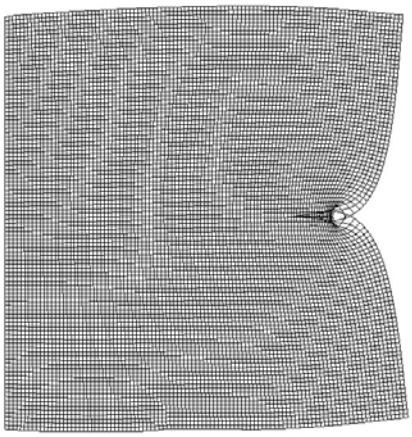

(e) Penalized Coulomb.

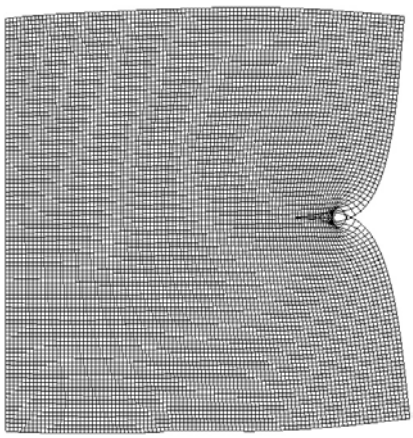

(f) Coulomb thanks to the fixed point method.

Figure 3.13: Results for the third contact case with a friction coefficient equal to 0.5

Chapter 4

Plasticity

Contents

4.1 Introduction

When the behaviour of a material is to be studied, the linearized elasticity approximation can be done when considering small strain and constraint as well as a slow loading speed or a small loading time. However if we are not in these particular cases the material does not behave linearly anymore and the non linearities cannot be ignored. Thus when performing some tests on a cylindircal mechanical specimen [199], ith as been remarked, once a specific constraint is reached, a great variety of behaviours which, for the most, present high non linearities and are irreversible, see figure 4.1 and figure 4.3(b). There is a moment when the elasticity approximation is not correct anymore. This phenomenon is called plasticity and comes from microscopic mechanical defects. For instance in metals it is due to the movement of the dislocations in the crystal lattice, in concrete it is due to the development of a network of microcracks.

Consequently, taking plasticity into account is of great importance in the study of structures. Indeed plastic areas tend to irreversibly deform more than elastic ones. This could lead to structural integrity dangers and sometimes to breaking. In this case, the designer often tries to avoid the creation of plastic regions by controlling the internal constraints. But plasticity could also be useful when for instance the breaking of a piece is meant to protect other parts which are difficult to repair or which should absolutely not collapse (like the use of a circuit breaker in electricity). Eventually there are materials, called ductile, which can suffer big deformations after the elastic phase (without collapsing) and the designer can take advantage of this property by allowing plastic areas and by trying to distribute the constraint in the structure the most uniformly as possible. Another difficulty which is out of the scope of the cases considered in this thesis is that the plastic behaviour of a material highly depends on the temperature. Thus a metal which is ductile at room temperature can be brittle, the opposite of ductile, at low temperature which means that the constraint rapidly decreases to zero with the growth of the strain after the elastic part. This particular dependency explained several famous accidents as the breaks of the Sully-sur-Loire bridge and the Schenectady, a Liberty ship [199].

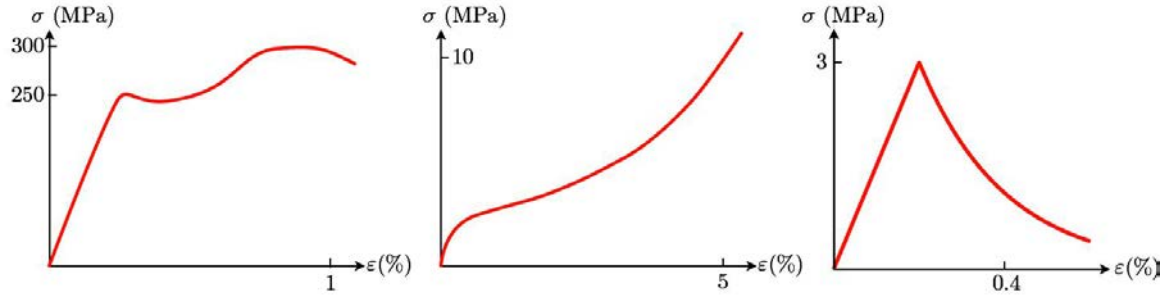

(a) Simplified plastic behaviours during a uniaxial traction test, on the left for a steel, in the center for an elastomer and on the right for concrete. Taken from [199].

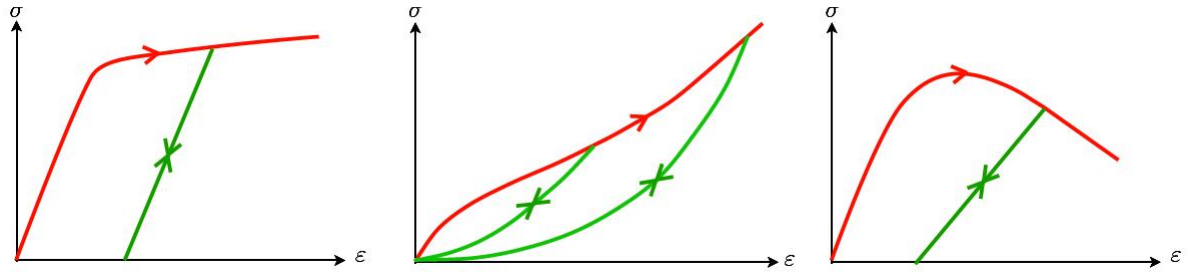

(b) Simplified plastic behaviours during a cycle loading-unloading-reloading, on the left for a steel, in the center for an elastomer and on the right for concrete. Taken from [199].

Figure 4.1: Plastic behaviours

From a mechanical point of view plasticity was first studied by Tresca, Saint Venant, Lévy and Bauschinger in the nineteenth century and in the next century by Prandtl, Von Mises and Reuss. From a mathematical point of view the study was started by Prager, Drucker and Hill and thanks to the theory of variational inequalities and convex analysis by Moreau [210], Duvaut and J.-L. Lions [98]. Since then a lot of articles were published on the subject investigating the well posedness of these problems. We particularly mention Suquet [277], Temam [283] and more recently Dal Maso [79], [80], [81],[82], [83]. In the following we will mainly refer to the monographs of Han and Reddy [124], Bensoussan and Frehse [30], Fuchs and Seregin [115], Temam [283] and Panagiotopoulos [229], the article of Löbach [190] and the thesis of Sauter [246].

This presentation focuses on static perfect plasticity also called the Hencky model. As pointed in [277], the Hencky plasticity is not mechanically relevant but for some very specific cases. It does not account for the path dependency shown by the experiments and thus is rather a non quadratic law. However it raises the same mathematical difficulties as the quasi-static case and when the numerical solution of the quasi-static evolution comes into question, a time discretization leads to a sequence of Hencky model to be solved. Finally for the shape optimization it will be easier to first study this steady problem as time-dependent problems lead to backward adjoint problems.

First we will present the mechanical laws of perfect plasticity, being a bit general at the begining to draw the context and studying a quasi-static evolution to infer the static model. Then the classical mathematical analysis of this model is given and some regularizations are discussed. Finally the different ways to numerically solve the plasticity equations are briefly investigated.

4.2 Mechanical laws

A first step to understand elasto-plasticity is to study toy systems composed of springs and Saint-Venant bodies, chapter 3 in [199]. We skip this step and focus on the construction of the plasticity laws. We choose to neglect the rate-dependence (there is no dependency on how fast the loads are applied) and the effects of temperature (the temperature remains constant). We take the notations of linearized elasticity in 1.3.3.

From thermodynamic considerations, we can deduce that the strain has to be additively decomposed into two parts ([124], chapter 3). The first one is the elastic part which we note e_e and the second one is the plastic strain: e_p. Then we have:

$$e(u) = e_e + e_p. \tag{4.1}$$

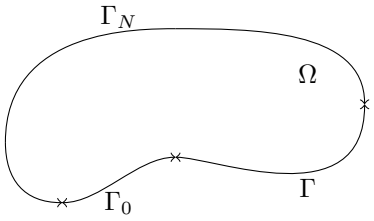

Figure 4.2: The open set Ω.

It has to be mentionned that if $e(u)$ is the symmetric part of the gradient of the displacement u, it is not the case for e_e and e_p which are however symmetric. The constraint tensor σ is only related to the elastic part:

$$\sigma = Ae_e, \tag{4.2}$$

and replacing it in the (4.1):

$$e(u) = A^{-1}\sigma + e_p. \tag{4.3}$$

The other fundamental ingredient is the elastic region and the yield surface. It means that as long as σ stays in a certain set called the elastic region the plastic rate is equal to zero: $\dot{e}_p = 0$. When σ reaches the yield surface which is the boundary of the elastic region, the plastic rate can vary. We suppose to simplify and also it is the only case we will study in this thesis that these regions are defined by a continuous function $\mathcal{F}$, called the yield function. Thus we call K the subset of symmetric order two tensors:

$$K = \left\{\tau \in \mathbb{M}_s^d | \mathcal{F}(\tau) \leq 0\right\}. \tag{4.4}$$

with $\mathbb{M}_s^d$ the space of symmetric tensors of order two in dimension d. The elastic region corresponds to $\mathcal{F}(\tau) < 0$ and the yield surface is defined by $\mathcal{F}(\tau) = 0$. When we are on the yield surface we have to define the evolution of the plastic strain e_p by giving the direction of the tensor without giving its norm [199]:

$$\dot{e}_p = \dot{\eta} g(\sigma). \tag{4.5}$$

This equality is called the flow rule. The function g defines the direction of the plastic deformation speed and depends on σ the stress. The parameter $\dot{\eta}$, which is a priori unknown, is the norm of this speed. This formulation is quite general and we focus now more specifically on perfect plasticity.

4.2.1 Drucker-Ilyushin postulate and Hill principle

The difficulty lies in the determining of the flow rule and therefore of g [199]. It is needed to rely on some physical principles which we sought as universal as possible. The second principle of thermodynamics gives, through the inequality of Clausius-Duhem, that the internal production of entropy has to be non negative during the evolution. In perfect plasticity this implies that the plastic dissipation should be non negative:

$$\sigma : \dot{e}_p \geq 0. \tag{4.6}$$

However this inequality is not selective and another principle is needed. Before giving it we define a deformation cycle and the deformation work [199].

Definition 4.2.1. *A deformation cycle is a path (a continuous application) $t \to e(t)$ from $[t_0, t_1]$ to $\mathbb{M}_s^d$ such that $e(t_0) = e(t_1)$.*

Definition 4.2.2. *If we take a deformation path $t \to e(t)$ compatible with the flow rule and its corresponding constraint path $t \to \sigma(t)$, the energy received by a volume element between t_0 and t_1 is:*

$$\mathcal{W} = \int_{t_0}^{t^1} \sigma(t) : \dot{e}(t)\, dt. \tag{4.7}$$

Then the postulate of Drucker-Ilyushin is:

Drucker-Ilyushin postulate The deformation work has to be non negative for every deformation cycle compatible with the flow rule

In fact this postulate is not used and we prefer to use another principle which is in certain cases equivalent to Drucker-Ilyushin principle ([199], 3.3.4):

Hill principle or maximum plastic work At every time when the plastic deformation rate is defined, the dissipated power is greater or equal to the power which would be dissipateed by every admissible stress tensor with the same plastic rate strain:

$$\sigma : \dot{e}_p \geq \tau : \dot{e}_p \ \forall \tau \in K \tag{4.8}$$

We note that this principle implies the Clausius-Duhem inequality as soon as $0 \in K$ and that it implies that if $\sigma \in K$ then $\dot{e}_p \in N_K(\sigma)$, as defined in 2.3.19. It also implies important properties for the flow rule and the elastic region ([199], 3.3.5) and ([124], 3.2 p 57).

Proposition 4.2.3. *A perfect elastoplastic material satisfies the maximum plastic work principle if and only if*

- *K is a convex set*
- *The plastic rate $\dot{e}_p$ is in the normal cone of K at the point σ and we have the following conditions on $\mathcal{F}$ and $\dot{\eta}$:*

$$\dot{\eta} \geq 0 \ \mathcal{F} \leq 0 \ \dot{\eta}\mathcal{F} = 0. \tag{4.9}$$

If ∂K is smooth in the neighborhood of σ it particularly means that:

$$\dot{e}_p = \dot{\eta} \frac{\partial \mathcal{F}}{\partial \sigma}(\sigma). \tag{4.10}$$

Finally we give a remark on the link between plastic incompressibility, the Hill principle and the form of the convex set K ([199], 3.3.6).

Definition 4.2.4. *The plastic flow is said to be incompressible if, at every time, $Tr(\dot{e}_p) = 0$.*

We recall the classical decomposition of a symmetric tensor of order two into a deviatoric part and into an hydrostatic (spherical) part. These two components belong to two complementary spaces. If we take σ a symmetric tensor of order two:

- its deviatoric part writes $\sigma_D = \sigma - \dfrac{Tr(\sigma)}{d} I$.
- its hydrostatic part writes $\sigma_H = \dfrac{Tr(\sigma)}{d} I$.

We note S the space of spherical tensors:

$$S = \{\tau \,|\, \exists \alpha \in \mathbb{R},\, \tau = \alpha I\}. \tag{4.11}$$

Proposition 4.2.5. *A perfect elastoplastic material which satisfies the maximum plastic work principle has an incompressible plastic flow if and only if the convex set K is invariant by translation in the direction of the spherical tensors:*

$$\forall \tau \in K,\ \forall p \in \mathbb{R},\ \ \tau + pI \in S \Leftrightarrow\ \forall t,\ Tr\left(\dot{e}_p(t)\right) = 0. \tag{4.12}$$

Plastic incompressibility means that the volume remains constant as the dislocations move. In the following the criteria used will imply plastic incompressiblity.

4.2.2 The mechanical problem

We can sum up the different equations which characterize the evolution of the perfect elastoplastic material, supposing the Hill principle satisfied. To get static equations we only remove the dependency on the time and the plastic rate $\dot{e}_p$ becomes e_p:

$$\begin{cases} e(u) & = e_p + A^{-1}\sigma & \text{in } \Omega \\ e_p : (\tau - \sigma) & \leq 0 & \forall \tau \in K \\ \sigma \in K & & \\ -\operatorname{div}(\sigma) & = f & \text{in } \Omega \\ u & = 0 & \text{on } \Gamma_0 \\ \sigma n & = g & \text{on } \Gamma_N \\ \sigma n & = 0 & \text{on } \Gamma. \end{cases} \tag{4.13}$$

We note that there is no need to write the flow rule as its form is implied by the maximum plastic work principle.

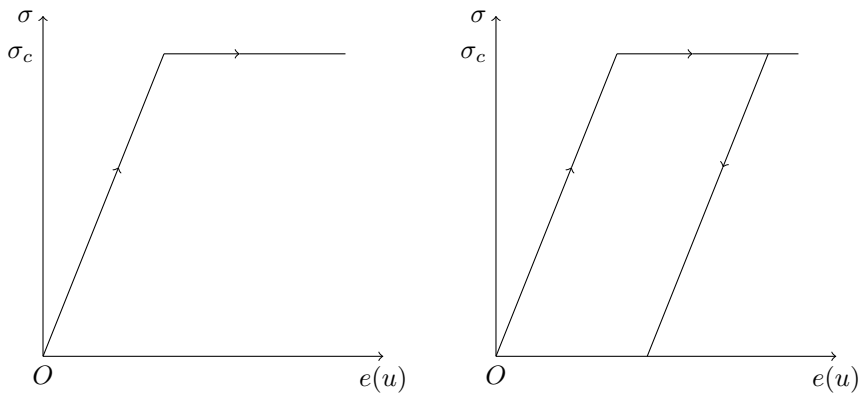

(a) Hencky's law (b) Quasi-static law

Our final remark on this mechanical problem is that these equations could have been infered without the mechanical reasoning, just by looking at the curve of σ with respect to $e(u)$ in a 1D test [98], see figure 4.3(b) for the curve. Looking at the quasistatic evolution, we write the variation of the strain:

$$de(u) = de_p + de_e$$

and

$$d\sigma = Ade_e.$$

Then we can derive the following conditions

$$\begin{cases} de_p = 0 \text{ when } \sigma < \sigma_c \\ \text{ or } (\sigma = \sigma_c \text{ and } d\sigma < 0) \\ de_p \geq 0 \text{ when } \sigma = \sigma_c \text{ and } d\sigma = 0 \end{cases}$$

which is equivalent to:

$$\begin{cases} de_p(\tau - \sigma) \leq 0, \ \forall \tau \\ \text{such that } \tau \leq \sigma_c \text{ and } \sigma \leq \sigma_c \\ de_p d\sigma = 0. \end{cases}$$

Finally substituing de_p by e_p (or $\dot{e}_p$ in the quasistatic case) and $d\sigma$ by $\dot{\sigma}$ we get the plastic conditions in dimension 1, noticing that $\dot{e}_p\dot{\sigma} = 0$ can be deduced from the conditions $\dot{e}_p(\tau - \sigma) \leq 0, \ \forall \tau$ as soon as σ is differentiable with respect to the time. Then we get the Hencky model by replacing $\dot{e}_p$ by e_p.

4.2.3 Two particular yield functions

There are two famous criteria which are used in perfect plasticity:

- The Tresca criterion
- The Von Mises criterion

The Tresca criterion

This criterion relies on the fact that σ is a symmetric tensor of order two. This means that it can be diagonalised and that its eigenvalues are real. We call $(\sigma_i)_{1 \leq i \leq d}$ its eigenvalues. The idea is to control the maximal shear stress which gives the following yield function:

$$\mathcal{F}(\sigma) = \frac{1}{2} \max_{1 \leq i,j \leq d} |\sigma_i - \sigma_j| - \sigma_c, \tag{4.14}$$

where $\sigma_c > 0$ is a scalar threshold.

The domain K is convex and invariant by translation in the direction of the spherical tensors ([199], 3.4.2). It means that the plasticity flow is incompressible. For more details we refer to [199], 3.4.2 and [124], 3.3.

The Von Mises criterion

The Von Mises criterion is defined by, ([199], 3.4.1 and [124], 3.3):

$$\mathcal{F}(\sigma) = \sqrt{\sigma_D : \sigma_D} - \sigma_c = |\sigma_D| - \sigma_c \tag{4.15}$$

where $\sigma_c > 0$ is a scalar threshold.

As for the Tresca model, K is a convex set invariant by translation in the direction of the spherical tensor. Contrary to the Tresca model, the Von Mises criterion is smooth. In this thesis we will only consider this yield criterion.

In the following we briefly present different plasticity models which does not fulfill one of the assumptions made for the perfect elastoplasticity.

4.2.4 Associated plasticity or non associated plasticity

We have seen that the Hill principle implies that the strain rate is in the normal cone of K which has to be convex. The laws in which the strain rate is in the normal cone of K are called associated. We note that the flow rule can be associative without assuming the Hill principle.

Sometimes an associated flow law is not the right choice to model the plastic behavior of some materials, for instance concrete, soil and rock. Then taking G a multifunction from $\mathbb{M}_s^d$ to $\mathbb{M}_s^d$, with $\mathbb{M}_s^d$ the space of symmetric matrix of dimension d, the flow rule is taken as:

$$\dot{e}_p \in G(\sigma) \tag{4.16}$$

and G is not anymore the normal cone of K at the point σ. The multifunction G has to be specified explicitly and is not anymore depending on the yield function $\mathcal{F}$. There are two important such laws: the Mohr-Coulomb and Drucker-Prager laws. We refer to [124] (section 3.4 in particular) and [246] for more details on non associated flow rules and on these two particular laws.

4.2.5 Hardening

The plasticity is said to be perfect when the set K does not vary as time changes. When it is not the case we talk about hardening. The idea is that the development of the dislocations is hindered by the previous created dislocations and this could imply some resistance to further plastification, needing a stronger and stronger constraint. In uniaxial tests this can be seen in the figure 4.1(b) on the left test for instance.

To account for this phenomenon the idea is to add some internal variables. We refer to [199], 3.2.4, and the whole book of Han and Reddy [124] for a thorough analysis of plasticity with hardening.

4.3 Mathematical formulations

In this section, we would like to mathematically analyse the problem (4.13). For quasistatic evolutions we refer to [124], [229], [277], [276], [275] and [79], for the static case to [283], [190], [30], [115], [21].

First we recall some duality and convex analysis definitions and rewrite the plasticity conditions in this framework. Then we present a first approach doomed to fail and explain what are the problems encountered. Then the now classical approach of static perfect plasticity is given. We suppose that K is invariant by translation in the direction of the spherical tensors.

4.3.1 Duality Analysis

Fro convex analysis results and definitions we refer to 2.2.1 and the references given, for convex duality results we refer to [102]. Here we only give some definitions and apply them to the problem of perfect elastoplasticity.

Definition 4.3.1. *The Legendre-Fenchel conjugate of a function f from a normed vector space X to $\bar{\mathbb{R}} = \mathbb{R} \cup \{-\infty, +\infty\}$ is noted f^* and is defined for $x^* \in X^*$ by:*

$$f^*(x^*) = \sup_{x \in X} \{\langle x^*, x\rangle - f(x)\} \tag{4.17}$$

where $\langle \cdot, \cdot \rangle$ is the duality product between X^* and X.

Proposition 4.3.2. *If f is proper, convex and l.s.c. then so is f^* and we have:*

$$(f^*)^* = f. \tag{4.18}$$

Then we introduce the notion of subdifferential which is of a common use in the plasticity theory [229], [277]:

Definition 4.3.3. *Let f be a convex function on X. We define the subdifferential $\partial f(x)$ of f at the point x the (possibly empty) subset of X^* defined by:*

$$\partial f(x) = \{x^* \in X' \,|\, f(y) \geq f(x) + \langle x^*, y - x\rangle, \ \ \forall y \in X\} \tag{4.19}$$

The element of the subdifferential are called subgradients. See [75] for more details on this notion.

Finally we introduce the notion of normal cone to a convex set K, its indicator function and the associated support function:

Definition 4.3.4. *Let K be a subset $K \subset X$.*

- *Its indicator function is:*
$$\mathbb{1}_K = \begin{cases} 0, & x \in K \\ +\infty, & x \notin K. \end{cases} \tag{4.20}$$
We note that if K is nonempty, convex and closed, $\mathbb{1}_K$ is proper convex and l.s.c..

- *The support function is defined on X^* by:*
$$H_K(x^*) = \sup_{x \in K} \langle x^*, x \rangle \tag{4.21}$$

- *If K is a convex set we can define its normal cone (it is a generalization of the definition 2.3.19) at a point $x \in K$:*
$$N_K(x) = \{x^* \in X^* \mid \langle x^*, y - x \rangle \leq 0, \ \ \forall y \in K\} \tag{4.22}$$

Proposition 4.3.5. *Let K be a non empty subset of X:*
$$\mathbb{1}_K^* = H_K \tag{4.23}$$
and
$$\partial \mathbb{1}_K(x) = \begin{cases} \varnothing, & x \notin K \\ N_K(x), & x \in K. \end{cases} \tag{4.24}$$
If K is nonempty convex and closed then:
$$\mathbb{1}_K = H_K^* \tag{4.25}$$

Proof.
$$\mathbb{1}_K^* = \sup_{x \in X} \{\langle x^*, x \rangle - \mathbb{1}_K(x)\}$$
and if $x \notin K$, $\mathbb{1}_K = +\infty$. So we can limit the supremum on K and as $\mathbb{1}_K(x) = 0$ when $x \in K$, it implies (4.23).
Now we compute the subdifferential of the indicator function. Suppose first $x \notin K$ then $\mathbb{1}_K(x) = +\infty$. If $\partial \mathbb{1}_K(x)$ is not empty then it would exist x^* such that for every $y \in X$
$$\mathbb{1}_K(y) \geq \mathbb{1}_K(x) + \langle x^*, y - x \rangle.$$
Then taking $y \in K$ leads to a contradiction: $\partial \mathbb{1}_K(x)$ is empty.
Now suppose $x \in K$ then taking $x^* \in \partial \mathbb{1}_K(x)$ leads to the following inequality for every $y \in X$:
$$\mathbb{1}_K(y) \geq \langle x^*, y - x \rangle, \tag{4.26}$$
as $\mathbb{1}_K(x) = 0$. But when $y \notin K$, $\mathbb{1}_K(y) = +\infty$ therefore fulfilling the condition (4.26) is equivalent to be such that for every $y \in K$
$$0 \geq \langle x^*, y - x \rangle.$$
This is the characterization of the normal cone.
For (4.25) it suffices to apply the proposition 4.3.2. □

Having given these definitions we can come back to plasticity. K is a non-empty closed convex set. The maximum plastic work principle is equivalent to say that $e_p \in \partial \mathbb{1}_K(\sigma)$. We have the following duality result:

Proposition 4.3.6. *Saying that $e_p \in \partial \mathbb{1}_K(\sigma)$ is equivalent to say that $\sigma \in \partial H_K(e_p)$ and $\sigma \in K$.*

Proof. We suppose first that $e_p \in \partial \mathbb{1}_K(\sigma)$. Since $\partial \mathbb{1}_K(\sigma)$ is not empty it means that $\partial \mathbb{1}_K(\sigma) = N_K(\sigma)$ and $\sigma \in K$. It also means that for every $\tau \in K$:
$$\langle e_p, \tau \rangle \leq \langle e_p, \sigma \rangle$$
Passing to the supremum with respect to τ in this inequality gives
$$H_K(e_p) \leq \langle e_p, \sigma \rangle$$
and as $\sigma \in K$ we have the equality. It follows that for every f:
$$H_K(e_p) + \langle \sigma, f \rangle - \langle \sigma, e_p \rangle = \langle \sigma, f \rangle \leq H_K(f).$$

This exactly means that $\sigma \in \partial H_K(e_p)$.
Now we prove the opposite implication. As $\sigma \in \partial H_K(e_p)$ for every f:

$$H_K(f) \geq H_K(e_p) + \langle \sigma, f - e_p \rangle$$

and

$$\langle \sigma, f \rangle - H_K(f) \leq \langle \sigma, e_p \rangle - H_K(e_p)$$

Taking the supremum with respect to f changes the left handside into the conjugate of the support function which is the indicator function. As $\sigma \in K$ we get:

$$0 \leq \langle \sigma, e_p \rangle - H_K(e_p)$$

which implies that:

$$H_K(e_p) \leq \langle \sigma, e_p \rangle$$

and for every $\tau \in K$:

$$\langle e_p, \tau \rangle \leq \langle e_p, \sigma \rangle$$

and $e_p \in \partial \mathbb{1}_K(\sigma)$. □

Remark 4.3.7. *At this point we point out that this approach is interesting as it enables a generalization with the use of responsive maps and gauge which is detailed in [124], chapter 4.*

The goal of this section was to show that σ and e_p are somehow variables in duality. In plasticity the problems posed with respect to σ are under the dual form, the ones posed with respect to e_p are under the primal form, [246]. In the next part we give a first approach to address the existence and uniqueness of a solution to the perfect plasticity problem.

4.3.2 A first approach

In this first approach we suppose that $u \in H^1_{\Gamma_0}(\Omega)^d$. We also introduce the admissible set for σ. First we define the set

$$H_s(\mathrm{div}, \Omega, d) = \left\{ \tau \in L^2_s(\Omega)^{d \times d} \,|\, \mathrm{div}\sigma \in L^2(\Omega)^d \right\} \tag{4.27}$$

where by $L^2_s(\Omega)^{d\times d}$ we mean symmetric matrices of dimension d whose coefficients belong to $L^2(\Omega)$. This space is studied in [121] or [50]. The important fact is that it is a Hilbert space with following scalar product:

$$(\sigma, \tau)_{H_{\mathrm{div}}} = (\sigma, \tau)_{L^2} + (\mathrm{div}\sigma, \mathrm{div}\tau)_{L^2}. \tag{4.28}$$

The trace operator is not defined but we can define the normal trace operator γ_N which associates with $\tau \in H_s(\mathrm{div}, \Omega, d)$ its normal trace $\tau n \in H^{-\frac{1}{2}}(\partial\Omega, \mathbb{R}^d)$. So we can define:

$$\Sigma_{\mathrm{div}}(g) = \{ \tau \in H_s(\mathrm{div}, \Omega, d) \,|\, \gamma_N(\tau) = g \}. \tag{4.29}$$

Finally we define:

$$S(f, g) = \{ \tau \in \Sigma_{\mathrm{div}}(g) \,|\, -\mathrm{div}\sigma = f \text{ in } \Omega \} \tag{4.30}$$

We suppose $\sigma \in S(f, g)$. The following presentation is given in [283]. Its idea is to adpot the point of view of [210] and so to consider that:

$$\sigma \in \partial\psi(e(u)) \tag{4.31}$$

and by duality properties shown in [283] I.2:

$$e(u) \in \partial\psi^*(\sigma) \tag{4.32}$$

where ψ is a called a superpotential. See [277] and [229] for the same approach in the case of quasi-static evolution.

It has to be noticed that this is not the same formulation we found in the previous part. To stick to this presentation we need to reformulate our problem passing from (σ, e_p) to $(\sigma, e(u))$. It is not so difficult since:

$$e(u) = A^{-1}\sigma + e_p$$

Yet $e_p \in \partial \mathbb{1}_K(\sigma)$ so $e(u) - A^{-1}\sigma \in \partial \mathbb{1}_K(\sigma)$ and $e(u) = A^{-1}\sigma + \partial \mathbb{1}_K(\sigma)$

Proposition 4.3.8.

$$A^{-1}\sigma + \partial \mathbb{1}_K(\sigma) = \partial\psi^*(\sigma) \tag{4.33}$$

with $\psi^*(\sigma) = \dfrac{1}{2} A^{-1}\sigma : \sigma + \mathbb{1}_K(\sigma)$.

This proposition gives the ψ^* of (4.32).

Proof. From classical properties of subdifferential:

$$A^{-1}\sigma + \partial \mathbb{1}_K(\sigma) \subset \partial\left(\frac{1}{2}A^{-1}\sigma : \sigma + \mathbb{1}_K(\sigma)\right).$$

It remains to prove the inverse inclusion. If $\sigma \notin K$ both sets are empty and the property is proved. Otherwise we take $e \in \partial\psi^*(\sigma)$. Then for every $\tau \in K$:

$$\frac{1}{2}A^{-1}\tau : \tau \geq \frac{1}{2}A^{-1}\sigma : \sigma + \langle e, \tau - \sigma\rangle$$

As K is a nonempty convex set, we can take $\tau = \sigma + t(\phi - \sigma) \in K$ with $t \in [0,1]$ and $\phi \in K$ in the inequality. This gives with the symmetric properties of A:

$$\frac{t^2}{2}A^{-1}(\phi - \sigma) : (\phi - \sigma) + tA^{-1}\sigma : (\phi - \sigma) \geq t\langle e, \phi - \sigma\rangle.$$

Dividing by t and making t goes to 0 we get that for every $\phi \in K$:

$$\langle A^{-1}\sigma, \phi - \sigma\rangle \geq \langle e, \phi - \sigma\rangle$$

which exactly means that $e \in A^{-1}\sigma + \partial \mathbb{1}_K(\sigma)$ and the proposition is proved. □

The dual problem

Following the computation in [283] we end up with a maximisation problem solved by σ:

$$\sigma = \text{argmin}_{\tau \in S(f,g)}\psi^*(\tau) \tag{4.34}$$

which can be rewritten as:

$$\begin{cases} \text{Maximize } -\dfrac{1}{2}\displaystyle\int_\Omega A^{-1}\sigma : \sigma \, dx \\ \sigma \in K \\ \displaystyle\int_\Omega \sigma : \epsilon(v)\, dx = \int_\Omega f \cdot v \, dx + \int_{\Gamma_N} g \cdot v \, ds, \ \ \forall v \in H^1_{\Gamma_0}(\Omega)^d \end{cases} \tag{4.35}$$

which admits a variational inequality formulation: for every $\tau \in S(f,g) \cap K$ find $\sigma \in S(f,g) \cap K$ such that

$$\int_\Omega A^{-1}\sigma : (\tau - \sigma)\, dx \geq 0. \tag{4.36}$$

The theorem 4.1 in [283] or the theorem 6.1 in [98] give the existence and uniqueness of a solution.

Theorem 4.3.9. *If $S(f,g) \cap K \neq \emptyset$, the problem (4.35) has a unique solution*

The displacement problem

The first difficulty of the analysis of this problem is that contrary to the problem written with respect to the constraints σ we do not have an explicit expression of ψ. The problem to solve is then:

$$\begin{cases} \text{Minimize } \displaystyle\int_\Omega \psi(e(v))\, dx - \int_\Omega f \cdot v \, dx - \int_{\Gamma_N} g \cdot v \, ds \\ v \in H^1_{\Gamma_0}(\Omega)^d \end{cases} \tag{4.37}$$

Its study is done in [283] chapter I section 4 where it is proved that (4.35) is the dual problem of (4.37). Another interesting remark of theorem 4.1 in [283] is that, as soon as there exists a solution to the dual problem, the infimum of (4.37) is finite and equal to the supremum of (4.35).

However it is not possible to prove the existence of a solution to the displacement problem, written like (4.37). There are several ways to understand this issue. The first one is a mechanical understanding of plasticity. The dislocations in the material can produce displacement discontinuities of d-1 dimension [277], [283] chapter 6, chapter V written by Suquet section 3.4 in [211]. Furthermore the discontinuity can be created at the boundary of Ω and especially at Γ_0 preventing the limit condition from being fulfilled. This urges for a change of paradigm in the choice of the admissible space for the displacement.

Another way to observe this existence difficulty is to write the problem under a saddle point problem and work on the Lagrangian formulation ([246] sections 3.2 3.3 in chapter 2). Then the problem can be written under the form of variational inequality coupled with a variational equality. The displacement u plays the role of the Lagrangian multiplier:

$$\begin{cases} \displaystyle\int_\Omega \sigma : e(v)\,dx = \int_\Omega f\cdot v\,dx + \int_{\Gamma_N} g\cdot v\,ds,\ \ \forall v \in H^1_{\Gamma_0}(\Omega)^d \\ \displaystyle\int_\Omega A^{-1}\sigma : (\tau-\sigma)\,dx \geq \int_\Omega e(u) : (\tau-\sigma)\,dx,\ \ \forall \tau \in K. \end{cases} \tag{4.38}$$

Since the variational inequality is the characterization of the projection on K with the norm associated with the scalar product of A^{-1}, noting $P_K^{A^{-1}}$ this projection we have

$$\sigma = P_K^{A^{-1}}(Ae(u)) \tag{4.39}$$

and

$$\int_\Omega P_K^{A^{-1}}(Ae(u)) : e(v)\,dx = \int_\Omega f\cdot v\,dx + \int_{\Gamma_N} g\cdot v\,ds,\ \ \forall v \in H^1_{\Gamma_0}(\Omega)^d. \tag{4.40}$$

Then if we define the operator $T(u) = -\text{div}\left(P_K^{A^{-1}}(Ae(u))\right)$ this operator is mononotone but not strongly monotone ([246] chapter 2 3.6). Furthermore it is not coercive and has an anisotropic linear growth. This forbids the use of classical theory of monotone operator [242]. An extensive study of such problems is done in [295].

Counter-example for coercivity In the case of the Von Mises criterion an explicit expression of the projection can be written [296], [295] and [140]:

$$P_K^{A^{-1}}(\tau) = \tau - \max\left(0, 1 - \frac{\sigma_c}{|\tau_D|}\right)\tau_D. \tag{4.41}$$

This enables to easily show why there is no coercivity. This comes from the fact that K is of the form $K = K_D \oplus \mathbb{R}I$, where K_D is closed and bounded in the space of deviatoric tensors. We outline a particular example on a 2D-rectangle domain $[0,1]\times[0,1]$ and choose $\Gamma_0 = \{(x,y)\,|\,x=0\}$. The idea is to find a sequence of $u_n \in H^1_{\Gamma_0}(\Omega)^2$ such that $\lim_{n\to\infty}\|u_n\|_{H^1} = \infty$, where thanks to Korn inequality we define $\|u_n\|_{H^1} = \|e(u_n)\|_{L^2}$, and $\lim_{n\to\infty}\dfrac{\int_\Omega P_K^{A^{-1}}(Ae(u_n))e(u_n)\,dx}{\|u_n\|_{H^1}} \neq +\infty$. So we define:

$$u_n = (0, g_n(x)) \tag{4.42}$$

with

$$g_n(x) = A_n x \tag{4.43}$$

where A_n is a real positive sequence which tends to $+\infty$. We also choose $A_n \geq \dfrac{\sigma_c}{\sqrt{2}\mu}$ which implies that

$$1 - \frac{\sigma_c}{\sqrt{2}\mu A_n} \geq 0.$$

If we compute $e(u_n)$ we have that $e(u_n)_D = e(u_n)$ as its trace is null and $|e(u_n)| = |e(u_n)|_D = \dfrac{A_n}{\sqrt{2}}$ which tends to $+\infty$. Then we compute:

$$\begin{aligned} \langle P_K^{A^{-1}}(Ae(u_n)), e(u_n)\rangle &= \langle Ae(u_n), e(u_n)\rangle - \langle (1 - \frac{\sigma_c}{\sqrt{2}\mu A_n})Ae(u_n)_D, e(u_n)_D\rangle \\ &= \langle Ae(u_n)_H, e(u_n)_H\rangle + \langle \frac{\sigma_c}{\sqrt{2}\mu A_n}Ae(u_n)_D, e(u_n)_D\rangle \\ &= \langle \frac{\sigma_c}{\sqrt{2}\mu A_n}Ae(u_n)_D, e(u_n)_D\rangle \\ &= CA_n \end{aligned}$$

where C is a constant independent of n. As

$$\lim_{n\to\infty}\frac{\int_\Omega P_K^{A^{-1}}(Ae(u_n))e(u_n)\,dx}{\|u_n\|_{H^1}} = 2C$$

we have found a counter-example to the coercivity of the operator.

4.3.3 The classical equations of static perfect plasticity

We follow first the idea of [283]. The first thing which can be done is to relax the limit conditions in the admissible space and put some kind of internal penalization in the function to minimize to account for the conditions we removed. The idea is to seperate tangential and normal conditions. Indeed the discontinuities created by plasticity can only be created tangential to the boundary whereas the normal displacement remains continuous. So instead of asking $u = 0$ on Γ_0 we ask that $u \cdot n = 0$ on Γ_0. We also add in the functionnal to be minimized a term:

$$\int_{\Gamma_0} \psi_\infty \left(\mathcal{J}(-v_t)\right) \, ds \tag{4.44}$$

where $\psi_\infty(\xi) = H_{K_D}$ and $\mathcal{J}$ is a tensor defined by:

$$\mathcal{J}_{i,j}(p) = \frac{1}{2}\left(p_i n_j + p_j n_i\right) \tag{4.45}$$

Then to account for the possible discontinuities inside the domain, we replace H^1 regularity by a weaker regularity. We introduce the space of bounded deformation $BD(\Omega)$ which is similar to the space of bounded variation $BV(\Omega)$. There is an extensive study of this space in [276] and [283] II.2 II.3. Here we only give the definition of this space:

$$BD(\Omega) = \left\{u \in L^1(\Omega)^d \,|\, e(u) \in M_1(\Omega, \mathbb{R})^{d\times d}\right\} \tag{4.46}$$

and the associated norm:

$$\|u\|_{BD(\Omega)} = \|u\|_{L^1(\Omega)} + \sum_{i,j=1}^{d} \|(e(u))_{i,j}\|_{M_1(\Omega)}, \tag{4.47}$$

with $M_1(\Omega, \mathbb{R})$ being the space of bounded measure on Ω, which means that if $\mu \in M_1(\Omega, \mathbb{R})$ then μ is a measure and there exists $C > 0$ such that for every $\phi \in C_c^0(\Omega)$:

$$|\mu(\phi)| \leq C\|\phi\|_\infty. \tag{4.48}$$

We finally introduce the spaces:

$$U(\Omega) = \left\{v \in BD(\Omega) \,|\, \mathrm{div} v \in L^2(\Omega)^d\right\} \tag{4.49}$$

and

$$\mathcal{C}_a = \{v \in U(\Omega) \,|\, v \cdot n = 0 \text{ on } \Gamma_0\} \tag{4.50}$$

and the new problem for the displacement is given by:

$$\begin{cases} \text{Minimize } \displaystyle\int_\Omega \psi(e(v))\, dx + \int_{\Gamma_0} \psi_\infty\left(\mathcal{J}(-v_t)\right)\, ds - \int_\Omega f \cdot v\, dx - \int_{\Gamma_N} g \cdot v\, ds \\ v \in \mathcal{C}_a \end{cases} \tag{4.51}$$

The theorem 6.1 in [283] ensures that the infinmum value of (4.51) coincides with the one of (4.37). In section 7 after having given a sense to $\sigma : e(u)$ (as a measure), the author proved that for $f \in L^\infty(\Omega)^d$, $g \in L^1(\Gamma_N)^d$, Ω of C^2 regularity, the problem (4.51) and (4.35) are in duality in the sense that the value of the infimum for the displacement problem is equal to the value of supremum for the constraint problem. Then section 8 in [283] concludes the study by giving the existence of a displacement under several conditions (theorem 8.1):

Theorem 4.3.10. *We note $\mathbb{M}_s^d$ the space of symmetric matrix of dimension d. Let Ω be C^2, $f \in L^\infty(\Omega)^d$, $g \in L^\infty(\Gamma_N)^d$, if Γ_0 is not empty and the safe-load condition is fulfilled:*

$$\exists \bar{\sigma} \in S(f,g),\ \epsilon > 0 \text{ such that } \forall \xi \in \mathbb{M}_s^d \text{ with } |\xi| \leq \epsilon,\ \bar{\sigma}(x) + \xi \in K \text{ a.e. in } \Omega \tag{4.52}$$

then the displacement problem (4.51) *has a solution in $U(\Omega)$.*

Remark 4.3.11. *Note that there is not uniqueness of the displacement and that a counter-example can be found in [277].*

Remark 4.3.12. *The relaxation of the Dirichlet boundary conditions are not necessary. Instead we can define a space $BD(\overline{\Omega})$ and use the notion of external trace, see [277] 2.3. Then the problem can be put under the following weak formulation (see also [190] definition* 1.7*): find $(\sigma, u) \in K \times BD(\Omega)$ such that:*

$$\begin{cases} \displaystyle\int_\Omega \sigma : e(v)\, dx = \int_\Omega f \cdot v\, dx + \int_{\Gamma_N} g \cdot v\, ds,\ \ \forall v \in H^1_{\Gamma_0}(\Omega)^d \\ \displaystyle\int_\Omega A^{-1}\sigma : (\tau - \sigma)\, dx \geq -\langle u, \mathrm{div}(\tau - \sigma)\rangle,\ \ \forall \tau \in K \cap \Sigma_{\mathrm{div}}(g). \end{cases} \tag{4.53}$$

4.4 Perzyna penalization and other regularisations

In the previous section we briefly review the method developped in [283] to prove the existence of solutions the Hencky model. It has to be mentionned that for quasistatic evolution the usual method is to approximate the perfect elastoplastic problem by a formulation in which the superpotential is smooth. It was the case in the seminal work of Duvaut and Lions [98] and for complete results in the space $BD(\Omega)$ see [277] or [229] (otherwise for a direct approach see [79]). Our goal is to introduce the elasto-visco plastic model of Perzyna and give a brief analysis of the existence of solution and of the convergence to perfect elastoplasticity. Then we cite other classical regularisations which will not be used in this thesis.

4.4.1 Perzyna penalization

Formulation of the problem

There are several ways to introduce the Perzyna penalization. From the point of view of optimization it consists in taking the problem (4.35) and replacing the constraint that $\sigma \in K$ by an external penalization. The chosen penalisation involve the projection $P_K^{A^{-1}}$ and we add in the optimization problem, for a small $\eta > 0$:

$$\frac{1}{2\eta}\int_\Omega A^{-1}\left(\sigma - P_K^{A^{-1}}(\sigma)\right) : \left(\sigma - P_K^{A^{-1}}(\sigma)\right) dx. \tag{4.54}$$

This leads to the following system of variational equations:

$$\begin{cases} \displaystyle\int_\Omega \sigma^\eta : e(v)\, dx = \int_\Omega f\cdot v\, dx + \int_{\Gamma_N} g\cdot v\, ds, \ \ \forall v \in H^1_{\Gamma_0}(\Omega)^d \\ \displaystyle\int_\Omega A^{-1}\sigma^\eta : \tau\, dx + \frac{1}{\eta}\int_\Omega A^{-1}\left(\sigma^\eta - P_K^{A^{-1}}(\sigma^\eta)\right) : \tau = \int_\Omega e(u^\eta) : \tau\, dx, \ \ \forall \tau \in L^2_s(\Omega)^{d\times d}. \end{cases} \tag{4.55}$$

Another way to get this formulation, see [246], is to apply the Moreau-Yosida approximation of the indicator function of K. If we note $\mathbb{1}_K^\eta$ the Moreau-Yosida approximation we have:

$$\mathbb{1}_K^\eta(\sigma) = \frac{1}{2\eta}A^{-1}\left(\sigma - P_K^{A^{-1}}(\sigma)\right) : \left(\sigma - P_K^{A^{-1}}(\sigma)\right) dx = \frac{1}{2\eta}\left\|\sigma - P_K^{A^{-1}}(\sigma)\right\|^2_{A^{-1}}. \tag{4.56}$$

Then we can write the approximate condition for $e_p \in \partial\mathbb{1}_K(\sigma)$. As $\sigma \to \mathbb{1}_K^\eta(\sigma)$ is Fréchet differentiable (theorem 2.3.5), its subdifferential reduces to its gradient and we can write (pointwise) for the approximation e_p^η:

$$e_p^\eta = \frac{1}{\eta}A^{-1}\left(\sigma - P_K^{A^{-1}}(\sigma)\right). \tag{4.57}$$

This directly leads to (4.55) by integration of the plasticity equations (4.13), replacing the condition on e_p by (4.57).

This point of view also gives way to further simplification of the problem (4.55) which is a mixed variational problem. Indeed we can remove the variable σ.

From (4.57) we can deduce the expression of σ^η:

$$\sigma^\eta = Ae(u^\eta) - \frac{1}{\eta}\left(\sigma^\eta - P_K^{A^{-1}}(\sigma^\eta)\right). \tag{4.58}$$

This expression says that $Ae(u^\eta)$ is on the ray defined by σ^η and its projection and so it implies that (chapter 3 lemma 3.2 [246]):

$$P_K^{A^{-1}}(\sigma^\eta) = P_K^{A^{-1}}(Ae(u^\eta)). \tag{4.59}$$

This enables to write σ with respect to only u and transform the implicit definition into an explicit one:

$$\sigma^\eta = \frac{\eta}{1+\eta}Ae(u^\eta) + \frac{1}{1+\eta}P_K^\gamma(Ae(u^\eta)). \tag{4.60}$$

We can write the new nonlinear variational equation of the Perzyna visco elastoplasticity:

$$\int_\Omega \left(\frac{\eta}{1+\eta}Ae(u) + \frac{1}{1+\eta}P_K^\gamma(Ae(u))\right) : e(v)\, dx = \int_\Omega f\cdot v\, dx + \int_{\Gamma_N} g\cdot v\, ds \ \forall v \in H^1_{\Gamma_0}(\Omega)^d. \tag{4.61}$$

Mathematical Analysis

The Perzyna model was extensively studied and for the static case we refer to [283], [190] and [138]. Here we confine ourselves to formulate classical theorems on existence and uniqueness of solutions and on the convergence of the solution to a solution of perfect elastoplasticity as $\eta \to \infty$.

Theorem 4.4.1. *Under the safe-load condition* (4.52) *and with* $f \in L^2(\Omega)^d$ *and* $g \in L^2(\Gamma_N)^d$,*there exists a unique solution* $(\sigma_\eta, u_\eta) \in L^2_S(\Omega)^{d\times d} \times H^1_{\Gamma_0}(\Omega)^d$ *to the problem* (4.55), *where* $L^2_S(\Omega)^{d\times d}$ *is the set of matrices of d-dimension with coefficients in* $L^2(\Omega)$.

This theorem is proved in [283] chapter 3 section 1 theorem 1.1 and a proof in [138] proposition 4.4 is also done (with hardening, but the proof works without it).

Then we focus on the convergence of the model to the model of perfect elastoplasticity.

Theorem 4.4.2. *Under the safe-load condition* (4.52) *and with* $f \in L^d(\Omega)^d$ *and* $g \in C^0(\Gamma_N)^d$,

- σ_η *converges strongly in* $L^2_S(\Omega)^{d\times d}$ *to* σ, *the constraint tensor solution of the Hencky model* (4.37).
- *Up to a subsequence,* u_η *converges weakly in* $L^{\frac{d}{d-1}}(\Omega, \mathbb{R}^d)$ *and weakly in* $BD(\Omega)$ *to* u *the displacement solution of the Hencky model* (4.51).

The proof is given in [190]. In [283] the proof is done for σ and the weakly convergence of a subsequence of u_η is done in $U(\Omega)$ taking advantage of the compacity of the closed bounded sets in $BD(\Omega)$, with $f \in L^2(\Omega)^d$ and $g \in L^2(\Gamma_N)^d$. The above result is a bit more precise since $BD(\Omega)$ is continuously embedded in $L^{\frac{d}{d-1}}(\Omega, \mathbb{R}^d)$ (theorem 2.2 chapter 2 section 2 in [283]) notwithstanding the need of more regular f and g.

4.4.2 Other Regularizations

The Norton-Hoff viscoplasticity model

The idea of the Norton-Hoff model is to take a different superpotential defined in the case of Von Mises criterion by:

$$\psi^*_N(\tau) = \frac{1}{2}A^{-1}\tau : \tau + \frac{1}{N\sigma_c^{N-1}}|\sigma_D|^N. \tag{4.62}$$

The study of this problem is done in [30] (chapter 10) where it is used to prove that Hencky model admits solutions, in [283], chapter 1.2 and [284] (not assuming a Von Mises criterion) and in [277] for quasistatic evolution.

The existence and uniqueness of a solution is ensured (proposition 10.5 [30]) and the convergence (up to a subsequence) to solutions of the Hencky model also (theorem 10.8 and 10.12).

Hardening models

As said before, to account for hardening, one introduces some internal variables. The possible choices for the hardening model are numerous and convergence were only proved for particular cases. For instance in [283] chapter 3 section 1.3 the following model is introduced.

An euclidian vector space E_1 is introduced and a function ϕ, the hardening parameter, is introduced as a function from Ω to E_1. Then new convex sets are defined $\mathcal{K}_\eta \subset E \times E_1$ where η is a parameter meant to tend to 0. There are some important assumptions on $\mathcal{K}_\eta$:

$$\mathcal{K}_0 = K \times E_1 \tag{4.63}$$

and

$$\mathcal{K}_\eta \cap (E \times \{0\}) = K \times \{0\}. \tag{4.64}$$

Then the associated superpotential is defined by:

$$\psi^*_\eta(\tau, \xi) = \begin{cases} \frac{1}{2}A^{-1}\tau : \tau + \frac{1}{2}|\xi|^2 & \text{if } (\tau, \xi) \in \mathcal{K}_\eta \\ +\infty & \text{otherwise.} \end{cases} \tag{4.65}$$

Then the convergence of the solutions (σ_η, u_η) to solutions of perfect elastoplasticity is proved (up to subsequences for u_η) making strong assumptions, in particular the fact that the value of the primal and dual problems for the hardening model are equal and converge to the value given by the primal and dual problem of perfect elastoplasticity ((4.35) or (4.51)). However interesting examples are given for the Von Mises criterion where K takes the form:

$$K = \left\{\tau \in \mathbb{M}^3_s \,|\, |\tau_D| \leq \sigma_c\right\}. \tag{4.66}$$

and where the definition of $\mathcal{K}_\eta$ is either:

- $E_1 = \mathbb{R}$ and $\mathcal{K}_\eta = \left\{(\tau, \xi) \in \mathbb{M}^3_s \times \mathbb{R} \,|\, |\tau_D| \leq \sigma_c + \eta\xi\right\}$.
- $E_1 = (\mathbb{M}^3_s)_D$ and $\mathcal{K}_\eta = \left\{(\tau, \xi) \in \mathbb{M}^3_s \times E_1 \,|\, |\tau_D - \eta\xi| \leq \sigma_c\right\}$ which gives a problem not far from the the kinematic hardening model considered in [140].

For both cases the convergence is ensured. For the Hencky model we also refer to the article of [238] (linear hardening) in which some additional numerical approximation results are given. For dynamic and quasistatic problems we refer to [27] and [65].

4.5 Numerical plasticity

4.5.1 Numerical solver

In this final section, we briefly explain how to numerically compute the solutions of elasto perfectplasticity and Persyna viscoplasticity. We will focus on the formulations written with respect only to the displacement u as mixed formulations are much trickier to solve and demands a tough implementation effort ([50] for a general view of mixed formulations and for instance [155] and [124] for applications to plasticity).

For the perfect plasticity case it corresponds to the non linear variational equation (4.40). The approach which consists in using this formulation to solve the perfect plasticity problem is adopted in [296], [235], where the quasistatic problem is also solved by computing the solution of a sequence of such static problems. We focus on the Von Mises criterion as the projection can be explicitly computed (4.41). To discretize the equation (4.40) we use the finite element method, on a regular square mesh and Q_1 elements. This leads, as for contact problems, to a non linear problem which we solve thanks to a Newton method mixed with a fixed point method in the same way and for the same reasons given previously for the contact problems, section 3.4.3.

In the discretization, the term which is (a bit) unusual is the one making the deviatoric part of the strain appear:

$$\int_\Omega k(u(x))Ae(u)_D : e(v)_D \, dx = \int_\Omega 2\mu k(u(x))e(u)_D : e(v) \, dx \tag{4.67}$$

where k corresponds to the non-linear part, here the max function. If we take the same notations as in contact, the problem can be written under the following matrix form:

$$KU - K_D(U)U = F, \tag{4.68}$$

with $K_D(U)$ the matrix corresponding to the bilinear form:

$$(v, w) \to \int_\Omega 2\mu k(u(x))e(v)_D : e(w) \, dx. \tag{4.69}$$

The idea of the fixed point method is to compute a sequence U^n of solutions such that:

$$(K - K_D(U^n))U^{n+1} = F, \tag{4.70}$$

and U^0 arbitrary chosen. Finally we show how to discretize $e(u)_D : e(v)$ in 2D. We note ϕ^x_j the shape function at the node j for the x component and ϕ^y_j, the same for the component y. The linear span of the shape functions is V_h, with h the size of the side of an element. We note N the number of nodes. We can write:

$$u = \sum_{j=1}^{N} u^j_x \phi^x_j + u^j_y \phi^y_j$$

and the same for v:

$$v = \sum_{j=1}^{N} v^j_x \phi^x_j + v^j_y \phi^y_j.$$

Then we can compute:

$$e(u)_D : e(v) = \frac{1}{2}\frac{\partial v_x}{\partial x}\left(\frac{\partial u_x}{\partial x} - \frac{\partial u_y}{\partial y}\right) + \frac{1}{2}\frac{\partial v_y}{\partial y}\left(\frac{\partial u_y}{\partial y} - \frac{\partial u_x}{\partial x}\right) + \frac{1}{4}\left(\frac{\partial u_x}{\partial y} + \frac{\partial u_y}{\partial x}\right)\left(\frac{\partial v_x}{\partial y} + \frac{\partial v_y}{\partial x}\right). \tag{4.71}$$

We can developp:

$$e(u)_D : e(v) = \frac{1}{2}\left(\frac{\partial v_x}{\partial x}\frac{\partial u_x}{\partial x} - \frac{\partial v_x}{\partial x}\frac{\partial u_y}{\partial y} + \frac{\partial v_y}{\partial y}\frac{\partial u_y}{\partial y} - \frac{\partial v_y}{\partial y}\frac{\partial u_x}{\partial x} + \frac{\partial u_x}{\partial y}\frac{\partial v_x}{\partial y} + \frac{\partial u_x}{\partial y}\frac{\partial v_y}{\partial x} + \frac{\partial u_y}{\partial x}\frac{\partial v_x}{\partial y} + \frac{\partial u_y}{\partial x}\frac{\partial v_y}{\partial x}\right) \tag{4.72}$$

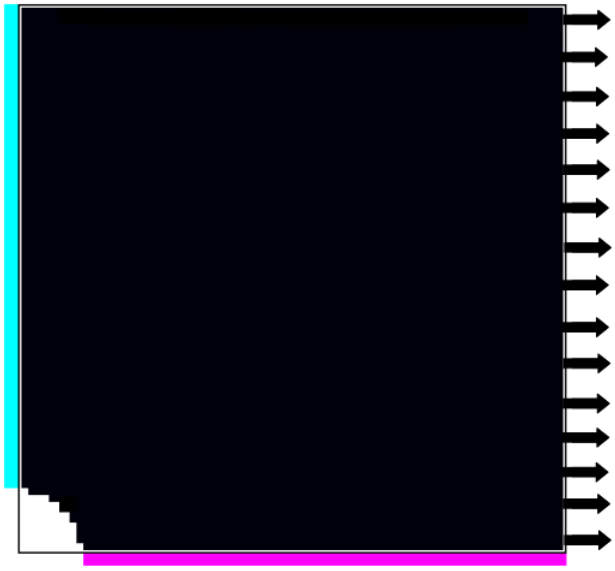

Figure 4.3: Load case for the numerical example.

Now we can use the discretized expression of u and v:

$$\begin{aligned} e(u)_D : e(v) = \frac{1}{2}\sum_{i,j=1}^{N} u_x^j v_x^i \left(\frac{\partial \phi_x^j}{\partial x}\frac{\partial \phi_x^i}{\partial x} + \frac{\partial \phi_x^j}{\partial y}\frac{\partial \phi_x^i}{\partial y}\right) + u_y^j v_y^i \left(\frac{\partial \phi_y^j}{\partial x}\frac{\partial \phi_y^i}{\partial x} + \frac{\partial \phi_y^j}{\partial y}\frac{\partial \phi_y^i}{\partial y}\right) \\ + u_y^j v_x^i \left(\frac{\partial \phi_y^j}{\partial x}\frac{\partial \phi_x^i}{\partial y} - \frac{\partial \phi_y^j}{\partial y}\frac{\partial \phi_x^i}{\partial x}\right) + u_x^j v_y^i \left(\frac{\partial \phi_x^j}{\partial y}\frac{\partial \phi_y^i}{\partial x} - \frac{\partial \phi_x^j}{\partial x}\frac{\partial \phi_y^i}{\partial y}\right), \end{aligned} \tag{4.73}$$

which enables to build the matrix $K_D(U^n)$ using quadrature formulae. We have to point out that the numerical solution which can be found will be more regular (H^1) than expected ($BD(\Omega)$ or $U(\Omega)$). A way to address this issue is to solve a regularized formulation which converges in a certain sense to the perfect elastoplastic problem. An error analysis is done in [238] for a regularization which corresponds to a linear hardening model.

One look at (4.61) shows that we do not need extra ingredients to discretize the Perzyna penalization formulation.

For further details and other approaches to the solution of such problems we refer to [261] and the part 2 of the thesis [246] which studied a large variety of method including the classical return algorithms, semi-smooth Newton approaches, active set methods and an augmented Lagrangian method derived from a generalized Moreau-Yosida penalisation. We also mention [296] for the static case, [124], [235] for the quasistatic case.

Remark 4.5.1. *In this part, we only focused on what is called the dual writing of the plasticity equations, that is to say a problem written with respect to the variable (σ, u), but the problem can be seen from the view of its primal formulation as introduced by Reddy in [236] written with respect to (e_p, u). We refer to the review [99] and to more recent articles, on quasistatic evolutions but also studying the static case, which answer some questions raised in this review: [79], [80], [81],[82] which in particular use the framework introduced in [192] and [204].*

4.5.2 Numerical examples

To illustrate this part we choose to solve a plasticity problem which is classical, see [296] and [235]. We place ourselves in plane stress. For the material parameters we take:

- The young modulus $E = 206900$.
- $\nu = 0.29$.
- $\sigma_c = 367.42346$

A rightward force is applied on the right side, the left side is clamped in the y direction and the bottom side on the x direction. There is a quarter of circle on the left bottom corner which is empty of matter. The square has a length and height of 2. We use Q_1 finite elements and a mesh which is a regular grid of 6400 elements.

For the problem (4.40) we plot on figure 4.4 the Von Mises criterion.

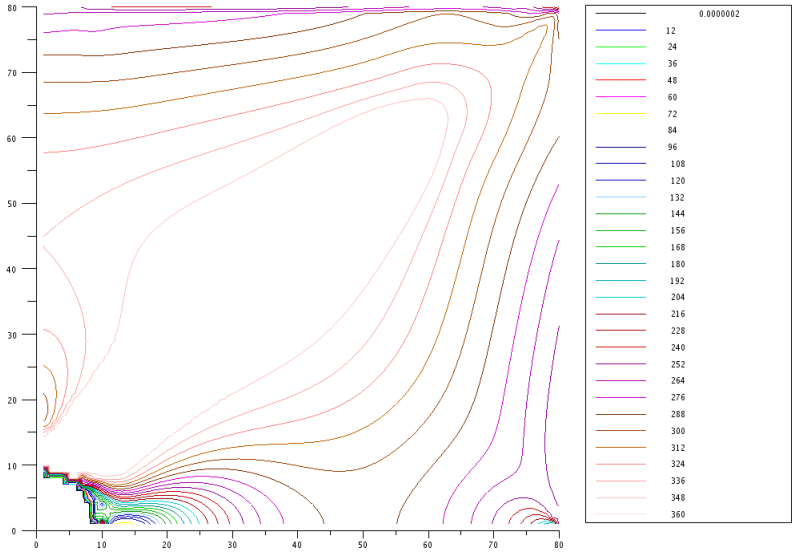

Figure 4.4: The Von Mises criterion for the problem (4.40).

Penalization	Maximal value of the Von Mises criterion
$\eta = 10^{-1}$	586.38837
$\eta = 10^{-2}$	412.24932
$\eta = 10^{-3}$	372.85277
$\eta = 10^{-4}$	367.98093
$\eta = 10^{-5}$	367.47936
$\eta = 10^{-6}$	367.42905
$\eta = 10^{-7}$	367.42402
$\eta = 10^{-8}$	367.42352
$\eta = 10^{-9}$	367.42347
$\eta = 10^{-10}$	367.42346

Table 4.1: Maximal value of the Von Mises criterion with respect to the penalization for the Perzyna model.

Then we solve the Perzyna model for different penalization parameter values. The results are collated in figure 4.5. We point out that the colour scales are not the same on each figures as the maximal value of the Von Mises depends on the penalisation and, as it can be seen on the table 4.1 and the figure 4.6, seems to converge to σ_c as the penalization tends to zero as expected.

Penalization	error on σ	error on U
$\eta = 10^{-1}$	0.0346282	0.0575211
$\eta = 10^{-2}$	0.0118671	0.0213725
$\eta = 10^{-3}$	0.0017787	0.0033636
$\eta = 10^{-4}$	0.0001893	0.0003611
$\eta = 10^{-5}$	0.0000190	0.0000363
$\eta = 10^{-6}$	0.0000019	0.0000036
$\eta = 10^{-7}$	0.0000002	0.0000004
$\eta = 10^{-8}$	1.902D-08	3.630D-08
$\eta = 10^{-9}$	1.886D-09	3.593D-09
$\eta = 10^{-10}$	1.730D-10	3.226D-10

Table 4.2: L^2-error on σ and U with respect to the penalization for the Perzyna model.

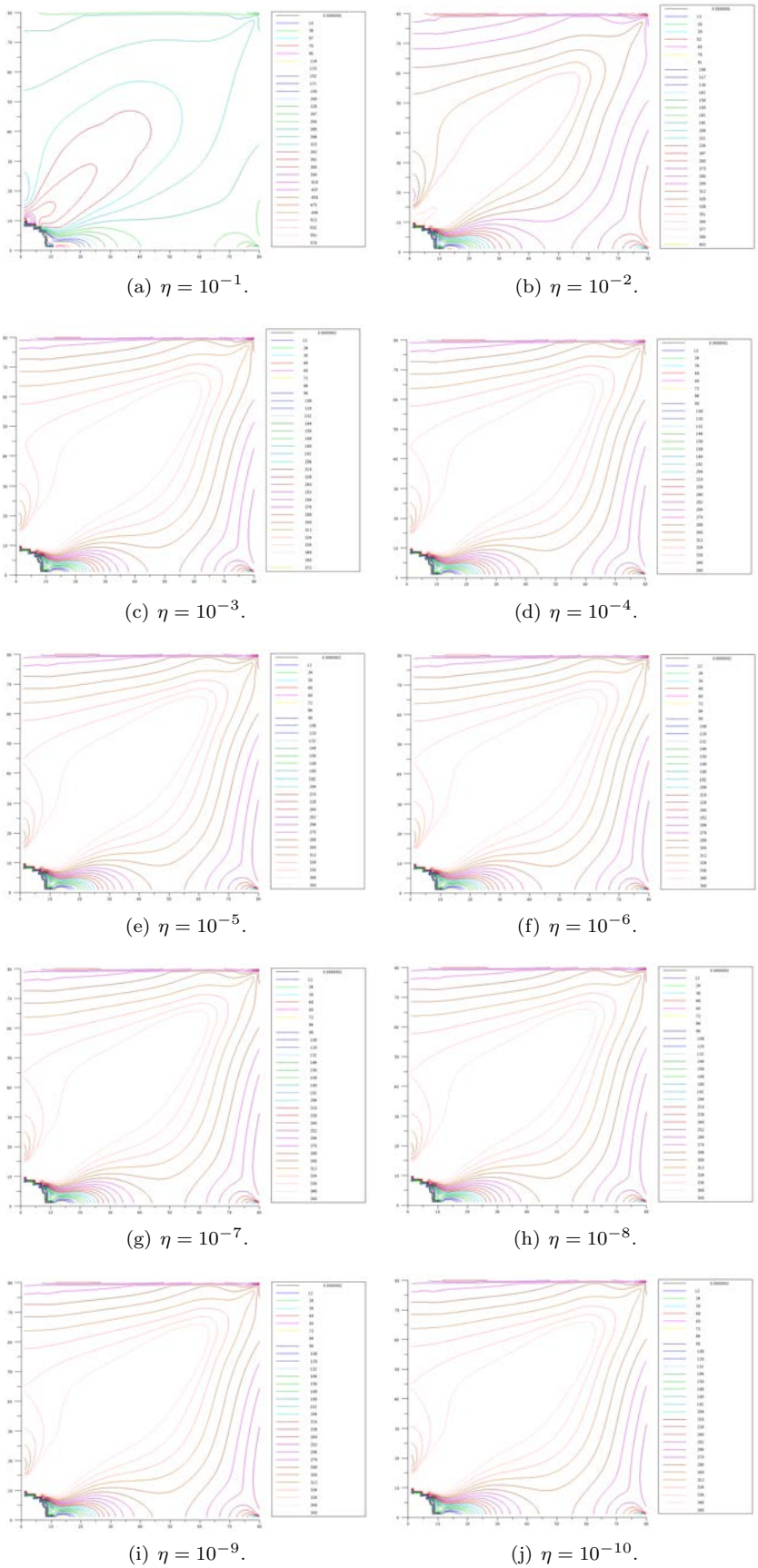

(a) $\eta = 10^{-1}$. (b) $\eta = 10^{-2}$.

(c) $\eta = 10^{-3}$. (d) $\eta = 10^{-4}$.

(e) $\eta = 10^{-5}$. (f) $\eta = 10^{-6}$.

(g) $\eta = 10^{-7}$. (h) $\eta = 10^{-8}$.

(i) $\eta = 10^{-9}$. (j) $\eta = 10^{-10}$.

Figure 4.5: Results for the Perzyna penalization for different penalization parameters η. We plot the Von Mises criterion with in black the elements which reached the Von Mises limit σ_c

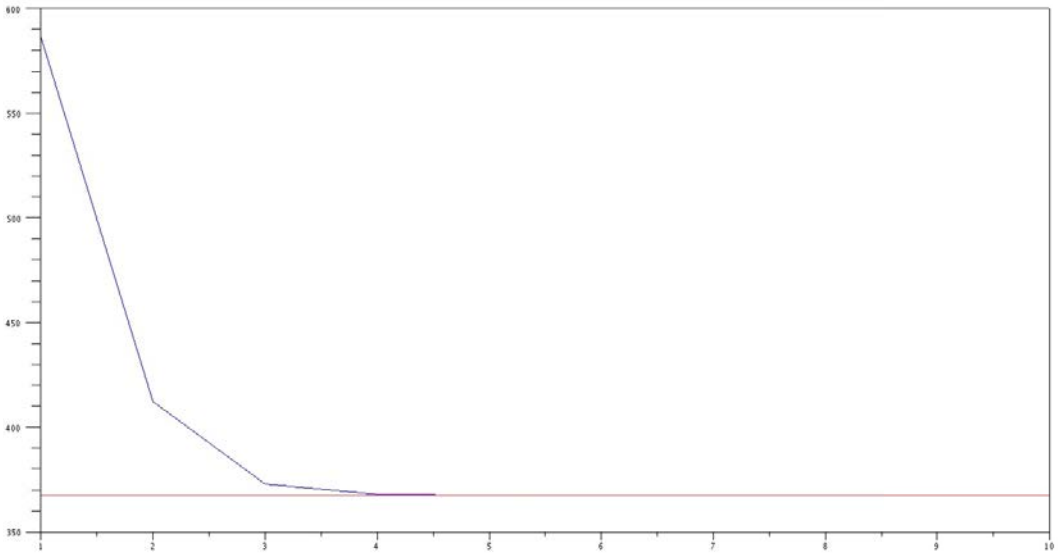

Figure 4.6: The maximal value of the Von Mises criterion with respect to $-log_{10}(\eta)$.

Part III

Shape Optimization

Chapter 5

Shape optimization for contact problems

Contents

5.1 Introduction

In this chapter we perform shape optimization for structure whose mechanical modelization includes some contact boundary conditions. From an industrial point of view, these kinds of boundary conditions are of great interest, as they enable a more detailed and accurate modelisation of boundary which could at first be approximately considered as fixed. The models used in this thesis were presented in chapter 3 where it was shown that the state equations could be put under the form of variational inequalites. From a mathematical point of view, variational inequalites tend to make the whole optimisation and, in particular, the sensitivity analysis, more intricate, as already pointed in section 2.4.4.

Indeed the shape optimisation of such problems present the same difficulties encountered in control theory of variational inequality. As remarked in [205] and [269], the frictionless contact solution can be written under the form of a projection onto a convex set, which is at most conically differentiable (see section 2.3.2). In [205], Mignot managed to derive optimality conditions, thanks to this weak differentiability. Using the conical derivative and writting the problem under a discretized form, Kocvara and al. [226] used a bundle algorithm to perform shape optimization. Another way to get optimality conditions, see [26], [12] and [285], is to write a sequence of penalised problems (see section 3.4.3 in the case of contact). This penalisation approach was used in numerical shape optimisation, for example in [94] using SIMP method, [228] and [165], using splines to parameterise the shape. Another similar approach is the

regularisation of the unilateral boundary conditions which was used in [273] and [272] in the context of SIMP method. Some authors, in [282] and [152], put the problem under a saddle point problem and use the so-called Lagrangian method presented in section 1.3.3 or in [5], ignoring the non differentiability of the Lagrangian multiplier arising in this formulation. We can also mention [66] and [187] where no derivative is computed and a genetic algorithm is used. As far as theoretical results are concerned we refer to [132], [134], [127], [130] where for a particular optimisation problem the proof of the existence of an optimum is done under assumptions of uniform Lipschitz regularity of the boundary, proving the result for the discretised case and passing to the limit.

When friction comes into question, the derivation becomes even more difficult. In [269], for the Tresca model (also called the prescribed friction model), a conical derivative is found out only for 2D cases and for specific directions. Once again, penalised and regularised formulations can be used such as in [164], [167], [12] and [274]. Theoretical results are also given for normal compliance model [171] in [172] and for Coulomb friction model in [128]. For this last model of friction the uniqueness of the contact solution is not ensured for the continuous model and examples of non uniqueness can be built. Consequently, in [31] and [32], the authors analysed the derivation of the discretised problem, which admits a unique solution for small coefficients, through the eye of subgradients calculus. Eventually, a thorough review of other results in shape optimization for contact problems can be found in [144].

In the first part, we give the proof of the existence of a conical Lagrangian derivative for the frictionless contact problem without auto-contact. The proof is largely inspired from [269] but we simplify it avoiding the decompositions of the solutions onto three subspaces. Moreover, even if we will not use this formula to perform shape optimization, numerous estimations done in this proof will be used in section 5.6.1. In the following part, we present the penalised and regularised models which will be used to compute shape gradients. We perform a sensitivity analysis of these formulations, which enables us to find the shape gradients of some criteria. Numerical examples, in 2D and 3D, are finally given where the contact zone is not optimized but the algorithm can choose to include it or not (or a part of it) in the shape.

In a the last part we try to optimize the place and the shape of the contact zone without changing the mesh we use. To do so, we present two possible ways to compute the solution of a frictionless contact problem without meshing the contact interface. For each one we give some numerical examples and discuss their potential drawbacks.

Finally the proof done in [269] for the conical differentiability of the Tresca model is given in an annex A.

In this whole chapter we consider a shape optimization problem of the following form:

Optimisation problem

Our goal is to minimize a certain function $J(\Omega)$ depending on u the displacement which solves one of the contact formulations given in sections 5.3.1 and 5.6 under constraints also depending on u noted $C(\Omega)$:

$$\begin{cases} \min J(\Omega) \\ \Omega \in \mathcal{U}_{ad} \\ u \text{ solution of (5.70), (5.118) or (5.131)} \\ C(\Omega) \leq 0 \end{cases} \tag{5.1}$$

where $\mathcal{U}_{ad}$ is the set of admissible shapes, see the section 1.1. The problem (5.70) is a general form of contact problems studied in this chapter, (5.118) and (5.131) are two approximations of the contact problem without friction.

5.2 Conical derivative of frictionless contact

5.2.1 Problem statement

The proof is very similar to the one done in section 2.3.2 for the obstacle problem with some additional difficulties. First, we somehow recall the studied problem:

$$\begin{cases} -\text{div}(Ae(u)) = f & \text{in } \Omega \\ u = 0 & \text{on } \Gamma_0 \\ Ae(u)n = g & \text{on } \Gamma_N \\ u \cdot n \leq 0 & \text{on } \Gamma_c \\ Ae(u)n \cdot n \leq 0 & \text{on } \Gamma_c \\ (u \cdot n)(Ae(u)n \cdot n) = 0 & \text{on } \Gamma_c \\ (Ae(u)n)_t = 0 & \text{on } \Gamma_c \end{cases} \tag{5.2}$$

which is equivalent to solve the following variational inequalities with $u \in K(\Omega)$:

$$\int_\Omega Ae(u) : e(v-u)\,dx \geq \int_\Omega f \cdot (v-u)\,dx + \int_{\Gamma_N} g \cdot (v-u)\,ds \ \forall v \in K(\Omega) \tag{5.3}$$

with $f \in L^2(\Omega)^d$ and $g \in L^2(\Gamma_N)^d$ and

$$K(\Omega) = \left\{ v \in H^1_{\Gamma_0}(\Omega)^d,\ v \cdot n \leq 0 \text{ on } \Gamma_c \right\}. \tag{5.4}$$

First we can notice that $K(\Omega)$ depends on Ω not only because it is a subset of $H^1_{\Gamma_0}(\Omega)^d$ but also because of the unit normal n. The first thing we should do is a variable change to transport our problem on the reference open set Ω_0. The problem is that $u \in K(\Omega)$ does not imply that $u(y+\theta(y)) \in K(\Omega_0)$ since the normal at a point y on $\partial\Omega_0$ is not generally the same as the one at $y+\theta(y)$ on $\partial\Omega$. First we recall the definition 1.3.11:

Definition 5.2.1. *We note $\bar{u}(\theta)$ the function defined for all $y \in \Omega_0$ by $\bar{u}(\theta)(y) = u\left((Id+\theta)(\Omega_0), y+\theta(y)\right)$.*

Proposition 5.2.2. *For $\theta \in W^{2,\infty}(\mathbb{R}^d, \mathbb{R}^d)$ we have:*

$$u \in K(\Omega) \Leftrightarrow (I+\nabla\theta)^{-1}\overline{u}(\theta) \in K(\Omega_0). \tag{5.5}$$

Proof. We just need to remind the proof of (1.20) where we had:

$$m(y+\theta(y)) =^t (I+\nabla\theta(y))^{-1} m^0(y) \tag{5.6}$$

with m and m^0 the (not normed) outward normal of respectively $\partial\Omega$ and $\partial\Omega_0$.

We have:

$$\langle \overline{u}(\theta), m(y+\theta(y)) \rangle \leq 0,$$

with (5.6):

$$\langle \overline{u}(\theta),^t (I+\nabla\theta(y))^{-1} m^0(y) \rangle \leq 0$$

and with the properties of the scalar product:

$$\langle (I+\nabla\theta(y))^{-1}\overline{u}(\theta), m^0(y) \rangle \leq 0.$$

The result follows □

For now on we fix $\theta \in W^{2,\infty}(\mathbb{R}^d, \mathbb{R}^d)$ such that $(Id+t\theta)(\Omega_0) = \Omega_t$ for $t > 0$. In the following we do not write Ω_t but Ω.

In the light of proposition 5.2.2, we define a new unknown:

Definition 5.2.3. *We note w the new unknown defined on Ω_0 by:*

$$w(\theta) = (I+\nabla\theta)^{-1}\overline{u}(\theta). \tag{5.7}$$

As we want to work with this new variable $w(\theta) \in K(\Omega_0)$, the problem (5.3) can be, by exactly doing the same change of variable on the test functions and transporting it on the reference domain Ω_0, rewritten as:

$$\begin{aligned}
&\forall \phi \in K(\Omega_0) \\
&\int_{\Omega_0} Ae'(\nabla[(I+\nabla\theta)w](I+\nabla\theta)^{-1}) : e'(\nabla[(I+\nabla\theta)(\phi-w)](I+\nabla\theta)^{-1}) |det(I+\nabla\theta)|\,dx \\
&\geq \int_{\Omega_0} f(y+\theta(y)) \cdot (I+\nabla\theta)(\phi-w)|det(I+\nabla\theta)|\,dx \\
&+ \int_{\partial\Gamma_N^0} g(y+\theta(y)) \cdot (I+\nabla\theta)(\phi-w)|det(I+\nabla\theta)||^t(I+\nabla\theta)^{-1}n|\,ds.
\end{aligned} \tag{5.8}$$

where we denote by e' the symmetric part of a matrix: if τ is a matrix, $e'(\tau) = \frac{1}{2}\left(\tau +^t \tau\right)$.

To shorten the calculations, the variational inequation (5.8) is written as:

$$a^\theta(w, \phi-w) \geq \langle F^\theta, \phi-w \rangle \tag{5.9}$$

with

$$\begin{aligned}
a^\theta(w,\phi) \quad = \quad & \int_{\Omega_0} Ae'(\nabla[(I+\nabla\theta)w](I+\nabla\theta)^{-1}) : e'(\nabla[(I+\nabla\theta)(\phi)](I+\nabla\theta)^{-1}) \\
& |det(I+\nabla\theta)|\,dx
\end{aligned} \tag{5.10}$$

and

$$\begin{aligned}
\langle F^\theta, \phi \rangle \quad = \quad & \int_{\Omega_0} f(y+\theta(y)) \cdot (I+\nabla\theta)(\phi-w)|det(I+\nabla\theta)|\,dx \\
& + \int_{\partial\Gamma_N^0} g(y+\theta(y)) \cdot (I+\nabla\theta)(\phi-w)|det(I+\nabla\theta)||^t(I+\nabla\theta)^{-1}n|\,ds.
\end{aligned} \tag{5.11}$$

5.2.2 Negligible terms

The first thing to do is to get a bilinear form which is independent of θ. We start first by the Taylor expansion of a^θ and F^θ.

For a^θ:

$$\begin{aligned} a^\theta(u,\phi) &= a^0(u,\phi) + \int_{\Omega_0} Ae'(\nabla u) : e'(\nabla\phi)\mathrm{div}(\theta)\,dx + \int_{\Omega_0} Ae'(\nabla u) : e'(\nabla(\nabla\theta\phi) - \nabla\phi\nabla\theta)\,dx \\ &\quad + \int_{\Omega_0} Ae'(\nabla(\nabla\theta u) - \nabla u\nabla\theta) : e'(\nabla\phi)\,dx + o(\theta) \\ &= a^0(u,\phi) + (a^0)'(\theta)(u,\phi) + o(\theta) \end{aligned} \tag{5.12}$$

where $o(\theta)$ is such that $|o(\theta)| \le o_1(\theta)\,\|u\|_{H^1}\,\|\phi\|_{H^1}$ with $o_1(\theta)$ independent of u and ϕ. The o have to be understood as $\lim_{\theta\to 0}\frac{|o(\theta)|}{\|\theta\|_{W^{2,\infty}}} = 0$ and $\lim_{\theta\to 0}\frac{|o_1(\theta)|}{\|\theta\|_{W^{2,\infty}}} = 0$.

For F^θ:

$$\begin{aligned} \langle F^\theta,\phi\rangle &= \langle F^0,\phi\rangle + \int_{\Omega_0} (\nabla f\theta)\cdot\phi + \mathrm{div}(\theta)(f\cdot\phi) - f\cdot(\nabla\theta\phi)\,dx \\ &\quad + \int_{\Gamma_N^0} (g\cdot\phi)\mathrm{div}(\theta) + (\nabla g\theta).\phi - (g\cdot\phi)({}^t\nabla\theta n\cdot n) - g\cdot(\nabla\theta\phi) + o(\theta) \\ &= \langle F^0,\phi\rangle + \langle (F^0)'(\theta),\phi\rangle + o(\theta) \end{aligned} \tag{5.13}$$

where $o(\theta)$ is such that $|o(\theta)| \le o_2(\theta)\,\|\phi\|_{H^1}$ with $o_2(\theta)$ independent of ϕ. The o have to be understood as $\lim_{\theta\to 0}\frac{|o(\theta)|}{\|\theta\|_{W^{2,\infty}}} = 0$ and $\lim_{\theta\to 0}\frac{|o_2(\theta)|}{\|\theta\|_{W^{2,\infty}}} = 0$. We rewrite (5.9):

$$\begin{aligned} a^0(w(\theta),\phi - w(\theta)) \;\ge\; & \langle F^0,\phi - w(\theta)\rangle + \langle F^\theta - F^0 - (F^0)'(\theta),\phi - w(\theta)\rangle \\ & + \langle (F^0)'(\theta),\phi - w(\theta)\rangle - (a^0)'(\theta)(w(0),\phi - w(\theta)) \\ & + a^0(w(0),\phi - w(\theta)) - a^\theta(w(0),\phi - w(\theta)) \\ & + (a^0)'(\theta)(w(0),\phi - w(\theta)) + a^0(w(\theta) - w(0),\phi - w(\theta)) \\ & - a^\theta(w(\theta) - w(0),\phi - w(\theta)). \end{aligned} \tag{5.14}$$

Definition 5.2.4. *We call l_1, l_2 and l_3 the following linear forms defined on $H^1_{\Gamma_0}(\Omega)^d$:*

$$\langle l_1,\phi\rangle = \langle F^\theta - F^0 - (F^0)'(\theta),\phi\rangle, \tag{5.15}$$

$$\langle l_2,\phi\rangle = a^0(w(0),\phi) - a^\theta(w(0),\phi) + (a^0)'(\theta)(w(0),\phi), \tag{5.16}$$

$$\langle l_3,\phi\rangle = a^0(w(\theta) - w(0),\phi - w(\theta)) - a^\theta(w(\theta) - w(0),\phi - w(\theta)). \tag{5.17}$$

Lemma 5.2.5. *l_1, l_2 and l_3 are $o(\theta)$ which means that $\lim_{\theta\to 0}\frac{|o(\theta)|}{\|\theta\|_{W^{2,\infty}}} = 0$.*

Proof. With (5.13) and (5.12) we directly conclude that $l_2 = o(\theta)$ and $l_1 = o(\theta)$. The difficult part is for l_3.

We have:

$$|\langle l_3,\phi\rangle| \le |(a^0)'(\theta)(w(\theta) - w(0),\phi)| + o_1(\theta)\,\|w(\theta) - w(0)\|_{H^1}\,\|\phi\|_{H^1}$$

and by using (5.12) and the expression of $(a^0)'(\theta)$

$$\begin{aligned} |\langle l_3,\phi\rangle| \;\le\; & C\,\|\mathrm{div}(\theta)\|_{L^\infty}\,\|w(\theta) - w(0)\|_{H^1}\,\|\phi\|_{H^1} \\ & + C\,\|w(\theta) - w(0)\|_{H^1}\,\|\nabla(\nabla\theta\phi) - \nabla\phi\nabla\theta\|_{L^2} \\ & + C\,\|\nabla(\nabla\theta(w(\theta) - w(0))) - \nabla(w(\theta) - w(0))\nabla\theta\|_{L^2}\,\|\phi\|_{H^1} \\ & + o_1(\theta)\,\|w(\theta) - w(0)\|_{H^1}\,\|\phi\|_{H^1}. \end{aligned} \tag{5.18}$$

We have to work on the last two terms of (5.18). As we have:

$$\|\nabla(\nabla\theta\phi) - \nabla\phi\nabla\theta\|_{L^2} \le (\|\nabla\theta\|_{L^\infty} + \|\theta\|_{W^{2,\infty}})\,\|\phi\|_{H^1}$$

and that

$$\|\nabla(\nabla\theta(w(\theta) - w(0))) - \nabla(w(\theta) - w(0))\nabla\theta\|_{L^2} \le (\|\nabla\theta\|_{L^\infty} + \|\theta\|_{W^{2,\infty}})\,\|w(\theta) - w(0)\|_{H^1},$$

we then get:

$$|\langle l_3,\phi\rangle| \;\le\; C\,\|\theta\|_{W^{2,\infty}}\,\|\phi\|_{H^1}\,\|w(\theta) - w(0)\|_{H^1} + o_1(\theta)\,\|w(\theta) - w(0)\|_{H^1}\,\|\phi\|_{H^1}. \tag{5.19}$$

In view of (5.19), using lemma 5.2.6:

$$\frac{|\langle l_3,\phi\rangle|}{\|\phi\|_{H^1}} \;\le\; C\,\|\theta\|^2_{W^{2,\infty}} + o(\theta)$$

and the lemma 5.2.5 is proved. □

Lemma 5.2.6. *We have:*

$$\|w(\theta) - w(0)\|_{H^1} \leq C \|\theta\|_{W^{2,\infty}} + o(\theta) \tag{5.20}$$

with $o(\theta)$ independent of $w(\theta)$ and $\lim_{\theta \to 0} \frac{|o(\theta)|}{\|\theta\|_{W^{2,\infty}}} = 0$.

Proof. We know that $w(\theta)$ is solution of (5.9):

$$a^\theta(w(\theta), \phi - w(\theta)) \geq \langle F^\theta, \phi - w(\theta) \rangle, \ \ \forall \phi \in K(\Omega_0)$$

and $w(0)$ is solution of:

$$a^0(w(0), \phi - w(0)) \geq \langle F^0, \phi - w(0) \rangle, \ \ \forall \phi \in K(\Omega_0). \tag{5.21}$$

We add (5.9) and (5.21) to find:

$$\begin{array}{rcl} a^0(w(\theta) - w(0), w(\theta) - w(0)) & \leq & \langle F^\theta - F^0, w(\theta) - w(0) \rangle + a^0(w(\theta), w(\theta) - w(0)) \\ & & -a^\theta(w(\theta), w(\theta) - w(0)) \\ & \leq & \left\|F^\theta - F^0\right\|_{H^{-1}} \|w(\theta) - w(0)\| \\ & & +C \|\theta\|_{W^{2,\infty}} \|w(\theta) - w(0)\|_{H^1} \|w(\theta)\|_{H^1} + o_1(t) \|w(\theta) - w(0)\|_{H^1} \|w(\theta)\|_{H^1} \end{array} \tag{5.22}$$

where we used the calculations done for (5.19). Moreover: $F^\theta - F^0 = (F^0)'(\theta) + o(\theta)$ and

$$\begin{array}{rcl} |\langle (F^0)'(\theta), \phi \rangle| & \leq & C \|\theta\|_{L^\infty(\Omega)} \|\phi\|_{L^2(\Omega)} + \|f\|_{L^2(\Omega)} \|\theta\|_{W^{1,\infty}(\Omega)} \|\phi\|_{L^2(\Omega)} + \\ & & C \|\phi\|_{L^2(\Omega)} \|f\|_{L^2(\Omega)} \|\theta\|_{W^{1,\infty}(\Omega)} + C \|g\|_{L^2(\Gamma_N)} \|\phi\|_{L^2(\Gamma_N)} \|\theta\|_{W^{1,\infty}(\Gamma_N)} + \\ & & C \|\theta\|_{L^\infty(\Gamma_N)} \|\phi\|_{L^2(\Gamma_N)} + C \|\phi\|_{L^2(\Gamma_N)} \|\theta\|_{W^{1,\infty}(\Gamma_N)} \end{array}$$

thanks to (5.13). It follows by trace theorem on H^1 that:

$$|\langle (F^0)'(\theta), \phi \rangle| \leq C \|\theta\|_{W^{2,\infty}} \|\phi\|_{H^1(\Omega)} \tag{5.23}$$

and then:

$$\left\|F^\theta - F^0\right\|_{H^{-1}} \leq C \|\theta\|_{W^{2,\infty}} + o_2(\theta).$$

Now we can find a bound for $\|w(\theta)\|_{H^1}$. As $0 \in K(\Omega_0)$, we have:

$$a^0(w(\theta), w(\theta)) \leq \langle F^\theta, w(\theta) \rangle + a^0(w(\theta), w(\theta)) - a^\theta(w(\theta), w(\theta)).$$

So using the coercivity of a^0 (let us call C_0 the coercivity constant) and the computations done for (5.19):

$$(C_0 - C \|\theta\| - o_1(t)) \|w(\theta)\|_{H^1} \leq \left\|F^\theta\right\|_{H^{-1}}.$$

Moreover:

$$\begin{array}{rcl} \left\|F^\theta\right\|_{H^{-1}} & \leq & \left\|F^0\right\|_{H^{-1}} + \left\|F^\theta - F^0\right\|_{H^{-1}} \\ & \leq & \left\|F^0\right\|_{H^{-1}} + C \|\theta\|_{W^{2,\infty}} + o(\theta), \end{array} \tag{5.24}$$

therefore for $\|\theta\|_{W^{2,\infty}}$ small enough, it enables us to conclude that $\|w(\theta)\|_{H^1}$ is bounded beyond.

Finally, using the coercivity of a^0 in (5.22), the boundedness of $\|w(\theta)\|_{H^1}$ and dividing by $\|w(\theta) - w(0)\|_{H^1}$, (5.20) is true.

□

5.2.3 The Lagrangian conical derivative

We now compute the Lagrangian conical derivative of $u(\theta)$, $Y(\theta, y)$.

Theorem 5.2.7. *The Lagrangian conical derivative of $u(\theta)$, $Y(\theta, y) \in S$ exists and is the solution of the following problem:*

$$\begin{array}{l} \forall \phi \in S \\ a^0(Y(\theta, y), \phi - Y(\theta, y)) \quad \geq \quad \langle (F^0)'(\theta), \phi - Y(\theta, y) \rangle - (a^0)'(\theta)(u(0), \phi - Y(\theta, y)) \\ \qquad\qquad\qquad\qquad\quad +a^0(\nabla\theta u(0), \phi - Y(\theta, y)) \end{array} \tag{5.25}$$

with:

$$S = \left\{ \phi \in W \,|\, \phi.n \leq (\nabla\theta u(0)).n \text{ q.e on } \{w(0).n = 0\} \text{ and } a^0(w(0), \phi) = \langle F^0, \phi \rangle + a^0(\nabla\theta u(0), \phi) \right\} \tag{5.26}$$

and:

$$W = \left\{ \phi \in H^1(\Omega) \,|\, \exists \psi \in H^1_{\Gamma_0}(\Omega_0)^d, \, \phi = \psi + \nabla\theta u(0) \right\}. \tag{5.27}$$

We recall that q.e. means quasi everywhere and was defined in section 2.2.3.

Proof. First we compute the conical derivative (defined in section 2.3.2) of $w(t\theta)$ with respect to t. We rewrite the problem (5.14) changing θ into $t\theta$:

$$\begin{aligned} a^0(w(t\theta),\phi-w(t\theta)) \quad \geq \quad & \langle F^0,\phi-w(t\theta)\rangle+\langle F^{t\theta}-F^0-(F^0)'(t\theta),\phi-w(t\theta)\rangle \\ & +\langle (F^0)'(t\theta),\phi-w(t\theta)\rangle-(a^0)'(t\theta)(w(0),\phi-w(t\theta)) \\ & +a^0(w(0),\phi-w(t\theta))-a^{t\theta}(w(0),\phi-w(t\theta)) \\ & +(a^0)'(t\theta)(w(0),\phi-w(t\theta))+a^0(w(t\theta)-w(0),\phi-w(t\theta)) \\ & -a^{t\theta}(w(t\theta)-w(0),\phi-w(t\theta)). \end{aligned} \tag{5.28}$$

We introduce three variables $G^0\in H^1_{\Gamma_0}(\Omega_0)^d$, $(G^0)'(\theta)\in H^1_{\Gamma_0}(\Omega_0)^d$ and $(K^0)'(\theta)\in H^1_{\Gamma_0}(\Omega_0)^d$, defined respectively as the solutions of the following variational equations: $\forall\phi\in H^1_{\Gamma_0}(\Omega_0)^d$

$$a^0(G^0,\phi)=\langle F,\phi\rangle, \tag{5.29}$$

$$a^0((G^0)'(\theta),\phi)=\langle (F^0)'(\theta),\phi\rangle, \tag{5.30}$$

$$a^0((K^0)'(\theta),\phi)=(a^0)'(\theta)(w(0),\phi). \tag{5.31}$$

We also note P_0 the projection on $K(\Omega_0)$ associated with a^0. Whence, we can write the problem (5.28) in the following way:

$$\begin{aligned} w(\theta) &= P_0(G^0+t(G^0)'(\theta)-t(K^0)'(\theta)+o(t)) \\ &= P_0(G^0+t(G^0)'(\theta)-t(K^0)'(\theta))+o(t). \end{aligned} \tag{5.32}$$

Lemma 5.2.9 and lemma 5.2.5 enable us to write:

$$w(\theta)=w(0)+tP_{S^{w(0)}(K(\Omega_0))}((G^0)'(\theta)-(K^0)'(\theta))+o(t) \tag{5.33}$$

with

$$S^{w(0)}(K(\Omega_0))=\left\{\phi\in H^1_{\Gamma_0}(\Omega_0)^d\,|\,\phi.n\leq 0 \text{ q.e on } \{w(0).n=0\} \text{ and } a^0(w(0),\phi)=\langle F^0,\phi\rangle\right\}$$

and $P_{S^{w(0)}(K(\Omega_0))}$ the projection on $S^{w(0)}(K(\Omega_0))$ associated with a^0.

As $w(\theta)=(I+\nabla\theta)^{-1}\overline{u}(\theta)$, noting $Y_w(\theta)$ the Lagrangian derivative of $w(\theta)$ we have $Y_w(\theta)=Y(\theta)-\nabla\theta\overline{u}(\theta)$ and we get (5.25). □

Remark 5.2.8. *We point out that the problem* (5.25) *has a unique solution since if we take Y a solution of this problem:*

$$Y_w(\theta)=Y-\nabla\theta\overline{u}(\theta)$$

and $Y_w(\theta)$ exists and is unique as it is the projection of $(G^0)'(\theta)-(K^0)'(\theta)$ on a closed convex set (see the proof of theorem 5.2.7).

We introduce T a linear application from $H^1_{\Gamma_0}(\Omega_0)^d$ to $H^{\frac{1}{2}}(\Gamma^0_c)$ defined as:

$$T(v)=v\cdot n.$$

We recall the notation (2.32). If K is a convex included in an Hilbert space H we note

$$S_y(K)=\{w\in H,\,\exists w_n\to w,\,\exists t_n>0,\,y+t_nw_n\in K\}$$

Lemma 5.2.9. *The following equality stands:*

$$S_y(K(\Omega_0))=\left\{\omega\in H^1_{\Gamma_0}(\Omega_0)^d, T(\omega)\leq 0 \text{ q.e when } T(y)=0\right\}. \tag{5.34}$$

and $K(\Omega_0)$ is polyhedric.

Proof. First we have: $K(\Omega_0)=\left\{u\in H^1_{\Gamma_0}(\Omega_0)^d, T(u)\leq 0\right\}$.

We introduce the following cone:

$$K_T(\Omega_0)=\{h\in R(T), h\leq 0\} \tag{5.35}$$

with $R(T)$ the range of T and $V^1=Ker(T)$ and V^2 its orthogonal.

T restricted to V^2 is a bijection from V^2 to $R(T)$. We note T^{-1} its inverse. As T is continuous, linear and bijective, T^{-1} is also continuous on $R(T)$. So:

$$T: H^1_{\Gamma_0}(\Omega_0)^d\to R(T)$$

$$T^{-1}: R(T)\to V^2.$$

We introduce a new convex cone $K_2(\Omega_0)=K(\Omega_0)\cap V^2$ and the three following convex cones can be defined:

$$S_{T(y)}(K_T(\Omega_0))=\{w\in R(T),\,\exists w_n\to w,\,\exists t_n>0,\,T(y)+t_nw_n\leq 0\}, \tag{5.36}$$

$$S_y(K(\Omega_0))=\left\{w\in H^1_{\Gamma_0}(\Omega_0)^d,\,\exists w_n\to w,\,\exists t_n>0,\,T(y)+t_nT(w_n)\leq 0\right\}, \tag{5.37}$$

$$S_y(K_2(\Omega_0)) = \left\{ w \in H^1_{\Gamma_0}(\Omega_0)^d \cap V^2,\ \exists w_n \to w,\ \exists t_n > 0,\ T(y) + t_n T(w_n) \leq 0 \right\}. \tag{5.38}$$

We prove that T is a bijection between: $S_y(K_2(\Omega_0))$ and $S_{T(y)}(K_T(\Omega_0))$.

If $w \in S_y(K_2(\Omega_0))$ then there exists w_n a sequence defined as in the definition (5.38). It follows that $T(w_n) \to T(w)$ and $T(y) + t_n T(w_n) \leq 0$ so $T(w) \in S_{T(y)}(K_T(\Omega_0))$ by (5.36).It follows that:

$$T(S_y(K_2(\Omega_0))) \subset S_{T(y)}(K_T(\Omega_0)).$$

If $w \in S_{T(y)}(K_T(\Omega_0))$ then $\exists w_n \to w$, $\exists t_n > 0$, $T(y) + t_n w_n \leq 0$. But $w_n \in R(T)$ therefore there exists a unique $z_n \in V^2$ such that $T(z_n) = w_n$ et $T(y) + t_n T^{-1}(z_n) \leq 0$. We then have $T^{-1}(w) \in S_y(K(\Omega_0))$, which implies:

$$T^{-1}(S_{T(y)}(K_T(\Omega_0))) \subset S_y(K_2(\Omega_0)).$$

These two inclusions give the surjectivity. The injectivity is given by the fact that if there exist $w_1 \in V^2$ and $w_2 \in V^2$ such that $T(w_1) = T(w_2)$, $(w_1 - w_2) \in V^1$ and by the orthogonality $w_1 = w_2$. So

$$T : S_y(K_2(\Omega_0)) \to S_{T(y)}(K_T(\Omega_0))$$

is a bijection.

We now use a property proved in [269] (Lemma 4.31), stating that $R(T)$ is a Dirichlet space in the sense of [205] (Definition 3.1) or [19]. Thanks to a result from [205] (Lemma 3.4):

$$S_{T(y)}(K_T(\Omega_0)) = \{ h \in R(T),\ h \leq 0 \text{ q.e when } T(y) = 0 \}.$$

The computations proving that T is a bijection by a slightly change also show that:

$$\omega \in S_y(K(\Omega_0)) \Rightarrow T(\omega) \in S_{T(y)}(K_T(\Omega_0))$$

and we get:

$$S_y(K(\Omega_0)) \subset \left\{ \omega \in H^1_{\Gamma_0}(\Omega_0)^d, T(\omega) \leq 0 \text{ q.e when } T(y) = 0 \right\}. \tag{5.39}$$

Moreover

$$S_y(K_2(\Omega_0)) \subset S_y(K(\Omega_0))$$

and the fact that T is a bijection gives that:

$$\left\{ \omega \in H^1_{\Gamma_0}(\Omega_0)^d \cap V^2, T(\omega) \leq 0 \text{ q.e when } T(y) = 0 \right\} \subset S_y(K_2(\Omega_0)).$$

As $V^1 \subset S_y(K(\Omega_0))$,

$$V^1 + \left\{ \omega \in H^1_{\Gamma_0}(\Omega_0)^d \cap V^2, T(\omega) \leq 0 \text{ q.e when } T(y) = 0 \right\} \subset S_y(K_2(\Omega_0))$$

and that:

$$\begin{aligned} &\left\{ \omega \in H^1_{\Gamma_0}(\Omega_0)^d, T(\omega) \leq 0 \text{ q.e when } T(y) = 0 \right\} \\ &= V^1 + \left\{ \omega \in H^1_{\Gamma_0}(\Omega_0)^d \cap V^2, T(\omega) \leq 0 \text{ q.e when } T(y) = 0 \right\}. \end{aligned}$$

Finally it follows that

$$\left\{ \omega \in H^1_{\Gamma_0}(\Omega_0)^d, T(\omega) \leq 0 \text{ q.e when } T(y) = 0 \right\} \subset S_y(K(\Omega_0)). \tag{5.40}$$

Thanks to (5.40) and (5.39), we recover the equality (5.34).
The polyhedricity of $K(\Omega_0)$ follows from theorems 3.1 and 3.2 in [205]. □

5.3 Penalised and regularised formulations

5.3.1 Formulations used in shape optimization

As our goal is to optimise thanks to a gradient algorithm and therefore to compute the derivative of some functions depending on the displacement u, we will not use the conical derivative computed (an example of this use in finite dimension can be found in [226]). We choose to take advantage of the penalised and regularised formulations presented in chapter 3. First we recall these formulations as we need to regularise the normal penalisation to be able to easily differentiate the solution u with respect to the shape. The variational equations are

- for the frictionless model

$$\int_\Omega Ae(u) : e(v)\, dx + j'_{N,\epsilon}(u, v) = \int_\Omega f \cdot v\, dx + \int_{\Gamma_N} g \cdot v\, ds. \quad \forall v \in H^1_{\Gamma_0}(\Omega)^d \tag{5.41}$$

with:

$$j'_{N,\epsilon}(u, v) = \frac{1}{\epsilon} \int_{\Gamma_c} \phi_r(u \cdot n) v \cdot n\, ds + \frac{1}{\epsilon} \int_S \phi_r([u] \cdot n_-)[v] \cdot n_-\, ds, \tag{5.42}$$

and

$$j_{N,\epsilon}(u) = \frac{1}{\epsilon} \left(\int_{\Gamma_c} \int_0^{u.n} \phi_r(t)\, dt\, ds + \int_S \int_0^{[u].n} \phi_r(t)\, dt\, ds \right). \tag{5.43}$$

- for the Tresca model

$$\int_\Omega Ae(u) : e(v)\,dx + j'_{\mathrm{tr},\eta}(u,v) + j'_{N,\epsilon}(u,v) = \int_\Omega f\cdot v\,dx + \int_{\Gamma_N} g\cdot v\,ds \quad \forall v \in H^1_{\Gamma_0}(\Omega)^d \tag{5.44}$$

where $j'_{\mathrm{tr},\eta}$ denote the derivative of $j_{\mathrm{tr},\eta}$ with respect to v with:

$$j_{\mathrm{tr},\eta}(v) = \int_{\Gamma_c} s\mathcal{N}_\eta(v_t)\,ds + \int_S s\mathcal{N}_\eta([v]_t)\,ds. \tag{5.45}$$

- for the Coulomb model:

$$\int_\Omega Ae(u) : e(v)\,dx + j'_{\mathrm{co},\epsilon,\eta}(u,v) + j'_{N,\epsilon}(u,v) = \int_\Omega f\cdot u\,dx + \int_{\Gamma_N} g\cdot u\,ds \quad \forall v \in H^1_{\Gamma_0}(\Omega)^d, \tag{5.46}$$

denoting

$$j'_{\mathrm{co},\epsilon,\eta}(u,v) = \int_{\Gamma_c} \frac{\mu}{\epsilon}\phi_r(u\cdot n)\mathcal{N}'_\eta(u_t)\cdot v_t\,ds + \int_S \frac{\mu}{\epsilon}\phi_r([u]\cdot n_-)\mathcal{N}'_\eta([u]_t)\cdot[v]_t\,ds \tag{5.47}$$

and $\mathcal{N}'_\eta$ the derivative of $\mathcal{N}_\eta$.

- for the Norton-Hoff model:

$$\int_\Omega Ae(u) : e(u)\,dx + j_{\mathrm{nh},\epsilon,\eta}(u,v) + j'_{N,\epsilon}(u,v) = \int_\Omega f\cdot v\,dx + \int_{\Gamma_N} g\cdot v\,ds \quad \forall v \in H^1_{\Gamma_0}(\Omega)^d, \tag{5.48}$$

noting

$$j_{\mathrm{nh},\epsilon,\eta}(u,v) = \int_{\Gamma_c} \frac{\mu}{\epsilon}\phi_r(u\cdot n)\mathcal{N}_\eta(u_t)^{\rho-1}u_t\cdot v_t\,ds + \int_S \frac{\mu}{\epsilon}\phi_r([u]\cdot n_-)\mathcal{N}_\eta([u]_t)^{\rho-1}[u]_t\cdot[v]_t\,ds. \tag{5.49}$$

- for the normal compliance model:

$$\int_\Omega Ae(u) : e(v)\,dx + j_{N,r,Nc}(u,v) + j'_{T,\eta,Nc}(u,v) = \int_\Omega f\cdot v\,dx + \int_{\Gamma_N} g\cdot v\,ds \quad \forall v \in H^1_{\Gamma_0}(\Omega)^d \tag{5.50}$$

with

$$j_{N,\mathrm{nc,r}}(u,v) = \int_{\Gamma_c} C_N\phi_r(u\cdot n)^{m_N}v\cdot n\,ds + \int_S C_N\phi_r([u]\cdot n_-)^{m_N}[v]\cdot n\,ds,$$

$$j'_{T,\mathrm{nc},\eta}(u,v) = \int_{\Gamma_c} C_T\phi_r(u\cdot n)^{m_T}\mathcal{N}'_\eta(u_t)\cdot v_t\,ds + \int_S C_T\phi_r([u]\cdot n_-)^{m_T}\mathcal{N}'_\eta([u]_t)\cdot[v]_t\,ds.$$

In chapter 3, the function ϕ_r was taken equal to $t \mapsto t\mathcal{H}(t)$ which is not differentiable. So we prefer using a regularized version of such functions, for instance, for a small parameter $\eta > 0$:

$$\phi_r^\eta(x) = \begin{cases} 0 & \text{for } x \in (-\infty;-\eta] \\ \dfrac{1}{4\eta}x^2 + \dfrac{1}{2}x + \dfrac{\eta}{4} & \text{for } x \in [-\eta;\eta] \\ x & \text{for } x \in [\eta;+\infty). \end{cases} \tag{5.51}$$

We ask ϕ_r^η to be positive, convex and increasing. We will note keep on writing the exponent η to simplify the notations. We also give the expression of $\mathcal{N}'_\eta$ for the particular case of the function (3.47) given in chapter 3:

$$\mathcal{N}'_\eta(x) = \begin{cases} \dfrac{x}{\|x\|} & \text{for } \|x\| \geq \eta \\ -\dfrac{1}{2\eta^3}\|x\|^2x + \dfrac{3}{2\eta}x & \text{for } \|x\| \leq \eta. \end{cases} \tag{5.52}$$

and we rewrite $\mathcal{N}'_\eta$:

$$\mathcal{N}'_\eta = \kappa_\eta(x)x \tag{5.53}$$

5.3.2 Existence and uniqueness for the penalised and regularised formulations

Theorem 5.3.1. *The problems* (5.44) *and* (5.41) *admit one and only one solution for* $f \in L^2(\Omega)^d$, $g \in L^2(\Gamma_N)^d$, ϕ_r *positive increasing and* $\mathcal{N}_\eta$ *convex positive.*

Proof. The same proof as for theorem 3.4.2 can be done but we propose another way to do it using the minimization problem formulation.
We introduce the function:

$$E(u) = \frac{1}{2}a(u,u) + \frac{1}{\epsilon}\left(\int_{\Gamma_c}\int_0^{u.n} \phi_r(t)\,dt\,ds + \int_S \int_0^{[u].n} \phi_r(t)\,dt\,ds\right) + j_\eta(u) - \int_{\Gamma_N} g\cdot u\,ds - \int_\Omega f\cdot u\,dx \tag{5.54}$$

with $a(u,u) = \int_\Omega Ae(u) : e(u)\,dx$ and $j_\eta(u) = 0$ for (3.44) and $j_\eta(u) = \int_{\Gamma_c} s\mathcal{N}_\eta(v_t)\,ds + \int_S\int_{\Gamma_c} s\mathcal{N}_\eta([v]_t)\,ds$ for (3.48). Thanks to Korn inequality, the part in $a(u,u)$ is strictly convex. We prove then that $\psi : u \to \int_{\Gamma_c} k\int_0^{u.n}\phi_r(t)\,dt\,ds$ is convex. We compute the Hessian of ψ:

$$D^2\psi(h,h') = \int_{\Gamma_c} k\phi_r'(u\cdot n)h'\cdot n\ h\cdot n\,ds$$

which is positive as ϕ_r' is positive. Moreover, since $\mathcal{N}_\eta$ is convex, j_η is convex, l.s.c.. So $u \to E(u)$ is strictly convex, l.s.c. on $H^1_{\Gamma_0}(\Omega)^d$. It is also bounded below as ϕ_r is non negative and an approximation of $x \to x\mathcal{H}(x)$ (for instance $\phi_r([u]\cdot n)$ is null when $[u]\cdot n$ is lesser than $-\eta$). It ensures the existence of a unique minimizer of E on $H^1_{\Gamma_0}(\Omega)^d$ thanks to theorem 2.2.4. To conclude we just need to remark that the optimality criterion is exactly (5.44) or (5.41), therefore both admit one and only one solution. □

Remark 5.3.2. *To compute the Hessian of* ψ *we use some regularity properties of* ϕ_r *proved in theorem 5.4.1.*

For (5.46) the existence is proved in chapter 3 of [100]. A proof similar to the one of (5.46) can be done for (5.48). In the case of the normal compliance model we refer to [123] for a particular case.

5.3.3 Convergence of the penalised solutions to the exact ones

Next we prove that the solutions of the regularized formulations for the Tresca model and the frictionless model converge to the solutions of the exact problems (3.23) and (5.3). We make the proof following the one of [97] done for frictionless contact. We also mention [96]. We consider the following variational inequation problems. The first one is (3.23) whose solution will be denoted by u. The second one is: find $u_\epsilon \in H^1_{\Gamma_0}(\Omega)^d$

$$a(u_\epsilon, v-u_\epsilon) + \frac{1}{\epsilon}j_N(v) - \frac{1}{\epsilon}j_N(u_\epsilon) + j_t(v) - j_t(u_\epsilon) \geq \langle F, v-u_\epsilon\rangle,\ \ \forall v \in H^1_{\Gamma_0}(\Omega)^d, \tag{5.55}$$

with j_N the normal penalisation which is not regularized and j_t the non-regularized friction term. We make the assumption that these terms are positive, convex and l.s.c.. We also suppose that $j_N(0) = j_t(0) = 0$ and that $j_N(v) = 0 \Leftrightarrow v \in K(\Omega)$. The third and last problem we consider is:

$$a(u_\epsilon^\eta, v-u_\epsilon^\eta) + \frac{1}{\epsilon}j_N^\eta(v) - \frac{1}{\epsilon}j_N^\eta(u_\epsilon^\eta) + j_t^\eta(v) - j_t^\eta(u_\epsilon^\eta) \geq \langle F, v-u_\epsilon^\eta\rangle,\ \ \forall v \in H^1_{\Gamma_0}(\Omega)^d, \tag{5.56}$$

where $\eta > 0$ is the regularisation parameter used to regularise the terms j_N and j_t. We assume that $|j_N(v) - j_N^\eta(v)| \leq C_t(\eta)$ and $|j_t(v) - j_t^\eta(v)| \leq C_N(\eta)$ with $C_N(\eta) \to 0$ and $C_t(\eta) \to 0$ when $\eta \to 0$. That is the case for the examples (3.47) and (5.51) taking $C_t(\eta) = C\eta$ with a specific constant C and $C_N(\eta) = C\eta$ for also a specific constant C since $|\mathcal{N}_\eta(x) - \|x\|| \leq \frac{9}{8}\eta$ and $|t\mathcal{H}(t) - \phi_r^\eta(t)| \leq \eta$.

Theorem 5.3.3. *The solution* u_ϵ^η *tends to* u_ϵ *as* $\eta \to 0$ *and we also have:*

$$\|u_\epsilon^\eta - u_\epsilon\|_{H^1} \leq \frac{1}{\epsilon}C_N(\eta) + C_t(\eta) \tag{5.57}$$

Proof. The proof is quickly done by taking $v = u_\epsilon^\eta$ into (5.55) and $v = u_\epsilon$ into (5.56) and adding both equations. Using the coercivity of the bilinear form a and the assumptions on j_N and j_t we get (5.57) which also implies the convergence. □

Theorem 5.3.4. *The solution* u_ϵ *tends to* u *strongly in* $H^1_{\Gamma_0}(\Omega)^d$ *as* $\epsilon \to 0$.

Proof. The first part of the proof is to prove that u_ϵ is bounded in $H^1_{\Gamma_0}(\Omega)^d$. Then we will be able to extract a subsequence converging weakly in H^1. In (5.55), we take $v = 0$ which implies, as $j_N(0) = 0$ and $j_t(0) = 0$:

$$a(u_\epsilon, u_\epsilon) + \frac{1}{\epsilon} j_N(u_\epsilon) + j_t(u_\epsilon) \leq \langle F, u_\epsilon \rangle. \tag{5.58}$$

Since all the terms are positive and thanks to the coercivity of the bilinear form a (we note C_0 the coercivity constant of a):

$$C_0 \|u_\epsilon\|^2_{H^1} \leq \langle F, u_\epsilon \rangle \leq \|F\|_{H^{-1}} \|u_\epsilon\|_{H^1}.$$

So:

$$\|u_\epsilon\| \leq \frac{\|F\|_{H^{-1}}}{C_0}. \tag{5.59}$$

Using that bound, we have:

$$0 \leq j_N(u_\epsilon) \leq \epsilon \frac{\|F\|^2_{H^{-1}}}{C_0}. \tag{5.60}$$

So there exists a subsequence of u_ϵ which converges weakly in $H^1_{\Gamma_0}(\Omega)^d$ to $\tilde{u}$. We note this subsequence u_{ϵ_n}.
The next step is to show that $\tilde{u}$ belongs to $K(\Omega)$. As j is convex l.s.c., it is also weakly l.s.c.. This implies:

$$j_N(\tilde{u}) \leq \liminf_{n\to\infty} j_N(u_{\epsilon_n}) = 0. \tag{5.61}$$

with (5.60). As $j(\tilde{u}) = 0$ we have $\tilde{u} \in K(\Omega)$.
One of the difficulties with the weak convergence is that we cannot pass to the limit in the variational inequation because of the term $a(u_{\epsilon_n}, v - u_{\epsilon_n})$. We want to show that $a(u_{\epsilon_n}, \tilde{u} - u_{\epsilon_n}) \to 0$. Take $v = \tilde{u}$ in (5.55):

$$a(u_{\epsilon_n}, \tilde{u} - u_{\epsilon_n}) + \frac{1}{\epsilon}(j_N(\tilde{u}) - j_N(u_{\epsilon_n})) + (j_t(\tilde{u}) - j_t(u_{\epsilon_n})) \geq \langle F, \tilde{u} - u_{\epsilon_n} \rangle.$$

As $\tilde{u} \in K(\Omega)$, $j_N(\tilde{u}) = 0$. Moreover $j_N(u_{\epsilon_n}) \geq 0$ so:

$$a(u_{\epsilon_n}, \tilde{u} - u_{\epsilon_n}) \geq \langle F, \tilde{u} - u_{\epsilon_n} \rangle + j_t(u_{\epsilon_n}) - j_t(\tilde{u}).$$

Now we want to pass to the lim inf. As j_t is convex l.s.c., we have

$$j_t(\tilde{u}) \leq \liminf_{n\to\infty} j_t(u_{\epsilon_n}). \tag{5.62}$$

It follows that:

$$\liminf_{n\to\infty} a(u_{\epsilon_n}, \tilde{u} - u_{\epsilon_n}) \geq 0. \tag{5.63}$$

For the lim sup we use the coercivity of a to state that:

$$a(\tilde{u} - u_{\epsilon_n}, \tilde{u} - u_{\epsilon_n}) \geq 0$$

which imples:

$$a(\tilde{u}, \tilde{u} - u_{\epsilon_n}) \geq a(u_{\epsilon_n}, \tilde{u} - u_{\epsilon_n})$$

Passing to the lim sup:

$$\limsup_{n\to\infty} a(u_{\epsilon_n}, \tilde{u} - u_{\epsilon_n}) \leq 0. \tag{5.64}$$

The inequality (5.64) together with (5.63) leads to

$$a(u_{\epsilon_n}, \tilde{u} - u_{\epsilon_n}) \to 0. \tag{5.65}$$

We can use this result to prove that $\liminf_{n\to\infty} j_t(u_{\epsilon_n}) = j(\tilde{u})$. Taking:

$$a(u_{\epsilon_n}, \tilde{u} - u_{\epsilon_n}) + j_t(\tilde{u}) \geq \langle F, \tilde{u} - u_{\epsilon_n} \rangle + j_t(u_{\epsilon_n}).$$

and passing to the lim inf leads to $j_t(\tilde{u}) \geq \liminf_{n\to\infty} j_t(u_{\epsilon_n})$ which with the inverse inequality (5.62) gives:

$$\liminf_{n\to\infty} j_t(u_{\epsilon_n}) = j(\tilde{u}). \tag{5.66}$$

Finally we show that $\lim_{n\to\infty} j_t(u_{\epsilon_n}) = j(\tilde{u})$. it suffices to take:

$$a(u_{\epsilon_n}, \tilde{u} - u_{\epsilon_n}) + j_t(\tilde{u}) \geq \langle F, \tilde{u} - u_{\epsilon_n} \rangle + j_t(u_{\epsilon_n}).$$

and to pass to the lim sup which yields $j_t(\tilde{u}) \geq \limsup_{n\to\infty} j_t(u_{\epsilon_n})$. With (5.66), it follows that:

$$\lim_{n\to\infty} j_t(u_{\epsilon_n}) = j(\tilde{u}). \tag{5.67}$$

In the variational inequality (5.55) we need to study the limit of the term $a(u_{\epsilon_n}, v - u_{\epsilon_n})$. Yet:

$$a(u_{\epsilon_n}, v - u_{\epsilon_n}) = a(u_{\epsilon_n}, v - \tilde{u}) + a(u_{\epsilon_n}, \tilde{u} - u_{\epsilon_n}).$$

This leads to the equality:

$$\lim_{n\to\infty} a(u_{\epsilon_n}, v - u_{\epsilon_n}) = a(\tilde{u}, v - \tilde{u}) \tag{5.68}$$

Taking $v \in K(\Omega)$ in (5.55), $j_N(v) = 0$ and as j_N is positive:

$$a(u_{\epsilon_n}, v - u_{\epsilon_n}) + j_t(v) - j_t(u_{\epsilon_n}) \geq \langle F, v - u_{\epsilon_n}\rangle, \ \ \forall v \in K(\Omega),$$

We can pass to the limit with (5.67) and (5.68): $\tilde{u} \in K(\Omega)$ such that:

$$a(\tilde{u}, v - \tilde{u}) + j_t(v) - j_t(\tilde{u}) \geq \langle F, v - \tilde{u}\rangle, \ \ \forall v \in K(\Omega), \tag{5.69}$$

which is the inequation (3.23). We have already proved that there exists a unique solution to (3.23). So $u = \tilde{u}$ and the uniqueness of u also implies that it is the whole sequence which weakly converges to u.
To prove the strong convergence we take $v = u$ in (5.55), $j_N(u) = 0$ and :

$$a(u_\epsilon, u_\epsilon - u) \leq \langle F, u_\epsilon - u\rangle - \frac{1}{\epsilon} j(u_\epsilon) + j_t(u) - j_t(u_\epsilon) \leq \langle F, u_\epsilon - u\rangle + j_t(u) - j_t(u_\epsilon)$$

Then using the coercivity of the bilinear form a:

$$C_0 \left\|u_\epsilon - u\right\|^2_{H^1} \leq a(u_\epsilon - u, u_\epsilon - u) = a(u_\epsilon, u_\epsilon - u) - a(u, u_\epsilon - u) \leq \langle F, u_\epsilon - u\rangle - a(u, u_\epsilon - u) + j_t(u) - j_t(u_\epsilon)$$

As $u_\epsilon \to u$ weakly in H^1, $j_t(u_\epsilon) \to j_t(u)$ and $a(u, u_\epsilon - u) \to 0$, we get $\left\|u_\epsilon - u\right\|_{H^1} \to 0$. □

A simple triangular inequality gives the following result:

Theorem 5.3.5. *The solution u^η_ϵ tends to u strongly in $H^1_{\Gamma_0}(\Omega)^d$ as $\epsilon \to 0$ and $\eta \to 0$ as soon as $\frac{1}{\epsilon} C_N(\eta)$, defined in theorem 5.3.3, tends to 0.*

Remark 5.3.6. *The article [70] gives estimations of the convergence for solutions regular enough and for Ω polyhedral in the discrete and continuous cases. See references therein for the convergence of finite element methods in contact problems with penalisation.*

We finally make the remark that (5.41), (5.44), (5.46), (5.48) and (5.50) can be written under the general following form: find $u \in H^1_{\Gamma_0}(\Omega)^d$ such that,

$$\int_\Omega Ae(u) : e(u)\, dx + \int_{S\cup\Gamma_c} j(u, v, n)\, ds = \int_\Omega f \cdot v\, dx + \int_{\Gamma_N} g \cdot v\, ds \ \ \forall v \in H^1_{\Gamma_0}(\Omega)^d. \tag{5.70}$$

5.4 Optimization and derivation of a criterion in the penalised case

5.4.1 Regularity of the regularised and penalised functions

The fact that ϕ_r is smooth does not imply it is Fréchet differentiable from $L^2(\Gamma_c)$ to $L^2(\Gamma_c)$, see section 4.3 in [286]. In fact, as ϕ_r is differentiable in $\mathbb{R}$ we have, for $x \in \mathbb{R}$: $\phi_r(x + h) = \phi_r(x) + \phi'_r(x)h + o(h)$ with $o(h)$ such that $\lim_{h\to 0} \frac{|o(h)|}{|h|} = 0$. When we want to pass to a differentiation in $L^2(\Gamma_c)$ it is possible that there exist directions $h \in L^2(\Gamma_c)$ such that $\lim_{h\to 0} \frac{\|o(h)\|_{L^2}}{\|h\|_{L^2}} \neq 0$. An example is given in [286] section 4.3.2 for the sine function at 0 or in [119] remark 5. On this point, we also mention the result in [175] saying that a Nemytskij operator (also called a superposition operator) $\Phi(u(x)) = \phi(x, u(x))$ is Fréchet differentiable in $L^p(E)$ if and only if $\phi(x, y)$ can be written as an affine function $\phi_0(x) + \phi_1(x)y$ with $\phi : E \times \mathbb{R} \to \mathbb{R}$, $\phi_0 \in L^p(E)$ and $\phi_1 \in L^\infty(E)$ where E is a bounded mesurable subset of $\mathbb{R}^d$. The fact that ϕ_r is smooth only implies the Gateaux differentiability at each point $x \in \Gamma_c$. But we can state the following theorem:

Theorem 5.4.1. *ϕ_r is differentiable from $H^{\frac{1}{2}}(\Gamma_c) \cap H^{\frac{1}{2}}(S)$ into $L^2(\Gamma_c) \cap L^2(S)$.*

Proof. We want to use the section 4.3.3 in [286] and the theorem 7 in [119]. First it is clear that ϕ'_r satisfies the Carathéodory condition which here means that $y \to \phi'_r(y)$ is continuous. We want to show that ϕ'_r maps $L^p(\Gamma_c) \cap L^p(S)$ into $L^r(\Gamma_c) \cap L^r(S)$ with $p > 2$ and $r = \frac{2p}{p-2}$. Then the theorem in [286] will imply that ϕ_r is Fréchet differentiable from $L^p(\Gamma_c) \cap L^p(S)$ into $L^2(\Gamma_c) \cap L^2(S)$. If $u \in H^{\frac{1}{2}}(\Gamma_c) \cap H^{\frac{1}{2}}(S)$, we can use Sobolev embeddings:

$$u \in L^p(\Gamma_c) \cap L^p(S)$$

with $\frac{1}{p} = \frac{1}{2} - \frac{\frac{1}{2}-\frac{1}{4}}{d-1}$ and $p = 2\frac{d-1}{d-\frac{3}{2}}$. Taking the notations of the theorem in [286] we have $q = 2$ and $r = 4(d-1)$. Due to the choice of the penalisation, ϕ_r' is bounded (depending on the parameter of penalisation). Moreover it is also globally Lipschitz continuous. So Lemma 4.11 in [286] implies that ϕ_r' maps $L^p(\Gamma_c) \cap L^p(S)$ into $L^\infty(\Gamma_c) \cap L^\infty(S)$. As $\partial\Omega$ is of finite measure, we have ϕ_r' maps $L^p(\Gamma_c) \cap L^p(S)$ into $L^r(\Gamma_c) \cap L^r(S)$. The Fréchet differentiability follows. □

Remark 5.4.2. *As $u \in H^1_{\Gamma_0}(\Omega)^d$, it follows that $u \cdot n \in H^{\frac{1}{2}}(\Gamma_c) \cap H^{\frac{1}{2}}(S)$ for Ω smooth enough. Then $u \to \phi_r(u \cdot n)$ is Fréchet differentiable from $H^1_{\Gamma_0}(\Omega)^d$ into $L^2(\Gamma_c) \cap L^2(S)$.*

Remark 5.4.3. *This result implied the continuity of ϕ_r from $H^{\frac{1}{2}}(\Gamma_c) \cap H^{\frac{1}{2}}(S)$ into $L^2(\Gamma_c) \cap L^2(S)$ which is needed for the proof of the existence of a solution to* (3.51) *and* (3.53).

Remark 5.4.4. *The regularisation term $\mathcal{N}_\eta$ is twice differentiable from $\mathbb{R}^d$ to $\mathbb{R}^d$. Moreover its derivative is bounded, so thanks to theorem* 8 *in [119] it is Gateaux differentiable from $L^2(\Gamma_c) \cap L^2(S)$ into $L^2(\Gamma_c) \cap L^2(S)$. As its second derivative is bounded by a linear function, it is also twice Fréchet differentiable from $H^{\frac{1}{2}}(\Gamma_c) \cap H^{\frac{1}{2}}(S)$ into $L^2(\Gamma_c) \cap L^2(S)$ thanks to theorem* 7 *in [119] applied two times. The proof is the same as in theorem 5.4.1.*

5.4.2 Shape gradient of a general criterion

We proceed to the computation of the gradient of a general criterion:

$$J(\Omega, u) = \int_\Omega m(u)\,dx + \int_{\Gamma_m} l(u)\,ds \tag{5.71}$$

where Γ_m will be the part of $\partial\Omega$ allowed to move during the optimization process, m and l are smooth functions and such that:

$$|m(u)| \leq C\left(1 + \|u\|^2\right) \tag{5.72}$$

$$|m'(u) \cdot h| \leq C'|u \cdot h| \tag{5.73}$$

and

$$|l(u)| \leq C\left(1 + \|u\|^2\right) \tag{5.74}$$

$$|l'(u) \cdot h| \leq C'|u \cdot h| \tag{5.75}$$

for every $h \in L^2(\Omega)^d$ and $u \in L^2(\Omega)^d$, and with $C > 0$ and $C' > 0$.

We will need an additional notation for the derivative of $(u, p, n) \to j(u, p, n)$ with respect to n which is a notion different from the normal derivative which will be noted $\partial_n \cdot$. Considering $\mathcal{J} : (u, p, \lambda) \to j(u, p, \lambda)$, $j(u, p, n) = \mathcal{J}(u, p, n)$ and the derivative with respect to n of $j(u, p, n)$ will be noted:

$$\frac{\partial j(u, p, n)}{\partial \lambda}. \tag{5.76}$$

Theorem 5.4.5. *Assume that $\Gamma_m \cap \Gamma_0 = \varnothing$, that $f \in H^1(\mathbb{R}^d)^d$ and $g \in H^2(\mathbb{R}^d)^d$, and that $u \in H^1_{\Gamma_0}(\Omega)^d$ is solution of* (5.70) *(supposing it exists and is unique). If we denote $J'(\Omega)(\theta)$ the Gateaux derivative of $J(\Omega)$ with respect to Ω in the direction $\theta \in W^{1,\infty}(\mathbb{R}^d, \mathbb{R}^d)$. We have:*

$$\begin{aligned} J'(\Omega)(\theta) = &\int_{\Gamma_m} (\theta \cdot n)(m(u) + Ae(u) : e(p) - f \cdot p)\,ds \\ &+ \int_{\Gamma_m} (\theta \cdot n)(Hl(u) + \partial_n l(u)) \\ &- \int_{\Gamma_N \cap \Gamma_m} (\theta \cdot n)(Hp \cdot g + \partial_n(p \cdot g))\,ds \\ &+ \int_{S \cup \Gamma_c} (\theta \cdot n)(Hj(u, p, n) + \partial_n(j(u, p, n))\,ds \\ &+ \int_{S \cup \Gamma_c} \frac{\partial j(u, p, n)}{\partial \lambda} \cdot n'(\theta)\,ds \end{aligned} \tag{5.77}$$

where p is defined as the solution of the following adjoint problem:

$$\begin{aligned} &\int_\Omega Ae(p) : e(\psi)\,dx + \int_\Omega m'(u) \cdot \psi\,dx + \int_{\Gamma_m} l'(u) \cdot \psi\,ds \\ &+ \int_{S \cup \Gamma_c} \frac{\partial j(u, p, n)}{\partial u} \cdot \psi\,ds = 0 \ \ \forall \psi \in H^1_{\Gamma_0}(\Omega)^d. \end{aligned} \tag{5.78}$$

H is the mean curvature: $H = \operatorname{div}(n)$, n' is the shape derivative of the normal (on S it is the shape derivative of n_-), $\partial_n f = \nabla f \cdot n$ for f a real function.

Proof. The proof relies on Cea's method [61], [5] or section 1.3.3. For a rigorous proof it would be needed to prove that u is Gateaux differentiable with respect to the shape. This could be done, as shown in section 1.3.3, by making in (5.70) a change of variable to transport the integral on Ω_0 such that $\Omega = (Id + t\theta)(\Omega_0)$. The proof is then exactly the same as in theorem 1.3.12. This leads to an equation of the type: $F(u,t) = 0$ with F differentiable with respect to t thanks to remark 5.4.4 and theorem 5.4.1 for the additional terms. Finally we apply the implicit function theorem in $t = 0$. This point proved, we apply the Lagrangian method, noting $u'(\theta)$ the shape derivative of u to find the expression of the gradient. Let us introduce the Lagrangian L with v and q in $H^1_{\Gamma_0}(\mathbb{R}^d)^d$:

$$\begin{aligned} L(v,q,n(\Omega),\Omega) &= \int_\Omega m(v)\,dx + \int_{\Gamma_m} l(v)\,ds + \int_\Omega Ae(v) : e(q)\,dx \\ &\quad \int_{S\cup\Gamma_c} j_N(v,q,n)\,ds + \int_{S\cup\Gamma_c} j_T(v,q,n)\,ds \\ &\quad -\int_\Omega f\cdot q\,dx - \int_{\Gamma_N} g\cdot q\,ds \end{aligned} \tag{5.79}$$

Since Γ_0 is fixed, there is no need of a Lagrange multiplier for the Dirichlet condition in the Lagrangian: $\Gamma_0 \subset \partial\Omega$ for every $\Omega \in \mathcal{U}_{ad}$. Moreover the functions q and v are in spaces independent of $\Omega \in \mathcal{U}_{ad}$. We note (u,p) a stationarity point of L. The state equation (5.70) can be retrieved by differentiating L with respect to q in the direction $\psi \in H^1_{\Gamma_0}(\mathbb{R}^d)^d$:

$$\langle \partial_q L(u,q,n,\Omega),\psi\rangle = 0 \ \ \forall \psi \in H^1_{\Gamma_0}(\mathbb{R}^d)^d$$

In the same way the equation solved by p (adjoint problem) can be found by derivating L with respect to v in the direction $\psi \in H^1_{\Gamma_0}(\mathbb{R}^d)^d$:

$$\langle \partial_u L,\psi\rangle = \int_\Omega Ae(v) : e(\psi)\,dx + \int_\Omega m'(u)\cdot\psi\,dx + \int_{\Gamma_m} l'(u)\cdot\psi\,ds \quad + \int_{S\cup\Gamma_c} \frac{\partial j(u,p,n)}{\partial u}\cdot\psi\,ds$$

and the adjoint problem can be deduced:

$$\langle \partial_u L(u,p,n,\Omega),\psi\rangle = 0 \ \ \forall \psi \in H^1_{\Gamma_0}(\mathbb{R}^d)^d$$

which gives (5.78).

To find the shape derivative of $J(\Omega)$, we remark that:

$$J(\Omega) = L(u(\Omega),q,n(\Omega),\Omega)$$

and differentiate the L with respect to the shape in the direction θ which gives:

$$\begin{aligned} J'(\Omega,\theta) &= L'(\Omega,u_\Omega,q,n_\Omega;\theta) \\ &= \partial_\Omega L(\Omega,u_\Omega,q,n_\Omega;\theta) + \partial_u L(\Omega,u_\Omega,q,n_\Omega;u'(\theta)) \\ &\quad + \langle \frac{\partial L(\Omega,u_\Omega,q,n_\Omega)}{\partial\lambda}, n'(\theta)\rangle. \end{aligned} \tag{5.80}$$

But as $u'(\theta)$ is in $H^1_{\Gamma_0}(\Omega)^d$, taking $q = p(\Omega)$ leads to:

$$\partial_u L(\Omega,u_\Omega,p(\Omega),n_\Omega;u'(\theta)) = 0.$$

Consequently:

$$J'(\Omega,\theta) = L'(\Omega,u_\Omega,p_\Omega,n_\Omega;\theta) = \partial_\Omega L(\Omega,u_\Omega,p_\Omega,n_\Omega;\theta) + \langle \frac{\partial L(\Omega,u_\Omega,p_\Omega,n_\Omega)}{\partial\lambda}, n'(\theta)\rangle. \tag{5.81}$$

By using the formulae of theorem 1.3.4, we recover (5.77). □

Remark 5.4.6. *With the theorem 5.4.1, we can prove that the solution u of the frictonless contact model is Fréchet shape differentiable. Moreover, in 2D, $\mathcal{N}_\eta$ can be seen as a function from $\mathbb{R}$ into $\mathbb{R}$ and the proof of theorem 5.4.1 can then be adapted to this function.*

Remark 5.4.7. *The derivative found here is only correct when the solution u exists and is unique. Despite this fact, we will use it even for the models where no uniqueness results are proven.*

5.4.3 Adjoint formulae

For the numerical applications we explicitly write the adjoint problems we need to solve with $p \in H^1_{\Gamma_0}(\Omega)^d$:

- for the frictionless model

$$\int_\Omega Ae(p) : e(v)\,dx + j''_{N,\epsilon}(p,v) = -\int_\Omega m'(u)\cdot\psi\,dx - \int_\Gamma l'(u)\cdot\psi\,ds \ \ \forall v \in H^1_{\Gamma_0}(\Omega)^d \tag{5.82}$$

with:

$$j''_{N,\epsilon}(p,v) = \frac{1}{\epsilon}\int_{\Gamma_c} \phi'_r(u\cdot n)p\cdot n\ v\cdot n\,ds + \frac{1}{\epsilon}\int_S \phi'_r([u]\cdot n_-)[p]\cdot n_-\ [v]\cdot n_-\,ds. \tag{5.83}$$

- for the Tresca model by

$$\int_\Omega Ae(p) : e(v)\,dx + j^{1\prime\prime}_{\mathrm{tr},\eta}(p,v) + j^{2\prime\prime}_{\mathrm{tr},\eta}(p,v) + j''_{N,\epsilon}(u,v) = -\int_\Omega m'(u)\cdot\psi\,dx - \int_\Gamma l'(u)\cdot\psi\,ds \quad \forall v \in H^1_{\Gamma_0}(\Omega)^d \tag{5.84}$$

where

$$j^{1\prime\prime}_{\mathrm{tr},\eta}(p,v) = \int_{\Gamma_c} s\kappa_\eta(u_t)p_t\cdot v_t\,ds + \int_S s\kappa_\eta([u]_t)[p]_t\cdot[v]_t\,ds, \tag{5.85}$$

$$j^{2\prime\prime}_{\mathrm{tr},\eta}(p,v) = \int_{\Gamma_c} s\kappa'_\eta(u_t)\cdot v_t u_t\cdot p_t\,ds + \int_S s\kappa'_\eta([u]_t)\cdot[v]_t[u]_t\cdot[p]_t\,ds. \tag{5.86}$$

- for the Coulomb model:

$$\begin{aligned}&\int_\Omega Ae(p) : e(v)\,dx + j^{1\prime\prime}_{\mathrm{co},\epsilon,\eta}(p,v) + j^{2\prime\prime}_{\mathrm{co},\epsilon,\eta}(p,v) + j^{3\prime\prime}_{\mathrm{co},\epsilon,\eta}(p,v) + j''_{N,\epsilon}(p,v)\\ &= -\int_\Omega m'(u)\cdot\psi\,dx - \int_\Gamma l'(u)\cdot\psi\,ds \quad \forall v\in H^1_{\Gamma_0}(\Omega)^d,\end{aligned} \tag{5.87}$$

denoting

$$j^{1\prime\prime}_{\mathrm{co},\epsilon,\eta}(p,v) = \int_{\Gamma_c}\frac{\mu}{\epsilon}\phi_r(u\cdot n)\kappa_\eta(u_t)p_t\cdot v_t\,ds + \int_S\frac{\mu}{\epsilon}\phi_r([u]\cdot n_-)\kappa_\eta([u]_t)[p]_t\cdot[v]_t\,ds, \tag{5.88}$$

$$j^{2\prime\prime}_{\mathrm{co},\epsilon,\eta}(p,v) = \int_{\Gamma_c}\frac{\mu}{\epsilon}\phi_r(u\cdot n)\kappa'_\eta(u_t)\cdot v_t u_t\cdot p_t\,ds + \int_S\frac{\mu}{\epsilon}\phi_r([u]\cdot n_-)\kappa'_\eta([u]_t)\cdot[v]_t[u]_t\cdot[p]_t\,ds, \tag{5.89}$$

$$j^{3\prime\prime}_{\mathrm{co},\epsilon,\eta}(p,v) = \int_{\Gamma_c}\frac{\mu}{\epsilon}\phi'_r(u\cdot n)v\cdot n\mathcal{N}'_\eta(u_t)\cdot p_t\,ds + \int_S\frac{\mu}{\epsilon}\phi_r([u]\cdot n_-)[v]\cdot n_-\mathcal{N}'_\eta([u]_t)\cdot[p]_t\,ds. \tag{5.90}$$

- for the Norton-Hoff model:

$$\begin{aligned}&\int_\Omega Ae(p) : e(v)\,dx + j^{1\prime}_{\mathrm{nh},\epsilon,\eta}(p,v) + j^{2\prime}_{\mathrm{nh},\epsilon,\eta}(p,v) + j^{3\prime}_{\mathrm{nh},\epsilon,\eta}(p,v) + j''_{N,\epsilon}(p,v)\\ &= -\int_\Omega m'(u)\cdot\psi\,dx - \int_\Gamma l'(u)\cdot\psi\,ds \quad \forall v\in H^1_{\Gamma_0}(\Omega)^d,\end{aligned} \tag{5.91}$$

noting

$$j^{1\prime}_{\mathrm{nh},\epsilon,\eta}(u,v) = \int_{\Gamma_c}\frac{\mu}{\epsilon}\phi_r(u\cdot n)\mathcal{N}_\eta(u_t)^{\rho-1}p_t\cdot v_t\,ds + \int_S\frac{\mu}{\epsilon}\phi_r([u]\cdot n_-)\mathcal{N}_\eta([u]_t)^{\rho-1}[p]_t\cdot[v]_t\,ds, \tag{5.92}$$

$$\begin{aligned}j^{2\prime}_{\mathrm{nh},\epsilon,\eta}(u,v) &= \int_{\Gamma_c}\frac{\mu}{\epsilon}(\rho-1)\phi_r(u\cdot n)\mathcal{N}_\eta(u_t)^{\rho-2}\mathcal{N}'_\eta(u_t)\cdot v_t u_t\cdot p_t\,ds\\ &\quad + \int_S\frac{\mu}{\epsilon}(\rho-1)\phi_r([u]\cdot n_-)\mathcal{N}_\eta([u]_t)^{\rho-2}\mathcal{N}'_\eta([u]_t)\cdot[v]_t[u]_t\cdot[p]_t\,ds,\end{aligned} \tag{5.93}$$

$$j^{3\prime}_{\mathrm{nh},\epsilon,\eta}(u,v) = \frac{\mu}{\epsilon}\phi'_r(u\cdot n)v\cdot n\mathcal{N}_\eta(u_t)^{\rho-1}p_t\cdot u_t\,ds + \int_S\frac{\mu}{\epsilon}\phi'_r([u]\cdot n_-)[v]\cdot n_-\mathcal{N}_\eta([u]_t)^{\rho-1}[p]_t\cdot[u]_t\,ds. \tag{5.94}$$

- for the normal compliance model:

$$\begin{aligned}&\int_\Omega Ae(p) : e(v)\,dx + j'_{N,r,Nc}(p,v) + j^{1\prime\prime}_{T,\eta,Nc}(p,v) + j^{2\prime\prime}_{T,\eta,Nc}(p,v) + j^{3\prime\prime}_{T,\eta,Nc}(p,v)\\ &= \int_\Omega f\cdot v\,dx + \int_{\Gamma_N} g\cdot v\,ds \quad \forall v\in H^1_{\Gamma_0}(\Omega)^d,\end{aligned} \tag{5.95}$$

with

$$\begin{aligned}j'_{N,\mathrm{nc,r}}(p,v) &= \int_{\Gamma_c} C_N m_N\phi_r(u\cdot n)^{m_N-1}\phi'_r(u\cdot n)p\cdot n\,v\cdot n\,ds\\ &\quad + \int_S C_N m_N\phi_r([u]\cdot n_-)^{m_N-1}\phi'_r([u]\cdot n_-)[p]\cdot n\,[v]\cdot n\,ds,\end{aligned} \tag{5.96}$$

$$j^{1\prime\prime}_{T,\mathrm{nc},\eta}(p,v) = \int_{\Gamma_c} C_T\phi_r(u\cdot n)^{m_T}\kappa_\eta(u_t)p_t\cdot v_t\,ds + \int_S C_T\phi_r([u]\cdot n_-)^{m_T}\kappa_\eta([u]_t)[p]_t\cdot[v]_t\,ds, \tag{5.97}$$

$$j^{2\prime\prime}_{T,\mathrm{nc},\eta}(p,v) = \int_{\Gamma_c} C_T\phi_r(u\cdot n)^{m_T}\kappa'_\eta(u_t)\cdot v_t p_t\cdot u_t\,ds + \int_S C_T\phi_r([u]\cdot n_-)^{m_T}\kappa'_\eta([u]_t)\cdot[v]_t\,[p]_t\cdot[u]_t\,ds, \tag{5.98}$$

$$\begin{aligned}j^{3\prime\prime}_{T,\mathrm{nc},\eta}(p,v) &= \int_{\Gamma_c} C_T m_T\phi_r(u\cdot n)^{m_T-1}\phi'_r(u\cdot n)v\cdot n\mathcal{N}'_\eta(u_t)\cdot p_t\,ds\\ &\quad + \int_S C_T m_T\phi_r([u]\cdot n_-)^{m_T-1}\phi'_r([u]\cdot n_-)[v]\cdot n_-\mathcal{N}'_\eta([u]_t)\cdot[p]_t\,ds.\end{aligned} \tag{5.99}$$

For the particular example of (5.52) we have:

$$k'(x) == \begin{cases} -\dfrac{x}{\|x\|^3} & \text{for } \|x\| \geq \eta \\ -\dfrac{1}{\eta^3}x & \text{for } \|x\| \leq \eta. \end{cases} \tag{5.100}$$

5.4.4 Criteria

Compliance and volume

In some numerical examples we will use these two classical criteria which can be written under the form of (5.71). For the compliance:

$$m_{Comp}(u) = f \cdot u$$

$$l_{Comp}(u) = g \cdot u$$

For the volume:

$$m_{vol}(u) = 1$$

$$l_{vol}(u) = 0$$

Contact pressure

The contact pressure, which is always non-positive see (3.9), is the force which is applied on the structure at the contact surface. It takes the following form: $Ae(u)n \cdot n$ on Γ_c and $Ae(u|_{S_-})n_- \cdot n_-$ on S. In the penalised and regularised formulations the contact pressure P_N can be written in terms of u:

$$P_N = \begin{cases} -\dfrac{1}{\epsilon}\phi_r(u \cdot n) & \text{on } \Gamma_c \\ -\dfrac{1}{\epsilon}\phi_r([u] \cdot n_-) & \text{on } S \end{cases} \tag{5.101}$$

where ϕ_r was defined in (5.51).

The various criteria we considered, depending on the contact pressure, are of the form:

$$l(u) = l_i(P_N(u), c)\mathbb{1}_{S \cup \Gamma_c}$$

where $\mathbb{1}_{S\cup\Gamma_c}$ is the characteristic function of $S \cup \Gamma_c$ and l_i will be defined according to which characteristic of the pressure we want to control.

Uniformisation If we want to make the pressure uniform on the contact zone around a constant c, we will use the following function:

$$l_1(P_N, c) = (P_N - c)^2 \tag{5.102}$$

with $c < 0$.

Minimising the maximum of the pressure We want P_N to be under a certain threshold $c < 0$. The first natural criterion which arises is of the type:

$$l_2(P_N, c) = \max(P_N - c, 0)^2.$$

However this could lead to a null gradient during the optimization process due, for example, to a null adjoint p when there is no point in contact. This could be an insurmountable obstacle when the initial shape in the optimisation process is such that there is no contact. Indeed the gradient does not indicate that contact is possible and how to reach a shape where there is an effective contact. So we change the definition of P_N by introducing the following function:

$$\phi_r^{th}(x) = \begin{cases} \phi_r(x) - \phi_r(0) & \text{if } x \geq 0 \\ \phi_r'(0)x & \text{otherwise.} \end{cases} \tag{5.103}$$

Then we define:

$$P_N = \begin{cases} -\dfrac{1}{\epsilon}\phi_r^{th}(u \cdot n) & \text{on } \Gamma_c \\ -\dfrac{1}{\epsilon}\phi_r^{th}([u] \cdot n_-) & \text{on } S \end{cases} \tag{5.104}$$

Now when $u \cdot n = 0$, the pressure is set to 0 and when $u \cdot n < 0$, the pressure is non negative and decreases linearly, giving a sense to an opposite pressure when there is no contact. Making the most of this new pressure formulation, we define the following criterion:

$$l_3(P_N, c) = \begin{cases} 1 - \dfrac{P_N}{c} & \text{if } P_N \leq 0 \\ e^{-\frac{P_N}{c}} & \text{if } P_N > 0. \end{cases} \tag{5.105}$$

The bigger $\dfrac{P_N}{c}$, the smaller is $l_3(P_N, c)$. We could also have taken:

$$l_4(P_N, c) = \begin{cases} 1 - \dfrac{P_N}{c} & \text{if } P_N \leq c \\ -\ln\left(\dfrac{P_N}{c}\right) & \text{if } P_N > c. \end{cases} \tag{5.106}$$

The numerical experiments done did not reveal much difference between these two functions. We also tried to use other functions than affine ones for the other part, such as functions behaving like arctan or square root, but the numerical results were not convincing.

5.5 Numerical examples

The way we solve the contact problems has already been discussed in section 3.4.3. We, another time, stress the fact that the robustness of the algorithm which solves the contact equations is crucial in the optimisation process. First because the optimisation can produce structures for which the finite element matrices are nearly singular. Secondly because we are solving problems whose solution is not always unique. This leads to difficulties which can be seen in the cases 11 and 12. The contact problems are solved thanks to the finite element method, by discretising the contact region and applying node to node contact conditions for the auto-contact part.

This section will be divided into two subsections corresponding respectively to 2D and 3D cases. In all the examples of this section the contact zone is fixed (non-optimizable) but the structure can choose to use it or not. In each subsection, different models will be used depending on the mechanical case. Except case 5, case 11 and 12, the domain D is a square of 2×2 discretized with 6400 square elements. For the other cases D is a square of 2×2 discretized with 2500 square elements. The penalisation coefficient ϵ is set to 10^{-7}. For the 3D cases only the sliding contact problem and Tresca friction contact problem have been tested. During the optimisation process, some shapes are rejected either because they do not fullfill the constraints or because they do not enable a decrease in the objective function. Due to this fact, for each example, both the number of iterations (shapes which were accepted) and the number of evaluations (all the shapes which were evaluated) are given.

5.5.1 Examples in 2D

In sliding contact

We present five examples where the volume is minimized under a compliance constraint. The potential contact zone is drawn in green, the arrows represent the forces and black zones the part of the boundary where Dirichlet conditions are prescribed, in all the directions (otherwise mentioned). There is no volume force and the results are compiled in table 5.1.

- Case 1, Dirichlet conditions are enforced on the whole left side and a downward force is applied on $(2, 1.5)$:

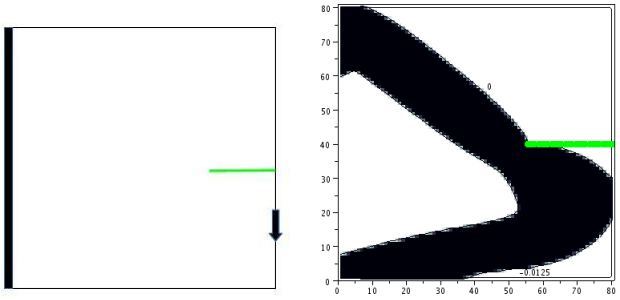

(a) Load case for case 1 (b) Final design for case 1

Figure 5.1: Case 1

- Case 2, Dirichlet conditions are enforced on the whole left side and a downward force is applied on $(2, 1.5)$. Case 1-2bis is the same case as 1 and 2 without the contact zone:

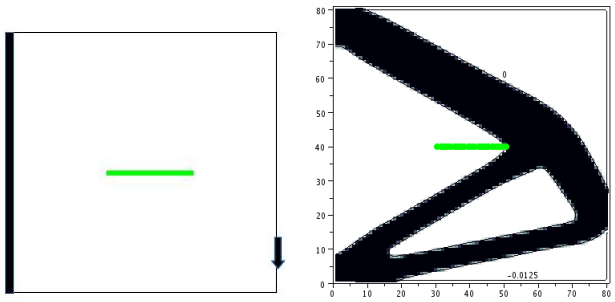

(a) Load case for case 2 (b) Final design for case 2

Figure 5.2: Case 2

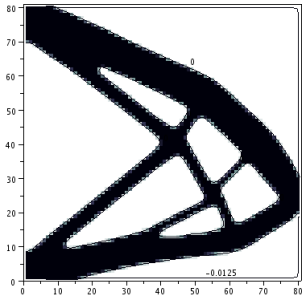

Figure 5.3: Final design for case 1-2bis

- Case 3, Dirichlet conditions are enforced on the whole left side and a rightward force is applied from $(2, 0.8)$ to $(2, 1.2)$. Case 3bis is similar without the contact area:

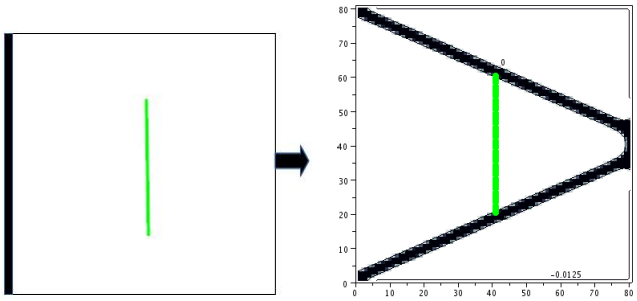

(a) Load case for case 3 (b) Final design for case 3

Figure 5.4: Case 3

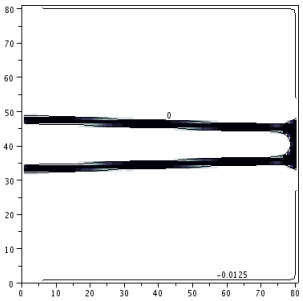

Figure 5.5: Final design for case 3bis

- Case 4, Dirichlet conditions are enforced on the whole left side and an upward force is applied on $(2, 1.5)$. Case 4bis is similar without the contact boundary conditions:

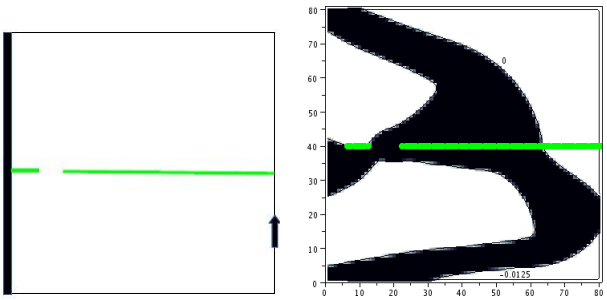

(a) Load case for case 4 (b) Final design for case 4

Figure 5.6: Case 4

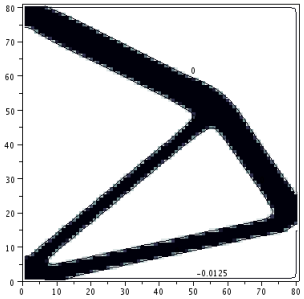

Figure 5.7: Final design for case 4bis

- Case 5, Dirichlet conditions are enforced on the part up to the left part of the L-shape and a downward force is applied on $(2, 1.6)$. Case 5bis corresponds to the same problem without the contact part:

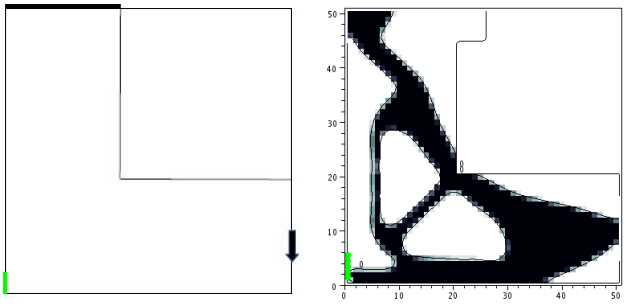

(a) Load case for case 5 (b) Final design for case 5

Figure 5.8: Case 5

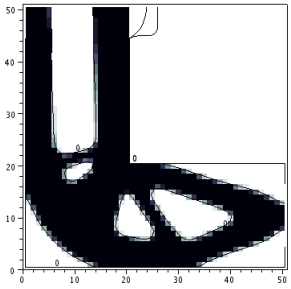

Figure 5.9: Final design for case 5bis

Cases	Volume	Compliance	Compliance Constraint	Iterations	Evaluations
1	1.6403	19.9999	20	66	92
2	1.45211	19.9998	20	67	95
1-2bis	1.41650	19.9997	20	22	38
3	0.35078	0.499995	0.5	82	110
3bis	0.248584	0.499993	0.5	31	47
4	1.69044	29.9999	30	64	95
4bis	0.928932	29.9841	30	28	46
5	1.15278	94.9829	95	18	36
5bis	1.64209	139.906	140	18	35

Table 5.1: Results for sliding contact cases and cases 1-2bis, 3bis, 4bis and 5bis.

In the cases 1, 2, and 3, the optimisation algorithm tends to avoid the contact zone which is not the case when this zone is removed. Indeed, due to the direction of the forces, this zone opens and no point is in contact. Including it in the structure would make the compliance increase which is made impossible by the constraint put on the compliance. In the case 4, the points of the contact zone are in contact and including them in the structure does not imply a too big increase of the compliance, despite the sliding occuring. In case 5, the contribution of the contact boundary conditions is underline by the fact, that for the same optimisation problem without them, even the full solution is not admissible (its compliance is about 118). We need to weaken the compliance constraint to give the possibility to the algorithm to work, as illustrated by case 5bis.

In the next three examples, the pressure criteria introduced earlier are used to obtain different kind of clamps. Apart from the case 6, in which the pressure criterion is minimized under volume and compliance constraints, we minimize the volume under compliance and pressure constraints. The results are presented in tables 5.2 and 5.3.

- Case 6, here the Dirichlet conditions on $(1.9, 0)$ and $(1.9, 2)$ are put only for the x (horizontal) part of the displacement and two forces are applied on $(1.8, 2)$ and $(1.8, 0)$. The pressure criterion used is l_3 with $c = -1.5$:

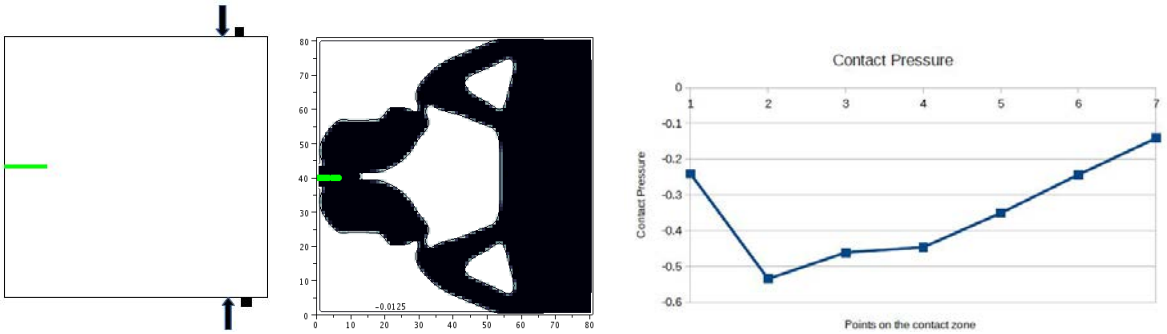

(a) Load case for case 6 (b) Final design for case 6 (c) Final pressure for case 6

Figure 5.10: Case 6

- Case 6bis, two forces are applied on $(1.8, 2)$ and $(1.8, 0)$ and the structure is fixed from $(2, 0.9)$ to $(2, 1.1)$. The pressure criterion used is l_3 with $c = -1.1$:

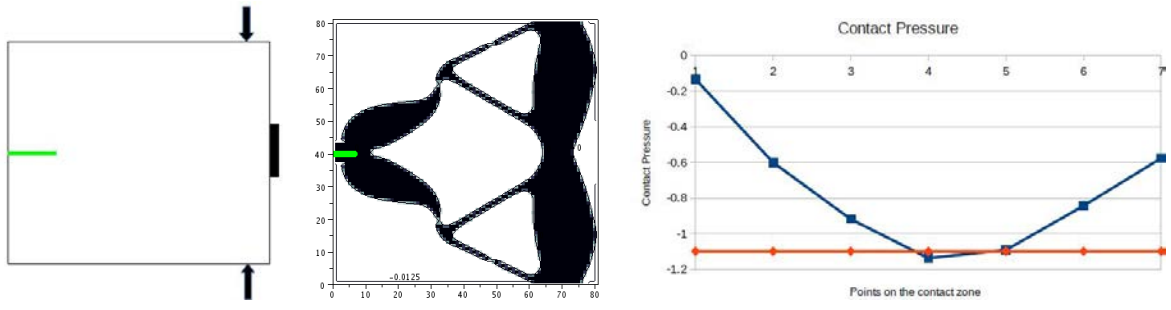

(a) Load case for case 6bis (b) Final design for case 6bis (c) Final pressure for case 6bis

Figure 5.11: Case 6bis

Cases	Press.	Compl.	Compl. Constr.	Vol.	Vol. constr.	Iterations	Evaluations
6	3.03302	8.32621	8.4	2.27271	2.7	16	23

Table 5.2: Results for the case 6.

- Case 7, two forces are applied on $(1.5, 2)$ and $(1.5, 0)$. The pressure criterion used is l_3 with $c = -0.9$:

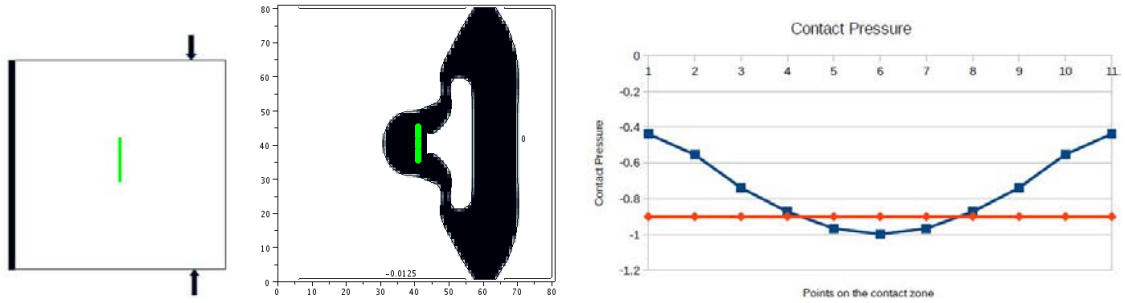

(a) Load case for case 7 (b) Final design for case 7 (c) Final pressure for case 7

Figure 5.12: Case 7

- Case 8, the downside is fixed and two forces are applied on $(0.2, 0)$ and $(1.8, 0)$. The pressure criterion used is l_1 with $c = -2$:

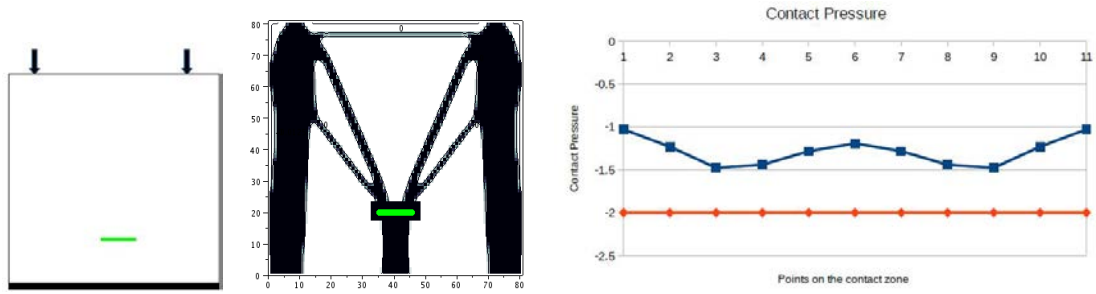

(a) Load case for case 8 (b) Final design for case 8 (c) Final pressure for case 8

Figure 5.13: Case 8

In example 6, the shape of a clamp is found, which manages to bring the forces from the right side to the left side keeping their direction. In example 6bis the Dirichlet part on the right side is used at the beginning of the optimisation process and is finally found to be useless. On the contrary, example 7 shows a mechanism which transforms the vertical forces into horizontal ones. Finally example 8 produces pilars that are not perpendicular to Dirichlet zone to put weight on the contact zone. It has to be noted that the computation of the contact pressure, thanks to the penalisation is not accurate since the displacement u is multiplied by the penalisation $\frac{1}{\epsilon}$. So u would need to be solved with a precision smaller than ϵ which is not the case here. Moreover it appears that the criteria used are very sensitive to small changes in the shape. This forbids the use of too tight pressure constraint, which explains that pointwise constraints are most of the time not fullfilled. These cases are however interesting as they give a hint of the shape really needed.

With friction

We give four cases of contact optimisation with friction. In each of them, the results for the sliding (no friction) contact, the Tresca model, the Norton Hoff model, the normal compliance model and the Coulomb model are shown. For normal compliance model $C_N = 1$, $m_N = 1$ and $m_T = 1$. We minimize the volume under a compliance constraint.

- Case 9, a force is applied on $(2, 1)$, the left side of the strucutre is fixed. The coefficient of friction used is 0.5 and for the Norton Hoff example $\rho = 0.1$. Case 9bis corresponds to the same problem without the two contact areas. Results can be found in table 5.4.

Cases	Vol.	Compl.	Compl. Constr.	Press.	Press. Constr.	Iterations	Evaluations
6bis	1.34868	10.9603	11	1.99976	2	251	275
7	0.971308	5.99801	6	1.49998	1.5	178	206
8	1.62217	14.9941	15	0.148007	0.15	24	40

Table 5.3: Results for the cases 6bis, 7 and 8

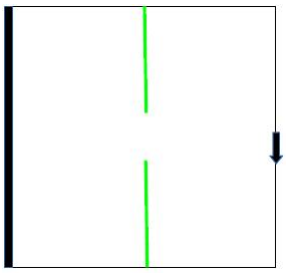

(a) Load case for case 9

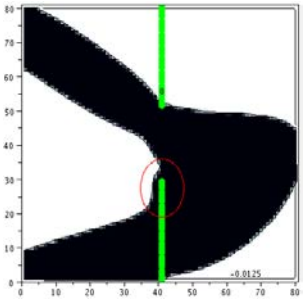

(b) Final design for frictionless contact

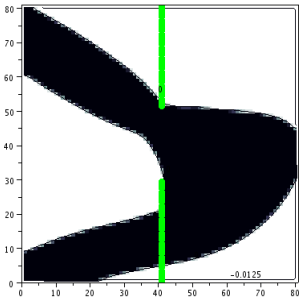

(c) Final design for the Tresca model

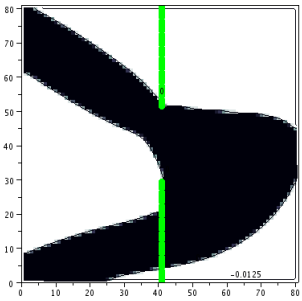

(d) Final design for the Norton-Hoff model

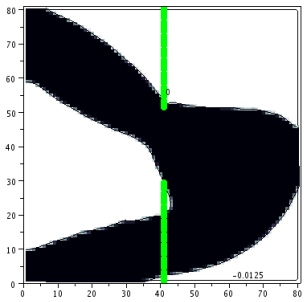

(e) Final design for the normal compliance model

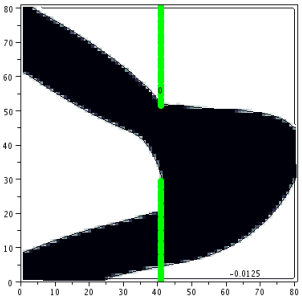

(f) Final design for the Coulomb model

Figure 5.14: Case 9.

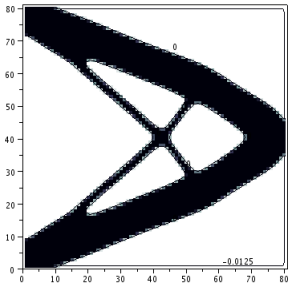

Figure 5.15: Final design for case 9bis (without contact).

In all the cases, the algorithm tends to avoid the upper contact zone which opens and keep the lower one. However, in sliding contact, the lower leg has to be hooked up to a part of the structure which is not in the contact zone. It is not the case in the friction cases as the friction keeps the lower leg connected to the structure (see the zone circled in red on the final design for frictionless contact and the equivalent zone on the models with

Cases	Volume	Compliance	Compliance Constraint	Iterations	Evaluations
Sliding contact	1.87253	19.9998	20	47	73
Tresca	1.76836	19.9999	20	47	73
Norton Hoff	1.76906	19.9999	20	41	67
Normal compliance	1.97197	19.9999	20	49	65
Coulomb	1.76948	19.9998	20	45	70
9bis	1.34787	19.9978	20	33	50

Table 5.4: Results for case 9 and 9bis.

friction). The case 9bis is meant to underline the impact of the contact on the optimised structure. The results are delivered in table 5.5.

- Case 10, a force is applied on $(1, 2)$. The coefficient of friction used is 1.3 and for the Norton Hoff example $\rho = 0.5$:

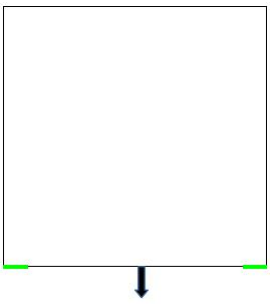

(a) Load case for case 10

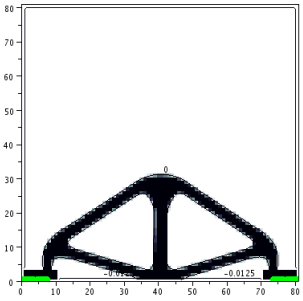

(b) Final design for frictionless contact

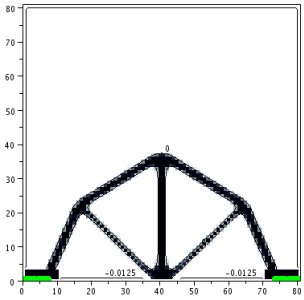

(c) Final design for the Tresca model

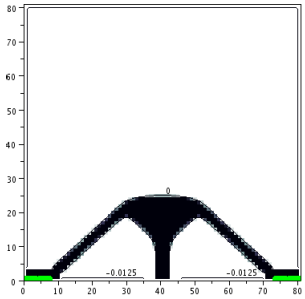

(d) Final design for the Norton-Hoff model

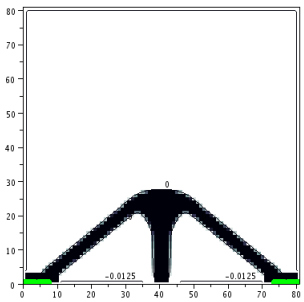

(e) Final design for the normal compliance model

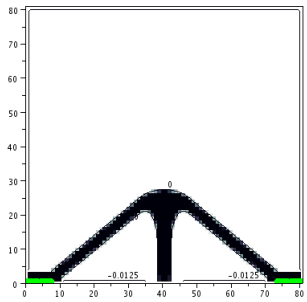

(f) Final design for the Coulomb model

Figure 5.16: Case 10.

In sliding contact the legs of the bridge have to be vertical to the contact zone to prevent sliding. Whereas in other cases, the friction stabilises the structure and enables the legs to incline.

- Case 11, Dirichlet conditions are enforced on the left up part of the L-shape and a downward force is applied on $(2, 1.6)$. The coefficient of friction used is 1.2 and for the Norton Hoff example $\rho = 0.6$. Results are given in

Cases	Volume	Compliance	Compliance Constraint	Iterations	Evaluations
Sliding contact	0.422235	21.9991	22	44	71
Tresca	0.302352	21.9957	22	45	71
Norton Hoff	0.309498	21.9995	22	44	65
Normal compliance	0.336178	21.9996	22	37	63
Coulomb	0.286532	21.9995	22	35	61

Table 5.5: Results for case 10.

table 5.6.

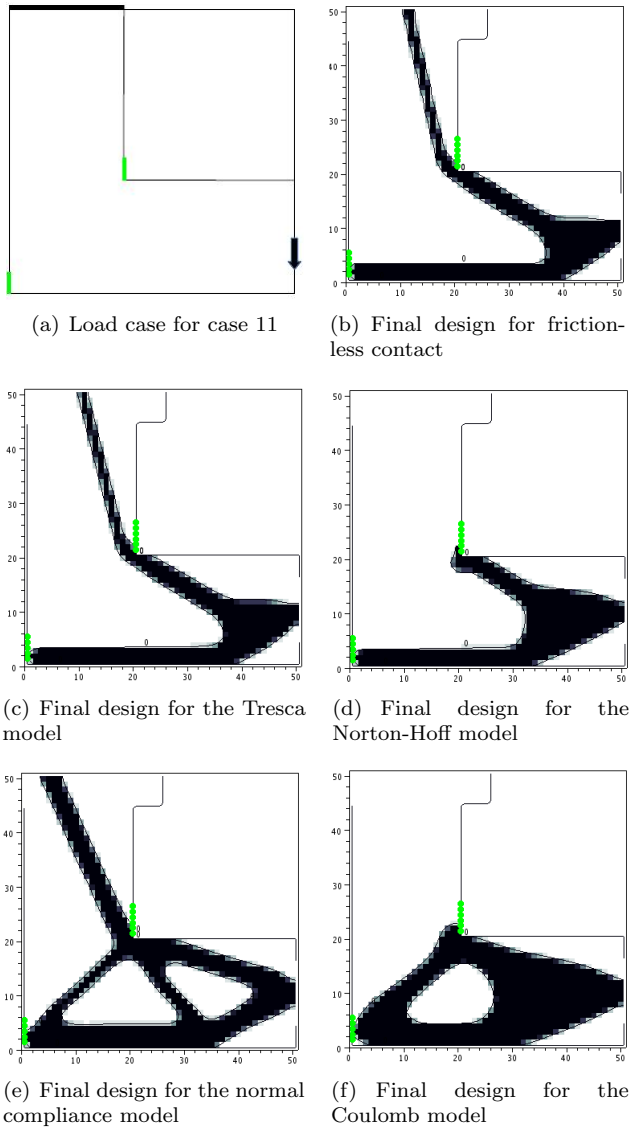

(a) Load case for case 11

(b) Final design for frictionless contact

(c) Final design for the Tresca model

(d) Final design for the Norton-Hoff model

(e) Final design for the normal compliance model

(f) Final design for the Coulomb model

Figure 5.17: Case 11.

The result in sliding contact can be compared with case 5. Here the algotihm makes use of the second contact zone and for Norton-Hoff model manages to use it to stabilise the structure without being connected to the Dirichlet boundary. In the case of Coulomb model, there is trouble in solving the contact problem which leads to a bad optimized result in terms of volume compared to the other models.

- Case 12, Dirichlet conditions are enforced from $(1.2, 0)$ to $(2, 0)$ and a downward force is applied on $(2, 1.6)$. The coefficient of friction used is 0.8 and for the Norton Hoff example $\rho = 0.6$. For the case 12bis, we only remove the contact zone. Results are shown in table 5.7

Cases	Volume	Compliance	Compliance Constraint	Iterations	Evaluations
Sliding contact	0.593907	94.9994	95	22	40
Tresca	0.59725	94.9014	95	18	34
Norton Hoff	0.550918	94.5404	95	18	34
Normal compliance	0.917105	94.1346	95	13	30
Coulomb	0.907396	94.9978	95	48	67

Table 5.6: Results for case 11.

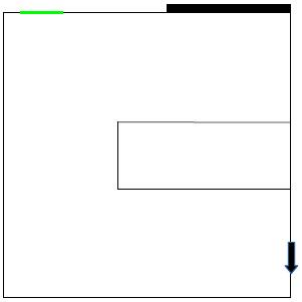

(a) Load case for case 12

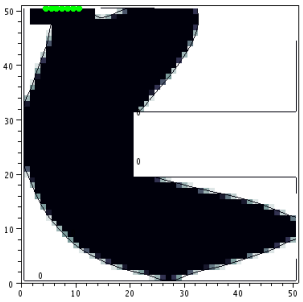

(b) Final design for frictionless contact

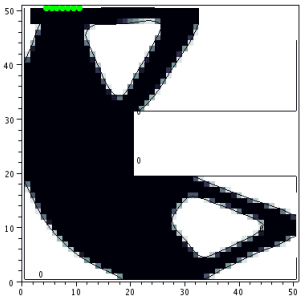

(c) Final design for the Tresca model

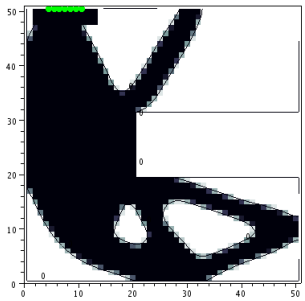

(d) Final design for the Norton-Hoff model

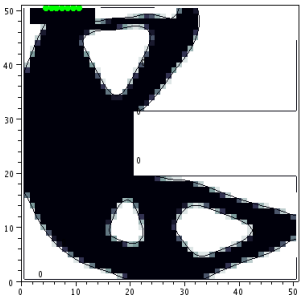

(e) Final design for the normal compliance model

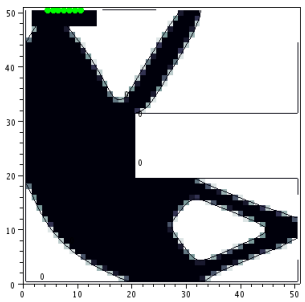

(f) Final design for the Coulomb model

Figure 5.18: Case 12.

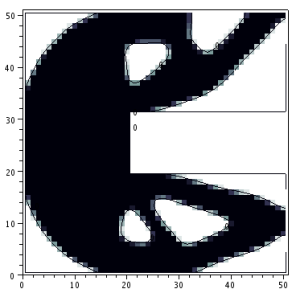

Figure 5.19: Final design for case 12bis

The contact area enables the structure to be only connected with the Dirichlet part by its left edge and to use less matter. The friction allows to slightly decrease the volume.

Cases	Volume	Compliance	Compliance Constraint	Iterations	Evaluations
Sliding contact	2.15435	149.999	150	16	32
Tresca	1.95836	149.989	150	14	29
Norton Hoff	1.87089	149.881	150	25	40
Normal compliance	1.94898	149.994	150	13	28
Coulomb	1.83706	149.997	150	20	39
12bis	2.39942	149.962	150	20	36

Table 5.7: Results for case 12 and 12bis.

5.5.2 Examples in 3D

The following cases were computed thanks to the finite element sofware SYSTUS of ESI-Group. In all of them the volume is minimised under compliance constraint. The friction coefficient is set to 0.01. To be sure that the models of sliding contact and Tresca were the same as in 2D, we choose to use node to node elements (string elements) for which we implement the penalisations adapted to the frictionless contact and the Tresca model.

- Case 13, for 97289 elements and 17290 nodes. The results are gathered in table 5.8.

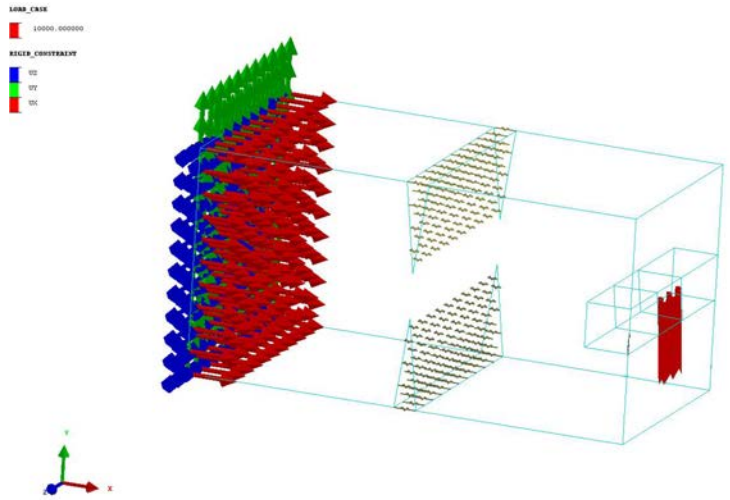

Figure 5.20: Load case for case 13.

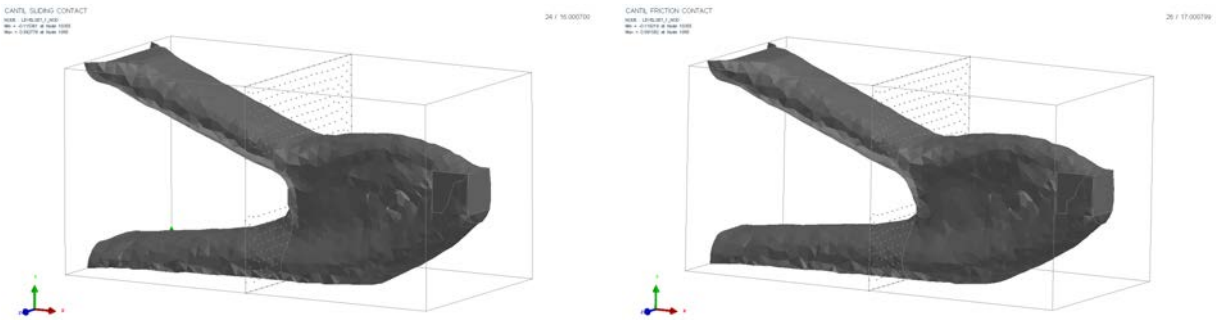

(a) Final design for frictionless contact

(b) Final design for the Tresca model

Figure 5.21: case 13.

This case is the equivalent of 2D case 9 but in 3D. There are two potential contact zones in the middle, the left side is fixed and a force is applied in the middle of the right side. We can make the same remark that in frictionless contact the lower leg needs to be hooked up to a part of the structure not containing the contact. This is not the case when friction is possible.

- Case 14, for 156417 elements and 27312 nodes. See table 5.9 for the results.

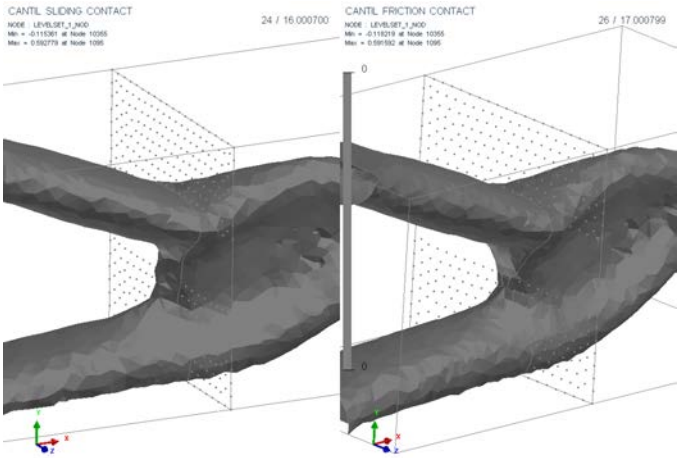

Figure 5.22: Comparison between without (left) and with (right) friction. We remark the small amount of matter needed only in the sliding case.

Cases	Volume	Compliance	Compliance Constraint	Iterations	Evaluations
Sliding contact	2.521889e-01	9.994017e+03	10000	15	23
Tresca	2.555368e-01	9.999298e+03	10000	17	25

Table 5.8: Results for case 13.

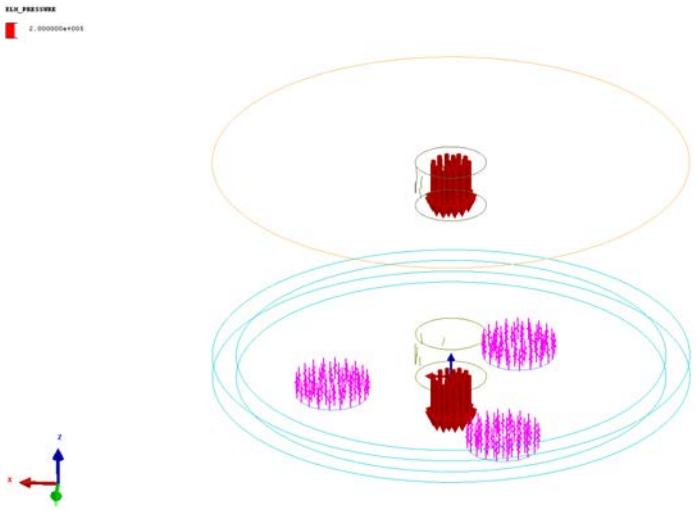

Figure 5.23: Load case for case 14.

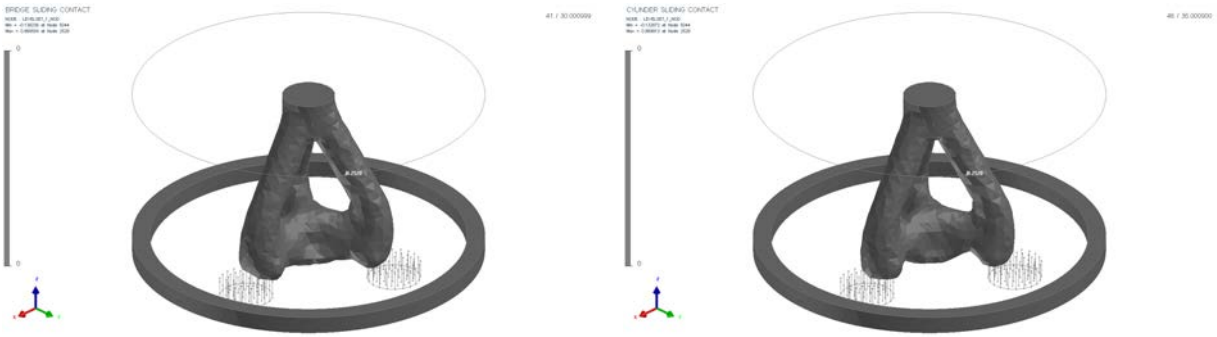

(a) Final design for frictionless contact

(b) Final design for the Tresca model

Figure 5.24: case 14.

Here there are three circular potential contact zones and the forces are applied on two small cylinders in the middle. A circular Dirichlet zone is put on the bottom, surrounding the structure. In both cases the contact

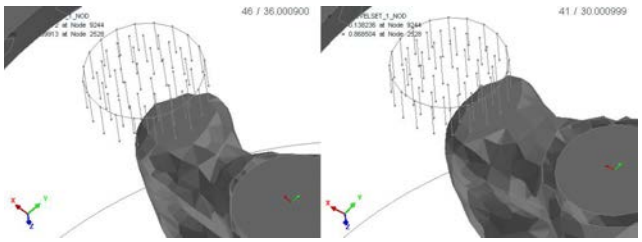

Figure 5.25: Comparison between with (left) and without (right) friction. We remark that the shape of the foot is larger when friction is present.

Cases	Volume	Compliance	Compliance Constraint	Iterations	Evaluations
Sliding contact	2.078838e-01	9.987082e+03	10000	29	40
Tresca	1.920865e-01	9.987843e+03	10000	36	45

Table 5.9: Results for case 14.

zones are enough to stabilise the structure and the Dirichlet zone is not used. Between frictionless and friction contact, slight changes appear in the shape of the three feet of the structure.

- Case 15, for 89475 elements and 15895 nodes. Table 5.10 shows the results.

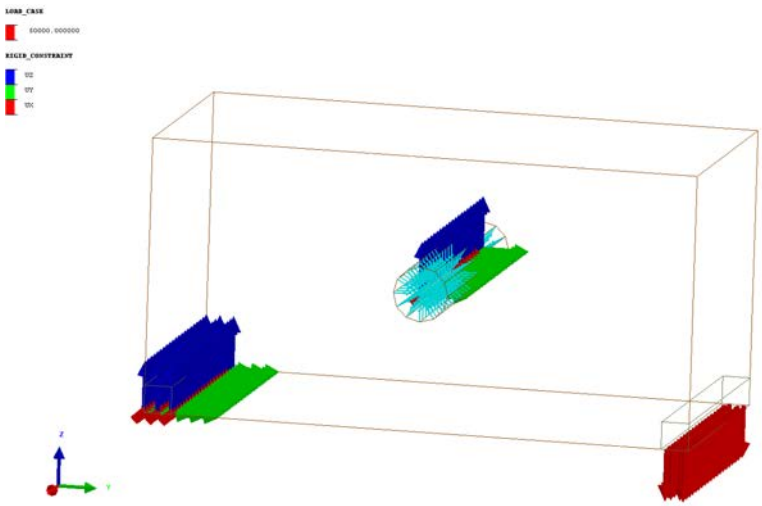

Figure 5.26: Load case for case 15.

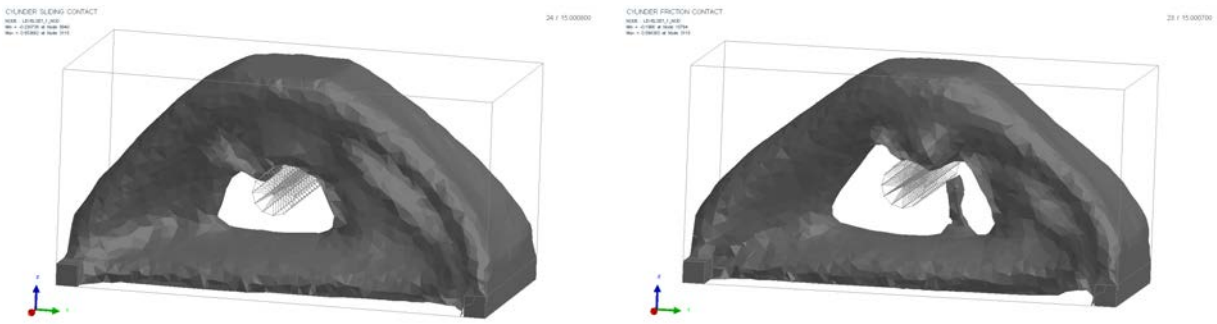

(a) Final design for frictionless contact

(b) Final design for the Tresca model

Figure 5.27: case 15.

The cylinder in the center and the bottom left side are completely fixed. A force is applied on the bottom right part. As the cylinder in the center is fixed, the algorithm uses it to stabilise the structure. In the frictionless

Cases	Volume	Compliance	Compliance Constraint	Iterations	Evaluations
Sliding contact	7.082515e-01	9.990895e+03	10000	14	23
Tresca	6.915364e-01	9.979266e+03	10000	14	22

Table 5.10: Results for case 15.

case it needs to turn around the cylinder as sliding is possible. In the friction case this is not needed anymore. But we remark that a small part of matter remains under the cylinder, going to it from the base. This part is not in contact but the tangential displacements are such that friction occurs (which is one of the problems of the Tresca model making it non mecanically correct, see section 3.4.3).

- Case 16, for 89475 elements and 15895 nodes. Table 5.11 gathers the results.

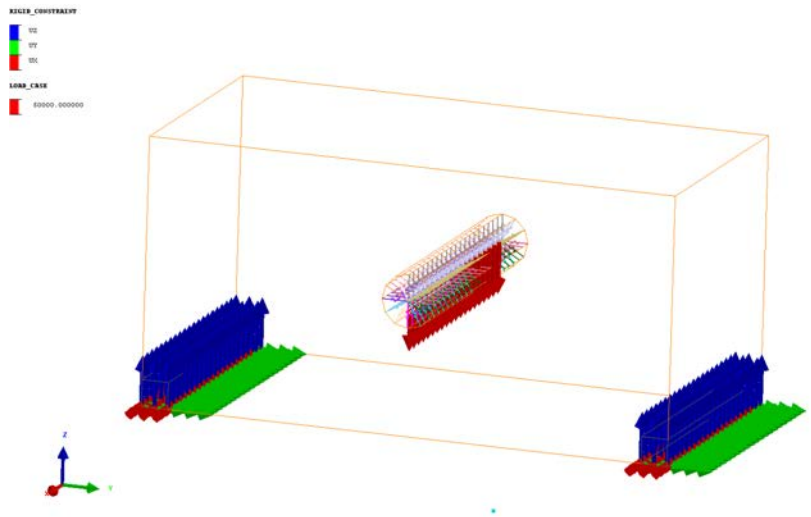

Figure 5.28: Load case for case 16.

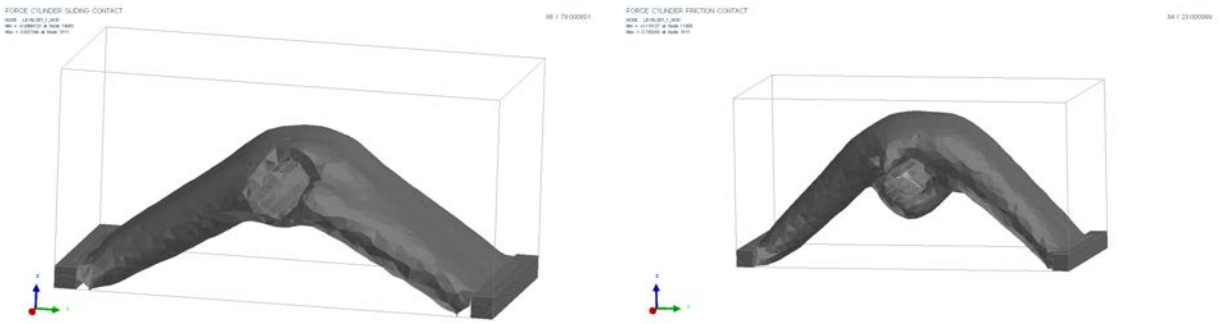

(a) Final design for frictionless contact

(b) Final design for the Tresca model

Figure 5.29: case 16.

A force is now applied on the cylinder and the left and right bottom parts are completely fixed. The cylinder is encircled by matter to be supported. The differences between the sliding and the friction case come from the fact that in the friction case the optimisation algorithm stopped prematurely due to convergence problems in the contact solver.

- Case 17, for 90205 elements and 16010 nodes. Table 5.12 presents the results.

The cylinder is fixed only in the y and x directions and a vertical force is applied on it. Forces are also applied on the extreme right and left parts. Finally we fixed two parts on the bottom. The structure only needs to support the cylinder and the forces on the left and right side. To perform that, it uses archways in order to lead

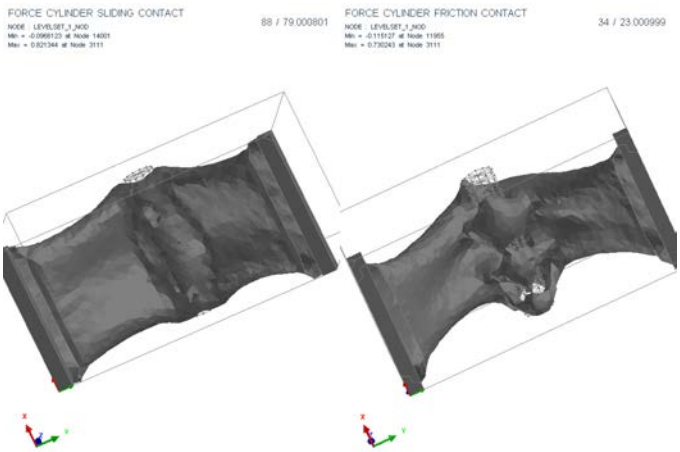

Figure 5.30: Comparison between without (left) and with (right) friction from below for case 16

Cases	Volume	Compliance	Compliance Constraint	Iterations	Evaluations
Sliding contact	3.293794e-01	9.997417e+03	10000	78	87
Tresca	3.322390e-01	9.860692e+03	10000	22	33

Table 5.11: Results for case 16.

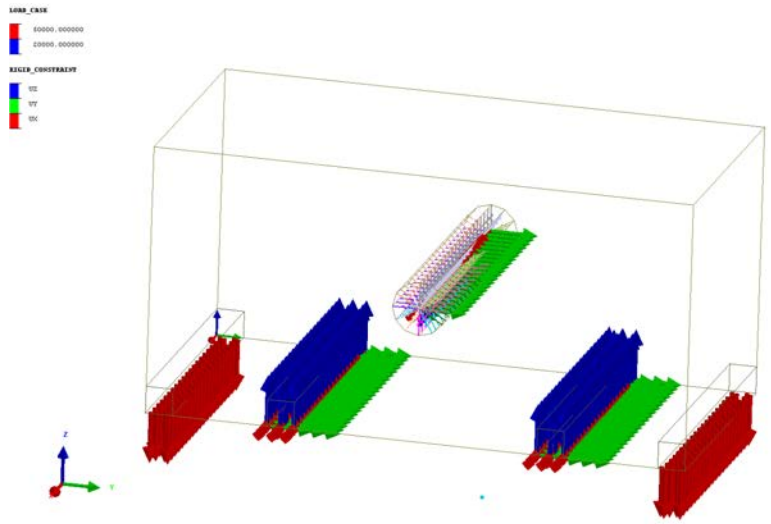

Figure 5.31: Load case for case 17.

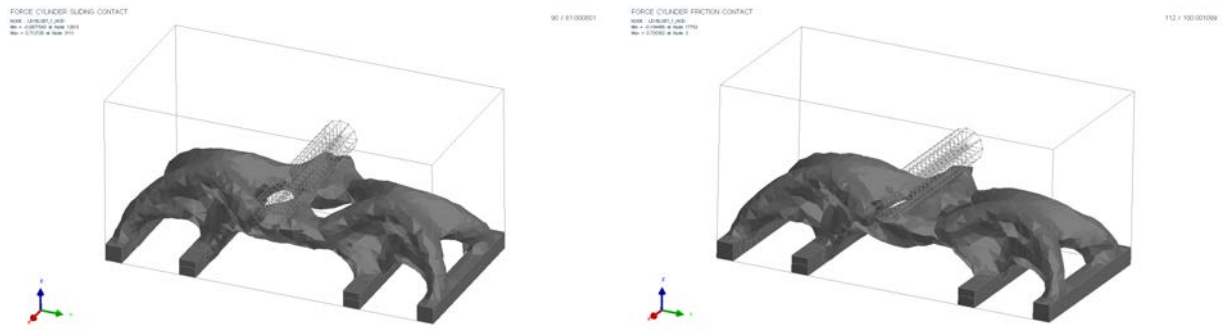

(a) Final design for frictionless contact

(b) Final design for the Tresca model

Figure 5.32: case 17.

to the middle of the structure forces on the sides, changing their direction in the opposite one and, this way, using them to support the force of the cylinder. Due to the Dirichlet conditions put on the cylinder, the fact that the results are the same with or without friction is not a surprise.

Cases	Volume	Compliance	Compliance Constraint	Iterations	Evaluations
Sliding contact	2.349350e-01	1.981722e+04	20000	81	89
Tresca	2.299134e-01	1.986286e+04	10000	100	111

Table 5.12: Results for case 17.

5.5.3 Conclusion

In conclusion, through all the examples shown in this part, the regularized and penalized formulations are proved to be good ways to cope with the non differentiability of problems having a unique solution. Despite the possible non uniqueness of its solution, the Norton Hoff model behaves well in this framework. On the contrary, the Coulomb model presents severe difficulties due to a bad convergence in the contact solver. It then appears that the crucial point is the robustness of the contact solver which has to converge in every situation for the optimization process to succeed. We can also point out that for contact solvers which use a Newton method, the adjoint method for computing the shape derivative is well suited. Indeed the adjoint solution p for a particular criterion j solved a problem of the form $Mp = f_{sec}$, where M is the transpose Newton matrix and f_{sec}, the right hand side, is the derivative of the criterion. This was of great help when we got to the implementation in the software of ESI group.
Concerning the criteria depending on the contact pressure, we have to be prudent on the conclusion, as the approximations made (Finite element method coupling with penalisation) does not enable a correct accuracy on the computed pressure. However these criteria can be used to create compliant mechanisms such as in case 6, 6bis and case 7 or in [197] or as in the case 8 to get a shape which tends to uniformize the pressure, keeping in mind that the threshold enforced in the numerical simulation can be very different from the real value.

To go beyond these results, we mention that the possibility of using subgradients algorithms, and, so of computing subgradients for the problems written under a variational inequation form, could also be investigated ([153] or [227]) to get a better accuracy on the contact pressure and to optimize with Coulomb friction [31]. Results are only shown when the problem is first discretized and the continuous case has not been studied yet. Further numerical studies are also to be made for this particular approach.

5.6 Optimizing the contact zone

In the continuity of the previous numerical examples, it could be interesting to optimize the potential contact zone as done in [180] where XFEM is used to compute the contact solution. This is the task we want to tackle in this part. Our goal is to perform the optimization with a fixed mesh. This means that the mesh will not vary during the optimization process, when the contact zone warps. Thus the mesh will not follow the contact zone and the algorithms used since now to compute the solutions of contact problems are useless.

We limit ourselves to the case of sliding auto-contact and present two possibilities, different from the XFEM method, to solve the mechanical problem. The first one is based on the idea of approximating the thin crack by an enlarged one. The second one makes the most of the idea introduced in [16] to account for unilateral contact in a crack propagation achieved, thanks to the phase field method. We recall the sliding auto-contact problem:

$$\begin{cases} -\operatorname{div}(Ae(u)) = f & \text{in } \Omega \\ u = 0 & \text{on } \Gamma_0 \\ Ae(u)n = g & \text{on } \Gamma_N \\ Ae(u)n = 0 & \text{on } \Gamma \\ [u]\cdot n_- \le 0,\ Ae(u_{|S_-})n_-\cdot n_- = Ae(u_{|S_+})n_-\cdot n_- \le 0,\ ([u]\cdot n_-)(Ae(u_{|S_-})n_-\cdot n_-) = 0 & \text{on } S \\ (Ae(u)n)_t = 0 & \text{on } S \end{cases} \tag{5.107}$$

and the associated variational inequality: find $u \in K(\Omega)$, such that

$$\int_\Omega Ae(u) : e(v-u)\,dx \ge \int_\Omega f\cdot(v-u)\,dx + \int_{\Gamma_N} g\cdot(v-u)\,ds \ \forall v \in K(\Omega) \tag{5.108}$$

with

$$K(\Omega) = \left\{ v \in H^1_{\Gamma_0}(\Omega)^d,\ [v\cdot n] \le 0 \text{ on } S \right\}. \tag{5.109}$$

5.6.1 Method 1: Enlarging the crack

The continuous model

Our idea is to approximate the crack S by a slot whose thickness is small, bounded by a small parameter $\epsilon > 0$. Indeed it is tantamount to replace the crack by a hole of small thickness, as shown in figure 5.33.

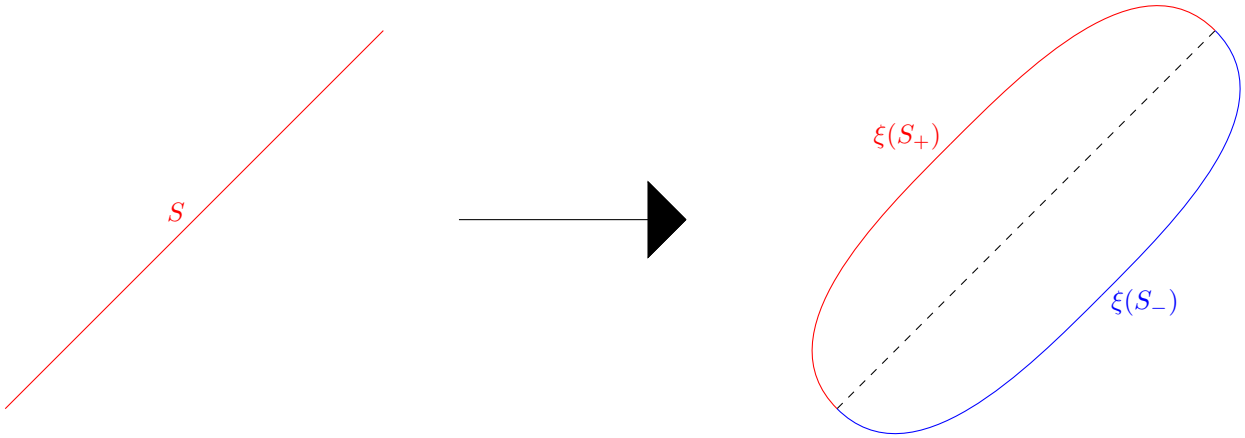

Figure 5.33: We replace the crack S on the left by a hole on the right

To be able to define the new problem, we take a function $\xi \in W^{2,\infty}\left(\mathbb{R}^d \setminus S, \mathbb{R}^d \setminus \omega\right)$ discontinuous on S such that the boundary of the hole is defined by $(I+\xi)(S_+ \cup S_-)$, ξ is null on $\Gamma_0 \cup \Gamma_N$ and $I+\xi$ is a C^1 diffeomorphism. We note ω the hole and $\Omega_\xi = \Omega \setminus \omega$ and define the jump $[\cdot]_\xi$ through the hole of a function defined in Ω_ξ by:

$$[v]_\xi = v_{|S_-}(x_- + \xi(x_-)) - v_{|S_+}(x_+ + \xi(x_+)) \tag{5.110}$$

where, if $x \in S$, x_+ is the corresponding point on S_+ and x_- the corresponding point on S_-. Then we can write the approximate formulation under the following variational formulation:

$$\int_{\Omega_\xi} Ae(u_\xi) : e(v-u_\xi)\,dx \geq \int_{\Omega_\xi} f\cdot(v-u_\xi)\,dx + \int_{\Gamma_N} g\cdot(v-u_\xi)\,ds \;\forall v \in K_\xi(\Omega_\xi) \tag{5.111}$$

with

$$K_\xi(\Omega_\xi) = \left\{ v \in H^1_{\Gamma_0}(\Omega)^d,\, [v\cdot n]_\xi \leq 0 \text{ on } S \right\}. \tag{5.112}$$

At this point we can remark that we are nearly in the same framework as for the computation of the conical derivative for the frictionless contact case. So we can apply the proposition 5.2.2:

$$u_\xi \in K_\xi(\Omega_\xi) \Leftrightarrow (I+\nabla\xi)^{-1}\overline{u}(\xi) \in K(\Omega). \tag{5.113}$$

We introduce the variable change of definition 5.7 and the problem can be put under the form (5.9), with a simplified F^ξ term as ξ is null on Γ_N:

$$\begin{aligned} \langle F^\xi, \phi\rangle \quad = \quad & \int_{\Omega_0} f(y+\xi(y))\cdot(I+\nabla\xi)(\phi-w)|det(I+\nabla\xi)|\,dx \\ & + \int_{\partial\Gamma_N} g(y)\cdot(\phi-w)\,ds. \end{aligned} \tag{5.114}$$

The result found in lemma 5.2.6 are true in the present case:

$$\|w(\xi)-w(0)\|_{H^1} \leq C\,\|\xi\|_{W^{2,\infty}} + o(\xi) \tag{5.115}$$

with $\lim\limits_{\xi\to 0} \dfrac{|o(\xi)|}{\|\xi\|_{W^{2,\infty}}} = 0$.

Theorem 5.6.1. *The function $\overline{u}(\xi)$ converges to the solution u of* (5.108)*. And we have:*

$$\|\overline{u}(\xi,x)-\overline{u}(0)\|_{H^1} \leq C\,\|\xi\|_{W^{2,\infty}} + o(\xi) \tag{5.116}$$

Proof. Thanks to the triangular inequality, we get:

$$\|\overline{u}(\xi,x)-\overline{u}(0)\|_{H^1} = \|(I+\nabla\xi)(w(\xi)-w(0))\|_{H^1} \leq C\,\|\xi\|_{W^{2,\infty}} + o(\xi). \tag{5.117}$$

This gives the convergence and the wanted estimation. □

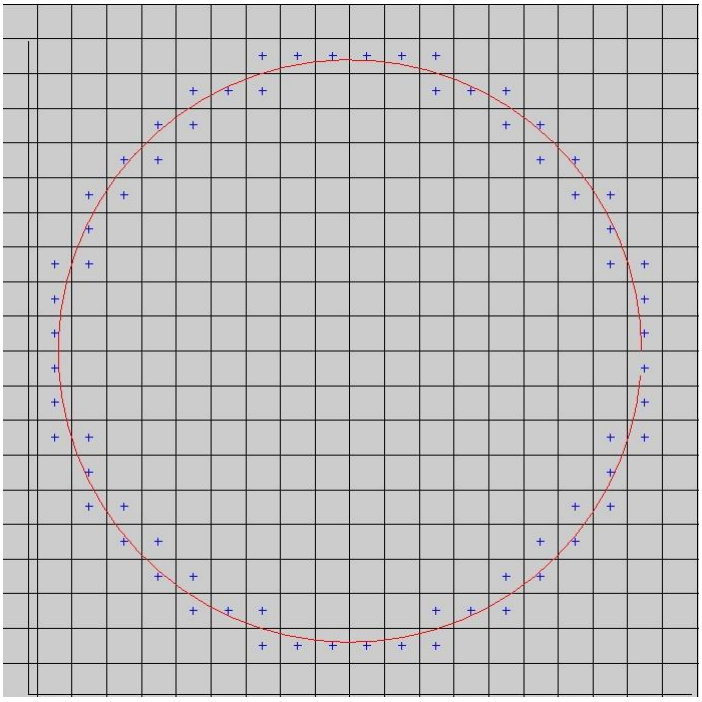

Figure 5.34: The elements marked by a blue cross of the slot for S (in red) being a circle

A penalised version of the approximate contact model

Adopting the same paradigm as in sections 5.3 and 5.4, we want to use a penalised formulation of our approximate model to be able to compute shape gradients. The formulation we propose is then: find $u_\xi \in H^1_{\Gamma_0}(\Omega)^d$ such that for every $v \in H^1_{\Gamma_0}(\Omega)^d$:

$$\int_{\Omega_\epsilon} Ae(u) : e(v)\,dx + \frac{1}{\epsilon}\int_S \phi_r([u\cdot n]_\xi)[v\cdot n]_\xi\,ds = \int_{\Omega_\xi} f\cdot v\,dx + \int_{\Gamma_N} g\cdot v\,ds. \tag{5.118}$$

We emphasize the fact that the normal is inside the jump $[\cdot]_\xi$ since it is possible that the two normals differ from S_+ to S_-.

On numerical implementation

We solve the approximate problem by the means of the finite element method as explained in chapter 3. The additional difficulty comes from the definition of S and of the approximate slot of small thickness. First, to define the crack S, we use two level set functions and more precisely two signed distance functions (only one if the crack is a closed contour), see figure 5.61. Then we choose to take for the slot the area covered by the elements crossed by S, which also enables to define the boundary of the slot. For instance for S being a circle, we mark with a blue cross in figure 5.34 the elements of the slot. These elements should be void elements but, to avoid working with singular matrices, we associate to them a small density mimicking the void (as done in section 1.3.4).

The next step is to compute the matrix corresponding to the term $\int_S \phi_r([u\cdot n]_\theta)[v\cdot n]_\theta\,ds$. As S is not discretized we have to compute this integral using the points near S, basically the points of the elements of the slot. Then taking one of these points we compute the jump of u by going on the other side of the crack, following the normal, at the boundary of the slot. On figure 5.35 this procedure is shown for the particular case of a circle: taking a node in green we find its associate node to calculate the jump in yellow.

Let $x \in S$ be given, we make the assumption that the normal in x_+, x_- and x have the same direction. This approximation can prove to be true if S is a closed smooth contour and the slot is well-chosen or, for a non closed contour S, if we estimate the integral term with nodes which are not too close from ∂S.

In the numerical examples, some cases include a volumic zone ω_0 where we want to enforce Dirichlet boundary limits (this volumic zone is clamped). To numerically account for this Dirichlet condition, we use a penalisation term which is added in the variational equation when solving the approximate contact problem:

$$\frac{1}{\epsilon_D}\int_{\omega_0} v\cdot u_\theta\,dx. \tag{5.119}$$

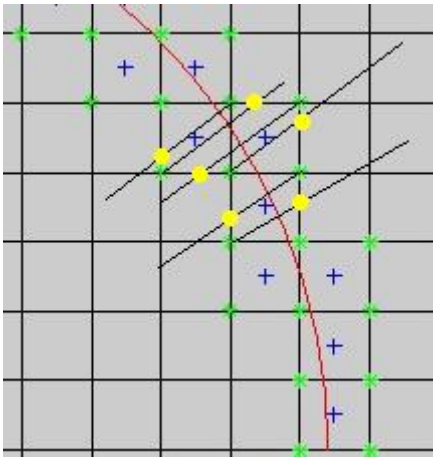

Figure 5.35: For a point in green we find its associate point in yellow to compute the jump

with $\epsilon_D > 0$ a small parameter, equal to 10^{-7} in the numerical examples.

Numerical Examples

We test our method on two simple cases. The first one is a compression case and the second one an expansion case. To be able to make some comparisons with the exact solution, the contact zone is meshed. We take a square box of side length equal to 2, discretized by a grid of square elements of length side noted h.

Compression example The left side is embedded, a contact zone is placed from $(1.05, 0.8)$ to $(1.05, 1.2)$. A force is applied on at $(2, 1)$ in the leftward direction, see figure 5.36.

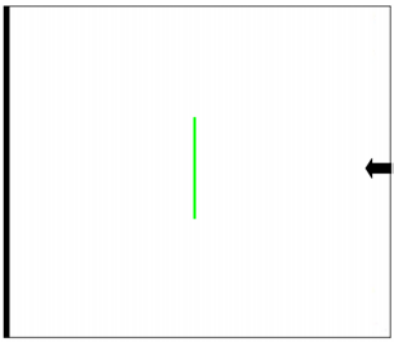

Figure 5.36: Load case for the compression case, using the enlarging crack method.

The difficulty in making a comparison between the exact solution and the approximate is that, despite the fact that the solutions are computed on the same mesh, we cannot make a node to node comparison if we want to see the convergence because of the kind of convergence proved in theorem 5.6.1. So we choose to plot some sections of the displacement in the x direction and in the y direction with respect to h the length of a square element side. For the y direction, we choose to do a section for $x = 1.05$ and for the x direction for $y = 1$ and for $x = 1.05$. See figures 5.37, 5.38 and 5.39 for the results.

On figure 5.37, the comparison is a node to node comparison. On figures 5.38 and 5.39, we make a comparison in the spirit of theorem 5.6.1. The crack we consider is vertical. We note S_- the left side and S_+ the right side. The contact zone being vertical and the mesh being a grid, the contact zone is exactly discretized and belongs to a column of the grid. We choose to number these columns from left to right and denote c the number of the column including the crack. Then, the hole ω has for boundary a part of the column $c - 1$ and $c + 1$. On figures 5.38 and 5.39, the comparison is made node to node outside the crack and, on the contact zone, is made between the exact values on S_- and the approximate values of the associated points of the column $c - 1$. In table 5.13, errors, computed doing this transformation for S_- and S_+ are gathered.

On figure 5.37, we see a plate where the contact zone lies. It is in fact the hole ω which behaves like a rigid material. On figure 5.39, we observe that the vertical component of the displacement is well approximate on the crack and, on figure 5.38, that, near the crack boundary, the horizontal component is not well computed.

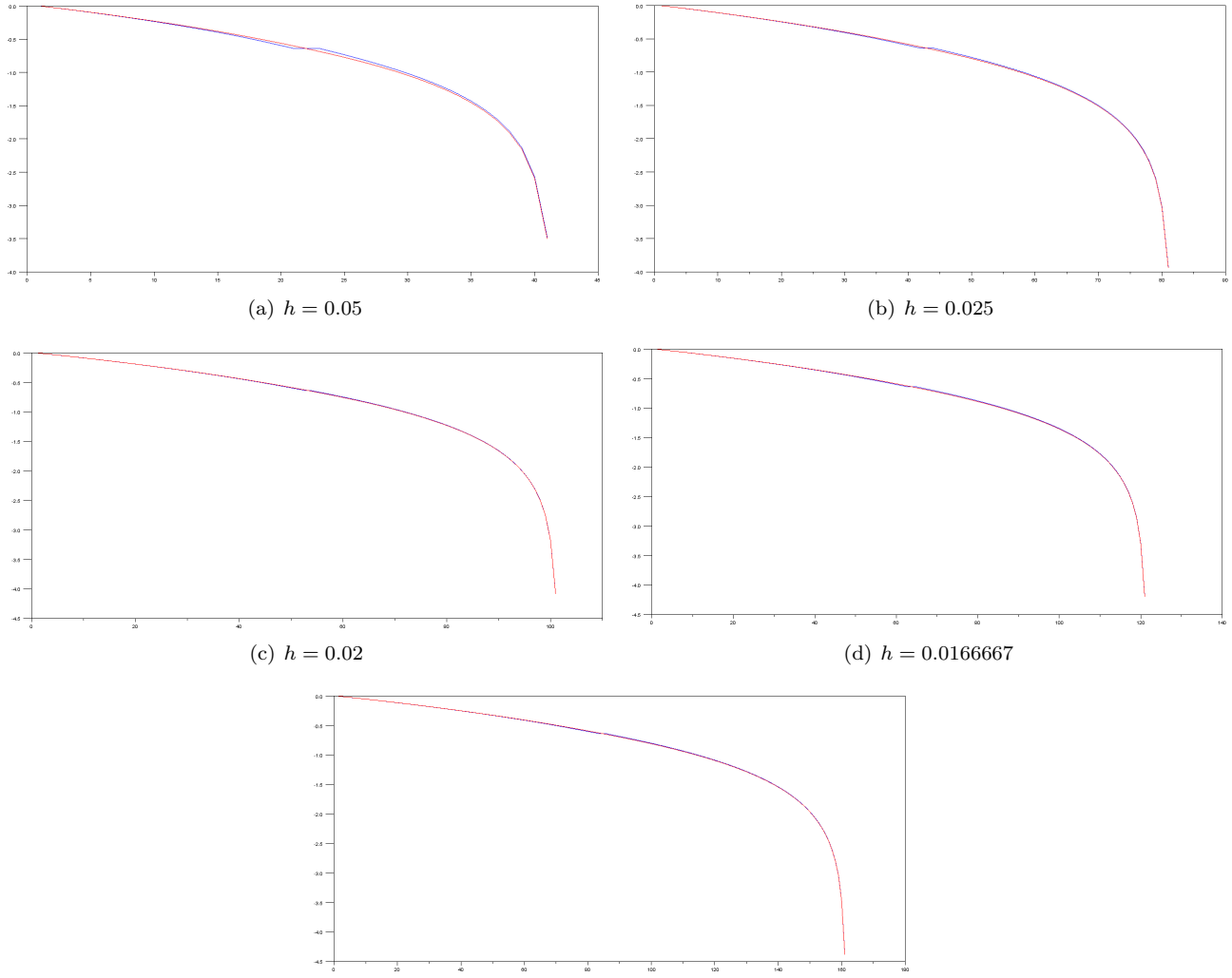

(a) $h = 0.05$ (b) $h = 0.025$

(c) $h = 0.02$ (d) $h = 0.0166667$

(e) $h = 0.0125$

Figure 5.37: Compression example. Section $y = 1$ of the x component of the displacement for the enlarging crack. The exact solution is in red and the approximate one in blue.

Expansion example The load case is the same but for a force which is now opposite, figure 5.40. We plot the same curves as in the compression example, see figures 5.41, 5.42 and 5.43, and compile the errors, computed in the same way as in the compression case in table 5.14

On figure 5.41, we clearly see the jump at the contact zone, with a delay due to the hole (which plays the role of the void in this case). On figure 5.43, we observe more difficulties to approximate the vertical displacement on the contact zone than for the compression case. On the contrary, on figure 5.42, the boundary of the crack causes less problems in the approximation of the horizontal displacement.

5.6.2 Shape optimization with an enlarging crack

Shape gradients of a general criterion

We can state the following theorem on shape gradients which notably differs from theorem 5.4.5 by the fact that the boundary Γ_0 can move. We also remove the subscript ξ for the sake of clarity. we make the same assumptions on m

h	Error L_2	Error L^∞
0.05	0.0244048	0.0420902
0.025	0.0125630	0.0224742
0.02	0.0046426	0.0112086
0.0166667	0.0084175	0.0155137
0.0125	0.0063213	0.0119325

Table 5.13: Errors with respect to length side of an element for the enlarging crack for the compression test.

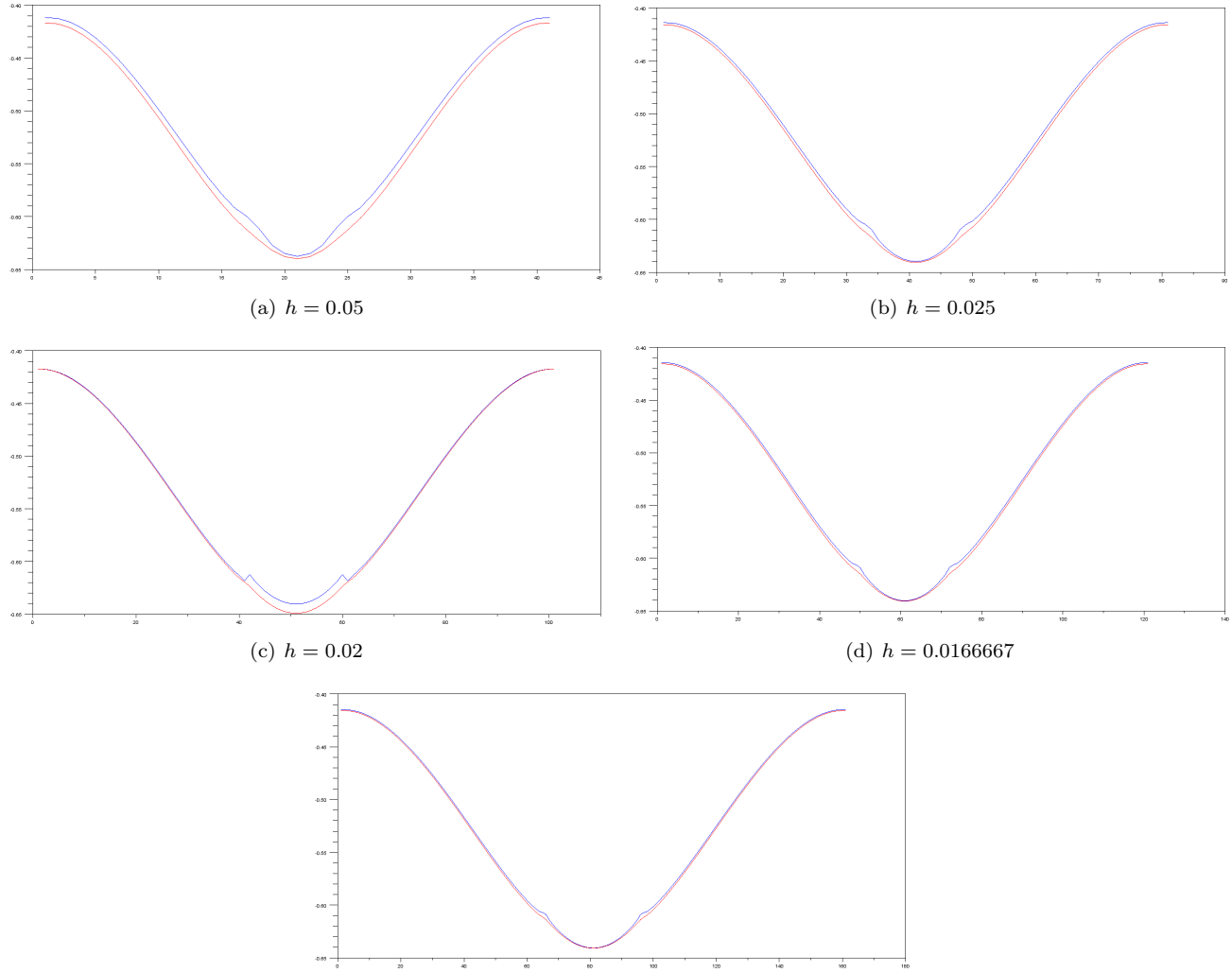

(a) $h = 0.05$

(b) $h = 0.025$

(c) $h = 0.02$

(d) $h = 0.0166667$

(e) $h = 0.0125$

Figure 5.38: Compression example. Section $x = 1.05$ of the x component of the displacement for the enlarging crack. The exact solution is in red and the approximate one in blue.

and l as in theorem 5.4.5.

Theorem 5.6.2. *Assume that $f \in H^1(\mathbb{R}^d)^d$ and $g \in H^2(\mathbb{R}^d)^d$, and that u is solution of* (5.118)*. If we denote $J'(\Omega)(\theta)$*

h	Error L_2	Error L^∞
0.05	0.0192680	0.0512890
0.025	0.0119889	0.0343586
0.02	0.0117159	0.0590228
0.0166667	0.0088889	0.0259891
0.0125	0.0071123	0.0210672

Table 5.14: Errors with respect to length side of an element for the enlarging crack for the expansion test.

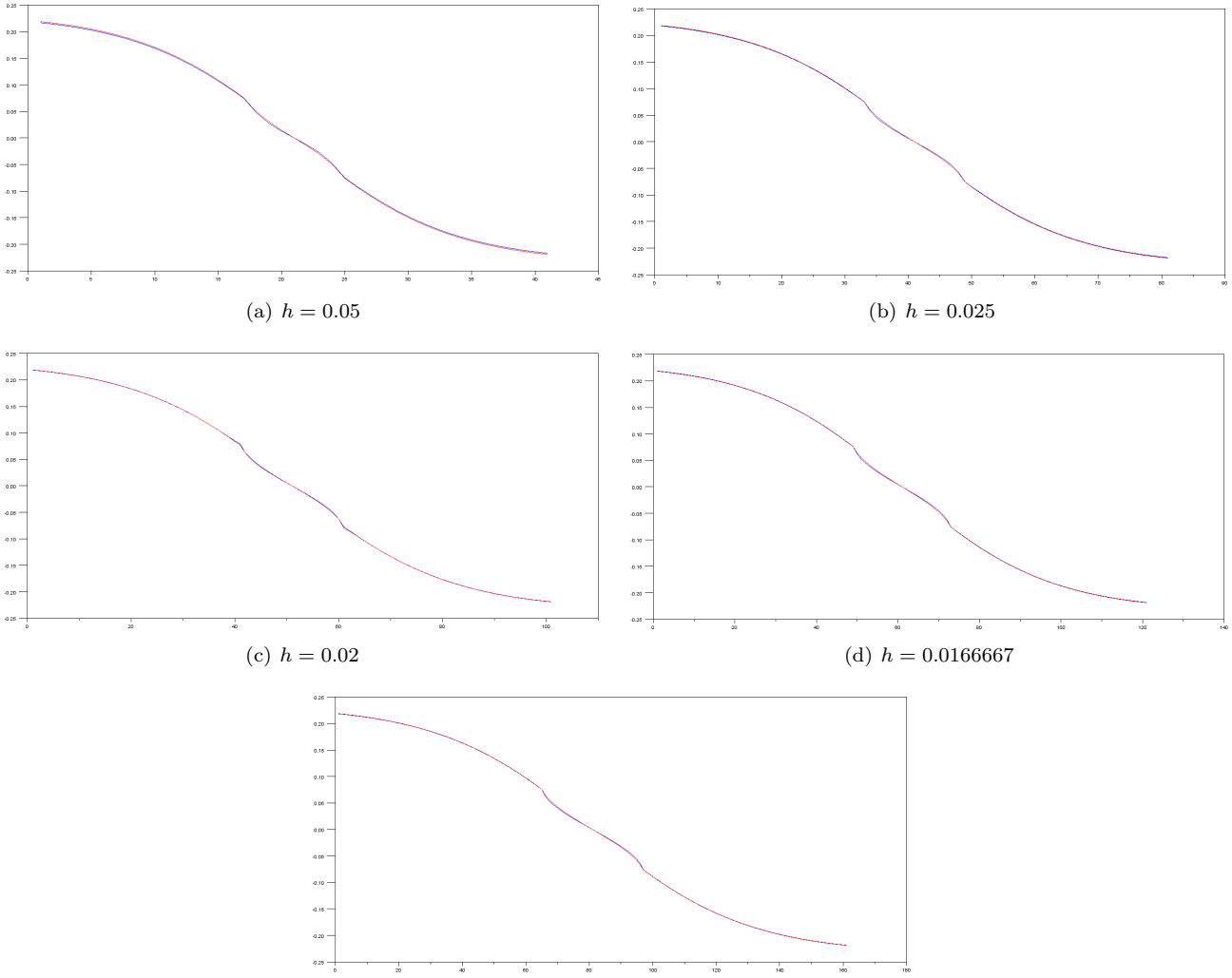

(a) $h = 0.05$ (b) $h = 0.025$

(c) $h = 0.02$ (d) $h = 0.0166667$

(e) $h = 0.0125$

Figure 5.39: Compression example. Section $x = 1.05$ of the y component of the displacement for the enlarging crack.The exact solution is in red and the approximate one in blue.

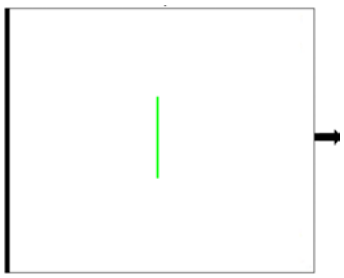

Figure 5.40: Load case for the expansion case, using the enlarging crack method.

the Gateaux derivative of $J(\Omega)$ *with respect to* Ω *in the direction* $\theta \in W^{1,\infty}(\mathbb{R}^d, \mathbb{R}^d)$. *We have:*

$$
\begin{aligned}
J'(\Omega)(\theta) = & \int_{\Gamma_m} (\theta \cdot n)(m(u) + Ae(u) : e(p) - f \cdot p)\, ds \\
& + \int_{\Gamma_m} (\theta \cdot n)(Hl(u) + \partial_n l(u)) \\
& - \int_{\Gamma_N \cap \Gamma_m} (\theta \cdot n)(Hp \cdot g + \partial_n (p \cdot g))\, ds \\
& + \frac{1}{\epsilon} \int_S (\theta \cdot n)(H\phi_r([u \cdot n])[p \cdot n] + \partial_n \left(\phi_r([u \cdot n])[p \cdot n]\right)\, ds \\
& + \frac{1}{\epsilon} \int_S \phi_1([u \cdot n])[p \cdot n']\, ds + \frac{1}{\epsilon} \int_S \phi_1'([u \cdot n])[u \cdot n']\ [p \cdot n]\, ds \\
& - \int_{\Gamma_0 \cap \Gamma_m} (\theta \cdot n) \left(H \left(Ae(p)n \cdot u + p \cdot Ae(u)n + l'(u)\right) + \partial_n \left(Ae(p)n \cdot u + p \cdot Ae(u)n + l'(u)\right)\right)\, ds
\end{aligned}
\tag{5.120}
$$

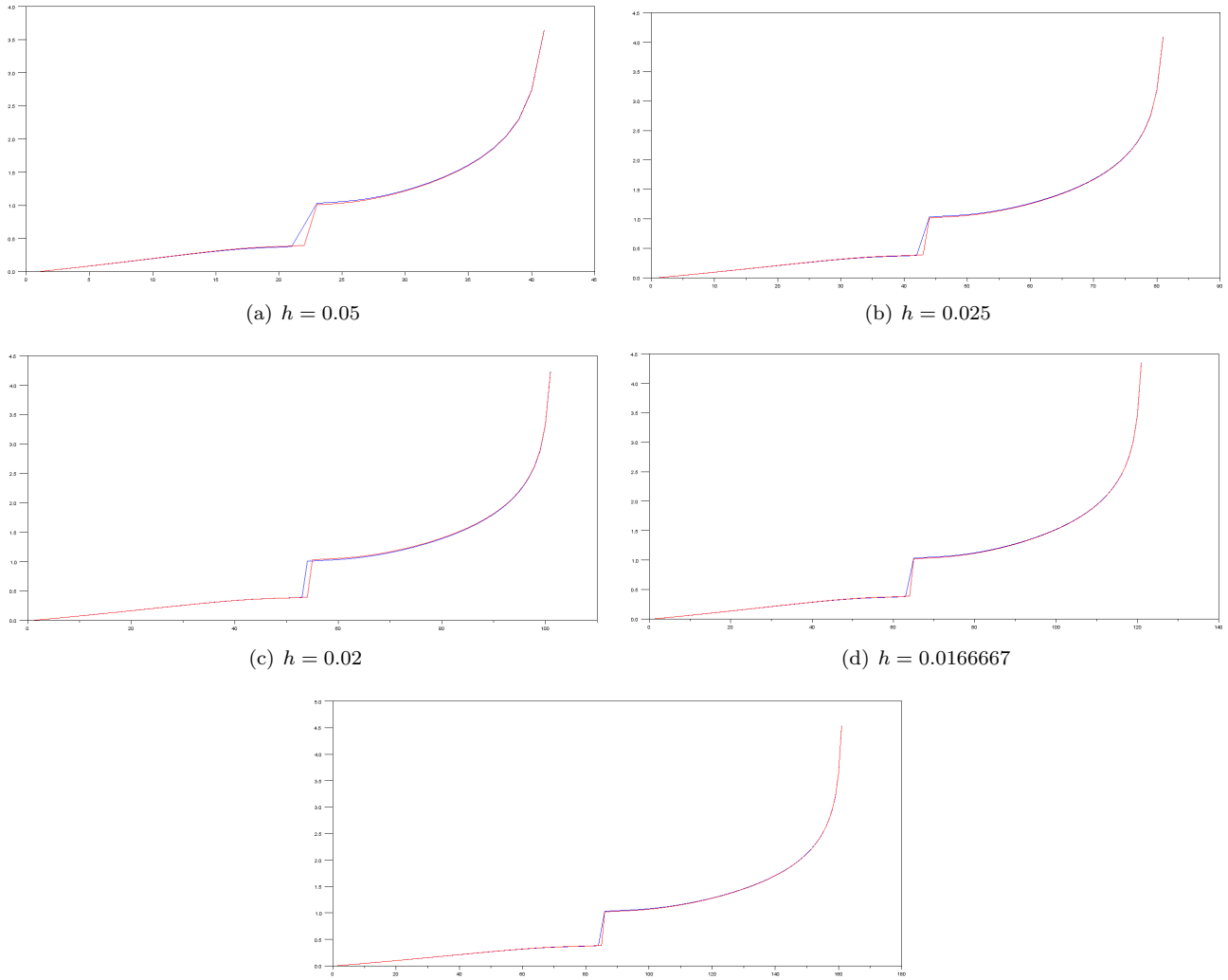

(a) $h = 0.05$ (b) $h = 0.025$

(c) $h = 0.02$ (d) $h = 0.0166667$

(e) $h = 0.0125$

Figure 5.41: Expansion example. Section $y = 1$ of the x component of the displacement for the enlarging crack. The exact solution is in red and the approximate one in blue.

where p is defined as the solution of the following adjoint problem:

$$\begin{aligned}&\int_\Omega Ae(p) : e(\psi)\,dx + \int_\Omega m'(u)\cdot\psi\,dx + \int_{\Gamma_m\setminus\Gamma_0} l'(u)\cdot\psi\,ds \\ &+ \frac{1}{\epsilon}\int_S \phi_1'([u\cdot n])[p\cdot n][\psi\cdot n]\,ds = 0 \ \ \forall\psi\in H^1_{\Gamma_0}(\Omega)^d.\end{aligned} \tag{5.121}$$

H is the mean curvature: $H = \operatorname{div}(n)$, n' is the shape derivative of the normal, $\partial_n f = \nabla f\cdot n$ for f a real function. In the integral on S, H and n, when n is not in a jump, have to be taken as the mean curvature and the normal of S.

Proof. It is possible to rigorously prove the existence of a Lagrangian derivative of u using the same method as in the proof of theorem 5.4.5. We limit ourselves to the application of Céa's method to find the expression of the gradient. Since $\Gamma_m\cap\Gamma_0\neq\varnothing$ the method is different. Let us introduce the Lagrangian L with v, q and μ in $H^1_{\Gamma_0}(\mathbb{R}^d)^d$:

$$\begin{aligned}L(v,q,n(\Omega),\mu,\Omega) \quad = \quad &\int_\Omega m(v)\,dx + \int_{\Gamma_m} l(v)\,ds - \int_\Omega \operatorname{div}(Ae(v))\cdot q\,dx \\ &+\frac{1}{\epsilon}\int_S (\phi_r([v\cdot n]_\theta)n_{|S_{-\theta}} + Ae(v)n_{|S_{-\theta}})\cdot q_{|S_{-\theta}}\,ds \\ &-\frac{1}{\epsilon}\int_S (\phi_r([v\cdot n]_\theta)n_{|S_{+\theta}} + Ae(v)n_{|S_{+\theta}})\cdot q_{|S_{+\theta}}\,ds \\ &+\int_\Gamma Ae(v)n\cdot q\,ds - \int_\Omega f\cdot q\,dx - \int_{\Gamma_N}(g - Ae(v)n)\cdot q\,ds \\ &+\int_{\Gamma_0} v\cdot\mu\,ds\end{aligned} \tag{5.122}$$

The functions q, μ and v are in spaces independent of $\Omega\in\mathcal{U}_{ad}$. We note (u,p,μ^*) a stationarity point of L. The state

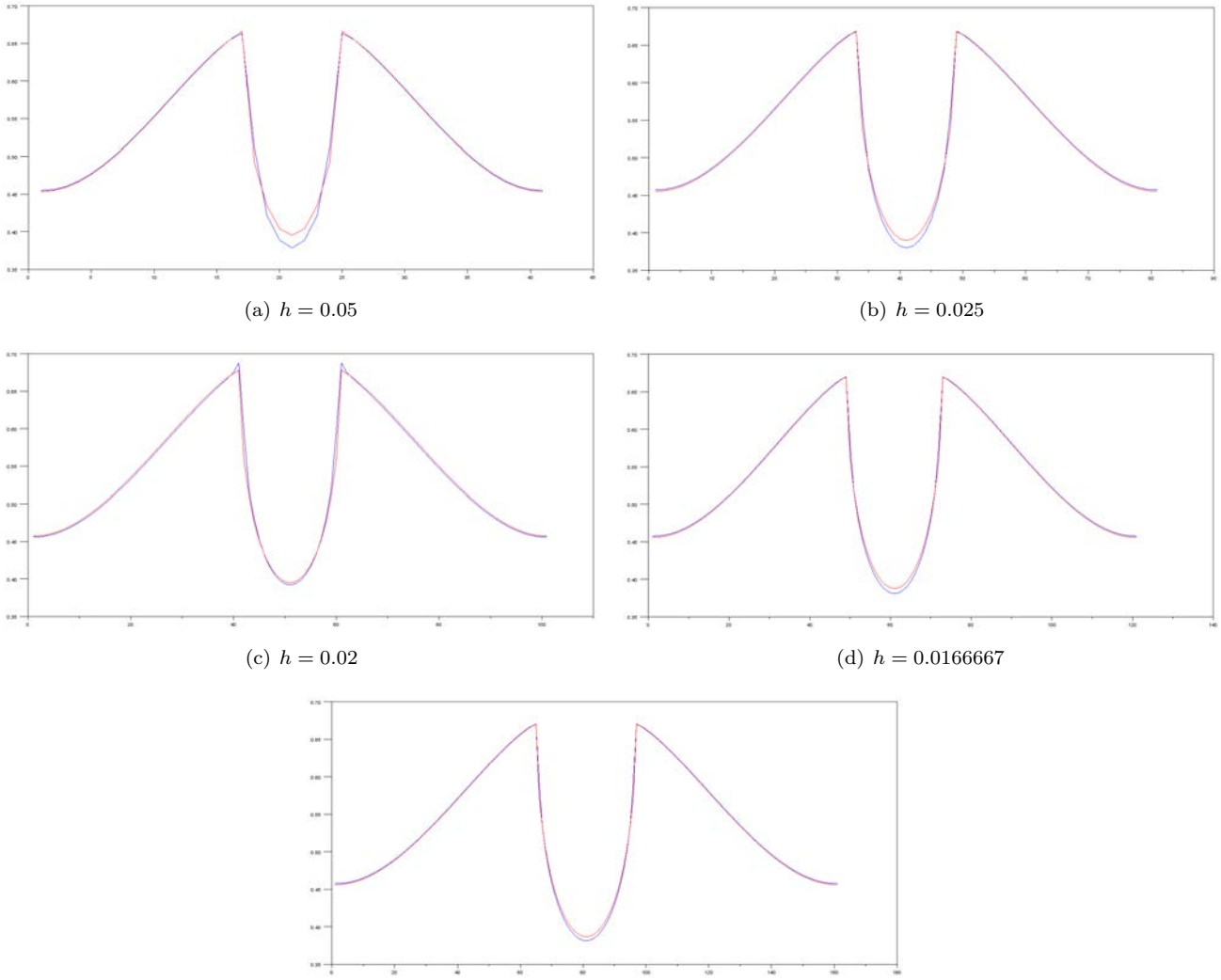

(a) $h = 0.05$ (b) $h = 0.025$

(c) $h = 0.02$ (d) $h = 0.0166667$

(e) $h = 0.0125$

Figure 5.42: Expansion example. Section $x = 1.05$ of the x component of the displacement for the enlarging crack. The exact solution is in red and the approximate one in blue.

equation (5.70) can be retrieved by differentiating L with respect to q in the direction $\psi \in H^1_{\Gamma_0}(\mathbb{R}^d)^d$:

$$\langle \partial_q L(u, q, n, \mu, \Omega), \psi \rangle = 0 \ \ \forall \psi \in H^1_{\Gamma_0}(\mathbb{R}^d)^d$$

and L with respect to μ for the boundary condition on Γ_0.
In the same way the equation solved by p (adjoint problem) can be found by derivating L with respect to v in the direction $\psi \in H^1_{\Gamma_0}(\mathbb{R}^d)^d$:

$$\begin{aligned}\langle \partial_v L, \psi \rangle = &\int_\Omega m'(u) \cdot \psi \, dx + \int_{\Gamma_m} l'(u) \cdot \psi \, ds - \int_\Omega \operatorname{div}(Ae(\psi)) \cdot q \, dx \\ &+ \frac{1}{\epsilon} \int_S (\phi_r'([u \cdot n]_\theta)[\psi \cdot n]_\theta n_{|S_-\theta} + Ae(\psi) n_{|S_-\theta}) \cdot q_{|S_-\theta} \, ds \\ &- \frac{1}{\epsilon} \int_S (\phi_r'([u \cdot n]_\theta)[\psi \cdot n]_\theta n_{|S_+\theta} + Ae(\psi) n_{|S_+\theta}) \cdot q_{|S_+\theta} \, ds \\ &+ \int_{\Gamma_0} \psi \cdot \mu \, ds + \int_\Gamma Ae(\psi) n \cdot q \, ds + \int_{\Gamma_N} Ae(\psi) n \cdot q \, ds\end{aligned}$$

and the adjoint problem can be deduced:

$$\langle \partial_u L(u, p, n, \mu, \Omega), \psi \rangle = 0 \ \ \forall \psi \in H^1_{\Gamma_0}(\mathbb{R}^d)^d.$$

To attain (5.121), we have to work a little more. First applying the Green formula:

$$-\int_\Omega \operatorname{div}(Ae(\psi)) \cdot q \, dx = \int_\Omega Ae(\psi) : e(q) \, dx - \int_{\partial\Omega} Ae(\phi) n \cdot q \, ds,$$

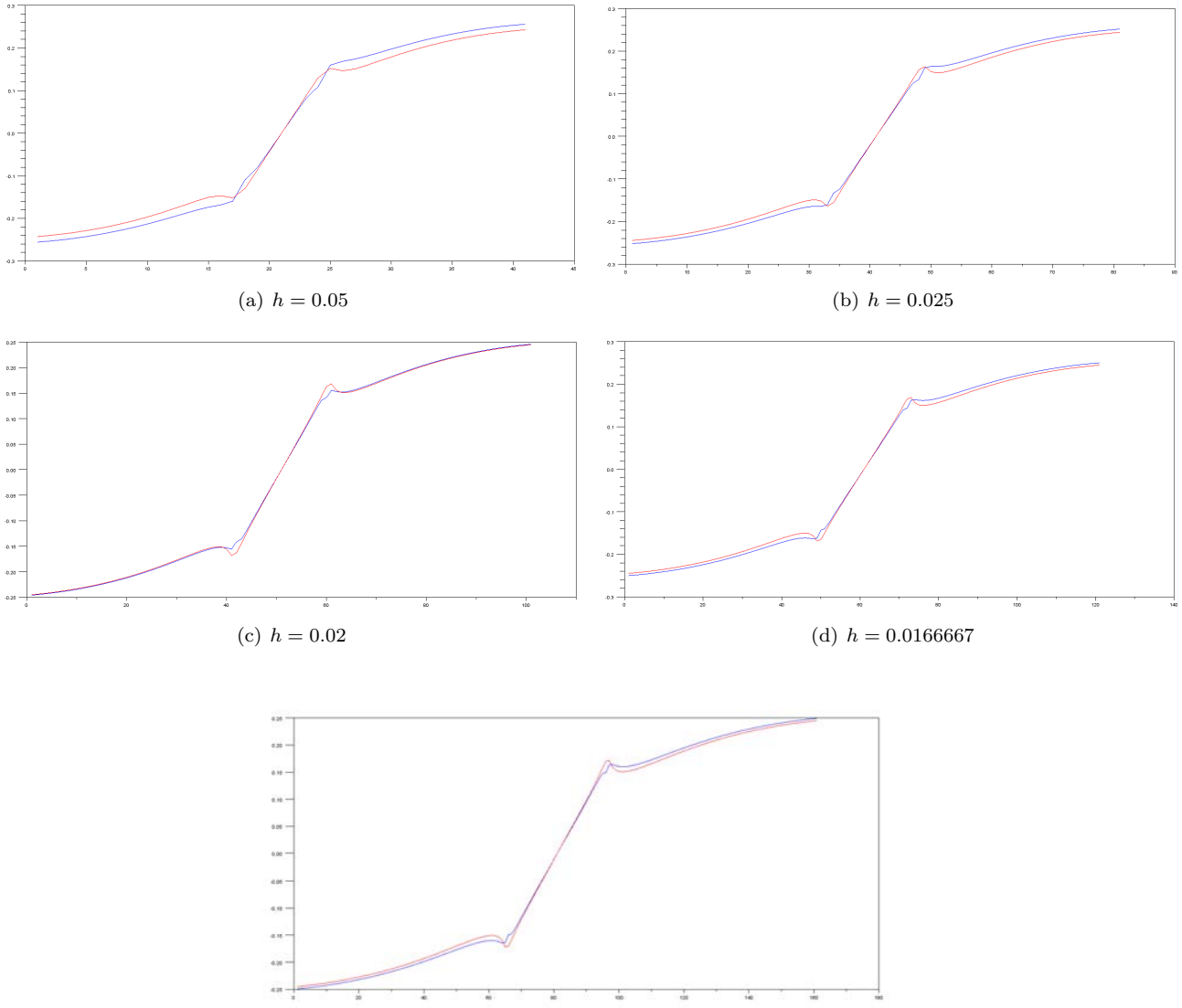

(a) $h = 0.05$ (b) $h = 0.025$

(c) $h = 0.02$ (d) $h = 0.0166667$

(e) $h = 0.0125$

Figure 5.43: Expansion example. Section $x = 1.05$ of the y component of the displacement for the enlarging crack. The exact solution is in red and the approximate one in blue.

and

$$\int_\Omega m'(u)\cdot\psi\,dx + \int_{\Gamma_m} l'(u)\cdot\psi\,ds - \int_\Omega Ae(\psi):e(p)\,dx$$
$$+\frac{1}{\epsilon}\int_S(\phi_r'([u\cdot n]_\theta)[\psi\cdot n]_\theta[p\cdot n]_\theta\,ds + \int_{\Gamma_0}\psi\cdot\mu - Ae(\psi)n\cdot p\,ds = 0.$$

Taking $\psi \in C_0^\infty$ we have $-\mathrm{div}(Ae(p)) = j'(u)$.Taking $\psi = 0$ on $\partial\Omega\setminus\Gamma_0$ such that $Ae(\psi)n = 0$ implies that:

$$\int_{\Gamma_0}\psi(l'(u)+\mu+Ae(p)n))\,dx = 0.$$

It yields that:

$$\mu^* = -l'(u) - Ae(p)n. \tag{5.123}$$

Furthermore taking $\psi = 0$ on Γ_0 and making $Ae(\psi)n$ vary gives $p = 0$ on Γ_0. We retrieve (5.121).
To find the shape derivative of $J(\Omega)$, we remark that for any q and μ:

$$J(\Omega) = L(u(\Omega), q, n(\Omega), \mu, \Omega)$$

and differentiate the L with respect to the shape in the direction θ which gives:

$$\begin{aligned} J'(\Omega,\theta) &= L'(\Omega, u_\Omega, q, n_\Omega, \mu;\theta)\\ &= \partial_\Omega L(\Omega, u_\Omega, q, n_\Omega, \mu;\theta) + \partial_u L(\Omega, u_\Omega, q, n_\Omega, \mu; u'(\theta))\\ &+ \langle\frac{\partial L(\Omega, u_\Omega, q, n_\Omega, \mu)}{\partial\lambda}, n'(\theta)\rangle. \end{aligned} \tag{5.124}$$

But as $u'(\theta)$ is in $H^1_{\Gamma_0}(\Omega)^d$, taking $q = p(\Omega)$ and $\mu = \mu^*$ leads to:

$$\partial_u L(\Omega, u_\Omega, p(\Omega), n_\Omega, \mu; u'(\theta)) = 0.$$

In conclusion:

$$J'(\Omega,\theta) = L'(\Omega, u_\Omega, p_\Omega, n_\Omega, \mu; \theta) = \partial_\Omega L(\Omega, u_\Omega, p_\Omega, n_\Omega, \mu; \theta) + \langle \frac{\partial L(\Omega, u_\Omega, p_\Omega, n_\Omega, \mu)}{\partial \lambda}, n'(\theta)\rangle. \tag{5.125}$$

By using the formulae of theorem 1.3.4, we recover (5.120). □

On numerical implementation

To be able to apply the method to find a descent direction, explained in section 1.3.4, it is needed to rewrite, in the gradient given by theorem 5.6.2, the term:

$$\int_S \phi_1([u\cdot n])[p\cdot n']\, ds.$$

Using the assumption made on the normal we have:

$$\int_S \phi_1([u]\cdot n_-)[p]\cdot n'_-\, ds.$$

As the crack is defined through a signed distance function, we can apply lemma 1.3.8:

$$n'_- = -\nabla_t(\theta\cdot n_-).$$

Then applying a classical integration by part, see [137] proposition 5.4.9:

$$\int_S \phi_1([u]\cdot n_-)[p]\cdot n'_-\, ds = \int_S (\theta\cdot n_-)\left(-\mathrm{div}_t(\phi_1([u]\cdot n_-)[p]) + H\phi_1([u]\cdot n_-)[p]\cdot n_-\right) ds \tag{5.126}$$

with, for v a vector:

$$\mathrm{div}_t(v) = \mathrm{div}(v) - \nabla v n_- \cdot n_-.$$

Numerical examples, with a fixed contact zone

We introduce seven examples which will be performed with this method and, also, with the phase field method presented in section 5.6.3. Moreover, three of them will be reused for a mobile contact zone. In all these examples, keep in mind that there is no friction assumed. The design domain D is a square of length 2, discretized with 6400 elements. We use Q1 finite elements. For all examples, we minimise the volume under a compliance constraint. We force, near loads applications, Dirichlet zones and the contact circle zones, a certain amount of material to remain. These zones are non optimisable. The results are gathered in the table 5.15.

The nail 1 A disc full of material is in $(1,1)$. Its radius is taken equal to 0.21. The circle which is the boundary of the disc is a contact zone. Inside the circle there is a Dirichlet zone which takes the form of a disk of radius equal to 0.11. The structure is embedded on the right and left bottom side. A downward force is applied at $(1,0)$, see figure 5.44. The final design is given on figure 5.45. The structure uses the Dirichlet zones on its sides to stabilize itself.

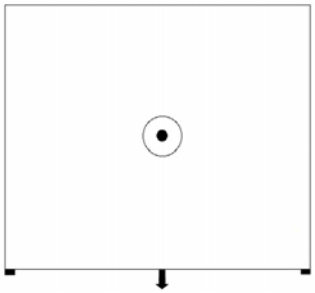

Figure 5.44: Load case for nail 1.

The nail 2 A disc full of material is in $(1,1.6)$. Its radius is taken equal to 0.21. The circle which is the boundary of the disc is a contact zone. Inside the circle there is a Dirichlet zone which takes the form of a disk of radius equal to 0.11. The structure is embedded on the left bottom side and on the bottom of the left side. A downward force is applied at $(2,0.4)$, see figure 5.46. The final design is given on figure 5.47. We remark that the structure does not need the Dirichlet zone on the left.

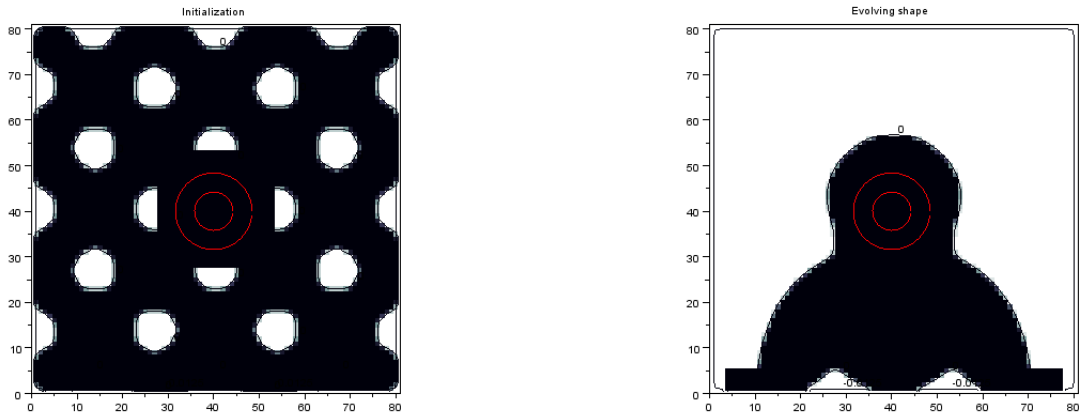

(a) Initialisation (b) Final design

Figure 5.45: The nail 1 case, for the enlarging crack.

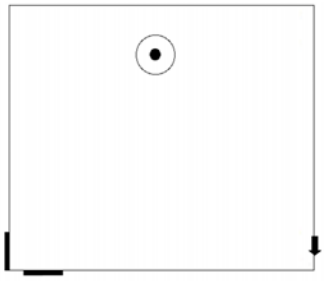

Figure 5.46: Load case for nail 2.

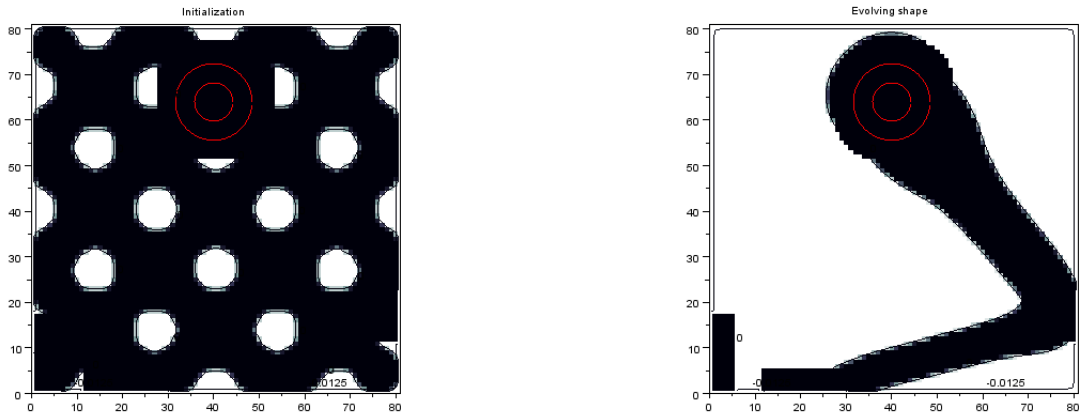

(a) Initialisation (b) Final design

Figure 5.47: The nail 2 case, for the enlarging crack.

The nail 3 A disc full of material is in $(0.75, 1.6)$. Its radius is taken equal to 0.21. The circle, which is the boundary of the disc, is a contact zone. Inside the circle, there is a Dirichlet zone which takes the form of a disk of radius equal to 0.11. The structure is embedded on the left of the bottom side. A rightward force is applied at $(2, 0.4)$, see figure 5.48. The final design is given on figure 5.49. It is interesting to compare this example with the nail 2. For nail 3, the thickest bar is the one making the link between the Dirichlet zone and the force which is rightward, the action of the nail is not predominant. It is the contrary for nail 2 where the force is downward.

The nail 4 A disc full of material is in $(1.35, 1)$. Its radius is taken equal to 0.21. The circle, which is the boundary of the disc, is a contact zone. Inside the circle there is a Dirichlet zone which takes the form of a disk of radius equal to 0.11. The structure is embedded on the left bottom side and on the bottom of the left side. A rightward force is applied between $(0.4, 2)$ and $(0.6, 2)$, see figure 5.50. The final design is given on figure 5.51.

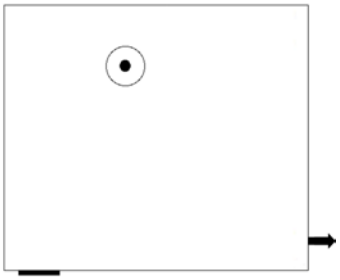

Figure 5.48: Load case for nail 3.

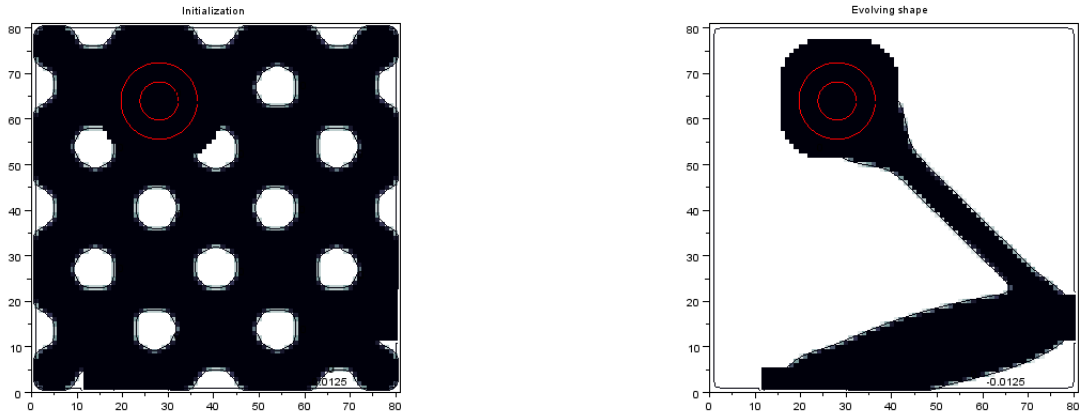

(a) Initialisation (b) Final design

Figure 5.49: The nail 3 case, for the enlarging crack.

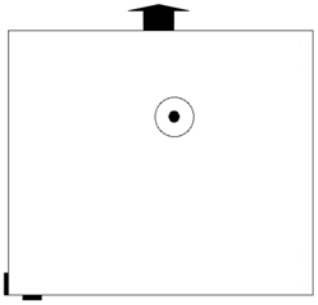

Figure 5.50: Load case for nail 4.

The nail 5 A disc full of material is in $(1.75, 1)$. Its radius is taken equal to 0.21. The circle, which is the boundary of the disc, is a contact zone. Inside the circle there is a Dirichlet zone which takes the form of a disk of radius equal to 0.11. The structure is embedded on the right bottom side. A downward force is applied at $(1, 0)$, see figure 5.52. The final design is given on figure 5.53.

Expansion case We take a crack from $(1.05, 0.8)$ to $(1.05, 1.2)$. The left side of the structure is embedded and a rightward force is applied at $(2, 1)$, see figure 5.54. The final design is given on figure 5.55. Surprisingly and contrary to the case 3 in section 5.5.1 the algorithm keeps material around the contact zone. In fact, the numerical implementation was done assuming material around the contact zone, therefore removing material on the contact zone leads to huge compliance.

The slanting crack The structure is embedded on the left bottom side and on the bottom of the left side. A crack is defined from $(0.7, 0.5)$ to $(1.75, 1.75)$. An upward force is set at $(2, 2)$, see figure 5.56. The final design is given on figure 5.57.

Numerical examples, with a mobile contact zone

In all the following examples, we assume that the nail can move on the horizontal direction but not on the vertical direction. We use the Lagrangian optimisation technique explained in section 1.3.4. The results are compiled in table

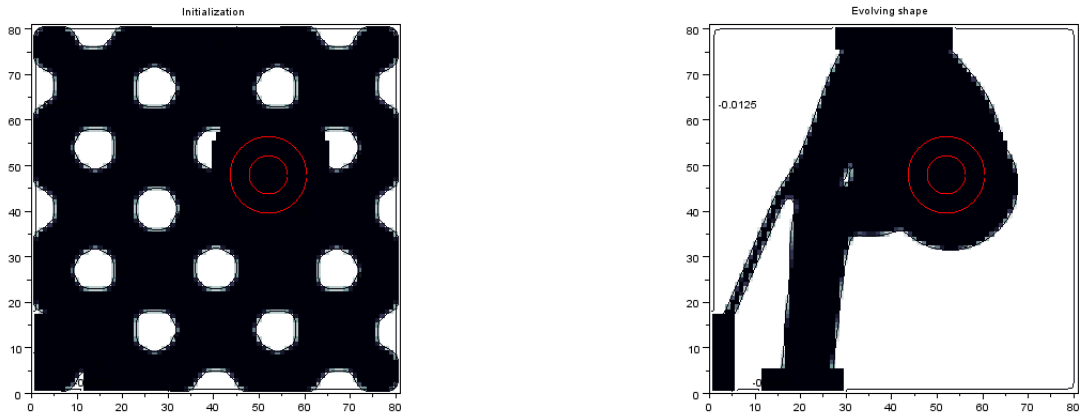

(a) Initialisation (b) Final design

Figure 5.51: The nail 4 case, for the enlarging crack.

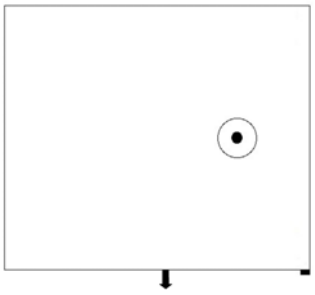

Figure 5.52: Load case for nail 5.

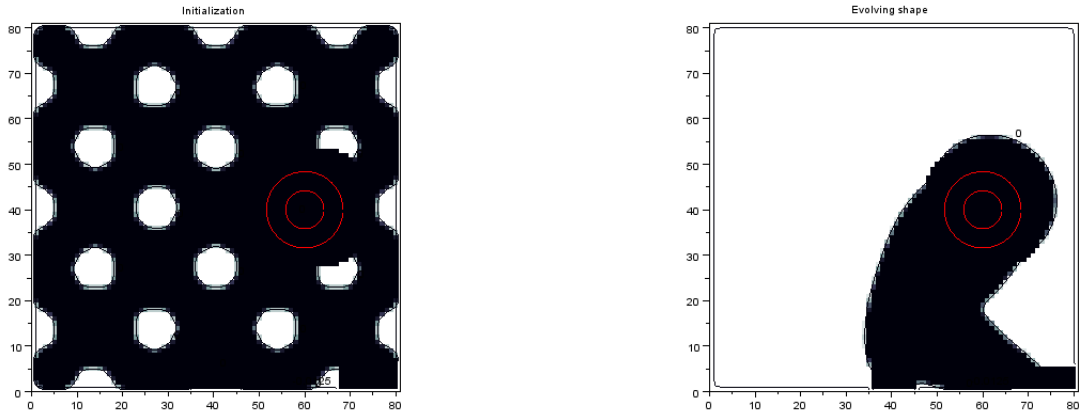

(a) Initialisation (b) Final design

Figure 5.53: The nail 5 case, for the enlarging crack.

5.16.

The nail 1 The Lagrangian multiplier is taken equal to 0.1. The circle starts from $(0.3, 1)$ and finishes at $(0.910046, 1)$. The results are given in figure 5.58. We observe that the nail arrives near (1,1), which should be its optimal place, but stops before. In fact, as the nail starts from the left, the structure is not symmetric from the first iteration. It is stabilized by the thin bar linking it to the Dirichlet zone. Further steps in the algorithm would break this bar and the structure would not be admissible for the compliance constraint. That is why the algorithm stops.

The nail 2 The Lagrangian multiplier is taken equal to 0.1. The circle starts from $(0.3, 1.6)$ and finishes at $(1.74, 1.6)$. The results are given in figure 5.59. The nail goes as far as it can on the right to align with the downward force.

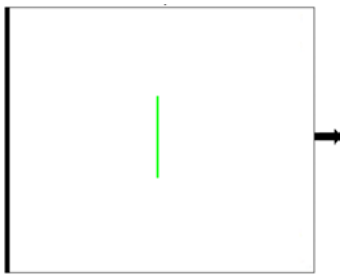

Figure 5.54: Load case for the expansion case.

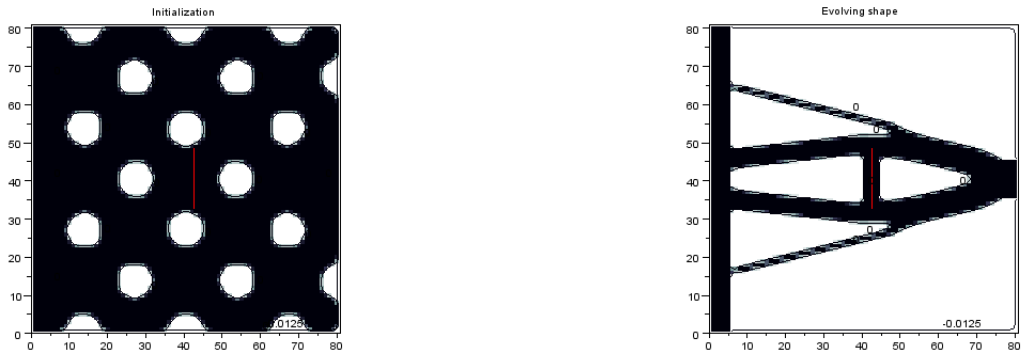

(a) Initialisation (b) Final design

Figure 5.55: The expansion case, for the enlarging crack

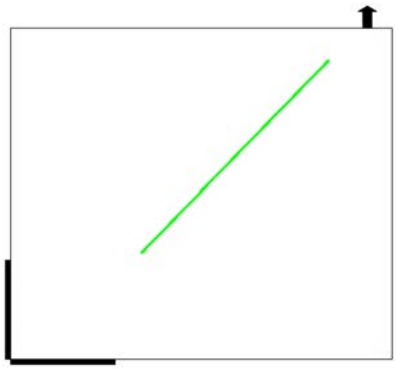

Figure 5.56: Load case for the slanting crack case.

The nail 5 The Lagrangian multiplier is taken equal to 0.1. The circle starts from $(0.3, 1)$ and finishes at $(0.964673, 1)$. The results are given in figure 5.60. Like for nail 1, a thin bar remains, linking the Dirichlet zone to the structure. This bar is necessary since the nail does not reach the point $(1, 1)$.

5.6.3 Method 2: Phase field contact

This second approximate formulation is taken from [16]. This article considers the evolution of a brittle fracture thanks to a variational model, putting on the crack unilateral contact conditions. The study of brittle fracture thanks to variational methods was introduced in [110], [54], [112] and [111], presenting a model not far from the one used in image segmentation and given in [214] and also explored in [25]. The basic idea is to define an energy which has to be minimized on a set allowing jump-discontinuities. Thus the solution is searched in the space $SBV(\Omega)$, introduced in [13].

From a numerical point of view, it is not possible to work with such a space and regularisations are proposed. We mention the article [43] where a phase field is used and the references therein. For a review of the variational method introduced by Bourdin, Francfort and Marigo we refer to [44]. In [16], the authors take into account unilateral contact boundary conditions, which seems to be rarely made in the literature. Anyway, our goal is not to solve a brittle fracture problem, but only to use the way the contact problem is solved thanks to the phasefield method. Our goal is also to compare this method with the previous one presented in section 5.6.1.

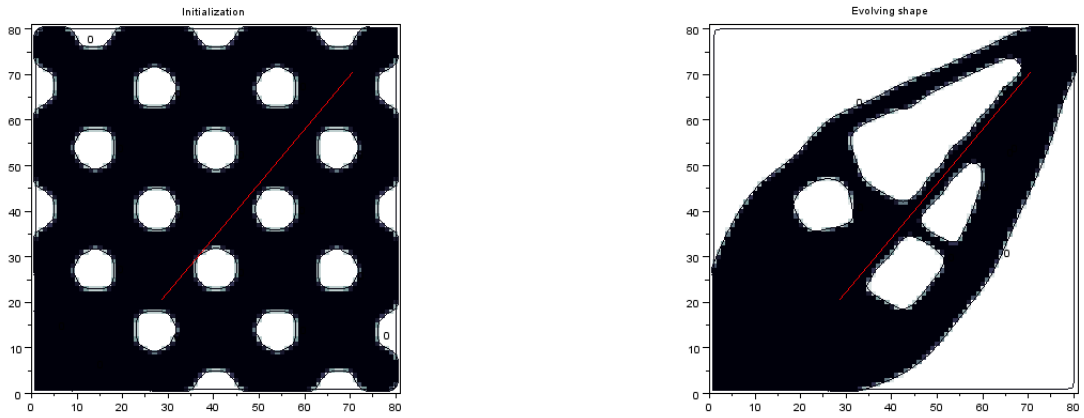

(a) Initialisation (b) Final design

Figure 5.57: The slanting crack case, for the enlarging crack

Cases	Volume	Compliance	Compliance Constraint	Iterations	Evaluations
nail 1	1.37545	4.1999	4.2	18	40
nail 2	1.22707	13.9999	14	39	61
nail 3	1.14657	6.49997	6.5	42	64
nail 4	1.53651	789.912	790	18	39
nail 5	1.06407	7.99998	8	48	25
Expansion	0.937077	7.99982	8	39	65
Slanting	2.08885	54.9993	55	74	103

Table 5.15: Results for the enlarging crack when the contact zone is fixed

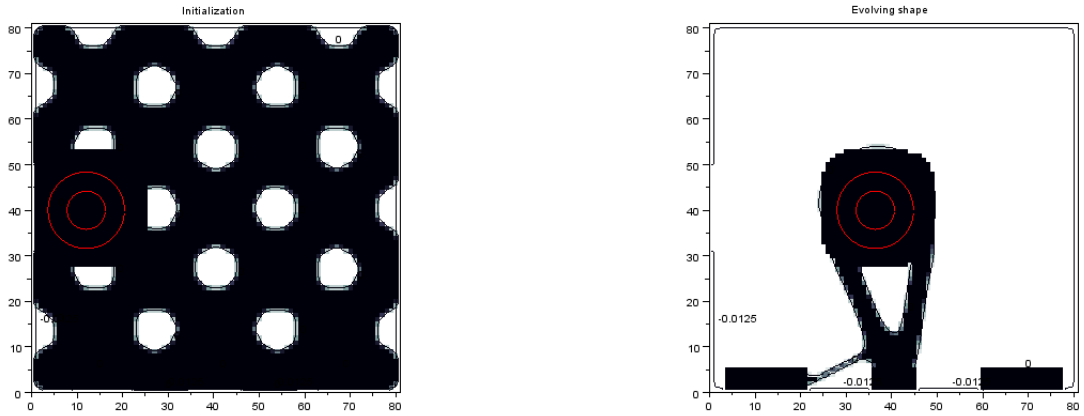

(a) Initialisation (b) Final design

Figure 5.58: The nail 1 case for a mobile contact zone, for the enlarging crack.

The continuous model

We take the notations of section 5.6.1. Instead of considering the crack S, we replace it by an enlarged open zone ω on which we define a function $\alpha : \mathbb{R}^d \to [0,1]$. This function is smooth, equal to 1 on the crack S, strictly positive on ω and 0 in $\mathbb{R}^d \setminus \omega$. This function can be seen as an evanescent enlarged crack.

In linearized elasticity, the problem can be put under the form of an optimization problem with an energy to be minimized of the form:

$$\frac{1}{2}\int_\Omega Ae(u) : e(u) - \langle F, u\rangle. \tag{5.127}$$

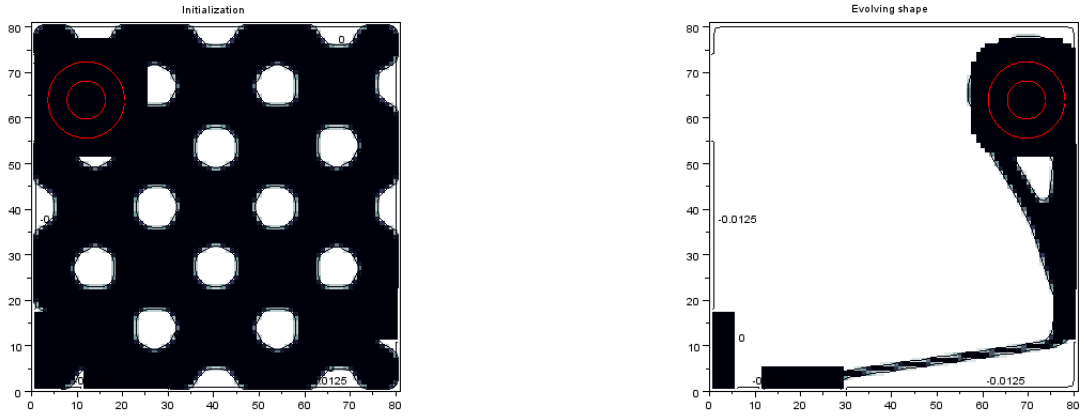

(a) Initialisation (b) Final design

Figure 5.59: The nail 2 case for a mobile contact zone, for the enlarging crack.

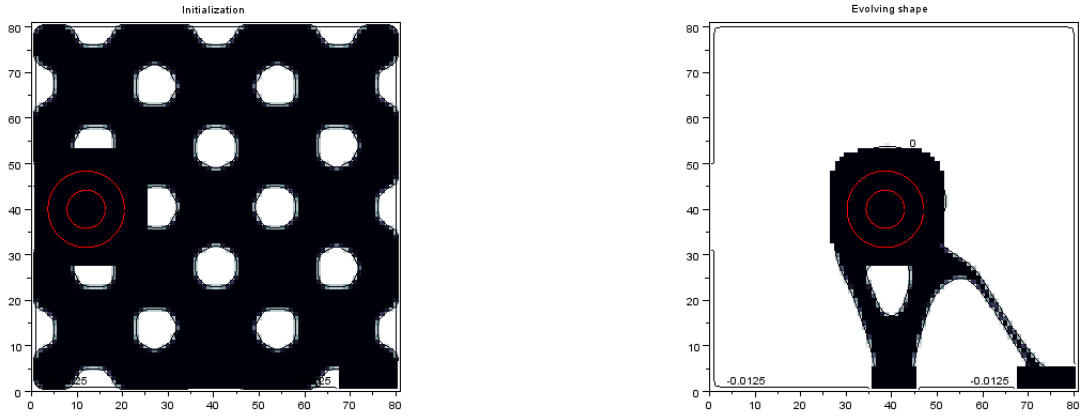

(a) Initialisation (b) Final design

Figure 5.60: The nail 5 case for a mobile contact zone, for the enlarging crack.

with:

$$Ae(u) : e(u) = \frac{1}{2}\lambda tr(e(u))^2 + \mu e(u) : e(u) = \frac{1}{2}\left(\lambda + \frac{2}{d}\mu\right) tr(e(u))^2 + \mu e(u)_D : e(u)_D.$$

If we note $k_0 = \left(\lambda + \frac{2}{d}\mu\right)$ this rewrites:

$$Ae(u) : e(u) = k_0 \frac{tr(e(u))^2}{2} + \mu e(u)_D : e(u)_D. \tag{5.128}$$

Yet the volume variation is measured by $tr(e(u))$ and if $tr(e(u)) > 0$ it means that the volume grows (expansion) and if $tr(e(u)) < 0$ the volume decreases (compression). The part $e(u)_D : e(u)_D$ accounts for the shear. If we want to put some contact boundary conditions on the crack S, we need to allow the expansion and the sliding. This means that on the crack S we want to remove the term $e(u)_D : e(u)_D$ and the term $tr(e(u))$ when it is positive. These remarks

Cases	Lagrangian	Volume	Compliance	Iterations	Evaluations
nail 1	1.52728	0.681501	8.45783	65	132
nail 2	2.00003	0.721471	12.7856	67	150
nail 5	1.50061	0.66886	8.31748	101	180

Table 5.16: Results for the enlarging crack when the contact zone is optimisable.

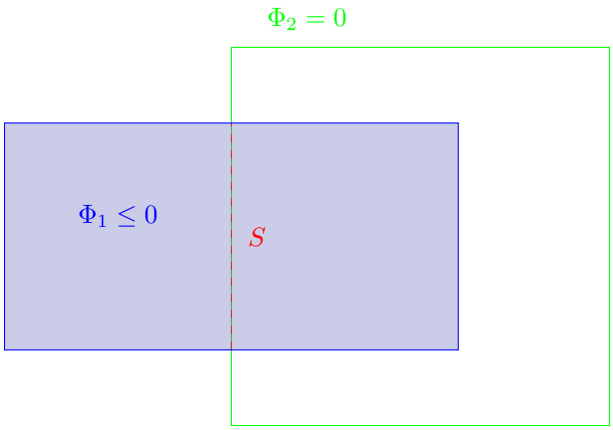

Figure 5.61: The crack S in red is defined by two level sets function Φ_2 and Φ_1: $S = \{\Phi_2 = 0\} \cap \{\Phi_1 \leq 0\}$. In green $\{\Phi_2 = 0\}$ and in blue $\{\Phi_1 \leq 0\}$.

lead to the following approximate energy:

$$W(u,\alpha) = k_0 \frac{tr^-(e(u))^2}{2} + \left((1-\alpha)^2 + k_l\right)\left(k_0 \frac{tr^+(e(u))^2}{2} + \mu e(u)_D : e(u)_D\right). \tag{5.129}$$

with $tr^-(\tau) = \max(0, -tr(\tau))$, $tr^+(\tau) = \max(0, tr(\tau))$ and k_l a small parameter for avoiding singular matrices during the numerical simulations.

Then we can write the variational equation associated with this new problem: find $u \in H^1_{\Gamma_0}(\Omega)^d$ such that for every $v \in H^1_{\Gamma_0}(\Omega)^d$:

$$\begin{aligned} &\int_\Omega k_0 \left(\left((1-\alpha)^2 + k_l\right) tr^+(e(u)) - tr^-(e(u))\right) tr(e(v))\, dx + \int_\Omega 2\mu \left((1-\alpha)^2 + k_l\right) e(u)_D : e(v)_D\, dx \\ &= \int_\Omega f \cdot v\, dx + \int_{\Gamma_N} g \cdot v\, ds. \end{aligned} \tag{5.130}$$

For the derivation of shape gradient, we also propose a regularised variational formulation: find $u \in H^1_{\Gamma_0}(\Omega)^d$ such that for every $v \in H^1_{\Gamma_0}(\Omega)^d$:

$$\begin{aligned} &\int_\Omega k_0 \left(\left((1-\alpha)^2 + k_l\right) \phi_r\left(tr(e(u))\right) - \phi_r\left(-tr(e(u))\right)\right) tr(e(v))\, dx + \int_\Omega 2\mu \left((1-\alpha)^2 + k_l\right) e(u)_D : e(v)_D\, dx \\ &= \int_\Omega f \cdot v\, dx + \int_{\Gamma_N} g \cdot v\, ds. \end{aligned} \tag{5.131}$$

The function α will be, in numerical examples, defined by (5.134).

About numerical implementation

To build the phase field α we need to define S. For this purpose, we use two level set functions (which are taken as signed distance functions), Φ_1 and Φ_2. We choose Φ_2 with the constraint that $\Phi_2 = 0$ on S. If the crack S is not a closed contour, the function Φ_2 cannot be taken only equal to 0 on S. Thence we use the function Φ_1 to caracterize the points where $\Phi_2 = 0$ which are really on S. We give an example on figure 5.61 for S being a segment.

Then we define α with the help of two functions α_2 and α_1 from $\mathbb{R}$ to $\mathbb{R}$ define as

$$\alpha_1(t) = \begin{cases} \frac{1}{l^4}t^4 - \frac{2}{l^2}t^2 + 1 & \text{if } 0 \leq t \leq l \\ 1 & \text{if } t < 0 \\ 0 & \text{otherwise.} \end{cases} \tag{5.132}$$

$$\alpha_2(t) = \begin{cases} \frac{1}{l^4}t^4 - \frac{2}{l^2}t^2 + 1 & \text{if } -l \leq t \leq l \\ 0 & \text{otherwise.} \end{cases} \tag{5.133}$$

Then we can define α on $\mathbb{R}^d$ as:

$$\alpha(x) = \alpha_1(\Phi_1(x))\alpha_2(\Phi_2(x)). \tag{5.134}$$

with $2l$ the thickness of the phase field.

h	Error L_2	Error L^∞
0.05	0.0965776	0.1225639
0.025	0.0274282	0.0365011
0.02	0.0246058	0.0398827
0.0166667	0.0260514	0.0510645
0.0125	0.0187123	0.0404695

Table 5.17: Errors with respect to length side of an element for the phase field method for the compression test.

Numerical examples

We test our method on the same two simple cases as for the enlarging crack. The first one is a compression case, figure 5.36 and the second one an expansion case, figure 5.40. The variable l is taken equal to $2h$.

Compression example Again we choose to plot some sections of the displacement in the x direction and in the y direction with respect to h the length of a square element side. For the y direction, we choose to do a section for $x = 1.05$ and for the x direction for $y = 1$ and for $x = 1.05$. See figures 5.62, 5.63 and 5.64 for the results. The comparisons are made on a node to node basis and the error are given in table 5.17.

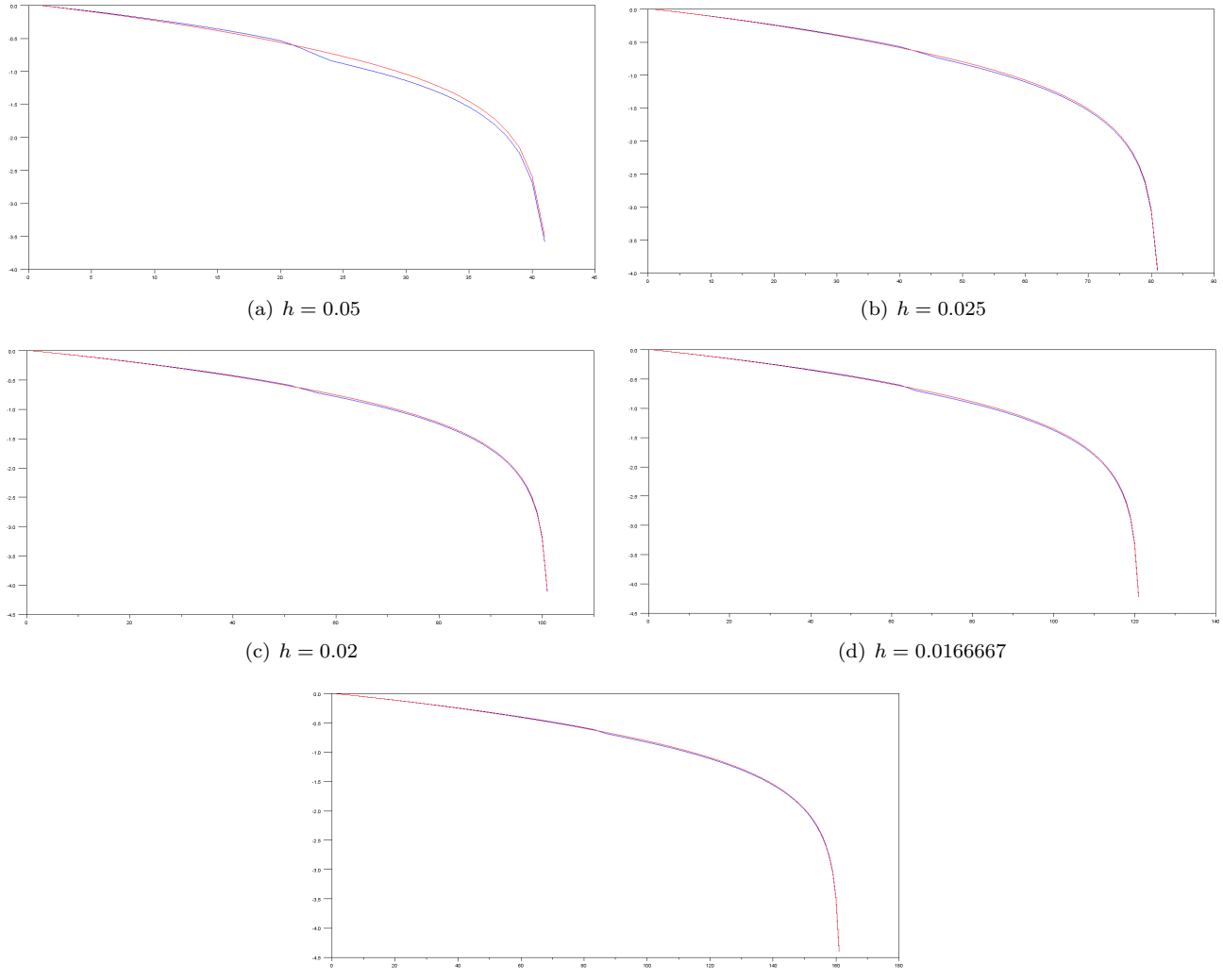

(a) $h = 0.05$

(b) $h = 0.025$

(c) $h = 0.02$

(d) $h = 0.0166667$

(e) $h = 0.0125$

Figure 5.62: Compression example. Section $y = 1$ of the x component of the displacement for the phase field method. The exact solution is in red and the approximate one in blue.

On figure 5.62, where the enlarging crack method has created a plate, we see that the phase field method nearly linearly approximate the displacement. On figure 5.63, the method seems to converge to the exact solution with, like for the enlarging crack method, problem on the boundary of the contact zone. In contrast the vertical component of the displacement seems to suffer from a bad approximation.

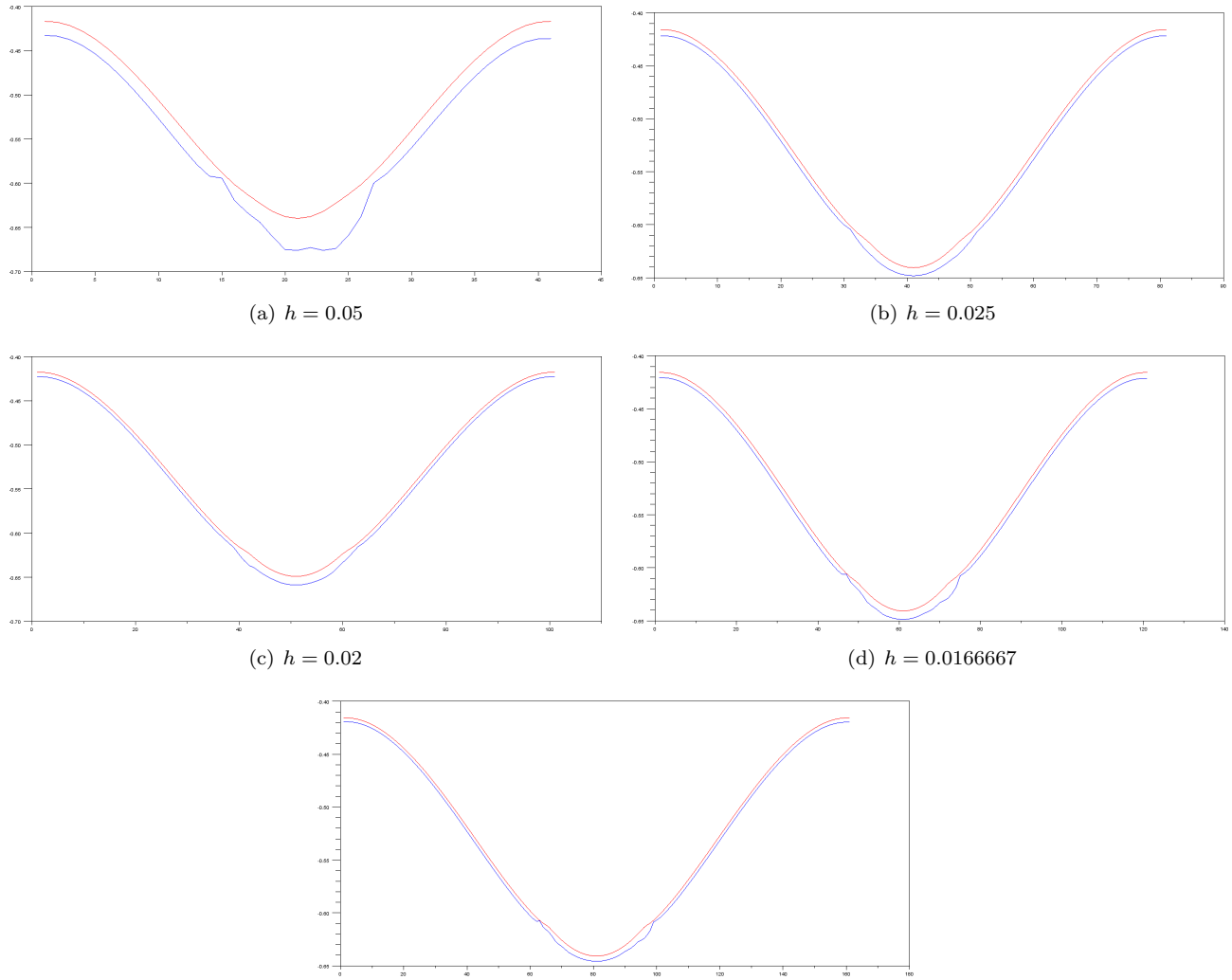

(a) $h = 0.05$

(b) $h = 0.025$

(c) $h = 0.02$

(d) $h = 0.0166667$

(e) $h = 0.0125$

Figure 5.63: Compression example. Section $x = 1.05$ of the x component of the displacement for the phase field method. The exact solution is in red and the approximate one in blue.

Expansion example We plot the same curves as in the compression example, see figures 5.65 and 5.66 except for the one comparing the x component on the section defined by $x = 1.05$. In fact, as we do not have a convergence proof to the exact solution, it is difficult to know which comparisons can be made. Thus a node to node error calculation and comparison is not really appropriate.

On this example, for both cases, the phase field method does not well approximate the contact problem. On figure 5.65 the jump is not sharp enough and on figure 5.66 the same problems can be seen as in the compression case. In fact, this advocates for a change in the form of the phasefield we took. We suggest this new formula for α_2:

$$\alpha_2(t) = \begin{cases} \dfrac{1}{l^4}(t+l)^4 - \dfrac{2}{l^2}(t+l)^2 + 1 & \text{if } -2l \leq t \leq -l \\ 1 & \text{if } -l \leq t \leq l \\ \dfrac{1}{l^4}(t-l)^4 - \dfrac{2}{l^2}(t-l)^2 + 1 & \text{if } l \leq t \leq 2l \\ 0 & \text{otherwise.} \end{cases} \tag{5.135}$$

For instance for $h = 120$ and $l = h$, we get the results of figure 5.67. We recover a better approximation in the expansion case losing accuracy on the compression case.

5.6.4 Shape optimization with phase field contact

One possible way to perform shape optimization with this model is to use the theory of phase field presented in the references given in section 1.1. We choose in a first approach not to use this theory and to do the shape optimization with respect to Φ_1 and Φ_2 which are assumed to be signed distance functions of smooth domain. We mainly make this choice because it exempts us from the coding related to the optimization with a phase field and it enables us to

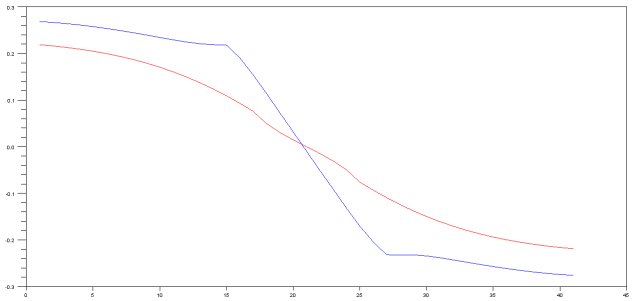

(a) $h = 0.05$

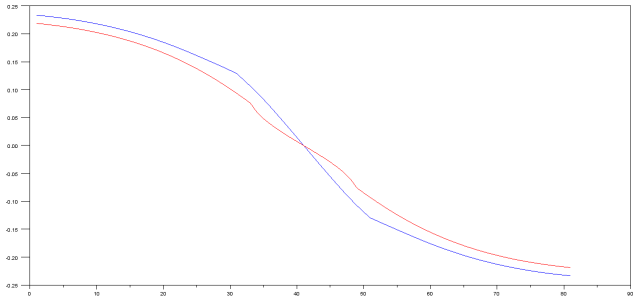

(b) $h = 0.025$

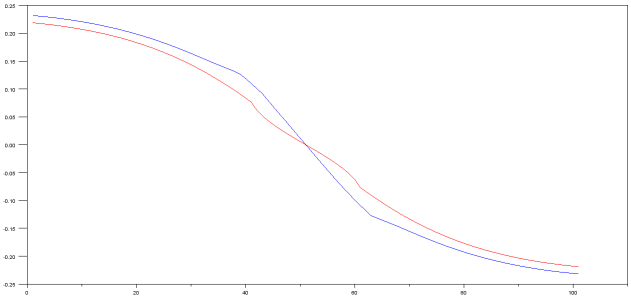

(c) $h = 0.02$

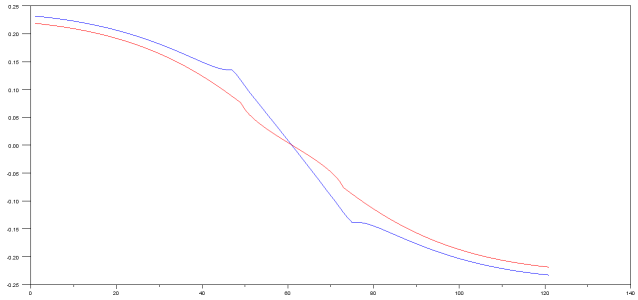

(d) $h = 0.0166667$

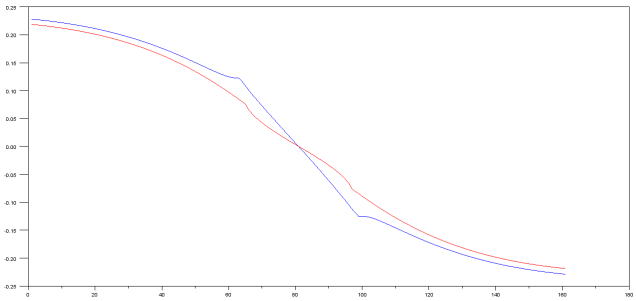

(e) $h = 0.0125$

Figure 5.64: Compression example. Section $x = 1.05$ of the y component of the displacement for the phase field method. The exact solution is in red and the approximate one in blue.

come back to the framework of level set functions. So, the first thing we do is to recall some important theorem on the shape derivative of the signed distance function which can be found in [202], [84] and [90]. Then we compute the shape gradient of a general criterion, detail some numerical points and give numerical examples.

Shape derivative of the signed distance function

The signed distance function was defined in chapter 1, (1.11). We give some additional definitions:

Definition 5.6.3. *Let $\Omega \subset \mathbb{R}^d$ be a Lipschitz bounded open set.*

- *For any $x \in \mathbb{R}^d$, $\Pi_{\partial\Omega}(x) = \left\{ y_0 \in \partial\Omega \,|\, |x - y_0| = \inf_{y \in \partial\Omega} |x - y| \right\}$ is the set of projections of x on $\partial\Omega$. It is a closed subset of $\partial\Omega$. When it is reduced to one point, it is denoted as $p_{\partial\Omega}(x)$ and it is called the projection of x onto $\partial\Omega$.*
- *We define the skeleton of $\partial\Omega$ as $\Sigma = \left\{ x \in \mathbb{R}^d \,|\, d_\Omega^2 \text{ is not differentiable at } x \right\}$.*
- *For $x \in \partial\Omega$, we note $ray_{\partial\Omega}(x) = \left\{ y \in \mathbb{R}^d \,|\, d_\Omega \text{ is differentiable at } y \text{ and } p_{\partial\Omega}(y) = x \right\}$. Equivalently $ray_{\partial\Omega}(x) = p_{\partial\Omega}^{-1}(x)$*

Then we give some results which can be found in [90] chapter 7 theorems 3.1, 3.3 and [14].

Proposition 5.6.4.

- *Let $x \in \mathbb{R}^d \setminus \partial\Omega$ and $y \in \Pi_{\partial\Omega}(x)$. If $\partial\Omega$ is C^1 in a neighbourhood of y then:*

$$\frac{x - y}{d_\Omega(x)} = n(y)$$

where $n(y)$ is the unit outward normal vector to Ω at y.

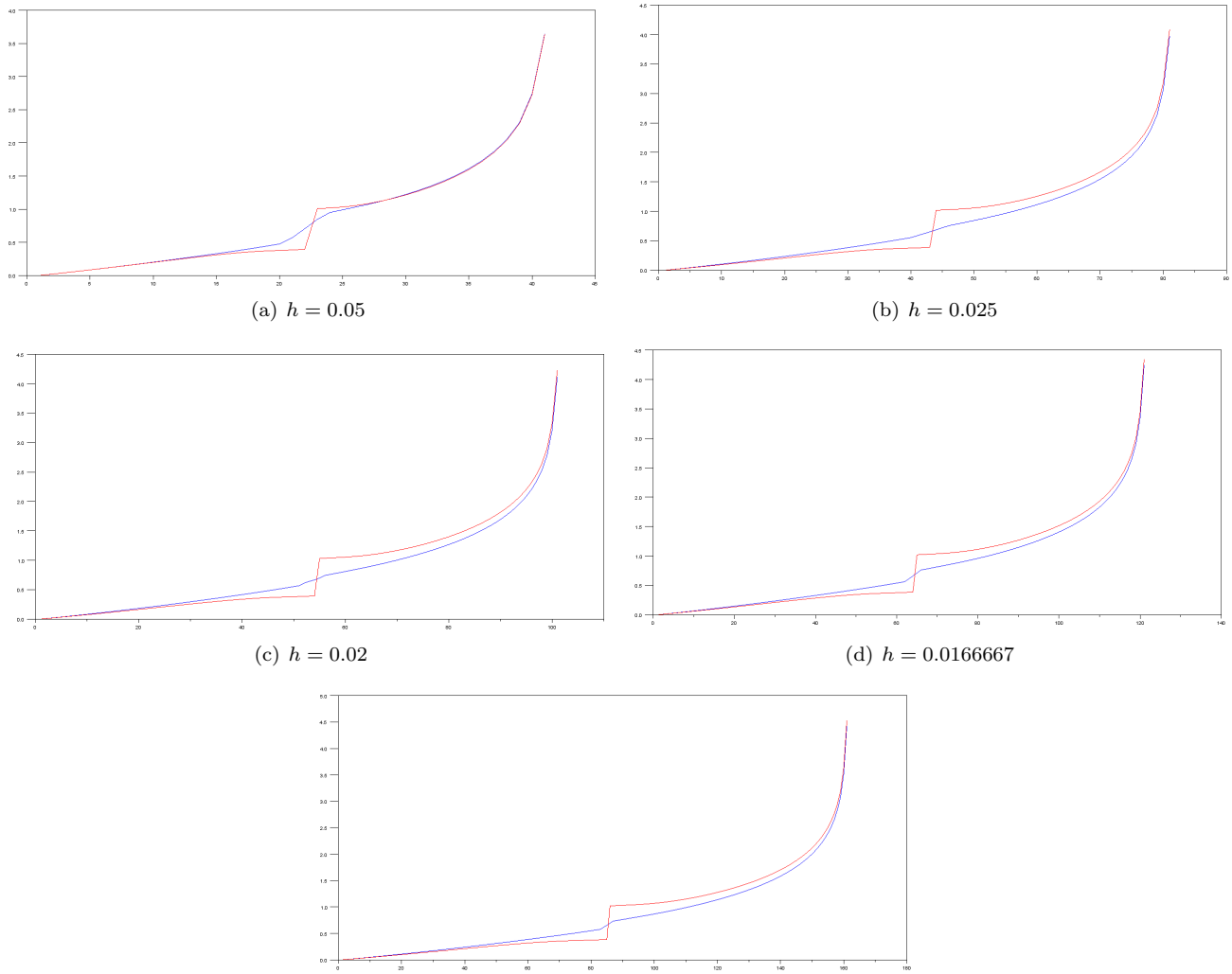

(a) $h = 0.05$

(b) $h = 0.025$

(c) $h = 0.02$

(d) $h = 0.0166667$

(e) $h = 0.0125$

Figure 5.65: Expansion example. Section $y = 1$ of the x component of the displacement for the phase field method. The exact solution is in red and the approximate one in blue.

- *A point $x \notin \partial\Omega$ has a unique projection $p_{\partial\Omega}(x)$ onto $\partial\omega$ if and only if $x \notin \Sigma$. In such a case, it satisfies:*

$$d(x, \partial\Omega) = |p_{\partial\Omega}(x) - x|$$

$$\nabla d_\Omega(x) = n(p_{\partial\Omega}(x)) = \frac{x - p_{\partial\Omega}(x)}{d_\omega(x)}$$

- *As a consequence of Rademacher's theorem, Σ has zero Lebesgue measure in $\mathbb{R}^d$. Furthermore when Ω is C^2, $\overline{\Sigma}$ has zero Lebesgue measure [198].*

- *For every $x \in \mathbb{R}^d$, $p \in \Pi_{\partial\Omega}(x)$, $t \in [0, 1]$ denoting $x_t = p + t(x - p)$ the points of $ray_{\partial\Omega}(x)$ lying between p and x, we have $d_{\partial\Omega}(x_t) = td_{\partial\Omega}(x)$ and $\Pi_{\partial\Omega}(x_t) \subset \Pi_{\partial\Omega}(x)$.*

- *If Ω is of class C^k, for $k \geq 2$, then $d_{\partial\Omega}$ is C^k in a tubular neighborhood of $\partial\Omega$. in that case d_Ω is differentiable at any point $x \in \partial\Omega$, and at such a point: $\nabla d_\Omega(x) = n(x)$.*

We are now able to state a result proved in [84] and [89] on the shape differentiability of the signed distance function of Ω:

Proposition 5.6.5. *Let Ω be bounded open set of class C^1. For every $x \in \mathbb{R}^d$, the function $t \mapsto d_{\Omega_{t\theta}}(x)$ is right-differentiable at $t = 0$, and if $x \in \Omega$:*

$$\frac{d}{dt}\left(d_{\Omega_{t\theta}}(x)\right) = -\inf_{x \in \Pi_{\partial\Omega}(x)} \theta(y) \cdot n(y) \tag{5.136}$$

and if $x \in^c \overline{\Omega}$:

$$\frac{d}{dt}\left(d_{\Omega_{t\theta}}(x)\right) = -\sup_{x \in \Pi_{\partial\Omega}(x)} \theta(y) \cdot n(y) \tag{5.137}$$

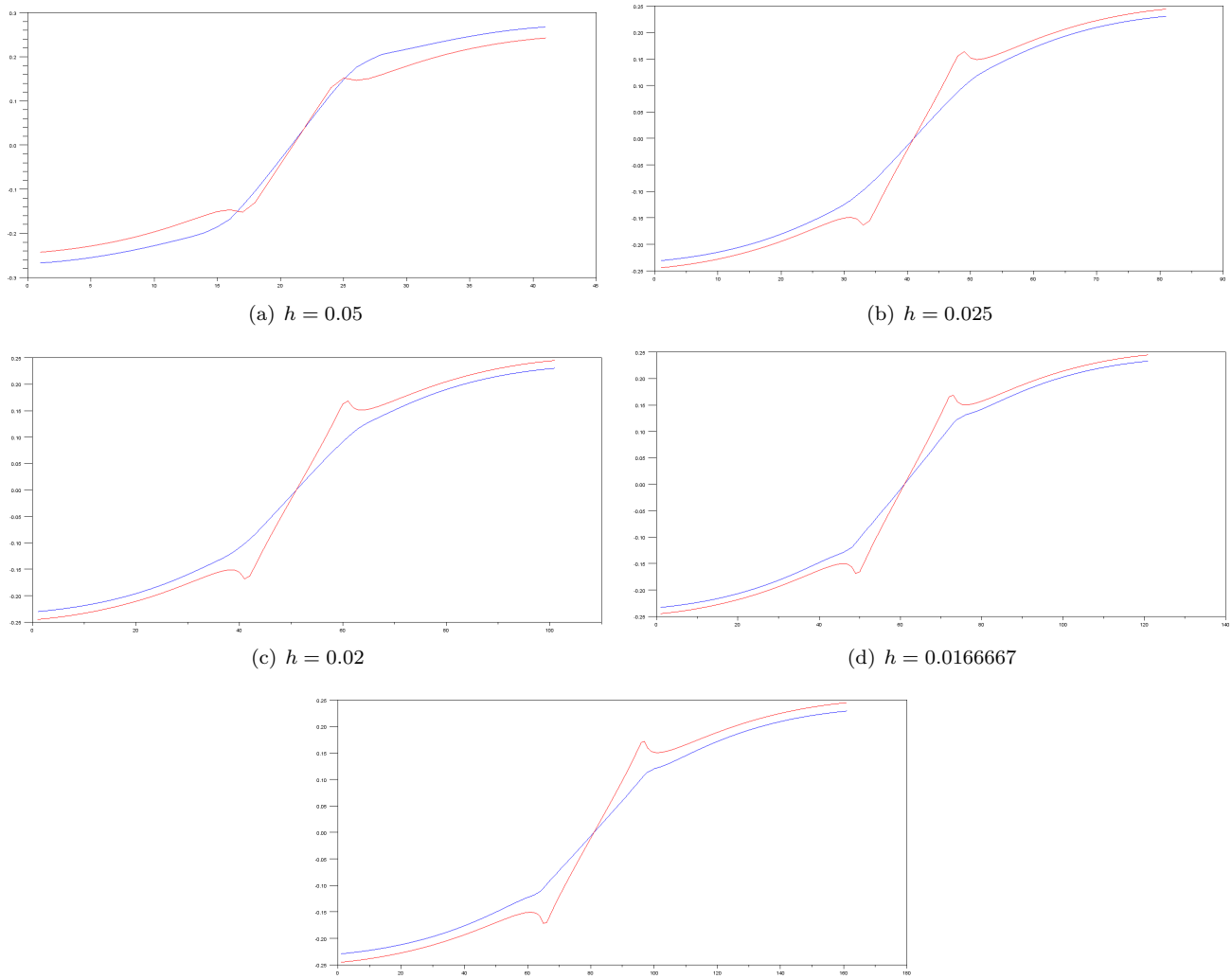

(a) $h = 0.05$ (b) $h = 0.025$

(c) $h = 0.02$ (d) $h = 0.0166667$

(e) $h = 0.0125$

Figure 5.66: Expansion example. Section $x = 1.05$ of the y component of the displacement for the phase field method. The exact solution is in red and the approximate one in blue.

If furthermore $x \notin \Sigma$, *then* $\theta \mapsto d_{\Omega_\theta}(x)$ *is Gateaux differentiable at* $\theta = 0$, *and its derivative* $d'_\Omega(\theta)(x)$ *is for every* $\theta \in W^{1,\infty}(\mathbb{R}^d, \mathbb{R}^d)$*:*

$$d'_\Omega(\theta)(x) = -\theta(p_{\partial\Omega}(x)) \cdot n(p_{\partial\Omega}(x)) \tag{5.138}$$

This particularly implies the following proposition (its proof can be found in [84]) for the derivation of a criterion dependent on the signed distance function and defined on a fixed domain D:

Proposition 5.6.6. *Assume* Ω *is a bounded domain of class* C^1, *and* $j : \mathbb{R}^d_x \times \mathbb{R}_s \to \mathbb{R}$ *a* C^1 *function. Define the function:*

$$J(\Omega) = \int_D j(x, d_\Omega(x))\, dx. \tag{5.139}$$

The application $\theta \mapsto J((Id + \theta)(\Omega))$, *from* $W^{1,\infty}(\mathbb{R}^d, \mathbb{R}^d)$ *into* $\mathbb{R}$, *is Gateaux-differentiable at* $\theta = 0$ *and its derivative at* Ω *is:*

$$J'(\Omega) = -\int_D \frac{\partial j}{\partial s}(x, d_\Omega(x))\theta(p_{\partial\Omega}(x)) \cdot n(p_{\partial\Omega}(x))\, dx. \tag{5.140}$$

Shape gradient of a criterion in the phase field model

We are now able to find the shape gradient of a general criterion. We take the same notations as in theorems 5.4.5 and 5.6.2 and note ω_1 the set defined by $\phi_1 \leq 0$ and ω_2 the set defined by $\phi_2 \leq 0$. Still the Dirichlet boundary can change and the same properties as in theorem 5.4.5 are assumed on m and l.

Theorem 5.6.7. *Assume, that* $f \in H^1(\mathbb{R}^d)^d$ *and* $g \in H^2(\mathbb{R}^d)^d$, *and that* u *is solution of* (5.131). *If we denote*

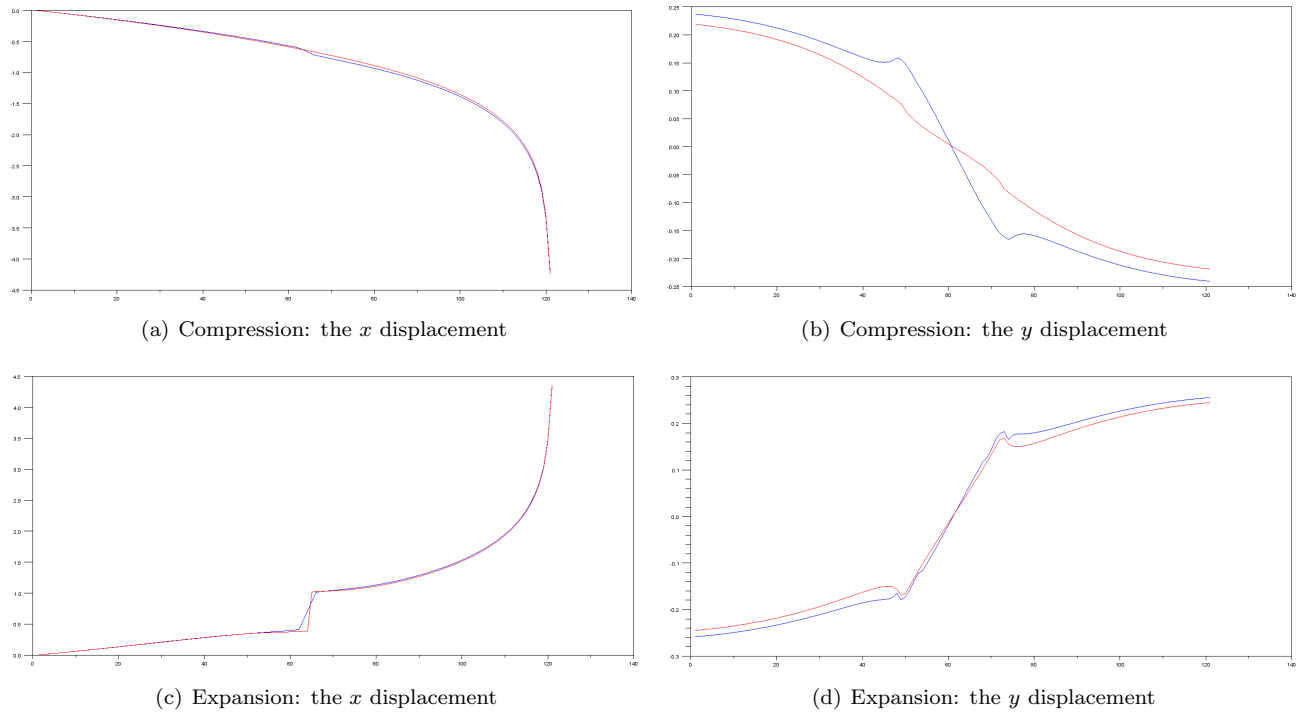

(a) Compression: the x displacement

(b) Compression: the y displacement

(c) Expansion: the x displacement

(d) Expansion: the y displacement

Figure 5.67: Compression and expansion examples with the definition of the phase field (5.135). For the x displacement, the section is defined by $y = 1$, for the y displacement by $x = 1.05$. The exact solution is in red and the approximate one in blue.

$J'(\Omega)(\theta)$ the Gateaux derivative of $J(\Omega)$ with respect to Ω in the direction $\theta \in W^{1,\infty}(\mathbb{R}^d, \mathbb{R}^d)$. We have:

$$\begin{aligned}
J'(\Omega)(\theta) = &\int_{\Gamma_m} (\theta \cdot n)(m(u) - f \cdot p)\, ds \\
&+ \int_{\Gamma_m} (\theta \cdot n)(Hl(u) + \partial_n l(u)) \\
&- \int_{\Gamma_N \cap \Gamma_m} (\theta \cdot n)(Hp \cdot g + \partial_n (p \cdot g))\, ds \\
&+ \int_{\Gamma_m} (\theta \cdot n) k_0 \left(\left((1-\alpha)^2 + k_l \right) \phi_r \left(tr(e(u)) \right) - \phi_r \left(-tr(e(u)) \right) \right) tr(e(p))\, ds \\
&+ \int_{\Gamma_m} (\theta \cdot n) 2\mu \left((1-\alpha)^2 + k_l \right) e(u)_D : e(v)_D\, ds \\
&- \int_{\Omega} \left(k_0 \phi_r \left(tr(e(u)) \right) tr(e(p)) + 2\mu e(u)_D : e(p)_D \right) 2\alpha'(1-\alpha)\, dx \\
&- \int_{\Gamma_0 \cap \Gamma_m} (\theta \cdot n) \left(H \left(Ae(p)n \cdot u + p \cdot Ae(u)n + l'(u) \right) + \partial_n \left(Ae(p)n \cdot u + p \cdot Ae(u)n + l'(u) \right) \right) ds
\end{aligned} \tag{5.141}$$

where α' is the shape derivative of the phase field α:

$$\alpha'(\Phi_1, \Phi_2) = -\theta(p_{\omega_1}) \cdot n(p_{\omega_1}) \alpha_2(\Phi_2) \dot{\alpha}_1(\Phi_1) - \theta(p_{\omega_2}) \cdot n(p_{\omega_2}) \alpha_1(\Phi_1) \dot{\alpha}_2(\Phi_2). \tag{5.142}$$

and p is defined as the solution of the following adjoint problem:

$$\begin{aligned}
&\int_{\Omega} k_0 \left(\left((1-\alpha)^2 + k_l \right) \phi_r' \left(tr(e(u)) \right) tr(e(\psi)) + \phi_r' \left(-tr(e(u)) tr(e(\psi)) \right) \right) tr(e(p))\, dx \\
&+ \int_{\Omega} 2\mu \left((1-\alpha)^2 + k_l \right) e(p)_D : e(\psi)_D\, dx + \int_{\Omega} m'(u) \cdot \psi\, dx + \int_{\Gamma_m \setminus \Gamma_0} l'(u) \cdot \psi\, ds = 0 \ \ \forall \psi \in H^1_{\Gamma_0}(\Omega)^d.
\end{aligned} \tag{5.143}$$

H is the mean curvature: $H = \operatorname{div}(n)$, $\partial_n f = \nabla f \cdot n$ for f a real function and

$$\dot{\alpha}_1(t) = \begin{cases} \dfrac{4}{l^4} t^3 - \dfrac{4}{l^2} t & \text{if } 0 \le t \le l \\ 0 & \text{otherwise.} \end{cases} \tag{5.144}$$

$$\dot{\alpha}_2(t) = \begin{cases} \dfrac{4}{l^4} t^3 - \dfrac{4}{l^2} t & \text{if } -l \le t \le l \\ 0 & \text{otherwise.} \end{cases} \tag{5.145}$$

Proof. The proof is similar to the one made for theorem 5.6.2. It suffices to treat the variable α as n was treated. □

On numerical implementation

To be able to apply the method to find a descent direction, explained in section 1.3.4, it is needed to rewrite, in the gradient given by theorem 5.6.7, the term:

$$\int_\Omega \left(k_0\phi_r\left(tr(e(u))\right)tr(e(p)) + 2\mu e(u)_D : e(p)_D\right) 2\alpha'(1-\alpha)\,dx.$$

In fact this term is of the form:

$$\int_\Omega -\theta(p_{\partial\omega_1})\cdot n(p_{\partial\omega_1})G_1(x) - \theta(p_{\partial\omega_2})\cdot n(p_{\partial\omega_2})G_2(x)\,dx. \tag{5.146}$$

We will use the coarea formula [64]:

Proposition 5.6.8. *Let X and Y be two smooth Riemannian manifolds of respective dimension $m \geq n$, and $f : X \to Y$ a surjective map of class C^1, whose differential $\nabla f(x) : T_xX \to T_{f(x)}Y$ is surjective for almost every $x \in X$. Let ϕ be an integrable function on X. Then:*

$$\int_X \phi(x)\,dx = \int_Y \int_{z\in f^{-1}(y)} \phi(z)\frac{1}{Jac(f)(z)}\,dz\,dy \tag{5.147}$$

where $Jac(f)(z)$ is the Jacobian of the function f

It is then proven in [202] corollary 3.3.11, applying this formula with $f = d_\Omega$, $X = \Omega$ and $Y = \partial\Omega$, that:

Corollary 5.6.9. *Let $\Omega \subset D$ be a C^2 bounded domain, and let ϕ be an integrable function over D. Then:*

$$\int_D \phi(x)\,dx = \int_{\partial\Omega}\left(\int_{ray_{\partial\Omega}(y)\cap D} \phi(z)\prod_{i=1}^{d-1}(1 + d_\Omega(z)\kappa_i(y))\,dz\right)dy \tag{5.148}$$

where z denotes a point in the ray emerging from $y \in \partial\Omega$, dz is the line integration along that ray and κ_i are the principal curvatures od $\partial\Omega$.

This theorem especially relies on the following lemma proved in [59] which also gives some regularity results on d_Ω and $p_{\partial\Omega}$:

Lemma 5.6.10. *Let $\Omega \subset D$ be a C^2 bounded domain. For $i = 1, \cdots, d-1$ κ_i are the principal curvatures of $\partial\Omega$ and e_i their associated directions. For every $x \in D$, and every $y \in \Pi_{\partial\Omega}(x)$ we have:*

$$-\kappa_i(y)d_\Omega(x) \leq 1,\ \ 1 \leq i \leq d-1 \tag{5.149}$$

Define Ξ the singular set of Ω which means that Ξ is the set of points $x \notin \Sigma$ that for some i, one of the inequality (5.149) is an equality. Then $\Sigma = \overline{\Sigma} \cup \Xi$ and $\overline{\Sigma}$ has zero Lebesgue measure. If $x \notin \overline{\Sigma}$, then all inequalities (5.149) are strict and d_Ω is twice differentiable at x. Its Hessian reads:

$$Hd_\Omega(x) = \sum_{i=1}^{d-1} \frac{\kappa_i(p_{\partial\Omega}(x))}{1 + \kappa_i(p_{\partial\Omega}(x))d_\Omega(x)} e_i(p_{\partial\Omega}(x)) \otimes e_i(p_{\partial\Omega}(x)). \tag{5.150}$$

Applying the corollary 5.6.9 to (5.146) give.

$$\begin{aligned}
&\int_{\partial\Omega_1} -\theta(y)\cdot n(y)\int_{ray_{\partial\Omega_1}(y)\cap\Omega} G_1(z)\prod_{i=1}^{d-1}(1 + d_\Omega(z)\kappa_i(y))\,dz\,dy \\
&\int_{\partial\Omega_2} -\theta(y)\cdot n(y)\int_{ray_{\partial\Omega_2}(y)\cap\Omega} G_2(z)\prod_{i=1}^{d-1}(1 + d_\Omega(z)\kappa_i(y))\,dz\,dy.
\end{aligned} \tag{5.151}$$

We also note that in (5.151) it suffices to integrate on the crack since G_1 and G_2 are null outside the enlarged evanescent phase field, in other word outside $\{\alpha > 0\}$. So, to compute the integral on the ray, we take the points of the elements cut by the crack S and for each of them find the ray which is normal to S and which passes through it. Then we find the intersections between a ray and the boundary of the phase field zone, $\{\alpha > 0\}$, and we integrate between these two points $G_k\prod_{i=1}^{d-1}(1 + d_\Omega(z)\kappa_i(y))$ thanks to a quadrature method.

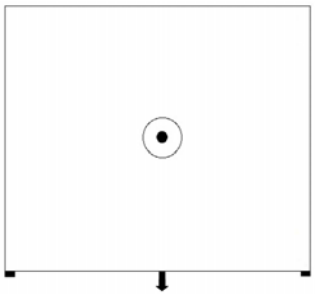

Figure 5.68: Load case for nail 1.

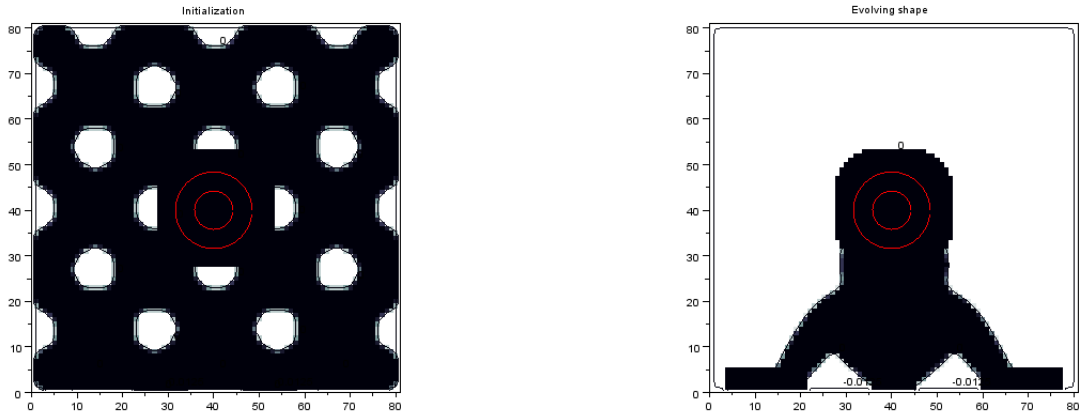

(a) Initialisation (b) Final design

Figure 5.69: The nail 1 case, with the phase field method

Numerical examples, with a fixed contact zone

We reuse the same examples as in section 5.6.1 and draw some comparisons. We use the phase field defined by (5.135) as we hope it will better take into account the expansion zones which are crucial in the value of the compliance and in the case of mechanical imbalances. The results are gathered in table 5.18.

The nail 1 We recall the load case on figure 5.68. The final design is given on figure 5.69.

The nail 2 We recall the load case on figure 5.70. The final design is given on figure 5.71.

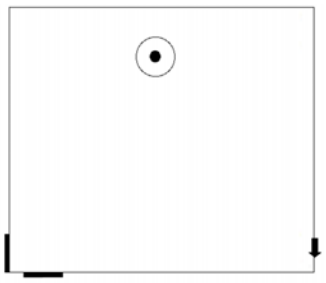

Figure 5.70: Load case for nail 2.

The nail 3 We recall the load case on figure 5.72. The final design is given on figure 5.73.

It is interesting to see that the three first results are comparable with the results found for the enlarging crack method. The difference lies in the value of the volume reach. For the phase field method, the algorithm manages to lower the volume a lot, comparing to the other method. It seems that the phase field method tends to add some stability to the structure.

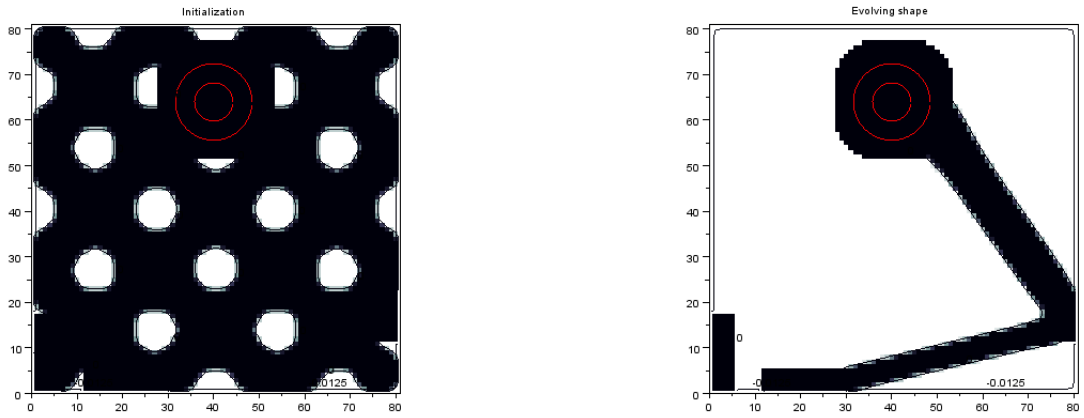

(a) Initialisation (b) Final design

Figure 5.71: The nail 2 case, with the phase field method

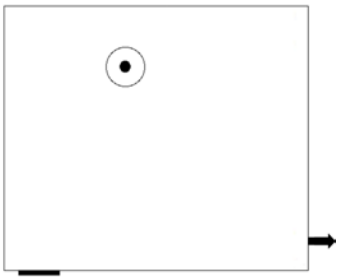

Figure 5.72: Load case for nail 3.

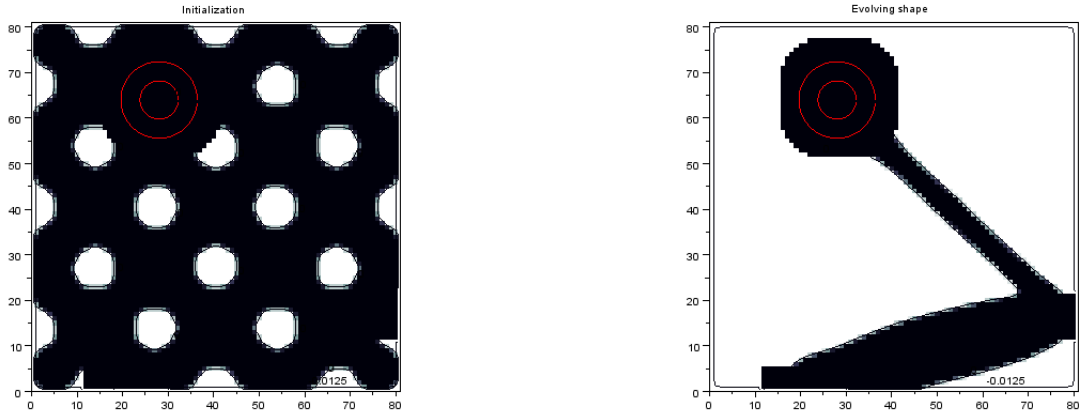

(a) Initialisation (b) Final design

Figure 5.73: The nail 3 case, with the phase field method

The nail 4 We recall the load case on figure 5.74. The final design is given on figure 5.75. This result confirms the observation made on the impact of the phase field method on stability. The structure does not use the vertical embedded zone and is lighter comparing to the enlarging crack case, see figure 5.51.

The nail 5 We recall the load case on figure 5.76. The final design is given on figure 5.77.

Expansion case We recall the load case on figure 5.78. The final design is given on figure 5.79.

The slanting crack We recall the load case on figure 5.80. The final design is given on figure 5.81. The two last cases show the difficulties of the algorithm to handle what happens near the crack.

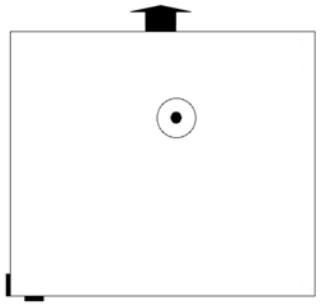

Figure 5.74: Load case for nail 4.

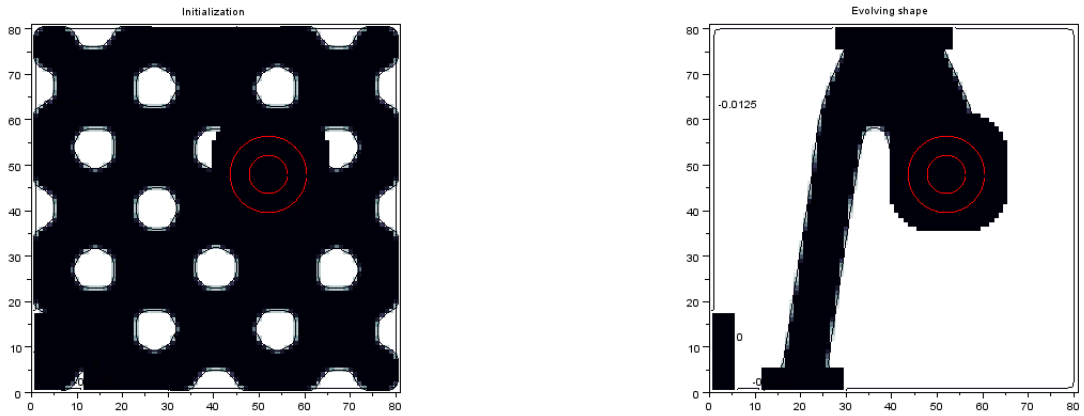

(a) Initialisation (b) Final design

Figure 5.75: The nail 4 case, with the phase field method

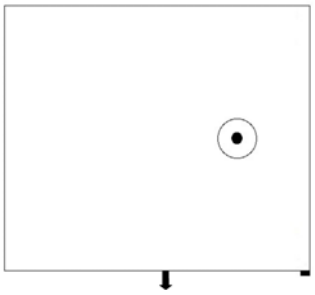

Figure 5.76: Load case for nail 5.

Numerical examples, with a mobile contact zone

In all these examples we assume that the nail can move on the horizontal direction. We use the Lagrangian optimisation technique explained in section 1.3.4. The results are compiled in table 5.19.

The nail 1 The circle starts from $(0.3, 1)$ and finishes at $(0.879777, 1)$. The results are given in figure 5.82. The final design keeps a thin bar on the left to be linked to a Dirichlet zone as in the corresponding example for the enlarging crack method.

The nail 2 The circle starts from $(0.3, 1.6)$ and finishes at $(1.56284, 1.6)$. The results are given in figure 5.83.

The nail 3 The Lagrangian multiplier is taken equal to 0.1. The circle starts from $(0.7, 1.6)$ and finishes at $(0.535555, 1)$. The results are given in figure 5.84. In the case of the enlarging crack method, the example did not converge. We notice that the structure holds thanks to the Dirichlet zone and that the role of the nail is small.

The nail 5 The circle starts from $(0.3, 1)$ and finishes at $(1.0315, 1)$. The results are given in figure 5.85. The structure counterbalances the fact that its abscissa is greater than 1, thanks to a thicker bar on the left.

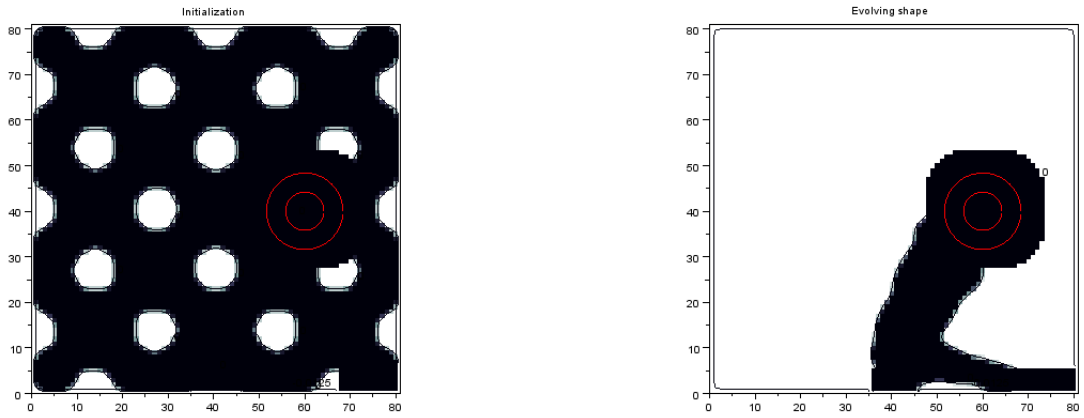

(a) Initialisation (b) Final design

Figure 5.77: The nail 5 case, with the phase field method

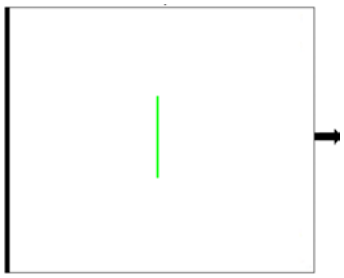

Figure 5.78: Load case for the expansion case.

(a) Initialisation (b) Final design

Figure 5.79: The expansion case, with the phase field method

5.6.5 Conclusion

Through all the examples we manage to treat shape optimization for frictionless contact without meshing the contact zone. Focusing on the approximation of the contact problem, the enlarging crack method is endowed with a better accuracy than the phase field method. As a matter of fact, it seems that the phase field method, where the crack opens, does not completely disconnect the two parts of the crack and that, on the parts in contact, the predicted sliding is mitigated. Thus the shape optimisation algorithm evaluates a reduced compliance for some structures and judges them admissible whereas it would not be the case using the enlarging crack method.
We also point out that the phase field method is dependent on the choice of the expression of the phase field chosen. The enlarging crack method is more intrinsic in this sense. We also show that the implemented solvers did not enable the algorithm to remove material on the contact zone see figure 5.55 and 5.79: it is coherent with the the numerical assumption made that there is always material near the crack.

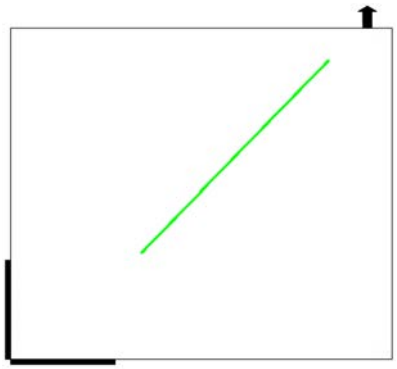

Figure 5.80: Load case for the slanting crack case.

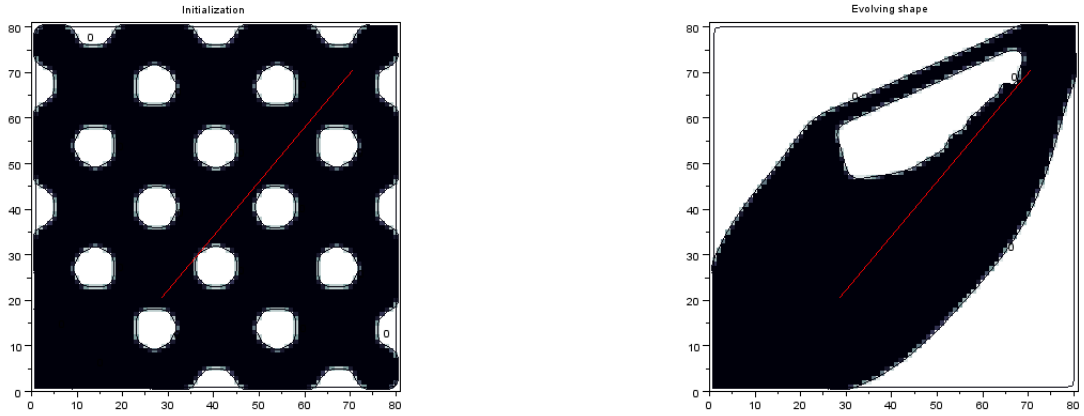

(a) Initialisation (b) Final design

Figure 5.81: The slanting crack case, with the phase field method

During the study of this section, there were some issues which were not raised. The first one is that the computation of the gradient for the enlarging crack method is much more delicate than for the phase field method. In fact, the boundary terms in the gradient (5.120) include normal derivatives of functions depending on the jump multiplied by the penalisation. To compute these terms, we use a finite differences approach which leads to bad approximations of the gradient values which, amongst others, are too big with respect to the values on the other parts of the boundary. This raises concerns when we do the optimization of the contact zone and of the shape of the structure in the meantime. On the simple example of a contact zone only allowed to be translated in a fixed direction, we manage to get some decent results by detecting the oscillations of the nail and forbidding them. In gradient (5.141) induced by the phase field, this complication disappears.

Another issue is the mesh dependency. On the example of the nail 5 we plot the compliance with respect to the location of the contact (and Dirichlet) circle center, which we move every $h/4 = 0.0625$ from 0.3 to 1.74. We do it for three cases. The first one is done removing the contact zone, there is only the Dirichlet area. For the second one, we do the contrary by removing the Dirichlet zone and keeping the contact zone. The third one shows the plot when both are kept. On figure 5.86, we observe that for both methods, moving the contact and Dirichlet zone lead to an oscillated compliance. These oscillations are similar from an element to another element, following the same pattern.

Cases	Volume	Compliance	Compliance Constraint	Iterations	Evaluations
nail 1	1.05064	4.1999	4.2	40	300
nail 2	0.954718	13.9999	14	54	79
nail 3	1.06363	6.49997	6.5	49	74
nail 4	1.18375	789.996	790	29	50
nail 5	0.761065	7.96966	8	29	47
Expansion	0.998301	7.99974	8	19	44
Slanting	2.19328	54.9688	55	31	52

Table 5.18: Results for the phase field method when the contact zone is fixed

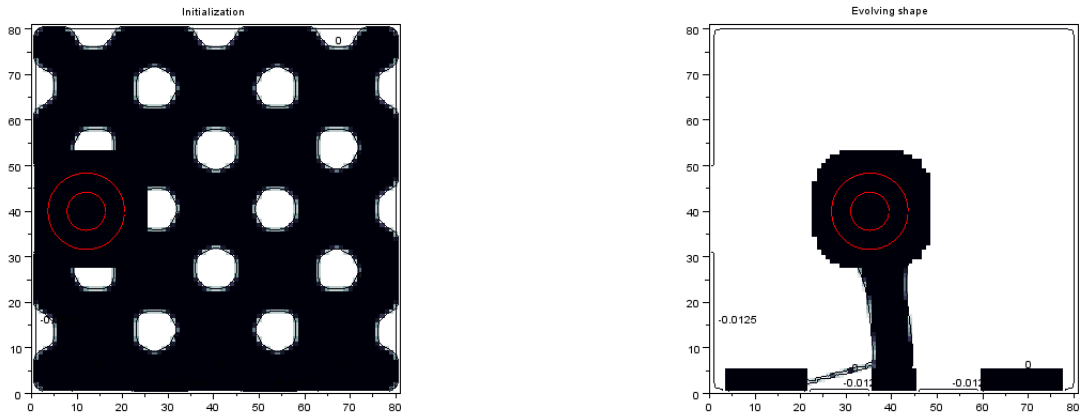

(a) Initialisation (b) Final design

Figure 5.82: The nail 1 case for a mobile contact zone, with the phase field method.

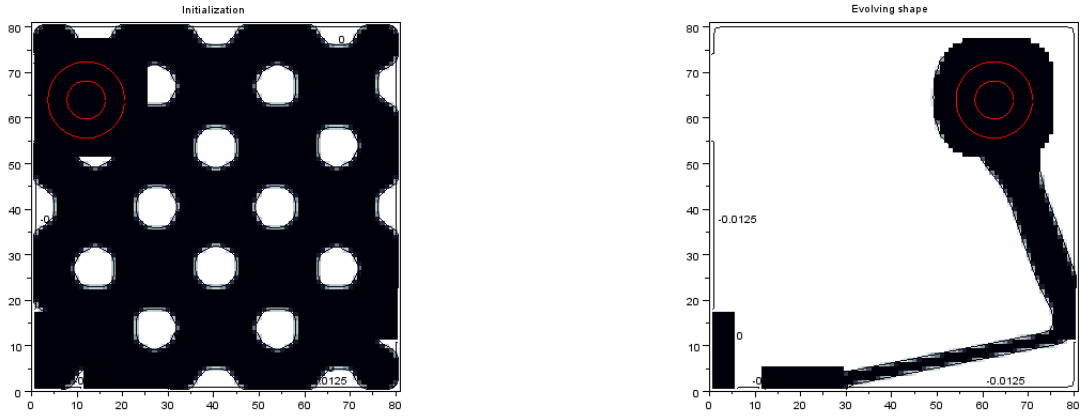

(a) Initialisation (b) Final design

Figure 5.83: The nail 2 case for a mobile contact zone, with the phase field method.

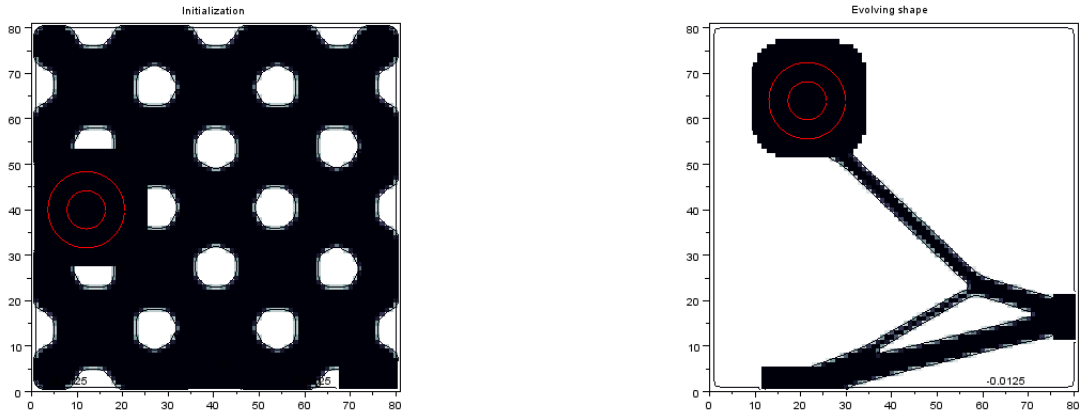

(a) Initialisation (b) Final design

Figure 5.84: The nail 3 case for a mobile contact zone, with the phase field method.

This dependency is amplified in case of contact: for the enlarging crack, the hole ω is numerically defined thanks to the mesh and a slight change in the crack location can completely change the thickness of ω. For the phase field method, the difficulty is similar since we use the mesh to approximate the phase field α.

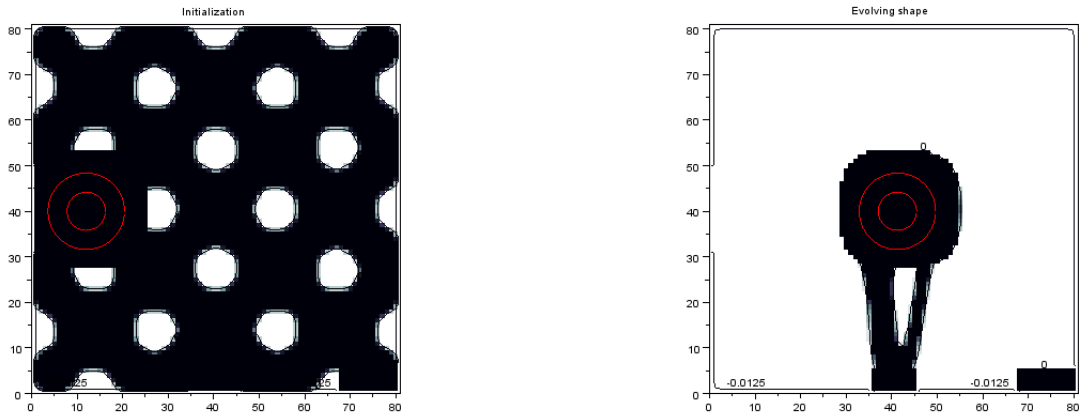

(a) Initialisation (b) Final design

Figure 5.85: The nail 5 case for a mobile contact zone, with the phase field method.

Cases	Lagrangian	Volume	Compliance	Iterations	Evaluations
nail 1	1.24804	0.65468	5.93356	19	74
nail 2	1.81288	0.795411	10.1747	16	61
nail 3	1.76969	0.788385	9.8131	17	67
nail 5	1.22542	0.591563	6.33857	17	180

Table 5.19: Results for the phase field method when the contact zone is optimisable.

As mentioned in the introduction of this chapter, in [180], the same kind of problems is considered using XFEM, focusing on the optimisation of the contact zone without optimising the shape of the structure. They considered the example of a kind of a screw we do not manage to solve at this stage for several reasons. They consider a square full of material in which there is a contact zone which, at the beginning of the optimisation, is a kind of semicircle supported by the right side of the square. The right side of the square included in the semicircle is fixed and a force is applied on the whole right side, see figure 5.87. The optimisation problem consists of minimising the displacement of the points on which the force is applied under a perimeter constraint. Thus the goal is that the initial smooth contact zone covers with small protrusions whose sizes are controlled by the perimeter constraint. In our attempts, these protusions appeared with even some contact loops, but we do not manage to tightly control their size. Then, it was impossible to rely on the two approximation methods introduced in this chapter, since the mesh was sometimes too coarse to catch the convolution produced.

We end this conclusion by talking a little bit of the optimisation strategy. As stated the gradient induced by the enlarging crack method is not easy to compute. We could solve the contact problem with this method and use the expression of the gradient given by the phase field method (with the solution of the enlarging crack) in the optimisation. Moreover, we choose to perform shape optimisation of the contact zone and the shape of the structure at once. We could imagine to do these optimisations sequentially, making some optimisation steps for the contact zone, then performing some optimisation steps for the structure shape and then making a loop.

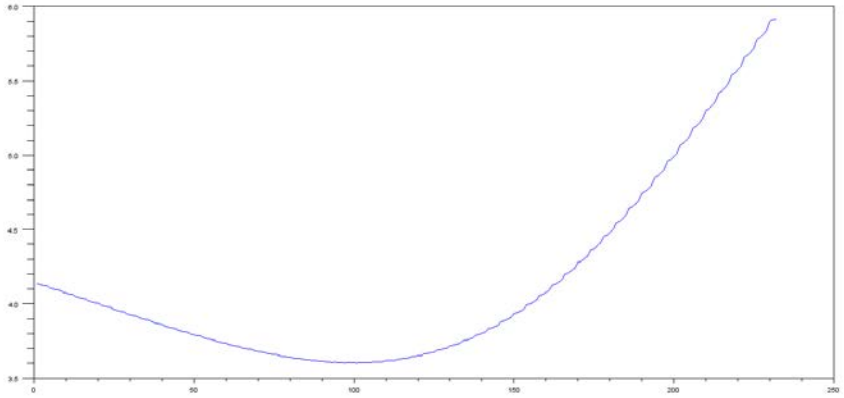

(a) Dirichlet zone moving

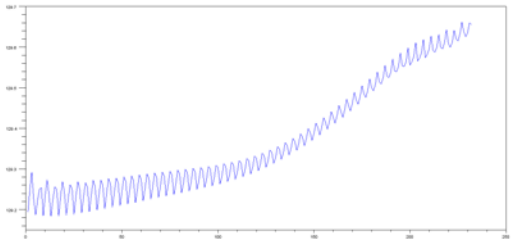

(b) Enlarging crack, contact zone moving

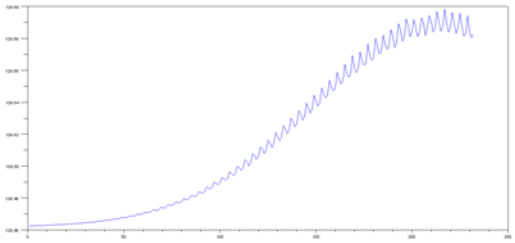

(c) Phase field method, contact zone moving

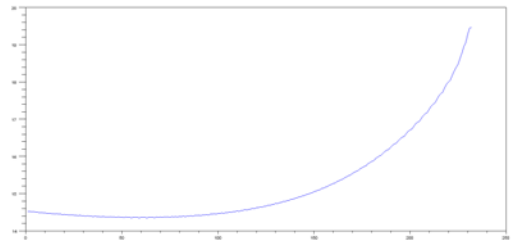

(d) Enlarging crack, both zones moving

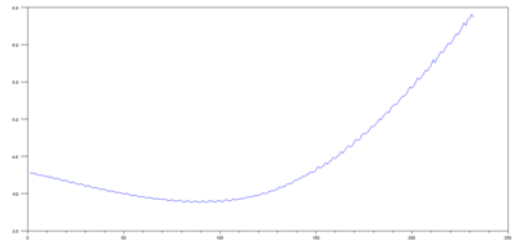

(e) Phase field method, both zones moving

Figure 5.86: The evolution of the compliance in the example of the nail 5, translating the center on the horizontal direction from $\frac{h}{4}$ on each step

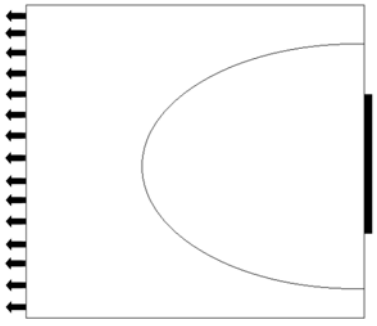

Figure 5.87: Load case for the screw case.

Chapter 6

Shape optimisation for static plasticity

Contents

6.1 Introduction

The importance of taking plasticity into account in the design of structure was already presented in chapter 4. In shape optimisation, there is an additional possible advantage to account for this phenomenon. The designs found, when a simple elastic behaviour is considered, often include small bars and areas where the stress is high. The optimisation process cannot foresee that theses particular areas can lead to the appearance of crack and the collapse of the structure, making the optimised solution ineffective in reality and non admissible. One idea is to forbid small thickness in the structure [202] or to apply constraints on the maximal value taken by the Von Mises criterion (or the Tresca criterion). This last possibility leads to great difficulty as this constraint amount to constrain every point of the structure, therefore it is impossible to use it, in its basic formulation. That is why numerous propositions were made of aggregation functions to account for these pointwise constraints, though not managing to completely respect them. On this subject, we mention, [8] [18] (with topological derivative), [183], [181] (using the SIMP method and regional stress constraints), [191] (using the SIMP method and an aggregated K-S function), [292] (using a the levelset method and a criterion defined only on the region where the constraint is violated), [299] (using the level set method and a maximum square aggregation function). Thus, it is also interesting for this particular reason to regard the plasticity behaviour of the structure.

In this chapter, we only consider the Hencky model. As stated in chapter 4, the problem can be put under a mixed form including a variational inequation and a variational equation. As previously pointed out in chapter 5, there is no chance for this problem to be Fréchet or Gateaux differentiable. One solution, which was largely investigated in the framework of control theory for problems with hardening, is the use of a regularised penalised problem to get rid of the variational inequality. On this issue we mention, for the static case, [138], [140], [141], [88] (using a primal formulation), [142], [36] (for a second order optimality condition), for the quasi-static case [289] and for other plastic models [87] and [162].

In shape optimization, the first case which was considered was the one of beam structure and frame optimization which is addressed for instance in [159], [120], [281], [157], [2], [230], [161]. We point out the particular case of [302], where periodical microstructures are used. From a theoretical point of view, in [269], in chapter 4.8, the shape derivative of an elasto-plastic torsion problem is computed and, in chapter 4.9, the shape derivative of the stress tensor is calculated in the case of the visco-plastic model of Perzyna (see section 4.4). There also exist numerous articles where, for a particular optimisation problem, the existence of a solution is proved for the continuous and discrete case with a uniform Lipschitz assumption on the boundary. The discrete solution is then proved to converge to the continuous one. In [146] or in [133] and [135], the analysis is done in the framework of the Hencky model for a criterion depending only on σ. In [148], the analysis is done for axisymmetric bodies. In [147], the same analysis is done in the

case of the Prandtl-Reuss model of elasto-plasticity (dynamic plasticity). In [233] strain-hardening is added. Finally [95] and [131] (for numerical results) deal with a particular elasto-plasticity model (introduced by Washizu in [294]).

From a numerical point of view some authors use conical derivatives inside a bundle algorithm to optimise the shape, see [241] and [174]. Another way to proceed is to differentiate the radial return algorithm (the generalized Newton method, see [246] chapter 8). The differentiation is analysed in [287], [184] and [203]. This procedure was applied in various articles, using the Von Mises criterion. In [201] and [250], the authors consider linear isotropic hardening/softening. They use, first, the SIMP method and finish the shape optimization using splines to parametrize the boundary to recover smooth shapes. In [164] rate-independent elasto-plasticity and contact friction are taken into account. For the shape optimization, splines are used. In [166], the same is done but for finite deformation elasto-plasticity. In [160], the elato-plastic model is the same but the derivative is computed differently. It also performs two-phase optimisation thanks to the SIMP method. For perfect plasticity we mention [101], using the boundary perturbation method.

In this chapter, we adopt the same point of view as in chapter 5. We will use regularised and penalised problems to approximate the solutions of the Hencky model with a Von Mises criterion. First we present two regularized plastic models. One is directly derived from the Perzyna model presented in section 4.4, the other one is, in a certain sense, a regularization of the projection in the case of the Von Mises criterion. We prove the existence and uniqueness of a solution for these two regularised problems and that both regularised solutions converge to the solution of the Hencky model.

In a second part, we analyse the differentiability with respect to the shape and compute shape gradients. Finally, some numerical examples are presented in 2D.

6.2 Regularized models

6.2.1 Regularization of the Perzyna model

Statement of the model

The Perzyna model was introduced in chapter 4, section 4.4 and the corresponding equation was given in (4.61). We recall this equation:

$$\int_\Omega \left(\frac{\eta}{1+\eta} Ae(u_\eta) + \frac{1}{1+\eta} P_K^{A^{-1}}(Ae(u_\eta)) \right) : e(v)\, dx = \int_\Omega f \cdot v\, dx + \int_{\Gamma_N} g \cdot v\, ds \ \forall v \in H^1_{\Gamma_0}(\Omega)^d. \tag{6.1}$$

If we want to derive the solution with respect to the shape, we need to regularise the term $P_K^{A^{-1}}$. This could be easily done in the case of the Von Mises criterion since we know the expression of the projection (4.41):

$$P_K^{A^{-1}}(\tau) = \tau - \max\left(0, 1 - \frac{\sigma_c}{|\tau_D|}\right) \tau_D. \tag{6.2}$$

The only part we need to regularise is the max function. We use the function:

$$f_\gamma(t) = \begin{cases} \dfrac{1}{4\gamma} t^2 + \dfrac{1}{2} t + \dfrac{\gamma}{4} & t \in [-\gamma, \gamma] \\ \max(t, 0) & \text{otherwise.} \end{cases} \tag{6.3}$$

The regularised projection is now:

$$P_K^\gamma(\tau) = \tau - f_\gamma\left(1 - \frac{\sigma_c}{|\tau_D|}\right) \tau_D. \tag{6.4}$$

The equation of the regularised Perzyna model can then be written: find $u \in H^1_{\Gamma_0}(\Omega)^d$ such that,

$$\int_\Omega \left(\frac{\eta}{1+\eta} Ae(u_\eta^\gamma) + \frac{1}{1+\eta} P_K^\gamma(Ae(u_\eta^\gamma)) \right) : e(v)\, dx = \int_\Omega f \cdot v\, dx + \int_{\Gamma_N} g \cdot v\, ds \ \forall v \in H^1_{\Gamma_0}(\Omega)^d. \tag{6.5}$$

or in a mixed form which will be needed for the mathematical analysis: find $\sigma_\gamma^\eta \in L^2_s(\Omega)^{d\times d}$ and $u_\gamma^\eta \in H^1_{\Gamma_0}(\Omega)^d$ such that:

$$\begin{cases} \displaystyle\int_\Omega \sigma_\gamma^\eta : e(v)\, dx = \int_\Omega f \cdot v\, dx + \int_{\Gamma_N} g \cdot v\, ds, \ \ \forall v \in H^1_{\Gamma_0}(\Omega)^d \\ \displaystyle\int_\Omega A^{-1}\sigma_\gamma^\eta : \tau\, dx + \frac{1}{1+\eta} \int_\Omega A^{-1} f_\gamma\left(1 - \frac{\sigma_c}{|\sigma_\gamma^\eta|_D}\right) (\sigma_\gamma^\eta)_D : \tau = \int_\Omega e(u_\gamma^\eta) : \tau\, dx, \ \ \forall \tau \in L^2_s(\Omega)^{d\times d}. \end{cases} \tag{6.6}$$

Mathematical analysis

We give two theorems stating that the solution of (6.5) exists, is unique and converges to the solution of the Hencky model. For the existence and uniqueness, the proof is the same as the one for proposition 2.8 in [140] with hardening.

Theorem 6.2.1. *Under the safe-load condition* (4.52) *and* $f \in L^2(\Omega)^d$ *and* $g \in L^2(\Gamma_N)^d$*,there exists a unique solution* $(\sigma_\eta^\gamma, u_\eta^\gamma) \in L^2_S(\Omega)^{d\times d} \times H^1_{\Gamma_0}(\Omega)^d$ *to the problem* (6.5)*, where* $L^2_S(\Omega)^{d\times d}$ *is the set of matrices of d-dimension with coefficients in* $L^2(\Omega)$*.*

For the convergence we have to adapt the proof in [190] chapter 2. We recall some definitions given in 4:

$$\Sigma_{\text{div}}(g) = \{\tau \in H_s(\text{div}, \Omega, d) \,|\, \gamma_N(\tau) = g\}\,, \tag{6.7}$$

$$S(f,g) = \{\tau \in \Sigma_{\text{div}}(g) \,|\, -\text{div}\sigma = f \text{ in } \Omega\}\,. \tag{6.8}$$

First we state a lemma to place ourselves in the same framework as the one of the Perzyna model.

Lemma 6.2.2. *The function* $\tau \to f_\gamma\left(1 - \dfrac{\sigma_c}{|\tau|_D}\right)\tau_D$ *from* $\mathbb{M}^d_s$ *into* $\mathbb{M}^d_s$ *is the derivative of the function:*

$$\tau \to F_\gamma\left(1 - \frac{\sigma_c}{|\tau|_D}\right) = \int_{-\gamma}^{1-\frac{\sigma_c}{|\tau|_D}} f_\gamma(t)\frac{\sigma_c^2}{(1-t)^3}\,dt. \tag{6.9}$$

Moreover F_γ *is convex.*

Proof. First we compute the derivative of the function in $]-\gamma, 1-\epsilon$ for every $\epsilon > 0$:

$$x \to F_\gamma(x) = \int_{-\gamma}^{x} f_\gamma(t)\frac{\sigma_c^2}{(1-t)^3}\,dt \tag{6.10}$$

which is $f_\gamma(x)\dfrac{\sigma_c^2}{(1-x)^3}$. Then the derivative of $\tau \to 1 - \dfrac{\sigma_c}{|\tau|_D}$ is:

$$\tau \to \sigma_c \frac{\sigma_D}{|\sigma|^3_D}.$$

Applying the chain rule we get the result. For the convexity of F_γ, we differentiate the function $\tau \to f_\gamma\left(1 - \dfrac{\sigma_c}{|\sigma|_D}\right)\tau_D$ with σ given. This gives the Hessian which is a bilinear positive form and implies the convexity. □

The following lemma is the equivalent result of theorem 2.1 in [190]:

Lemma 6.2.3. *For the solution of the regularised Perzyna model, if we assume* γ *small enough there exist three constants* $C_1 > 0$*,* $C_2 > 0$ *and* $C_3 > 0$ *such that:*

$$\left\|\sigma_\eta^\gamma\right\|_{L^2} \le C_1 \tag{6.11}$$

$$\left\|\frac{1}{\eta}F_\gamma\left(1 - \frac{\sigma_c}{|\sigma_\gamma^\eta|_D}\right)\right\|_{L^1} \le C_2 \tag{6.12}$$

$$\left\|\frac{1}{\eta}f_\gamma\left(1 - \frac{\sigma_c}{|\sigma_\gamma^\eta|_D}\right)\left(\sigma_\eta^\gamma\right)_D\right\|_{L^1} \le C_2 \tag{6.13}$$

Proof. First we make a remark. Let $\overline{\sigma}$ satisfying the safe load condition. This especially implies that $\overline{\sigma} \in S(f,g)$. Then there exists $\delta > 0$ such that:

$$|\overline{\sigma}|_D - \sigma_c \le -\delta.$$

This means that:

$$1 - \frac{\sigma_c}{|\overline{\sigma}|_D} \le -\frac{\delta}{\sigma_c - \delta}.$$

So taking γ small enough ($\dfrac{\delta}{\sigma_c - \delta} \ge \gamma$), which is assumed in the sequel, we have:

$$F_\gamma\left(1 - \frac{\sigma_c}{|\overline{\sigma}|_D}\right) = 0.$$

We adopt some notations:

$$a^{-1}(\sigma,\tau) = \int_\Omega A^{-1}\sigma : \tau\,dx$$

and we note $F_\gamma(\tau)$ and $F'_\gamma(\tau) = f_\gamma(\tau)\tau_D$ instead of:

$$F_\gamma\left(1 - \frac{\sigma_c}{|\tau|_D}\right),$$

$$F'_\gamma\left(1 - \frac{\sigma_c}{|\tau|_D}\right) = f_\gamma\left(1 - \frac{\sigma_c}{|\tau|_D}\right)\tau_D.$$

We test the regularized Perzyna formulation with $\sigma^\eta_\gamma - \overline{\sigma}$, doing an integration by part:

$$a^{-1}(\sigma^\eta_\gamma, \sigma^\eta_\gamma - \overline{\sigma}) + \frac{1}{\eta}\int_\Omega A^{-1} f_\gamma\left(1 - \frac{\sigma_c}{|\sigma^\eta_\gamma|_D}\right)(\sigma^\eta_\gamma)_D : \left(\sigma^\eta_\gamma - \overline{\sigma}\right)\, dx = -\int_\Omega u^\eta_\gamma \cdot \operatorname{div}(\sigma^\eta_\gamma - \overline{\sigma})\, dx \tag{6.14}$$

Since $\sigma^\eta_\gamma \in S(f,g)$ and $\overline{\sigma} \in S(f,g)$, in Ω, $\operatorname{div}(\sigma^\eta_\gamma) = \operatorname{div}(\overline{\sigma}) = -f$. So, the last term in the equality is equal to 0. Moreover we know that F_γ is positive and convex. The fact that it is convex implies:

$$F_\gamma(\sigma^\eta_\gamma) - F_\gamma(\overline{\sigma}) \leq F'_\gamma(\sigma^\eta_\gamma) : \sigma^\eta_\gamma - \overline{\sigma}. \tag{6.15}$$

Yet $F_\gamma(\overline{\sigma}) = 0$ which yields:

$$\int_\Omega A^{-1} f_\gamma(\sigma^\eta_\gamma)(\sigma^\eta_\gamma)_D : \sigma^\eta_\gamma - \overline{\sigma}\, dx \geq 0. \tag{6.16}$$

since $A^{-1}(\sigma^\eta_\gamma)_D = \dfrac{1}{2\mu}(\sigma^\eta_\gamma)_D$. It follows that:

$$a^{-1}(\sigma^\eta_\gamma, \sigma^\eta_\gamma - \overline{\sigma}) \leq 0 \tag{6.17}$$

and adding $-a^{-1}(\overline{\sigma}, \sigma^\eta_\gamma - \overline{\sigma})$ on both side:

$$a^{-1}(\sigma^\eta_\gamma - \overline{\sigma}, \sigma^\eta_\gamma - \overline{\sigma}) \leq -a^{-1}(\overline{\sigma}, \sigma^\eta_\gamma - \overline{\sigma}). \tag{6.18}$$

We use the coercivity (on the left hand side, noting C_0 the coercivity constant) and the continuity (on the right hand side, noting C_c the continuity constant) of a^{-1} to get:

$$C_0 \left\|\sigma^\eta_\gamma - \overline{\sigma}\right\|^2_{L^2} \leq C_c \left\|\overline{\sigma}\right\| \left\|\sigma^\eta_\gamma - \overline{\sigma}\right\|. \tag{6.19}$$

So we have proved that $\left\|\sigma^\eta_\gamma - \overline{\sigma}\right\|_{L^2}$ is smaller than a constant which, in particular, implies (6.11).
Now taking (6.14) and adding on each side $-a^{-1}(\overline{\sigma}, \sigma^\eta_\gamma - \overline{\sigma})$:

$$a^{-1}(\sigma^\eta_\gamma - \overline{\sigma}, \sigma^\eta_\gamma - \overline{\sigma}) + \frac{1}{\eta}\int_\Omega A^{-1} f_\gamma\left(\sigma^\eta_\gamma\right)(\sigma^\eta_\gamma)_D : \left(\sigma^\eta_\gamma - \overline{\sigma}\right)\, dx = -a^{-1}(\overline{\sigma}, \sigma^\eta_\gamma - \overline{\sigma}). \tag{6.20}$$

Thanks to the coercivity of a^{-1}, the first term is positive so:

$$\frac{1}{\eta}\int_\Omega A^{-1} f_\gamma\left(\sigma^\eta_\gamma\right)(\sigma^\eta_\gamma)_D : \left(\sigma^\eta_\gamma - \overline{\sigma}\right)\, dx \leq C_c \left\|\overline{\sigma}\right\| \left\|\sigma^\eta_\gamma - \overline{\sigma}\right\| \leq C_2. \tag{6.21}$$

Using (6.15) this yields that

$$\left\|\frac{1}{\eta} F_\gamma(\sigma^\eta_\gamma)\right\|_{L^1} \leq C_2. \tag{6.22}$$

This implies the last estimate as:

$$\begin{aligned}\left\|\frac{1}{\eta} F'_\gamma(\sigma^\eta_\gamma)\right\|_{L^1} &= \frac{2}{\delta} \sup_{\|\chi\|_{L^\infty} \leq \frac{\delta}{2}} \langle \frac{1}{\eta} F'_\gamma(\sigma^\eta_\gamma), \chi\rangle \\ &\leq \frac{2}{\delta} \sup_{\|\chi\|_{L^\infty} \leq \frac{\delta}{2}} \left(\langle \frac{1}{\eta} F'_\gamma(\sigma^\eta_\gamma), \chi - \sigma^\eta_\gamma + \overline{\sigma}\rangle + \langle \frac{1}{\eta} F'_\gamma(\sigma^\eta_\gamma), \sigma^\eta_\gamma - \overline{\sigma}\rangle\right)\end{aligned} \tag{6.23}$$

At this point we make two remarks. The first one is that thanks to the convexity of F_γ:

$$\int_\Omega F_\gamma(\sigma^\eta_\gamma) - F_\gamma(\chi + \overline{\sigma})\, dx \geq \langle F'_\gamma(\sigma^\eta_\gamma), \chi - \sigma^\eta_\gamma + \overline{\sigma}\rangle.$$

Secondly we can take γ small enough to ensure that $F_\gamma(\chi + \overline{\sigma}) = 0$, which we can assume since $|\chi + \overline{\sigma}|_D - \sigma_c \leq -\dfrac{\delta}{2}$. So:

$$\begin{aligned}\left\|\frac{1}{\eta} F'_\gamma(\sigma^\gamma_\eta)\right\|_{L^1} &\leq \frac{2}{\delta} \sup_{\|\chi\|_{L^\infty} \leq \frac{\delta}{2}} \left(\int_\Omega \frac{1}{\eta} F_\gamma(\sigma^\eta_\gamma) - \frac{1}{\eta} F_\gamma(\chi + \overline{\sigma})\, dx\right) + \langle \frac{1}{\eta} F'_\gamma(\sigma^\eta_\gamma), \sigma^\eta_\gamma - \overline{\sigma}\rangle \\ &\leq \frac{2}{\delta} \sup_{\|\chi\|_{L^\infty} \leq \frac{\delta}{2}} \left(\int_\Omega \frac{1}{\eta} F_\gamma(\sigma^\eta_\gamma)\, dx\right) + \sup_{\|\chi\|_{L^\infty} \leq \frac{\delta}{2}} \left(\int_\Omega \frac{1}{\eta} F_\gamma(\chi + \overline{\sigma})\, dx\right) + \langle \frac{1}{\eta} F'_\gamma(\sigma^\eta_\gamma), \sigma^\eta_\gamma - \overline{\sigma}\rangle \\ &\leq \frac{2}{\delta} 2C_2\end{aligned} \tag{6.24}$$

and the estimate (6.13) is proved thanks to (6.21) and (6.22). □

Lemma 6.2.4. *For the solution of the regularised Perzyna model, if we assume γ small enough there exist two constants $C_4 > 0$, $C_5 > 0$ such that:*

$$\left\|e(u_\gamma^\eta)\right\|_{L^2} \leq C_4 \left(1 + \frac{1}{\eta}\right), \tag{6.25}$$

$$\left\|u_\gamma^\eta\right\|_{H^1} \leq C_5 \left(1 + \frac{1}{\eta}\right). \tag{6.26}$$

Proof. First we prove a boundedness result on $f_\gamma\left(1 - \frac{\sigma_c}{|\sigma_\gamma^\eta|_D}\right)(\sigma_\gamma^\eta)_D$ in $L^2(\Omega)^{d\times d}$.

$$\int_\Omega f_\gamma\left(\sigma_\gamma^\eta\right)^2 (\sigma_\gamma^\eta)_D : (\sigma_\gamma^\eta)_D \leq \left\|\sigma_\gamma^\eta\right\|_{L^2}^2 \tag{6.27}$$

thanks to the fact that $t \to f_\gamma\left(1 - \frac{\sigma_c}{t}\right)$ is smaller than one and positive.
Taking the second equation in (6.6) with $\tau = e(u_\eta^\gamma)$ gives:

$$\int_\Omega A^{-1}\sigma_\gamma^\eta : e(u_\eta^\gamma)\, dx + \frac{1}{\eta}\int_\Omega A^{-1} f_\gamma\left(\sigma_\gamma^\eta\right)(\sigma_\gamma^\eta)_D : e(u_\eta^\gamma) = \int_\Omega e(u_\gamma^\eta) : e(u_\eta^\gamma)\, dx. \tag{6.28}$$

This implies that:

$$\left\|e(u_\gamma^\eta)\right\|_{L^2}^2 \leq \left\|A^{-1}\sigma_\gamma^\eta\right\|_{L^2}\left\|e(u_\gamma^\eta)\right\|_{L^2} + \frac{1}{\eta}\left\|A^{-1} f_\gamma\left(\sigma_\gamma^\eta\right)(\sigma_\gamma^\eta)_D\right\|_{L^2}\left\|e(u_\gamma^\eta)\right\|_{L^2}. \tag{6.29}$$

Using the properties of A^{-1}, the estimation (6.27) and (6.11) gives:

$$\left\|e(u_\gamma^\eta)\right\|_{L^2} \leq C_4 \left(1 + \frac{1}{\eta}\right), \tag{6.30}$$

and thanks to Korn inequality:

$$\left\|u_\gamma^\eta\right\|_{H^1} \leq C_5 \left(1 + \frac{1}{\eta}\right). \tag{6.31}$$

□

Lemma 6.2.5. *Assuming γ small enough, there exist two constants $C_6 > 0$, $C_7 > 0$ such that:*

$$\left\|e(u_\gamma^\eta)\right\|_{L^1} \leq C_6, \tag{6.32}$$

$$\left\|u_\gamma^\eta\right\|_{L^{\frac{d}{d-1}}} \leq C_7. \tag{6.33}$$

Proof. Taking the second equation in (6.6), we get pointwise:

$$A^{-1}\left(\sigma_\gamma^\eta + f_\gamma\left(\sigma_\gamma^\eta\right)(\sigma_\gamma^\eta)_D\right) = e(u_\gamma^\eta) \tag{6.34}$$

Integrating on Ω, using (6.11) and (6.13) leads to (6.32). For (6.33) it suffices to use the Korn inequality given in [190] appendix D theorem $D.2$ third point. □

Theorem 6.2.6. *Under the safe-load condition* (4.52) *and with $f \in L^d(\Omega)^d$ and $g \in C^0(\Gamma_N)^d$,*

- *σ_γ^η converges strongly in $L^2_S(\Omega)^{d\times d}$ to σ, the constraint tensor solution of the Hencky model* (4.53).
- *Up to a subsequence, u_γ^η converges weakly in $L^{\frac{d}{d-1}}(\Omega, \mathbb{R}^d)$ and weakly in $BD(\Omega)$ to u the displacement solution of the Hencky model* (4.53).

Proof. We start by the convergence of σ_γ^η. Thanks to (6.11), there exists a subsequence $\sigma_{\gamma_l}^{\eta_l}$ converging weakly in $L^2_S(\Omega)^{d\times d}$ to a function $\tilde{\sigma}$. Our goal is to prove that $\sigma = \tilde{\sigma}$. We note E the energy function defined for every $\tau \in L^2_S(\Omega)^{d\times d}$ by:

$$E(\tau) = \frac{1}{2}a^{-1}(\tau, \tau). \tag{6.35}$$

This energy was already introduced in (4.35). Indeed the solution of the Hencky model σ minimises it in $S(f, g)$. We define two open sets $\omega_\eta = \{x \in \Omega \,|\, d(x, \partial\Omega) > \eta\}$, $\omega_{\frac{\eta}{2}}^c = \left\{x \in \Omega \,|\, d(x, \partial\Omega) < \frac{\eta}{2}\right\}$ and a function $\phi_\gamma^\eta \in C^\infty(\Omega, \mathbb{R})$ such that $\phi_\gamma^\eta = 1$ on $\partial\Omega \cup \omega_{\frac{\eta}{2}}^c$ and $\frac{1}{\gamma+1}$ in ω_η.We prove that $E(\tilde{\sigma}) \leq E\left(\phi_\gamma^\eta\sigma\right)$.
We test (6.6) with $\sigma_\gamma^\eta - \phi_\gamma^\eta\sigma$ and apply the Green formula:

$$a^{-1}(\sigma_\gamma^\eta, \sigma_\gamma^\eta - \phi_\gamma^\eta\sigma) + \frac{1}{\eta}\int_\Omega A^{-1} f_\gamma\left(\sigma_\gamma^\eta\right)(\sigma_\gamma^\eta)_D : \left(\sigma_\gamma^\eta - \phi_\gamma^\eta\sigma\right) dx = -\int_\Omega u_\gamma^\eta \cdot \left(f - \operatorname{div}(\phi_\gamma^\eta\sigma)\right) dx, \tag{6.36}$$

Then we can use the usual convexity argument to say that:

$$\int_\Omega F_\gamma(\sigma_\gamma^\eta) - F_\gamma(\phi_\gamma^\eta\sigma)\,dx \leq \int_\Omega A^{-1} f_\gamma\left(\sigma_\gamma^\eta\right)(\sigma_\gamma^\eta)_D : \left(\sigma_\gamma^\eta - \phi_\gamma^\eta\sigma\right)\,dx. \tag{6.37}$$

The term $F_\gamma(\sigma_\gamma^\eta) \geq 0$, consequently:

$$\int_\Omega A^{-1} f_\gamma\left(\sigma_\gamma^\eta\right)(\sigma_\gamma^\eta)_D : \left(\sigma_\gamma^\eta - \phi_\gamma^\eta\sigma\right)\,dx \geq -\int_\Omega F_\gamma(\phi_\gamma^\eta\sigma)\,dx.$$

Then with (6.36) we deduce that:

$$a^{-1}(\sigma_\gamma^\eta,\sigma_\gamma^\eta) \leq a^{-1}(\sigma_\gamma^\eta,\phi_\gamma^\eta\sigma) - \int_\Omega u_\gamma^\eta\cdot\left(f - \operatorname{div}(\phi_\gamma^\eta\sigma)\right)\,dx + \frac{1}{\eta}\int_\Omega F_\gamma(\phi_\gamma^\eta\sigma)\,dx. \tag{6.38}$$

Thanks to Young's inequality on $a^{-1}(\sigma_\gamma^\eta,\phi_\gamma^\eta\sigma)$:

$$a^{-1}(\sigma_\gamma^\eta,\sigma_\gamma^\eta) \leq a^{-1}(\phi_\gamma^\eta\sigma,\phi_\gamma^\eta\sigma) - \int_\Omega u_\gamma^\eta\cdot\left(f - \operatorname{div}(\phi_\gamma^\eta\sigma)\right)\,dx + \frac{1}{\eta}\int_\Omega F_\gamma(\phi_\gamma^\eta\sigma)\,dx. \tag{6.39}$$

To conclude:

$$E(\sigma_\gamma^\eta) \leq E\left(\phi_\gamma^\eta\sigma\right) - \int_\Omega u_\gamma^\eta\cdot\left(f - \operatorname{div}(\phi_\gamma^\eta\sigma)\right)\,dx + \frac{1}{\eta}\int_\Omega F_\gamma(\phi_\gamma^\eta\sigma)\,dx. \tag{6.40}$$

We have $E\left(\phi_\gamma^\eta\sigma\right)$ converging to $E\left(\sigma\right)$. Moreover thanks to the Hölder inequality:

$$\int_\Omega \left|u_\gamma^\eta\cdot\left(f - \operatorname{div}(\phi_\gamma^\eta\sigma)\right)\right|\,dx \leq \left\|u_\gamma^\eta\right\|_{L^{\frac{d}{d-1}}}\left\|f - \operatorname{div}(\phi_\gamma^\eta\sigma)\right\|_{L^d}$$

and, thanks to lemma 6.2.5 and the fact that $\left\|f - \operatorname{div}(\phi_\gamma^\eta\sigma)\right\|_{L^d} \to 0$, this term converges to 0.
The next step is to prove that $\dfrac{1}{\eta}\displaystyle\int_\Omega F_\gamma(\phi_\gamma^\eta\sigma)\,dx$ converges to 0. First we remark that $F_\gamma(\phi_\gamma^\eta\sigma) = 0$ almost everywhere on ω_η since $|\phi_\gamma^\eta\sigma|_D = |\phi_\gamma^\eta||\sigma|_D \leq \dfrac{\sigma_c}{\gamma+1}$ which implies $1 - \dfrac{\sigma_c}{|\phi_\gamma^\eta\sigma|_D} \leq -\gamma$.

$$\begin{aligned} 0 \leq \int_\Omega F_\gamma(\phi_\gamma^\eta\sigma)\,dx &= \int_{\Omega\setminus\omega_\eta}\int_{-\gamma}^{1-\frac{\sigma_c}{|\phi_\gamma^\eta\sigma|_D}} \frac{f_\gamma(t)\sigma_c^2}{(1-t)^3}\,dt\,dx \\ &\leq \int_{\Omega\setminus\omega_\eta}\int_{-\gamma}^{0} \frac{f_\gamma(t)\sigma_c^2}{(1-t)^3}\,dt\,dx \end{aligned} \tag{6.41}$$

thanks to the positivity of the integrand and that $\sigma \in K(\Omega)$. Moreover $t \to f_\gamma(t)$ and $t \to \dfrac{1}{(1-t)^3}$ are increasing:

$$\begin{aligned} \int_\Omega F_\gamma(\phi_\gamma^\eta\sigma)\,dx &\leq \int_{\Omega\setminus\omega_\eta} \gamma f_\gamma(0)\sigma_c^2\,dx \\ &\leq \eta\gamma f_\gamma(0)\sigma_c^2 \end{aligned} \tag{6.42}$$

using for the last inequality the definition of ω_η and the smoothness of Ω (at least C^2, see [179] theorem 8.24 for the calculation of the volume of a tubular neigbourhood). As $f_\gamma(0) \to 0$ when $\gamma \to 0$, we have $\displaystyle\int_\Omega F_\gamma(\phi_\gamma^\eta\sigma)\,dx \to 0$ when $(\gamma,\eta) \to 0$.
As E is convex l.s.c. we have:

$$E(\tilde\sigma) \leq \liminf_{l\to\infty} E(\sigma_{\gamma_l}^{\eta_l}) \leq E(\sigma). \tag{6.43}$$

We need to prove that $\tilde\sigma \in K(\Omega)\cap S(f,g)$. The fact that $\tilde\sigma \in S(f,g)$ is straightforward using the first equality in (6.6) and taking the limit:

$$\int_\Omega \tilde\sigma : e(v)\,dx = \int_\Omega f\cdot v\,dx + \int_{\Gamma_N} g\cdot v\,ds \tag{6.44}$$

Applying the Green formula gives the result.
The fact that $\tilde\sigma \in K(\Omega)$ is harder to prove. Thanks to (6.13) we have:

$$\int_\Omega F_\gamma(\sigma_\gamma^\eta)\,dx \leq \eta C_3. \tag{6.45}$$

Using that $F_\gamma(\sigma_\gamma^\eta) \geq F_0(\sigma_\gamma^\eta)$, the convexity of F_0 and the fact that it is l.s.c. gives:

$$F_0(\tilde\sigma) \leq \liminf_{l\to\infty} F_0(\sigma_\gamma^\eta) \leq \liminf_{l\to\infty} F_\gamma(\sigma_\gamma^\eta) \tag{6.46}$$

So:

$$\int_\Omega F_0(\tilde{\sigma})\,dx \leq \int_\Omega \liminf_{l\to\infty} F_\gamma(\sigma_\gamma^\eta)\,dx \leq \liminf_{l\to\infty} \int_\Omega F_\gamma(\sigma_\gamma^\eta)\,dx = 0. \tag{6.47}$$

As F_0 is positive this implies that $F_0(\tilde{\sigma}) = 0$ almost everywhere, which implies that $\tilde{\sigma} \leq \sigma_c$ almost everywhere: $\tilde{\sigma} \in K(\Omega)$.
Yet the solution of the Hencky model σ is unique so $\tilde{\sigma} = \sigma$. But as the limit is unique it is the whole sequence σ_γ^η which weakly converges to σ. Moreover thanks to (6.43) we have:

$$\lim_{(\eta,\gamma)\to 0} a^{-1}(\sigma_\gamma^\eta, \sigma_\gamma^\eta) = a^{-1}(\sigma,\sigma),$$

which implies that $a^{-1}(\sigma - \sigma_\gamma^\eta, \sigma - \sigma_\gamma^\eta) \to 0$ and with the coercivity of a^{-1} the strong convergence in $L^2_S(\Omega)^{d\times d}$.
Thanks to (6.33) and (6.32) we have $\|u_\gamma^\eta\|_{BD}$ which is bounded, since $L^{\frac{d}{d-1}}(\Omega)^d \subset L^1(\Omega)^d$ and $\|e(u)\|_{M_1} \leq \|e(u)\|_{L_1}$. So using (3.4) in chapter II section 3 in [283] gives the existence of a subsequence $u_{\gamma_l}^{\eta_l}$ which weakly converges to $\tilde{u} \in BD(\Omega)$.
Thanks to (6.33) and to the fact that $BD(\Omega) \subset L^{\frac{d}{d-1}}(\Omega)^d$ (continuously) we can also take this subsequence to weakly converge to $\tilde{u} \in L^{\frac{d}{d-1}}(\Omega)^d$.
We take $\tau \in K(\Omega) \cap \Sigma_{\text{div}}(g)$ and note $\tau_\gamma^\eta = \phi_\gamma^\eta \tau$. We test the second equality in (6.6) with $\left(\sigma_{\gamma_l}^{\eta_l} - \tau_\gamma^\eta\right)$:

$$a^{-1}\left(\sigma_\gamma^\eta, \sigma_{\gamma_l}^{\eta_l} - \tau_{\gamma_l}^{\eta_l}\right) + \frac{1}{\eta}\int_\Omega A^{-1} f_\gamma\left(1 - \frac{\sigma_c}{|\sigma_\gamma^\eta|_D}\right)(\sigma_\gamma^\eta)_D : \left(\sigma_{\gamma_l}^{\eta_l} - \tau_{\gamma_l}^{\eta_l}\right) = -\int_\Omega u_\gamma^\eta \cdot \text{div}\left(\sigma_{\gamma_l}^{\eta_l} - \tau_{\gamma_l}^{\eta_l}\right)\,dx. \tag{6.48}$$

Using the usual convexity result for F_γ we get:

$$\int_\Omega F_\gamma(\sigma_\gamma^\eta) - F_\gamma(\tau_\gamma^\eta)\,dx \leq \int_\Omega A^{-1} f_\gamma\left(\sigma_\gamma^\eta\right)(\sigma_\gamma^\eta)_D : \left(\sigma_\gamma^\eta - \tau_\gamma^\eta\right)\,dx.$$

and $\int_\Omega F_\gamma(\sigma_\gamma^\eta)\,dx \geq 0$ yields:

$$-\int_\Omega u_\gamma^\eta \cdot f - \text{div}\left(\tau_\gamma^\eta\right)\,dx \leq a^{-1}\left(\sigma_\gamma^\eta, \tau_\gamma^\eta - \sigma_{\gamma_l}^{\eta_l}\right) + \frac{1}{2\mu\eta}\int_\Omega F_\gamma(\tau_\gamma^\eta)\,dx. \tag{6.49}$$

Then $\frac{1}{\eta}\int_\Omega F_\gamma(\tau_\gamma^\eta)\,dx$ converges to 0 which can be proven as in (6.42). It remains to pass to the limit in the (6.49).
We use the fact that $\tau_\gamma^\eta \to \tau$ strongly in $H_s(\text{div}, \Omega, d)$ to state that: for every $\tau \in K(\Omega) \cap \Sigma_{\text{div}}(g)$

$$-\int_\Omega \tilde{u} \cdot (f - \text{div}\tau)\,dx \leq a^{-1}(\sigma, \tau - \sigma). \tag{6.50}$$

This last inequality implies that $\tilde{u} \in BD(\Omega)$ is solution of the Hencky problem. □

6.2.2 A second regularisation derived for the Von Mises criterion

Another idea to get a compatible model with shape optimization is to focus on the formulation (4.40), used in numerical applications and address the non smoothness and ill-posedness. So first we introduce the operator:

Definition 6.2.7.

$$T\ :\ u \in H^1_{\Gamma_0}(\Omega)^d \to T(u) \in \left(H^1_{\Gamma_0}(\Omega)^d\right)^*$$

where $T(u)$ is defined for every $v \in H^1_{\Gamma_0}(\Omega)^d$ as:

$$\int_\Omega P_K^{A^{-1}}(Ae(u)) : e(v)\,dx.$$

T is monotone and is not coercive. To gain these two properties and the smoothness, we define the following regularized projection:

$$P_\gamma(\tau) = (1+\gamma)\,\tau - f_\gamma\left(1 - \frac{\sigma_c}{|\tau_D|}\right)\tau_D. \tag{6.51}$$

and the new operator:

Definition 6.2.8.

$$T_\gamma\ :\ u \in H^1_{\Gamma_0}(\Omega)^d \to T_\gamma(u) \in \left(H^1_{\Gamma_0}(\Omega)^d\right)^*$$

where $T_\gamma(u)$ is defined for every $v \in H^1_{\Gamma_0}(\Omega)^d$ as:

$$\int_\Omega P_\gamma(Ae(u)) : e(v)\,dx.$$

The function f_γ in 6.51 can be defined as in (6.3). But basically we only need the chosen function to fulfill the following properties:
We want it to be equal to the max outside $[-\gamma,\gamma]$, to be smooth enough on $\mathbb{R}$, convex, increasing and for $t\in\mathbb{R}^+$, $f_\gamma\left(1-\frac{\sigma_c}{t}\right)$ stays between 0 and 1. We also need $t\in\mathbb{R}^+\to t-tf_\gamma\left(1-\frac{\sigma_c}{t}\right)$ to be increasing and we note that $t\in\mathbb{R}^+\to f_\gamma\left(1-\frac{\sigma_c}{t}\right)$ is decreasing.

Then we have:

$$\sigma = P_\gamma\left(Ae\left(u\right)\right). \tag{6.52}$$

Next we prove the strict monotonicity and the coercivity of T_γ.

Monotonicity

Theorem 6.2.9. *T_γ is a monotone operator.*

Proof. We take u and v in $H^1_{\Gamma_0}(\Omega)^d$.

$$\begin{aligned}
&\left(P_\gamma\left(Ae\left(v\right)\right)-P_\gamma\left(Ae\left(u\right)\right),e\left(v-u\right)\right)_{L^2}-\gamma\left(Ae\left(v-u\right),e\left(v-u\right)\right)_{L^2}\\
&=\left(Ae\left(v-u\right),e\left(v-u\right)\right)_{L^2}\\
&-\left(f_\gamma\left(1-\frac{\sigma_c}{|\left[Ae\left(v\right)\right]_D|}\right)\left[Ae\left(v\right)\right]_D-f_\gamma\left(1-\frac{\sigma_c}{|\left[Ae\left(u\right)\right]_D|}\right)\left[Ae\left(u\right)\right]_D,e\left(v-u\right)\right)_{L^2}\\
&=\left(\left[Ae\left(v-u\right)\right]_D,\left[e\left(v-u\right)\right]_D\right)_{L^2}+\left(\left[Ae\left(v-u\right)\right]_{D^\perp},\left[e\left(v-u\right)\right]_{D^\perp}\right)_{L^2}\\
&-\left(f_\gamma\left(1-\frac{\sigma_c}{|\left[Ae\left(v\right)\right]_D|}\right)\left[Ae\left(v\right)\right]_D-f_\gamma\left(1-\frac{\sigma_c}{|\left[Ae\left(u\right)\right]_D|}\right)\left[Ae\left(u\right)\right]_D,e\left(v-u\right)\right)_{L^2}\\
&=\left(\left[Ae\left(v-u\right)\right]_{D^\perp},\left[e\left(v-u\right)\right]_{D^\perp}\right)_{L^2}+\left(\left(1-f_\gamma\left(1-\frac{\sigma_c}{|\left[Ae\left(v\right)\right]_D|}\right)\right)\left[Ae\left(v\right)\right]_D,\left[e\left(v-u\right)\right]_D\right)_{L^2}\\
&-\left(\left(1-f_\gamma\left(1-\frac{\sigma_c}{|\left[Ae\left(u\right)\right]_D|}\right)\right)\left[Ae\left(u\right)\right]_D,\left[e\left(v-u\right)\right]_D\right)_{L^2}
\end{aligned} \tag{6.53}$$

we will note for $w\in H^1_{\Gamma_0}(\Omega)^d$, $p_\gamma\left(w\right)=1-f_\gamma\left(1-\frac{\sigma_c}{|\left[Ae\left(w\right)\right]_D|}\right)\geq 0$. Then we rewrite (6.53):

$$\begin{aligned}
&\left(P_\gamma\left(Ae\left(v\right)\right)-P_\gamma\left(Ae\left(u\right)\right),e\left(v-u\right)\right)_{L^2}-\gamma\left(Ae\left(v-u\right),e\left(v-u\right)\right)_{L^2}\\
&=\left(\left[Ae\left(v-u\right)\right]_{D^\perp},\left[e\left(v-u\right)\right]_{D^\perp}\right)_{L^2}+\left(p_\gamma\left(v\right)\left[Ae\left(v\right)\right]_D,\left[e\left(v-u\right)\right]_D\right)_{L^2}\\
&-\left(p_\gamma\left(u\right)\left[Ae\left(u\right)\right]_D,\left[e\left(v-u\right)\right]_D\right)_{L^2}
\end{aligned} \tag{6.54}$$

Remarking that $\left[A\tau\right]_{D^\perp}:\left[\tau'\right]_{D^\perp}=\frac{1}{d}\left(2\mu+d\lambda\right)\left(Tr\left(\tau\right)^2\right)$ the first term is non negative. We investigate next the sign of

$$p_\gamma\left(v\right)\left[Ae\left(v\right)\right]_D:\left[e\left(v-u\right)\right]_D-p_\gamma\left(u\right)\left[Ae\left(u\right)\right]_D:\left[e\left(v-u\right)\right]_D \tag{6.55}$$

for $x\in\Omega$, which will be omitted in the following. We will use the fact that

$$\left[A\tau\right]_D:\left[\tau'\right]_D=2\mu\left[\tau_D\right]:\left[\tau'\right]_D. \tag{6.56}$$

1. First we suppose that $p_\gamma\left(v\right)\geq p_\gamma\left(u\right)$. Then there are three possible cases:
   a) $\left[Ae\left(v\right)\right]_D:\left[e\left(v-u\right)\right]_D\geq 0$
   b) $\left[Ae\left(v\right)\right]_D:\left[e\left(v-u\right)\right]_D\leq 0$ and $\left[Ae\left(u\right)\right]_D:\left[e\left(v-u\right)\right]_D\geq 0$
   c) $\left[Ae\left(v\right)\right]_D:\left[e\left(v-u\right)\right]_D\leq 0$ and $\left[Ae\left(u\right)\right]_D:\left[e\left(v-u\right)\right]_D\leq 0$

   a) If $\left[Ae\left(v\right)\right]_D:\left[e\left(v-u\right)\right]_D\geq 0$ then $p_\gamma\left(v\right)\left[Ae\left(v\right)\right]_D:\left[e\left(v-u\right)\right]_D\geq p_\gamma\left(u\right)\left[Ae\left(v\right)\right]_D:\left[e\left(v-u\right)\right]_D$ and

$$\begin{aligned}
&p_\gamma\left(v\right)\left[Ae\left(v\right)\right]_D:\left[e\left(v-u\right)\right]_D-p_\gamma\left(u\right)\left[Ae\left(u\right)\right]_D:\left[e\left(v-u\right)\right]_D\\
&\geq p_\gamma\left(u\right)\left(\left[Ae\left(v\right)\right]_D:\left[e\left(v-u\right)\right]_D-\left[Ae\left(u\right)\right]_D:\left[e\left(v-u\right)\right]_D\right)\\
&\geq 0
\end{aligned} \tag{6.57}$$

   b) If $\left[Ae\left(v\right)\right]_D:\left[e\left(v-u\right)\right]_D\leq 0$ and $\left[Ae\left(u\right)\right]_D:\left[e\left(v-u\right)\right]_D\geq 0$ then $p_\gamma\left(u\right)\left[Ae\left(u\right)\right]_D:\left[e\left(v-u\right)\right]_D\leq p_\gamma\left(v\right)\left[Ae\left(u\right)\right]_D:\left[e\left(v-u\right)\right]_D$. It follows that:

$$-p_\gamma\left(u\right)\left[Ae\left(u\right)\right]_D:\left[e\left(v-u\right)\right]_D\geq -p_\gamma\left(v\right)\left[Ae\left(u\right)\right]_D:\left[e\left(v-u\right)\right]_D \tag{6.58}$$

   and:

$$\begin{aligned}
&p_\gamma\left(v\right)\left[Ae\left(v\right)\right]_D:\left[e\left(v-u\right)\right]_D-p_\gamma\left(u\right)\left[Ae\left(u\right)\right]_D:\left[e\left(v-u\right)\right]_D\\
&\geq p_\gamma\left(v\right)\left(\left[Ae\left(v\right)\right]_D:\left[e\left(v-u\right)\right]_D-\left[Ae\left(u\right)\right]_D:\left[e\left(v-u\right)\right]_D\right)\\
&\geq 0
\end{aligned} \tag{6.59}$$

c) If $[Ae(v)]_D : [e(v-u)]_D \leq 0$ and $[Ae(u)]_D : [e(v-u)]_D \leq 0$ we can rewrite (6.55), using (6.56):

$$p_\gamma(v)\left(2\mu|\,[e(v)]_D\,|^2 - [Ae(v)]_D : [e(u)]_D\right) - p_\gamma(u)\left([Ae(v)]_D : [e(u)]_D - 2\mu|\,[e(u)]_D\,|^2\right) \tag{6.60}$$

Using again (6.56):

$$p_\gamma(v)\,2\mu\left(|\,[e(v)]_D\,|^2 - [e(v)]_D : [e(u)]_D\right) - p_\gamma(u)\,2\mu\left([e(v)]_D : [e(u)]_D - |\,[e(u)]_D\,|^2\right) \tag{6.61}$$

We develop and use Cauchy Schwarz inequality:

$$\begin{array}{l} 2\mu\left[p_\gamma(v)\,|\,[e(v)]_D\,|^2 + p_\gamma(u)\,|\,[e(u)]_D\,|^2 - p_\gamma(v)\,[e(v)]_D : [e(u)]_D - p_\gamma(u)\,[e(v)]_D : [e(u)]_D\right] \\ \geq 2\mu\left[p_\gamma(v)\,|\,[e(v)]_D\,|^2 + p_\gamma(u)\,|\,[e(u)]_D\,|^2 - p_\gamma(v)\,|\,[e(v)]_D\,||\,[e(u)]_D\,|\right. \\ \left. -p_\gamma(u)\,|\,[e(v)]_D\,||\,[e(u)]_D\,|\right] \\ \geq 2\mu\left[p_\gamma(v)\,|\,[e(v)]_D\,|\left(|\,[e(v)]_D\,| - |\,[e(u)]_D\,|\right) + p_\gamma(u)\,|\,[e(u)]_D\,|\left(|\,[e(u)]_D\,| - |\,[e(v)]_D\,|\right)\right] \\ \geq 2\mu\left(|\,[e(u)]_D\,| - |\,[e(v)]_D\,|\right)\left(p_\gamma(u)\,|\,[e(u)]_D\,| - p_\gamma(v)\,|\,[e(v)]_D\,|\right) \end{array} \tag{6.62}$$

Since $t \in \mathbb{R}^+ \to 1 - f_\gamma\left(1 - \frac{\sigma_c}{t}\right)$ is decreasing, $p_\gamma(v) \geq p_\gamma(u)$ meaning that

$$1 - f_\gamma\left(1 - \frac{\sigma_c}{|\,[Ae(v)]_D\,|}\right) > 1 - f_\gamma\left(1 - \frac{\sigma_c}{|\,[Ae(u)]_D\,|}\right) \tag{6.63}$$

implies that $|\,[e(u)]_D\,| \geq |\,[e(v)]_D\,|$ (with $|\,[Ae(\cdot)]_D\,|$ playing the role of t and with (6.56)). As $t \in \mathbb{R}^+ \to t - tf_\gamma\left(1 - \frac{\sigma_c}{t}\right)$ is increasing,

$$2\mu\left(p_\gamma(u)\,|\,[e(u)]_D\,| - p_\gamma(v)\,|\,[e(v)]_D\,|\right) \geq 0$$

with $2\mu|\,[e(\cdot)]_D\,|$ playing the role of t and finally:

$$p_\gamma(v)\,[Ae(v)]_D : [e(v-u)]_D - p_\gamma(u)\,[Ae(u)]_D : [e(v-u)]_D \geq 0 \tag{6.64}$$

2. Eventually, we suppose that $p_\gamma(v) \leq p_\gamma(u)$ which implies

$$|\,[e(u)]_D\,| \leq |\,[e(v)]_D\,|.$$

Thanks to Cauchy-Schwarz inequality and (6.56):

$$p_\gamma(v)\,[Ae(v)]_D : [e(v-u)]_D \geq 2\mu p_\gamma(v)\left(|\,[e(v)]_D\,|^2 - |\,[e(v)]_D\,||\,[e(u)]_D\,|\right) \tag{6.65}$$

$$p_\gamma(u)\,[Ae(u)]_D : [e(v-u)]_D \leq 2\mu p_\gamma(u)\left(|\,[e(v)]_D\,||\,[e(u)]_D\,| - |\,[e(u)]_D\,|^2\right) \tag{6.66}$$

It follows that:

$$\begin{array}{l} p_\gamma(v)\,[Ae(v)]_D : [e(v-u)]_D - p_\gamma(u)\,[Ae(u)]_D : [e(v-u)]_D \\ \geq 2\mu\left[p_\gamma(v)\left(|\,[e(v)]_D\,|^2 - |\,[e(v)]_D\,||\,[e(u)]_D\,|\right) - p_\gamma(u)\left(|\,[e(v)]_D\,||\,[e(u)]_D\,| - |\,[e(u)]_D\,|^2\right)\right] \\ \geq 2\mu\left[p_\gamma(v)\,|\,[e(v)]_D\,|\left(|\,[e(v)]_D\,| - |\,[e(u)]_D\,|\right) - p_\gamma(u)\,|\,[e(u)]_D\,|\left(|\,[e(v)]_D\,| - |\,[e(u)]_D\,|\right)\right] \\ \geq 2\mu\left(p_\gamma(v)\,|\,[e(v)]_D\,| - p_\gamma(u)\,|\,[e(u)]_D\,|\right)\left(|\,[e(v)]_D\,| - |\,[e(u)]_D\,|\right) \\ \geq 0 \end{array} \tag{6.67}$$

As $|\,[e(u)]_D\,| \leq |\,[e(v)]_D\,|$ and since $t \in \mathbb{R}^+ \to t - tf_\gamma\left(1 - \frac{\sigma_c}{t}\right)$ is increasing,

$$2\mu\left(p_\gamma(v)\,|\,[e(v)]_D\,| - p_\gamma(u)\,|\,[e(u)]_D\,|\right) \geq 0$$

with $2\mu|\,[e(\cdot)]_D\,|$ playing the role of t.

So for every $x \in \Omega$, (6.55) is non negative and therefore the operator T is strictly monotone. □

Coercivity

Theorem 6.2.10. *T_γ is coercive.*

Proof. The calculations give:

$$\begin{array}{rl} \left(P_\gamma(Ae(v)), e(v)\right)_{L^2} &= (1+\gamma)\left(Ae(v), e(v)\right)_{L^2} - \left(f_\gamma\left(1 - \frac{\sigma_c}{|\,[Ae(v)]_D\,|}\right)[Ae(v)]_D, e(v)\right)_{L^2} \\ &\geq (1+\gamma)\left(Ae(v), e(v)\right)_{L^2} - \left([Ae(v)]_D, [e(v)]_D\right)_{L^2} \\ &= \gamma\left(Ae(v), e(v)\right)_{L^2} + \left([Ae(v)]_{D^\perp}, [e(v)]_{D^\perp}\right)_{L^2} \end{array} \tag{6.68}$$

which implies the coercivity. □

Existence and uniqueness

Lemma 6.2.11. *T is hemicontinuous.*

Proof. We need to prove that for every $(u,v) \in (H^1_{\Gamma_0}(\Omega)^d)^2$ the function from $\mathbb{R}$ to $\mathbb{R}$:

$$t \to \left(P_\gamma\left(Ae\left(u\right)+tAe\left(v\right)\right),e\left(v\right)\right)_{L^2} \tag{6.69}$$

is continuous. Rewritting the regularized projection:

$$\begin{aligned}\left(P_\gamma\left(Ae\left(u\right)+tAe\left(v\right)\right),e\left(v\right)\right)_{L^2} =& \left(1+\gamma\right)\left(Ae\left(u\right)+tAe\left(v\right),e\left(v\right)\right)_{L^2}\\ &-\left(f_\gamma\left(1-\frac{\sigma_c}{|\left[Ae\left(u+tv\right)\right]_D|}\right)\left[Ae\left(u+tv\right)\right]_D,e\left(v\right)\right)_{L^2}\end{aligned} \tag{6.70}$$

as f_γ is Lipschitz, the hemicontinuity follows. □

Lemma 6.2.12. *T is a bounded operator.*

Proof. We need to prove that for u in a bounded subset of $H^1_{\Gamma_0}(\Omega)^d$, $T\left(u\right)$ stays in a bounded subset of $\left(H^1_{\Gamma_0}(\Omega)^d\right)^*$:

$$\left\|T\left(u\right)\right\| = \sup_{v\in H^1_{\Gamma_0}(\Omega)^d}\frac{\left\langle T\left(u\right),v\right\rangle}{\left\|v\right\|_{H^1_{\Gamma_0}(\Omega)^d}} \tag{6.71}$$

As

$$\begin{aligned}\left\|T\left(u\right)\right\| &\leq \left\|P_\gamma\left(Ae\left(u\right)\right)\right\|_{L^2}\\ &\leq \left(1+\gamma\right)\left\|Ae\left(u\right)\right\|_{L^2}+\left\|f_\gamma\left(1-\frac{\sigma_c}{|\left[Ae\left(u\right)\right]_D|}\right)\left[Ae\left(u\right)\right]_D\right\|_{L^2}\\ &\leq \left(1+\gamma\right)\left\|Ae\left(u\right)\right\|_{L^2}+\left\|\left[Ae\left(u\right)\right]_D\right\|_{L^2}\end{aligned} \tag{6.72}$$

if u stays in a bounded subset of $H^1_{\Gamma_0}(\Omega)^d$, so do $T\left(u\right)$ in $\left(H^1_{\Gamma_0}(\Omega)^d\right)^*$. □

Theorem 6.2.13. *The regularised problem: find $u \in H^1_{\Gamma_0}(\Omega)^d$ such that,*

$$\int_\Omega P_\gamma\left(Ae\left(u\right)\right):\epsilon(v)\,dx = \int_\Omega f\cdot v\,dx+\int_{\Gamma_N} g\cdot v\,ds\ \forall v\in H^1_{\Gamma_0}(\Omega)^d, \tag{6.73}$$

admits a unique solution. The associated regularised stress tensor σ is defined as:

$$\sigma = P_\gamma\left(Ae\left(u\right)\right).$$

Proof. Thanks to the strict monotonicity, the coercivity, the hemicontinuity and the boundness, we apply a classical theorem 2.2.9 which ensures the existence and uniqueness of a solution. □

Remark 6.2.14. *Thanks to the coercivity of the operator we could also have used theorem* 1.1 *in [139], the assumptions being satisfied (the Lipschitz condition* 1.6 *in this article is clearly true for the operator $P_\gamma\left(A\cdot\right)$. In fact, this theorem will be used in the next section to study the differentiability of the model with respect to the shape as it gives an additional regularity result. The aim of the proof given here is, first, to show why the projection operator or the simple regularized projection P^γ_K are not strictly monotone and coercive and, secondly, to explain what was the idea behind the definition of the operator P_γ.*

Convergence to the static perfect plasticity case

We note u^2_γ and σ^2_γ the solutions of the regularized problem (6.73).

Theorem 6.2.15. *Under the safe-load condition* (4.52) *and with $f \in L^d(\Omega)^d$ and $g \in C^0(\Gamma_N)^d$, the solution u^2_γ converges weakly, up to a subsequence, in $L^{\frac{d}{d-1}}(\Omega,\mathbb{R}^d)$ and weakly in $BD(\Omega)$ to a displacement u solution to the Hencky model.*

Proof. The idea is to use the proof done for Perzyna penalisation. We take the problem:

$$\begin{cases}\displaystyle\int_\Omega \sigma^3_\gamma : e(v)\,dx = \frac{1}{1+\gamma}\left(\int_\Omega f\cdot v\,dx+\int_{\Gamma_N} g\cdot v\,ds\right)\ \forall v\in H^1_{\Gamma_0}(\Omega)^d\\ \displaystyle\int_\Omega A^{-1}\sigma^3_\gamma:\tau\,dx+\int_\Omega A^{-1}\left(\sigma^3_\gamma-P^{A^{-1}}_K(\sigma^3_\gamma)\right):\tau = \int_\Omega e(u^3_\gamma):\tau\,dx\ \forall\tau\in K.\end{cases} \tag{6.74}$$

which can be simplied into a variational equation:

$$\int_\Omega \sigma^3_\gamma : e(v)\,dx = \frac{1}{1+\gamma}\left(\int_\Omega f\cdot v\,dx+\int_{\Gamma_N} g\cdot v\,ds\right)\ \forall v\in H^1_{\Gamma_0}(\Omega)^d \tag{6.75}$$

with

$$\sigma_\gamma^3 = Ae(u) - \frac{1}{1+\gamma} f_\gamma \left(1 - \frac{\sigma_c}{|Ae(u)|_D}\right) (Ae(u))_D = P_\gamma^2 (Ae(u)).$$

We note that the variational equation (6.74) is in fact equivalent to solve:

$$\int_\Omega P_\gamma^2 (Ae(u)) : e(v)\, dx = \frac{1}{1+\gamma} \left(\int_\Omega f \cdot v\, dx + \int_{\Gamma_N} g \cdot v\, ds \right) \ \forall v \in H^1_{\Gamma_0}(\Omega)^d. \tag{6.76}$$

Yet $(1+\gamma)P_\gamma^2(\tau) = P_\gamma(\tau)$ for every $\tau \in L^2_S(\Omega)^{d\times d}$, so $u_\gamma^3 = u_\gamma^2$. We need to prove that, up to a subsequence, u_γ^3 converges weakly in $L^{\frac{d}{d-1}}(\Omega, \mathbb{R}^d)$ and weakly in $BD(\Omega)$ to a displacement u solution of the Hencky model. We adapt the proof of theorem 6.2.6, since the function f and g are now replaced by $\frac{1}{1+\gamma} f$ and $\frac{1}{1+\gamma} g$. In fact lemmas, 6.2.4, 6.2.5 are still valid since we did not use the first equation in (6.74) and the safe load condition. The lemma 6.2.3 is also still true. Taking $\overline{\sigma}$ given by the safe load condition, we define $\overline{\sigma}_\gamma = \frac{1}{1+\gamma}\overline{\sigma}$. We have to remake the proof of lemma 6.2.3 changing $\overline{\sigma}$ into $\overline{\sigma}_\gamma$. First we have:

$$|\overline{\sigma}_\gamma|_D - \sigma_c \leq -\frac{\delta + \sigma_c \gamma}{1+\gamma}$$

which implies that:

$$1 - \frac{\sigma_c}{|\overline{\sigma}_\gamma|_D} \leq -\frac{\delta + \sigma_c\gamma}{\sigma_c - \delta} \leq \frac{\delta}{\sigma_c - \delta}$$

So we still have (for γ small enough) $F_\gamma(\overline{\sigma}_\gamma) = 0$. Everything is correct until (6.19) which we rewrite in our framework:

$$C_0 \left\| \sigma_\gamma^\eta - \overline{\sigma}_\gamma \right\|_{L^2}^2 \leq C_c \left\| \overline{\sigma}_\gamma \right\|_{L^2} \left\| \sigma_\gamma^\eta - \overline{\sigma}_\gamma \right\|_{L^2}. \tag{6.77}$$

As we have

$$\left\| \overline{\sigma}_\gamma \right\|_{L^2} = \frac{1}{1+\gamma} \left\| \overline{\sigma} \right\|_{L^2} \leq \left\| \overline{\sigma} \right\|_{L^2}$$

and $\left\| \overline{\sigma} - \overline{\sigma}_\gamma \right\|_{L^2} = \frac{\gamma}{1+\gamma} \left\| \overline{\sigma} \right\|_{L^2}$ using the fact that γ is taken small enough and a simple triangular inequality leads to $\left\| \sigma_\gamma^\eta - \overline{\sigma} \right\|_{L^2}$ is smaller than a constant. The remaining of the proof is then the same, the computation of (6.24) being valid, since taking χ such that $\|\chi\|_{L^\infty} \leq \frac{\delta}{2}$, :

$$|\xi + \overline{\sigma}_\gamma|_D - \sigma_c \leq \frac{\delta}{2} - \frac{\delta + \sigma_c\gamma}{1+\gamma}$$

which is negative as soon as $\gamma < 1$.
We pass to the convergence of σ_γ^3 and u_γ^3. We focus on adapting the proof of theorem 6.2.6. In our case $\gamma = \eta$ and the proof of the convergence of σ_γ^3 and u_γ^3 is simpler than in 6.2.6 since, instead of taking $\phi_\gamma^\eta \sigma$ and $\phi_\gamma^\eta \tau$, it suffices to take $\frac{1}{1+\eta}\sigma$ from (6.36) and $\frac{1}{1+\eta}\tau$ from (6.48). Indeed for (6.36) it enables to erase the terms $-\int_\Omega u_\gamma^\eta \cdot \left(\mathrm{div}(\sigma_\gamma^3) - \frac{1}{1+\eta}\mathrm{div}(\sigma) \right) dx = 0$ and $F_\gamma(\frac{1}{1+\eta}\sigma) = 0$. For (6.48), we have $F_\gamma(\frac{1}{1+\eta}\tau) = 0$.
At this point, we make the remark that if we would have defined the operator

$$P_\gamma^\eta(\tau) = (1+\eta)\,\tau - f_\gamma \left(1 - \frac{\sigma_c}{|\tau_D|}\right) \tau_D,$$

instead of P_γ, the result, proved here, is still true but for the proof of the convergence we need to use $\frac{1}{1+\eta}\phi_\gamma^\eta \sigma$ and $\frac{1}{1+\eta}\phi_\gamma^\eta \tau$ with $\phi_\gamma^\eta = \frac{1+\eta}{1+\gamma}$ on ω_η (instead of $\frac{1}{1+\gamma}$).
We conclude that u_γ^3 converges weakly in $L^{\frac{d}{d-1}}(\Omega, \mathbb{R}^d)$ and weakly in $BD(\Omega)$ to a displacement u solution of the Hencky model and that σ_γ^3 converges strongly in $L^2_S(\Omega)^{d\times d}$ to σ, the constraint tensor solution of the Hencky model. It is consequently also the case for u_γ^2. □

Theorem 6.2.16. *Under the safe-load condition* (4.52) *and with $f \in L^d(\Omega)^d$ and $g \in C^0(\Gamma_N)^d$, the solution σ_γ^2 converges, as γ goes to 0, strongly in $L^2_S(\Omega)^{d\times d}$ to σ, the stress tensor solution of the Hencky model.*

Proof. The proof of theorem 6.2.15 gives that $(1+\gamma)\sigma_\gamma^3 = \sigma_\gamma^2$ almost everywhere and this implies that:

$$\left\| \sigma_\gamma^3 - \sigma_\gamma^2 \right\|_{L^2} \leq \gamma \left\| \sigma_\gamma^3 \right\|_{L^2}.$$

As the convergence of σ_γ^3 is strong in $L^2_S(\Omega)^{d\times d}$, $\left\| \sigma_\gamma^3 \right\|_{L^2}$ is bounded and the result is proved. □

Remark 6.2.17. *Remark that the proof of theorem 6.2.15 gives also a way to prove the existence and uniqueness of the solution of the problem* (6.73).

Penalization	Maximal value of the Von Mises criterion
$\eta = 10^{-1}$	586.7835
$\eta = 10^{-2}$	412.68502
$\eta = 10^{-3}$	373.15242
$\eta = 10^{-4}$	368.0169
$\eta = 10^{-5}$	367.48303
$\eta = 10^{-6}$	367.42942
$\eta = 10^{-7}$	367.42406
$\eta = 10^{-8}$	367.42352
$\eta = 10^{-9}$	367.42347
$\eta = 10^{-10}$	367.42346

Table 6.1: Maximal value of the Von Mises criterion with respect to the penalization for the second regularized problem, corresponding to the example of section 6.2.2

Penalization	error on σ	error on u
$\eta = 10^{-1}$	0.0416052	0.0575211
$\eta = 10^{-2}$	0.0166839	0.0213725
$\eta = 10^{-3}$	0.0027445	0.0033636
$\eta = 10^{-4}$	0.0002976	0.0003611
$\eta = 10^{-5}$	0.0000300	0.0000363
$\eta = 10^{-6}$	0.0000030	0.0000036
$\eta = 10^{-7}$	0.0000003	0.0000004
$\eta = 10^{-8}$	3.001D-08	3.630D-08
$\eta = 10^{-9}$	2.985D-09	3.593D-09
$\eta = 10^{-10}$	2.830D-10	3.226D-10

Table 6.2: L^2-error on σ and U with respect to the penalization for the second regularized problem.

Numerical results

We illustrate the solutions given by this model, using the same example as in section 4.5.2. We solve the second regularised problems (6.73) for different penalization parameter values. The results are collated in figure 6.1. We point out that the colour scales are not the same on each figures as the maximal value of the Von Mises depends on the penalisation. As it can be seen on the table 6.1 and the figure 6.2, the maximal value of the Von Mises criterion seems, as expected, to converge to $\sigma_c = 367.42346$ as the penalization tends to zero. The solution (σ, u) also converges as shown in table 6.2.

6.2.3 Conclusion on the two proposed regularisations

For the Von Mises criterion, the two formulations introduced in this section are quite similar. They are tantamount to redefine σ by one of these formulae:

1. for the Perzyna penalisation

$$\sigma = Ae(u) - \frac{1}{1+\eta} f_\gamma \left(1 - \frac{\sigma_c}{|Ae(u)|_D}\right) (Ae(u))_D$$

2. for the second proposition

$$\sigma = (1+\gamma)Ae(u) - f_\gamma \left(1 - \frac{\sigma_c}{|Ae(u)|_D}\right) (Ae(u))_D \,.$$

In each case, the problem reduces to a non-linear variational equation:

$$\int_\Omega \sigma : e(v)\, dx = \int_\Omega f \cdot v\, dx + \int_{\Gamma_N} g \cdot v\, ds \;\forall v \in H^1_{\Gamma_0}(\Omega)^d \tag{6.78}$$

6.3 Derivation and optimization

As far as optimisation is concerned, we need to investigate the differentiability of the operator $\tau \to f_\gamma \left(1 - \frac{\sigma_c}{|\tau|_D}\right)$. As f_γ is a smooth Lipschitz function from $\mathbb{R}$ to $\mathbb{R}$, it is Gateaux differentiable. It has no chance to be Fréchet differentiable from $L^2(\Omega)$ to $L^2(\Omega)$. However, as it is proved for the Perzyna penalisation in [140] it is Fréchet differentiable from

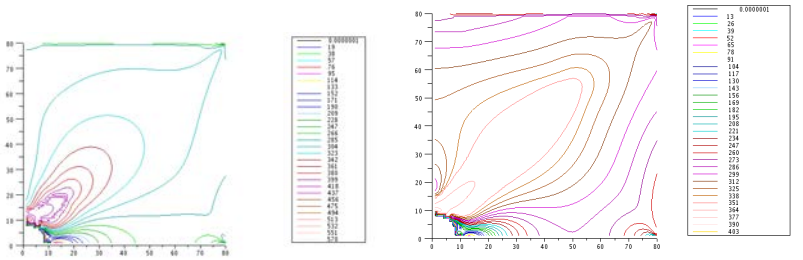

(a) $\eta = 10^{-1}$. (b) $\eta = 10^{-2}$.

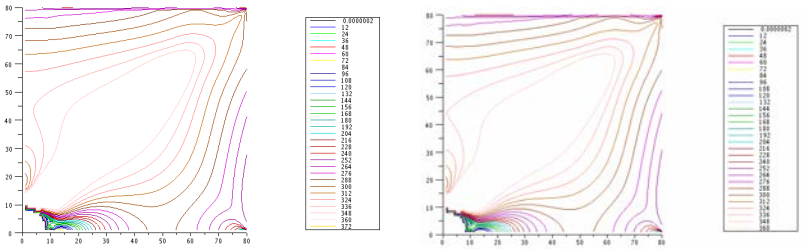

(c) $\eta = 10^{-3}$. (d) $\eta = 10^{-4}$.

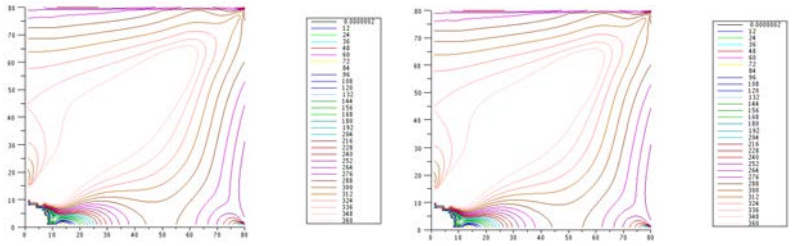

(e) $\eta = 10^{-5}$. (f) $\eta = 10^{-6}$.

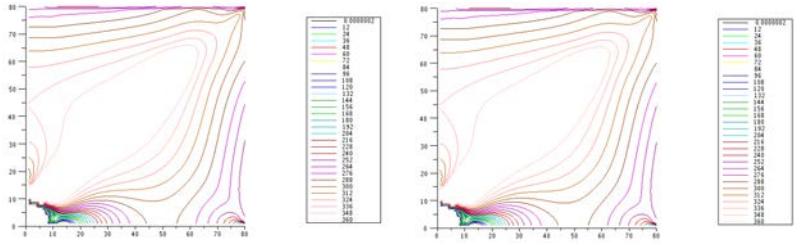

(g) $\eta = 10^{-7}$. (h) $\eta = 10^{-8}$.

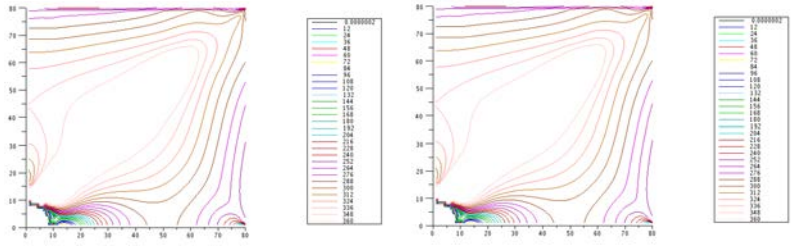

(i) $\eta = 10^{-9}$. (j) $\eta = 10^{-10}$.

Figure 6.1: Results for the second regularisation for different penalization parameters γ. We plot the level sets of the Von Mises criterion.

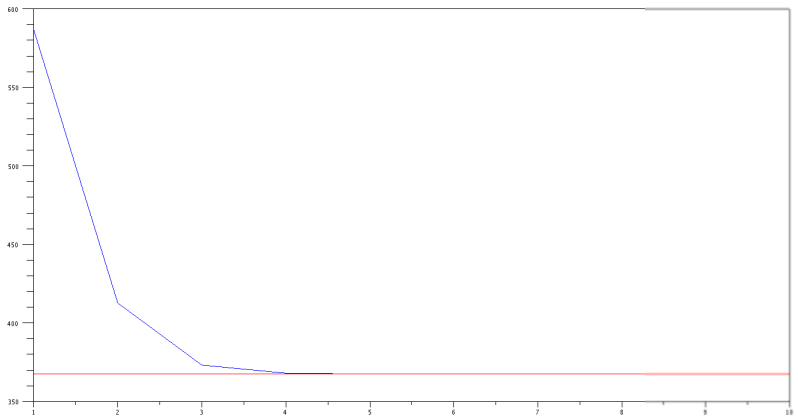

Figure 6.2: The maximal value of the Von Mises criterion with respect to $-log_{10}(\eta)$ for the second regularisation, corresponding to the example of section 6.2.2

$L^{2+\delta}(\Omega)$ to $L^2(\Omega)$ with $\delta > 0$. So we need our solution to be a little smoother than $H^1(\Omega)^d$ and it is the case by applying theorem 1.1 of [139], implying that $u \in W^{1,p}(\Omega)^d$ with $p \in [2, \overline{p}]$ and $\overline{p} = 2 + \delta > 2$. Both regularisations are Fréchet differentiable with respect to u.

6.3.1 Computation of the gradients

We proceed now to the computation of the gradient of a general criterion:

$$J(\Omega, u) = \int_\Omega m(u)\, dx + \int_{\Gamma_m} l(u)\, ds \tag{6.79}$$

where Γ_m will be the part of $\partial\Omega$ allows to move during the optimization process, m and l are smooth functions. We also suppose that, a.e.:

$$|m(u)| \leq C\left(1 + \|u\|^2\right) \tag{6.80}$$

$$|m'(u) \cdot h| \leq C'|u \cdot h| \tag{6.81}$$

and

$$|l(u)| \leq C\left(1 + \|u\|^2\right) \tag{6.82}$$

$$|l'(u) \cdot h| \leq C'|u \cdot h| \tag{6.83}$$

for every $h \in L^2(\Omega)^d$ and $u \in L^2(\Omega)^d$, and with $C > 0$ and $C' > 0$.

Theorem 6.3.1. *Assume that $\Gamma_m \cap \Gamma_0 = \emptyset$, that $f \in H^1(\mathbb{R}^d)^d$ and $g \in H^2(\mathbb{R}^d)^d$ and that u is solution of (6.78). If we denote $J'(\Omega)(\theta)$ the Gateaux derivative of $J(\Omega)$ with respect to Ω in the direction θ. We have:*

$$\begin{aligned} J'(\Omega)(\theta) = &\int_{\Gamma_m} (\theta \cdot n)(m(u) - f \cdot p)\, ds \\ &+ \int_{\Gamma_m} (\theta \cdot n)(Hl(u) + \partial_n l(u)) \\ &- \int_{\Gamma_N \cap \Gamma_m} (\theta \cdot n)(Hp \cdot g + \partial_n (p \cdot g))\, ds \\ &+ \int_{\Gamma_m} (\theta \cdot n)\,(\sigma : e(p)) \end{aligned} \tag{6.84}$$

where $p \in H^1_{\Gamma_0}(\Omega)^d$ is defined as the solution of the following adjoint problem:

$$\begin{aligned} &\alpha \int_\Omega Ae(p) : e(\psi)\, dx - \beta \int_\Omega f_\gamma \left(1 - \frac{\sigma_c}{|Ae(u)|_D}\right) (Ae(p))_D : e(\psi)_D\, dx \\ &- \beta \int_\Omega f'_\gamma \left(1 - \frac{\sigma_c}{|Ae(u)|_D}\right) \frac{\sigma_c}{|Ae(u)|^3_D} Ae(u)_D : e(\psi)_D\ Ae(u)_D : e(p)_D\, dx \\ &= -\int_\Omega m'(u) \cdot \psi\, dx - \int_\Gamma l'(u) \cdot \psi\, ds\ \forall \psi \in H^1_{\Gamma_0}(\Omega)^d \end{aligned} \tag{6.85}$$

with:

- $\alpha = 1$ *and* $\beta = \dfrac{1}{1+\eta}$ *for the Perzyna regularisation,*
- $\alpha = 1+\eta$ *and* $\beta = 1$ *for the second plasticity regularisation*

and H *the mean curvature:* $H = \operatorname{div}(n)$.

Proof. It is possible to rigorously prove the existence of a Lagrangian derivative of u using the same method as in the proof of theorem 5.4.5. We limit ourselves to the application of Céa's method to find the expression of the gradient, noting $u'(\theta)$ the shape derivative of u. Let us introduce the Lagrangian L with v and q in $H^1_{\Gamma_0}(\mathbb{R}^d)^d$:

$$\begin{aligned} L(v,q,\Omega) \quad = \quad & \int_\Omega m(v)\,dx + \int_\Gamma l(v)\,ds + \alpha \int_\Omega Ae(v) : e(q)\,dx \\ & -\beta \int_\Omega f_\gamma \left(1 - \frac{\sigma_c}{|Ae(v)|_D}\right) (Ae(v))_D : e(q)_D\,dx \\ & - \int_\Omega f \cdot q\,dx - \int_{\Gamma_N} g \cdot q\,ds \end{aligned} \tag{6.86}$$

with α and β depending on the model chosen as stated in theorem 6.3.1.
Since Γ_0 is fixed, there is no need of a Lagrangian multiplier for the Dirichlet condition in the Lagrangian: $\Gamma_0 \subset \partial\Omega$ for every $\Omega \in \mathcal{U}_{ad}$. Moreover the functions q and v are in spaces independent of $\Omega \in \mathcal{U}_{ad}$. We note (u,p) a stationarity point of L. The state equation (5.70) can be retrieved by differentiating L with respect to q in the direction $\psi \in H^1_{\Gamma_0}(\mathbb{R}^d)^d$:

$$\langle \partial_q L(u,q,\Omega), \psi \rangle = 0 \ \ \forall \psi \in H^1_{\Gamma_0}(\mathbb{R}^d)^d$$

In the same way the equation solved by p (adjoint problem) can be found by derivating L with respect to v in the direction $\psi \in H^1_{\Gamma_0}(\mathbb{R}^d)^d$:

$$\begin{aligned} \langle \partial_u L, \psi \rangle = & \alpha \int_\Omega Ae(p) : e(\psi)\,dx - \beta \int_\Omega f_\gamma \left(1 - \frac{\sigma_c}{|Ae(u)|_D}\right) (Ae(p))_D : e(\psi)_D\,dx + \int_\Omega m'(u)\cdot\psi\,dx \\ & + \int_\Gamma l'(u)\cdot\psi\,ds - \beta \int_\Omega f'_\gamma \left(1 - \frac{\sigma_c}{|Ae(u)|_D}\right) \frac{\sigma_c}{|Ae(u)|^3_D} Ae(u)_D : e(\psi)_D \ Ae(u)_D : e(p)_D\,dx \end{aligned}$$

and the adjoint problem can be deduced:

$$\langle \partial_u L(u,p,\Omega), \psi \rangle = 0 \ \ \forall \psi \in H^1_{\Gamma_0}(\mathbb{R}^d)$$

which gives (6.85). To find the shape derivative of $J(\Omega)$, we remark that:

$$J(\Omega) = L(u(\Omega), q, \Omega)$$

and differentiate the L with respect to the shape in the direction θ which gives:

$$\begin{aligned} J'(\Omega,\theta) &= L'(\Omega, u_\Omega, q, n_\Omega; \theta) \\ &= \partial_\Omega L(\Omega, u_\Omega, q; \theta) + \partial_u L(\Omega, u_\Omega, q; u'(\theta)) \end{aligned} \tag{6.87}$$

But as $u'(\theta)$ is in $H^1_{\Gamma_0}(\Omega)^d$, taking $q = p(\Omega)$ leads to:

$$\partial_u L(\Omega, u_\Omega, p(\Omega), n_\Omega; u'(\theta)) = 0.$$

Consequently:

$$J'(\Omega,\theta) = L'(\Omega, u_\Omega, p_\Omega; \theta) = \partial_\Omega L(\Omega, u_\Omega, p_\Omega; \theta) \tag{6.88}$$

By using the formulae of theorem 1.3.4, we recover (6.84). □

6.3.2 Criteria

For the numerical example we will use three criteria which can be written under the form of (6.79).

Volume

the volume:

$$m_{vol}(u) = 1$$

$$l_{vol}(u) = 0.$$

Case	Volume	Displacement	Constraint	Iter.	Eval.
Elastic	1.35746	7.99968e-07	8e-07	32	56
Perzyna	2.42645	7.99909e-07	8e-07	28	51
Sec. Reg.	2.42656	7.99909e-07	8e-07	28	51

Table 6.3: Results for the cantilever

Displacement

A criterion on the displacement of the part of the boundary where the force is applied:

$$m_{Disp}(u) = 0$$

$$l_{Disp}(u) = \|u\|^2 \mathbb{1}_{\Gamma_N}.$$

6.3.3 Numerical examples

We consider five two-dimensional examples. In all the examples $\eta = \gamma = 10^{-10}$ and the nonlinear variational equations are solved thanks to finite elements as explained in section 4.5.1. In every example, we force a small amount of material to remain near the loading and embedded zones (this zones cannot be optimised) and no volume force is applied.

Cantilever

For this example we use a grid mesh of 6400 Q1-elements. The design domain has a length and a height of 2. A constant force equal to 1.1 is applied in the middle of the right side (from $(2, 0.9)$ to $(2, 1.1)$) and the left side is clamped. The volume is optimized under a displacement constraint. For the material characteristic we take: $E = 1960$, $\nu = 0.3$ and $\sigma_c = 0.95$. Results are given in table 6.3.

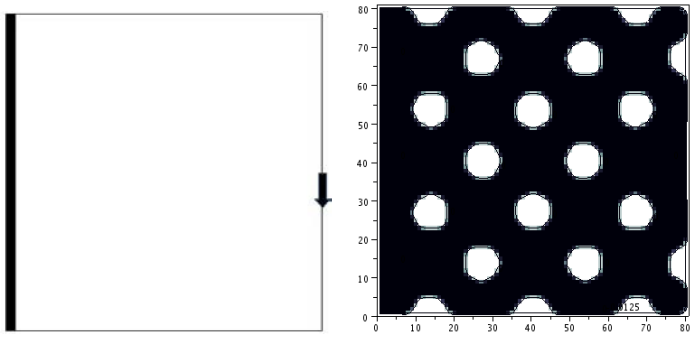

(a) Load case (b) Initialisation

Figure 6.3: Cantilever

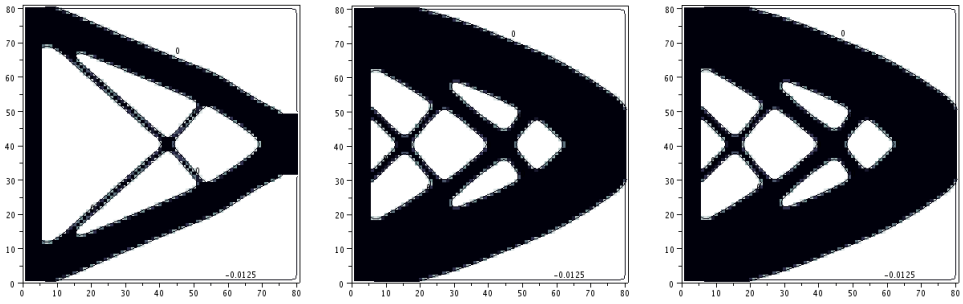

(a) Without plasticity (b) Perzyna penalisation (c) Second regularisation

Figure 6.4: Cantilever, final designs

On this example, we observed that taking plasticity into account produces heavier structures. Indeed the algorithm try to avoid the appearance of plastic zone which are less rigid and implies greater displacements. We also remark that the two different plasticity models give a similar final design and that plasticity zones occur near the load conditions.

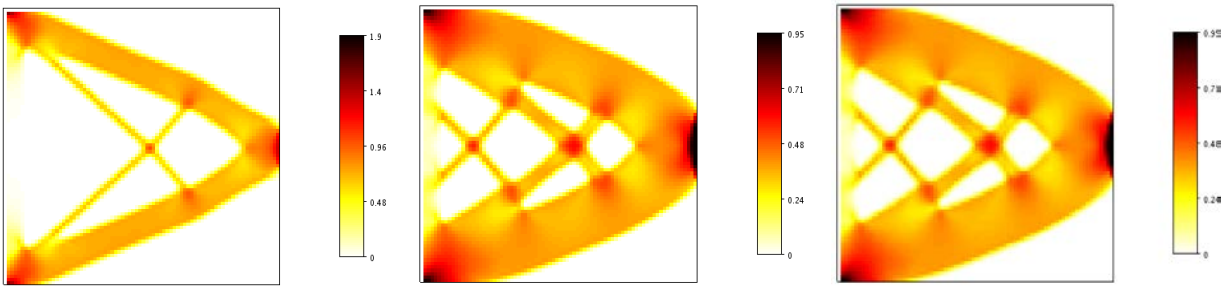

(a) Von Mises for the elasticity case (b) Von Mises for Perzyna penalisation (c) Von Mises for the second regularisation

Figure 6.5: Cantilever, Von Mises for the final designs. We point out that the color scale differs between elasticity and plasticity.

Bridge

The right and left sides are clamped. The design domain has a length equal to 4 and a height of 1. A constant force equal to 30 is applied on the middle of the upper side from $(1.748, 1)$ to $(2.25, 1)$. The volume is optimized under a displacement constraint. For the material characteristic we take: $E = 1.8 * 10^5$, $\nu = 0$ and $\sigma_c = 70$. Results are gathered in table 6.4.

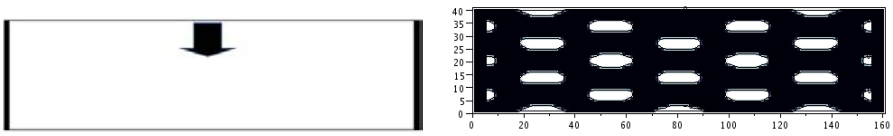

(a) Load case (b) Initialisation

Figure 6.6: Bridge

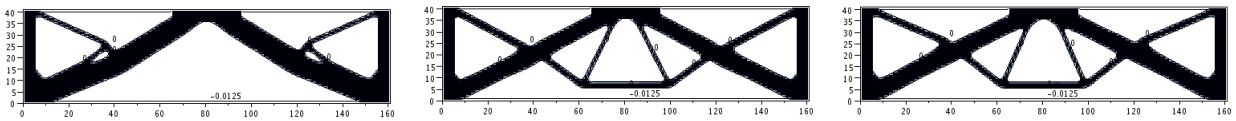

(a) Without plasticity (b) Perzyna penalisation (c) Second regularisation

Figure 6.7: Bridge, final designs

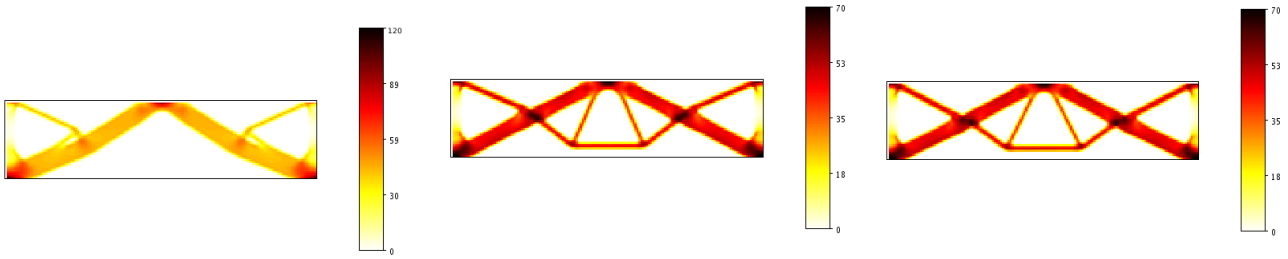

(a) Von Mises for the elasticity case (b) Von Mises for Perzyna penalisation (c) Von Mises for the second regularisation

Figure 6.8: Bridge, Von Mises for the final designs. We point out that the color scale differs between elasticity and plasticity.

On this example, we note that the algorithm did not take the same path when plasticity is considered. Here the two plasticity regularisations give shapes which are more different than in the case of the cantilever and plasticity zones appear not only near the loading zone but also at the meeting point of different bars. The fact that, in plastic cases, the volume is better than in the elastic case could be explained by the different paths taken by the algorithm.

Pylon 1

For this example we use a grid mesh of 6400 Q1-elements. The design domain has a length and a height of 2. The structure is fixed on the bottom right and on the bottom of the left side. A constant force equal to 2 is applied on

Case	Volume	Displacement	Constraint	Iter.	Eval.
Elastic	1.39414	8.99939e-07	9e-07	47	74
Perzyna	1.38493	8.99537e-07	9e-07	42	70
Sec. Reg.	1.364	8.99995e-07	9e-07	51	81

Table 6.4: Results for the bridge

the left of the upper side from $(0.1, 2)$ to $(0.35, 2)$. The volume is optimized under a displacement constraint. For the material characteristic we take: $E = 1960$, $\nu = 0.3$ and $\sigma_c = 2$. Results are shown in table 6.5.

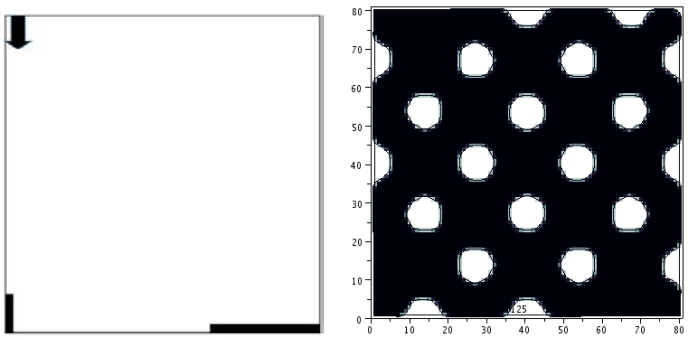

(a) Load case (b) Initialisation

Figure 6.9: Pylon 1

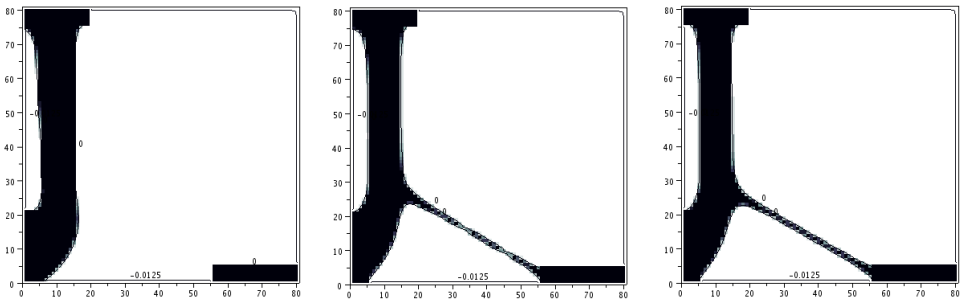

(a) Without plasticity (b) Perzyna penalisation (c) Second regularisation

Figure 6.10: Pylon 1, final designs

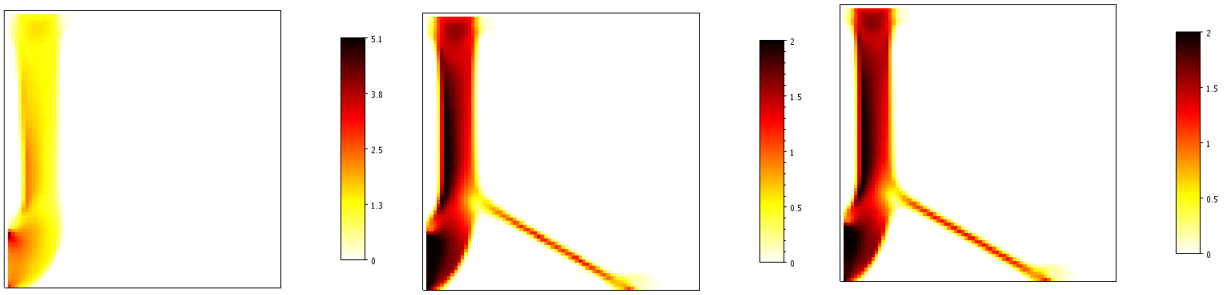

(a) Von Mises for the elasticity case (b) Von Mises for Perzyna penalisation (c) Von Mises for the second regularisation

Figure 6.11: Pylon 1, Von Mises for the final designs. We point out that the color scale differs between elasticity and plasticity.

On this example, there is a clear difference between the elastic case and the plastic cases. In the elastic case, the connection with the Dirichlet conditions on the bottom right is not needed whereas in the plastic case, the algorithm does not manage to remove it. We note also that the final values of the volume are quite the same in every case.

Case	Volume	Displacement	Constraint	Iter.	Eval.
Elastic	0.682463	7.99926e-07	8e-07	602	683
Perzyna	0.682525	7.9992e-07	8e-07	501	547
Sec. Reg.	0.676969	7.99838e-07	8e-07	297	349

Table 6.5: Results for the Pylon 1

The Y

For this example we use a grid mesh of 6400 Q1-elements. The design domain has a length and a height of 2. The left side is fixed. A constant force equal to 1.3 is applied on the top right side from $(2, 0.1)$ to $(2, 0.5)$ and on the bottom right side $(2, 1.5)$ to $(2, 1.9)$. The volume is optimized under a displacement constraint. For the material characteristic we take: $E = 1960$, $\nu = 0.3$ and $\sigma_c = 1$. Results are collated in table 6.6.

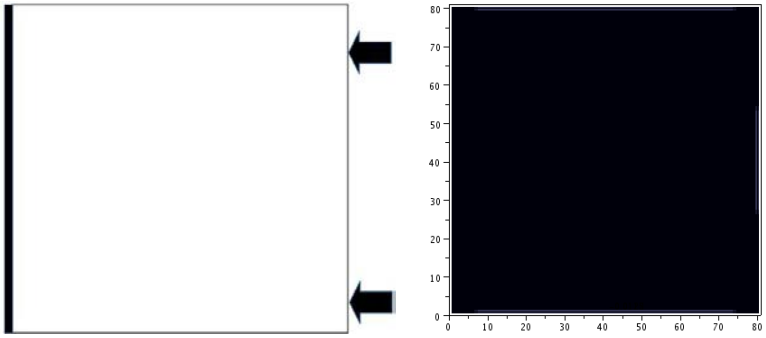

(a) Load case (b) Initialisation

Figure 6.12: The Y

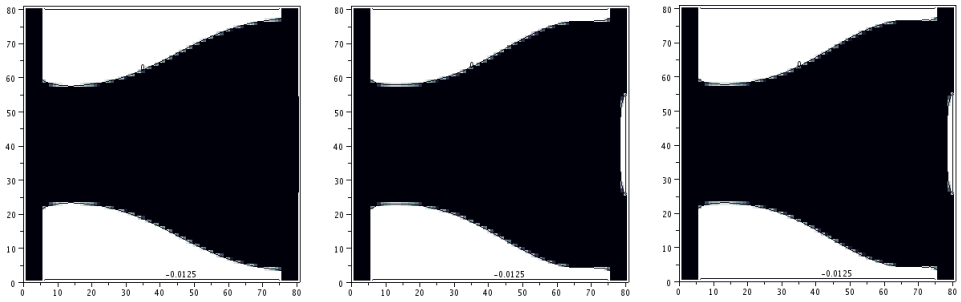

(a) Without plasticity (b) Perzyna penalisation (c) Second regularisation

Figure 6.13: The Y, final designs

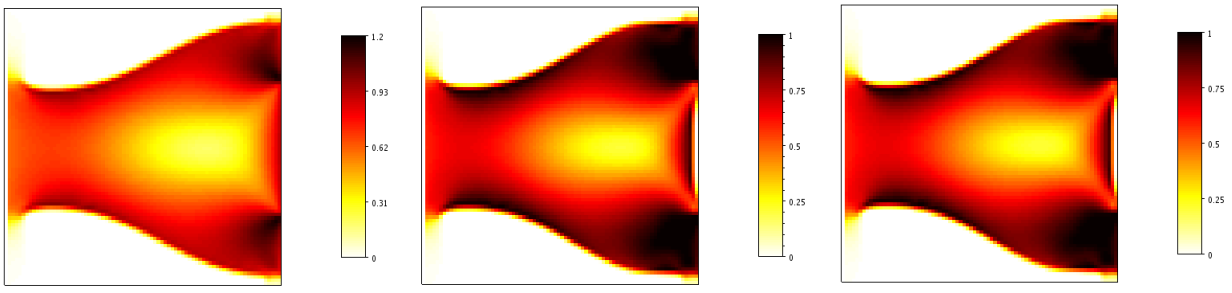

(a) Von Mises for the elasticity case (b) Von Mises for Perzyna penalisation (c) Von Mises for the second regularisation

Figure 6.14: The Y, Von Mises for the final designs. We point out that the color scale differs between elasticity and plasticity.

The elastic and plastic case take quite the same optimisation path but in the elastic case the volume of the final is slightly lower.

Case	Volume	Displacement	Constraint	Iter.	Eval.
Elastic	2.74181	7.9999e-07	8e-07	39	62
Perzyna	2.77577	7.99989e-07	8e-07	103	128
Sec. Reg.	2.77554	7.99993e-07	8e-07	69	94

Table 6.6: Results for the Y

Pylon 2

The structure is fixed on the bottom left, right and middle. The design domain has a length equal to 2 and a height of 1 A constant force equal to 40 is applied on the middle of the top from $(0.8, 1)$ to $(1.2, 1)$. The volume is optimized under a displacement constraint. For the material characteristic we take: $E = 3000$, $\nu = 0$ and $\sigma_c = 70$. Results are presented in table 6.7.

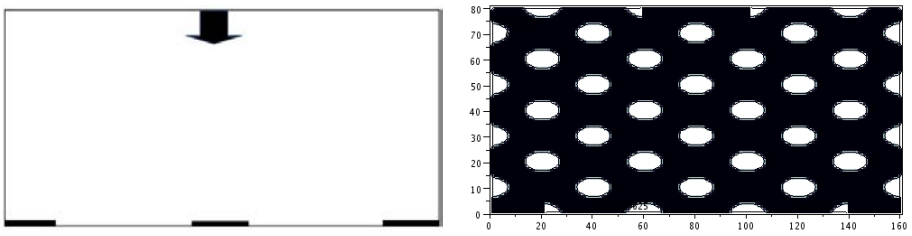

(a) Load case (b) Initialisation

Figure 6.15: Pylon 2

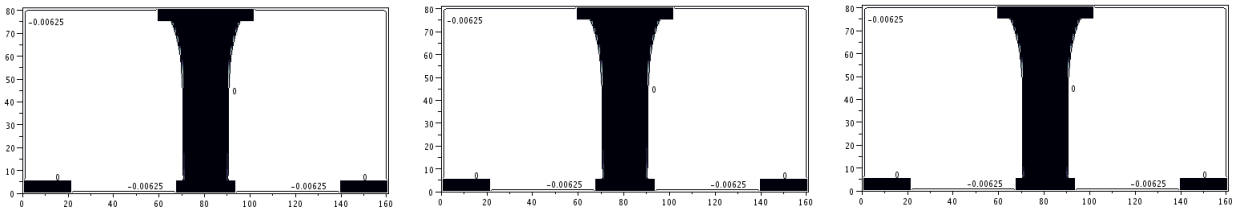

(a) Without plasticity (b) Perzyna penalisation (c) Second regularisation

Figure 6.16: Pylon 2, final designs

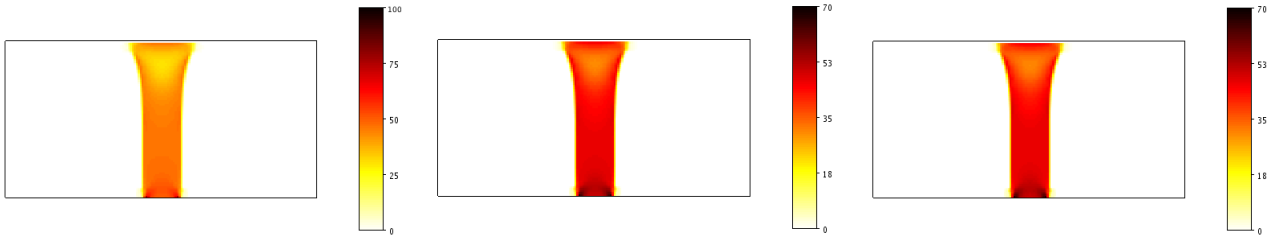

(a) Von Mises for the elasticity case (b) Von Mises for Perzyna penalisation (c) Von Mises for the second regularisation

Figure 6.17: Pylon 2, Von Mises for the final designs. We point out that the color scale differs between elasticity and plasticity.

The same remark as for the previous example of the Y can be made. In the elastic case the volume is slightly lower but it is not really significant.

Case	Volume	Displacement	Constraint	Iter.	Eval.
Elastic	0.320939	8.99997e-07	9e-07	79	104
Perzyna	0.321082	8.9998e-07	9e-07	102	130
Sec. Reg.	0.321073	8.99981e-07	9e-07	144	173

Table 6.7: Results for the Pylon 2

Appendices

Appendix A

Conical derivative for the Tresca model

Contents

A.1 Introduction

In this annex we give the proof of a result which can be found in [269], trying to give more details and simplifying the proof a little bit. We place ourselves in $\mathbb{R}^2$, without crack. The main idea is to rewrite the problem under the form a saddle point problem. This yields two problems to differentiate which are variational inequalities of the first kind. For these two problems we can hope to be allowed to use the conical derivative of the projection (if the convex on which we project is polyhedric).

We finally make the remark that the conical derivative is found with two restrictions. The first restriction already mentioned is the one of the dimension. It is crucial to be in dimension 2, otherwise it would not be possible to use the tangent vector in (A.10). Then the variable ξ in the max should be searched in $\left(H^{\frac{1}{2}}(\Gamma_c)^n\right)^*$ and this would prevent the bilinear form b^0 (defined in (A.18)) from being coercive (proposition A.2.7). The second restriction lies in the assumption (A.2). The conical derivative found is only valid in the particular directions θ verifying this property which is not the case for every $\theta \in W^{2,\infty}(\mathbb{R}^2,\mathbb{R}^2)$. This last assumption cannot be removed if we want to use the simplified expression (A.10) which is fundamental when we want to pass to the saddle point formulation. In this annex, $\theta \in W^{2,\infty}(\mathbb{R}^2,\mathbb{R}^2)$.

A.2 A saddle point problem

The first step is to put our variational problem under the form of an optimization problem (this formulation has already been given in (3.24)):

Theorem A.2.1. *The problem* (3.23) *is equivalent to the following problem: find $u \in K(\Omega)$ such that*

$$u = \underset{\phi\in K(\Omega)}{\operatorname{argmin}} \left(J(\phi) = \frac{1}{2}\int_\Omega Ae(\phi) : e(\phi)\, dx - \langle F,\phi\rangle + j(\phi)\right). \tag{A.1}$$

with $j(\phi) = \displaystyle\int_{\Gamma_c} s|\phi_t|$ *and* $\langle F,\phi\rangle = \displaystyle\int_\Omega f\cdot\phi\, dx + \int_{\Gamma_N} G\cdot\phi\, ds$

Next we make the classical variable change $T = Id + t\theta$ and take the new variable $z = (I+\nabla\theta)^{-1}\overline{u}(\theta)$ as in the case of the conical derivative for contact without friction (5.7). We also make the following technical assumption (corresponding to the assumption A_1 in [269] chapter 4, (4.343)): There exist $t_0 > 0$ such that for every $0 < t < t_0$ we have:

$$(I+t\nabla\theta)n = \frac{{}^t(I+t\nabla\theta)^{-1}n}{\|{}^t(I+t\nabla\theta)^{-1}n\|^2}. \tag{A.2}$$

Since we limit ourselves to the dimension 2 we note τ the tangent vector associated with n such that:

$$\phi_t = |\phi\cdot\tau|\,\tau \tag{A.3}$$

Remark A.2.2. *It seems difficult to clearly understand what the assumption* (A.2) *implies on the direction* θ*. However, we propose to formally write the power series of the right hand side with respect to* t *in* 0*. We use the fact that:*

$$\left(I + t^t\nabla\theta\right)^{-1} = \sum_{i=0}^{+\infty}(-1)^i t^i \left({}^t\nabla\theta\right)^i$$

So:

$$\frac{{}^t(I+t\nabla\theta)^{-1}n}{\|{}^t(I+t\nabla\theta)^{-1}n\|^2} = \frac{\sum_{k=0}^{+\infty}(-1)^k t^k \left({}^t\nabla\theta\right)^k n}{1+\sum_{0\le i,0\le j,\, i+j\neq 0}(-1)^{i+j}t^{i+j}\left({}^t\nabla\theta\right)^{i+j}}.$$

The assumption (A.2) *means that:*

$$(I+t\nabla\theta)n = \sum_{k=0}^{+\infty}\sum_{l=0}^{+\infty}\left(\sum_{0\le i,0\le j,\, i+j\neq 0}(-1)^{i+j}t^{i+j}\left({}^t\nabla\theta\right)^{i+j}\right)^l (-1)^k t^k \left({}^t\nabla\theta\right)^k n.$$

It is difficult to rearrange the term in the serie but for the first order it implies that:

$$\left({}^t\nabla\theta + \nabla\theta\right)n = 2\left({}^t\nabla\theta n\cdot n\right)n. \tag{A.4}$$

Since we are in two dimension this gives the following constraint:

$$\left({}^t\nabla\theta + \nabla\theta\right)n\cdot\tau = 0, \tag{A.5}$$

since the constraint on the normal part is satisfied by every direction. For the second order we have:

$$\left({}^t\nabla\theta n\cdot{}^t\nabla\theta n\right)n + 2\left(\nabla\theta n\cdot n\right)\nabla\theta n = 2\left(\nabla\theta n\cdot n\right)^2 n + \left({}^t\nabla\theta\right)^2 n. \tag{A.6}$$

Again the normal part is satisfied by every direction. It only constrains the tangential part:

$$2\left(\nabla\theta n\cdot n\right)\nabla\theta n\cdot\tau = \left({}^t\nabla\theta\right)n\cdot\left(\nabla\theta\right)n. \tag{A.7}$$

Lemma A.2.3. *After the variable change* $T = Id + \theta$ *in the integral and after making the variable change:* $\phi = (I+\nabla\theta)\psi$*, corresponding to same change of variable made on* $\overline{u}(\theta)$*, to work with test function such that* $\psi\cdot T \in K(\Omega_0)$*,* $J(\phi)$ *becomes:*

$$J^\theta(\psi) = \frac{1}{2}a^\theta(\psi,\psi) - \langle F^\theta,\psi\rangle + j^\theta(\psi) \tag{A.8}$$

where a^θ *is defined by* (5.10)*,* F^θ *by* (5.11) *and:*

$$j^\theta(\psi) = \int_{\Gamma_c^0} s\circ T|det(I+\nabla\theta)|\|{}^t(I+\nabla\theta)^{-1}n\||(I+\nabla\theta)(\psi\circ T)_t|\,ds. \tag{A.9}$$

Proof. For a^θ and F^θ the proof was done in (5.8). We only need to focus on j and we remove the t variable for the sake of clarity.

$$j^\theta(\psi) = \int_{\Gamma_c^0} s\circ T|det(I+\nabla\theta)|\|{}^t(I+\nabla\theta)^{-1}n\||(I+\nabla\theta)\psi\circ T - ((I+\nabla\theta)\psi\circ T\cdot n\circ T)n\circ T|\,ds,$$

using (5.6):

$$n\circ T = \frac{{}^t(I+\nabla\theta)^{-1}n}{\|{}^t(I+\nabla\theta)^{-1}n\|},$$

consequently:

$$\left((I+\nabla\theta)\psi\circ T\cdot n\circ T\right)n\circ T = (\psi\circ T\cdot n)\frac{{}^t(I+\nabla\theta)^{-1}n}{\|{}^t(I+\nabla\theta)^{-1}n\|^2},$$

using the assumption (A.2):

$$\left((I+\nabla\theta)\psi\circ T\cdot n\circ T\right)n\circ T = (\psi\circ T\cdot n)(I+\nabla\theta)n$$

and the expression of j^θ can be simplified:

$$j^\theta(\psi) = \int_{\Gamma_c^0} s\circ T|det(I+\nabla\theta)|\|{}^t(I+\nabla\theta)^{-1}n\||(I+\nabla\theta)(\psi\circ T)_t|\,ds.$$

□

To put the problem under a saddle point problem we remark that:

$$j^\theta(\psi) = \max_{\xi\in\Lambda} \int_{\Gamma_c^0} r_\theta s\circ T\xi\cdot(\psi\circ T)\,ds \tag{A.10}$$

and we note

$$r_\theta = |det(I+\nabla\theta)|\,\left|{}^t(I+\nabla\theta)^{-1}n\right|\,|(I+\nabla\theta)\tau|\,, \tag{A.11}$$

$$\Lambda = \left\{\|\xi\|_{L^\infty}\le 1, \xi\in L^\infty(\Gamma_c^0)\right\}. \tag{A.12}$$

For now we take $\psi\circ T^{-1}$ instead of ψ.

Definition A.2.4. *We define the following Lagrangian on $H^1_{\Gamma_0^0}(\Omega)^d\times(H^{\frac12}(\Gamma_c^0))'$:*

$$\mathcal{L}(\psi,\xi) = \frac12 a^\theta(\psi,\psi) - \langle F^\theta,\psi\rangle + \int_{\Gamma_c^0} s\circ T\xi\tau\cdot\psi r_\theta\,ds \tag{A.13}$$

and the saddle point problem can be written as:
Find $z(\theta)\in K(\Omega_0)$ and $\lambda(\theta)\in\Lambda$ such that

$$\forall\psi\in K(\Omega_0),\ \forall\xi\in\Lambda,\ \mathcal{L}(z(\theta),\xi)\le\mathcal{L}(z(\theta),\lambda(\theta))\le\mathcal{L}(\psi,\lambda(\theta)). \tag{A.14}$$

Proposition A.2.5. *The problem* (A.14) *is equivalent to the following variational inequalities:*
Find $z(\theta)\in K(\Omega_0)$ and $\lambda(\theta)\in\Lambda$ such that:

$$\forall\gamma\in K(\Omega_0),\ a^\theta(z(\theta),\gamma-z(\theta)) - \langle F^\theta,\gamma-z(\theta)\rangle + \int_{\Gamma_c^0} s\circ T\lambda(\theta)\tau\cdot(\gamma-z(\theta))r_\theta\,ds\ge 0, \tag{A.15}$$

$$\forall\xi\in\Lambda,\ b^\theta(\lambda(\theta),\xi-\lambda(\theta))\ge\int_{\Gamma_c^0}(\xi-\lambda(\theta))\,\tau\cdot\omega(\theta)r_\theta s\circ T\,ds, \tag{A.16}$$

with $\Psi^\theta(\xi)$ the solution of the following variational inequality in $H_{n_0}=\left\{\phi\in H^1_{\Gamma_0^0}(\Omega)^d \text{ such that } \phi\cdot n=0 \text{ on } \Gamma_c^0\right\}$: find $\Psi^\theta(\xi)\in H_{n_0}$ such that for every $\phi\in H_{n_0}$:

$$a^\theta(\Psi^\theta(\xi),\phi) = \int_{\Gamma_c^0} r_\theta s\circ T\xi\tau\cdot\phi\,ds, \tag{A.17}$$

$\omega(\theta)=\Psi^\theta(\lambda(\theta))+z(\theta)$ *and*

$$b^\theta(\lambda,\xi) = \int_{\Gamma_c^0}\tau\cdot\Psi^\theta(\lambda)\xi r_\theta s\circ T\,ds. \tag{A.18}$$

Proof. For (A.15), we take the second inequality in (A.14):

$$\frac12 a^\theta(\psi,\psi) - \frac12 a^\theta(z(\theta),z(\theta)) - \langle F^\theta,\gamma-z(\theta)\rangle + \int_{\Gamma_c^0} r_\theta s\circ T\lambda(\theta)(\gamma-z(\theta))\cdot\tau\,ds\ge 0.$$

Taking $\psi = z(\theta)+\alpha(\gamma-z(\theta))$ with $\gamma\in K(\Omega_0)$ and $\alpha\in[0,1]$, which is in the convex $K(\Omega_0)$; dividing by α and $t\to 0$ gives (A.15).
Taking (A.15) for real, we compute:

$$\frac12 a^\theta(\psi-z(\theta),\psi-z(\theta)) = \frac12 a^\theta(\psi,\psi) + \frac12 a^\theta(z(\theta),z(\theta)) - a^\theta(\psi,z(\theta)).$$

So:

$$\begin{aligned}\frac12 a^\theta(\psi,\psi) - \frac12 a^\theta(z(\theta),z(\theta)) &= \frac12 a^\theta(\psi-z(\theta),\psi-z(\theta)) - a^\theta(z(\theta),z(\theta)) + a^\theta(z(\theta),\psi)\\ &= \frac12 a^\theta(\psi-z(\theta),\psi-z(\theta)) + a^\theta(z(\theta),\psi-z(\theta)).\end{aligned}$$

Using (A.15) and the coercivity of a^θ:

$$\frac12 a^\theta(\psi,\psi) - \frac12 a^\theta(z(\theta),z(\theta)) \ge \langle F^\theta,\gamma-z(\theta)\rangle - \int_{\Gamma_c^0} r_\theta s\circ T\lambda(\theta)(\gamma-z(\theta))\cdot\tau\,ds$$

which gives the second inequality in (A.14).
For (A.16), we take the first inequality in (A.14):

$$\int_{\Gamma_c^0} r_\theta s\circ T\lambda(\theta)\tau\cdot z(\theta)\,ds \ge \int_{\Gamma_c^0} r_\theta s\circ T\xi z(\theta)\cdot\tau\,ds$$

using that $\omega(\theta)=\Psi^\theta(\lambda(\theta))+z(\theta)$ we find the equivalence with (A.16). □

Proposition A.2.6. *$\omega(\theta)$ is the solution of the following inequation in $K(\Omega_0)$:*

$$a^\theta(\omega(\theta), \gamma - \omega(\theta)) \geq \langle F^\theta, \gamma - \omega(\theta)\rangle \tag{A.19}$$

Proof. Taking (A.16) and remarking that for every $v \in K(\Omega_0)$, $\gamma = v + \Psi^\theta(\lambda(\theta)) \in K(\Omega_0)$, we obtain:

$$\forall v \in K(\Omega),\ a^\theta(z(\theta), v - \omega(\theta)) - \langle F^\theta, v - \omega(\theta)\rangle + \int_{\Gamma_c^0} r_\theta s \circ T\lambda(\theta)(v - \omega(\theta)) \cdot \tau\, ds \geq 0$$

Since $z(\theta) = \omega(\theta) - \Psi^\theta(\lambda(\theta))$ and:

$$a^\theta(\Psi^\theta(\lambda(\theta)), (v - \omega(\theta))) = \int_{\Gamma_c^0} r_\theta s \circ T\lambda(\theta)\tau \cdot (v - \omega(\theta))\, ds,$$

we conclude that $\omega(\theta)$ is the solution of (A.19). □

Now we study the properties of b^0.

Proposition A.2.7. *The form b^0 is bilinear, symetric, continuous and coercive on $H^{\frac{1}{2}}(\Gamma_c^0)'$*

Proof. The fact that b^θ is bilinear is obvious as $\Psi^\theta(\xi)$ is the solution of a variational equation linear in ξ.

For the symmetry, which is true for b^θ:

$$\begin{aligned} b^\theta(\xi, \lambda) &= \int_{\Gamma_c^0} \tau \cdot \Psi^\theta(\xi)\lambda r_\theta s \circ T\, ds \\ &= a^\theta(\Psi^\theta(\lambda), \Psi^\theta(\xi)) \\ &= a^\theta(\Psi^\theta(\xi), \Psi^\theta(\lambda)) \\ &= \int_{\Gamma_c^0} \tau \cdot \Psi^\theta(\lambda)\xi r_\theta s \circ T\, ds \\ &= b^\theta(\lambda, \xi) \end{aligned}$$

We prove now that b^0 is continuous.

$$\begin{aligned} |b^0(\xi, \lambda)| &= \left| \int_{\Gamma_c^0} \Psi^0(\xi) \cdot \tau\lambda s\, ds \right| \\ &\leq \|s\|_{L^\infty} \int_{\Gamma_c^0} \left|\Psi^0(\xi) \cdot \tau\lambda\right| ds \\ &\leq C' \left\|\Psi^0(\xi) \cdot \tau\right\|_{H^{\frac{1}{2}}} \|\lambda\|_{\left(H^{\frac{1}{2}}\right)^*} \end{aligned}$$

We then use the continuity of the trace on Ω_0: $\left\|\Psi^0(\xi) \cdot \tau\right\|_{H^{\frac{1}{2}}} \leq C_1 \left\|\Psi^0(\xi)\right\|_{H^1}$ and with $C_1 \left\|\Psi^0(\xi)\right\|_{H^1} \leq C_2 \|\lambda\|_{H^{\frac{1}{2}}}$ using the equation (A.17).

Finally the coercivity:

$$\begin{aligned} |b^0(\xi, \xi)| &= |a^0(\Psi^0(\xi), \Psi^0(\xi))| \\ &= \left\|\Psi^0(\xi))\right\|_{H^1}^2 \end{aligned}$$

but:

$$\left\|\Psi^0(\xi))\right\|_{H^1} \geq C\sqrt{a^0(\Psi^0(\xi), \Psi^0(\xi))}$$

and

$$\begin{aligned} \sqrt{a^0(\Psi^0(\xi), \Psi^0(\xi))} &= \sup_{\substack{\|\phi\| \leq 1 \\ \phi \in H^1}} \left|a^0(\Psi^0(\xi), \phi)\right| \\ &= \sup_{\substack{\|\phi\| \leq 1 \\ \phi \in H^1}} \left| \int_{\Gamma_c^0} s\phi\tau\xi\, ds \right| \\ &= \|\xi\|_{\left(H^{\frac{1}{2}}\right)^*} \end{aligned}$$

due to the surjectivity of the trace. It enables us to conclude that b^0 is coercive. □

A.3 Derivation of the saddle point problem : $\lambda(\theta)$

In the next part we will use the definitions given in section 5.2: (5.12) and (5.13). Moreover it is clear that $\Psi^\theta(\xi)$ admits a shape derivative and, thanks to section 5.2, that $\omega(t\theta)$ admits a conical shape derivative. First we focus on the derivative of $\lambda(\theta)$. The spirit of the proof is the same as in sections 5.2.2 and 5.2.3.

First we define some spaces which will be needed in the following

Definition A.3.1.

$$C_{\lambda(0)}(\Lambda) = \left\{ w \in \left(H^{\frac{1}{2}}(\Gamma_c^0) \right)^*,\ \exists t > 0,\ \lambda(0) + tw \in \Lambda \right\} \tag{A.20}$$

and its closure in $\left(H^{\frac{1}{2}}(\Gamma_c^0) \right)^*$*:*

$$S_{\lambda(0)}(\Lambda) = \overline{C_{\lambda(0)}(\Lambda)}^{\left(H^{\frac{1}{2}}(\Gamma_c^0) \right)^*} \tag{A.21}$$

The Taylor expansion of b^θ is given by:

$$\begin{aligned} b^\theta(\lambda,\xi) &= b^0(\lambda,\xi) + \int_{\Gamma_c^0} s\xi Y_{\Psi^0(\lambda)}(\theta)\cdot\tau\, ds + \int_{\Gamma_c^0} \xi\Psi^0(\lambda)\cdot\tau\left(\nabla s\cdot\theta + s r_0'(\theta)\right) ds + o(\theta) \\ &= b^0(\lambda,\xi) + (b^0)'(\theta)(\lambda,\xi) + o(\theta) \end{aligned} \tag{A.22}$$

where $r_0'(\theta) = (\mathrm{div}(\theta) - {}^t\nabla\theta n\cdot n) + \nabla\tau\cdot\tau)$ and $|o(\theta)| \le o_3(\theta)\,\|\lambda\|_{\left(H^{\frac{1}{2}}\right)^*}\,\|\xi\|_{\left(H^{\frac{1}{2}}\right)^*}$ with $o_3(\theta)$ independent of λ and ξ. We also specify that $\lim_{\theta\to 0}\frac{|o(\theta)|}{\|\theta\|_{W^{2,\infty}}} = 0$ and $\lim_{\theta\to 0}\frac{|o_3(\theta)|}{\|\theta\|_{W^{2,\infty}}} = 0$.

We also write the Taylor expansion of $\langle \Xi^{t\theta}, \xi\rangle = \int_{\Gamma_c^0} \xi\tau\cdot\omega(t\theta) r_{t\theta} s\circ T\, ds$:

$$\begin{aligned} \langle \Xi^{t\theta},\xi\rangle &= \langle \Xi^0,\xi\rangle + t\int_{\Gamma_c^0}\omega(0)\cdot\tau\xi(s r_0'(\theta) + \nabla s\cdot\theta) + t\int_{\Gamma_c^0} s\xi Y_{\omega(0)}(\theta)\cdot\tau\, ds + o(t) \\ &= \langle \Xi^0,\xi\rangle + t\langle (\Xi^0)'(\theta),\xi\rangle + o(t) \end{aligned} \tag{A.23}$$

where $|o(t)| \le o_4(t)\,\|\xi\|_{\left(H^{\frac{1}{2}}\right)^*}$ with $o_4(t)$ independent of ξ.

Next, we rewrite the inequation (A.16) in the following way:

$$\begin{aligned} b^0(\lambda(t\theta),\xi-\lambda(t\theta)) \ge\ & \langle \Xi^0,\xi-\lambda(t\theta)\rangle + \langle \Xi^{t\theta} - \Xi^0 - (\Xi^0)'(t\theta),\xi-\lambda(t\theta)\rangle \\ & + \langle (\Xi^0)'(t\theta),\xi-\lambda(t\theta)\rangle + (b^0)'(t\theta)(\lambda(0),\xi-\lambda(t\theta)) \\ & + b^0(\lambda(0),\xi-\lambda(t\theta)) - b^{t\theta}(\lambda(0),\xi-\lambda(t\theta)) + (b^0)'(t\theta)(\lambda(0),\xi-\lambda(t\theta)) \\ & + b^0(\lambda(t\theta)-\lambda(0),\xi-\lambda(t\theta)) - b^{t\theta}(\lambda(t\theta)-\lambda(0),\xi-\lambda(t\theta)). \end{aligned} \tag{A.24}$$

Definition A.3.2. *We define* l_1*,* l_2 *and* l_3 *the following linear forms defined on* $H^{\frac{1}{2}}(\Gamma_c^0)^*$*:*

$$\langle l_1,\xi\rangle = \langle \Xi^\theta - \Xi^0 - t(\Xi^0)'(\theta),\xi\rangle, \tag{A.25}$$

$$\langle l_2,\xi\rangle = b^0(\lambda(0),\xi) - b^\theta(\lambda(0),\xi) + (b^0)'(\theta)(\lambda(0),\xi), \tag{A.26}$$

$$\langle l_3,\xi\rangle = b^0(\lambda(\theta)-\lambda(0),\xi) - b^\theta(\lambda(\theta)-\lambda(0),\xi). \tag{A.27}$$

Theorem A.3.3. $\lambda(\theta)$ *is conically differentiable and its conical derivative is the solution of:*

$$\forall\xi\in S_\Lambda^{\lambda(0)},\ b^0(Y_{\lambda(0)}(\theta),\xi - Y_{\lambda(0)}(\theta)) \ge \langle (\Xi^0)'(\theta),\xi - Y_{\lambda(0)}(\theta)\rangle - (b^0)'(\theta)(\lambda(0),\xi - Y_{\lambda(0)}(\theta)). \tag{A.28}$$

Proof. We take (A.24) to derive with respect to t. With lemma A.3.4 and lemma A.3.8 referring to [205] theorem 2.1 we can write:

$$\begin{aligned} \lambda(\theta) &= P_\Lambda^{b^0}\left(B^{-1}(\Xi^0) + tB^{-1}((\Xi^0)'(\theta)) - tB^{-1}((b^0)'(\theta)(\lambda(0))) + o(t)\right) \\ &= P_\Lambda^{b^0}\left(B^{-1}(\Xi^0) + tB^{-1}((\Xi^0)'(\theta)) - tB^{-1}((b^0)'(\theta)(\lambda(0)))\right) + o(t) \\ &= \lambda(0) + tP_{S_\Lambda^{\lambda(0)}}^{b^0}\left(B^{-1}((\Xi^0)'(\theta)) - B^{-1}((b^0)'(\theta)(\lambda(0)))\right) + o(t) \end{aligned}$$

where B^{-1} is the operator which associates to every $\phi\in H^{\frac{1}{2}}(\Gamma_c^0)$ the solution λ of

$$b^0(\lambda,\xi) = \langle\phi,\xi\rangle.$$

So $Y_{\lambda(0)}(\theta)$ is the solution of the following variational inequality:

$$\forall\xi\in S_\Lambda^{\lambda(0)},\ b^0(Y_{\lambda(0)}(\theta),\xi - Y_{\lambda(0)}(\theta)) \ge \langle (\Xi^0)'(\theta),\xi - Y_{\lambda(0)}(\theta)\rangle - (b^0)'(\theta)(\lambda(0),\xi - Y_{\lambda(0)}(\theta))$$

□

Lemma A.3.4. l_1 *is such that its norm in* $H^{\frac{1}{2}}(\Gamma_c^0)^*$ *is a* $o(t)$*.* l_2 *and* l_3 *are* $o(\theta)$ *and by* $o(\theta)$ *we mean that* $\lim_{\theta\to 0}\frac{|o(\theta)|}{\|\theta\|_{W^{2,\infty}}} = 0$.

Proof. The definition of l_1 and l_2 ensures that they are respectively $o(t)$ and $o(\theta)$. We just need to focus on l_3.

$$|\langle l_3, \xi\rangle| \leq |(b^0)'(\theta)(\lambda(\theta)-\lambda(0),\xi)| + o_3(t)\left\|\lambda(\theta)-\lambda(0)\right\|_{\left(H^{\frac{1}{2}}\right)^*}\left\|\xi\right\|_{\left(H^{\frac{1}{2}}\right)^*} \tag{A.29}$$

and with (A.22):

$$\begin{aligned}
|(b^0)'(\theta)(\lambda(\theta)-\lambda(0),\xi)| &\leq (\left\|\nabla s\right\|_{L^\infty}\left\|\theta\right\|_{L^\infty} + C\left\|s\right\|_{L^\infty}\left\|\theta\right\|_{W^{1,\infty}})\int_{\Gamma_c^0}\left|\xi\Psi^0(\lambda(\theta)-\lambda(0))\cdot\tau\right| ds \\
&\quad + \left\|s\right\|_{L^\infty}\int_{\Gamma_c^0}\left|\xi(Y_{\Psi^0(\lambda(\theta)-\lambda(0))}(\theta))\cdot\tau\right| ds \\
&\leq C\left\|s\right\|_{W^{1,\infty}}\left\|\theta\right\|_{W^{1,\infty}}\left(\left\|\xi\right\|_{\left(H^{\frac{1}{2}}\right)^*}\left\|\Psi^0(\lambda(\theta)-\lambda(0))\cdot\tau\right\|_{H^{\frac{1}{2}}}\right) \\
&\quad + \left\|s\right\|_{W^{1,\infty}}\left\|\xi\right\|_{\left(H^{\frac{1}{2}}\right)^*}\left\|Y_{\Psi^0(\lambda(\theta)-\lambda(0))}(\theta)\cdot\tau\right\|_{H^{\frac{1}{2}}}.
\end{aligned}$$

But lemmas A.3 and A.3.6 give:

$$\left|(b^0)'(\theta)(\lambda(\theta)-\lambda(0),\xi)\right| \leq C\left\|s\right\|_{W^{1,\infty}}\left\|\xi\right\|_{\left(H^{\frac{1}{2}}\right)^*}\left\|\theta\right\|_{W^{1,\infty}}\left\|\lambda(\theta)-\lambda(0))\right\|_{\left(H^{\frac{1}{2}}\right)^*}. \tag{A.30}$$

Finally, using the lemma A.3.7 and (A.29), l_3 is $o(\theta)$

□

Lemma A.3.5. *There exist a constant $C>0$ such that:*

$$\left\|\Psi^0(\lambda(\theta)-\lambda(0))\cdot\tau\right\| \leq C\left\|\lambda(\theta)-\lambda(0))\right\|_{\left(H^{\frac{1}{2}}\right)^*}. \tag{A.31}$$

Proof.

$$a^0(\Psi^0(\lambda(\theta)-\lambda(0)),\phi) = \int_{\Gamma_c^0}(\lambda(\theta)-\lambda(0))\,\phi\cdot\tau\, ds.$$

Using the coercivity of a^0 and the trace inequality on Ω_0:

$$\left\|\Psi^0(\lambda(\theta)-\lambda(0))\cdot\tau\right\| \leq C\left\|\lambda(\theta)-\lambda(0))\right\|_{\left(H^{\frac{1}{2}}\right)^*}.$$

□

Lemma A.3.6. *There exists a constant $C>0$ such that:*

$$\left\|Y_{\Psi^0(\lambda(\theta)-\lambda(0))}(\theta)\cdot\tau\right\|_{H^{\frac{1}{2}}} \leq C\left\|\lambda(\theta)-\lambda(0))\right\|_{\left(H^{\frac{1}{2}}\right)^*}\left\|\theta\right\|_{W^{2,\infty}}. \tag{A.32}$$

Proof. In view of (A.17) the Lagrangian derivative of $\Psi^0(\lambda(\theta)-\lambda(0))$, $Y_{\Psi^0(\lambda(\theta)-\lambda(0))}(\theta)$ is the solution of the following variational equality:

$$a^0(Y_{\Psi^0(\lambda(\theta)-\lambda(0))}(\theta),\phi) + (a^0)'(\theta)(\Psi^0(\lambda(\theta)-\lambda(0)),\phi) = \int_{\Gamma_c^0}(r_0'(\theta)s+\nabla s\cdot\theta)(\lambda(\theta)-\lambda(0))\phi\cdot\tau\, ds \tag{A.33}$$

for every $\phi\in H^1_{\Gamma_0^0}(\Omega)^d$ such that $\phi\cdot n=0$ on Γ_c^0.

Let us call C_0 the coercivity constant of a^0. Then:

$$\begin{aligned}
C_0\left\|Y_{\Psi^0(\lambda(\theta)-\lambda(0))}(\theta)\right\|^2_{H^1} &\leq C\left\|\lambda(\theta)-\lambda(0))\right\|_{\left(H^{\frac{1}{2}}\right)^*}\left\|Y_{\Psi^0(\lambda(\theta)-\lambda(0))}(\theta)\cdot\tau\right\|_{H^{\frac{1}{2}}}\left\|\theta\right\|_{W^{2,\infty}}\left\|g\right\|_{W^{1,\infty}} \\
&\quad + \left|(a^0)'(\theta)(\Psi^0(\lambda(\theta)-\lambda(0)),Y_{\Psi^0(\lambda(\theta)-\lambda(0))})\right|.
\end{aligned} \tag{A.34}$$

To bound $|(a^0)'(\theta)(\Psi^0(\lambda(\theta)-\lambda(0)),Y_{\Psi^0(\lambda(\theta)-\lambda(0))})|$ we use the computations done in (5.18) and (5.19). Terms of $\left\|\Psi^0(\lambda(\theta)-\lambda(0))\right\|_{H^1}$ appear which we manage to bound by $\left\|\lambda(\theta)-\lambda(0))\right\|_{\left(H^{\frac{1}{2}}\right)^*}$ thanks to lemma A.3, therefore (A.34) reduces to:

$$\left\|Y_{\Psi^0(\lambda(\theta)-\lambda(0))}(\theta)\right\|^2_{H^1} \leq C\left\|\lambda(\theta)-\lambda(0))\right\|_{\left(H^{\frac{1}{2}}\right)^*}\left\|Y_{\Psi^0(\lambda(\theta)-\lambda(0))}(\theta)\cdot\tau\right\|_{H^1}\left\|\theta\right\|_{W^{2,\infty}},$$

using the continuity of the trace for the term $\left\|Y_{\Psi^0(\lambda(\theta)-\lambda(0))}(\theta)\cdot\tau\right\|_{H^{\frac{1}{2}}}$ in (A.34). Dividing by $\left\|Y_{\Psi^0(\lambda(\theta)-\lambda(0))}(\theta)\right\|_{H^1}$ and using again the continuity of the trace we prove lemma A.3.6. □

Lemma A.3.7. *There exists a constant $C>0$ such that*

$$\left\|\lambda(\theta)-\lambda(0)\right\| \leq C\left\|\theta\right\|_{W^{2,\infty}} + o(\theta) \tag{A.35}$$

where $o(\theta)$ is independent of $\lambda(\theta)$, with $\lim_{\theta\to 0}\dfrac{|o(\theta)|}{\left\|\theta\right\|_{W^{2,\infty}}} = 0$

Proof. Calling C_0' the coercivity constant of b^0 we have:

$$C_0' \left\|\lambda(\theta)-\lambda(0)\right\|^2_{\left(H^{\frac{1}{2}}\right)^*} \leq b^0(\lambda(\theta)-\lambda(0),\lambda(\theta)-\lambda(0))$$

but using (A.16) we have:

$$\begin{aligned} C_0' \left\|\lambda(\theta)-\lambda(0)\right\|^2_{\left(H^{\frac{1}{2}}\right)^*} &\leq \int_{\Gamma_c^0} \left|\left(\lambda(\theta)-\lambda(0)\right)\tau\cdot\omega(\theta) r_\theta s\circ T - s\omega(0)\cdot\tau\right| ds \\ &\quad -b^\theta(\lambda(\theta),\lambda(\theta)-\lambda(0)) + b^0(\lambda(\theta),\lambda(\theta)-\lambda(0)) \\ &\leq \|s\|_{L^\infty}\left\|\lambda(\theta)-\lambda(0)\right\|_{\left(H^{\frac{1}{2}}\right)^*}\left\|\tau\cdot\omega(\theta)r_\theta-\omega(0)\cdot\tau\right\|_{H^{\frac{1}{2}}} \\ &\quad +C\|\theta\|_{W^{2,\infty}}\left\|\lambda(\theta)-\lambda(0)\right\|_{\left(H^{\frac{1}{2}}\right)^*}\left\|\lambda(\theta)\right\|_{\left(H^{\frac{1}{2}}\right)^*} \end{aligned} \tag{A.36}$$

using for the last line the beginning of the proof of lemma A.3.4. Next we want to bound $\left\|\tau\cdot\omega(\theta)r_\theta-\omega(0)\cdot\tau\right\|_{H^{\frac{1}{2}}}$, using the trace inequality:

$$\left\|\tau\cdot\omega(\theta)r_\theta-\omega(0)\cdot\tau\right\|_{H^{\frac{1}{2}}} \leq \left\|\omega(\theta)r_\theta-\omega(0)\right\|_{H^1}$$

but $r_\theta = 1+\mathrm{div}(\theta) - {}^t\nabla\theta n\cdot n + \nabla\tau\cdot\tau + o(\theta)$ so:

$$\left\|\tau\cdot\omega(\theta)r_\theta-\omega(0)\cdot\tau\right\|_{H^{\frac{1}{2}}} \leq \left\|(\omega(\theta)-\omega(0))\cdot\tau\right\|_{H^1} + \left\|(1-r_\theta)\omega(\theta)\cdot\tau\right\|_{H^1} + o(\theta)\left\|\omega(\theta)\right\|_{H^1}.$$

Then we can use the calculations of (5.20) and the fact that $\left\|\omega(\theta)\right\|_{H^1}$ is bounded for $\|\theta\|_{W^{2,\infty}}$ small enough. Thus:

$$\left\|\tau\cdot\omega(\theta)r_\theta-\omega(0)\cdot\tau\right\|_{H^{\frac{1}{2}}} \leq C\|\theta\|_{W^{2,\infty}} + o(\theta) \tag{A.37}$$

and:

$$C_0'\left\|\lambda(\theta)-\lambda(0)\right\|_{\left(H^{\frac{1}{2}}\right)^*} \leq C\|\theta\|_{W^{2,\infty}}\left(1+\left\|\lambda(\theta)\right\|_{\left(H^{\frac{1}{2}}\right)^*}\right) + o(\theta).$$

The last step is to show that $\left\|\lambda(\theta)\right\|_{\left(H^{\frac{1}{2}}\right)^*}$ is bounded for $\|\theta\|_{W^{2,\infty}}$ small enough.

As $0\in\Lambda$:

$$b^0(\lambda(\theta),\lambda(\theta)) \leq \langle\Xi^\theta,\lambda(\theta)\rangle + b^0(\lambda(\theta),\lambda(\theta)) - b^\theta(\lambda(\theta),\lambda(\theta)).$$

Using the coercivity of b^0, the computations done for (A.29) and (A.30):

$$\left(C_0' - C\|\theta\|_{W^{2,\infty}} - o(t)\right)\left\|\lambda(\theta)\right\|^2_{\left(H^{\frac{1}{2}}\right)^*} \leq \left\|\Xi^\theta\right\|_{H^{\frac{1}{2}}}.$$

Moreover:

$$\begin{aligned} \left\|\Xi^\theta\right\|_{H^{\frac{1}{2}}} &\leq \left\|\Xi^0\right\|_{H^{\frac{1}{2}}} + \left\|\Xi^\theta-\Xi^0\right\|_{H^{\frac{1}{2}}} \\ &\leq \left\|\Xi^0\right\|_{H^{\frac{1}{2}}} + C\|\theta\|_{W^{2,\infty}} + o(\theta), \end{aligned}$$

where for the last line we have used (A.37). This gives the boundedness of $\left\|\lambda(\theta)\right\|_{\left(H^{\frac{1}{2}}\right)^*}$ and finally:

$$C_0'\left\|\lambda(\theta)-\lambda(0)\right\|_{\left(H^{\frac{1}{2}}\right)^*} \leq C\|\theta\|_{W^{2,\infty}} + o(\theta).$$

□

Lemma A.3.8. *We introduce the sets:*

$$I_1 = \{x\in\Gamma_c,\ |\lambda(0)|=1\}, \tag{A.38}$$

$$I_1^+ = \{x\in\Gamma_c,\ \lambda(0)=1\}, \tag{A.39}$$

$$I_1^- = \{x\in\Gamma_c,\ \lambda(0)=-1\}. \tag{A.40}$$

We make the assumption that these sets are sufficiently regular as in [265]. We have:

$$S_{\lambda(0)}(\Lambda) = \left\{w\in\left(H^{\frac{1}{2}}(\Gamma_c^0)\right)^*,\ w\leq 0 \text{ on } I_1^+ \text{ and } w\geq 0 \text{ on } I_1^-\right\} \tag{A.41}$$

where by $w\leq 0$ on I_1^+ we mean that for every $\phi\in C_0^\infty(\Gamma_c^0)$ with support in I_1^+ and $\phi\geq 0$: $\langle w,\phi\rangle_{\left(H^{\frac{1}{2}}(\Gamma_c^0)\right)'}\leq 0$. The definition of $w\geq 0$ on I_1^- is similar. Moreover:

$$S^{\lambda(0)}(\Lambda) = S_{\lambda(0)}(\Lambda)\cap X[B^{-1}(\Xi^0)] = \overline{C_{\lambda(0)}(\Lambda)\cap X[B^{-1}(\omega(0)\cdot\tau)]}^{\left(H^{\frac{1}{2}}(\Gamma_c)\right)^*} \tag{A.42}$$

with

$$X[B^{-1}(\Xi^0)] = X_\omega = \left\{\mu\in\left(H^{\frac{1}{2}}(\Gamma_c^0)\right)' \mid \langle\mu,\overline{u}(0)\rangle = 0\right\} \tag{A.43}$$

Proof. The proof is inspired by the proof of lemma 1 in [265]. We replace Γ_c^0 by Γ_c for the sake of simplicity (the computations are done only on Γ_c^0). First we prove the lemma in $L^2(\Gamma_c)$.

It is clear that $\Lambda \subset L^2(\Gamma_c)$. To compute the closure in $L^2(\Gamma_c)$ of $C_{\lambda(0)}(\Lambda)$ we use the bipolar theorem as [205] (2. "Etude des projections" for the notations and in part 3 "différentiabilité des a-projections" for an example). Let be $u \in \left(C_{\lambda(0)}(\Lambda)\right)^0_{L^2}$ then

$$\forall z \in \Lambda,\ \int_{\Gamma_c} u(z-\lambda(0))\,ds \leq 0.$$

Separating Γ_c into two parts:

$$\forall z \in \Lambda,\ \int_{\Gamma_c \setminus I_1} u(z-\lambda(0))\,ds + \int_{I_1} u(z-\lambda(0))\,ds \leq 0.$$

Taking $z = \lambda(0) + \epsilon u$ on a compact K of $\Gamma_c \setminus I_1$, 0 otherwise, with ϵ such that $z \in \Lambda$ it follows:

$$\int_K |u|^2\,ds \leq 0$$

therefore u is 0 on every compact included in $\Gamma_c \setminus I_1$ and so u is non null on I_1 only. So:

$$\forall z \in \Lambda,\ \int_{I_1} u(z-\lambda(0))\,ds \leq 0.$$

Dividing the integral on I_1 into two integrals on I_1^+ and I_1^-, we have a.e. on I_1^+, $z-\lambda(0) \leq 0$ and a.e. on I_1^-, $z-\lambda(0) \geq 0$. As the inequality is true for every $z \in \Lambda$ this is equivalent to $u \geq 0$ a.e. on I_1^+ and $u \leq 0$ a.e. on I_1^-. This yields

$$\begin{aligned}\left(C_{\lambda(0)}(\Lambda)\right)^0_{L^2} &= \big\{u \in L^2(\Gamma_c),\ u \text{ zero a.e. on } \Gamma_c \setminus I_1,\\ &\qquad \text{such that } u \geq 0 \text{ a.e. on } I_1^+ \text{ and } u \leq 0 \text{ a.e. on } I_1^-\big\}.\end{aligned} \tag{A.44}$$

Using the bipolar theorem:

$$S_{\lambda(0)}(\Lambda)_{L^2} = \left(\left(C_{\lambda(0)}(\Lambda)\right)^0_{L^2}\right)^0_{L^2}. \tag{A.45}$$

therefore:

$$S_{\lambda(0)}(\Lambda)_{L^2} = \left\{w \in L^2(\Gamma_c),\ \forall u \in \left(C_{\lambda(0)}(\Lambda)\right)^0_{L^2},\ \int_{I_1} u \cdot w\,ds \leq 0\right\} \tag{A.46}$$

Then taking $w \in S_{\lambda(0)}(\Lambda)_{L^2}$ we use the property:

$$\forall u \in \left(C_{\lambda(0)}(\Lambda)\right)^0_{L^2},\ \int_{I_1} uw\,ds \leq 0$$

which is equivalent to

$$w \leq 0 \text{ a.e on } I_1^+ \text{ and } w \geq 0 \text{ a.e. on } I_1^-.$$

This implies:

$$\begin{aligned}S_{\lambda(0)}(\Lambda)_{L^2} &= \big\{w \in L^2(\Gamma_c),\ w(x)\lambda(0)(x) \leq 0 \text{ a.e in } I_1\big\}\\ &= \big\{w \in L^2(\Gamma_c),\ w \leq 0 \text{ a.e. on } I_1^+ \text{ and } w \geq 0 \text{ a.e. on } I_1^-\big\}\end{aligned} \tag{A.47}$$

and applying theorem 3.1 and 3.2 in [205] ($L^2(\Gamma_c)$ is a Dirichlet space):

$$S_{\lambda(0)}(\Lambda)_{L^2} \cap X_\omega = \overline{X_\omega \cap C_{\lambda(0)}(\Lambda)}^{L^2}. \tag{A.48}$$

It remains to compute the closure of $S_{\lambda(0)}(\Lambda)_{L^2}$ in $\left(H^{\frac{1}{2}}(\Gamma_c)\right)^*$.

Let $w_n \in S_{\lambda(0)}(\Lambda)_{L^2}$ converging to w in $\left(H^{\frac{1}{2}}(\Gamma_c)\right)^*$. This means that:

$$\forall \psi \in H^{\frac{1}{2}}(\Gamma_c),\ \langle w_n, \psi\rangle \to \langle w, \psi\rangle.$$

Yet

$$\begin{aligned}\big\{w \in L^2(\Gamma_c),\ w(x)\cdot\lambda(0)(x) \text{ a.e in } I_1\big\} &= \Big\{w \in L^2(\Gamma_c),\ \forall \phi \in L^2(I_1),\ \phi \geq 0,\\ &\qquad \int_{I_1^+} \phi w\,ds \leq 0 \text{ and } \int_{I_1^-} \phi w\,ds \geq 0\Big\}.\end{aligned}$$

Consequently:

$$\int_{I_1^+} w_n \phi\,ds = \langle w_n, \phi\rangle \leq 0,\ \forall \phi \in L^2(\Gamma_c).$$

And when $n \to +\infty$; $\langle w, \phi \rangle \leq 0$ which means that: $w \leq 0$ on I_1^+. The same holds for I_1^-. We have proved that:

$$S_{\lambda(0)}(\Lambda) \subset \left\{ w \in \left(H^{\frac{1}{2}}(\Gamma_c) \right)^*,\ w \leq 0 \text{ on } I_1^+ \text{ and } w \geq 0 \text{ on } I_1^- \right\}.$$

For the inverse inclusion we again use the bipolar theorem with the bilinear form b^0 which is coercive:

$$\left(S_{\lambda(0)}(\Lambda)_{L^2}\right)_b^0 = \left\{ \xi \in \left(H^{\frac{1}{2}}(\Gamma_c) \right)^* \mid \forall \zeta \in L^2(\Gamma_c) \text{ such that a.e on } I_1,\ \zeta\lambda(0) \leq 0,\ \langle \xi, \Psi^0(\lambda) \cdot \tau \rangle \leq 0 \right\}$$

and

$$S_{\lambda(0)}(\Lambda) = \left(\left(S_{\lambda(0)}(\Lambda)_{L^2}\right)_b^0 \right)_b^0 = \left\{ \mu \in \left(H^{\frac{1}{2}}(\Gamma_c) \right)^* \mid \forall \xi \in \left(S_{\lambda(0)}(\Lambda)_{L^2}\right)_b^0,\ \langle \mu, \Psi^0(\xi) \cdot \tau \rangle \leq 0 \right\}.$$

Let $w \in \left\{ w \in \left(H^{\frac{1}{2}}(\Gamma_c) \right)^*,\ w \leq 0 \text{ on } I_1^+ \text{ and } w \geq 0 \text{ on } I_1^- \right\}$ and $\xi \in \left(S_{\lambda(0)}(\Lambda)_{L^2}\right)_b^0$ then:

$$\forall \zeta \in L^2(\Gamma_c) \text{ such that a.e on } I_1,\ \zeta\lambda(0) \leq 0,\ \langle \xi, \Psi^0(\zeta) \cdot \tau \rangle \leq 0$$

Using the density of $L^2(\Gamma_c)$ in $\left(H^{\frac{1}{2}}(\Gamma_c) \right)^*$ it follows that:

$$\forall \zeta \in \left(H^{\frac{1}{2}}(\Gamma_c) \right)^* \text{ such that on } I_1^+,\ \zeta \leq 0 \text{ and } \zeta \geq 0 \text{ on } I_1^-,\ \langle \xi, \Psi^0(\zeta) \cdot \tau \rangle \leq 0.$$

Taking $\zeta = w$ and using the symmetry of b^0 we get $w \in S_{\lambda(0)}(\Lambda)$. Then:

$$S_{\lambda(0)}(\Lambda) = \left\{ w \in \left(H^{\frac{1}{2}}(\Gamma_c) \right)^*,\ w \leq 0 \text{ on } I_1^+ \text{ and } w \geq 0 \text{ on } I_1^- \right\} \tag{A.49}$$

and doing the same computation for $\overline{X_\omega \cap C_{\lambda(0)}(\Lambda)}^{\left(H^{\frac{1}{2}}(\Gamma_c) \right)^*}$:

$$S_{\lambda(0)}(\Lambda) \cap X_\omega = \overline{X_\omega \cap C_{\lambda(0)}(\Lambda)}^{\left(H^{\frac{1}{2}}(\Gamma_c) \right)^*} \tag{A.50}$$

and the lemma is proved. □

A.4 Derivation of the saddle point problem : $z(\theta)$

Again, we rewrite the variational inequation (A.15):

$$\begin{array}{rcl} a^0(z(t\theta), \gamma - z(t\theta)) & \geq & \langle F^0, \gamma - z(t\theta) \rangle + \langle F^{t\theta} - F^0 - t(F^0)'(\theta), \gamma - z(t\theta) \rangle \\ & & + \langle t(F^0)'(\theta), \gamma - z(t\theta) \rangle - t(a^0)'(\theta)(w(0), \gamma - z(t\theta)) \\ & & \langle G^0, \gamma - z(t\theta) \rangle + \langle G^{t\theta} - G^0 - t(G^0)'(\theta), \gamma - z(t\theta) \rangle \\ & & + \langle t(G^0)'(\theta), \gamma - z(t\theta) \rangle \\ & & + a^0(w(0), \gamma - z(t\theta)) - a^{t\theta}(w(0), \gamma - z(t\theta)) + t(a^0)'(\theta)(w(0), \gamma - z(t\theta)) \\ & & + a^0(w(t\theta) - w(0), \gamma - z(t\theta)) - a^{t\theta}(w(t\theta) - w(0), \gamma - z(t\theta)) \end{array} \tag{A.51}$$

where:

$$\langle G^\theta, \gamma \rangle = \int_{\Gamma_c^0} r_\theta s \circ T\lambda(\theta)\tau \cdot \gamma \, ds \tag{A.52}$$

and the Taylor expansion of G^θ is:

$$\begin{array}{rcl} \langle G^\theta, \gamma \rangle & = & \langle G^0, \gamma \rangle + \displaystyle\int_{\Gamma_c^0} s\lambda(0) r_0'(\theta)\gamma \cdot \tau \, ds \\ & & + \displaystyle\int_{\Gamma_c^0} s Y_{\lambda(0)}(\theta)\gamma \cdot \tau \, ds + \int_{\Gamma_c^0} \nabla s \cdot \theta\lambda(0)\gamma \cdot \tau \, ds + o(\theta) \\ & = & \langle G^0, \gamma \rangle + \langle (G^0)'(\theta), \gamma \rangle + o(\theta) \end{array} \tag{A.53}$$

Definition A.4.1. *We call l_1, l_2 and l_3 the following linear forms defined on $H^1_{\Gamma_0}(\Omega)^d$:*

$$\langle l_1, \gamma \rangle = \langle F^{t\theta} - F^0 - (F^0)'(t\theta), \gamma \rangle, \tag{A.54}$$

$$\langle l_2, \gamma \rangle = a^0(z(0), \gamma) - a^{t\theta}(w(0), \gamma) + (a^0)'(t\theta)(w(0), \gamma), \tag{A.55}$$

$$\langle l_3, \gamma \rangle = a^0(z(t\theta) - w(0), \gamma) - a^{t\theta}(z(t\theta) - z(0), \gamma), \tag{A.56}$$

$$\langle l_4, \gamma \rangle = \langle G^0, \gamma \rangle + \langle G^{t\theta} - G^0 - t(G^0)'(\theta), \gamma \rangle. \tag{A.57}$$

Lemma A.4.2. *l_1, l_2, l_3 and l_4 are such that their norm in $(H^1_{\Gamma_0}(\Omega)^d)^*$ is a $o(t)$.*

Proof. l_1, l_2, and l_4 are clearly $o(t)$. It remains to work on l_3.

It is clear that the proof of lemma 5.2.5 can be done for l_3 in our case from the begining to (5.19). To complete the proof it is needed to prove a lemma equivalent to lemma 5.2.6 but for our problem. In fact there is one thing to change in the proof: the right hand side which becomes:

$$\langle F^{t\theta}, \gamma - z(t\theta)\rangle - \int_{\Gamma_c^0} s \circ Tr_{t\theta}\lambda(t\theta)(\gamma - z(t\theta)) \cdot \tau \, ds$$

and which is not reduced to $\langle F^{t\theta}, \gamma - z(t\theta)\rangle$ anymore. First we define:

$$\langle M(\theta), \gamma\rangle = \int_{\Gamma_c^0} r_\theta s \circ T\lambda(\theta)\gamma \cdot \tau \, ds. \tag{A.58}$$

In view of the proof of lemma 5.2.6, we just need to prove an inequality of the form:

$$\|M(t\theta) - M(0)\|_{H^{-1}} \leq Ct \|\theta\|_{W^{2,\infty}} + o(t). \tag{A.59}$$

First we compute the Taylor expansion of $M(t\theta)$:

$$\begin{aligned} \langle M(t\theta), \gamma\rangle &= \langle M(0), \gamma\rangle + t\int_{\Gamma_c^0} sY_{\lambda(0)}(\theta)\gamma \cdot \tau \, ds \\ &\quad + t\int_{\Gamma_c^0} (sr_0'(\theta) + \nabla g \cdot \theta)\lambda(0)\gamma \cdot \tau \, ds + o(t) \\ &= \langle M(0), \gamma\rangle + t\langle (M^0)'(\theta), \gamma\rangle + o(t) \end{aligned} \tag{A.60}$$

where $|o(t)| \leq o_5(t)\|\gamma\|_{H^1}$ where $o_5(t)$ is independent of γ. First we bound:

$$|\langle (M^0)'(\theta), \gamma\rangle| \leq C\|\theta\|_{W^{1,\infty}} \|\lambda(0)\|_{\left(H^{\frac{1}{2}}\right)^*} \|\gamma\|_{H^{\frac{1}{2}}} + C\|\gamma\|_{H^{\frac{1}{2}}} \left\|Y_{\lambda(0)}(\theta)\right\|_{\left(H^{\frac{1}{2}}\right)^*}. \tag{A.61}$$

We need to bound $\left\|Y_{\lambda(0)}(\theta)\right\|_{\left(H^{\frac{1}{2}}\right)^*}$. To do that, take (A.28) with $\xi = 0$, using coercivity of b^0,(A.23) and (A.30):

$$\begin{aligned} C_0' \left\|Y_{\lambda(0)}(\theta)\right\|^2_{\left(H^{\frac{1}{2}}\right)^*} &\leq \langle (\Xi^0)'(\theta), Y_{\lambda(0)}(\theta)\rangle + (b^0)'(\theta)(\lambda(0), Y_{\lambda(0)}(\theta)) \\ &\leq C\|\theta\|_{W^{1,\infty}} \|\omega(0)\cdot\tau\|_{H^{\frac{1}{2}}} \left\|Y_{\lambda(0)}(\theta)\right\|_{\left(H^{\frac{1}{2}}\right)^*} + C\left\|Y_{\lambda(0)}(\theta)\right\|_{\left(H^{\frac{1}{2}}\right)^*} \left\|Y_{\omega(0)}(\theta)\right\|_{H^{\frac{1}{2}}} \\ &\quad + C\|\lambda(0)\|_{\left(H^{\frac{1}{2}}\right)^*} \left\|Y_{\Psi^0(\lambda(0))}(\theta)\right\|_{\left(H^{\frac{1}{2}}\right)}. \end{aligned} \tag{A.62}$$

Again we need to bound $\left\|Y_{\omega(0)}(\theta)\right\|_{H^{\frac{1}{2}}}$. Thanks to (5.33), $Y_{\omega(0)}(\theta)$ is the solution of the following variational inequation in $S^{\omega(0)}(K(\Omega_0))$:

$$a^0(Y_{\omega(0)}(\theta), \gamma - Y_{\omega(0)}(\theta)) \geq \langle (F^0)'(\theta), \gamma - Y_{\omega(0)}(\theta)\rangle - (a^0)'(\theta)(w(0), \gamma - Y_{\omega(0)}(\theta)). \tag{A.63}$$

Taking $\phi = 0$, using the coercivity of a^0, (5.18) and (5.19) and (5.23):

$$\left\|Y_{\omega(0)}(\theta)\right\|_{H^1} \leq C\|\theta\|_{W^{2,\infty}}(1 + \|\omega(0)\|_{H^1}).$$

Using the trace theorem:

$$\left\|Y_{\omega(0)}(\theta)\right\|_{H^{\frac{1}{2}}} \leq C\|\theta\|_{W^{2,\infty}}(1 + \|\omega(0)\|_{H^1})$$

and then

$$\left\|Y_{\lambda(0)}(\theta)\right\|_{\left(H^{\frac{1}{2}}\right)^*} \leq C\|\theta\|_{W^{2,\infty}}.$$

Eventually:

$$|\langle (M^0)'(\theta), \gamma\rangle| \leq C\|\theta\|_{W^{2,\infty}} \|\gamma\|_{H^{\frac{1}{2}}} \tag{A.64}$$

and the trace theorem enables to conclude that:

$$|\langle M(\theta) - M(0), \gamma\rangle| \leq Ct\|\theta\|_{W^{2,\infty}} \|\gamma\|_{H^1} + o_5(t)\|\gamma\|_{H^1}$$

which gives (A.59). Then we can finish the proof exactly as in lemma 5.2.6 and lemma 5.2.5.

□

Theorem A.4.3. *The Lagrangian conical derivative of $u(\theta)$, $Y_{u(0)}(\theta)$ is the solution of the following inequation in S:*

$$\begin{aligned} a^0(Y_{u(0)}(\theta), \phi - Y_{u(0)}(\theta)) &\geq \langle (F^0)'(\theta), \phi - Y_{u(0)}(\theta)\rangle - (a^0)'(\theta)(u(0), \phi - Y_{u(0)}(\theta)) \\ &\quad -\langle (M^0)'(\theta), \phi - Y_{u(0)}(\theta)\rangle + a^0(\nabla\theta u(0), \phi - Y_{u(0)}(\theta)) \end{aligned} \tag{A.65}$$

with:

$$S = \left\{\phi \in W,\ \phi.n \leq (\nabla\theta u(0)).n \text{ q.e on } w(0).n = 0 \text{ and } a^0(w(0), \phi) = \langle F^0, \phi\rangle + a^0(\nabla\theta u(0), \phi)\right\} \tag{A.66}$$

and:

$$W = \left\{\phi \in H^1(\Omega)^d,\ \exists\psi \in H^1_{\Gamma_0}(\Omega_0)^d,\ \phi = \psi + \nabla\theta u(0)\right\}. \tag{A.67}$$

Proof. As we have lemma A.4.2, and that the inequation solved by $z(\theta)$ is in $K(\Omega_0)$ (as it was the case for contact problem without friction), the proof of the theorem is exactly the same as theorem 5.2.7

□

Bibliography

[1] T. Abballe, M. Albertelli, G. Allaire, A. Caron, P. Conraux, L. Dall 'olio, C. Dapogny, C. Dobrzynski, B. Jeannin, F. Jouve, D. Lachouette, T. Le Sommer, K. Maquin, G. Michailidis, M. Siavelis, and V. Srithammavanh. RODIN project, Topology Optimization 2.0? *Actes du congrès "simulation" de la société des ingénieurs de l'automobile (SIA), Montigny le Bretonneux, 18-19 mars*, Mar. 2015.

[2] B. A. Akbora, R. B. Corotis, and J. H. Ellis. Optimization of structural frames with elastic and plastic constraints. *Civil Engineering Systems*, 10(2):147–169, 1993.

[3] S. S. Akmal, N. M. Nam, and J. Veerman. On a convex set with nondifferentiable metric projection. *Optimization Letters*, 9(6):1039–1052, 2015.

[4] E. Alba. *Parallel evolutionary computations*, volume 22. springer, 2006.

[5] G. Allaire. *Conception optimale de structures*, volume 58 of *Mathématiques & Applications (Berlin)*. Springer-Verlag, Berlin, 2007.

[6] G. Allaire. *Shape optimization by the homogenization method*, volume 146. Springer Science & Business Media, 2012.

[7] G. Allaire, F. De Gournay, F. Jouve, and A. Toader. Structural optimization using topological and shape sensitivity via a level set method. *Control and cybernetics*, 34(1):59, 2005.

[8] G. Allaire and F. Jouve. Minimum stress optimal design with the level set method. *Engineering analysis with boundary elements*, 32(11):909–918, 2008.

[9] G. Allaire, F. Jouve, and A.-M. Toader. A level-set method for shape optimization. *Comptes Rendus Mathématique*, 334(12):1125–1130, 2002.

[10] G. Allaire, F. Jouve, and A.-M. Toader. Structural optimization by the level-set method. *International Series of Numerical Mathematics, Vol. 147*, pages 1–15, 2003.

[11] G. Allaire and R. V. Kohn. Optimal design for minimum weight and compliance in plane stress using extremal microstructures. *European journal of mechanics. A. Solids*, 12(6):839–878, 1993.

[12] A. Amassad, D. Chenais, and C. Fabre. Optimal control of an elastic contact problem involving tresca friction law. *Nonlinear Analysis, 48*, pages 1107–1135, 2002.

[13] L. Ambrosio. Existence theory for a new class of variational problems. *Archive for Rational Mechanics and Analysis*, 111(4):291–322, 1990.

[14] L. Ambrosio. Lecture notes on geometric evolution problems, distance function and viscosity solutions. *Centre National de la Recherche Scientifique*, 1997.

[15] L. Ambrosio and G. Buttazzo. An optimal design problem with perimeter penalization. *Calculus of Variations and Partial Differential Equations*, 1(1):55–69, 1993.

[16] H. Amor, J.-J. Marigo, and C. Maurini. Regularized formulation of the variational brittle fracture with unilateral contact: numerical experiments. *Journal of the Mechanics and Physics of Solids*, 57(8):1209–1229, 2009.

[17] S. Amstutz and H. Andrä. A new algorithm for topology optimization using a level-set method. *Journal of Computational Physics*, 216(2):573–588, 2006.

[18] S. Amstutz and A. A. Novotny. Topological optimization of structures subject to von mises stress constraints. *Structural and Multidisciplinary Optimization*, 41(3):407–420, 2010.

[19] A. Ancona. *Théorie du potentiel dans les espaces fonctionnels à forme coercive*. Cours 3ème cycle multig. Université Paris VI, 1973.

[20] J. Andersson. Optimal regularity and free boundary regularity for the signorini problem. *St. Petersburg Mathematical Journal, Volume 24 (Number 3)*, pages 371–386, 2013.

[21] G. Anzellotti and M. Giaquinta. Existence of the displacements field for an elasto-plastic body subject to hencky's law and von mises yield condition. *manuscripta mathematica*, 32(1-2):101–136, 1980.

[22] I. Athanasopoulos and L. A. Caffarelli. Optimal regularity of lower-dimensional obstacle problems. *Journal of Mathematical Sciences*, 132(3):274–284, 2006.

[23] I. Athanasopoulos, L. A. Caffarelli, and S. Salsa. The structure of the free boundary for lower dimensional obstacle problems. *American journal of mathematics*, 130(2):485–498, 2008.

[24] C. Baiocchi and A. Capelo. *Variational and quasivariational inequalities: applications to free boundary problems*. A Wiley-Interscience publication. Wiley, 1984.

[25] L. Bar, T. F. Chan, G. Chung, M. Jung, L. A. Vese, N. Kiryati, and N. Sochen. Mumford and shah model and its applications to image segmentation and image restoration. *Handbook of Mathematical Methods in Imaging*, pages 1539–1597, 2015.

[26] V. Barbu. *Optimal control of variational inequalities*, volume 100 of *Research Notes in Mathematics*. Pitman (Advanced Publishing Program), Boston, MA, 1984.

[27] S. Bartels, A. Mielke, and T. Roubicek. Quasi-static small-strain plasticity in the limit of vanishing hardening and its numerical approximation. *SIAM Journal on Numerical Analysis*, 50(2):951–976, 2012.

[28] M. P. Bendsøe and N. Kikuchi. Generating optimal topologies in structural design using a homogenization method. *Computer methods in applied mechanics and engineering*, 71(2):197–224, 1988.

[29] M. P. Bendsøe and O. Sigmund. *Topology optimization: theory, methods, and applications*. Springer Science & Business Media, 2013.

[30] A. Bensoussan and J. Frehse. *Regularity results for nonlinear elliptic systems and applications*, volume 151. Springer Science & Business Media, 2013.

[31] P. Beremlijski, J. Haslinger, M. Kocvara, and J. Outrata. Shape optimization in contact problems with coulomb friction. *SIAM J. Optim Vol. 13, No 2*, pages 561–587, 2002.

[32] P. Beremlijski, J. Haslinger, J. Outrata, and R. Patho. Shape optimization in contact problems with coulomb friction and a solution-dependent friction coefficient. *SIAM J. Control Optim. Vol. 52, No 5*, pages 3371–3400, 2014.

[33] M. Bergounioux. Optimal control of an obstacle problem. *Applied Mathematics and Optimization*, 36(2):147–172, 1997.

[34] M. Bergounioux. Optimal control of problems governed by abstract elliptic variational inequalities with state constraints. *SIAM Journal on Control and Optimization*, 36(1):273–289, 1998.

[35] M. Bergounioux and F. Mignot. Optimal control of obstacle problems: existence of lagrange multipliers. *ESAIM: Control, Optimisation and Calculus of Variations*, 5:45–70, 2000.

[36] T. Betz and C. Meyer. Second-order sufficient optimality conditions for optimal control of static elastoplasticity with hardening. *ESAIM: Control, Optimisation and Calculus of Variations*, 21(1):271–300, 2015.

[37] L. Blank, H. Garcke, L. Sarbu, T. Srisupattarawanit, V. Styles, and A. Voigt. Phase-field approaches to structural topology optimization. In *Constrained Optimization and Optimal Control for Partial Differential Equations*, pages 245–256. Springer, 2012.

[38] P. Boieri, F. Gastaldi, and D. Kinderlehrer. Existence, uniqueness, and regularity results for the two-body contact problem. *Appl. Math. Optim., 15*, pages 251–277, 1987.

[39] J. F. Bonnans and E. Casas. An extension of pontryagin's principle for state-constrained optimal control of semilinear elliptic equations and variational inequalities. *SIAM Journal on Control and Optimization*, 33(1):274–298, 1995.

[40] J. F. Bonnans and A. Shapiro. *Perturbation analysis of optimization problems*. Springer Series in Operations Research. Springer-Verlag, New York, 2000.

[41] B. Bourdin and A. Chambolle. Design-dependent loads in topology optimization. *ESAIM: Control, Optimisation and Calculus of Variations*, 9:19–48, 2003.

[42] B. Bourdin and A. Chambolle. The phase-field method in optimal design. In *IUTAM Symposium on Topological Design Optimization of Structures, Machines and Materials*, pages 207–215. Springer, 2006.

[43] B. Bourdin, G. A. Francfort, and J.-J. Marigo. Numerical experiments in revisited brittle fracture. *Journal of the Mechanics and Physics of Solids*, 48(4):797–826, 2000.

[44] B. Bourdin, G. A. Francfort, and J.-J. Marigo. The variational approach to fracture. *Journal of elasticity*, 91(1-3):5–148, 2008.

[45] V. Braibant and C. Fleury. Shape optimal design using b-splines. *Computer Methods in Applied Mechanics and Engineering*, 44(3):247–267, 1984.

[46] H. Brézis. Equations et inéquations non linéaires dans les espaces vectoriels en dualité. 18(1):115–175, 1968.

[47] H. Brézis, P. G. Ciarlet, and J. L. Lions. *Analyse fonctionnelle: théorie et applications*, volume 91. Dunod Paris, 1999.

[48] H. Brézis and S. G. Contrôle dans les inéquations variationelles elliptiques. *Bulletin de la S.M.F. tome 96*, pages 153–180, 1968.

[49] H. Brézis and G. Stampacchia. Sur la régularité de la solution d'inéquations elliptiques. *Bulletin de la Société Mathématique de France*, 96:153–180, 1968.

[50] F. Brezzi and M. Fortin. *Mixed and hybrid finite element methods*, volume 15. Springer Science & Business Media, 2012.

[51] D. Bucur and G. Buttazzo. Variational methods in shape optimization problems, 2005.

[52] T. Burczyński, A. Długosz, and W. Kuś. Parallel evolutionary algorithms in shape optimization of heat radiators. *Journal of Theoretical and Applied Mechanics*, 44(2):351–366, 2006.

[53] M. Burger. A framework for the construction of level set methods for shape optimization and reconstruction. *Interfaces and Free boundaries*, 5(3):301–329, 2003.

[54] G. Buttazzo. *Energies on BV and variational models in fracture mechanics*, volume 5 of *GAKUTO Internat. Ser. Math. Sci. Appl.* Gakkōtosho, Tokyo, 1995.

[55] L. A. Caffarelli. The regularity of free boundaries in higher dimensions. *Acta Mathematica*, 139(1):155–184, 1977.

[56] L. A. Caffarelli. The obstacle problem revisited. *Journal of Fourier Analysis and Applications*, 4(4):383–402, 1998.

[57] L. A. Caffarelli and N. M. Riviere. Smoothness and analyticity of free boundaries in variational inequalities. *Annali della Scuola Normale Superiore di Pisa-Classe di Scienze*, 3(2):289–310, 1976.

[58] L. A. Caffarelli and N. M. Riviere. Asymptotic behavior of free boundaries at their singular points. *Annals of Mathematics*, 106(2):309–317, 1977.

[59] P. Cannarsa and P. Cardaliaguet. Representation of equilibrium solutions to the table problem of growing sandpiles. *Journal of the European Mathematical Society*, 6(4):435–464, 2004.

[60] A. Capatina. Inéquations variationnelles et problèmes de contact avec frottement. *Preprint Series IMAR*, 10:1–210, 2011.

[61] J. Cea. Conception optimale ou identification de formes, calcul rapide de la dérivée directionnelle de la fonction coût. *Modélisation mathématiques et analyse numérique 20-3*, pages 371–402, 1986.

[62] A. Chambolle. A density result in two-dimensional linearized elasticity, and applications. *Archive for rational mechanics and analysis*, 167(3):211–233, 2003.

[63] D. Chamoret, K. Qiu, and M. Domaszewski. Optimization of truss structures by a stochastic method. *International Journal for Simulation and Multidisciplinary Design Optimization*, 3(1):321–325, 2009.

[64] I. Chavel. *Riemannian geometry: a modern introduction*, volume 98. Cambridge university press, 2006.

[65] K. Chełmiński. Perfect plasticity as a zero relaxation limit of plasticity with isotropic hardening. *Mathematical methods in the applied sciences*, 24(2):117–136, 2001.

[66] W.-H. Chen and C.-R. Ou. Shape optimization in contact problems with desired contact traction distribution on the specified contact surface. *Computational Mechanics 15*, pages 534–545, 1995.

[67] D. Chenais. On the existence of a solution in a domain identification problem. *Journal of Mathematical Analysis and Applications*, 52(2):189–219, 1975.

[68] F. Chouly. An adaptation of nitsche´ method to the tresca friction problem. *Journal of Mathematical Analysis and Applications*, 411(1):329–339, 2014.

[69] F. Chouly and P. Hild. A nitsche-based method for unilateral contact problems: numerical analysis. *SIAM Journal on Numerical Analysis*, 51(2):1295–1307, 2013.

[70] F. Chouly and P. Hild. On the convergence of the penalty method for unilateral contact problems. *Applied Numerical Mathematics 65*, pages 27–40, 2013.

[71] F. Chouly, P. Hild, and Y. Renard. Symmetric and non-symmetric variants of nitsches method for contact problems in elasticity: theory and numerical experiments. *Mathematics of Computation*, 84(293):1089–1112, 2015.

[72] P. W. Christensen and A. Klarbring. *An Introduction to Structural Optimization*, volume 153 of *Solid Mechanics and Its Applications*. Springer Netherlands, 2009.

[73] C. Ciarcià and P. Daniele. New existence theorems for quasi-variational inequalities and applications to financial models. *European Journal of Operational Research*, 251(1):288–299, 2016.

[74] P. Ciarlet. *Mathematical elasticity, vol. 1. Three-dimensional elasticity*. Elsevier Science Publishers, 1988.

[75] F. H. Clarke. *Optimization and nonsmooth analysis*, volume 5. Siam, 1990.

[76] M. Cocu. Existence of solutions of signorini problems with friction. *International Journal of Engineering Science*, 22(5):567 – 575, 1984.

[77] M. G. Crandall and P.-L. Lions. Viscosity solutions of hamilton-jacobi equations. *Transactions of the American Mathematical Society*, 277(1):1–42, 1983.

[78] A. Curnier and P. Alart. A generalized Newton method for contact problems with friction. *J. de Mécanique Théorique et Appliquée, special issue entitled "Numerical Methods in Mechanics of Contact involving Friction"*, pages 67–82, 1988.

[79] G. Dal Maso, A. DeSimone, and M. G. Mora. Quasistatic evolution problems for linearly elastic–perfectly plastic materials. *Archive for rational mechanics and analysis*, 180(2):237–291, 2006.

[80] G. Dal Maso, A. DeSimone, M. G. Mora, and M. Morini. A vanishing viscosity approach to quasistatic evolution in plasticity with softening. *Archive for Rational Mechanics and Analysis*, 189(3):469–544, 2008.

[81] G. Dal Maso, A. DeSimone, and F. Solombrino. Quasistatic evolution for cam-clay plasticity: a weak formulation via viscoplastic regularization and time rescaling. *Calculus of Variations and Partial Differential Equations*, 40(1-2):125–181, 2011.

[82] G. Dal Maso, A. DeSimone, and F. Solombrino. Quasistatic evolution for cam-clay plasticity: properties of the viscosity solution. *Calculus of Variations and Partial Differential Equations*, 44(3-4):495–541, 2012.

[83] G. Dal Maso and R. Scala. Quasistatic evolution in perfect plasticity as limit of dynamic processes. *Journal of Dynamics and Differential Equations*, 26(4):915–954, 2014.

[84] C. Dapogny. *Shape optimization, level set methods on unstructured meshes and mesh evolution*. Theses, Université Pierre et Marie Curie - Paris VI, Dec. 2013.

[85] P. Davis and P. Rabinowitz. *Methods of Numerical Integration*. Dover Books on Mathematics Series. Dover Publications, 2007.

[86] F. De Gournay. Velocity extension for the level-set method and multiple eigenvalues in shape optimization. *SIAM journal on control and optimization*, 45(1):343–367, 2006.

[87] J. C. De los Reyes. Optimization of mixed variational inequalities arising in flow of viscoplastic materials. *Computational Optimization and Applications*, 52(3):757–784, 2012.

[88] J. C. De los Reyes, R. Herzog, and C. Meyer. *Optimal control of static elastoplasticity in primal formulation*. Techn. Univ., Fak. für Mathematik, 2013.

[89] M. C. Delfour and J. P. Zolésio. Shape identification via metrics constructed from the oriented distance function. *Control and Cybernetics*, 34(1):137, 2005.

[90] M. C. Delfour and J.-P. Zolésio. *Shapes and geometries: metrics, analysis, differential calculus, and optimization*, volume 22. Siam, 2011.

[91] J.-P. Demailly. *Analyse numérique et équations différentielles*. EDP sciences, 2012.

[92] J. J. Dennis and R. Schnabel. *Numerical methods for unconstrained optimization and nonlinear equations*, volume 16 of *Classics in Applied Mathematics*. Society for Industrial and Applied Mathematics (SIAM), Philadelphia, PA, 1996. Corrected reprint of the 1983 original.

[93] D. Dentcheva. On differentiability of metric projections onto moving convex sets. *Annals of Operations Research*, 101(1-4):283–298, 2001.

[94] B. Desmorat. Structural rigidity optimization with frictionless unilateral contact. *International Journal of Solids and Structures, Volume 44, Issues 3-4*, pages 1132–1144, 2007.

[95] Z. Dimitrovová. A new methodology to establish upper bounds on open-cell foam homogenized moduli. *Structural and Multidisciplinary Optimization*, 29(4):257–271, 2005.

[96] S. Drabla and M. Sofonea. Analysis of a signorini problem with friction. *IMA journal of applied mathematics*, 63(2):113–130, 1999.

[97] S. Drabla, M. Sofonea, and B. Teniou. Analysis of a frictionless contact problem for elastic bodies. 69(1), 1998.

[98] G. Duvaut and J. Lions. *Les inéquations en mécanique et en physique*. Dunod, Paris, 1972. Travaux et Recherches Mathématiques, No. 21.

[99] F. Ebobisse and B. D. Reddy. Some mathematical problems in perfect plasticity. *Computer methods in applied mechanics and engineering*, 193(48):5071–5094, 2004.

[100] C. Eck, J. Jarusek, and M. Krbec. *Unilateral contact problems*, volume 270 of *Pure and Applied Mathematics (Boca Raton)*. Chapman & Hall/CRC, Boca Raton, FL, 2005. Variational methods and existence theorems.

[101] W. Egner, Z. Kordas, and M. Życzkowski. Optimal plastic shape design via the boundary perturbation method. *Structural optimization*, 8(2-3):145–155, 1994.

[102] I. Ekeland and R. Temam. *Convex analysis and variational problems*. SIAM, 1976.

[103] L. C. Evans. *Partial differential equations*. Graduate studies in mathematics. American Mathematical Society, Providence (R.I.), 1998. Réimpr. avec corrections : 1999, 2002.

[104] L. C. Evans and R. F. Gariepy. *Measure theory and fine properties of functions*. CRC press, 2015.

[105] B. Farshi and A. Alinia-ziazi. Sizing optimization of truss structures by method of centers and force formulation. *International Journal of Solids and Structures*, 47(18-19):2508–2524, 2010.

[106] O. Faugeras and R. Keriven. Variational principles, surface evolution, PDE's, level set methods, and the stereo problem. *IEEE Trans. Image Process.*, 7(3):336–344, 1998.

[107] A. V. Fiacco. Sensitivity analysis for nonlinear programming using penalty methods. *Mathematical programming*, 10(1):287–311, 1976.

[108] G. Fichera. Sul problema elastostatico di Signorini con ambigue condizioni al contorno. *Atti Accad. Naz. Lincei, VIII. Ser., Rend., Cl. Sci. Fis. Mat. Nat.*, 34:138–142, 1963.

[109] S. Fitzpatrick and R. Phelps. Differentiability of the metric projection in hilbert space. *Transactions of the American Mathematical Society*, 270(2):483–501, 1982.

[110] I. Fonseca and G. A. Francfort. Relaxation inbv versus quasiconvexification in w 1, p; a model for the interaction between fracture and damage. *Calculus of Variations and Partial Differential Equations*, 3(4):407–446, 1995.

[111] G. Francfort and J.-J. Marigo. Une approche variationnelle de la mécanique du défaut. In *ESAIM: Proceedings*, volume 6, pages 57–74. EDP Sciences, 1999.

[112] G. A. Francfort and J.-J. Marigo. Revisiting brittle fracture as an energy minimization problem. *Journal of the Mechanics and Physics of Solids*, 46(8):1319–1342, 1998.

[113] J. Frehse. On the smoothness of solutions of variational inequalities with obstacles. In *Proc. Semester Partial Diff. Eq., Banach Center, Warszawa*, 1978.

[114] A. Friedman. Optimal control for variational inequalities. *SIAM Journal on Control and Optimization*, 24(3):439–451, 1986.

[115] M. Fuchs and G. Seregin. *Variational methods for problems from plasticity theory and for generalized Newtonian fluids*. Springer Science & Business Media, 2000.

[116] S. Garreau, P. Guillaume, and M. Masmoudi. The topological asymptotic for pde systems: the elasticity case. *SIAM journal on control and optimization*, 39(6):1756–1778, 2001.

[117] C. Ghaddar, Y. Maday, and A. T. Patera. Analysis of a part design procedure. *Numerische Mathematik*, 71(4):465–510, 1995.

[118] R. Glowinsky, J. Lions, and R. Trémolières. *Analyse numérique des inéquations variationnelles. Tome 1.* Dunod, Paris, 1976. Théorie générale premiéres applications, Méthodes Mathématiques de l'Informatique, 5.

[119] H. Goldberg, W. Kampowsky, and F. Tröltzsch. On nemytskij operators in lp-spaces of abstract functions. *Mathematische Nachrichten*, 155(1):127–140, 1992.

[120] A. Grigusevicius and S. Kalanta. Optimization of elastic-plastic beam structures with hardening using finite element method. *Foundations of Civil and Environmental Engineering*, (6):31–52, 2005.

[121] P. Grisvard. Elliptic problems in nonsmooth domains, 1985.

[122] R. T. Haftka and R. V. Grandhi. Structural shape optimization-a survey. *Computer methods in applied mechanics and engineering*, 57(1):91–106, 1986.

[123] W. Han. On the numerical approximation of a frictional contact problem with normal compliance. *Numer. Funct. Anal. Optim., 17*, pages 307–321, 1996.

[124] W. Han and B. D. Reddy. *Plasticity: mathematical theory and numerical analysis*, volume 9. Springer Science & Business Media, 2012.

[125] A. Haraux. How to differentiate the projection on a convex set in hilbert space. some applications to variational inequalities. *J. Math. Soc. Japan, Vol. 29, No. 4*, 1977.

[126] J. Haslinger. Approximation of the signorini problem with friction, obeying coulomb law. *Math. Methods Appl. Sci., 5, No. 3*, pages 422–437, 1983.

[127] J. Haslinger. Shape optimization in contact problems. *Equadiff 6, Proceedings of the International Conference on Differential Equations and Their Applications*, pages 445–450, 1986.

[128] J. Haslinger. Signorini problem with coulomb law of friction. shape optimization in contact problems. *International Journal for Numerical methods in engineering, vol. 34*, pages 223–231, 1992.

[129] J. Haslinger et al. *Introduction to shape optimization: theory, approximation, and computation*, volume 7. Siam, 2003.

[130] J. Haslinger and A. Klarbring. Shape optimization in unilateral contact problems using generalized reciprocal energy as objective functional. *Nonlinear Analysis, Theory, Methods and Applications, Vol. 21, No. 11*, pages 815–834, 1993.

[131] J. Haslinger and R. Mäkinen. Shape optimization of elasto-plastic bodies under plane strains: sensitivity analysis and numerical implementation. *Structural optimization*, 4(3-4):133–141, 1992.

[132] J. Haslinger and P. Neittaanmäki. On the existence of optimal shapes in contact problems. *Numer. funct. anal. and optimiz., 7(2 and 3)*, pages 107–124, 1985.

[133] J. Haslinger and P. Neittaanmäki. On the existence of optimal shapes in contact problems—perfectly plastic bodies. *Computational mechanics*, 1(4):293–299, 1986.

[134] J. Haslinger and P. Neittaanmäki. Shape optimization in contact problems. approximation and numerical realization. *Mathematical Modelling and Numerical Analysis, Vol. 21, No. 2*, pages 269–291, 1987.

[135] J. Haslinger, P. Neittaanmäki, and T. Tiihonen. Shape optimization in contact problems. 1. design of an elastic body. 2. design of an elastic perfectly plastic body. In *Analysis and Optimization of Systems*, pages 29–39. Springer, 1986.

[136] L. L. V. Helms. *Potential theory*. Springer, 2009.

[137] A. Henrot and M. Pierre. *Variation et optimisation de formes*, volume 48 of *Mathématiques & Applications (Berlin) [Mathematics & Applications]*. Springer, Berlin, 2005. Une analyse géométrique. [A geometric analysis].

[138] R. Herzog and C. Meyer. Optimal control of static plasticity with linear kinematic hardening. *ZAMM-Journal of Applied Mathematics and Mechanics/Zeitschrift für Angewandte Mathematik und Mechanik*, 91(10):777–794, 2011.

[139] R. Herzog, C. Meyer, and G. Wachsmuth. Integrability of displacement and stresses in linear and nonlinear elasticity with mixed boundary conditions. *Journal of Mathematical Analysis and Applications*, 382(2):802–813, 2011.

[140] R. Herzog, C. Meyer, and G. Wachsmuth. C-stationarity for optimal control of static plasticity with linear kinematic hardening. *SIAM Journal on Control and Optimization*, 50(5):3052–3082, 2012.

[141] R. Herzog, C. Meyer, and G. Wachsmuth. B-and strong stationarity for optimal control of static plasticity with hardening. *SIAM Journal on Optimization*, 23(1):321–352, 2013.

[142] R. Herzog, C. Meyer, and G. Wachsmuth. Optimal control of elastoplastic processes: Analysis, algorithms, numerical analysis and applications. In *Trends in PDE Constrained Optimization*, pages 27–41. Springer, 2014.

[143] P. Hild. Two results on solution uniqueness and multiplicity for the linear elastic friction problem with normal compliance. *Nonlinear Analysis 71*, pages 5560–5571, 2009.

[144] D. Hilding, A. Klarbring, and J. Petersson. Optimization of structures in unilateral contact. *ASME Appl Mech Rev, vol 52, No 4*, pages 1–4, 1999.

[145] M. Hintermüller and A. Laurin. Optimal shape design subject to elliptic variational inequalities. *SIAM J. Control. Optim., Vol. 49, No 3*, pages 1015–1047, 2011.

[146] I. Hlaváček. Shape optimization of elastoplastic bodies obeying hencky's law. *Aplikace matematiky*, 31(6):486–499, 1986.

[147] I. Hlaváček. Shape optimization of an elasto-perfectly plastic body. *Aplikace matematiky*, 32(5):381–400, 1987.

[148] I. Hlaváček. Shape optimization of elasto-plastic axisymmetric bodies. *Applications of Mathematics*, 36(6):469–491, 1991.

[149] R. B. Holmes. Smoothness of certain metric projections on hilbert space. *Transactions of the American Mathematical Society*, 184:87–100, 1973.

[150] K. Ito and K. Kunisch. Optimal control of elliptic variational inequalities. *Applied Mathematics and Optimization*, 41(3):343–364, 2000.

[151] K. Ito and K. Kunisch. *Lagrange multiplier approach to variational problems and applications*, volume 15. SIAM, 2008.

[152] T. Iwai, A. Sugimoto, T. Aoyama, and H. Azegami. Shape optimization problem of elastic bodies for controlling contact pressure. *JSIAM Letters Vol.2*, pages 1–4, 2010.

[153] J. Jarusek and J. V. Outrata. On sharp necessary optimality conditions in control of contact problems with strings. *Nonlinear Analysis: Theory, Methods & Applications*, 67(4):1117–1128, 2007.

[154] K. Jittorntrum. Solution point differentiability without strict complementarity in nonlinear programming. In *Sensitivity, Stability and Parametric Analysis*, pages 127–138. Springer, 1984.

[155] C. Johnson. A mixed finite element method for plasticity problems with hardening. *SIAM Journal on Numerical Analysis*, 14(4):575–583, 1977.

[156] J.-L. Joly and U. Mosco. A propos de l'existence et de la régularité des solutions de certaines inéquations quasi-variationnelles. *Journal of Functional Analysis*, 34(1):107–137, 1979.

[157] S. Kaliszky, J. Logo, and T. Havady. Optimal design of elasto-plastic structures under various loading conditions and displacement constraints. *Periodica Polytechnica. Civil Engineering*, 33(3-4):107, 1989.

[158] C. Kane and M. Schoenauer. Topological optimum design using genetic algorithms. *Control and Cybernetics*, 25:1059–1088, 1996.

[159] R. Karkauskas. Optimization of elastic-plastic geometrically non-linear lightweight structures under stiffness and stability constraints. *Journal of Civil Engineering and Management*, 10(2):97–106, 2004.

[160] J. Kato, H. Hoshiba, S. Takase, K. Terada, and T. Kyoya. Analytical sensitivity in topology optimization for elastoplastic composites. *Structural and Multidisciplinary Optimization*, 52(3):507–526, 2015.

[161] M. Khanzadi and S. M. Tavakkoli. Optimal plastic design of frames using evolutionary structural optimization. *International Journal of Civil Engineering*, 9(3), 2011.

[162] A. Khludnev. Optimal control in one-dimensional elastic-plastic models. *Journal of applied mechanics and technical physics*, 32(5):760–763, 1991.

[163] N. Kikuchi and J. T. Oden. *Contact problems in elasticity: a study of variational inequalities and finite element methods*, volume 8. siam, 1988.

[164] N. H. Kim, K. K. Choi, and J. Chen. Shape design sensitivity analysis and optimization of elasto-plasticity with frictional contact. *AIAA Journal, Vol. 38, No. 9*, pages 1742–1753, 2000.

[165] N. H. Kim, K. K. Choi, J. Chen, and Y. Park. Meshless shape design sensitivity analysis and optimization for contact problem with friction. *Computational Mechanics 25*, pages 157–168, 2000.

[166] N. H. Kim, K. K. Choi, and J. S. Chen. Structural optimization of finite deformation elastoplasticity using continuum-based shape design sensitivity formulation. *Computers & Structures*, 79(20):1959–1976, 2001.

[167] N. H. Kim, Y. H. Park, and K. K. Choi. Optimization of a hyper-elastic structure with multibody contact using continuum-based shape design sensitivity analysis. *Structural and multidisciplinary optimization*, 21(3):196–208, 2001.

[168] D. Kinderlehrer and L. Nirenberg. Regularity in free boundary problems. *Annali della Scuola Normale Superiore di Pisa-Classe di Scienze*, 4(2):373–391, 1977.

[169] D. Kinderlehrer and G. Stampacchia. *An introduction to variational inequalities and their applications*, volume 88 of *Pure and Applied Mathematics*. Academic Press, Inc. [Harcourt Brace Jovanovich, Publishers], New York-London, 1980.

[170] U. Kirsch. On singular topologies in optimum structural design. *Structural Optimization*, 2(3):133–142, 1990.

[171] A. Klarbring, A. Mikelic, and M. Shillor. On friction problems with normal compliance. *Nonlinear analysis theory methods and applications, Vol 13, No 8*, pages 935–955, 1989.

[172] A. Klarbring, A. Mikelic, and M. Shillor. Optimal shape design in contact problems with normal compliance and friction. *Appl. Math. Lett. Vol.5, No 2*, pages 51–55, 1992.

[173] D. Knees and A. Schröder. Global spatial regularity for elasticity models with cracks, contact and other nonsmooth constraints. *Math. Meth. Appl. Sci., 35*, pages 1859–1884, 2012.

[174] M. Kocvara and J. V. Outrata. Shape optimization of elasto-plastic bodies governed by variational inequalities. *Boundary Control and Variation*, page 261, 1994.

[175] M. A. Krasnoselskiĭ, P. P. Zabreĭko, E. I. Pustylnik, and P. E. Sobolevskiĭ. *Integral operators in spaces of summable functions*. Noordhoff International Publishing, Leiden, 1976. Translated from the Russian by T. Ando, Monographs and Textbooks on Mechanics of Solids and Fluids, Mechanics: Analysis.

[176] A. S. Kravchuk and P. J. Neittaanmäki. *Variational and quasi-variational inequalities in mechanics*, volume 147. Springer Science & Business Media, 2007.

[177] J. Kruskal. Two convex counterexamples: A discontinuous envelope function and a nondifferentiable nearest-point mapping. *Proceedings of the American Mathematical Society*, 23(3):697–703, 1969.

[178] P. Laborde and Y. Renard. Fixed point strategies for elastostatic frictional contact problems. *Math. Meth. Appl. Sci., 31*, pages 415–441, 2008.

[179] J. Lafontaine. *Introduction aux variétés différentielles*. EDP sciences, 2012.

[180] M. Lawry and K. Maute. Level set topology optimization of problems with sliding contact interfaces. *Struct Multidisc Optim, Vol. 52, Issue 6*, pages 1107–1119, 2015.

[181] C. Le, J. Norato, T. Bruns, C. Ha, and D. Tortorelli. Stress-based topology optimization for continua. *Structural and Multidisciplinary Optimization*, 41(4):605–620, 2010.

[182] H. Le Dret. *Équations aux dérivées partielles elliptiques non linéaires*. Springer, 2013.

[183] E. Lee, K. A. James, and J. R. Martins. Stress-constrained topology optimization with design-dependent loading. *Structural and Multidisciplinary Optimization*, 46(5):647–661, 2012.

[184] T. Lee, J. Arora, and V. Kumar. Shape design sensitivity analysis of viscoplastic structures. *Computer methods in applied mechanics and engineering*, 108(3):237–259, 1993.

[185] A. B. Levy. Sensitivity of solutions to variational inequalities on banach spaces. *SIAM Journal on Control and Optimization*, 38(1):50–60, 1999.

[186] H. Lewy and G. Stampacchia. On the regularity of the solution of a variational inequality. *Communications on Pure and Applied Mathematics*, 22(2):153–188, 1969.

[187] W. Li, G. Steven, and Y. Xie. Shape design for two-and three-dimensional contact problems using an evolutionary method. *International Journal of Computational Engineering Science*, 2(02):181–198, 2001.

[188] J. L. Lions and E. Magenes. *Non-homogeneous boundary value problems and applications*, volume 1. Springer Science & Business Media, 2012.

[189] X. Liu, W.-J. Yi, Q. Li, and P.-S. Shen. Genetic evolutionary structural optimization. *Journal of Constructional Steel Research*, 64(3):305 – 311, 2008.

[190] D. Löbach. *Interior stress regularity for the Prandtl Reuss and Hencky model of perfect plasticity using the Perzyna approximation*. Number 386. Rheinische Friedrich-Wilhelms-Universität, Mathematisches Institut, 2007.

[191] Y. Luo, M. Y. Wang, and Z. Kang. An enhanced aggregation method for topology optimization with local stress constraints. *Computer Methods in Applied Mechanics and Engineering*, 254:31–41, 2013.

[192] A. Mainik and A. Mielke. Existence results for energetic models for rate-independent systems. *Calculus of Variations and Partial Differential Equations*, 22(1):73–99, 2005.

[193] K. Malanowski. Differentiability with respect to parameters of solutions to convex programming problems. *Mathematical Programming*, 33(3):352–361, 1985.

[194] K. Malanowski. Stability and sensitivity of solutions to nonlinear optimal control problems. *Applied Mathematics and Optimization*, 32(2):111–141, 1995.

[195] K. Malanowski. Remarks on differentiability of metric projections onto cones of nonnegative functions. *Journal of Convex Analysis*, 10(1):285–294, 2003.

[196] R. Malladi, J. A. Sethian, and B. C. Vemuri. A fast level set based algorithm for topology-independent shape modeling. *Journal of Mathematical Imaging and Vision*, 6(2-3):269–289, 1996.

[197] N. D. Mankame and G. K. Ananthasuresh. Topology optimization for synthesis of contact-aided compliant mechanisms using regularized contact modeling. *International Conference on Modeling, Simulation and Optimization for Design of Multi-disciplinary Engineering Systems 24-26 September, Goa, India*, 2004.

[198] C. Mantegazza, A. C. Mennucci, et al. Hamilton-jacobi equations and distance functions on riemannian manifolds. *Applied Mathematics and Optimization*, 47(1):1–26, 2003.

[199] J.-J. Marigo. *Plasticité et Rupture*. Ecole Polytechnique, July 2012. Lecture.

[200] J. Martins, J. Oden, and M. Shillor. Models and computational methods for dynamic friction phenomena. *Comput. Methods Appl. Mech. Engrg. 52*, pages 527–634, 1985.

[201] K. Maute, S. Schwarz, and E. Ramm. Adaptive topology optimization of elastoplastic structures. *Structural Optimization*, 15(2):81–91, 1998.

[202] G. Michailidis. *Manufacturing Constraints and Multi-Phase Shape and Topology Optimization via a Level-Set Method*. Theses, Ecole Polytechnique X, Jan. 2014.

[203] P. Michaleris, D. A. Tortorelli, and C. A. Vidal. Tangent operators and design sensitivity formulations for transient non-linear coupled problems with applications to elastoplasticity. *International Journal for Numerical Methods in Engineering*, 37(14):2471–2499, 1994.

[204] A. Mielke. Evolution of rate-independent systems. *Handbook of differential equations: Evolutionary equations*, 2:461–559, 2006.

[205] F. Mignot. Contrôle dans les inéquations variationelles elliptiques. *Journal of Functional Analysis*, 22(2):130–185, 1976.

[206] I. Milne, R. Ritchie, and B. Karihaloo. *Comprehensive structural integrity*. Elsevier Science, 2003.

[207] R. Monneau. *Problèmes de frontières libres, EDP elliptiques non linéaires et applications(en combustion, supraconductivité et élasticité)*. PhD thesis, Paris 6, 1999.

[208] R. Monneau. A brief overview on the obstacle problem. In *European Congress of Mathematics*, pages 303–312. Springer, 2001.

[209] R. Monneau. On the number of singularities for the obstacle problem in two dimensions. *The Journal of Geometric Analysis*, 13(2):359–389, 2003.

[210] J. J. Moreau. Evolution problem associated with a moving convex set in a hilbert space. *Journal of Differential Equations*, 26(3):347 – 374, 1977.

[211] J. J. Moreau and P. D. Panagiotopoulos. *Nonsmooth mechanics and applications*, volume 302. Springer, 2014.

[212] U. Mosco. *Implicit variational problems and quasi variational inequalities*. Springer, 1976.

[213] W. Mulder, S. Osher, and J. A. Sethian. Computing interface motion in compressible gas dynamics. *Journal of Computational Physics*, 100(2):209–228, 1992.

[214] D. Mumford and J. Shah. Optimal approximations by piecewise smooth functions and associated variational problems. *Communications on pure and applied mathematics*, 42(5):577–685, 1989.

[215] D. J. Munk, G. A. Vio, and G. P. Steven. Topology and shape optimization methods using evolutionary algorithms: a review. *Structural and Multidisciplinary Optimization*, 52(3):613–631, 2015.

[216] Y. Murase, R. Kano, and N. Kenmochi. Elliptic quasi-variational inequalities and applications. *DYNAMICAL SYSTEMS*, pages 583–591, 2009.

[217] F. Murat and J. Simon. Etude de problèmes d'optimal design. In *IFIP Technical Conference on Optimization Techniques*, pages 54–62. Springer, 1975.

[218] F. Murat and S. Simon. Etudes de problèmes d'optimal design. *Lecture Notes in Computer Science 41, Springer Verlag, Berlin*, pages 54–62, 1976.

[219] J. Nocedal and S. Wright. *Numerical optimization*. Springer Science & Business Media, 2006.

[220] D. Noll. Directional differentiability of the metric projection in hilbert space. *Pacific Journal of Mathematics*, 170(2):567–592, 1995.

[221] M. A. Noor. Sensitivity analysis for quasi-variational inequalities. *Journal of Optimization Theory and Applications*, 95(2):399–407, 1997.

[222] A. A. Novotny and J. Sokołowski. *Topological derivatives in shape optimization*. Springer Science & Business Media, 2012.

[223] S. Osher and R. Fedkiw. *Level set methods and dynamic implicit surfaces*, volume 153 of *Applied Mathematical Sciences*. Springer-Verlag, New York, 2003.

[224] S. Osher and J. Sethian. Front propagating with curvature dependent speed: algorithms based on hamilton-jacobi formulations. *J. Comp. Phys., 78*, pages 12–49, 1988.

[225] S. J. Osher and F. Santosa. Level set methods for optimization problems involving geometry and constraints. *Journal of Computational Physics*, 171(1):272 – 288, 2001.

[226] J. Outrata. On the numerical solution of a class of stackelberg problems. *Methods and Models of Operations Research 34*, pages 255–277, 1990.

[227] J. Outrata, J. Jarusek, and J. Stará. On optimality conditions in control of elliptic variational inequalities. *Set-Valued and Variational Analysis*, 19(1):23–42, 2011.

[228] I. Paczelt and T. Szabo. Optimal shape design for contact problems. *Structural Optimization 7*, pages 66–75, 1994.

[229] P. D. Panagiotopoulos. *Inequality Problems in Mechanics and Applications: Convex and nonconvex energy functions*. Springer Science & Business Media, 2012.

[230] C. B. Pedersen. Topology optimization of 2d-frame structures with path-dependent response. *International Journal for Numerical Methods in Engineering*, 57(10):1471–1501, 2003.

[231] A. Petrosyan, H. Shahgholian, N. N. Uraltseva, and H. Shahgholian. *Regularity of free boundaries in obstacle-type problems*, volume 136. American Mathematical Society Providence (RI), 2012.

[232] O. Pironneau. *Optimal shape design for elliptic systems*. Springer Series in Computational Physics. Springer-Verlag, New York, 1984.

[233] V. Pištora. Shape optimization of an elasto-plastic body for the model with strain-hardening. *Aplikace matematiky*, 35(5):373–404, 1990.

[234] C. Pozzolini. *Continuation contact problems for plates*. Theses, Université de Provence - Aix-Marseille I, Jan. 2009.

[235] R. Rannacher and F.-T. Suttmeier. A posteriori error estimation and mesh adaptation for finite element models in elasto-plasticity. *Computer Methods in Applied Mechanics and Engineering*, 176(1):333–361, 1999.

[236] B. D. Reddy. Existence of solutions to a quasistatic problem in elastoplasticity. In *Progress in partial differential equations: calculus of variations, applications (Pont-à-Mousson, 1991)*, volume 267 of *Pitman Res. Notes Math. Ser.*, pages 299–311. Longman Sci. Tech., Harlow, 1992.

[237] Y. Renard. Generalized newton's methods for the approximation and resolution of frictional contact problems in elasticity. *Computer Methods in Applied Mechanics and Engineering*, 256:38–55, 2013.

[238] S. Repin. Errors of finite element methods for perfect plasticity. *Math. Mod. Meth. Appl. Sci*, 5:587–604, 1996.

[239] R. T. Rockafellar. *Convex analysis*. Princeton university press, 2015.

[240] J.-F. Rodrigues. *Obstacle problems in mathematical physics*, volume 134. Elsevier, 1987.

[241] E. Rohan and J. Whiteman. Shape optimization of elasto-plastic structures and continua. *Computer Methods in Applied Mechanics and Engineering*, 187(1):261–288, 2000.

[242] T. Roubíček. *Nonlinear partial differential equations with applications*, volume 153. Springer Science & Business Media, 2013.

[243] G. Rozvany. On design-dependent constraints and singular topologies. *Structural and Multidisciplinary Optimization*, 21(2):164–172, 2001.

[244] G. Rozvany and T. Birker. On singular topologies in exact layout optimization. *Structural optimization*, 8(4):228–235, 1994.

[245] L. I. Rudin and S. Osher. Total variation based image restoration with free local constraints. In *Image Processing, 1994. Proceedings. ICIP-94., IEEE International Conference*, volume 1, pages 31–35. IEEE, 1994.

[246] M. Sauter. *Numerical analysis of algorithms for infinitesimal associated and non-associated elasto-plasticity*. PhD thesis, Karlsruher Inst. für Technologie, Diss., 2010, 2010.

[247] D. G. Schaeffer. An example of generic regularity for a non-linear elliptic equation. *Archive for Rational Mechanics and Analysis*, 57(2):134–141, 1974.

[248] R. Schumann. Regularity for signorini's problem in linear elasticity. *manuscripts math. 63*, pages 255–291, 1989.

[249] H. Schwarz. *Gesammelte Mathematische Abhandlungen*, volume 2. Berlin J. Springer, 1890.

[250] S. Schwarz, K. Maute, and E. Ramm. Topology and shape optimization for elastoplastic structural response. *Computer Methods in Applied Mechanics and Engineering*, 190(15):2135–2155, 2001.

[251] J. Sethian. *Level set methods and fast marching methods*, volume 3 of *Cambridge Monographs on Applied and Computational Mathematics*. Cambridge University Press, Cambridge, second edition, 1999. Evolving interfaces in computational geometry, fluid mechanics, computer vision, and materials science.

[252] J. Sethian and P. Smereka. Level set methods for fluid interfaces. *Annual Review of Fluid Mechanics*, 35(1):341–372, 2003.

[253] J. A. Sethian and A. Wiegmann. Structural boundary design via level set and immersed interface methods. *Journal of computational physics*, 163(2):489–528, 2000.

[254] A. Shapiro. Directional differentiability of metric projections onto moving sets at boundary points. *Journal of mathematical analysis and applications*, 131(2):392–403, 1988.

[255] A. Shapiro. Sensitivity analysis of nonlinear programs and differentiability properties of metric projections. *SIAM Journal on Control and Optimization*, 26(3):628–645, 1988.

[256] A. Shapiro. On concepts of directional differentiability. *Journal of optimization theory and applications*, 66(3):477–487, 1990.

[257] A. Shapiro. Directionally nondifferentiable metric projection. *Journal of optimization theory and applications*, 81(1):203–204, 1994.

[258] A. Shapiro. Existence and differentiability of metric projections in hilbert spaces. *SIAM Journal on Optimization*, 4(1):130–141, 1994.

[259] A. Shapiro. Differentiability properties of metric projections onto convex sets. *Journal of Optimization Theory and Applications*, 169(3):953–964, 2016.

[260] M. Šilhavỳ. Differentiability of the metric projection onto a convex set with singular boundary points. *Journal of Convex Analysis*, 22(4):969–997, 2015.

[261] J. C. Simo and T. J. Hughes. *Computational inelasticity*, volume 7. Springer Science & Business Media, 2006.

[262] J. Simon. Differentiation with respect to the domain in boundary value problems. *Num. Funct. Anal. Optimiz, 2*, pages 649–687, 1980.

[263] M. Sofonea and A. Matei. *Variational inequalities with applications: a study of antiplane frictional contact problems*, volume 18. Springer Science & Business Media, 2009.

[264] M. Sofonea and A. Matei. *Mathematical models in contact mechanics*. Number 398. Cambridge University Press, 2012.

[265] J. Sokolowski. Sensitivity analysis of contact problems with prescribed friction. *Applied Mathematics and Optimization, 18, No. 2*, pages 99–117, 1988.

[266] J. Sokolowski and A. Zochowski. On the topological derivative in shape optimization. *SIAM journal on control and optimization*, 37(4):1251–1272, 1999.

[267] J. Sokolowski and A. Żochowski. Topological derivatives of shape functionnals for elasticity systems. *Mechanics of Structures and Machines*, 29(3):331–349, 2001.

[268] J. Sokołowski and A. Żochowski. Modelling of topological derivatives for contact problems. *Numerische Mathematik*, 102(1):145–179, 2005.

[269] J. Sokolowski and J.-P. Zolesio. *Introduction to shape optimization*, volume 16 of *Springer Series in Computational Mathematics*. Springer-Verlag, Berlin, 1992. Shape sensitivity analysis.

[270] J. Steiner and K. Weierstrass. *Jacob Steiner: Gesammelte Werke*. Number vol. 2. De Gruyter, 1882.

[271] J. Strain. Semi-lagrangian methods for level set equations. *Journal of Computational Physics*, 151(2):498–533, 1999.

[272] N. Strömberg and A. Klarbring. Topology optimization of structures with contact constraints by using a smooth formulation and a nested approach. *8th Wolrd Congress on Strucutral and Multidisciplinary Optimization*, 2009.

[273] N. Strömberg and A. Klarbring. Topology optimization of structures in unilateral contact. *Struct Multidisc Optim, 41*, pages 57–64, 2010.

[274] S. Stupkiewicz, J. Lengiewicz, and J. Korelc. Sensitivity analysis for frictional contact problems in the augmented lagrangian formulation. *Computer Methods in Applied Mechanics and Engineering 199*, pages 2165–2176, 2010.

[275] P. M. Suquet. Sur un nouveau cadre fonctionnel pour les équations de la plasticité. *CR Acad. Sci. Paris Sér. AB*, 286:1129–1132, 1978.

[276] P. M. Suquet. Un espace fonctionnel pour les équations de la plasticité. In *Annales de la Faculté des sciences de Toulouse: Mathématiques*, volume 1, pages 77–87. Université Paul Sabatier, 1979.

[277] P. M. Suquet. Sur les équations de la plasticité: existence et régularité des solutions. *J. Mécanique*, 20(1):3–39, 1981.

[278] V. Šverák. On optimal shape design. *Journal de mathématiques pures et appliquées*, 72(6):537–551, 1993.

[279] A. Świech and E. V. Teixeira. Regularity for obstacle problems in infinite dimensional hilbert spaces. *Advances in Mathematics*, 220(3):964–983, 2009.

[280] A. Takezawa, S. Nishiwaki, and M. Kitamura. Shape and topology optimization based on the phase field method and sensitivity analysis. *Journal of Computational Physics*, 229(7):2697–2718, 2010.

[281] L. Tao and D. Zichen. Design optimization for truss structures under elasto-plastic loading condition. *Acta Mechanica Solida Sinica*, 19(3):264–274, 2006.

[282] N. Tardieu and A. Constantinescu. On the determination of elastic coefficients from indentation experiments. *Inverse Problems*, 16(3):577–588, 2000.

[283] R. Temam. *Problèmes mathématiques en plasticité, volume 12 of Méthodes Mathématiques de l'Informatique [Mathematical Methods of Information Science]*. Gauthier-Villars, Montrouge, 1983.

[284] R. Temam. A generalized norton-hoff model and the prandtl-reuss law of plasticity. *Archive for Rational Mechanics and Analysis*, 95(2):137–183, 1986.

[285] A. Touzaline. Optimal control of a frictional contact problem. *Acta Mathematicae Applicatae Sinica, English Series*, 31(4):991–1000, 2015.

[286] F. Tröltzsch. *Optimal control of partial differential equations*, volume 112 of *Graduate Studies in Mathematics*. American Mathematical Society, Providence, RI, 2010. Theory, methods and applications, Translated from the 2005 German original by Jürgen Sprekels.

[287] C. A. Vidal and R. B. Haber. Design sensitivity analysis for rate-independent elastoplasticity. *Computer Methods in Applied Mechanics and Engineering*, 107(3):393–431, 1993.

[288] J.-L. Vié. *Second-order derivatives for shape optimization with a level-set method*. PhD thesis, Université Paris Est, 2016.

[289] G. Wachsmuth. Optimal control of quasi-static plasticity with linear kinematic hardening, part i: Existence and discretization in time. *SIAM Journal on Control and Optimization*, 50(5):2836–2861, 2012.

[290] G. Wachsmuth. Strong stationarity for optimal control of the obstacle problem with control constraints. *SIAM Journal on Optimization*, 24(4):1914–1932, 2014.

[291] J. Wang, J. Periaux, and M. Sefrioui. Parallel evolutionary algorithms for optimization problems in aerospace engineering. *Journal of Computational and Applied Mathematics*, 149(1):155 – 169, 2002. Scientific and Engineering Computations for the 21st Century - Me thodologies and Applications Proceedings of the 15th Toyota Conference.

[292] M. Y. Wang and L. Li. Shape equilibrium constraint: a strategy for stress-constrained structural topology optimization. *Structural and Multidisciplinary Optimization*, 47(3):335–352, 2013.

[293] M. Y. Wang, X. Wang, and D. Guo. A level set method for structural topology optimization. *Computer methods in applied mechanics and engineering*, 192(1):227–246, 2003.

[294] K. Washizu. *Variational Methods in Elasticity and Plasticity*. 01. Elsevier Science & Technology, 1974.

[295] C. Wieners. *Orthogonal projections onto convex sets and the application to problems in plasticity*. Citeseer, 1999.

[296] C. Wieners. Nonlinear solution methods for infinitesimal perfect plasticity. *ZAMM-Journal of Applied Mathematics and Mechanics/Zeitschrift für Angewandte Mathematik und Mechanik*, 87(8-9):643–660, 2007.

[297] P. Wriggers. *Computational contact mechanics*. Springer Science & Business Media, 2006.

[298] P. Wriggers and U. Nackenhorst. *Analysis and Simulation of Contact Problems (Lecture Notes in Applied and Computational Mechanics)*, volume 1. Springer, 1 edition, 2006.

[299] Q. Xia, T. Shi, S. Liu, and M. Y. Wang. A level set solution to the stress-based structural shape and topology optimization. *Computers & Structures*, 90:55–64, 2012.

[300] Y. M. Xie and G. P. Steven. *Evolutionary Structural Optimization*. Springer, 1997.

[301] T. Yamada, K. Izui, S. Nishiwaki, and A. Takezawa. A topology optimization method based on the level set method incorporating a fictitious interface energy. *Computer Methods in Applied Mechanics and Engineering*, 199(45):2876–2891, 2010.

[302] K. Yuge and N. Kikuchi. Optimization of a frame structure subjected to a plastic deformation. *Structural optimization*, 10(3-4):197–208, 1995.

[303] E. H. Zarantonello. *Projections on convex sets in Hilbert space and spectral theory*. University of Wisconsin, 1971.

[304] S. Zhou and M. Y. Wang. Multimaterial structural topology optimization with a generalized cahn–hilliard model of multiphase transition. *Structural and Multidisciplinary Optimization*, 33(2):89–111, 2007.